CHEMICAL RESEARCH, DEVELOPMENT & ENGINEERING CENTER

CRDEC-CR-062

FOUR TECHNIQUES TO MEASURE COMPLEX REFRACTIVE INDICES OF LIQUIDS AND SOLIDS AT CARBON DIOXIDE LASER WAVELENGTHS IN THE INFRARED SPECTRAL REGION

David M. Wieliczka
Marvin R. Querry

UNIVERSITY OF MISSOURI-KANSAS CITY
Kansas City, MO 64110

January 1990

U.S. ARMY ARMAMENT MUNITIONS CHEMICAL COMMAND

Aberdeen Proving Ground, Maryland 21010-5423

Disclaimer

The findings in this report are not to be construed as an official Department of the Army position unless so designated by other authorizing documents.

Distribution Statement

Approved for public release; distribution is unlimited.

UNCLASSIFIED
SECURITY CLASSIFICATION OF THIS PAGE

REPORT DOCUMENTATION PAGE

Form Approved OMB No. 0704-0188

1a. REPORT SECURITY CLASSIFICATION UNCLASSIFIED	1b. RESTRICTIVE MARKINGS
2a. SECURITY CLASSIFICATION AUTHORITY	3. DISTRIBUTION/AVAILABILITY OF REPORT Approved for public release; distribution is unlimited.
2b. DECLASSIFICATION/DOWNGRADING SCHEDULE	
4. PERFORMING ORGANIZATION REPORT NUMBER(S) CRDEC-CR-062	5. MONITORING ORGANIZATION REPORT NUMBER(S)
6a. NAME OF PERFORMING ORGANIZATION University of Missouri-Kansas City 6b. OFFICE SYMBOL (If applicable)	7a. NAME OF MONITORING ORGANIZATION
6c. ADDRESS (City, State, and ZIP Code) Kansas City, MO 64110	7b. ADDRESS (City, State, and ZIP Code)
8a. NAME OF FUNDING/SPONSORING ORGANIZATION CRDEC 8b. OFFICE SYMBOL (If applicable) SMCCR-RSP-P	9. PROCUREMENT INSTRUMENT IDENTIFICATION NUMBER DAAA15-85-K-0013
8c. ADDRESS (City, State, and ZIP Code) Aberdeen Proving Ground, MD 21010-5423	10. SOURCE OF FUNDING NUMBERS PROGRAM ELEMENT NO. / PROJECT NO. / TASK NO. / WORK UNIT ACCESSION NO.

11. TITLE (Include Security Classification)
Four Techniques to Measure Complex Refractive Indices of Liquids and Solids at Carbon Dioxide Laser Wavelengths in the Infrared Spectral Region

12. PERSONAL AUTHOR(S)
Wieliczka, David M., and Querry, Marvin R.

13a. TYPE OF REPORT	13b. TIME COVERED	14. DATE OF REPORT (Year, Month, Day)	15. PAGE COUNT
Contractor	FROM 85 Aug TO 88 Sep	1990 January	462

16. SUPPLEMENTARY NOTATION
COR: Merrill E. Milham, SMCCR-RSP-P, (301) 671-3854

17. COSATI CODES			18. SUBJECT TERMS (Continue on reverse if necessary and identify by block number)
FIELD	GROUP	SUB-GROUP	Absorption, Refractive indices, Reflectance, Carbon dioxide laser, Optical constants, Infrared
20	06		

19. ABSTRACT (Continue on reverse if necessary and identify by block number)
Four techniques were developed to determine the optical constants of liquids and solids. Two cells were designed and constructed to obtain the optical constants of liquids, a wedge-shaped cell and an internal reflectance cell. The wedge-shaped cell was used to determine the optical constants of 11 liquids in the spectral range 500 - 12500 cm^{-1}. The techniques of Querry and Avery were used in conjunction with the internal reflectance cell to obtain the complex refractive index of water and SF-96. The complex refractive indices of illite, kaolin, and montmorillinite were obtained from applying the techniques of Querrys and Averys. The error associated with each of the four techniques was also examined and is summarized.

20. DISTRIBUTION/AVAILABILITY OF ABSTRACT ☒ UNCLASSIFIED/UNLIMITED ☐ SAME AS RPT. ☐ DTIC USERS	21. ABSTRACT SECURITY CLASSIFICATION UNCLASSIFIED
22a. NAME OF RESPONSIBLE INDIVIDUAL SANDRA J. JOHNSON	22b. TELEPHONE (Include Area Code) (301) 671-2914 22c. OFFICE SYMBOL SMCCR-SPS-T

DD Form 1473, JUN 86 *Previous editions are obsolete.*

SECURITY CLASSIFICATION OF THIS PAGE
UNCLASSIFIED

SUMMARY

STATEMENT OF PROBLEM

The goals of this project were to develop four techniques to determine the optical constants of liquids and solids. Ihe four techniques originally proposed were: 1) Avery's method, 2) Querry's method, 3) Ellipsometry, and 4) Transmittance. In addition two devices were to be designed and constructed, a thin wedge-shaped cell and an internal reflectance accessory, to be used in determining the complex refractive index of liquids.

SUMMARY OF RESULTS

The two devices, the wedge-shaped cell and internal reflectance device, were designed and constructed. Both were used by graduate students in conjunction with a Perkin-Elmer 580B spectrophotometer to assure proper functioning of the units. The theses describing this work and their results are given in appendices 1.4 and 2.2. After testing the cells in the Perkin-Elmer the cells were positioned on the CO_2 laser system and used to obtain the complex refractive index of the same liquids. Due to an unknown and as yet unfound source of noise, the results obtained with the CO_2 laser are extremely poor. The noise with the internal reflectance accessory was large enough to preclude calculation of the complex refractive index.

The two techniques, Querry and Avery, were implemented with the CO_2 laser. The samples being studied were pressed pellets of illiie, kaolin, and monimorilliniie. Again, the results obtained with the CO_2 laser were extremely noisy as compared to the complex refractive index obtained with the Perkin-Elmer system by Querry. The error analysis of these two techniques indicate the need for extreme accuracy in measuring the reflection coefficients prior to determination of the complex refractive index. The roughness of the pellet surfaces does not lend itself to the accuracy necessary for these techniques.

Of the four techniques originally proposed, three were completed. The ellipsometry could not be completed due to problems with alignment of the reflection polarizers. The polarizers which were purchased were to have an angular output divergence of 2 mrad; the best we could align the polarizers was to 4 mrad. With this divergence, the output beam would precess in a circle of 4 mm diameter at a distance of 50 cm, the polarizer - detector separation distance. The technique of ellipsometry requires the rotation of two polarizers in order to acquire the necessary data. With the polarizers in their present condition, this would require the repositioning of the sample and detector for each angle of the polarizer in which the reflected intensity is to be measured. This would require a time period of approximately 10 minutes per polarization position, over 1 hour per wavelength and approximately 1 week per sample to acquire data for the entire wavelength region accessible by the CO_2 laser. Due to this difficulty, the technique of ellipsometry was not completed.

Although the data obtained with the CO_2 laser was quite noisy, we were confident of the equipment and computer programs which were used in obtaining the results. The wedge-shaped cell and the internal reflectance accessory when used in conjunction with the Perkin-Elmer instrument provided accurate results for the complex refractive index. The computer programs used to compute the complex refractive index using Querry's method and Avery's method have been debugged and tested to assure proper operation. The only failure was the inability to obtain an accurate measure of the carbon dioxide laser. Once this inability is removed, the complex refractive index as measured with the laser should be as accurate as that obtained with the Perkin-Elmer instrument.

RECOMMENDATIONS

The techniques which have been developed within this project have been shown to be valid techniques in obtaining the complex refractive index of both solids and liquids. The project should not be completely abandoned due to the noise encountered with the carbon dioxide laser. It is felt that the noise can be reduced with time and additional resources. Several items which would improve the acquisition system are: 1) IEE-488 interface board for the IBM computer system - allowing computer control of the lock-in amplifiers; 2) a more sensitive power meter allowing a better monitor of the laser output; 3) replacement of the pyroelectric detectors as they may be the source of the instability; and 4) a chamber constructed around the system to allow for purging of the optical path the infrared laser follows.

PREFACE

The work described in this report was authorized under Contract No. DAAA15-85-K-0013. This work was started in August 1985 and completed in September 1988.

The use of trade names or manufacturers' names in this report does not constitute an official endorsement of any commercial products. This report may not be cited for purposes of advertisement.

This report has been approved for release to the public.

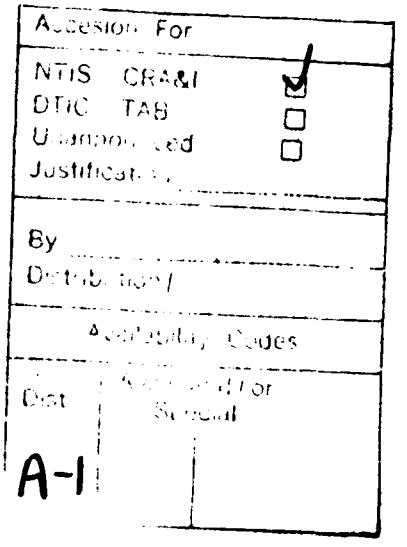

Blank

CONTENTS

LIST OF FIGURES

CHAPTER 1

APPENDIX 1.4

LIST OF TABLES

CHAPTER 1

APPENDIX 1.4

FOUR TECHNIQUES TO MEASURE COMPLEX REFRACTIVE INDICES OF LIQUIDS AND SOLIDS AT CARBON DIOXIDE LASER WAVELENGTHS IN THE INFRARED SPECTRAL REGION

I. THIN WEDGE-SHAPED CELL

a. INTRODUCTION

Many techniques exist for determining the complex refractive index of media. The technique we discuss here leads to a determination of the Lambert Absorption coefficient, $\alpha(\nu)$, from which follows the extinction coefficient, $k(\nu)$. Both of these quantities are functions of the wavenumber of the incident light, ν.

The time average flow of energy through a media is given by the relationship:

$$\langle \underline{S} \rangle = \frac{1}{2} \mathrm{Re}\left\{ \frac{c}{4\pi} \underline{E}(\underline{x}) \times \underline{H}(\underline{x}) \right\} \qquad (1.1)$$

Substitution for $\underline{E}$ and $\underline{H}$ by the expressions for an electromagnetic wave gives:

$$\langle \underline{S} \rangle = \langle \underline{S}_o \rangle \, e^{-2\beta(\underline{\kappa} \cdot \underline{x})} \qquad (1.2)$$

with $$\beta = \frac{2\pi\nu}{c} \sqrt{\mu\varepsilon} \left\{ \frac{-1 + \sqrt{1 + (2\sigma/\nu\varepsilon)^2}}{2} \right\} \qquad (1.3)$$

where ν is the wavenumber of the EM wave, $\underline{\kappa}$ is the propagation vector, ε is the dielectric function, μ is the magnetic permeability, and σ is the conductivity. One can obtain a physical interpretation of β if a comparison of the electromagnetic theory is made with the theory presented by Lambert[1]. Lambert showed that if homogeneous radiant energy strikes an absorbing medium, the amount absorbed will depend on the frequency of the radiation, the nature of the absorber, and the thickness of the absorber. If a parallel beam of homogeneous radiation of intensity I is incident on an isotropic, homogeneous sample with smooth, plane surfaces at normal

incidence, the decrease in intensity in a thickness dx of the sample due to absorption is given by:

$$-\frac{dI}{dx} = \alpha\, I, \qquad (1.4)$$

where α is known as the Lambert Absorption coefficient. For a finite sample width x we can integrate eq. 1.4 to obtain:

$$I = I_o\, e^{-\alpha x}, \qquad (1.5)$$

where I_o and I are the incident and transmitted intensities, respectively. A comparison of equations 1.2 and 1.5 lead to the identification:

$$\alpha = 2\beta \qquad (1.6)$$

The relationship between the Lambert absorption coefficient and the extinction coefficient (the imaginary part of the complex refractive index) is then given by:

$$\alpha(\nu) = 4\,\pi\,\nu\,k(\nu). \qquad (1.7)$$

Equations 1.5 and 1.7 provide a method of determining the extinction coefficient of an isotropic, homogeneous material. Experimentally, one requires a sample of known thickness with smooth parallel surfaces. The measurement of the fractional transmittance, T, given by the ratio of I/I_o, then provides the Lambert absorption coefficient from which the extinction coefficient can be determined. This technique is viable provided the sample thickness can be accurately determined. For samples with a low absorption coefficient a large sample thickness can be employed and therefore the thickness can be accurately determined through the use of mechanical devices, micrometer or calipers. Samples with large absorption coefficients, implying the need to employ thin samples, leads to the use of indirect measurements of the sample thickness. In addition to the difficulties associated with the determination of the sample thickness two other difficulties arise; 1) accurate measurement of the incident and transmitted intensity, and 2) the type of sample to be studied, i.e. solid, liquid, or gas.

In order to apply this technique to liquids a suitable cell was constructed which has a thin wedge shaped geometry (a complete description is given in the next section), allowing one to vary the sample thickness by translating the cell. Consider two transmission measurements performed with

the same frequency ν and at two vertical positions of the cell providing two sample thicknesses, x_1 and x_2. The fractional transmittance at each position is given by:

$$T(x_1,\nu) = T_a(\nu)\, T_s(\nu)\, \exp[-2d\alpha_w(\nu) - x_1\alpha_s(\nu)], \qquad (1.8)$$

where T_a and T_s are the spectral transmittance at the air-window and sample-window interfaces, respectively , α_w and α_s are the Lambert absorption coefficients of the windows and sample, respectively, and d is the window thickness. The Lambert absorption coefficient can then be determined by:

$$\alpha(\nu) = \frac{\ln\left[\, T(x_1,\nu)/T(x_2,\nu)\right]}{(x_2 - x_1)}, \qquad (1.9)$$

where $x_1 = z_1 \tan\varphi$, and φ is the vertex angle of the wedge-shaped volume and z_1 is the distance the wedge-shaped volume is translated perpendicular to the incident beam direction. Notice by performing the ratio of the fractional transmittance at two positions the effects due to the air-window and sample-window interfaces as well as absorption by the windows is removed.

The results we present in this report were obtained by measuring the fractional transmittance at many positions of the cell and applying a pseudo - linear least squares approach to equation 1.9. The natural logarithm of the ratio of the fractional transmittance is linear in the relative displacement of the cell, with the slope of the line being the Lambert absorption coefficient. Consider N transmittance values, T_i, each measured at a cell position z_i. From this set of N values we can compute N-1 distinct combinations of the N transmittance values. We define R_j as the average of the ratio of the fractional transmittance values associated with a relative increase in sample thickness given by $\bar{Z}_j = (z_i - z_{i+j})\tan\varphi$, and σ_j as the standard deviation of the R_j values. The natural logarithm of the R_j values are then linear in $\bar{Z}_j$. An example is worked in detail below with four fractional transmittance values.

Given transmittance values T_1, T_2, T_3, T_4 measured at positions z_1, z_2, z_3, z_4, respectively, produces three distinct combinations for the ratios of the transmittance values given by:

$$\left.\begin{aligned} R_1 &= (T_1/T_2 + T_2/T_3 + T_3/T_4)/3 & \mathcal{Z}_1 &= (z_2 - z_1)\tan\varphi \\ R_2 &= (T_1/T_3 + T_2/T_4)/2 & \mathcal{Z}_2 &= (z_3 - z_1)\tan\varphi \\ R_3 &= T_1/T_4 & \mathcal{Z}_3 &= (z_4 - z_1)\tan\varphi \end{aligned}\right\} \quad (1.10)$$

The standard deviation is defined as:

$$\sigma_1 = \left\{(1-1)^{-1} \sum_{1=1}^{1-1} [R_1 - (T_1/T_{1+1})]^2\right\}^{1/2} \quad (1.11)$$

The least squares fitting routine then fits the $\ln(R_1)$ versus $\mathcal{Z}_1$. The slope, intercept and standard deviation of these quantities are given in eqns. 1.12 thru 1.15.

Slope
$$\alpha = \frac{(M-1)\left[\Sigma \ln(R_1)\mathcal{Z}_1\right] - \left[\Sigma \mathcal{Z}_1\right]\left[\Sigma \ln(R_1)\right]}{(M-1)\left[\Sigma \mathcal{Z}_1^2\right] - \left[\Sigma \mathcal{Z}_1\right]^2}, \quad (1.12)$$

Intercept
$$A = \frac{\left[\Sigma \mathcal{Z}_1^2\right]\left[\Sigma \ln(R_1)\right] - \left[\Sigma \mathcal{Z}_1\right]\left[\Sigma \mathcal{Z}_1 \ln(R_1)\right]}{(M-1)\left[\Sigma \mathcal{Z}_1^2\right] - \left[\Sigma \mathcal{Z}_1\right]^2}, \quad (1.13)$$

STD slope
$$\sigma_\alpha = \frac{(M-1)\,\sigma_y^2}{(M-1)\left[\Sigma \mathcal{Z}_1^2\right] - \left[\Sigma \mathcal{Z}_1\right]^2}, \quad (1.14)$$

STD Intercept
$$\sigma_A = \frac{\sigma_y^2\left[\Sigma \mathcal{Z}_1^2\right]}{(N-1)\left[\Sigma \mathcal{Z}_1^2\right] - \left[\Sigma \mathcal{Z}_1\right]^2}, \quad (1.15)$$

where
$$\sigma_y = \frac{1}{(M-2)} \sum (\ln(R_1) - A - \alpha\,\mathcal{Z}_1)^2, \quad (1.16)$$

and M is the number of $\mathcal{Z}$,R data pairs. The computer program to calculate

these values is given in the program listed in appendix 1.2 called WMENU, in subroutine RATIO.

b. CALIBRATION OF THE CELL

The vertex angle φ of the empty wedge-shaped volume between the windows was determined by measuring the interference pattern for a HeNe laser beam reflected from the respective window-air and air-window interfaces. A complete description of the formation of the interference fringes for a wedge-shaped volume can be found in Born and Wolf[2]. Figure 1.1 shows the pertinent geometry associated with the wedge shaped volume in reference to the production of the interference fringes. The optical path length difference between SAP and SBCDP is given by:

$$\Lambda = 2\, n'z \tan \varphi \cos \theta', \qquad (1.17)$$

and the phase difference associated with this optical path length difference is given by:

$$\Delta\phi = 2\, \pi\, \Lambda / \lambda_o = 4\, \pi\, n'z \tan \varphi \cos \theta' / \lambda_o, \qquad (1.18)$$

where λ_o is the wavelength of the incident light in vacuum, n' is the index of refraction of the medium between the windows which make up the wedge-shaped volume, θ' is the angle of incidence within the wedge-shaped volume, and z is the distance the cell is translated. Taking into account the phase shift upon reflection at the window-air boundary we have for minimum interference:

$$(2m+1)\pi = 4\, \pi\, n'z \tan \varphi \cos \theta' / \lambda_o \pm \pi. \qquad (1.19)$$

From Eq. 1.19 we have for the tangent of the wedge angle:

$$\tan \varphi = m\, \lambda_o / (2\, n'z \cos \theta') \qquad (1.20)$$

If we consider near normal incidence, $\cos \theta' \cong 1$, and air as the media in the wedge-shaped volume Eq. 1.20 reduces to:

$$\tan \varphi = m\, \lambda_o / 2\, z \qquad (1.21)$$

Eq. 1.21 indicates the vertex angle can be determined by translating the cell a distance z and counting the number of maxima, m as the cell is translated.

In the most recent version of the wedge-shaped cell a stepper motor has been attached, allowing the cell to be positioned under computer control. As the stepper motor/translator vertically displaces the cell, the pattern of interference fringes is acquired in digital form using an entrance slit assembly preceeding a photomultiplier tube. The output of the photomultiplier tube is appropriately connected to an A/D channel of a Data Acquisition and Control Adapter installed in an IBM PS-2 model 30 computer (the computer program, FMENU, used in obtaining the interference pattern and

in performing the Fourier transform is given in appendix 1.1). An interference pattern that was obtained in this manner is shown in Fig. 1.2. As the cell was translated in the vertical z direction, the intensity I(z) of the interference pattern is given by:

$$I(z) = A + B \cos(4\pi z \nu_o \tan\varphi + \rho), \qquad (1.22)$$

where A and B are constants, $\nu_o = 15{,}802.8\ cm^{-1}$ is the wavenumber of the HeNe laser light, φ is the vertex angle of the wedge-shaped volume, and ρ is an arbitrary phase factor. The Fourier transform of Eq. 1.22 gives:

$$I(\nu) = \sqrt{2\pi}\left\{ A\,\delta(\gamma) + B\,[\,\delta(\gamma-\zeta)\,e^{i\rho} + \delta(\gamma+\zeta)\,e^{-i\rho}]\right\}, \qquad (1.23)$$

where $\gamma = 2\pi\nu$, and $\zeta = 4\pi\nu_o \tan\varphi$. Thus,

$$\tan\varphi = \nu/(2\nu_o) = m/(2\nu_o N\,\Delta z), \qquad (1.24)$$

where m is the integer position of $\delta(\gamma-\zeta)$ in the interval $0 \le m \le (N/2)-1$ of the Digital Fast Fourier Transform (DFFT) used in this work, N is the number of data points in the digitized interference pattern, and Δz is the incremental z direction displacement of the cell between data points in the digitized interference pattern. In Eq. 1.24 we used the relations $\nu = m\Delta\nu$ and $N = (\Delta z \Delta\nu)^{-1}$. Comparison of Eqs. 1.21 and 1.24 demonstrate that m in Eq. 1.24 is the number of minima, or maxima, in the digitized interference pattern. In Fig. 1.3 we present the DFFT of the interference pattern shown in Fig. 1.2. The inset in the upper right corner is an enlargement of the region of the DFFT spectrum of interest.

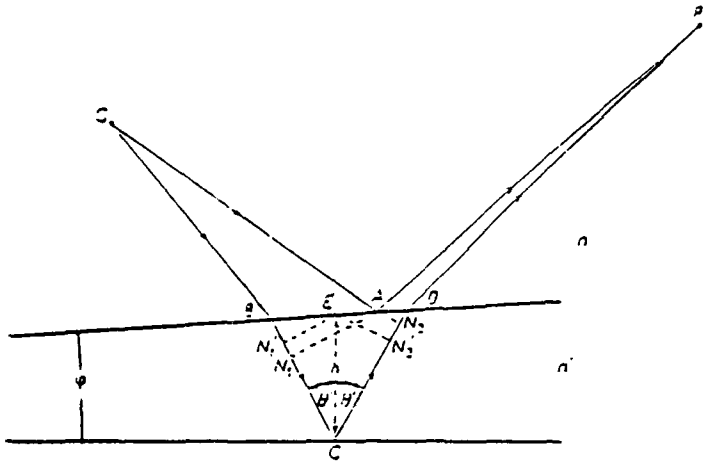

$$\Delta\mathcal{S} = n(SB + DP - SA - AP) + n'(BC + CD),$$

$$nSA \sim nSB + n'BN_1,$$

$$nAP \sim nDP + n'N_2D,$$

$$\Delta\mathcal{S} \sim n'(N_1'C + CN_2'),$$

$$N_1C + CN_2 \sim N_1'C + CN_2',$$

$$N_1'C = CN_2' = h\cos\theta',$$

The optical path difference

$$\Delta\mathcal{S} = 2n'h\cos\theta',$$

FIG. 1.1 Geometry for determination of optical path length difference for a wedge-shaped volume.

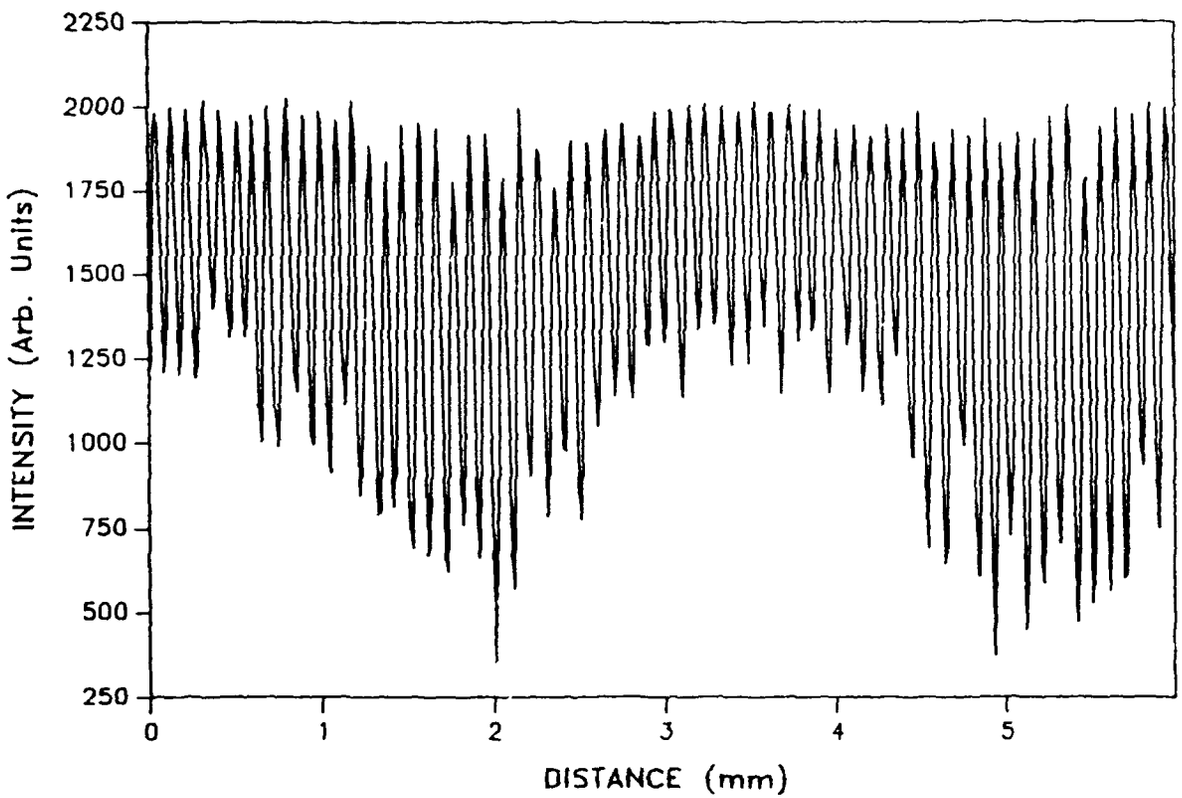

FIG. 1.2 Interference pattern obtained by stepping the wedge-shaped cell and measuring the reflected He-Ne laser intensity.

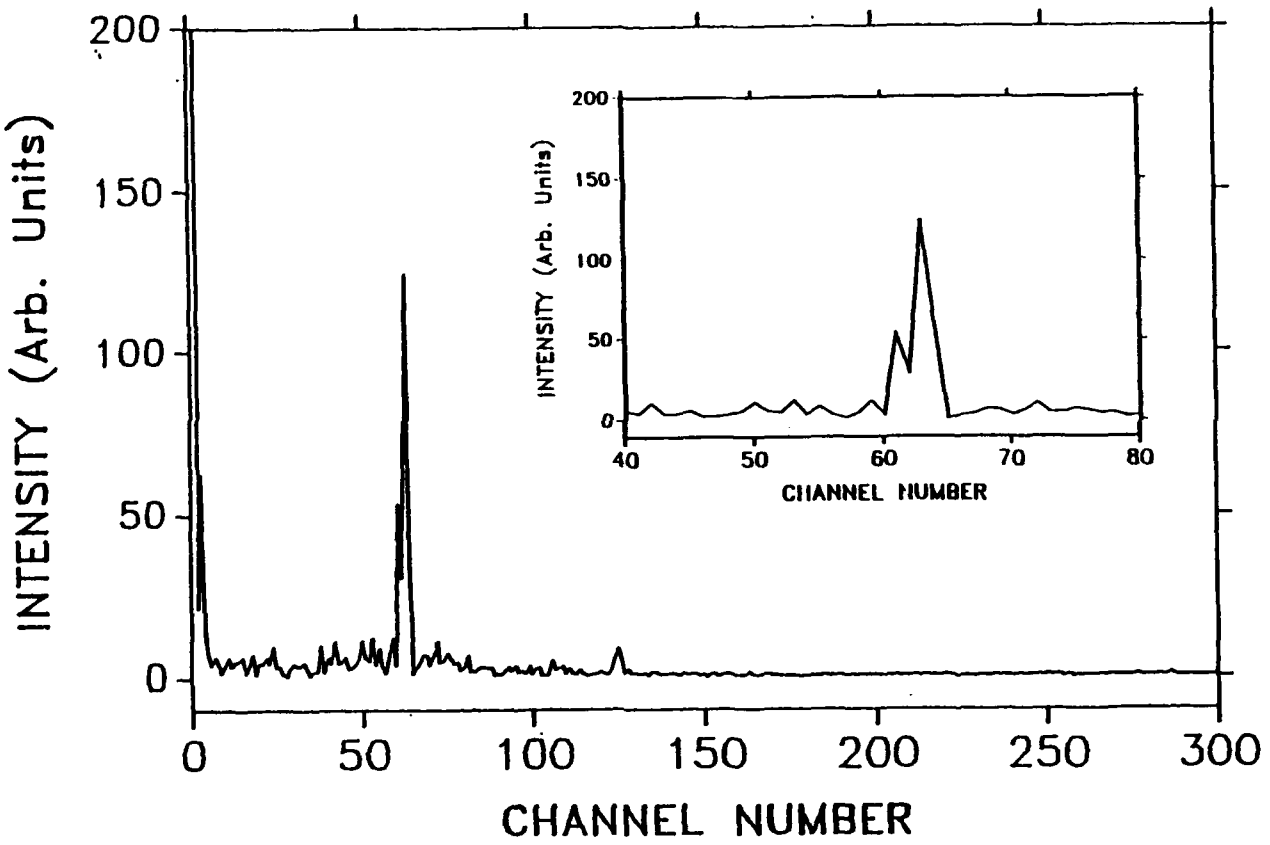

FIG. 1.3 Fast Fourier Transform of the interference pattern in FIG. 1.2. The inset is an expanded scale of the peak near channel number 60.

c. ERROR ANALYSIS

The error in the Lambert absorption coefficient can be evaluated using the theory of the propagation of error. In general for a function of several variables $q(x,\ldots,z)$ with uncertainties $\delta x,\ldots,\delta z$ the uncertainty in q is

$$\delta q = \sqrt{\left(\frac{\partial q}{\partial x}\,\delta x\right)^2 + \ldots\ldots + \left(\frac{\partial q}{\partial z}\,\delta z\right)^2}\ , \qquad (1.25)$$

where the uncertainties in $x,\ldots,z$ have been assumed to be independent and random. In applying Eq. 1.25 we shall examine the error in determining the vertex angle first using Eq. 1.24 and then use the error in the vertex angle to examine the error in the Lambert absorption coefficient using Eq. 1.9. The two equations of importance are given below.

$$\alpha(\nu) = \frac{\ln\left[\, T(x_1,\nu)/T(x_2,\nu)\right]}{(x_2 - x_1)}\ , \qquad (1.9)$$

$$\tan\varphi = \nu/(2\nu_o) = m/(2\nu_o N\,\Delta z), \qquad (1.24)$$

The fractional error in the tangent of the vertex angle can be shown to be given by:

$$\frac{\delta(\tan\varphi)}{\tan\varphi} = \left\{ \left(\frac{\delta m}{m}\right)^2 + \left(\frac{\delta(\Delta z)}{\Delta z}\right)^2 \right\}^{1/2}\ , \qquad (1.26)$$

where m is the number of interference fringes in the pattern and Δz is the incremental distance the cell is translated. From our measurements we can assign values of $\delta m = 1$, $\delta(\Delta z) = 0.0001$ mm, $50 \le m \le 100$, and $\Delta z = 0.01$ mm. Substitution into Eq. 1.26 gives for the fractional error in the tangent of the apex angle a maximum value of 2%. The uncertainty in the fringe count contributes approximately half to the uncertainty in the tangent of the vertex angle.

The fractional uncertainty in the Lambert absorption coefficient can be determined in the same fashion and is given by:

$$\frac{\delta\alpha}{\alpha} = \left\{ \left[\frac{\delta(\tan\varphi)}{\tan\varphi}\right]^2 + \left[\frac{\delta(Z_j)}{Z_j}\right]^2 + \frac{2}{(\ln(R_j))^2}\left[\left[\frac{\delta I_i}{I_i}\right]^2 + \left[\frac{\delta I_{oi}}{I_{oi}}\right]^2\right]\right\}^{1/2} \tag{1.27}$$

From the previous discussion of the error in the tangent of the vertex angle the first quantity under the quadratic is 2%, the second quantity is associated with the error in positioning the cell andis on the order of 2%, the last two quantities deal with the uncertainty in measuring the incident and transmitted intensities. We have assumed the fractional uncertainty is the same for any two measurements of the transmitted flux. If we have $\delta I/I = 5\%$ for both the incident and transmitted intensities and $0.2 \leq R_j \leq 0.9$ then the fractional uncertainty in the Lambert absorption coefficient can range from $7\% \leq (\delta\alpha/\alpha) \leq 95\%$. The uncertainty as determined by Eq. 1.27 is valid for a direct determination of the Lambert absorption coefficient, i.e. employing only two transmittance measurements to determine the absorption coefficient. The uncertainty in α is reasonable provided the value R_j is below 0.3.

This value can be reduced dramatically by applying a linear least squares fit to the plot of $\log(R_j)$ vs Z_j. The error using this technique can be determined using Eq. 1.14 and reduces the fractional error to a value of 5% or less.

d. DESCRIPTION OF THE CELL

An exploded view of the wedge-shaped cell is shown in Fig. 1.4. The cell comprises:

a rectangular stainless steel cell holder 1 measuring 16.25 x 7.8 x 2.23 cm^3 with rectangular hole measuring 5.23 x 2.54 x 2.23 cm^3 centered therethrough, with threaded holes 7',7'',8',8'' to receive set screws with rounded tips, with threaded holes therein to receive ball plungers 9' and 9'', with stainless steel posts 5',5'',6', and 6'' mounted thereon as shown in Fig. 1.4, with threaded holes in the top to receive screws for attaching holder 1 via a stainless steel angle piece to Unislide translator 17, with side threaded holes therein for mounting rectangular stainless steel pieces 4' and 4'', with eight threaded holes therein to receive screws for mounting toggle clamps 2' and 2'' thereon, and with two holes therethrough for receiving reducing manifolds 15' and 15'';

toggle clamps 2' and 2'' mounted on 1 as shown in Fig. 1.4;

spring plungers 3' and 3'' mounted in the heads of 2' and 2'', respectively;

rectangular stainless steel pieces 4' and 4'' mounted on 1, and with threaded holes therein to receive ball plungers 10' and 10'';

stainless steel posts 5', 5'',6', and 6'' mounted on 1 as shown in Fig. 1.4;

stainless steel feeler gauge stock 11 for mounting below posts 6' and 6'' and in slot between 1 and rectangular pieces 4' and 4'', and for mounting between windows 21' and 21'';

reducing manifolds 12' and 12'' for respectively filling and venting the cell;

stainless steel channel holders 13' and 13'' to receive and protect manifolds 12' and 12'', respectively;

teflon spacers 14' and 14'' mounted on manifolds 13' and 13'', respectively, and for pressing against side edges of windows 21' and 21'' thus sealing the side edges;

tubing reducers 15' and 15'' connected respectively by shrinkable tubing to one side of manifolds 12' and 12'', for connecting on the opposite side of one of said mainfolds to a syringe for filling the cell with liquid, and for opening the opposite side of other said manifold to vent cell during filling;

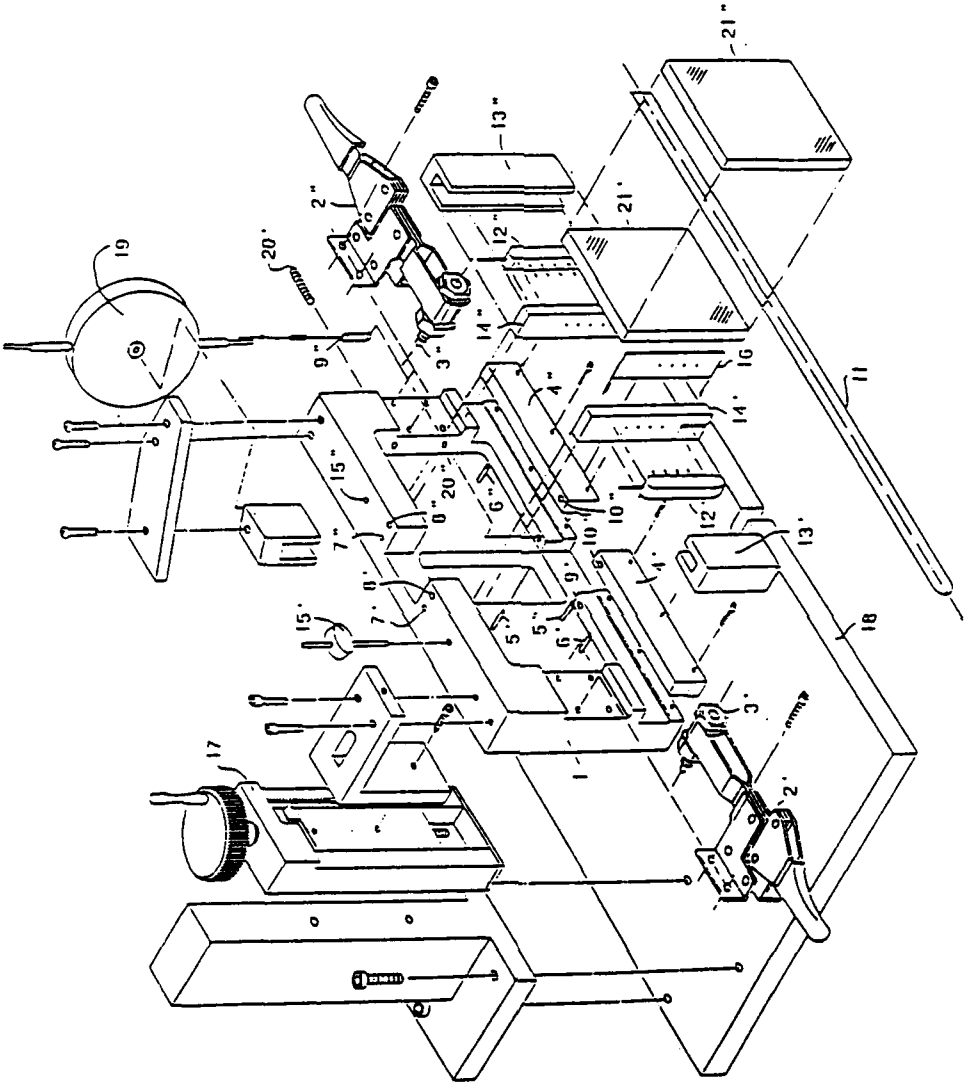

FIG. 1.4 Exploded view of the wedge-shaped cell.

rectangular stainless steel piece 16' mounting between 12' and 14', and resting in contact with stainless steel posts 5' and 5'';

Unislide translator 17' with manually operated crank for adjusting vertical displacement between 1 and 18, with 17' mounted on vertical standard, and with vertical standard mounted on base plate 18 as shown in Fig. 1.4;

base plate 18 for mounting cell holder in sample compartment of spectrophotometer;

dial indicator 19 mounted on 1, as shown in Fig. 1.4, and for measuring vertical displacement between 1 and 18;

machine screws 20' and 20'' in threaded holes in 1 for applying horizontal force to 13'' and thus sealing sides of cell by forcing 14' and 14'' in contact with windows 21' and 21'';

two ZnSe or uv grade fused silica windows 21' and 21'' measuring 25 x 25 x 0.6 cm^3.

In the most current version of the cell holder, the manual crank on Unislide translator 17 was replaced with a computer controlled stepper motor. To mount the stepper motor, four cylindrical posts were end mounted vertically on base 18, and the stepper motor was then mounted on the opposite ends of said posts so the shaft of said motor is co-axial with the drive screw of the Unislide translator 17.

Before assembly the components of the cell are cleaned in acetone, methyl alcohol, or ethyl alcohol in an ultrasonic cleaner. The cell is then assembled as follows. Attach rectangular stainless steel pieces 4' and 4'' to holder 1 using six threaded machine screws as indicated in Fig. 1.4. Attach toggle clamps 2' and 2'' to holder 1. Connect holder 1, Unislide 17, and base plate 18 as indicated in Fig. 1.4. connect dial indicator 19 to holder 1 as indicated in Fig. 1.4.

Place manifolds 12' and 12'' in stainless steel channel holders 13' and 13'', respectively. Place stainless steel rectangular piece 16 on 12', and teflon spacers 14' and 14'' respectively on 12' and 12''. Place assembled units (13', 12', 16, 14') and (13'', 12'', 14'') in holder 1 as shown in Fig. 1.4. Use shrinkable tubing through appropriate holes in 1 to connect reducers 15' and 15'' to 12' and 12'', respectively.

Place window 21' flat against the side of holder 1 as indicated in Fig. 1.4. Window 21' is held in rigid vertical position by set screws 7' and 7'' and ball plungers 9' and 9''. Apply a very thin layer of vacuum grease along the top edge-face of window 21'. Apply very thin layer of vacuum

grease to both surfaces of feeler stock 11, then place 11 horizontally in slot between 1 and 4', 1 and 4'', and in contact with lower edge of window 21'. Place 21'' in holder 1 with top edge in contact with window 21', and with bottom edge in contact with feeler stock 11. Window 21'' is held rigid vertical position by set screws 8' and 8'' and ball plungers 10' and 10''. Toggle clamps 2' and 2'' are then closed so spring plungers 3' and 3'' gently but resiliently contact the surface of window 21''. Finally, tighten set screws 20' and 20'' thus applying force to 13'', causing 16 to contact 5' and 5'', and causing 14' and 14'' to contact windows 21' and 21''. The teflon spacers 14' and 14'' seal the sides of the cell, and the vacuum grease seals the top and bottom edges of the cell.

After measuring the wedge angle φ, the cell was filled with the liquid sample. A syringe containing the liquid was attached to a tube on the upper side of reducer 15' and the liquid was injected throught the reducer, shrinkable tubing, and manifold 12' into the cell. This procedure was performed very slowly and carefully, otherwise air bubbles remained in the cell or the seals ruptured causing leakage. During this process manifold 12'' and reducer 15'' were open to vent the air in the cell. When the cell was full, the syringe was removed and the tubes connected to the top of reducers 15' and 15'' were sealed with pinch clamps. In tests the cell has remained sealed for several days without leakage.

e. ACQUISITION OF DATA

After the tangent of the vertex angle is determined and the cell is successfully filled with the liquid sample to be studied the CO_2 laser is turned on and allowed to stabilize, a period of 30 minutes is normally needed to stabilize the Edinburgh CO_2 laser. During this time the computer program WMENU, given in appendix 1.2 is loaded and all electrical connections are checked and the A/D converters are tested to assure proper working order.

The procedure for acquiring data for each line available from the CO_2 laser is given below.

1. The cell is positioned such that the CO_2 laser beam is transmitted through the thinnest part, i.e. near the vertex.
2. The CO_2 laser is then tuned to the appropriate line and the dither stabilizer unit is activated.
3. The sample and reference lock-in amplifiers are adjusted with respect to phase, amplitude, and time constant.
4. The operating parameters are input into the computer to be stored with the data.
5. Control of the stepper motor is turned over to the computer program.
6. The sample and reference lock-ins and the power meter are read at each position of the cell.
7. The amplitudes of the lock-ins and power meter are displayed on the screen allowing the operator to monitor the data acquisition process. If the noise appears large the operator can abort the acquisition of data with no data stored to disk.
8. If the scan is completed the program automatically calculates the values R_i and Z_i and computes the best fit line. The results of the fitting procedure provide the Lambert absorption coefficient and the uncertainty as determined from the fit to the raw data.
9. The data pairs Z, ln(R) are plotted on an Hewlett-Packard plotter along with the standard deviation of ln(R). The results of the fitting procedure are used to superimpose a straight line onto the data.
10. The cell is returned to the starting position and procedures 2 thru 9 are repeated.

Table 1.1 is a listing of raw data as taken by the computer system. The digital values as read by the A/D converter have been converted to the approriate reading from the lock-in. The data was obtained on June, 27, 1988.

The scan parameters were

Tan φ = 2.44E-03
Wavelength = 10.22 μm
Step size = 0.2 mm
Number of steps = 40
Sample Lock-in Scale = 0.005 V
Reference Lock-in Scale = 0.005 V
Power Meter Scale = 1 W
Time Constant = 0.1 sec.
Number of A/D readings to average = 10

TABLE 1.1

Raw transmission data from wedge-shaped cell

Sample Position (cm)	Sample Lock-In (Volts)	Reference Lock-in (Volts)	Power Meter (Watts)
0.20000E-01	0.21724E-02	0.32183E-02	0.83408E+00
0.40000E-01	0.21035E-02	0.32146E-02	0.82939E+00
0.60000E-01	0.20320E-02	0.32048E-02	0.82510E+00
0.80000E-01	0.19543E-02	0.32073E-02	0.82847E+00
0.10000E+00	0.18948E-02	0.32153E-02	0.82622E+00
0.12000E+00	0.18298E-02	0.32139E-02	0.82480E+00
0.14000E+00	0.17629E-02	0.32058E-02	0.82681E+00
0.16000E+00	0.17109E-02	0.32156E-02	0.82578E+00
0.18000E+00	0.16533E-02	0.32131E-02	0.82554E+00
0.20000E+00	0.15940E-02	0.32097E-02	0.82769E+00
0.22000E+00	0.15381E-02	0.32200E-02	0.82690E+00
0.24000E+00	0.14885E-02	0.32012E-02	0.82510E+00
0.26000E+00	0.14480E-02	0.32212E-02	0.82349E+00
0.28000E+00	0.13884E-02	0.32122E-02	0.83369E+00
0.30000E+00	0.13474E-02	0.32200E-02	0.82524E+00
0.32000E+00	0.12996E-02	0.32136E-02	0.82236E+00
0.34000E+00	0.12571E-02	0.32122E-02	0.83037E+00
0.36000E+00	0.12124E-02	0.32217E-02	0.82656E+00
0.38000E+00	0.11602E-02	0.32039E-02	0.82344E+00
0.40000E+00	0.11157E-02	0.32104E-02	0.82808E+00
0.42000E+00	0.10857E-02	0.32173E-02	0.82212E+00
0.44000E+00	0.10376E-02	0.32112E-02	0.82407E+00
0.46000E+00	0.99951E-03	0.32151E-02	0.82646E+00
0.48000E+00	0.96875E-03	0.32019E-02	0.82300E+00
0.50000E+00	0.93848E-03	0.32080E-02	0.82578E+00
0.52000E+00	0.90405E-03	0.32178E-02	0.82793E+00
0.54000E+00	0.86279E-03	0.32085E-02	0.82705E+00
0.56000E+00	0.83545E-03	0.32021E-02	0.82427E+00
0.58000E+00	0.79932E-03	0.32065E-02	0.82480E+00
0.60000E+00	0.77295E-03	0.32058E-02	0.82769E+00
0.62000E+00	0.74414E-03	0.32061E-02	0.82168E+00
0.64000E+00	0.72388E-03	0.31953E-02	0.82441E+00
0.66000E+00	0.68970E-03	0.31973E-02	0.82920E+00
0.68000E+00	0.67627E-03	0.32017E-02	0.82236E+00
0.70000E+00	0.64258E-03	0.31885E-02	0.82539E+00
0.72000E+00	0.61670E-03	0.31904E-02	0.82603E+00
0.74000E+00	0.59570E-03	0.31914E-02	0.82134E+00
0.76000E+00	0.56958E-03	0.32048E-02	0.82461E+00
0.78000E+00	0.54077E-03	0.31912E-02	0.82324E+00
0.80000E+00	0.53345E-03	0.32024E-02	0.82427E+00

The forty intensity readings given in Table 1.1 provide 39 unique sample thicknesses. Table 1.2 lists the natural logarithm of the averages of the ratios for each of these sample thicknesses and the standard deviation for each value. The linear least square fit to this data provides a Lambert absorption coefficient of 740.3 ± 0.6 cm^{-1}

The data from Table 1.1 is presented in graphical form in Fig. 1.5. The readings from the sample and reference lock-ins are indicated by the symbols filled circles and plus symbols, respectively, and are associated with the left axis. The power meter readings are represented by the stars and are associated with the right axis. Notice the smooth exponential decay in the sample lock-in readings and the almost constant reference lock-in readings. The power meter readings were not used in any calculations but were measured as a check of the reference lock-in.

The natural logarithm of the ratios of these intensities are plotted versus the relative sample thickness in Fig. 1.6. Superimposed on this graph is the linear least squares fit to the data. Notice the excellent agreement between the linear fit and the computed data values. The vertical error bars for each data point represent the standard deviation of the $Ln(R_j)$ computed from the raw data. The last data point does not have a standard deviation associated with it since the ratio is for the largest relative sample thickness and only one value can be determined.

TABLE 1.2

Ln(R) versus $\mathcal{Z}$

Wavelength = 10.220 μm (978.47 cm $)^{-1}$

Sample Thickness $\mathcal{Z}$ (cm)	Ln(R)	$\sigma_{Ln(R)}$
0.48726E-04	0.35904E-01	0.73207E-02
0.97451E-04	0.72406E-01	0.79011E-02
0.14618E-03	0.10874E+00	0.89730E-02
0.19490E-03	0.14464E+00	0.10526E-01
0.24363E-03	0.18063E+00	0.12355E-01
0.29235E-03	0.21649E+00	0.12269E-01
0.34108E-03	0.25205E+00	0.13010E-01
0.38980E-03	0.28814E+00	0.13486E-01
0.43853E-03	0.32390E+00	0.13923E-01
0.48726E-03	0.36006E+00	0.15647E-01
0.53598E-03	0.39607E+00	0.17629E-01
0.58471E-03	0.43248E+00	0.18855E-01
0.63343E-03	0.46866E+00	0.19727E-01
0.68216E-03	0.50495E+00	0.21565E-01
0.73088E-03	0.54107E+00	0.21414E-01
0.77961E-03	0.57709E+00	0.20795E-01
0.82834E-03	0.61336E+00	0.21285E-01
0.87706E-03	0.64993E+00	0.22235E-01
0.92579E-03	0.68629E+00	0.22652E-01
0.97451E-03	0.72209E+00	0.24403E-01
0.10232E-02	0.75854E+00	0.25453E-01
0.10720E-02	0.79435E+00	0.26213E-01
0.11207E-02	0.82984E+00	0.27479E-01
0.11694E-02	0.86560E+00	0.26738E-01
0.12181E-02	0.90169E+00	0.25360E-01
0.12669E-02	0.93763E+00	0.25647E-01
0.13156E-02	0.97323E+00	0.25875E-01
0.13643E-02	0.10090E+01	0.23781E-01
0.14130E-02	0.10440E+01	0.24576E-01
0.14618E-02	0.10800E+01	0.26522E-01
0.15105E-02	0.11155E+01	0.26841E-01
0.15592E-02	0.11524E+01	0.24435E-01
0.16079E-02	0.11880E+01	0.26839E-01
0.16567E-02	0.12265E+01	0.21464E-01
0.17054E-02	0.12641E+01	0.20376E-01
0.17541E-02	0.13014E+01	0.23628E-01
0.18028E-02	0.13408E+01	0.14409E-01
0.18516E-02	0.13752E+01	0.13835E-01
0.19003E-02	0.13993E+01	----------

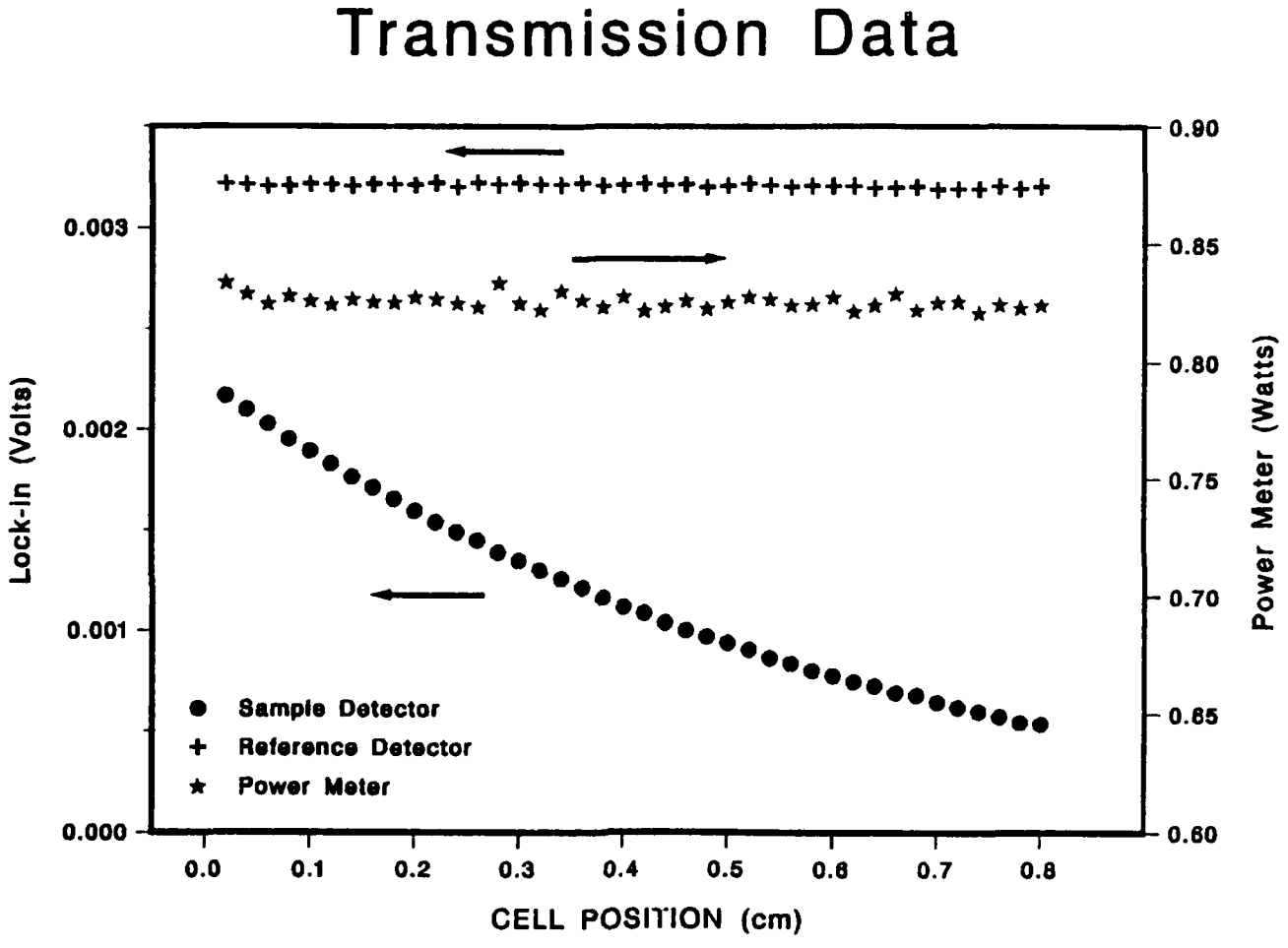

FIG. 1.5 Typical raw data obtained with the CO_2 laser. Solid circles represent the sample lock-in reading, plus symbols the reference lock-in reading, and stars the power meter reading. The power meter readings are associated with the right axis.

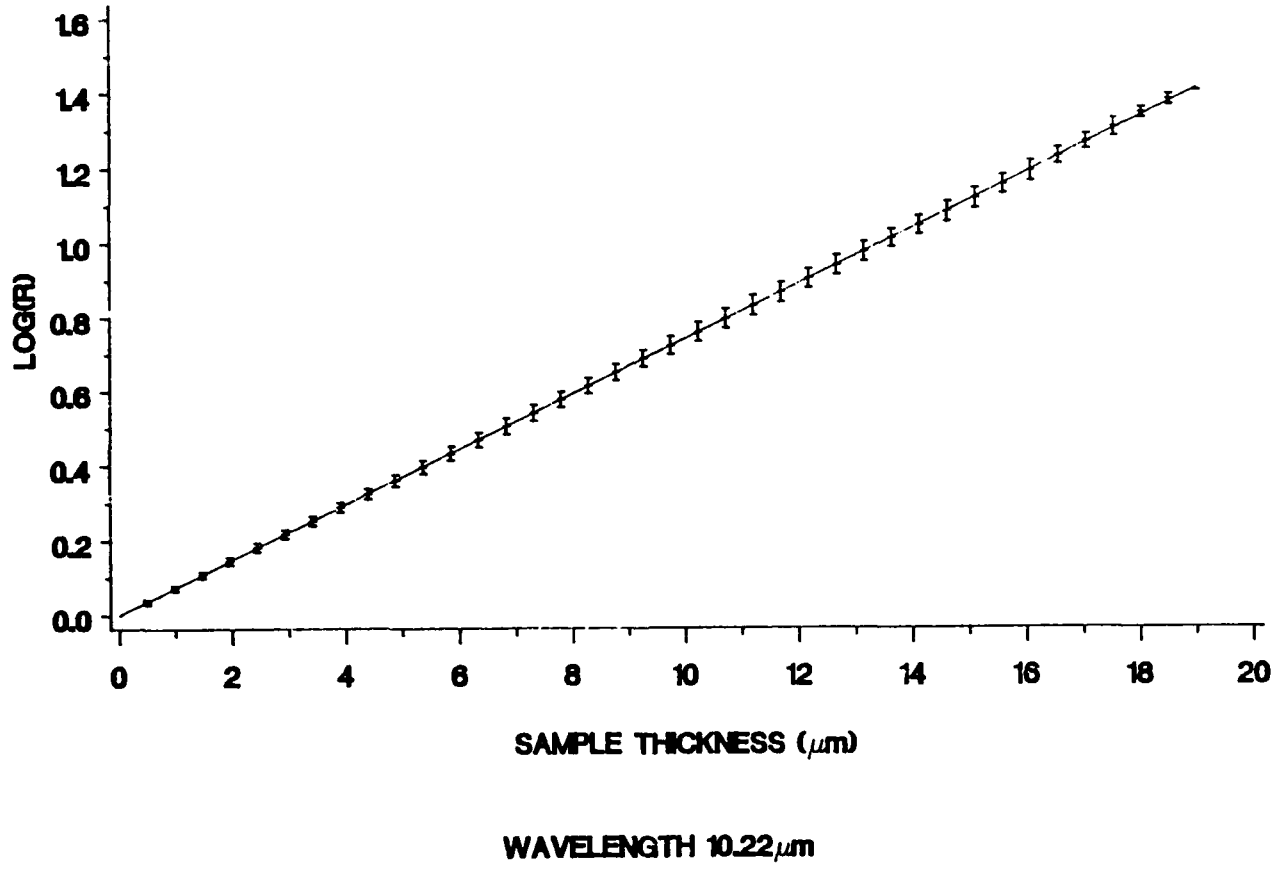

FIG. 1.6 Data from FIG. 1.5 reduced to determine the Lambert absorption coefficient. The vertical bars associated with each data point represent the standard deviation of the log(R) for that sample translation value. The straight line is the best fit line determined through least squares fitting.

f. RESULTS

The wedge shaped cell was employed to obtain extinction coefficients for five liquids. In this section we present the results and provide a discussion of these experiments.

The results for water are presented graphically in Fig. 1.7 and in a tabular form in Table 1.3. The solid line in Fig. 1.7 represents values determined by Weng[3] for the extinction coefficient in this spectral range, the data obtained with the CO_2 laser are represented by the plus symbols and have error bars which are given by the standard deviation of the slope as determined from the linear least squares fitting routine. Table 1.2 provides the wavenumber, extinction coefficient and standard deviation of the extinction coefficient. From the table one can observe the reasonable uncertainty associated with the computed values of the extinction coefficient and would conclude the extinction coefficients were accurately determined, with the exception of a few data points. A quick glance at Fig. 1.7 indicates the results may be accurately determined but are not precise. The scatter in the values for k indicate the error entering the experiment is random. We have not been able to positively identify the source of this error but have several ideas concerning its origin. A discussion of the possible errors will be left for the next section.

TABLE 1.3

Extinction Coefficient for Water

Wavenumber cm^{-1}	Extinction Coefficient k	σ_k	Percent Uncertainty
928.94	7.9522E-02	3.5166E-03	4.4222E+00
934.93	8.2382E-02	3.5419E-03	4.2993E+00
936.77	8.0022E-02	9.1688E-03	1.1458E+01
940.56	8.5544E-02	1.9519E-02	2.2818E+01
942.42	6.7411E-02	1.7819E-03	2.6433E+00
944.20	6.7273E-02	1.3133E-02	1.9521E+01
945.98	5.6295E-02	3.5063E-03	6.2285E+00
947.78	6.9473E-02	7.4842E-03	1.0773E+01
949.49	7.6584E-02	8.2690E-03	1.0797E+01
951.20	6.7353E-02	2.6007E-03	3.8613E+00
952.93	6.2640E-02	4.5935E-03	7.3331E+00
954.56	6.1277E-02	2.0555E-03	3.3545E+00
970.50	5.9552E-02	1.0513E-03	1.7653E+00
971.91	5.4634E-02	4.0300E-04	7.3764E-01
973.24	5.2435E-02	2.2179E-03	4.2298E+00
974.66	5.0925E-02	1.5737E-03	3.0903E+00
975.90	4.8646E-02	1.3963E-03	2.8704E+00
980.87	4.5925E-02	6.9049E-04	1.5035E+00
982.13	5.9898E-02	6.1213E-03	1.0220E+01
983.19	4.0724E-02	6.0602E-03	1.4881E+01
986.49	4.2312E-02	7.6235E-03	1.8017E+01
1031.57	5.6561E-02	2.2126E-02	3.9118E+01
1035.52	5.1231E-02	3.3664E-03	6.5710E+00
1037.45	5.5219E-02	2.4190E-03	4.3806E+00
1039.39	5.0708E-02	6.4546E-03	1.2729E+01
1045.04	4.8098E-02	2.1300E-03	4.4284E+00
1046.90	3.9027E-02	7.0448E-04	1.8051E+00
1048.66	4.4686E-02	5.8680E-03	1.3132E+01
1050.53	4.5267E-02	4.2524E-03	9.3940E+00
1052.19	4.1476E-02	7.6939E-04	1.8550E+00
1053.96	3.5626E-02	3.5447E-03	9.9499E+00
1055.63	4.1336E-02	1.2215E-03	2.9551E+00
1071.93	4.3802E-02	6.3678E-03	1.4538E+01
1076.08	3.0190E-02	2.7106E-03	8.9785E+00
1077.35	2.3928E-02	1.3673E-03	5.7142E+00
1078.63	3.3411E-02	9.6241E-04	2.8805E+00
1079.91	4.9247E-02	2.6625E-03	5.4063E+00
1081.08	8.4879E-02	7.9844E-02	9.4068E+01
1082.37	3.2051E-02	2.9443E-03	9.1864E+00

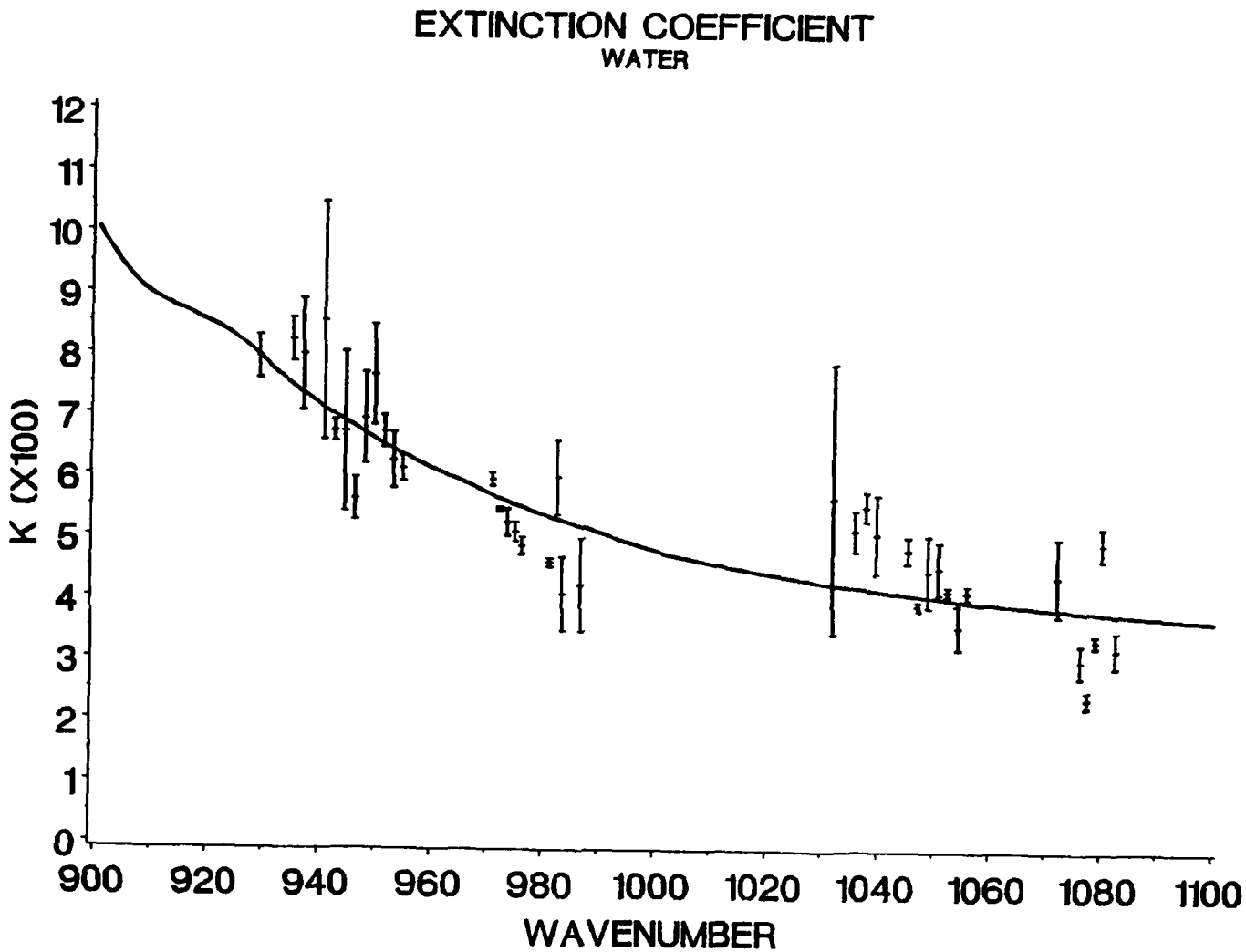

FIG. 1.7 Extinction coefficient for water in the 900 to 1100 cm^{-1} spectral region, the k values have been multiplied by 100. The solid line is data from Shengshan Weng's thesis. The data obtained with the CO_2 laser is represented by the plus symbols and the error bars are +/- one standard deviation.

The results for SF-96 are presented in Figs. 1.8 and 1.9 are given in Table 1.4. Fig. 1.7 is an overview of the entire spectral range available to the CO_2 laser with Fig. 1.8 being an expanded scale. The solid line in these figures is data obtained by using the wedge shaped cell in a Perkin-Elmer IR spectrophotometer (see S. Wengs thesis in appendix 1.4). The extinction coefficients determined with the Perkin-Elmer instrument have a fractional uncertainty of 2-5%. Again the results obtained with the laser are not in agreement with the results form the Perkin-Elmer instrument. The agreement becomes worse as the extinction coefficient increases.

The results for DMMP are given in Figs. 1.10 and 1.11 and in Table 1.5. The agreement between the data obtained with the laser and the data obained with the Perkin-Elmer instrument is again poor. The agreement is better in the region of low extinction coefficient.

The results for DIMP are shown in Figs. 1.12, 1.13 and 1.14 and in Table 1.6. The discussion of the results for water, SF-96, and DMMP is again applicable here. In addition the data obtained at 1030 - 1060 cm^{-1} show even poor agreement at small extinction coefficients.

The results for DEP are shown in Figs. 1.15 and 1.16 and in Table 1.7. The agreement between the two methods of measuring the extinction coefficient is again very poor.

TABLE 1.4

Extinction coefficient for SF-96

Wavenumber cm^{-1}	Extinction Coefficient k	σ_k	Percent Uncertainty
926.96	1.4815E-02	3.4614E-04	2.3364E+00
928.94	1.4353E-02	4.5574E-04	3.1752E+00
931.01	1.4399E-02	7.6141E-04	5.2878E+00
932.92	1.5437E-02	1.2931E-03	8.3768E+00
934.93	6.6369E-03	1.9005E-03	2.8635E+01
936.77	1.8125E-02	2.1930E-03	1.2100E+01
938.70	2.3881E-02	1.5893E-03	6.6554E+00
940.56	5.6538E-03	6.2744E-04	1.1098E+01
942.42	2.1432E-02	1.4990E-03	6.9942E+00
944.20	7.8900E-03	5.7345E-04	7.2680E+00
947.78	2.5646E-02	2.6509E-03	1.0336E+01
949.49	1.8713E-02	9.4371E-04	5.0431E+00
951.20	1.4526E-02	1.1291E-03	7.7729E+00
952.93	1.4551E-02	1.0856E-03	7.4606E+00
969.09	3.6275E-02	4.4717E-03	1.2327E+01
970.50	3.2426E-02	1.3461E-03	4.1512E+00
971.91	3.2102E-02	3.6802E-03	1.1464E+01
973.24	2.9943E-02	7.1954E-04	2.4030E+00
974.66	2.9407E-02	1.7169E-03	5.8383E+00
975.90	3.3477E-02	1.0444E-03	3.1198E+00
977.23	4.0857E-02	2.1798E-03	5.3351E+00
978.47	5.2419E-02	3.7317E-03	7.1189E+00
979.72	4.8873E-02	5.3017E-03	1.0848E+01
980.87	4.1274E-02	1.1705E-03	2.8360E+00
986.49	5.7138E-02	6.2137E-03	1.0875E+01
982.13	6.2091E-02	2.1874E-02	3.5229E+01
983.19	4.3718E-02	5.4719E-02	1.2516E+02
1035.52	2.7242E-02	1.9576E-02	7.1861E+01
1037.45	1.0437E-01	1.7548E-01	1.6813E+02
1043.19	7.6768E-02	1.1092E-01	1.4448E+02
1045.04	5.8066E-01	3.0748E+00	5.2954E+02
1048.66	2.9849E-01	5.4829E-01	1.8369E+02
1050.53	4.2707E-01	9.9174E-01	2.3222E+02

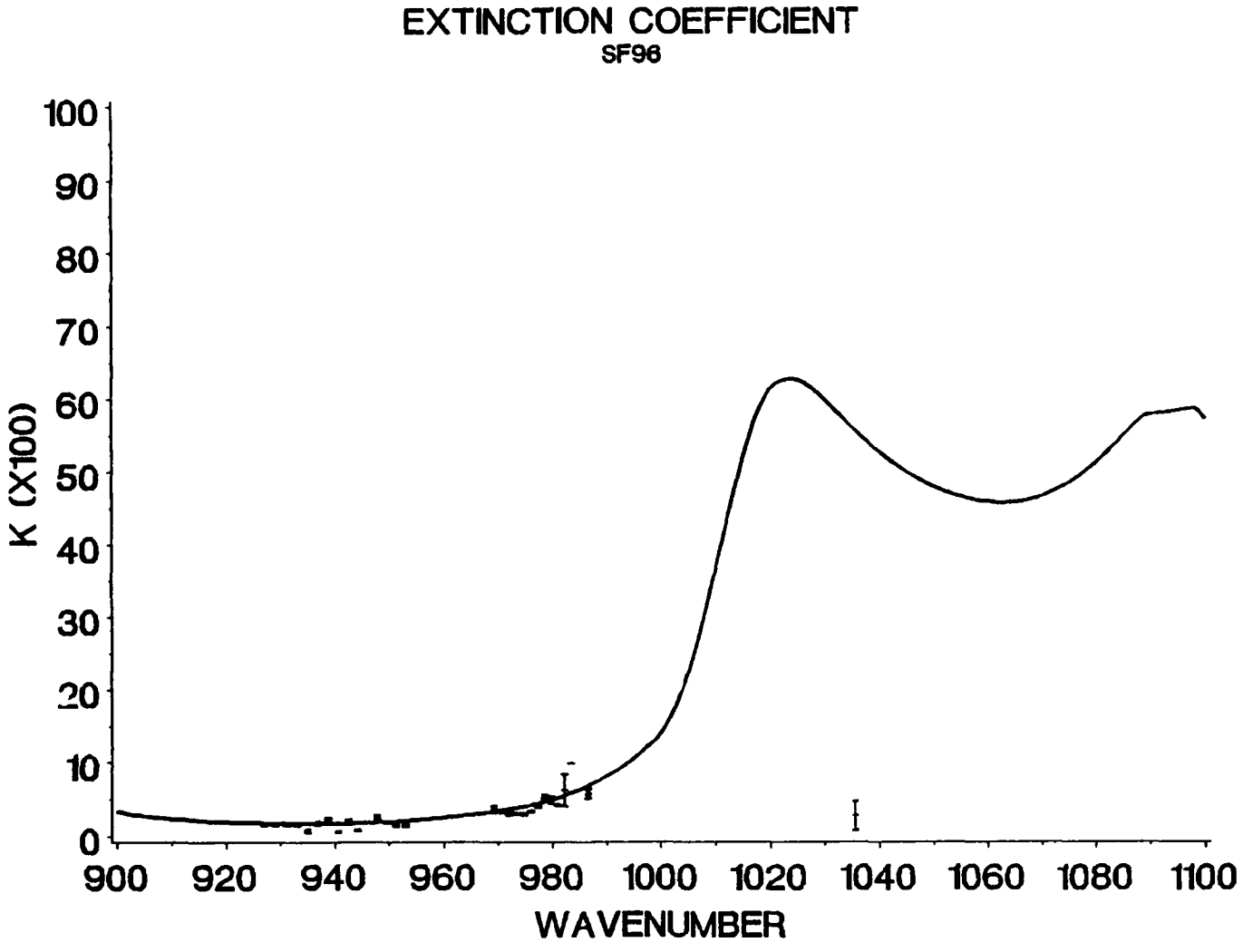

FIG. 1.8 Extinction coefficient for SF-96 in the wavenumber region 900 to 1100 cm^{-1}. The k values have been multiplied by 100. The solid line is data from Shengshan Weng's thesis. The data obtained with the CO_2 laser is represented by the plus symbols and the error bars are +/- one standard deviation.

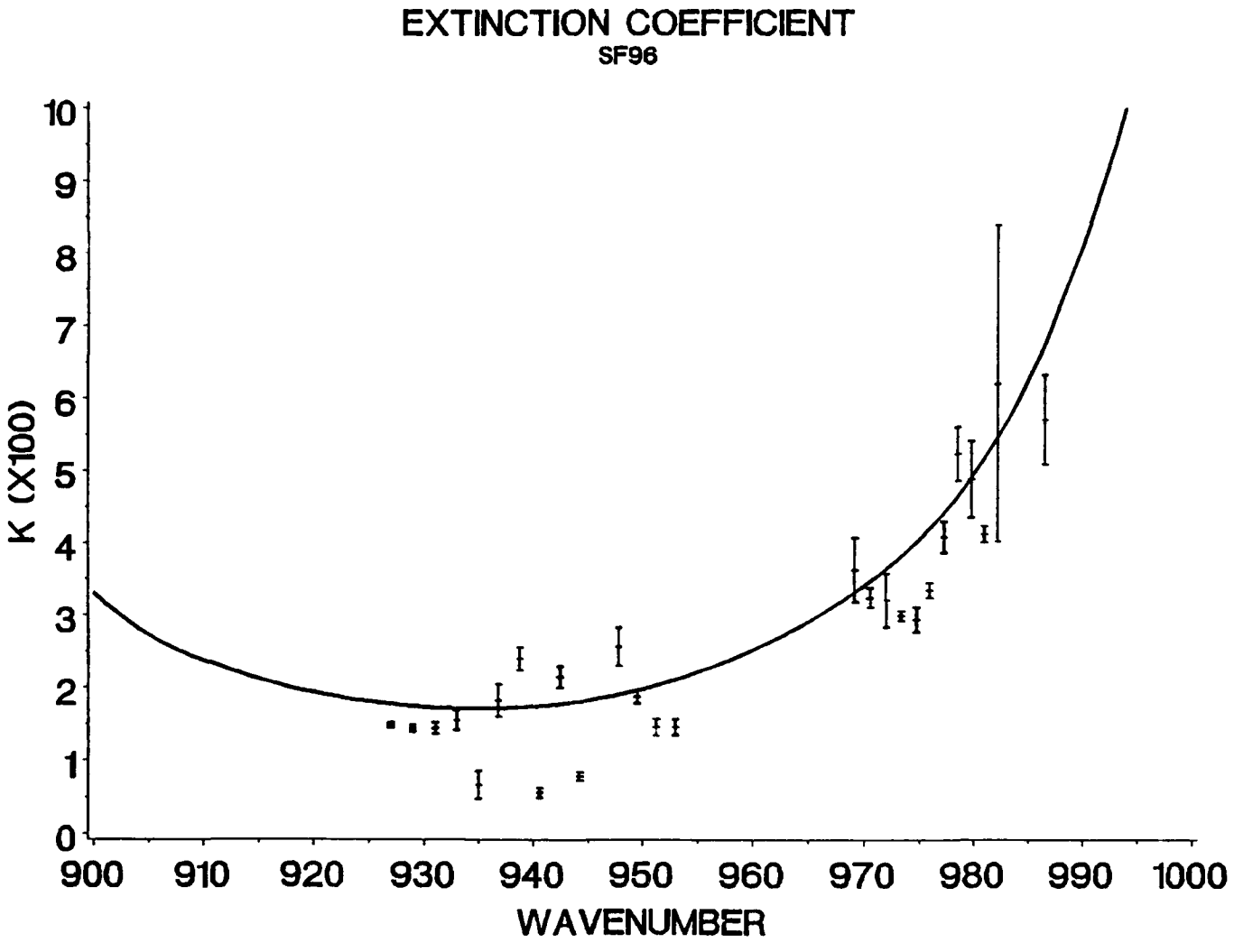

FIG. 1.9 Extinction coefficient for SF-96 in the wavenumber region 900 to 1000 cm^{-1}. The k values have been multiplied by 100. The solid line is data from Shengshan Weng's thesis. The data obtained with the CO_2 laser is represented by the plus symbols and the error bars are +/- one standard deviation.

TABLE 1.5

Extinction Coefficient for DMMP

Wavenumber cm^{-1}	Extinction Coefficient k	σ_k	Percent Uncertainty
928.94	1.1193E-01	2.8273E-02	2.5259E+01
931.01	8.2118E-02	1.0865E-03	1.3230E+00
932.92	7.5154E-02	1.4935E-03	1.9872E+00
934.93	4.9124E-02	5.2508E-04	1.0689E+00
936.77	3.5527E-02	3.3028E-04	9.2968E-01
938.70	4.7937E-02	5.8740E-04	1.2254E+00
940.56	3.9216E-02	3.4164E-04	8.7117E-01
942.42	2.6544E-02	3.3725E-04	1.2705E+00
944.20	2.6297E-02	1.1214E-03	4.2642E+00
945.98	2.9994E-02	1.0598E-03	3.5333E+00
947.78	3.1017E-02	1.4159E-03	4.5647E+00
949.49	2.5621E-02	5.5399E-04	2.1622E+00
951.20	2.6841E-02	8.8027E-04	3.2796E+00
952.93	3.1740E-02	5.5842E-04	1.7594E+00
954.56	3.3434E-02	5.8197E-04	1.7407E+00
969.09	3.2676E-02	4.4712E-04	1.3684E+00
970.50	2.6844E-02	9.4312E-04	3.5133E+00
971.91	2.4061E-02	7.1610E-04	2.9762E+00
973.24	2.1826E-02	7.3598E-04	3.3720E+00
975.90	2.2083E-02	1.0105E-03	4.5757E+00
977.23	2.3058E-02	8.8508E-04	3.8384E+00
978.47	2.4928E-02	7.6278E-04	3.0599E+00
979.72	2.4918E-02	3.4391E-04	1.3802E+00
980.87	3.1127E-02	7.0385E-03	2.2612E+01
982.13	2.5796E-02	8.2460E-04	3.1967E+00
983.19	2.4446E-02	1.1657E-03	4.7684E+00
1035.52	6.2486E-04	1.5172E-01	2.4281E+04
1037.45	7.4406E-01	2.8424E-02	3.8201E+00
1039.39	3.0850E-02	1.3933E-02	4.5165E+01
1043.19	5.6774E-01	1.3669E-01	2.4075E+01
1045.04	5.3841E-01	2.4414E-02	4.5344E+00
1048.66	2.9230E-01	3.3088E-01	1.1320E+02
1050.53	6.8413E-01	2.6433E+00	3.8638E+02
1052.19	6.0164E-01	3.8817E-02	6.4519E+00
1077.35	1.9964E-01	9.4714E-03	4.7443E+00
1078.63	1.3121E-01	2.2930E-03	1.7475E+00
1081.08	1.5346E-01	9.0250E-03	5.8808E+00

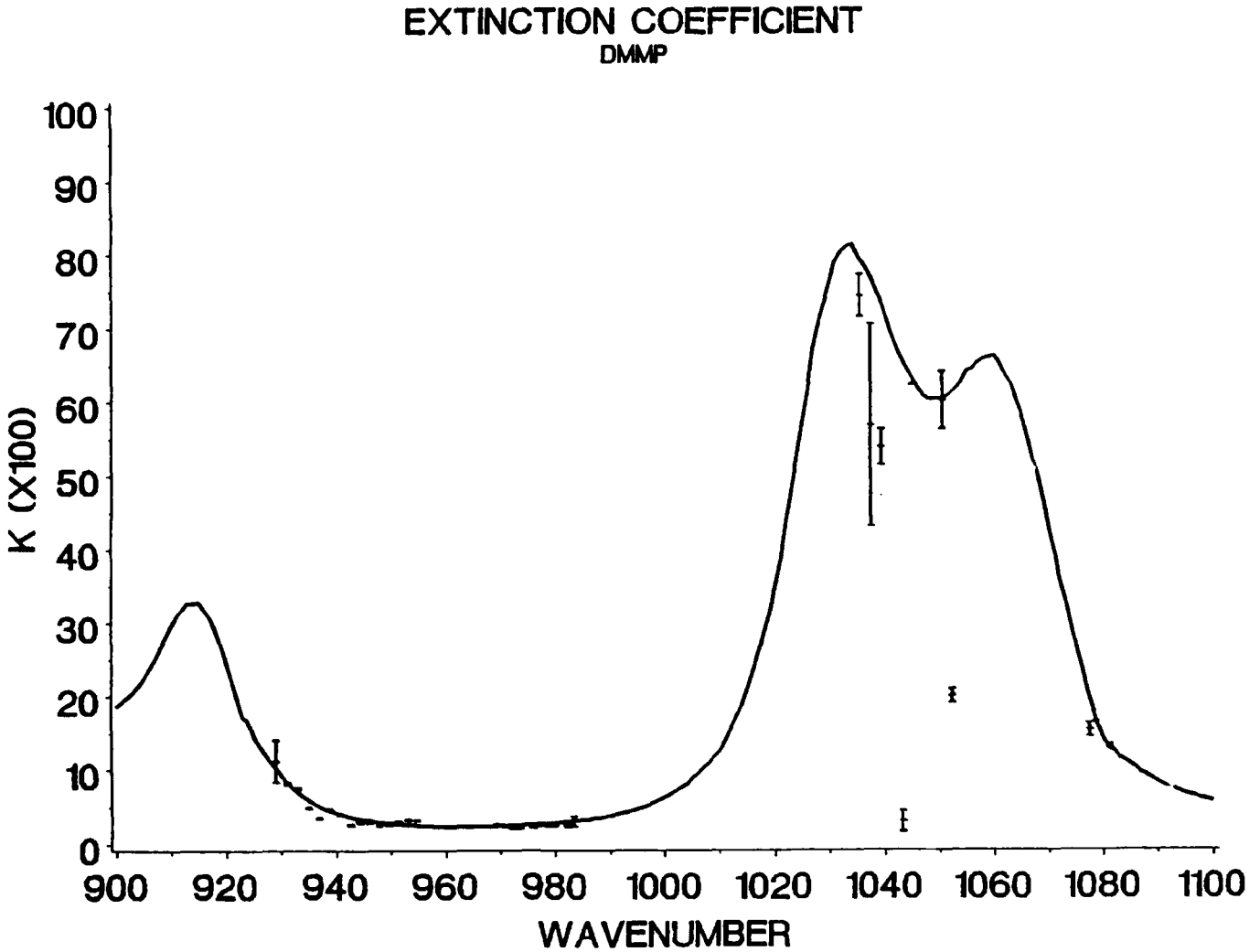

FIG. 1.10 Extinction coefficient for DMMP in the wavenumber region 900 to 1100 cm^{-1}. The k values have been multiplied by 100. The solid line is data from Shengshan Weng's thesis. The data obtained with the CO_2 laser is represented by the plus symbols and the error bars are +/- one standard deviation.

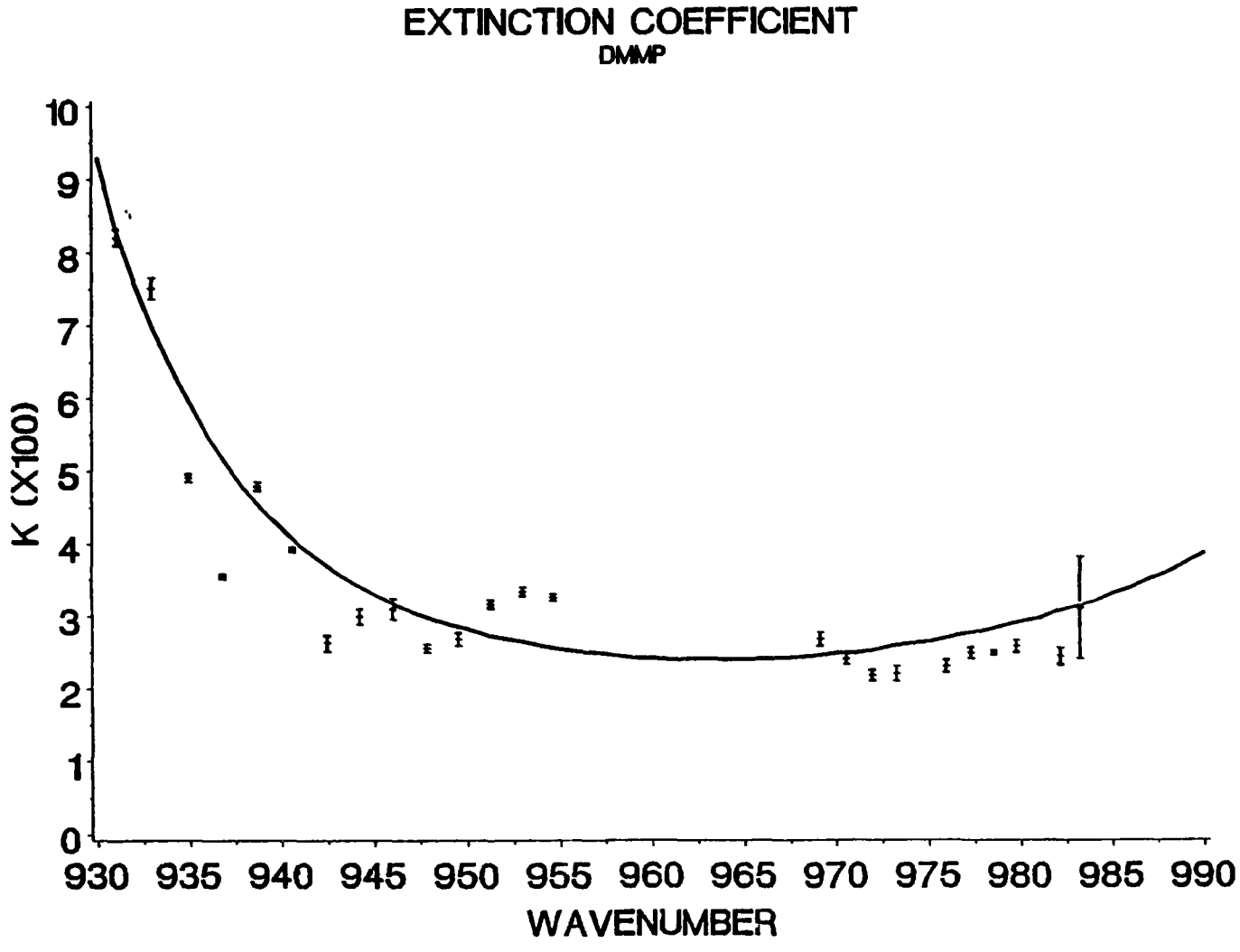

FIG. 1.11 Extinction c efficient for DMMP in the wavenumber region 930 to 990 cm^{-1}. The k values have been multiplied by 100. The solid line is data from Shengshan Weng's thesis. The data obtained with the CO_2 laser is represented by the plus symbols and the error bars are +/- one standard deviation.

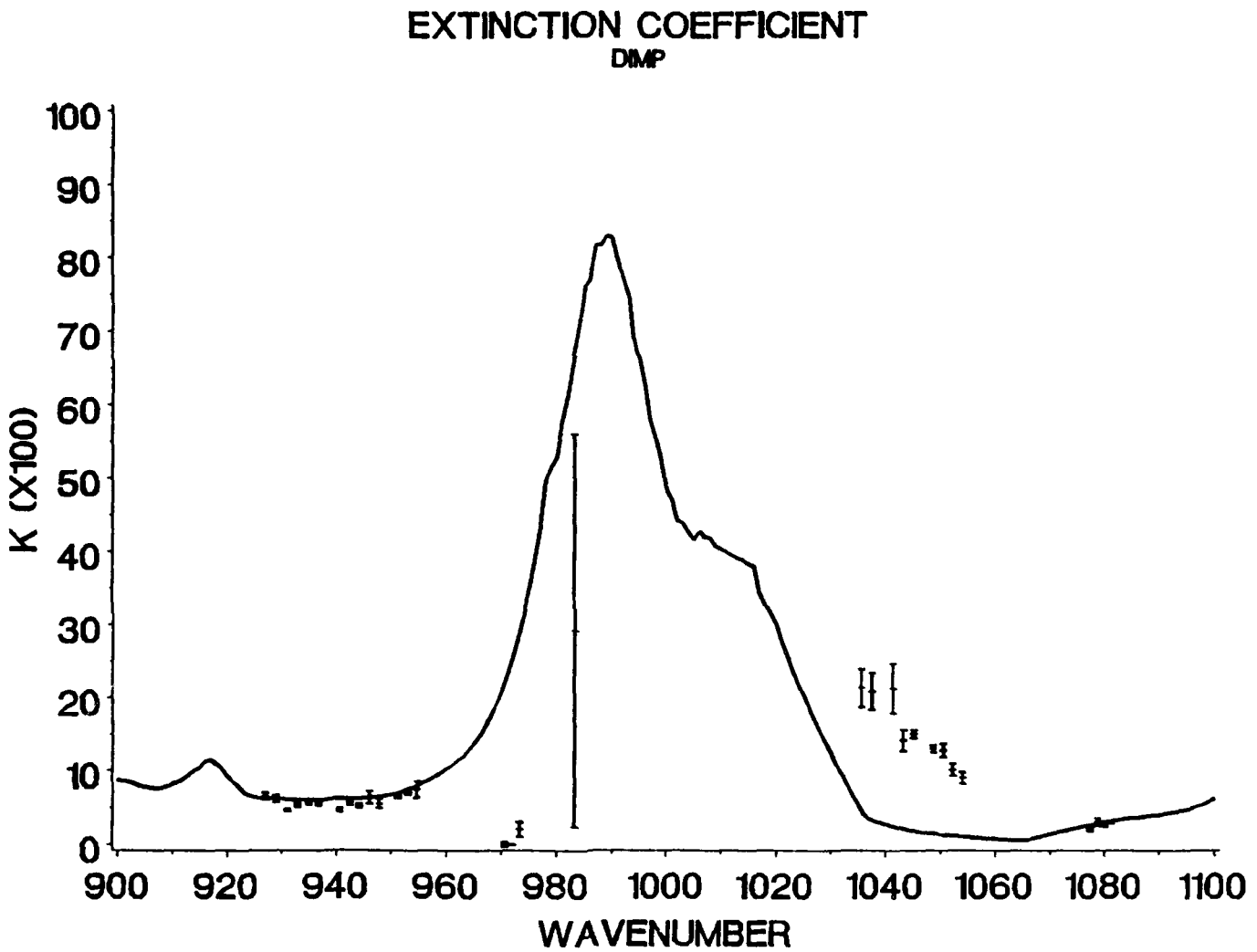

FIG. 1.12 Extinction coefficient for DIMP in the wavenumber region 900 to 1100 cm^{-1}. The k values have been multiplied by 100. The solid line is data from Shengshan Weng's thesis. The data obtained with the CO_2 laser is represented by the plus symbols and the error bars are +/- one standard deviation.

TABLE 1.6

Extinction Coefficient for DIMP

Wavenumber cm^{-1}	Extinction Coefficient k	σ_k	Percent Uncertainty
926.96	6.5435E-02	4.6936E-03	7.1729E+00
928.94	6.2046E-02	4.7790E-03	7.7024E+00
931.01	4.6316E-02	1.4005E-03	3.0237E+00
932.92	5.3394E-02	2.6158E-03	4.8990E+00
934.93	5.6080E-02	2.1344E-03	3.8059E+00
936.77	5.6430E-02	3.1860E-03	5.6460E+00
940.56	4.6369E-02	2.7676E-03	5.9686E+00
942.42	5.6630E-02	3.9873E-03	7.0411E+00
944.20	5.2272E-02	2.0666E-03	3.9536E+00
945.98	6.3569E-02	8.7368E-03	1.3744E+01
947.78	5.5481E-02	6.0266E-03	1.0863E+01
951.20	6.5228E-02	1.4765E-03	2.2636E+00
952.93	7.0378E-02	2.1701E-03	3.0834E+00
954.56	7.4847E-02	1.1031E-02	1.4738E+01
969.09	1.3261E-02	6.1072E-02	4.6055E+02
970.50	6.5360E-04	3.0655E-03	4.6903E+02
971.91	1.1119E-04	4.8553E-04	4.3667E+02
973.24	2.0667E-02	9.8507E-03	4.7663E+01
983.19	2.9271E-01	2.6834E-01	9.1675E+01
1035.52	2.1354E-01	2.6375E-02	1.2352E+01
1037.45	2.0894E-01	2.5434E-02	1.2173E+01
1041.34	2.1288E-01	3.4261E-02	1.6094E+01
1043.19	1.4124E-01	1.4826E-02	1.0497E+01
1045.04	1.5020E-01	5.3398E-03	3.5552E+00
1048.66	1.2984E-01	4.6696E-03	3.5965E+00
1050.53	1.2766E-01	9.0464E-03	7.0862E+00
1052.19	1.0104E-01	8.1868E-03	8.1022E+00
1053.96	9.0402E-02	7.7305E-03	8.5513E+00
1077.35	2.1527E-02	2.1149E-03	9.8241E+00
1078.63	3.0936E-02	4.7694E-03	1.5417E+01
1079.91	2.8357E-02	3.8533E-03	1.3589E+01
1081.08	3.1230E-02	2.3248E-03	7.4440E+00

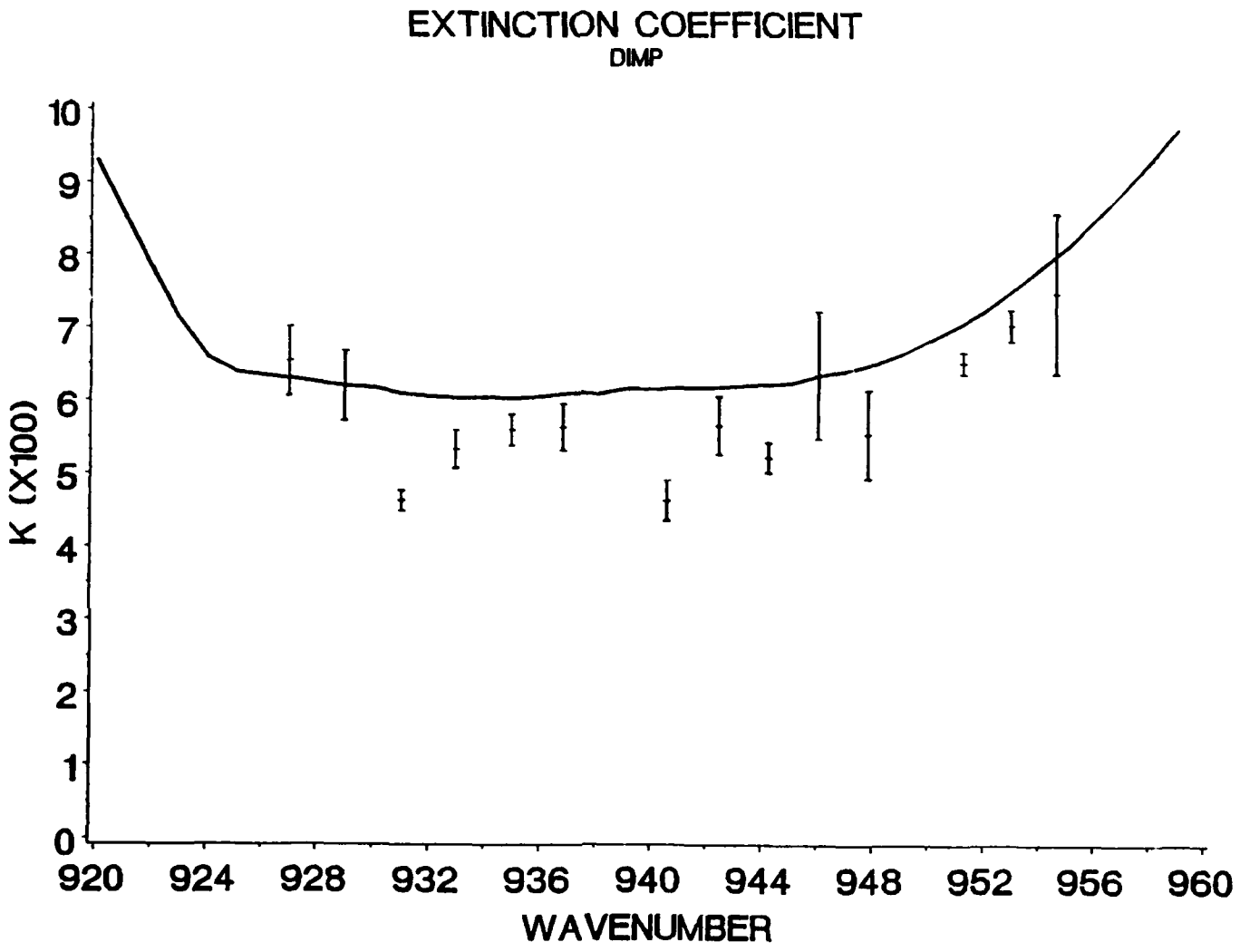

FIG. 1.13 Extinction coefficient for DIMP in the wavenumber region 920 to 960 cm^{-1}. The k values have been multiplied by 100. The solid line is data from Shengshan Weng's thesis. The data obtained with the CO_2 laser is represented by the plus symbols and the error bars are +/- one standard deviation.

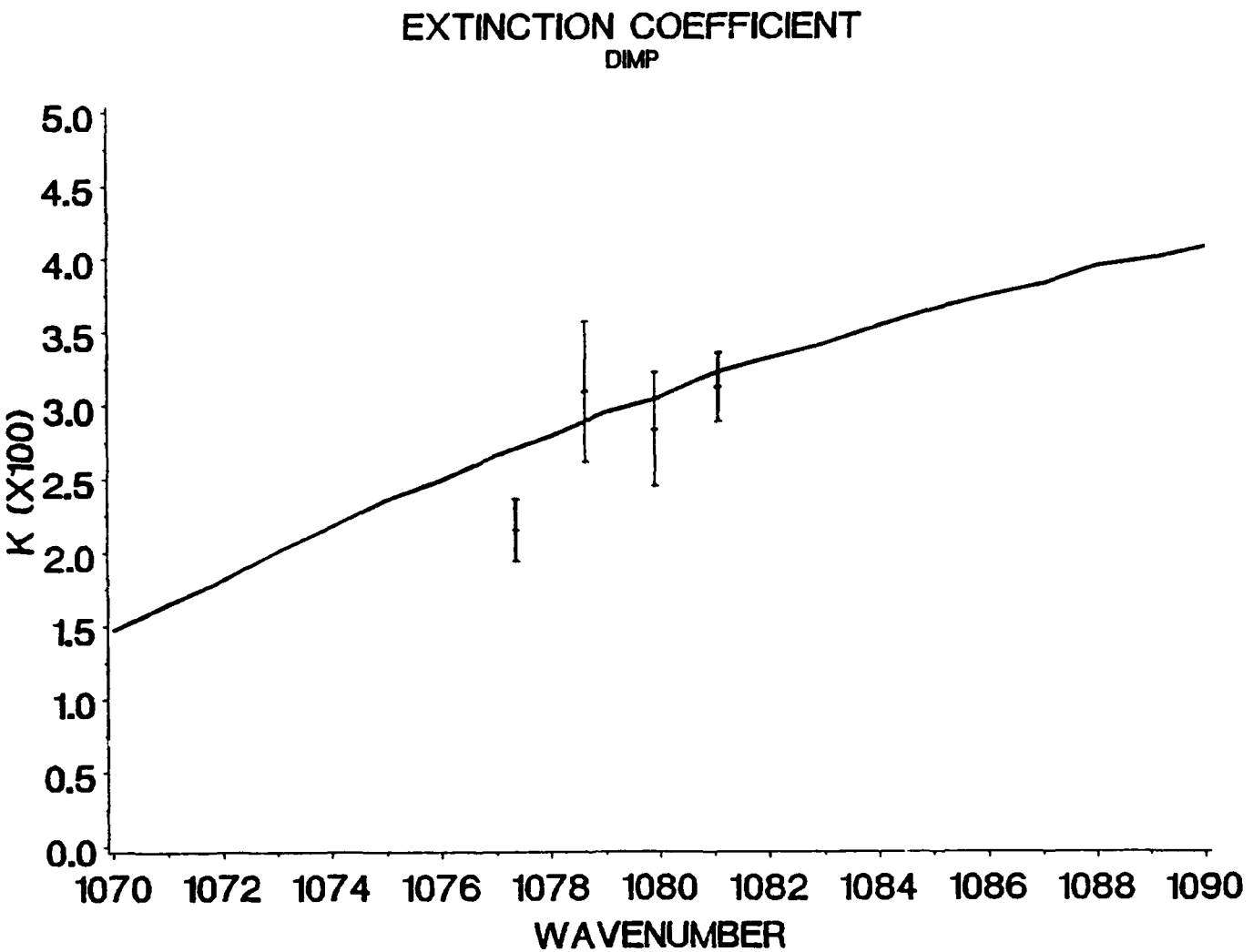

FIG. 1.14 Extinction coefficient for DIMP in the wavenumber region 1070 to 1090 cm^{-1}. The k values have been multiplied by 100. The solid line is data from Shengshan Weng's thesis. The data obtained with the CO_2 laser is represented by the plus symbols and the error bars are +/- one standard deviation.

TABLE 1.7

Extinction Coefficient for DEP

Wavenumber cm^{-1}	Extinction Coefficient k	σ_k	Percent Uncertainty
926.96	1.5496E-03	2.1977E-04	1.4182E+01
928.94	2.0078E-03	8.2274E-03	4.0977E+02
954.56	4.1078E-03	2.9236E-04	7.1172E+00
969.09	8.4471E-03	3.7593E-04	4.4504E+00
970.50	8.6114E-03	1.0356E-03	1.2026E+01
973.24	4.9073E-03	4.5192E-04	9.2092E+00
974.66	4.8816E-03	2.2877E-04	4.6864E+00
975.90	5.2341E-03	9.1369E-04	1.7457E+01
977.23	4.5393E-03	7.2735E-04	1.6023E+01
978.47	4.6906E-03	1.9015E-04	4.0537E+00
979.72	1.0897E-02	6.0748E-04	5.5745E+00
980.87	6.4198E-03	3.7311E-04	5.8120E+00
982.13	8.6407E-03	7.5143E-04	8.6965E+00
983.19	7.4744E-03	2.6038E-04	3.4836E+00
984.35	1.1905E-02	1.9456E-03	1.6342E+01
1033.49	3.2957E-02	2.7046E-03	8.2063E+00
1035.52	5.0390E-02	1.4786E-03	2.9342E+00
1039.39	3.1839E-02	6.9480E-03	2.1822E+01
1041.34	3.4477E-02	5.2525E-03	1.5235E+01
1043.19	8.1636E-02	1.0710E-03	1.3119E+00
1045.04	9.0491E-02	7.4357E-02	8.2171E+01
1048.66	3.0192E-02	7.4936E-04	2.4820E+00
1050.53	2.6916E-02	6.1486E-04	2.2844E+00
1052.19	2.3962E-02	9.7979E-04	4.0889E+00
1053.96	2.3552E-02	4.6064E-04	1.9558E+00
1055.63	2.3451E-02	6.2229E-04	2.6536E+00
1076.08	2.3792E-01	1.6982E-02	7.1377E+00
1078.63	1.5247E-01	1.8064E-02	1.1847E+01
1077.35	1.9534E-01	1.0527E-02	5.3891E+00

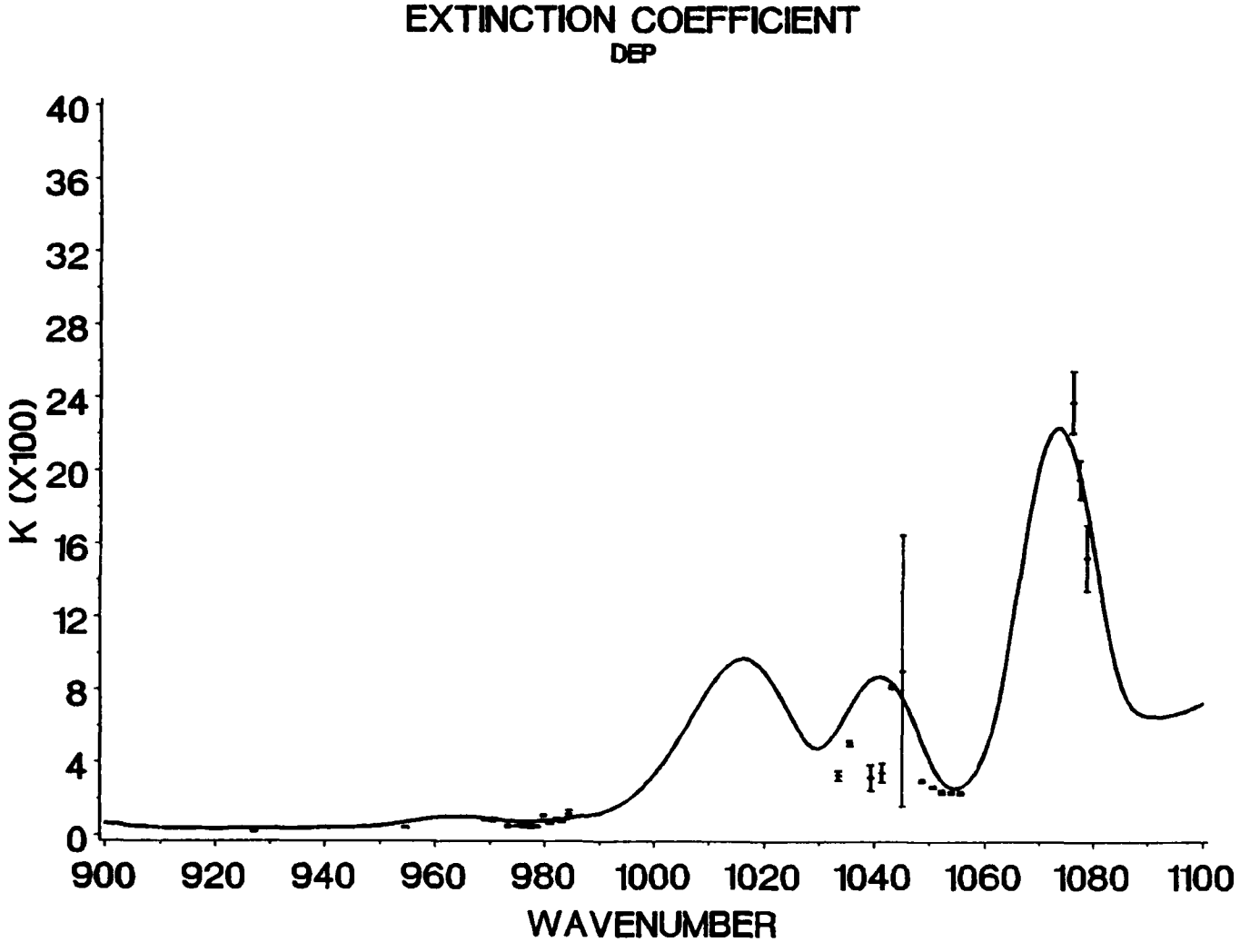

FIG. 1.15 Extinction coefficient for DEP in the wavenumber region 900 to 1100 cm^{-1}. The k values have been multiplied by 100. The solid line is data from Shengshan Weng's thesis. The data obtained with the CO_2 laser is represented by the plus symbols and the error bars are +/- one standard deviation.

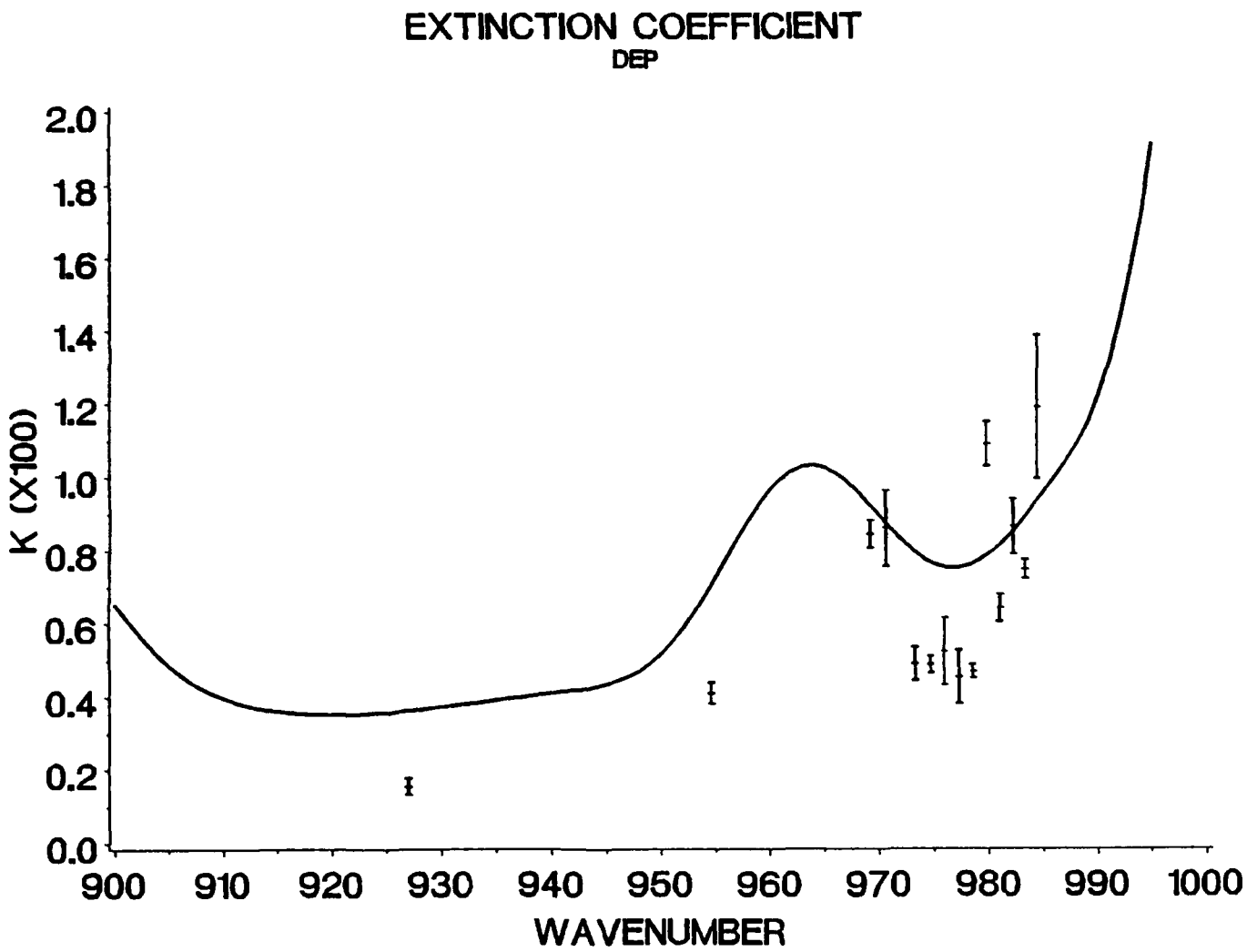

FIG. 1.16 Extinction coefficient for DEP in the wavenumber region 900 to 1000 cm^{-1}. The k values have been multiplied by 100. The solid line is data from Shengshan Weng's thesis. The data obtained with the CO_2 laser is represented by the plus symbols and the error bars are +/- one standard deviation.

g. CONCLUSION

As previously stated the results obtained using the CO_2 laser provide reasonable accuracy in determining the extinction coefficient with the wedge shaped cell. A comparison of the results obtained with the laser to those obtained with a conventional IR spectrophotometer indicate considerable disagreement between the two light sources. We believe the results obtained with the Perkin-Elmer instrument provide the more precise values for the extinction coefficient. We have examined the experimental setup with the laser in an attempt to isolate the source of error. The effects we have examined are listed below.

1. Instability of the pyroelectric detectors.

The detectors were examined using both a secondary heat source, soldering iron, and by placing a polarizer between the laser and the detector. The signal produced by the soldering iron, assuming it was a point source, decreased as the iron was moved further from the detector. Rotation of the polarizer provided the characteristic intensity profile as a function of polarizer angle.

2. Instability of the laser

The power output of the laser was monitored for both short and long time periods. The short term stability was below 2% and the long term stability was ≅ 2%. Three detectors were used in these studies, a power meter, and two pyroelectric detectors. All detectors registered simultaneous changes in the power output. The measurements on the laser stability and the detector response provided confidence in the method used to compensate the transmitted data for any changes in the incident intensity.

3. Inaccurate determination of the vertex angle

The Fourier transform technique employed in determining the vertex angle was tested by the normal procedure of counting the fringes as the cell was transmitted. The Fourier transform technique consistently provided more accurate results for the vertex angle than any other method that was attempted. In addition if the vertex angle were inaccurate the effect this would produce on the final results would be a constant multiplicative factor. We observe a more random fluctuation in the extinction coefficients.

4. Inaccurate positioning of the cell

The stepper motor was monitored on a routine basis to assure the incremental cell position was accurate during the scan. The results of repeated tests indicated the cell could be positioned to within a 2% error. In addition the technique used to determine the Lambert absorption coefficient averages over many positions of the cell which would minimize the inaccuracy of positioning the cell even further. If the cell were positioned inaccurately the effect would be observed in large error bars in plots similar to Fig. 1.6.

5. Phase shift

Since the pyroelectric detectors function only with an AC signal the phase between the optical chopper and the signal from the detectors was examined as a function of time and cell position. No appreciable shift in phase, which would result in a shift in lock-in reading, was observed. Again the averaging of the ratios would minimize the effects due to this change in phase.

6. Electrical interference

All precautions were made to minimize the effects due to ground loops and to shield against the RF generated by the laser and the stepper motor power supply.

Based on the sources of error which have been ruled out by the previous discussion we have only one suggestion as to the source of the error. An examination of the data indicates the error is large in regions where the Lambert absorption coefficient is largest. This would indicate two possible sources; 1) sample heating and 2) non-linear effects. The greater the abosrption coefficient the more heat is absorbed by the sample and thus the more motion associated with the thin film of fluid sandwiched between the ZnSe windows. This fluid flow changes the effective sample thickness. The effect would be random depending on the laser power output the absorption coefficient and the sample thickness. The presence of non-linear effects is difficult to confirm. The maximum power output of the laser is 4 W. This power is reduced after transmission through three beam splitters and one polarizer to an effective intensity at the sample of ≈1 W in a spot size of 3 mm, diameter. This provides an extremely high power density at the sample at could be the source of the error we observe.

[1]J.H. Lambert, Photometria, sive de mensura et gradibus luminis, colorum, et umbrae, 1760.

[2]M. Born and E. Wolf, Principles of Optics (Pergamon Press, 1970), pp. 281-288.

[3]Shengshan Weng, Masters thesis private communication, also attached as an appendix.

Blank

h. APPENDIX 1.1

Program FMENU

h. Appendix 1.1

Program FMENU

Listing of the program which computes the vertex angle of the wedge-shaped volume.

```
1 REM THIS PROGRAM HAS BEEN DEVELOPED AND WRITTEN BY DR. DAVID WIELICZKA
2 REM FOR USE WITH AN IBM PS/2 MODEL 30 COMPUTER AND A COMPUMOTOR CX57-83
3 REM STEPPER MOTOR AND CONTROLLER.
4 REM THE PROJECT WAS FUNDED BY CRDEC UNDER CONTRACT DAAA-15-85-K-0013
5 REM DATE WRITTEN SEPTEMBER 19, 1987
10 'NAME:  Data Acquisition And Control (DAAC)
20 '       HEADER for BASICA
30 '
40 'FILE NAME:  DACHDR.BAS
50 '
60 'DOS DEVICE NAME:  DAAC
70 '
80 'RESERVED FUNCTION NAMES:
90 '           AINM, AINS, AINSC, AOUM, AOUS,
100 '           BINM, BINS, BITINS, BITOUS, BOUM, BOUS,
110 '           CINM, CINS, CSET, DELAY
120 'RESERVED DEF SEG VALUE NAME:  DSEG
130 '
140 'NAMES DEFINED AND USED BY HEADER:
150 '           ADAPT%, AI, COUNT, FOUND%,
160 '           HNAME$, SG%, STAT%
170 '
180 '
190 'When using the BASICA Interpreter, this header
200 'must be executed before any function calls are
210 'made that access the DAAC adapter.  It initializes
220 'a number of variables for each function call.  These
230 'variables are reserved and should not be used except
240 'to access the DAAC adapter.  This routine also does a
250 'DEF SEG to the segment where the DAAC Device Driver
260 '(DAC.COM) is loaded.  If you execute a DEF SEG to
270 'access other hardware, you must DEF SEG to the segment
280 'of the DAAC Device Driver before any subsequent
290 'calls to access the DAAC adapter.
300 '
310 '
320 FOUND% = 0
330 SG% = &H2E
340 'Start searching the interrupt vectors until you find
350 'one that points to the DAAC device driver.
360 'Do a DEF SEG to that segment.
370 WHILE ((SG% <= &H3E) AND (FOUND% = 0))
380       DEF SEG = 0
390       DSEG = PEEK(SG%) + PEEK(SG% + 1) * 256
400       DEF SEG = DSEG
```

```
410       HNAME$=""
420       FOR AI=10 TO 17
430               HNAME$ = HNAME$ + CHR$(PEEK(AI))
440       NEXT AI
450       IF HNAME$ = "DAAC    " AND PEEK(18) + PEEK(19) <> 0 THEN FOUND% = 1
460       SG% = SG% + 4
470 WEND
480 IF FOUND% = 0 THEN PRINT "ERROR: DEVICE DRIVER DAC.COM NOT FOUND" : END
490 'Now initialize all function name variables for calls
500 'to access the device driver.
510 AINM        = PEEK(&H13) * 256 + PEEK(&H12)
520 AINS        = PEEK(&H15) * 256 + PEEK(&H14)
530 AINSC       = PEEK(&H17) * 256 + PEEK(&H16)
540 AOUM        = PEEK(&H19) * 256 + PEEK(&H18)
550 AOUS        = PEEK(&H1B) * 256 + PEEK(&H1A)
560 BINM        = PEEK(&H1D) * 256 + PEEK(&H1C)
570 BINS        = PEEK(&H1F) * 256 + PEEK(&H1E)
580 BITINS      = PEEK(&H21) * 256 + PEEK(&H20)
590 BITOUS      = PEEK(&H23) * 256 + PEEK(&H22)
600 BOUM        = PEEK(&H25) * 256 + PEEK(&H24)
610 BOUS        = PEEK(&H27) * 256 + PEEK(&H26)
620 CINM        = PEEK(&H29) * 256 + PEEK(&H28)
630 CINS        = PEEK(&H2B) * 256 + PEEK(&H2A)
640 CSET        = PEEK(&H2D) * 256 + PEEK(&H2C)
650 DELAY       = PEEK(&H2F) * 256 + PEEK(&H2E)
660 'Finally, execute any call to re-initialize the
670 'device driver from any former invocation of BASIC.
680 ADAPT% = 0
690 COUNT = 1
700 STAT% = 0
710 CALL DELAY (ADAPT%, COUNT, STAT%)
720 '
730 'End of DAAC BASICA Header
740 '
1000 REM FRINGE MENU
1010 REM $DYNAMIC
1020 REM ************************************************************
1030 REM VARIABLE LIST
1040 REM A----ASCII VALUE FOR INKEY
1050 REM B(1)-TANGENT OF ANGLE
1060 REM B(2)-STEP SIZE IN MM
1070 REM B(3)-NUMBER OF STEPS
1080 REM B(4)-WAVELENGTH IN METERS
1090 REM B(5)-DIRECTION OF MOTION +/-=UP/DOWN
1100 REM P---STRING VARIABLE FOR INKEY
1110 REM Q(1)-FILENAME
1120 REM Q(2)-COMMENT
1130 REM O - 1 DIMENSION ARRAY OF DIMENSION 9, MENU LABELS
1140 REM ************************************************************
1150 OPTION BASE 1 'ALL ARRAYS BEGIN WITH VALUE 1
1160 DEFSNG A-H 'VARIABLES BEGINNING WITH THE LETTERS A THRU H ARE SINGLE PREC
1170 DEFINT I-N 'VARIABLES BEGINNING WITH THE LETTERS I THRU N ARE INTEGERS
1180 DEFDBL T-Z 'VARIABLES BEGINNING WITH THE LETTERS T THRU Z ARE DOUBLE PREC
1190 DEFSTR O-S 'VARIABLES BEGINNING WITH THE LETTERS O THRU S ARE STRINGS
```

```
1200 DIM Q(2),B(5),O(9)
1210 O(1)="FILENAME FOR FRINGE DATA: "
1220 O(2)="COMMENT: "
1230 O(3)="TANGENT OF WEDGE ANGLE: "
1240 O(4)="STEP SIZE IN MM: "
1250 O(5)="NUMBER OF STEPS: "
1260 O(6)="WAVELENGTH IN METERS: "
1270 O(7)="POSITION CELL"
1280 O(8)="ACQUIRE DATA"
1290 O(9)="EXIT"
1300 CLS 'CLEAR SCREEN
1310 REM************************
1320 REM PRINT MENU TO SCREEN
1330 REM BESIDE EACH MENU ITEM LIST THE CORRESPONDING LETTER TO STIKE TO
1340 REM BRANCH TO THAT ROUTINE.
1350 REM ALSO LIST THE DATA ASSOCIATED WITH THE MENU ITEM IF KNOWN
1360 REM************************
1370 FOR I=1 TO 2
1380 PRINT "(";CHR$(64+I);") ";O(I);Q(I)
1390 NEXT I
1400 FOR I=3 TO 6
1410 PRINT "(";CHR$(64+I);") ";O(I);B(I-2)
1420 NEXT I
1430 FOR I=7 TO 9
1440 PRINT "(";CHR$(64+I);") ";O(I)
1450 NEXT I
1460 PRINT "PRESS THE APPROPRIATE KEY TO CONTINUE!!"
1470 REM LOOP THRU INKEY FUNCTION TO DETERMINE THE ROUTINE TO BRANCH TO
1480 P=INKEY$: IF P="" THEN 1480
1490 REM SUBSTRACT ASCII OFFSET FOR LETTER A
1500 A=ASC(P)-64
1510 IF A<3 GOTO 1560 'BRANCH TO 460 FOR STRING INPUT
1520 IF A<7 GOTO 1690 'BRANCH TO 560 FOR NUMERIC INPUT
1530 IF A>9 GOTO 1480 'IF A GREATER THAN 9 RETURN TO INKEY FUNCTION
1540 A=A-6 'SUBTRACT ADDITIONAL OFFSET TO USE ON A GOTO COMMAND
1550 ON A GOTO 1730,1780,2090
1560 REM INPUT A STRING VARIABLE
1570 ON A GOTO 1580,1650
1580 PRINT O(A);
1590 INPUT Q(A) 'INPUT FILENAME TO STORE THE FRINGE DATA IN
1600 OPEN Q(A) FOR OUTPUT AS #1:PRINT #1,DATE$
1610 GOTO 1300
1620 REM************************
1630 REM FILENAME MUST HAVE BEEN CHOSEN PRIOR TO INPUTING COMMENT
1640 REM************************
1650 PRINT O(A);
1660 INPUT Q(A) 'INPUT COMMENT TO STORE WITH DATA
1670 PRINT #1,Q(A):CLOSE #1
1680 GOTO 1300
1690 REM INPUT A REAL VARIABLE
1700 PRINT O(A);
1710 INPUT B(A-2)
1720 GOTO 1300
1730 REM POSITION CELL
```

```
1740 REM THE FOLLOWING SUBROUTINE WILL POSITION THE CELL AT THE TOP OR BOTTOM
1750 REM THE POSITION DEPENDS ON THE VALUE OF B(5)
1760 GOSUB 4000
1770 GOTO 1300
1780 REM ACQUIRE DATA
1790 FOR J=1 TO 2 'MAKE SURE A FILENAME AND COMMENT HAVE BEEN INPUT
1800 IF Q(J)="" THEN 1990 'IF EITHER Q(1) OR Q(2) ARE EMPTY PRINT ERROR
1810 NEXT J
1820 FOR J=2 TO 5 'MAKE SURE ALL SCAN PARAMETERS HAVE BEEN SET
1830 IF B(J)=0 THEN 2010 'IF ANY ARE ZERO PRINT ERROR MESSAGE
1840 IF B(3)>1190 THEN 2030 'MAKE SURE NUMBER OF DATA POINTS IS LESS THAN 1190
1850 IF B(3)*B(2)>40 THEN 2050 'MAKE SURE SCAN RANGE IS LESS THAN 40 MM.
1860 NEXT J
1870 FOR J=1 TO 2 'SEND FILENAME AND COMMENT TO PRINTER
1880 LPRINT "          ";Q(J)
1890 NEXT J
1900 FOR J=2 TO 4 'SEND SCAN PARAMETERS TO PRINTER
1910 LPRINT "          ";O(J+2);B(J)
1920 NEXT J
1930 GOSUB 6000
1940 GOTO 1300
1950 REM****************************************
1960 REM THE FOLLOWING LINES ARE THE ERROR MESSAGES ASSOCIATED WITH
1970 REM THE CHECK OF ALL SCAN PARAMETERS.
1980 REM****************************************
1990 CLS:LOCATE 15,1:PRINT "NOT ALL STRINGS ARE INPUT"
2000 GOTO 2060
2010 CLS:LOCATE 15,1:PRINT "SCAN PARAMETER HAS NOT BEEN INITIALIZED!!!"
2020 GOTO 2060
2030 CLS:LOCATE 15,1:PRINT "TO MANY STEPS REDUCE NUMBER OF STEPS"
2040 GOTO 2060
2050 CLS:LOCATE 15,1:PRINT "REDUCE NUMBER OF STEPS OR STEP SIZE"
2060 LOCATE 18,1:PRINT "STRIKE ANY KEY TO RETURN TO THE MENU"
2070 P=INKEY$:IF P="" THEN 2070
2080 GOTO 1300
2090 END
2100 REM
2110 REM
2120 REM
2130 REM
2140 REM
4000 REM SUBROUTINE PSIT
4010 REM THIS SUBROUTINE POSITIONS THE CELL AT THE TOP OR BOTTOM OF
4020 REM THE VERTEX.
4030 REM****************************************
4040 REM VARIABLE LIST
4050 REM SMOVE - 7 ELEMENT ARRAY CONTAINING COMMAND TO START CONTINUOUS
4060 REM         MOTION OF MOTOR DRIVE
4070 REM SNIT - 20 ELEMENT ARRAY TO INITIALIZE STEPPER MOTOR
4080 REM STA  - 3 ELEMENT ARRAY TO EXAMINE LIMIT SWITCH STATUS
4090 REM SSET - 12 ELEMENT ARRAY TO SET THE STEP SIZE OF THE MOTOR
4100 REM SSET - 12 ELEMENT ARRAY TO SET THE STEP SIZE OF THE MOTOR
4110 REM SZERO - 2 ELEMENT ARRAY TO SET CURRENT POSITION OF MOTOR AS
4120 REM         ABSOLUTE ZERO
```

```
4130 REM SHALT - 1 ELEMENT ARRAY TO STOP THE MOTOR INSTANTANEOUSLY
4140 REM STAM - 2 ELEMENT ARRAY TO CHECK MOTOR STATUS
4150 REM FLAG -
4160 REM J - DUMMY VARIABLE TO READ STATUS OF SERIAL PORT
4170 REM R - DUMMY VARIABLE TO READ ECHO OF STEPPER MOTOR CONTROLLER
4180 REM P - INKEY VARIABLE
4190 DIM SNIT(20),SMOVE(7),STA(3),SSET(12),SZERO(2),SHALT(1),STAM(2)
4200 SNIT(1)="L":SNIT(2)="D":SNIT(3)="0":SNIT(4)=" ":SNIT(5)="A"
4210 SNIT(6)="0":SNIT(7)="1":SNIT(8)=" ":SNIT(9)="V":SNIT(10)="0"
4220 SNIT(11)="1":SNIT(12)=" ":SNIT(13)="S":SNIT(14)="C":SNIT(15)="1"
4230 SNIT(16)=" ":SNIT(17)="S":SNIT(18)="C":SNIT(19)="A":SNIT(20)="1"
4240 SMOVE(1)="H":SMOVE(2)="+":SMOVE(3)=" ":SMOVE(4)="M":SMOVE(5)="C"
4250 SMOVE(6)=" ":SMOVE(7)="G"
4260 STA(1)="8":STA(2)="R":STA(3)="A"
4270 SSET(1)="M":SSET(2)="N":SSET(3)=" ":SSET(4)="D":SSET(5)="+"
4280 SSET(6)="2":SSET(7)="5":SSET(8)="6":SSET(9)="0":SSET(10)="0"
4290 SSET(11)=" ":SSET(12)="G"
4300 SZERO(1)="P":SZERO(2)="Z"
4310 SHALT(1)="S"
4320 STAM(1)="8":STAM(2)="R"
4330 FLAG=0
4340 REM THE FOLLOWING COMMANDS ARE SENT TO INITIALIZE THE STEPPER
4350 REM MOTOR CONTROLLER
4360 REM LD0 - ENABLE LIMIT SWITCHES
4370 REM A01 - SET ACCELARATION TO 1 REV/SEC/SEC
4380 REM V01 - SET VELOCITY TO 1 REV/SEC
4390 REM SC1 - SET STANDBY CURRENT TO 1/8 OF MAX.
4400 REM SCA1 - SET STANDBY CURRENT AFTER EACH MOVE TO 1/8 MAX.
4410 OPEN "COM1:9600,N,8,1" AS #3 ' OPEN SERIAL PORT 1 FOR COMMUNICATION
4420 FOR I=1 TO 20 'INITIALIZE STEPPER MOTOR CONTROLLER
4430 J=INP(&H3FD) 'SEE IF SERIAL PORT IS READY TO SEND A CHARACTER
4440 IF J<>96 GOTO 4430 'LOOP TO 4290 IF SERIAL PORT NOT READY
4450 PRINT #3,SNIT(I); 'SEND OUT SINGLE CHARACTER NO CARRIAGE RETURN
4460 IF EOF(3) THEN 4460 'WAIT FOR ECHO FROM STEPPER MOTOR CONTROLLER
4470 R=INPUT$(1,#3) 'INPUT ECHO FROM CONTROLLER
4480 NEXT I
4490 PRINT #3,CHR$(13); 'SEND CARRIAGE RETURN TO TERMINATE COMMAND
4500 IF EOF(3) THEN 4500 'WAIT FOR ECHO FROM CONTROLLER
4510 R=INPUT$(1,#3) 'READ ECHO FROM CONTROLLER
4520 PRINT "POSITION CELL AT TOP(T) OR BOTTOM(B) OF WEDGE"
4530 P=INKEY$: IF P="" THEN 4530
4540 REM THE FOLLOWING COMMANDS DIRECT THE MOTOR TO MOVE EITHER CLOCKWISE
4550 REM OR COUNTER-CLOCKWISE AND TO MOVE CONTINUOUSLY
4560 REM H- MOVE IN CCW DIRECTION
4570 REM H+ MOVE IN CW DIRECTION
4580 REM MC MOVE CONTINUOUSLY
4590 REM G GO
4600 PRINT "TYPE <ESC> IF YOU WISH TO STOP THE MOTOR"
4610 IF P="B" THEN SMOVE(2)="-"
4620 IF P="T" THEN SMOVE(2)="+"
4630 FOR I=1 TO 7  'SEND COMMAND TO CONTROLLER
4640 J=INP(&H3FD) 'EXAMINE SERIAL PORT
4650 IF J<>96 GOTO 4640 'LOOP IF SERIAL PORT NOT READY
4660 PRINT #3,SMOVE(I); 'SEND SINGLE CHARACTER
```

```
4670 IF EOF(3) THEN 4670  'WAIT FOR ECHO
4680 R=INPUT$(1,#3)  'READ IN ECHO
4690 NEXT I
4700 PRINT #3,CHR$(13);  'TERMINATE COMMAND
4710 IF EOF(3) THEN 4710 'WAIT FOR ECHO
4720 R=INPUT$(1,#3)  'READ IN ECHO
4730 REM 8RA CHECK STATUS LIMIT SWITCHES
4740 REM LIMIT SWITCHES TELL IF MOTOR IS STILL RUNNING OR NOT
4750 FOR I=1 TO 3 'SEND OUT LIMIT SWITCH COMMAND
4760 J=INP(&H3FD) 'SEE IF SERIAL PORT IS READY FOR CHARACTER
4770 IF J<>96 THEN 4760 'LOOP IF SERIAL PORT NOT READY
4780 PRINT #3,STA(I); 'SEND SINGLE CHARACTER TO SERIAL PORT
4790 IF EOF(3) THEN 4790 'WAIT FOR ECHO
4800 R=INPUT$(1,#3) 'READ IN ECHO
4810 NEXT I
4820 PRINT #3,CHR$(13);  'TERMINATE COMMAND
4830 IF EOF(3) THEN 4830 'WAIT FOR ECHO
4840 R=INPUT$(1,#3) 'READ IN ECHO
4850 IF EOF(3) THEN 4850 'READ IN STATUS OF LIMIT SWITCHES
4860 INPUT #3,R 'INPUT CHARACTER
4870 P1=INKEY$  'CHECK TO SEE IF ESC KEY HAS BEEN STRUCK
4880 IF P1=CHR$(27) THEN FLAG=-1:GOTO 5350  'IF ESC KEY STRUCK EXIT
4890 REM EXAMINE THE STATUS RETURNED BY STEPPER MOTOR CONTROLLER
4900 REM IF STATUS IS LESS THAN "A" OR GREATER THAN "O" THEN
4910 REM REPEAT CHECK OF LIMIT SWITCHES
4920 REM IF LIMIT SWITCHES SET CONTINUE
4930 IF (RIGHT$(R,1)<"A") OR (RIGHT$(R,1)>"O") GOTO 4750
4940 REM AFTER LIMIT SWITCHES ARE SET MOVE MOTOR TWO REVOLUTIONS
4950 '  IN OPPOSITE DIRECTION TO REMOVE BACKLASH IN DRIVE SCREW
4960 REM D25600 G MOVE 2 REVOLUTIONS IN CW DIRECTION
4970 REM D-25600 G MOVE 2 REVOLUTIONS IN CCW DIRECTION
4980 IF P="B" THEN SSET(5)="+":B(5)=+1
4990 IF P="T" THEN SSET(5)="-":B(5)=-1
5000 FOR I=1 TO 12 'SEND OUT COMMAND TO MOVE TWO REVOLUTIONS
5010 J=INP(&H3FD)
5020 IF J<>96 GOTO 5010
5030 PRINT #3,SSET(I);
5040 IF EOF(3) THEN 5040
5050 R=INPUT$(1,#3)
5060 NEXT I
5070 PRINT #3,CHR$(13);
5080 IF EOF(3) THEN 5080
5090 R=INPUT$(1,#3)  'TERMINATE COMMAND TO MOVE TWO REVOLUTIONS
5100 FOR I=1 TO 2  'SEND OUT COMMAND TO SEE IF MOTOR HAS STOPPED
5110 J=INP(&H3FD)
5120 IF J<>96 THEN 5110
5130 PRINT #3,STAM(I);
5140 IF EOF(3) THEN 5140
5150 R=INPUT$(1,#3)
5160 NEXT I
5170 PRINT #3,CHR$(13);
5180 IF EOF(3) THEN 5180
5190 R=INPUT$(1,#3)   'TERMINATE COMMAND TO SEE IF MOTOR HAS STOPPED
5200 IF EOF(3) THEN 5200
```

```
5210 INPUT #3,R  'INPUT RESPONSE TO PREVIOUS COMMAND
5220 IF R<>"*R" GOTO 5100  'REPEAT COMMAND IF RESPONSE NOT CORRECT
5230 REM PZ SET CURRENT POSITION AS ABSOLUTE ZERO
5240 FOR I=1 TO 2 'SET CURRENT MOTOR POSITION TO ABSOLUTE ZERO
5250 J=INP(&H3FD)
5260 IF J<>96 THEN 5250
5270 PRINT #3,SZERO(I);
5280 IF EOF(3) THEN 5280
5290 R=INPUT$(1,#3)
5300 NEXT I
5310 PRINT #3,CHR$(13);
5320 IF EOF(3) THEN 5320
5330 R=INPUT$(1,#3) 'TERMINATE COMMAND TO SET ABSOLUTE ZERO
5340 IF FLAG<>-1 GOTO 5430 'IF ESC KEY NOT STRUCK BRANCH TO 5200
5350 J=INP(&H3FD) 'IF ESC KEY STRUCK SEND COMMAND TO STOP MOTOR
5360 IF J<>96 THEN 5350
5370 PRINT #3,SHALT(1)
5380 IF EOF(3) THEN 5380
5390 R=INPUT$(1,#3)
5400 PRINT #3,CHR$(13);
5410 IF EOF(3) THEN 5410
5420 R=INPUT$(1,#3) 'TERMINATE COMMAND TO STOP MOTOR
5430 CLOSE #3  'CLOSE SERIAL COMMUNICATION
5440 RETURN
5450 REM
5460 REM
5470 REM
5480 REM
5490 REM
6000 REM SUBROUTINE TO ACQUIRE AND ANALYZE FRINGE DATA
6010 REM PARAMETER LIST
6020 REM A--ASCII VALUE FOR INKEY
6030 REM B(1)--TANGENT OF WEDGE ANGLE
6040 REM B(2)--STEP SIZE IN MM
6050 REM B(3)--NUMBER OF STEPS
6060 REM B(4)--WAVELENGTH OF LIGHT
6070 REM B(5)--DIRECTION OF MOTOR MOTION
6080 REM DMAX--MAXIMUM VALUE OF REAL COEF. FROM FOURIER TRANS. ROUTINE
6090 REM GSPMM--STEPS PER MILLIMETER FOR STEPPER MOTOR
6100 REM GSIZE--NUMBER OF PULSES CORRESPONDING TO STEP SIZE B(2)
6110 REM HDTA1(2000)--REAL VALUES SENT TO FOURIER TRANS. ROUTINE
6120 REM HDTA2(2000)--IMAG. VALUES SENT TO FOURIER TRANS. ROUTINE
6130 REM IADAPT--DATA ACQ. ADAPTER NUMBER
6140 REM ICHAN--CHANNEL TO BE READ
6150 REM ICTRL--VALUE FOR CONTROL OF INTERRUPTS MUST BE ZERO
6160 REM IDEVICE--DEVICE NUMBER 9 FOR ALL A/D CALLS
6170 REM IDTA(2000)--A/D VALUES
6180 REM ISTAT--RETURN VALUE GIVING STATUS OF READ 0=SUCCESFUL READ
6190 REM IX--GRAPHICS VALUE FOR X POSITION OF CELL
6200 REM IY--GRAPHICS VALUE FOR A/D VALUE
6210 REM DFFT1(2000)--REAL COEF. RETURNED FROM FOURIER TRANS. ROUTINE
6220 REM DFFT2(2000)--IMAG. COEF. RETURNED FROM FOURIER TRANS. ROUTINE
6230 REM NSTEP--INTEGER VALUE OF NUMBER OF STEPS
6240 REM Q(1)--FILENAME
```

```
6250 REM Q(2)--COMMENT
6260 REM R--ECHO AND RESPONSE FROM STEPPER MOTOR CONTROLLER
6270 REM SINC--COMMAND SENT TO STEPPER MOTOR CONTROLLER TO DEFINE INCREMENT
6280 REM SGO--COMMAND SENT TO STEPPER MOTOR TO STEP PREDEFINED AMOUNT
6290 REM STAM--COMMAND SENT TO STEPPER MOTOR TO QUERY STATUS
6300 REM STA--COMMAND SENT TO STEPPER MOTOR CONTROLLER TO QUERY STATUS
6310 DIM IDTA(1200),HDTA1(1200),HDTA2(1200),DFFT1(1200),DFFT2(1200),
        DMAG(1200),SINC(7),SGO(1),STAM(2)
6320 SCREEN 2
6330 SINC(1)="D":SINC(2)="+":SINC(3)="2":SINC(4)="0"
6340 SINC(5)="0":SINC(6)="0":SINC(7)="0"
6350 SGO(1)="G"
6360 STAM(1)="8":STAM(2)="R"
6370 CLS
6380 REM DEFINE PARAMETERS NECESSARY FOR A/D CONVERSION
6390 IADAPT=0' ALL CALLS ARE TO DAC ADAPTER 0
6400 IDEVICE=9' DEVICE IS 9 FOR A/D CALLS
6410 ICHAN=3' READ CHANNEL 3 - PHOTOMULTIPLIER TUBE OUTPUT
6420 ICTRL=0
6430 ISTAT=0
6440 IX=0: IY=0
6450 NSTEP=CINT(B(3))
6460 GSPMM=20000' STEPS PER MILLIMETER
6470 GSIZE=GSPMM*B(2)'DETERMINE NUMBER OF STEPS TO MOVE MOTOR
6480 IF B(5)=1 THEN SINC(2)="+" 'SET CLOCKWISE MOTION
6490 IF B(5)=-1 THEN SINC(2)="-" 'SET COUNTER CLOCKWISE MOTION
6500 SSIZE=MID$((STR$(GSIZE)),2) 'DETERMINE SIZE OF COMMAND
6510 JSIZE=LEN(SSIZE) 'CONVERT STRING TO INTEGER
6520 FOR K=1 TO JSIZE
6530 SINC(K+2)=MID$(SSIZE,K,1)
6540 NEXT K
6550 JSIZE=JSIZE+2
6560 OPEN "COM1:9600,N,8,1" AS #3
6570 OPEN Q(1) FOR APPEND AS #1
6580 FOR K=1 TO JSIZE 'SEND STEP SIZE TO MOTOR
6590 J=INP(&H3FD)
6600 IF J<>96 THEN 6590
6610 PRINT #3,SINC(K);
6620 IF EOF(3) THEN 6620
6630 R=INPUT$(1,#3)
6640 NEXT K
6650 PRINT #3,CHR$(13);
6660 IF EOF(3) THEN 6660
6670 R=INPUT$(1,#3)  'TERMINATE COMMAND TO DEFINE STEP SIZE
6680 LOCATE 25,1:PRINT "TYPE <ESC> TO STOP ACQUISITION"
6690 FOR I=1 TO NSTEP  'BEGIN ACQUIRING DATA
6700 P=INKEY$ 'EXAMINE KEYBOARD BUFFER FOR <ESC> KEY
6710 IF P=CHR$(27) GOTO 7390 'IF <ESC> KEY STRUCK TERMINATE
6720 CALL AINS(IADAPT,IDEVICE,ICHAN,ICTRL,IDTA(I),ISTAT) 'READ A/D CHANNEL 3
6730 J=INP(&H3FD) 'SEND COMMAND TO STEP MOTOR
6740 IF J<>96 THEN 6730
6750 PRINT #3,SGO(1);
6760 IF EOF(3) THEN 6760
6770 R=INPUT$(1,#3)
```

```
6780 PRINT #3,CHR$(13);
6790 REM IF EOF(3) THEN 2810
6800 R=INPUT$(1,#3) 'TERMINATE COMMAND TO STEP MOTOR
6810 REM WHILE MOTOR IS STEPPING CALCULATE PIXEL POSITION TO DISPLAY
6820 IX=I*640!/B(3)
6830 REM DATA ON SCREEN WHILE IT IS ACQUIRED
6840 REM CONVERT A/D READING TO PIXEL VALUE
6850 IY=200-(IDTA(I)+2048)*.048828
6860 CIRCLE (IX,IY),2
6870 REM REDUCE A/D READING BY 1000 BEFORE SENDING IT TO FFT ROUTINE
6880 HDTA1(I)=CSNG(IDTA(I))/1000!
6890 HDTA2(I)=0
6900 FOR K=1 TO 2 'SEND COMMAND TO EXAMINE STATUS OF MOTOR
6910 J=INP(&H3FD)
6920 IF J<>96 THEN 6910
6930 PRINT #3,STAM(K);
6940 IF EOF(3) THEN 6940
6950 R=INPUT$(1,#3)
6960 NEXT K
6970 PRINT #3,CHR$(13);
6980 REM IF EOF(3) THEN 2960
6990 R=INPUT$(1,#3) 'TERMINATE MOTOR STATUS COMMAND
7000 REM IF EOF(3) THEN 2980
7010 INPUT #3,R  'INPUT RESPONSE TO MOTOR STATUS COMMAND
7020 IF R<>"*R" GOTO 6900 'IF INCORRECT RESPONSE REPEAT COMMAND
7030 NEXT I
7040 REM COMPUTE COMPLEX FAST FOURIER TRANSFORM OF FRINGE PATTERN
7050 GOSUB 10000
7060 REM SEND OUTPUT OF CFFT TO SCREEN AND PRINTER
7070 REM ONLY DISPLAY VALUES THAT ARE WITHIN 10% OF MAXIMUM VALUE
7080 PRINT "CHANNEL     REAL COEFF.     IMAGINERY COEFF.     MAGNITUDE"
7090 LPRINT "CHANNEL    REAL COEFF.     IMAGINARY COEFF.     MAGNITUDE"
7100 PRINT "0",DFFT1(1),DFFT2(1),SQR((DFFT1(1)^2)+(DFFT2(1)^2))
7110 DMAX=0
7120 FOR I=2 TO NSTEP
7130 DMAG(I)=SQR((DFFT1(I)^2)+(DFFT2(I)^2))
7140 IF DMAG(I)>DMAX THEN DMAX=DMAG(I)
7150 NEXT I
7160 M=0
7170 FOR I=2 TO NSTEP/2
7180 IF DMAG(I)<.1*DMAX THEN GOTO 7270
7190 PRINT I-1,DFFT1(I),DFFT2(I),DMAG(I)
7200 LPRINT "         ";I-1,DFFT1(I),DFFT2(I),DMAG(I)
7210 M=M+1
7220 IF INT(M/15)<>M/15 THEN GOTO 7270 'PAUSE FOR FULL SCREEN
7230 PRINT "STRIKE ANY KEY TO CONTINUE"
7240 P=INKEY$: IF P="" THEN 7240
7250 M=0
7260 CLS
7270 NEXT I
7280 INPUT "CHANNEL NUMBER FOR MAXIMUM MAGNITUDE: ",CH1
7290 LPRINT "          CHANNEL NUMBER FOR MAXIMUM MAGNITUDE: ",CH1
7300 B(1)=(B(4)*CH1*1000!)/(2*B(2)*B(3))
7310 LPRINT "          TANGENT OF WEDGE ANGLE: ",B(1)
```

```
7320 FOR I=1 TO 5  'STORE SCAN PARAMETERS ON DISK
7330 PRINT #1,B(I);
7340 NEXT I
7350 PRINT #1,
7360 FOR I=1 TO NSTEP 'STORE RAW DATA AND CFFT ON DISK
7370 PRINT #1,IDTA(I),DFFT1(I),DFFT2(I),DMAG(I)
7380 NEXT I
7390 CLOSE #1
7400 CLOSE #3
7410 RETURN
7420 REM
7430 REM
7440 REM
7450 REM
10000 REM SUBROUTINE FOR COMPUTING COMPLEX FFT
10005 REM DEVELOPED AND WRITTEN BY DAVID WIELICZKA
10010 CLS
10020 DIM NPR(12),DUM1(2000),DUM2(2000)
10030 DATA 2,3,5,7,11,13,17,19,23,29,31,37 'PRIME NUMBERS TO 37
10040 RESTORE
10050 FOR I=1 TO 12 'READ PRIMES TO SORT BY
10060 READ NPR(I)
10070 NEXT I
10080 FOR I=1 TO NSTEP 'ASSIGN DATA TO DUMMY VARIABLES
10090 DUM1(I)=HDTA1(I):DUM2(I)=HDTA2(I)
10100 NEXT I
10110 REM INITIALIZE LOOP PARAMETERS
10120 IAFT=1
10130 IBEF=NSTEP
10140 NXT=1
10150 REM DETERMINE IF THE NUMBER OF POINTS IS DIVISIBLE BY A PRIME
10160 IF (INT(IBEF/NPR(NXT)))*NPR(NXT)>=IBEF GOTO 10220
10170 NXT=NXT+1
10180 IF NXT<=12 GOTO 10160
10190 NOW=IBEF
10200 IBEF=1
10210 GOTO 10240
10220 NOW=NPR(NXT)
10230 IBEF=IBEF/NPR(NXT)
10240 BPI2=6.283185 '2(PI)
10250 ANGLE=BPI2/CSNG(NOW*IAFT)
10260 CANG=COS(ANGLE)
10270 HANG=-SIN(ANGLE)
10280 ARGR=1
10290 ARGI=0
10300 REM BEGIN LOOP TO DETERMINE COEFFICIENTS
10310 FOR J=1 TO NOW
10320 FOR IA=1 TO IAFT
10330 FOR IB=1 TO IBEF
10340 IVR=IA+IAFT*(IB-1+IBEF*(NOW-1))
10350 ER=DUM1(IVR)
10360 EI=DUM2(IVR)
10370 FOR IN=NOW-1 TO 1 STEP -1
10380 IV2=IA+IAFT*(IB-1+IBEF*(IN-1))
```

```
10390 ERT=ER*ARGR-EI*ARGI+DUM1(IV2)
10400 EIT=EI*ARGR+ER*ARGI+DUM2(IV2)
10410 ER=ERT
10420 EI=EIT
10430 NEXT IN
10440 IV3=IA+IAFT*(J-1+NOW*(IB-1))
10450 DFFT1(IV3)=ER
10460 DFFT2(IV3)=EI
10470 NEXT IB
10480 IF IAFT=1 GOTO 10530
10490 ARGRT=ARGR*CANG-ARGI*HANG
10500 ARGIT=ARGI*CANG+ARGR*HANG
10510 ARGR=ARGRT
10520 ARGI=ARGIT
10530 NEXT IA
10540 IF IAFT<>1 GOTO 10590
10550 ARGRT=ARGR*CANG-ARGI*HANG
10560 ARGIT=ARGI*CANG+ARGR*HANG
10570 ARGR=ARGRT
10580 ARGI=ARGIT
10590 NEXT J
10600 IF IBEF=1 GOTO 10660
10610 IAFT=IAFT*NOW
10620 FOR I=1 TO NSTEP
10630 DUM1(I)=DFFT1(I):DUM2(I)=DFFT2(I)
10640 NEXT I
10650 GOTO 10160
10660 RETURN
```

i. APPENDIX 1.2

Program WMENU

1. Appendix 1.2

Program WMENU

Program to acquire transmission data and compute the Lambert Absorption coefficient

```
10 'NAME:  Data Acquisition And Control (DAAC)
20 '       HEADER for BASICA
30 '
40 'FILE NAME:  DACHDR.BAS
50 '
60 'DOS DEVICE NAME:  DAAC
70 '
80 'RESERVED FUNCTION NAMES:
90 '          AINM, AINS, AINSC, AOUM, AOUS,
100 '          BINM, BINS, BITINS, BITOUS, BOUM, BOUS,
110 '          CINM, CINS, CSET, DELAY
120 'RESERVED DEF SEG VALUE NAME:  DSEG
130 '
140 'NAMES DEFINED AND USED BY HEADER:
150 '          ADAPT%, AI, COUNT, FOUND%,
160 '          HNAME$, SG%, STAT%
170 '
180 '
190 'When using the BASICA Interpreter, this header
200 'must be executed before any function calls are
210 'made that access the DAAC adapter.  It initializes
220 'a number of variables for each function call.  These
230 'variables are reserved and should not be used except
240 'to access the DAAC adapter.  This routine also does a
250 'DEF SEG to the segment where the DAAC Device Driver
260 '(DAC.COM) is loaded.  If you execute a DEF SEG to
270 'access other hardware, you must DEF SEG to the segment
280 'of the DAAC Device Driver before any subsequent
290 'calls to access the DAAC adapter.
300 '
310 '
320 FOUND% = 0
330 SG% = &H2E
340 'Start searching the interrupt vectors until you find
350 'one that points to the DAAC device driver.
360 'Do a DEF SEG to that segment.
370 WHILE ((SG% <= &H3E) AND (FOUND% = 0))
380       DEF SEG = 0
390       DSEG = PEEK(SG%) + PEEK(SG% + 1) * 256
400       DEF SEG = DSEG
410       HNAME$=""
420       FOR AI=10 TO 17
430             HNAME$ = HNAME$ + CHR$(PEEK(AI))
```

```
440       NEXT AI
450       IF HNAME$ = "DAAC    " AND PEEK(18) + PEEK(19) <> 0 THEN FOUND% = 1
460       SG% = SG% + 4
470 WEND
480 IF FOUND% = 0 THEN PRINT "ERROR: DEVICE DRIVER DAC.COM NOT FOUND" : END
490 'Now initialize all function name variables for calls
500 'to access the device driver.
510 AINM        = PEEK(&H13) * 256 + PEEK(&H12)
520 AINS        = PEEK(&H15) * 256 + PEEK(&H14)
530 AINSC       = PEEK(&H17) * 256 + PEEK(&H16)
540 AOUM        = PEEK(&H19) * 256 + PEEK(&H18)
550 AOUS        = PEEK(&H1B) * 256 + PEEK(&H1A)
560 BINM        = PEEK(&H1D) * 256 + PEEK(&H1C)
570 BINS        = PEEK(&H1F) * 256 + PEEK(&H1E)
580 BITINS      = PEEK(&H21) * 256 + PEEK(&H20)
590 BITOUS      = PEEK(&H23) * 256 + PEEK(&H22)
600 BOUM        = PEEK(&H25) * 256 + PEEK(&H24)
610 BOUS        = PEEK(&H27) * 256 + PEEK(&H26)
620 CINM        = PEEK(&H29) * 256 + PEEK(&H28)
630 CINS        = PEEK(&H2B) * 256 + PEEK(&H2A)
640 CSET        = PEEK(&H2D) * 256 + PEEK(&H2C)
650 DELAY       = PEEK(&H2F) * 256 + PEEK(&H2E)
660 'Finally, execute any call to re-initialize the
670 'device driver from any former invocation of BASIC.
680 ADAPT% = 0
690 COUNT = 1
700 STAT% = 0
710 CALL DELAY (ADAPT%, COUNT, STAT%)
720 '
730 'End of DAAC BASICA Header
740 '
1000 REM PROGRAM DEVELOPED AND WRITTEN BY DAVID WIELICZKA
1010 REM THIS ROUTINE ACQUIRES TRANSMISSION DATA AND COMPUTES THE
1020 REM LAMBERT ABSORPTION COEFFICIENT FROM THE TRANSMISSION DATA
1030 REM THE PROGRAM WAS WRITTEN UNDER THE SUPPORT OF CRDEC CONTRACT
1040 REM NUMBER DAAA-15-85-K-0013
1050 REM DATE WRITTEN SEPTEMBER 20, 1987
1060 REM WEDGE MENU
1070 REM $DYNAMIC
1080 OPTION BASE 1' ALL ARRAYS BEGIN WITH INDEX 1
1090 DEFSNG A-H 'ALL  VARIABLES BEGINNING WITH A THRU H ARE SINGLE PREC.
1100 DEFINT I-N 'ALL VARAIBLES BEGINNING WITH I THRU N ARE INTEGER
1110 DEFDBL T-Z 'ALL VARIABLES BEGINNING WITH T THRU Z ARE DOUBLE PREC.
1120 DEFSTR O-S 'ALL VARIABLES BEGINNING WITH O THRU S ARE STRINGS
1130 '**********************PARAMETER LIST*******************************
1140 'Q - ARRAY OF LENGTH 3 TO STORE FILENAMES AND COMMENT
1150 'B - ARRAY OF LENGTH 10 FOR SCAN PARAMETERS
1160 'B(1) - TANGENT OF VERTEX ANGLE
1170 'B(2) - WAVELENGTH IN MICRONS
1180 'B(3) - STEP SIZE IN MM
1190 'B(4) - NUMBER OF STEPS
1200 'B(5) - SAMPLE LOCK-IN SCALE
```

```
1210 'B(6) - REFERENCE LOCK-IN SCALE
1220 'B(7) - POWER METER SCALE
1230 'B(8) - TIME CONSTANT FOR LOCK-INS
1240 'B(9) - NUMBER OF A/D READINGS TO AVERAGE PER POINT
1250 'B(10) - DIRECTION OF TRAVEL FOR CELL
1260 'O - ARRAY OF LENGTH 16 FOR MENU LABELS
1265 '************************************************************
1266 DIM Q(3),B(10),O(16)
1270 O(1)="FILENAME FOR RAW DATA: "
1280 O(2)="FILENAME FOR LAC AND K: "
1290 O(3)="COMMENT: "
1300 O(4)="TANGENT OF WEDGE ANGLE: "
1310 O(5)="WAVELENGTH IN MICRONS: "
1320 O(6)="STEP SIZE IN MM: "
1330 O(7)="NUMBER OF STEPS: "
1340 O(8)="SAMPLE LOCK-IN SCALE: "
1350 O(9)="REFERENCE LOCK-IN SCALE: "
1360 O(10)="POWER METER SCALE: "
1370 O(11)="TIME CONSTANT: "
1380 O(12)="NUMBER OF A/D AVERAGES: "
1390 O(13)="POSITION CELL"
1400 O(14)="ACQUIRE DATA"
1410 O(15)="A/D CONVERSION CHECK"
1420 O(16)="EXIT"
1430 CLS:LOCATE 1,1
1440 REM DISPLAY MENU ON SCREEN
1450 FOR I=1 TO 3
1460 PRINT "(";CHR$(64+I);") ";O(I);Q(I)
1470 NEXT I
1480 FOR I=4 TO 12
1490 PRINT "(";CHR$(64+I);") ";O(I);B(I-3)
1500 NEXT I
1510 FOR I=13 TO 16
1520 PRINT "(";CHR$(64+I);") ";O(I)
1530 NEXT I
1540 PRINT "PRESS THE APPROPRIATE KEY TO CONTINUE!!"
1550 P=INKEY$: IF P="" THEN 1550
1560 A=ASC(P)-64  'SUBTRACT ASCII OFFSET FOR LETTER A
1570 IF A<1 GOTO 1550 'REPEAT INKEY IF INCORRECT KEY STRUCK
1580 IF A<4 GOTO 1630 'INPUT A STRING VARIABLE
1590 IF A<13 GOTO 1800  'INPUT A REAL VARIABLE
1600 IF A>16 GOTO 1550 'REPEAT INKEY IF INCORRECT KEY STRUCK
1610 A=A-12 'SUBTRACT ADDITIONAL OFFSET TO BRANCH TO SUBROUTINES
1620 ON A GOTO 1840,1870,2000,2030
1630 REM INPUT A STRING VARIABLE
1640 ON A GOTO 1660,1710,1760
1650 'INPUT FILENAME TO STORE RAW DATA
1660 PRINT O(A);
1670 INPUT Q(A)
1680 OPEN Q(A) FOR OUTPUT AS #1:PRINT #1,DATE$
1690 GOTO 1430
1700 'INPUT FILENAME TO STORE LAMBERT ABSORPTION COEFFICIENT
```

```
1710 PRINT O(A);
1720 INPUT Q(A)
1730 OPEN Q(A) FOR OUTPUT AS #2:PRINT #2,DATE$
1740 GOTO 1430
1750 'INPUT COMMENT TO STORE WITH BOTH DATA FILES
1760 PRINT O(A);
1770 INPUT Q(A)
1780 PRINT #1,Q(A):PRINT #2,Q(A):CLOSE #1:CLOSE #2
1790 GOTO 1430
1800 REM INPUT A REAL VARIABLE
1810 PRINT O(A);
1820 INPUT B(A-3)
1830 GOTO 1430
1840 REM POSITION CELL
1850 GOSUB 4000
1860 GOTO 1430
1870 REM ACQUIRE DATA
1880 FOR J=1 TO 3 'ASSURE BOTH FILES HAVE BEEN CREATED
1890 IF Q(J)="" THEN 1980
1900 NEXT J
1910 FOR J=1 TO 10 'ASSURE ALL SCAN PARAMETERS HAVE BEEN SET
1920 IF B(J)=0 THEN 1990
1930 NEXT J
1940 GOSUB 6000
1950 GOTO 1430
1960 'ERROR MESSAGES IF CHECKS OF FILENAMES AND SCAN PARAMETERS ARE
1970 'INCORRECT
1980 CLS:LOCATE 25,1:PRINT "NOT ALL STRINGS ARE INPUT":GOTO 1430
1990 CLS:LOCATE 25,1:PRINT "NOT ALL SCAN PARAMETERS ARE INPUT":GOTO 1430
2000 REM CHECK A/D
2010 GOSUB 11000
2020 GOTO 1430
2030 END
4000 REM SUBROUTINE PSIT
4010 REM THIS SUBROUTINE POSITIONS THE CELL AT THE TOP OR BOTTOM OF
4020 REM THE VERTEX.
4030 REM*****************************************
4040 REM VARIABLE LIST
4050 REM SMOVE - 7 ELEMENT ARRAY CONTAINING COMMAND TO START CONTINUOUS
4060 REM         MOTION OF MOTOR DRIVE
4070 REM SNIT - 20 ELEMENT ARRAY TO INITIALIZE STEPPER MOTOR
4080 REM STA  - 3 ELEMENT ARRAY TO EXAMINE LIMIT SWITCH STATUS
4090 REM SSET - 12 ELEMENT ARRAY TO SET THE STEP SIZE OF THE MOTOR
4100 REM SSET - 12 ELEMENT ARRAY TO SET THE STEP SIZE OF THE MOTOR
4110 REM SZERO - 2 ELEMENT ARRAY TO SET CURRENT POSITION OF MOTOR AS
4120 REM        . ABSOLUTE ZERO
4130 REM SHALT - 1 ELEMENT ARRAY TO STOP THE MOTOR INSTANTANEOUSLY
4140 REM STAM - 2 ELEMENT ARRAY TO CHECK MOTOR STATUS
4150 REM FLAG -
4160 REM J - DUMMY VARIABLE TO READ STATUS OF SERIAL PORT
4170 REM R - DUMMY VARIABLE TO READ ECHO OF STEPPER MOTOR CONTROLLER
4180 REM P - INKEY VARIABLE
```

```
4190 DIM SNIT(20),SMOVE(7),STA(3),SSET(12),SZERO(2),SHALT(1),STAM(2)
4200 SNIT(1)="L":SNIT(2)="D":SNIT(3)="0":SNIT(4)=" ":SNIT(5)="A"
4210 SNIT(6)="0":SNIT(7)="1":SNIT(8)=" ":SNIT(9)="V":SNIT(10)="0"
4220 SNIT(11)="1":SNIT(12)=" ":SNIT(13)="S":SNIT(14)="C":SNIT(15)="1"
4230 SNIT(16)=" ":SNIT(17)="S":SNIT(18)="C":SNIT(19)="A":SNIT(20)="1"
4240 SMOVE(1)="H":SMOVE(2)="+":SMOVE(3)=" ":SMOVE(4)="M":SMOVE(5)="C"
4250 SMOVE(6)=" ":SMOVE(7)="G"
4260 STA(1)="8":STA(2)="R":STA(3)="A"
4270 SSET(1)="M":SSET(2)="N":SSET(3)=" ":SSET(4)="D":SSET(5)="+"
4280 SSET(6)="2":SSET(7)="5":SSET(8)="6":SSET(9)="0":SSET(10)="0"
4290 SSET(11)=" ":SSET(12)="G"
4300 SZERO(1)="P":SZERO(2)="Z"
4310 SHALT(1)="S"
4320 STAM(1)="8":STAM(2)="R"
4330 FLAG=0
4340 REM THE FOLLOWING COMMANDS ARE SENT TO INITIALIZE THE STEPPER
4350 REM MOTOR CONTROLLER
4360 REM LD0 - ENABLE LIMIT SWITCHES
4370 REM A01 - SET ACCELARATION TO 1 REV/SEC/SEC
4380 REM V01 - SET VELOCITY TO 1 REV/SEC
4390 REM SC1 - SET STANDBY CURRENT TO 1/8 OF MAX.
4400 REM SCA1 - SET STANDBY CURRENT AFTER EACH MOVE TO 1/8 MAX.
4410 OPEN "COM1:9600,N,8,1" AS #3 ' OPEN SERIAL PORT 1 FOR COMMUNICATION
4420 FOR I=1 TO 20 'INITIALIZE STEPPER MOTOR CONTROLLER
4430 J=INP(&H3FD) 'SEE IF SERIAL PORT IS READY TO SEND A CHARACTER
4440 IF J<>96 GOTO 4430 'LOOP TO 4290 IF SERIAL PORT NOT READY
4450 PRINT #3,SNIT(I); 'SEND OUT SINGLE CHARACTER NO CARRIAGE RETURN
4460 IF EOF(3) THEN 4460 'WAIT FOR ECHO FROM STEPPER MOTOR CONTROLLER
4470 R=INPUT$(1,#3) 'INPUT ECHO FROM CONTROLLER
4480 NEXT I
4490 PRINT #3,CHR$(13); 'SEND CARRIAGE RETURN TO TERMINATE COMMAND
4500 IF EOF(3) THEN 4500 'WAIT FOR ECHO FROM CONTROLLER
4510 R=INPUT$(1,#3) 'READ ECHO FROM CONTROLLER
4520 PRINT "POSITION CELL AT TOP(T) OR BOTTOM(B) OF WEDGE"
4530 P=INKEY$: IF P="" THEN 4530
4540 REM THE FOLLOWING COMMANDS DIRECT THE MOTOR TO MOVE EITHER CLOCKWISE
4550 REM OR COUNTER-CLOCKWISE AND TO MOVE CONTINUOUSLY
4560 REM H- MOVE IN CCW DIRECTION
4570 REM H+ MOVE IN CW DIRECTION
4580 REM MC MOVE CONTINUOUSLY
4590 REM G GO
4600 PRINT "TYPE <ESC> IF YOU WISH TO STOP THE MOTOR"
4610 IF P="B" THEN SMOVE(2)="-"
4620 IF P="T" THEN SMOVE(2)="+"
4630 FOR I=1 TO 7  'SEND COMMAND TO CONTROLLER
4640 J=INP(&H3FD) 'EXAMINE SERIAL PORT
4650 IF J<>96 GOTO 4640 'LOOP IF SERIAL PORT NOT READY
4660 PRINT #3,SMOVE(I); 'SEND SINGLE CHARACTER
4670 IF EOF(3) THEN 4670  'WAIT FOR ECHO
4680 R=INPUT$(1,#3)  'READ IN ECHO
4690 NEXT I
4700 PRINT #3,CHR$(13);  'TERMINATE COMMAND
```

```
4710 IF EOF(3) THEN 4710 'WAIT FOR ECHO
4720 R=INPUT$(1,#3)  'READ IN ECHO
4730 REM 8RA CHECK STATUS LIMIT SWITCHES
4740 REM LIMIT SWITCHES TELL IF MOTOR IS STILL RUNNING OR NOT
4750 FOR I=1 TO 3 'SEND OUT LIMIT SWITCH COMMAND
4760 J=INP(&H3FD) 'SEE IF SERIAL PORT IS READY FOR CHARACTER
4770 IF J<>96 THEN 4760 'LOOP IF SERIAL PORT NOT READY
4780 PRINT #3,STA(I); 'SEND SINGLE CHARACTER TO SERIAL PORT
4790 IF EOF(3) THEN 4790 'WAIT FOR ECHO
4800 R=INPUT$(1,#3) 'READ IN ECHO
4810 NEXT I
4820 PRINT #3,CHR$(13);  'TERMINATE COMMAND
4830 IF EOF(3) THEN 4830 'WAIT FOR ECHO
4840 R=INPUT$(1,#3) 'READ IN ECHO
4850 IF EOF(3) THEN 4850 'READ IN STATUS OF LIMIT SWITCHES
4860 INPUT #3,R 'INPUT CHARACTER
4870 P1=INKEY$  'CHECK TO SEE IF ESC KEY HAS BEEN STRUCK
4880 IF P1=CHR$(27) THEN FLAG=-1:GOTO 5350  'IF ESC KEY STRUCK EXIT
4890 REM EXAMINE THE STATUS RETURNED BY STEPPER MOTOR CONTROLLER
4900 REM IF STATUS IS LESS THAN "A" OR GREATER THAN "O" THEN
4910 REM REPEAT CHECK OF LIMIT SWITCHES
4920 REM IF LIMIT SWITCHES SET CONTINUE
4930 IF (RIGHT$(R,1)<"A") OR (RIGHT$(R,1)>"O") GOTO 4750
4940 REM AFTER LIMIT SWITCHES ARE SET MOVE MOTOR TWO REVOLUTIONS
4950 ' IN OPPOSITE DIRECTION TO REMOVE BACKLASH IN DRIVE SCREW
4960 REM D25600 G MOVE 2 REVOLUTIONS IN CW DIRECTION
4970 REM D-25600 G MOVE 2 REVOLUTIONS IN CCW DIRECTION
4980 IF P="B" THEN SSET(5)="+":B(10)=+1
4990 IF P="T" THEN SSET(5)="-":B(10)=-1
5000 FOR I=1 TO 12 'SEND OUT COMMAND TO MOVE TWO REVOLUTIONS
5010 J=INP(&H3FD)
5020 IF J<>96 GOTO 5010
5030 PRINT #3,SSET(I);
5040 IF EOF(3) THEN 5040
5050 R=INPUT$(1,#3)
5060 NEXT I
5070 PRINT #3,CHR$(13);
5080 IF EOF(3) THEN 5080
5090 R=INPUT$(1,#3)  'TERMINATE COMMAND TO MOVE TWO REVOLUTIONS
5100 FOR I=1 TO 2  'SEND OUT COMMAND TO SEE IF MOTOR HAS STOPPED
5110 J=INP(&H3FD)
5120 IF J<>96 THEN 5110
5130 PRINT #3,STAM(I);
5140 IF EOF(3) THEN 5140
5150 R=INPUT$(1,#3)
5160 NEXT I
5170 PRINT #3,CHR$(13);
5180 IF EOF(3) THEN 5180
5190 R=INPUT$(1,#3)   'TERMINATE COMMAND TO SEE IF MOTOR HAS STOPPED
5200 IF EOF(3) THEN 5200
5210 INPUT #3,R  'INPUT RESPONSE TO PREVIOUS COMMAND
5220 IF R<>"*R" GOTO 5100  'REPEAT COMMAND IF RESPONSE NOT CORRECT
```

```
5230 REM PZ SET CURRENT POSITION AS ABSOLUTE ZERO
5240 FOR I=1 TO 2 'SET CURRENT MOTOR POSITION TO ABSOLUTE ZERO
5250 J=INP(&H3FD)
5260 IF J<>96 THEN 5250
5270 PRINT #3,SZERO(I);
5280 IF EOF(3) THEN 5280
5290 R=INPUT$(1,#3)
5300 NEXT I
5310 PRINT #3,CHR$(13);
5320 IF EOF(3) THEN 5320
5330 R=INPUT$(1,#3) 'TERMINATE COMMAND TO SET ABSOLUTE ZERO
5340 IF FLAG<>-1 GOTO 5430 'IF ESC KEY NOT STRUCK BRANCH TO 5200
5350 J=INP(&H3FD) 'IF ESC KEY STRUCK SEND COMMAND TO STOP MOTOR
5360 IF J<>96 THEN 5350
5370 PRINT #3,SHALT(1)
5380 IF EOF(3) THEN 5380
5390 R=INPUT$(1,#3)
5400 PRINT #3,CHR$(13);
5410 IF EOF(3) THEN 5410
5420 R=INPUT$(1,#3) 'TERMINATE COMMAND TO STOP MOTOR
5430 CLOSE #3  'CLOSE SERIAL COMMUNICATION
5440 RETURN
6000 REM SUBROUTINE TO ACQUIRE DATA
6010 '*********************PARAMETER LIST**********************
6020 'IDTA - ARRAY OF LENGTH 600 TO STORE DATA READ FOR A/D CHANNELS
6030 'C1 - ARRAY OF LENGTH 200 TO STORE SAMPLE LOCK-IN VALUES
6040 'C2 - ARRAY OF LENGTH 200 TO STORE REFERENCE LOCK-IN VALUES
6050 'C3 - ARRAY OF LENGTH 200 TO STORE POWER METER VALUES
6060 'SINC - ARRAY OF LENGTH 7 MOTOR COMMAND TO SET STEP SIZE
6070 'SGO - ARRAY OF LENGTH 1 MOTOR COMMAND TO START MOTOR
6080 'STAM - ARRAY OF LENGTH 2 MOTOR COMMAND TO EXAMINE STATUS OF MOTOR
6090 '***********************************************
6100 DIM IDTA(600),C1(200),C2(200),C3(200),SINC(7),SGO(1),STAM(2)
6110 SCREEN 2
6120 CLS
6130 'INITIALIZE MOTOR COMMANDS
6140 SINC(1)="D":SINC(2)="+":SINC(3)="2":SINC(4)="0":SINC(5)="0"
6150 SGO(1)="G"
6160 STAM(1)="8":STAM(2)="R"
6170 'INITIALIZE VARIABLES FOR A/D CONVERSION ROUTINE
6180 IADAPT=0' ALL CALLS ARE TO DAC ADAPTER 0
6190 IDEVICE=9' DEVICE IS 9 FOR A/D CALLS
6200 ICHANLO=0' SCAN BEGINNING WITH CHANNEL 0 - SAMPLE LOCKIN, 1-REF. LOCKIN
6210 ICHANHI=2' SCAN TO CHANNEL 2-POWER METER
6220 ICTRL=0
6230 IMODE=0
6240 ISTOR=0
6250 COUNT=B(9)' NUMBER OF A/D TO ACQUIRE
6260 ICT=CINT(B(9))
6270 IF B(8)<1! THEN CRATE=2!*(1/B(8)) ' RATE IS TWICE THE TIME CONSTANT
6280 IF B(8)>=1! THEN CRATE = 2! ' MINIMUM RATE IS 2 READS PER SECOND
6290 ISTAT=0
```

```
6300 IX=0: IY=0
6310 NSTEP=CINT(B(4))
6320 FOR K=1 TO 3 'ZERO DATA VALUES
6330 FOR I=1 TO NSTEP
6340 C1(I)=0: C2(I)=0: C3(I)=0
6350 NEXT I
6360 NEXT K
6370 GSPMM=20000' STEPS PER MILLIMETER
6380 GSIZE=GSPMM*B(3)'DETERMINE NUMBER OF STEPS TO MOVE MOTOR
6390 IF B(10)=1 THEN SINC(2)="+"
6400 IF B(10)=-1 THEN SINC(2)="-"
6410 SSIZE=MID$((STR$(GSIZE)),2)
6420 JSIZE=LEN(SSIZE)
6430 FOR K=1 TO JSIZE
6440 SINC(K+2)=MID$(SSIZE,K,1)
6450 NEXT K
6460 JSIZE=JSIZE+2
6470 OPEN Q(1) FOR APPEND AS #1 'OPEN RAW DATA FILE
6480 OPEN Q(2) FOR APPEND AS #2 'OPEN LAMBERT ABSORPTION FILE
6490 COM(1) ON
6500 OPEN "COM1:9600,N,8,1,RS" AS #3 'OPEN SERIAL PORT FOR COMMUNICATION
6510 FOR K=1 TO JSIZE 'SEND STEP SIZE COMMAND TO MOTOR CONTROLLER
6520 J=INP(&H3FD)
6530 IF J<>96 THEN 6520
6540 PRINT #3,SINC(K);
6550 IF EOF(3) THEN 6550
6560 R=INPUT$(1,#3)
6570 NEXT K
6580 PRINT #3,CHR$(13);    'TERMINATE STEP SIZE COMMAND
6590 IF EOF(3) THEN 6590
6600 R=INPUT$(1,#3)
6610 FOR I=1 TO 9 'STORE SCAN VALUES IN RAW DATA FILE
6620 PRINT #1,B(I);
6630 NEXT I
6640 PRINT #1,
6650 FOR I=1 TO NSTEP  'BEGIN ACQUIRING DATA
6660 CALL AINSC(IADAPT,IDEVICE,ICHANLO,ICHANHI,ICTRL,IMODE,ISTOR,COUNT,CRATE,
     IDTA(1),ISTAT)
6670 IF ISTAT<>0 THEN PRINT "A/D CONVERSION ERROR";ISTAT: END
6680 J=INP(&H3FD) 'SEND COMMAND TO STEP MOTOR PRESET AMOUNT
6690 IF J<>96 THEN 6680
6700 PRINT #3,SGO(1);
6710 IF EOF(3) THEN 6710
6720 R=INPUT$(1,#3)
6730 PRINT #3,CHR$(13);  'TERMINATE COMMAND TO STEP MOTOR
6740 IF EOF(3) THEN 6740
6750 R=INPUT$(1,#3)
6760 FOR J=1 TO ICT 'SEPARATE CHANNELS FROM A/D CONVERSION
6770 C1(I)=C1(I)+CSNG(IDTA((3*J)-2))
6780 C2(I)=C2(I)+CSNG(IDTA((3*J)-1))
6790 C3(I)=C3(I)+CSNG(IDTA(3*J))
6800 NEXT J
```

```
6810 'COMPUTE PIXEL VALUES TO DISPLAY DATA ON SCREEN DURING ACQUISITON
6820 IX=IX+CINT(B(3)*640/(B(3)*B(4)))
6830 C1(I)=C1(I)/B(9)
6840 C2(I)=C2(I)/B(9)
6850 C3(I)=C3(I)/B(9)
6860 PRINT #1,C1(I),C2(I),C3(I)
6870 C1(I)=(C1(I)-2048!)/2048!
6880 C2(I)=(C2(I)-2048!)/2048!
6890 C3(I)=(C3(I)-2048!)/2048!
6900 'DISPLAY DATA ON SCREEN DURING ACQUISITION
6910 IY1=200-CINT(C1(I)*200):CIRCLE(IX,IY1),1
6920 IY2=200-CINT(C2(I)*200):CIRCLE(IX,IY2),2
6930 IY3=200-CINT(C3(I)*200):CIRCLE(IX,IY3),3
6940 FOR K=1 TO 2 'SEND COMMAND TO DETERMINE IF MOTOR HAS STOPPED
6950 J=INP(&H3FD)
6960 IF J<>96 THEN 6950
6970 PRINT #3,STAM(K);
6980 IF EOF(3) THEN 6980
6990 R=INPUT$(1,#3)
7000 NEXT K
7010 PRINT #3,CHR$(13); 'TERMINATE STATUS COMMAND
7020 IF EOF(3) THEN 7020
7030 R=INPUT$(1,#3)  'INPUT RESPONSE TO STATUS COMMAND
7040 IF EOF(3) THEN 7040
7050 INPUT #3,R
7060 IF R<> "*R" GOTO 6940  'IF MOTOR STILL IN MOTION REPEAT STATUS COMMAND
7070 NEXT I  'ACQUIRE NEXT DATA POINT
7080 CLOSE #3 'END COMMUNICATION WITH MOTOR
7090 GOSUB 8000
7100 CLOSE #1
7110 CLOSE #2
7120 RETURN
8000 REM SUBROUTINE TO COMPUTE RATIOS AND DRAW FITTED LINE
8010 '*******************PARAMETER LIST*********************
8020 'D - ARRAY OF LENGTH 200 USED IN LEAST SQUARES FITTING ROUTINE
8030 'COEF - ARRAY OF LENGTH 4 COEFFICIENTS IN LEAST SQUARES FITTING
8040 'DX - ARRAY OF LENGTH 200 X VALUES FOR LEAST SQUARES FITTING
8050 'DS - STANDARD DEVIATION OF RATIOS
8060 'NDIFF - NUMBER OF DISTINCT RATIOS TO DETERMINE
8070 NDIFF=CINT(B(4))-1
8080 DIM D(200),COEF(4),DX(200),DS(200)
8090 FOR K=1 TO 4: COEF(K)=0!: NEXT K 'ZERO COEFFICIENTS
8100 PRINT #2,B(2),NDIFF 'STORE WAVELENGTH AND NUMBER OF DATA POINTS
8110 '  IN FILE FOR LAMBERT ABSORPTION COEFFICIENT
8120 FOR I=1 TO NDIFF  'BEGIN LOOP THROUGH POSSIBLE RATIOS
8130 D(I)=0!
8140 E=0
8150 FOR J=1 TO B(4)-I 'COMPUTE RATIOS WITH A CONSTANT SUBSCRIPT DIFFERENCE
8160 '                    OF I
8170 H=(C1(J)*C2(J+I))/(C1(J+I)*C2(J))
8180 D(I)=D(I)+H   'SUM OF RATIOS H
8190 E=E+H^2     'USED IN COMPUTING STANDARD DEVIATION OF H
```

```
8200 NEXT J
8210 D(I)=D(I)/(J-1)  'AVERAGE OF RATIOS WITH SUBSCRIPT DIFFERENCE OF I
8220 E=E/(J-1)
8230 DS(I)=E-(D(I)^2) 'VARIANCE OF D(I)
8240 DX(I)=B(3)*B(1)*I/10! 'COMPUTE X VALUES
8250 DS(I)=SQR(DS(I)/D(I))' CONVERT VARIANCE OF DATA INTO VARIANCE OF LN(DATA)
8260 D(I)=LOG(D(I))   'CONVERT DATA TO LOG FOR LEAST SQUARES FITTING
8270 PRINT #2,DX(I),D(I),DS(I)  'STORE VALUES IN LAMBERT ABS. FILE
8280 COEF(1)=COEF(1)+DX(I)'SUM OF X VALUES
8290 COEF(2)=COEF(2)+D(I)'SUM OF Y VALUES
8300 COEF(3)=COEF(3)+(DX(I)*D(I))'SUM OF X*Y VALUES
8310 COEF(4)=COEF(4)+(DX(I)^2)'SUM OF X VALUES SQUARED
8320 NEXT I
8330 DENOM=NDIFF*COEF(4)-(COEF(1)^2)  'DENOMINATOR IN LEAST SQUARES EQ.
8340 AINT=(COEF(4)*COEF(2)-COEF(1)*COEF(3))/DENOM  'INTERCEPT OF FIT
8350 BSLOP=(NDIFF*COEF(3)-COEF(1)*COEF(2))/DENOM   'SLOPE OF FIT
8360 DEV=0
8370 FOR I=1 TO NDIFF  'COMPUTE STANDARD DEVIATION OF Y
8380 F=D(I)-AINT-(BSLOP*DX(I))
8390 DEV=DEV+(F^2)
8400 NEXT I
8410 DEV=DEV/(NDIFF-2)
8420 DSLOP=NDIFF*DEV/DENOM  'STANDARD DEVIATION OF SLOPE
8430 DINT=DEV*COEF(4)/DENOM  'STANDARD DEVIATION OF INTERCEPT
8440 DEV=SQR(DEV):DSLOP=SQR(DSLOP):DINT=SQR(DINT)
8450 PRINT #2,BSLOP,AINT  'STORE SLOPE AND INTERCEPT
8460 PRINT #2,DEV,DSLOP,DINT  'STORE STD OF FIT-SLOPE-INTERCEPT
8470 DXMAX=0:DYMAX=0
8480 FOR I=1 TO NDIFF  'DETERMINE X AND Y MAXIMUM VALUES
8490 IF DX(I)>DXMAX THEN DXMAX=DX(I)
8500 IF D(I)>DYMAX THEN DYMAX=D(I)
8510 NEXT I
8520 GXSC=INT(LOG(DXMAX)/2.302585):GXSC=(10^(GXSC-1))' SCALE FACTOR TO DIVIDE
8530 GYSC=INT(LOG(DYMAX)/2.302585):GYSC=(10^(GYSC-1))' SCALE FACTOR TO DIVIDE
8540 FOR I=1 TO NDIFF 'SCALE ALL DATA FOR PLOTTING
8550 DX(I)=DX(I)/GXSC
8560 D(I)=D(I)/GYSC
8570 DS(I)=DS(I)/GYSC
8580 NEXT I
8590 AINT=AINT/GYSC
8600 BSLOP=BSLOP*GXSC/GYSC
8610 REM   plot program for the HP 7475A, accepts data points, slope,
8620 REM   y-intercept, y-deviation per y, and number of points,
8630 REM   for a LSQF plotting.
8640 REM   created by mark anthony pederson, 14 feb 88, for Dr. Wieliczka.
8650 REM
8660 REM SUB HPPLOT(DX!(1),D!(1),DS!(1),BSLOP!,AINT!,NDIFF%) STATIC
8670 REM
8680 REM initialisation.....................................................
8690   M1  = 10365  'plotter units x direction for 8.5"x 11" paper
8700   M2  = 7962   'plotter units y direction
8710   B1  = .15  'border, lower bounds, x and y, decimal percent
```

```
8720   B2  = .8  'border, upper bounds, where 100% are right and top edges
8730   J1  = B1*M1  'plotter units, left edge of plotting area
8740   J2  = B2*M1  'plotter units, right edge of plotting area
8750   K1  = B1*M2  'plotter units, lower edge of plotting area
8760   K2  = B2*M2  'plotter units, upper edge of plotting area
8770   M3  = 10     'x-tick divisions
8780   M4  = 10     'y-tick divisions
8790   BX  = 0      'maximum x data value, yet to be determined
8800   CX  = 0      'minimum x data value, yet to be determined
8810   BY  = 0      'maximum y data value, yet to be determined
8820   CY  = 0      'minimum y data value, yet to be determined
8830   P1  = "Distance"        'x-axis label
8840   P2  = "Intensity"       'y-axis label
8850   P3  = "Lambert sherbert" 'graph title
8860   Q   = "TEMP.DAT"        'temporary file used for buffering the printer
8870   N   = NDIFF
8880 REM
8890 REM find minimums and maximums in the data point set.....................
8900 FOR I=1 TO N
8910   D=DX(I) : E=D(I)  'done for speed efficiency
8920   IF BX<D THEN BX=D : GOTO 8940
8930   IF CX>D THEN CX=D
8940   IF BY<E THEN BY=E : GOTO 8960
8950   IF CY>E THEN CY=E
8960 NEXT I
8970 BX=((BX\M3)+1)*M3 :  BY=((BY\M4)+1)*M4   'rounding up user values
8980 REM
8990 REM open file buffer and send plotter initializers.....................
9000 OPEN Q FOR OUTPUT AS 4
9010 REM PRINT #4,"IN;SP1;";  'initialise plotter and select pen
9020 REM PRINT #4,CHR$(27);".I1;5;6;";
9030 PRINT #4,"IP0,0,";M1;",";M2;";"  'set up maximum pen reach for now
9040 REM
9050 REM draw outline of the plotting area.....................................
9060 PRINT #4,"PU";J1;",";K1;"PD";  'move pen to area origin, lower left
9070 PRINT #4,J2;",";K1;",";        'draw lower edge, x-axis
9080 PRINT #4,J2;",";K2;",";        'draw right edge
9090 PRINT #4,J1;",";K2;",";        'draw upper edge
9100 PRINT #4,J1;",";K1;"PU;"       'draw left edge, y-axis, and lift pen
9110 REM
9120 REM calibrate x-axis with tick marks and values.........................
9130 PRINT #4,"SR";1*(B2-B1);",";20*B1;";";  'set lettering size for values
9140 PRINT #4,"TL0,";10*D1;";"   'off-center tick, set tick size
9150 M9=(J2-J1)\M3              'tick spacing in plotter units
9160 M10=(BX-CX)\M3             'tick value increment in user units
9170 M11=0
9180 FOR I=J1 TO J2 STEP M9      'increment tick position
9190   PRINT #4,"PA";I;",";K1;"XT;"  'move and draw tick mark
9200 REM  PRINT #4,"CP";-LEN(STR$(M11))\2;",";-10/20;";"  'center for value
9210   PRINT #4,"CP";-1;",";-1;";"  'center for value
9220   PRINT #4,"LB";STR$(M11);CHR$(3);"PU;"  'print value
9230   M11=M11+M10               'increment tick value
```

```
9240 NEXT I
9250 REM
9260 REM label x-axis.....................................................
9270 PRINT #4,"PA";J2;",";K1;";"          'position at end of x-axis
9280 PRINT #4,"CP0,-1.5;"'space down to avoid writing overlap
9290 PRINT #4,"SR";2*(B2-B1);",";15*B1;";"  'set up reverse write
9300 PRINT #4,"PR";-(J2-J1)\2;",0;";  'center in the x direction
9310 PRINT #4,"CP";-LEN(P1)\2;",-.5;"     'offset for centering label
9320 PRINT #4,"LB";P1;CHR$(3)           'reverse write x-axis label
9330 REM
9340 REM calibrate y-axis with tick marks and values.....................
9350 PRINT #4,"DI0,-1;"            'rotate writing direction 90 degrees
9360 PRINT #4,"SR";1*(B2-B1);",";20*B1;";";  'set lettering size for values
9370 PRINT #4,"TL0,";10*B1;";"   'off-center tick, set tick size
9380 M9=(K2-K1)\M4              'tick spacing in plotter units
9390 M10=(BY-CY)\M4             'tick value increment in user units
9400 M11=0
9410 FOR I=K1 TO K2 STEP M9      'increment tick position
9420   PRINT #4,"PA";J1;",";I;"YT;"  'move and draw tick mark
9430   PRINT #4,"CP";-LEN(STR$(M11))\2;",";-1;";"  'center for value
9440   PRINT #4,"LB";STR$(M11);CHR$(3);"PU;"  'print value
9450   M11=M11+M10               'increment tick value
9460 NEXT I
9470 REM
9480 REM label y-axis.....................................................
9490 PRINT #4,"PA";J1;",";K2;";"   'move to end of y-axis
9500 PRINT #4,"CP0,";-15*B1;";";  'space down to avoid writing overlap
9510 PRINT #4,"SR";1*(B2-B1);",";20*B1;";"  'set up letter size
9520 PRINT #4,"PR0,";-(K2-K1)\2;";";  'center in the y direction
9530 PRINT #4,"CP";-LEN(P2)\2;",0;"     'offset for centering label
9540 PRINT #4,"LB";P2;CHR$(3)           'write y-axis label
9550 PRINT #4,"DI1,0;"   'rotate writing angle back to normal
9560 REM
9570 REM write graph title...............................................
9580 REM PRINT #4,"PU;PR";(J2-J1-LEN(P3))\2;",";K2;";"; 'goto top center minus
9590 REM PRINT #4,"SR";10*B1;",";20*B1;";";            'set letter size
9600 REM PRINT #4,"CP0,";-1.2;";LB";P3;CHR$(3) 'drop down space and write titl
9610 REM
9620 REM point plotting..................................................
9630 PRINT #4,"PU";J1;",";K1;";";  'move to origin
9640 PRINT #4,"IP";J1;",";K1;",";J2;",";K2;";";   'reset pen reach to plot are
9650 PRINT #4,"SC";CX;",";BX;",";CY;",";BY;";"  'turn scaling on for user unit
9660 PRINT #4,"TL.5,.5;"  'horizontal cross hair for data point
9670 FOR I=1 TO N
9680   PRINT #4,"PA";DX(I);",";D(I)+DS(I);",PD;";  'upper range for data
9690   PRINT #4,"PA";DX(I);",";D(I);"YT;";          'data point @ crosshair
9700   PRINT #4,"PA";DX(I);",";D(I)-DS(I);"PU;"    'lower range for data
9710 NEXT I
9720 REM
9730 REM lay down the LSQF line..........................................
9740 IF AINT<0 THEN AINT=0
9750 PRINT #4,"PA";CX;",";AINT;";";   'start at the y-intercept
```

```
9760 PRINT #4,"PD;PA";DX(N);",";DX(N)*BSLOP+AINT;"PU;"    'goto mx+b, draw the
9770 REM
9780 REM serial port file buffer unload.....................................
9790 CLOSE #4
9800 INPUT "Please turn the data switch to B.  Hit any key when completed! ",R
9810 OPEN Q FOR INPUT AS 4
9820 OPEN "COM1:9600,N,8,1,RS" AS 3
9830 PRINT #3,"IN;SP1;";   'initialise plotter and select pen
9840 PRINT #3,CHR$(27);".I80;5;6:";
9850 PRINT #3,"SP1;"
9860 WHILE NOT EOF(4)
9870   LINE INPUT #4,R
9880   J=LEN(R)
9890   FOR I=1 TO J
9900 K=INP(&H3FD)
9910 IF K<>96 THEN 9900
9920     PRINT #3,CHR$(5);
9930     S=INPUT$(1,#3)
9940 REM IF S<>CHR$(6) THEN 1500
9950 K=INP(&H3FD)
9960 IF K<>96 THEN 9950
9970     PRINT #3,MID$(R,I,1);
9980   NEXT I
9990 WEND
10000 PRINT #3,"SP;"
10010 CLOSE #4
10020 CLOSE #3
10030 INPUT "Please turn the data switch to A.  Hit any key when completed! ",
10040 REM
10050 REM
10060 REM end of program.....................................................
10070 RETURN
11000 REM SUBROUTINE TO TEST A/D CONVERSION
11010 DIM IDTA(3)
11020 CLS
11030 IADAPT=0' ALL CALLS ARE TO DAC ADAPTER 0
11040 IDEVICE=9' DEVICE IS 9 FOR A/D CALLS
11050 ICHANLO=0' SCAN BEGINNING WITH CHANNEL 0 - SAMPLE LOCKIN, 1-REF. LOCKIN
11060 ICHANHI=2' SCAN TO CHANNEL 2-POWER METER
11070 ICTRL=0
11080 ISTOR=0
11090 ISTAT=0
11100 IMODE=0
11110 COUNT=1
11120 CRATE=1
11130 CALL AINSC(IADAPT,IDEVICE,ICHANLO,ICHANHI,ICTRL,IMODE,ISTOR,COUNT,CRATE,
      IDTA(1),ISTAT)
11140 IF ISTAT<>0 THEN PRINT "A/D CONVERSION ERROR";ISTAT:END
11150 C1=C1+CSNG(IDTA(1))
11160 C2=C2+CSNG(IDTA(2))
11170 C3=C3+CSNG(IDTA(3))
11180 C1=(C1-2048!)*B(5)/2048!
```

```
11190 C2=(C2-2048!)*B(6)/2048!
11200 C3=(C3-2048!)*B(7)/2048!
11210 CLS
11220 PRINT "SAMPLE LOCK-IN SHOULD READ: ";C1
11230 PRINT
11240 PRINT "REFERENCE LOCK-IN SHOULD READ: ";C2
11250 PRINT
11260 PRINT "POWER METER SHOULD READ: ";C3
11270 LOCATE 10,10:PRINT "PRESS ANY KEY TO CONTINUE!!"
11280 S=INKEY$: IF S="" THEN 11280
11290 RETURN
```

Blank

j. APPENDIX 1.3

Construction Drawings of Cell

j. Appendix 1.3

Construction Drawings of Cell

Two dimensional drawings of the components of the wedge shaped cell. The expanded drawing numerically identifies the components which are listed below.

1. Main assembly which holds the windows
2. Hold down clamp
3. Spring plungers
4. Shim stock holders
5. Horizontal alignment pins
6. Vertical alignment pins
7. Back window adjustment screws
8. Front window adjustment screws
9. Ball plungers for back window
10. Ball plungers for front window
11. Shim stock
12. Input and output manifolds
13. Manifold covers
14. Teflon side seals
15. Reducing coupling
16. Stainless steel pressure plate
17. Unislide translation stage
18. Main base plate
19. Dial indicator
20. Horizontal adjustment screws
21. Windows

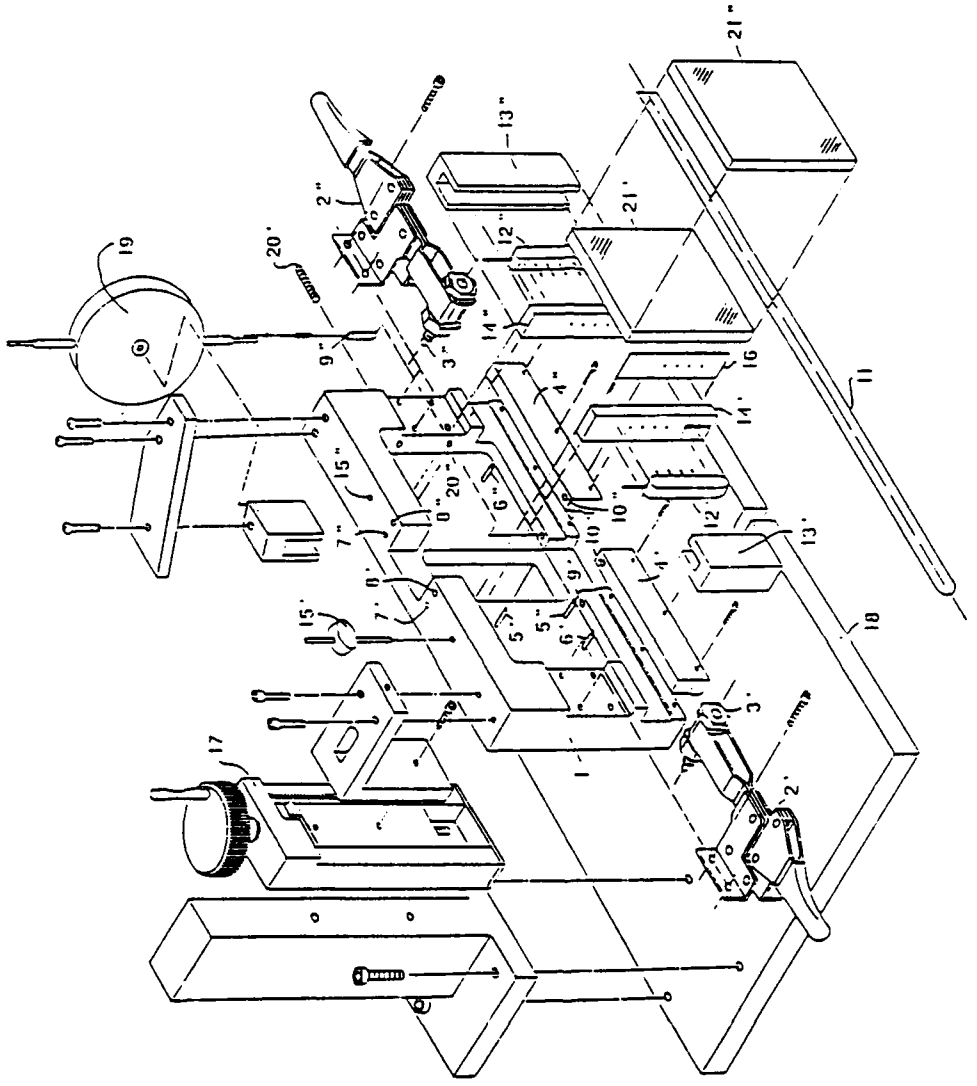

FIG. 1.4 Exploded view of the wedge-shaped cell.

ITEM# - 1

MATERIAL - STAINLESS STEEL

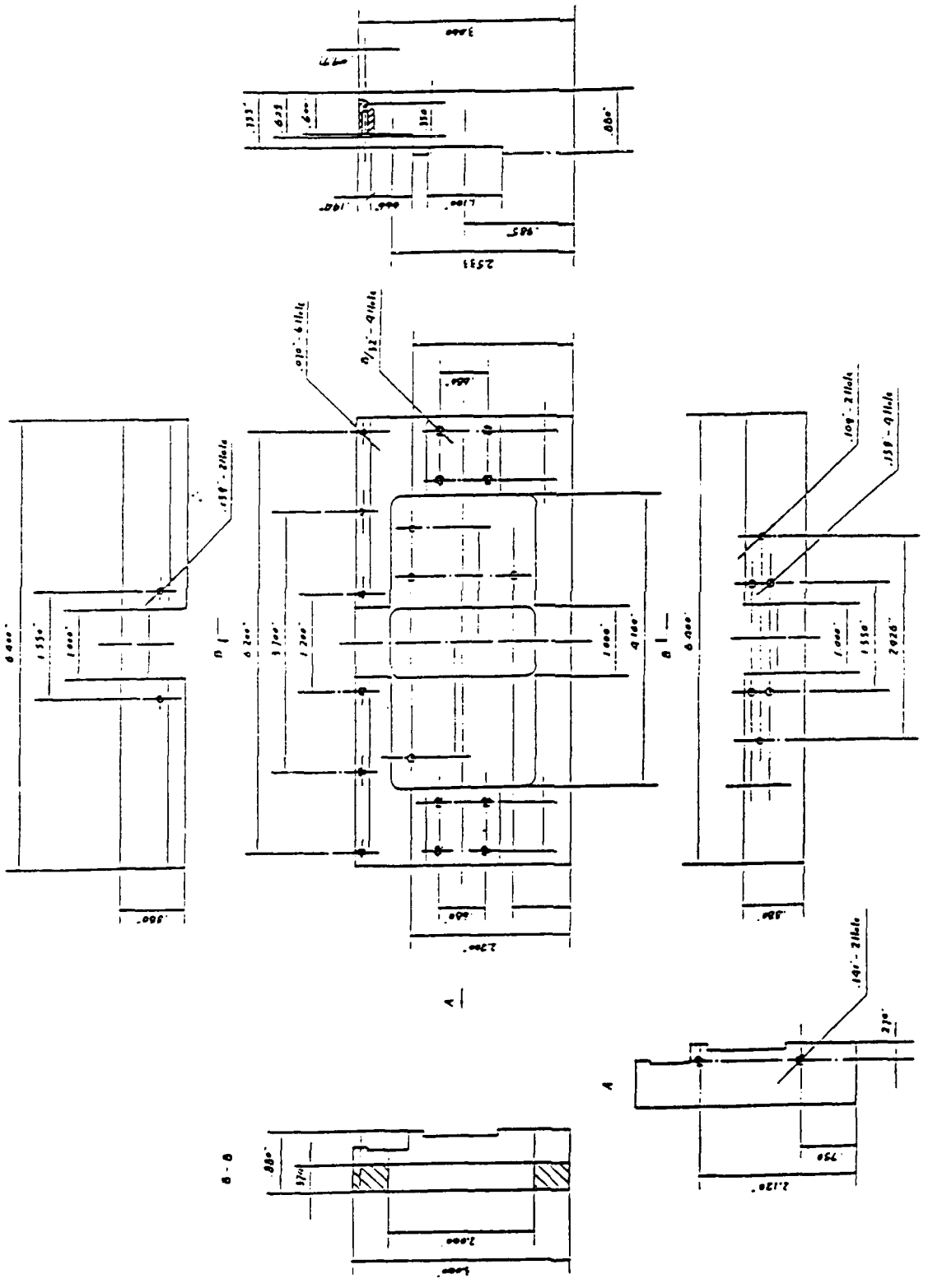

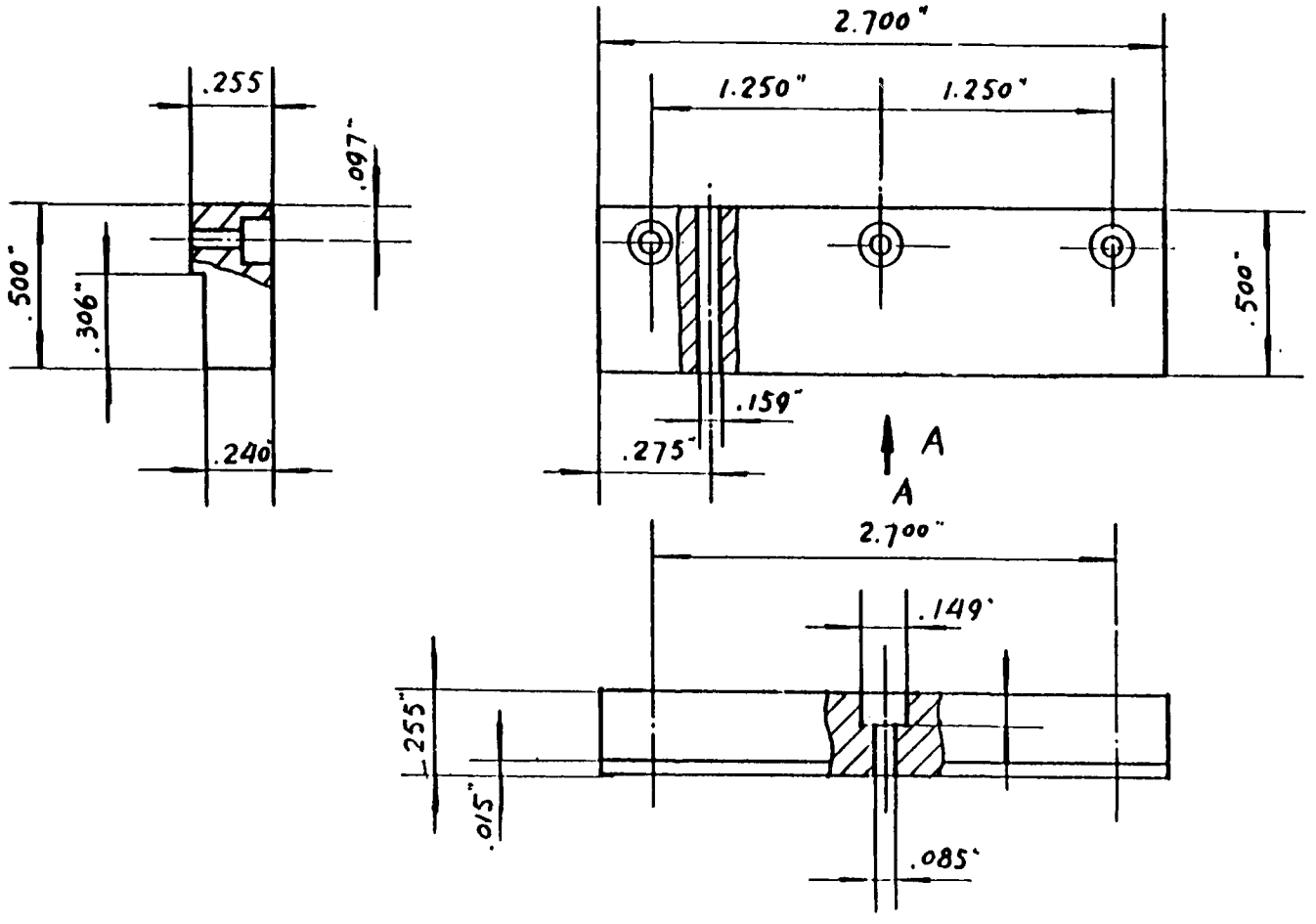

ITEM# - 4' 4"

MATERIAL - STAINLESS STEEL

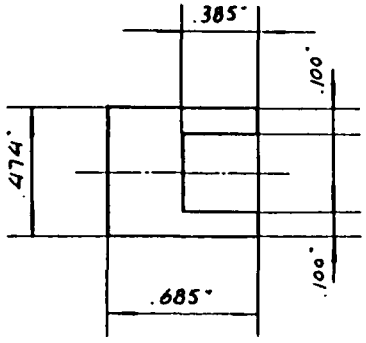

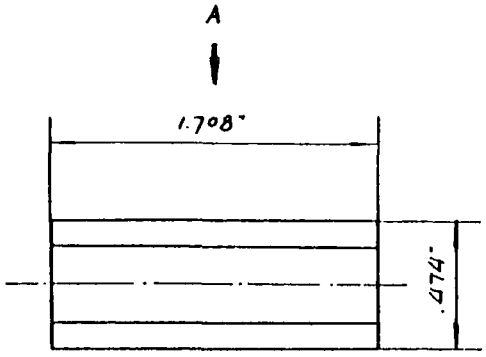

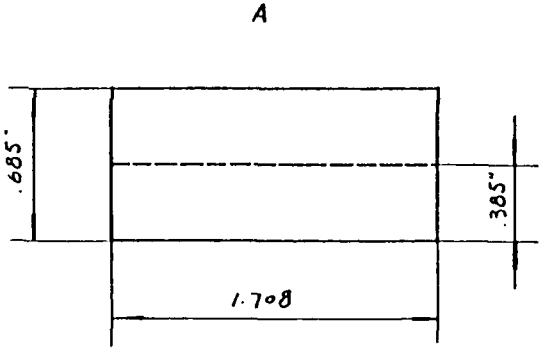

ITEM# - 13'

MATERIAL - STAINLESS STEEL

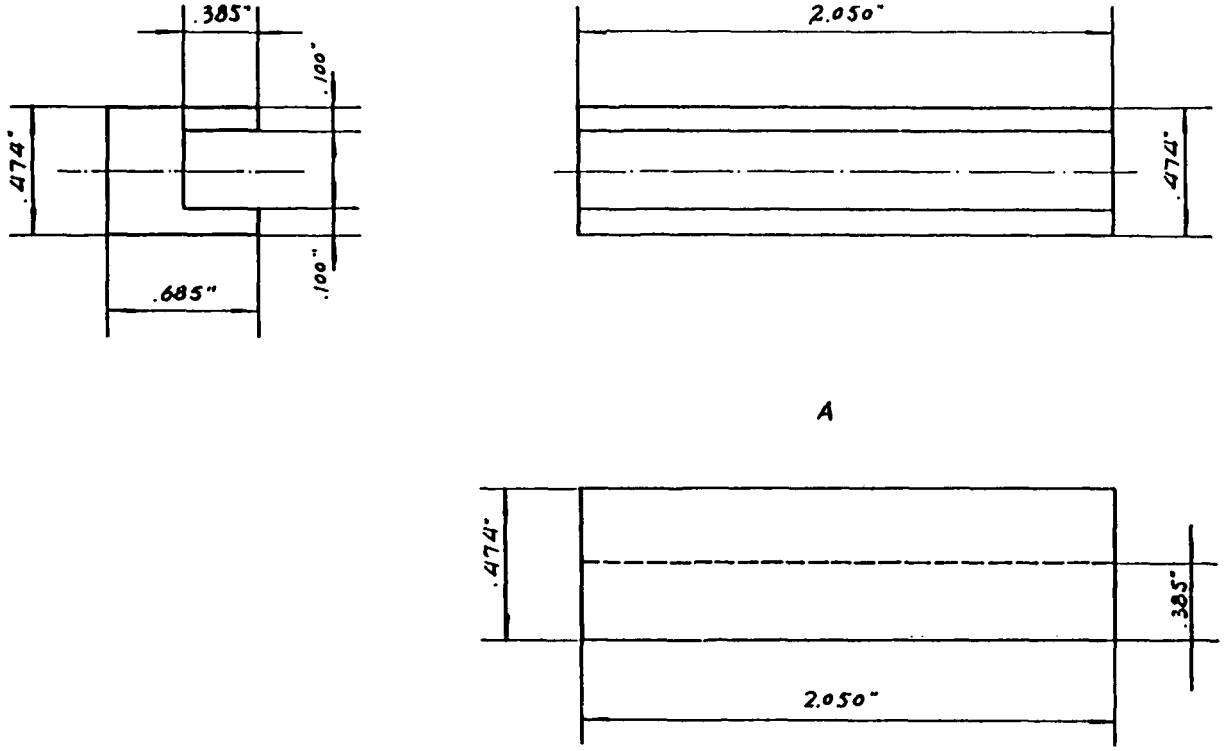

ITEM# - 13"

MATERIAL - STAINLESS STEEL

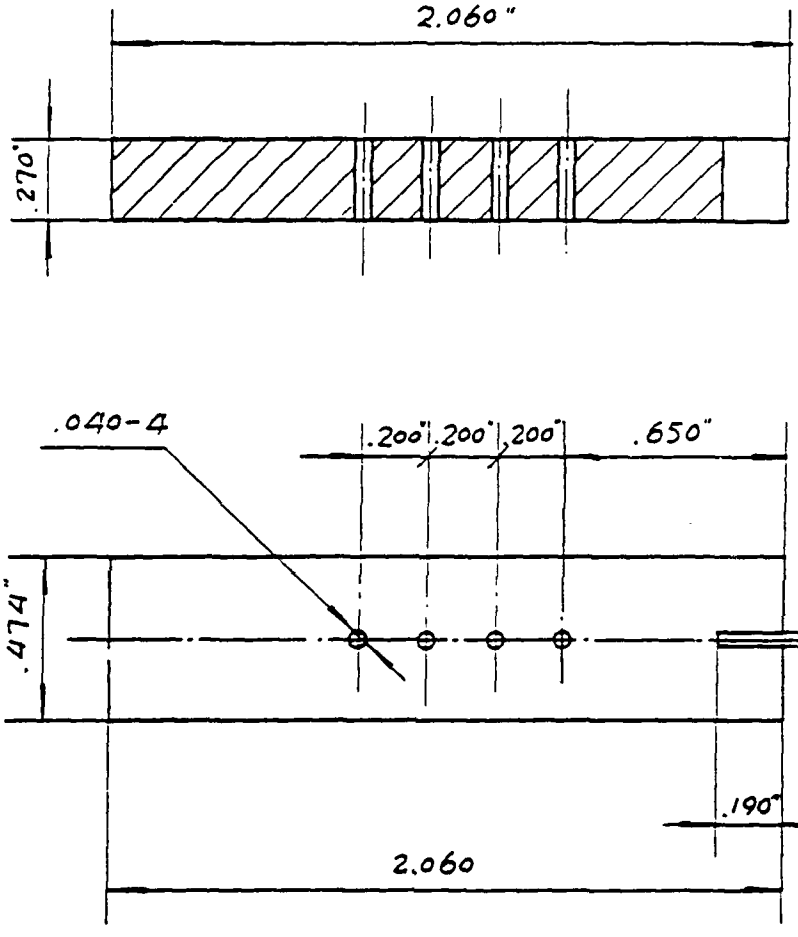

ITEM# - 14' 14"

MATERIAL - TEFLON

ITEM# - 18

MATERIAL - STAINLESS STEEL

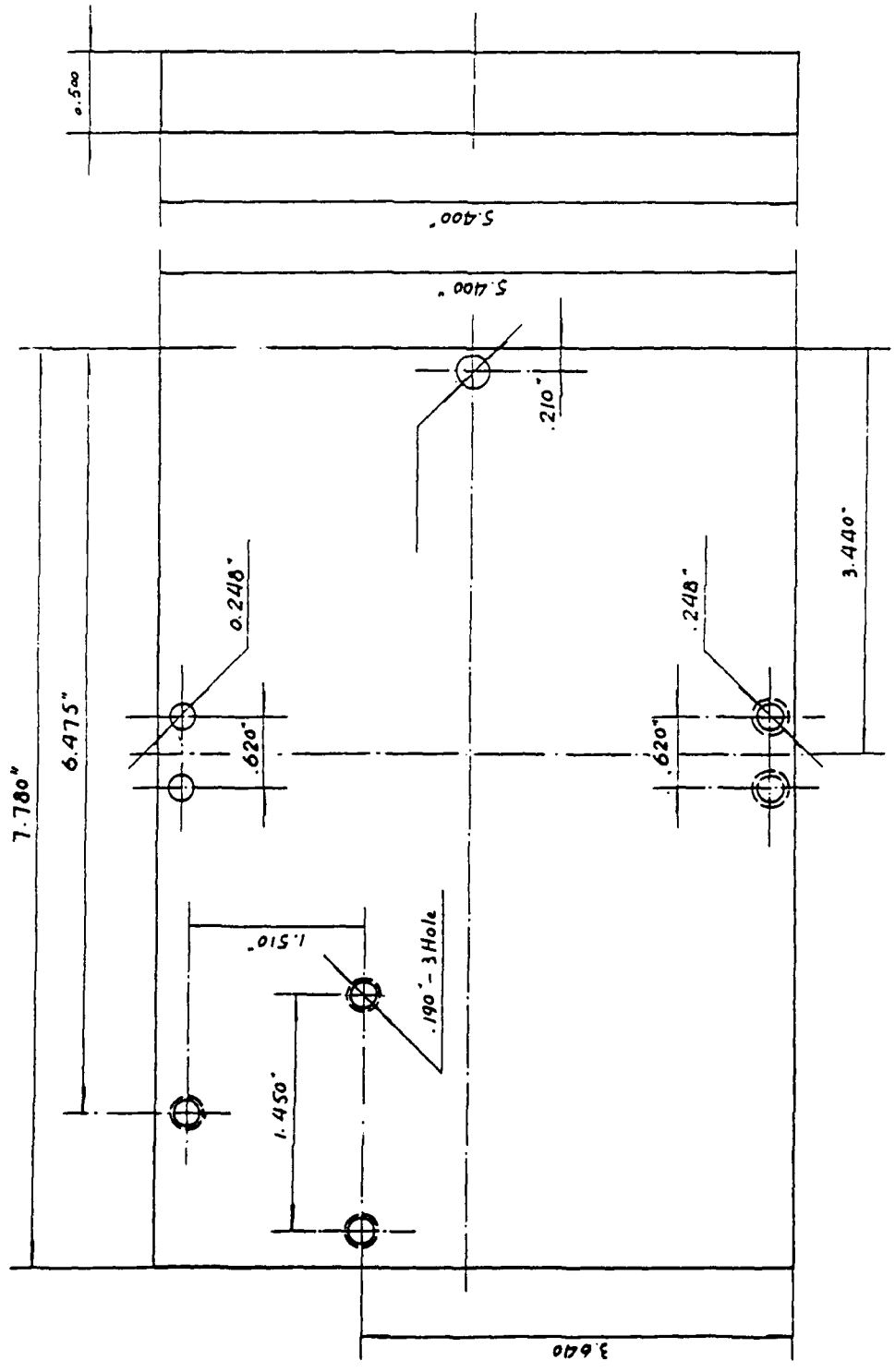

Blank

k. APPENDIX 1.4

Shengshan Weng's Thesis

k. Appendix 1.4

Shengshan Weng's Thesis

Master's thesis of Shengshan Weng using the wedge-shaped cell to determine the optical contsants of liquids. The cell was used in conjunction with a Perkin-Elmer 520B spectrophotometer.

COMPLEX REFRACTIVE INDICES OF SELECTED LIQUIDS

A THESIS IN
PHYSICS

Presented to the Faculty of the University
of Missouri-Kansas City in partial fulfillment of
the requirements of the degree

MASTER OF SCIENCE

by
SHENGSHAN WENG
B.S, Fudan University, 1982

Kansas City, Missouri
1987

This thesis has been renumbered to correspond with numbering in this contract report.

COMPLEX REFRACTIVE INDICES OF SELECTED LIQUIDS

Shengshan Weng, Master of Science

University of Missouri-Kansas City, 1987

ABSTRACT

A wedge-shaped-cell has been developed that avoids serious errors during the measurements on the Lambert absorption coefficient of liquids. After assembling the cell the vertex angle of the air wedge film is determined using the interference fringes produced from a He-Ne laser at near normal incidence. Without disassembling the cell, the sample fluid is injected into the wedge by employing a manifold and syringe. In this way we can accurately determine the sample thickness. The Lambert absorption coefficient and the imaginary parts of the complex refractive index of water, methyl alcohol, ethyl alcohol, SF96, fogoil, diesel fuel, ethyl sulfide, diethyl phthalate, dimethyl methylphosphonate, diisopropylmethylphosphonate, and glycerin in the range from 500 cm^{-1} to 12500 cm^{-1}, were measured. The range of the data is limited by the refractive index of the window material currently being used. This range can be extended into the visible and

infrared by employing fused silica and ZnSe windows, respectively. The real parts of the complex refractive index are calculated by Kramers-Kronig relations.

This abstract of 166 words is approved as to form and content.

David M. Wieliczka

David M. Wieliczka, Ph.D.

The undersigned, appointed by the Dean of Graduate Studies, have examined a thesis entitled "Complex Refractive Indices of Selected Liquids", presented by Shengshan Weng, a candidate for the degree of Master of Science and hereby certify that in their opinion it is worthy of acceptance.

David M. Wieliczka — Sept. 30 1987

David M. Wieliczka, Ph.D.
Department of Physics

Date

Marvin R. Querry — 30 Sept. 1987

Marvin R. Querry, Ph.D.
Department of Physics

Date

John R. Urani — 30 Sept. 1987

John R. Urani, Ph.D.
Department of Physics

Date

TABLE OF CONTENTS

LIST OF ILLUSTRATIONS

LIST OF TABLES

ACKNOWLEDGEMENT

I would like to thank the faculty of the Physics Department at the University of Missouri-Kansas City for their help and inspiration inside and outside the classroom.

I especially thank Drs. David M. Wieliczka and Marvin R. Querry for their guidance and valuable advice during this project. Without their encouragement, constant assistance, and advice, I could not imagine the completion of this thesis. I express my special gratitude to them here.

I also thank my colleagues and the entire staff of the Physics Department especially Cora Ferrer and Lewis Meloan for their friendship and assistance throughout this project.

This work was partially supported by U.S. Army CRDEC Contracts DAAA-15-85-K-0013 and DAAA-15-85-K-0004 (J. Embury and M. Milham).

CHAPTER I

INTRODUCTION

The study of the optical properties of liquids developed after 1870, following Maxwell's extraordinary theory of electromagnetic waves. There are several ways to determine the optical properties of an absorbing medium. One method is to determine the Lambert absorption coefficient $\alpha(\nu)$, from which the imaginary part of the complex refractive index $k(\nu)$ can be calculated as

$$k(\nu) = \frac{\alpha(\nu)}{4\pi\nu}. \qquad (1.1)$$

The complex refractive index $N(\nu)$ as a function of wavenumber is then defined as

$$N(\nu)=n(\nu)+ik(\nu), \qquad (1.2)$$

where the wave number, ν, is defined as the inverse of wavelength, and has units of cm^{-1}; $k(\nu)$ is called the extinction coefficient.

As shown in Eq. (1.2), k can be determined provided the Lambert absorption coefficient is known. One very common

experiment in determining α is using a wedge-shaped cell.[1] Two measurements of fractional spectral transmittance $T(\nu,Z)$ with the same frequency ν of electromagnetic radiation and with the same cell windows but with different thickness Z_1 and Z_2 of the absorbing liquid are needed. The transmittance measurements then provide:

$$\alpha(\nu) = \ln[T(\nu,Z_1)/T(\nu,Z_2)]/(Z_2-Z_1). \qquad (1.3)$$

The real part of the complex refractive index $n(\nu)$ can be calculated by Kramers-Kronig analysis. This procedure is usually difficult in practice, especially in the region of strong absorption because the absorption coefficent is difficult to measure except in thin films.

Reflection ellipsometry is useful in the strong absorption regions. The usual optical procedure is to measure the real parts of the complex reflectance $\vec{r} = \vec{r}(\omega)e^{i\theta(\omega)}$ at normal incidence over as wide a spectral range as possible. The imaginary part of the complex reflectance $\theta(\omega)$ is,

$$\theta(\omega_i) = \frac{2\omega i}{\pi} \int_0^\infty \frac{\ell nr(\omega)}{\omega^2 - \omega_i^2}\, d\,. \qquad (1.4)$$

The constants n, k, r, and θ are related as follows:

$$n = (1-r^2)/(1-2r\cos\theta+r^2) \quad (1.5)$$

$$k = (2r\sin\theta)/(1-2r\cos\theta+r^2). \quad (1.6)$$

As Eq. (1.4) indicates, the phase angle θ at a given frequency ω_i depends upon the reflectance amplitude $r(\omega)$ at all frequencies from zero to infinity. Unfortunately, it is not possible to know the reflectance amplitudes from zero to infinite frequency, and it is rather burdensome to measure reflectance very accurately for any extended range of frequencies. Also, experiments have demonstrated that,[1] for materials with optical constants in the range $k<0.2$ and $1<n<2$, no useful reflection spectra can be obtained.

For the purpose of determining accurate k values of liquids, the wedge-shaped cell technique is the most direct. A brief review of previous literature of this technique follows:

In 1962, Bauman[2] presented a variable-space cell and fixed liquid cell. The variable-space cell was designed using a frame spacer held by two windows. The liquid sample was filled by capillary action.

A 1971 paper by Robertson and Williams,[3] described the use of a unique absorption cell to measure the Lambert absorption coefficient for water in the spectral region

between 4000 and 288 cm^{-1} with two optically flat infrared transmitting windows of CaF_2 or KRS-5. Neoprene strips were used to seal the edges of the cell. The wedge varied uniformly from zero thickness at its vertex to 20 μm thickness at its base.

Tyler, Taylor, and Querry[4] published a paper in 1978, describing a thin-wedge-shaped cell for highly absorbent liquids. Liquids were held in the cell by surface tension. The wedge was formed using feeler stock, the maximum thickness of the wedge could be varied according to the application and surface tension of the sample. The cells described by the above authors served their purposes well.

The purpose of the present research is to:

1. Design a new wedge-shaped cell which can be used for general applications which require the cell to be sealed; to be able to study materials with high vapor pressure; also the cell must have a variable maximum thickness to compensate for the amplitude of the absorption coefficient; the cell must also be filled uniformly with the sample liquid to be studied.

2. Develope a complete experimental technique for the measurement of the Lambert absorption coefficient.

3. Measure the Lambert absorption coefficients of water, methyl alcohol, ethyl alcohol, SF96, fogoil, diesel

fuel, ethyl sulfide (DES), diethyl phthalate (DEP), dimethyl methylphosphonate (DMMP), diisopropylmethylphosphonate (DIMP), and glycerin in the spectral region between 12500 and 500 cm^{-1}. Employ a Varian Cary-2300 Spectrophotometer with fused silica windows in the spectral region between 12500 and 4000 cm^{-1} incremented by 1.0 nm, and a Perkin-Elmer 580B infrared spectrophotometer and ZnSe windows in the region between 4000 and 500 cm^{-1} incremented by 1 cm^{-1}.

4. Apply Kramers-Kronig relations to determine the real part of the complex refractive index of the samples listed above.

CHAPTER II

THEORY

Theory of Interference Fringes

When two coherent light beams are superimposed, the distribution of intensity in the region of superposition is found to vary from point to point between maxima which exceed the sum of the intensities in the beams, and minima which may be zero. This phenomenon is called interference. Born and Wolf[5] indicate that the total intensity I resulting from the superposition of two light beams is:

$$I = I_1 + I_2 + 2\sqrt{I_1 I_2}\cos\delta. \qquad (2.1a)$$

Evidently there will be maxima of intensity

$$I_{max} = I_1 + I_2 + 2\sqrt{I_1 I_2} \qquad (2.1b)$$

when $|\delta| = 0, 2\pi, 4\pi, \ldots$

and minima of intensity

$$I_{min} = I_1 + I_2 - \sqrt{2I_1 I_2} \qquad (2.1c)$$

when $|\delta| = \pi, 3\pi.....,$

where I_1 and I_2 are the intensities of two incident light beams and δ is the phase difference of the two beams.

If two plane-parallel plates are inclined to each other at a slight angle, interference fringes can be formed by light which has been internally and externally reflected from both plates; these fringes are localized at infinity, but are straight, have equal thickness and are parallel to the edge of the wedge. The complete theory of the formation of these fringes is presented in Born and Wolf.[5] The corresponding phase difference at the observer is, as shown in Fig. 1

$$\delta = \frac{4\pi}{\lambda_o} \, n'h \cos \theta', \tag{2.2}$$

where λ_o is the wavelength of the incident light; n' is the refractive index of the medium between the wedge cell; θ' is the angle of incidence at the upper surface; and h is the thickness of the wedge at the incident position. Taking into account the phase change of δ on reflection at one surface of the air film, there are, by (2.2) and (2.1), maxima of intensity at infinity when:

$$2n'h \cos \theta' \pm \frac{\lambda_o}{2} = m\lambda_o , \quad m = 1, 2, 3, \ldots \tag{2.3a}$$

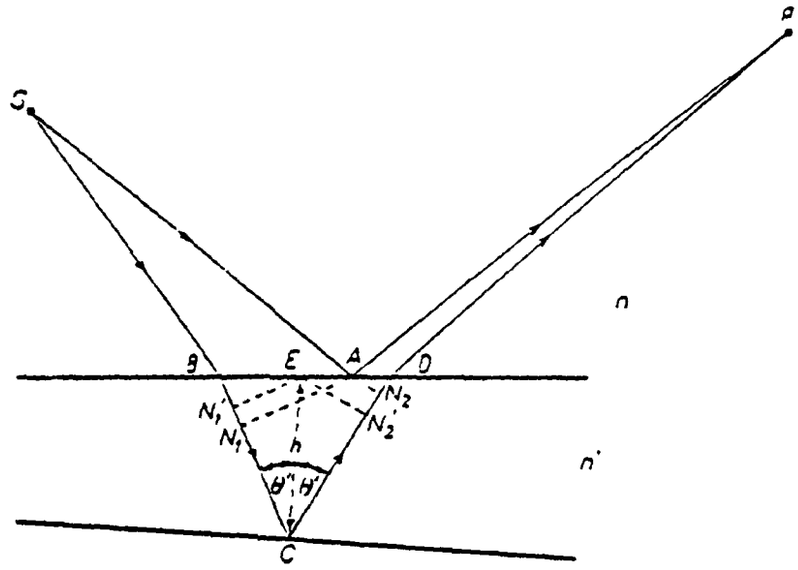

$$\Delta\mathscr{S} = n(SB + DP - SA - AP) + n'(EC + CD),$$

$$nSA \sim nSB + n'BN_1,$$

$$nAP \sim nDP + n'N_2D,$$

$$\Delta\mathscr{S} \sim n'(N_1C + CN_2).$$

$$N_1C + CN_2 \sim N_1'C + CN_2',$$

$$N_1'C = CN_2' = h\cos\theta',$$

The optical path difference

$$\Delta\mathscr{S} = 2n'h\cos\theta',$$

Fig. 1 Phase difference at observer.

and minima of intensity when

$$2\, n'h \cos\theta' \pm \frac{\lambda_o}{2} = m\lambda_o \,, \quad m_o = 1/2,\ 3/2,\ 5/2, \ldots \qquad (2.3b)$$

For near normal incidence, the condition (2.3b) for a dark fringe then becomes, with $\cos\theta' \approx 1$, and the wavelength $\lambda = \lambda_o/n'$ in air,

$$h = \frac{m\lambda}{2} \,, \qquad m = 0,\ 1,\ 2, \ldots \qquad (2.3c)$$

The position of observation depends on the type of windows and the medium between the two windows. For an air film between window plates, the index of the film is lower than that of the windows. The fringe patterns observed arise from interference between beams which, having been reflected at least once in the film, reach the observer by paths of different lengths. When the surfaces of the film have a low coefficient of reflection, the fringes are best seen by observing the light which emerges on the side of incidence. Such fringes are said to be seen by reflected light. The fringes due to interference between beams which emerge on the opposite side of the film are said to be viewed by transmitted light. They are very weak and not easy to observe when the coefficients of reflection are small, but they become very sharp and clear when the film

has a high reflection coefficient.

Laws of Absorption

In 1729, Bougner[6] observed that the fractional part of the energy, or intensity, absorbed in a thin layer of material depended upon the substance and upon the frequency of the incident radiation and was proportional to the thickness. Summation over a series of thin layers, or integration over a finite thickness, leads to an exponential relationship between transmitted intensity and thickness. Later Lambert[7] showed that if homogeneous radiant energy strikes an absorbing medium, the amount absorbed will depend on the frequency of the radiation, the nature of the absorber, and the thickness of the absorber. Let the radiant power, or intensity, of a beam of parallel, homogeneous radiation striking an isotropic, homogeneous sample with smooth, plane surfaces at normal incidence be represented by I. The decrease in intensity in a thickness dx of the sample due to absorption, may be written,

$$-\frac{dI}{dx} = \alpha I, \tag{2.4}$$

where α is a constant characteristic of the sample material and the frequency. For a finite path length, Δx,

$$-\int_{I_o}^{I} \frac{dI}{I} = \ln \frac{I_o}{I} = \alpha \Delta x \tag{2.5}$$

$$I = I_o e^{-\alpha x} \qquad (2.6)$$

The ratio, I/I_o, of transmitted to incident intensities is called the transmittance. The actual dimensions of the quantities I and I_o are unimportant as long as they are proportional to the energy of the beam. In practice they will be observed as a displacement on a chart.

In 1852 Beer[8] observed that for a given sample thickness the transmittance depended exponentially on the concentration of the absorbing species. This relationship may be combined with Equation (2.4) to give

$$-dI/dx = kcI \qquad (2.7)$$

$$\ell n\ I_o/I = kc\Delta x \qquad (2.8)$$

where k is the absorption coefficient per unit concentration and c is the concentration. A more convenient form, for most purposes, is obtained by converting to common logarithms

$$\log I_o/I = \log 1/T = A = abc. \qquad (2.9)$$

In this equation, I_o is the incident intensity; I is the intensity that will pass through a sample of thickness b; c

is the concentration of the sample; and a, the absorptivitiy, is the absorption constant characteristic of the sample and the frequency of the radiation. The absorbance, $A = \log(1/T)$, is more simply related to concentration than is the transmittance.

The Complex Refractive Index

James Clerk Maxwell,[9] in 1864, published an article defining what is generally conceded to be the crowning achievement of classical physics, the relation between electric and magnetic fields, and the realization that electromagnetic waves propagate with the speed of light, indicating strongly that light itself is in the form of an electromagnetic wave. Maxwell expressed the main result of his work in the form of four fundamental equations known as Maxwell's equations. In cgs units, Maxwell's equations are[10]

$$\Delta \cdot \vec{D} = 4\pi\rho \qquad (2.10a)$$

$$\Delta \cdot \vec{B} = 0 \qquad (2.10b)$$

$$\Delta \times \vec{E} + \frac{1}{c} \frac{\partial \vec{B}}{\partial t} = 0 \qquad (2.10c)$$

$$\Delta \times \vec{H} - \frac{1}{c} \frac{\partial \vec{D}}{\partial t} = \frac{4\pi}{c} \vec{J} \qquad (2.10d)$$

where $\vec{E}$ is the electric field $\vec{D}$ is the electric displacement, $\vec{B}$ is the magnetic induction; $\vec{H}$ is the magnetic field, $\vec{J}$ is the current density, ρ is the charge density, and c is the speed of electromagnetic wave propagation.

For a linear, homogeneous, isotropic, conducting and charge free material, the relations for $\vec{D}$, $\vec{H}$ and $\vec{J}$ are

$$\vec{D} = \varepsilon\vec{E} \tag{2.11a}$$

$$\vec{B} = \mu\vec{H} \tag{2.11b}$$

$$\vec{J} = \sigma\vec{E} \tag{2.11c}$$

$$\rho = 0 \tag{2.11d}$$

where ε is the dielectric function, μ is the magnetic permeability, and σ is the conductivity. Together with Equations (2.10) and (2.11) Maxwell's equations can be rewritten as:

$$\Delta \cdot \vec{E} = 0 \tag{2.12a}$$

$$\Delta \cdot \vec{H} = 0 \tag{2.12b}$$

$$\Delta \times \vec{E} = -\frac{\mu}{c}\frac{\partial \vec{H}}{\partial t} \tag{2.12c}$$

$$\nabla \times \vec{H} = \frac{1}{c} \frac{\partial \vec{E}}{\partial t} + \frac{4\pi\sigma}{c} \vec{E}. \qquad (2.12d)$$

The wave equations for $\vec{E}$ and $\vec{H}$ can be derived from Equations (2.12), the results are:

$$\nabla^2 \vec{H} - \frac{4\pi\mu\sigma}{c^2} \frac{\partial \vec{H}}{\sigma t} - \frac{\mu\epsilon}{c^2} \frac{\partial^2 \vec{H}}{\partial t^2} = 0 \qquad (2.13)$$

and

$$\nabla^2 \vec{E} - \frac{4\pi\mu\sigma}{c^2} \frac{\partial \vec{E}}{\partial t} - \frac{\partial\epsilon}{c^2} \frac{\partial^2 \vec{E}}{\partial t^2} = 0. \qquad (2.14)$$

The solutions of Equation (2.14) for a plane, transverse, and monochromatic wave is

$$\vec{E}(\vec{x},t) = \vec{E}_o e^{i(\vec{K}\cdot\vec{x}-\omega t)} \qquad (2.15a)$$

$$\vec{H}(\vec{x},t) = \frac{c}{\mu\omega} \vec{K} \times \vec{E} \qquad (2.15b)$$

where $\omega = 2\pi\nu$ is the angular frequency, and $\vec{K}$ is the wave vector. Substitution of Equation (2.15) into (2.14) gives

$$K^2 = \frac{\mu\epsilon\omega^2}{c^2} + i\left(\frac{4\pi\sigma\mu\omega}{c^2}\right). \qquad (2.16a)$$

Assuming K is complex, then

$$K = \alpha + i\beta \tag{2.16b}$$

$$\alpha = \frac{\omega}{c}\sqrt{\mu\varepsilon}\ \left\{\frac{1+\sqrt{1+(4\pi\sigma/\omega\varepsilon)^2}}{2}\right\}^{1/2}. \tag{2.17}$$

and

$$\beta = \frac{\omega}{c}\sqrt{\mu\varepsilon}\ \left\{\frac{-1+\sqrt{1+(4\omega\sigma/\omega\varepsilon)^2}}{2}\right\}^{1/2}. \tag{2.18}$$

The complex refractive index $N(\omega)$ of the medium is defined as the ratios of the phase velocity in vacuum to the phase velocity in the material medium namely,

$$N(\omega) = \frac{k_m}{k_o} = \frac{\partial+i\beta}{\partial_o} = n(\omega)+ik(\omega). \tag{2.19}$$

Comparing with Equations (2.17), (2.18), and (2.19), one obtains

$$n(\omega) = \sqrt{\mu\varepsilon}\left\{\frac{1+\sqrt{1+(4\pi\sigma/\omega\varepsilon)^2}}{2}\right\}^{1/2} \tag{2.20}$$

and

$$k(\omega) = \sqrt{\mu\varepsilon}\ \left\{\frac{-1+\sqrt{1+(4\omega\sigma/\omega\varepsilon)^2}}{2}\right\}^{1/2}. \tag{2.21}$$

The time averaged energy flow S is:

$$\langle \vec{S} \rangle = \frac{1}{2} \mathrm{Re}\{\frac{c}{4\pi}\} \vec{E} \times \vec{H}^{*} \}. \qquad (2.22)$$

Substituting equations (2.15) and (2.16b) into (2.22), then gives

$$\langle \vec{S} \rangle = \langle \vec{S}_{o} \rangle \; e^{-2\beta \vec{K} \cdot \vec{x}}. \qquad (2.23)$$

As we know, the intensity of radiation is proportional to the energy of the beam. Comparing Equation (2.6) with (2.23), the Lambert absorption coefficient can be defined as

$$\alpha_{L} = 2\beta. \qquad (2.24)$$

The relation between Lambert Absorption coefficient and the imaginary parts of complex refractive index is then

$$\alpha_{L}(\nu) = 4\pi\nu k(\nu) \qquad (2.25)$$

where ν is the wave number of the radiation source.

If a dielectric function is defined as $\varepsilon' = \varepsilon_{o} + i\frac{4\pi\sigma}{\omega}$ then

$$N(\nu) = n(\nu) + ik(\nu) = \sqrt{\mu(\nu)\,\varepsilon'(\nu)} \; . \qquad (2.26)$$

For nonmagnetic material $\mu(\nu) = 1$, and

$$N(\nu) = n(\nu) + ik(\nu) = \sqrt{\varepsilon'(\nu)}. \tag{2.27}$$

Thus the real part of the complex dielectric constant is

$$\varepsilon'_r(\nu) = n^2(\nu) + k^2(\nu). \tag{2.28}$$

The imaginary part of the complex dielectric constant is

$$\varepsilon'_i(\nu) = 2n(\nu)k(\nu). \tag{2.29}$$

The relations between the complex refractive index and the complex reflectance can be defined by the Fresnel Equations. The Fresnel equation with the electric field perpendicular to the plane of incidence is

$$r_s e^{i\phi} = \frac{\cos\theta_i - Z}{\cos\theta_i + Z} \tag{2.30}$$

where ϕ is the phase angle associated with reflection, $R = r_s^2$ is the reflection coefficient of the medium, θ_i is the angle of incidence, and Z is defined as

$$Z = \sqrt{N^2 - \sin^2\theta_i}. \tag{2.31}$$

For normal incidence, R and can be defined as

$$R(\nu) = \frac{[n(\nu)-1]^2+k^2(\nu)}{[n(\nu)+1]^2+k^2(\nu)} \qquad (2.32)$$

and

$$\phi(\nu) = \tan^{-1}[\frac{2k(\nu)}{n^2(\nu)-1+k^2(\nu)}]. \qquad (2.33)$$

As we showed above, the absorption coefficient of a medium is related to the complex refractive index. From the complex refractive index and reflectance measurements the dielectric function of the absorbing medium can be determined.

The Kramers-Kronig Relations

In 1952 Robinson[11] applied the Kramers-Kronig dispersion relationship to the determination of optical constants in the infrared region from normal incidence reflectance measurements. In the application of the Kramers-Kronig relations, we have to derive the relationship between the real part of the complex refractive index and the imaginary part of the complex refractive index.

As we know, the function $N(\omega)$ is dependent on the properties of the material medium, the incident electric field, the electric displacement in the medium, and the reflected electric field in the vacuum. This function

denotes the frequency response of the material medium to the electromagnetic wave.

If $F(\omega)$ represents the frequency response function of the real part of the complex refractive index

$$F(\omega) = N(\omega) - 1 \tag{2.34}$$

we can then define the time response function of the material medium as

$$G(t) = \frac{1}{\sqrt{2\pi}} \int_{-\infty}^{+\infty} F(\omega) e^{-i\omega t} d\omega. \tag{2.35}$$

The frequency response is thus given by

$$F(\omega) = \frac{1}{\sqrt{2\pi}} \int_{-\infty}^{+\infty} G(t) e^{i\omega t} dt. \tag{2.36}$$

Now, require $G(t)$ to be real and we obtain

$$G(t) - G^*(t) = \frac{1}{\sqrt{2\pi}} \int_{-\infty}^{+\infty} [F(\omega) - F^*(\omega)] e^{-i\omega t} d\omega = 0, \tag{2.37}$$

Then we have

$$F(\omega) = F^*(-\omega) \tag{2.38}$$

$$F_r(\omega) + iF_i(\omega) = F_r(-\omega) - iF_i(-\omega). \tag{2.39}$$

Real [$F(\omega)$] is an even (symmetric) function about $\omega=0$. Im[$F(\omega)$] is an odd (anti-symmetric) function about $\omega=0$. Thus, we can denote $F(\omega)$ as

$$F(\omega) = S(\omega) + iA(\omega) \tag{2.40}$$

where $S(\omega)$ and $A(\omega)$ are respectively the symmetric (real) and antisymmetric (imaginary) parts of $F(\omega)$. In this case,

$$S(\omega)=N_r(\omega)-1=n(\omega)-1 \tag{2.41}$$

$$A(\omega)=N_i(\omega)=k(\omega). \tag{2.42}$$

Substitution of Equation (2.40) into (2.35) yields

$$G(t) = \frac{1}{\sqrt{2\pi}} \int_{-\infty}^{+\infty} \{S(\omega)\cos(\omega t)+A(\omega)\sin(\omega t)\} d\ . \tag{2.43}$$

Equation (2.43) can be written as,

$$G(t) = G_S(t) + G_A(t), \tag{2.44}$$

where $G_S(t)$, $G_A(t)$ are symmetric and antisymmetric about $t=0$. Then, we obtain

$$G_S(t) = \frac{1}{\sqrt{2\pi}} \int_{-\infty}^{+\infty} S(\omega)e^{-i\omega t}d\omega \tag{2.45a}$$

$$G_A(t) = \frac{i}{\sqrt{2\pi}} \int_{-\infty}^{+\infty} A(\omega) e^{-i\omega t} d\omega. \qquad (2.45b)$$

The inverse Fourier transforms are,

$$S(\omega) = \frac{1}{\sqrt{2\pi}} \int_{-\infty}^{+\infty} G_S(t) e^{i\omega t} dt, \qquad (2.46a)$$

$$A(\omega) = \frac{-i}{\sqrt{2\pi}} \int_{-\infty}^{+\infty} G_A(t) e^{i\omega t} dt. \qquad (2.46b)$$

Next we apply the principle of causality to $G(t)=G_A(t)+G_S(t)$. The results are that

$$G_S(t) = -G_A(t) \quad \text{when } t<0 \text{ and} \qquad (2.47a)$$

$$G_S(t) = G_A(t) \quad \text{when } t>0, \qquad (2.47b)$$

These equations imply that the material does not respond until the EM-wave arrives at t=0.

Now we can relate the real and imaginary parts of the complex refractive index. As Equation (12.45a) shows

$$S(\omega_o) = \frac{1}{\sqrt{2\pi}} \int_{-\infty}^{+\infty} G_S(t) e^{i\omega_o t} dt. \qquad (2.48)$$

Applying condition (2.47), we have that

$$S(\omega_o) = \frac{1}{\sqrt{2\pi}} \{ -\int_{-\infty}^{o} G_A(t) e^{i\omega_o t} dt + \int_{o}^{\infty} G_A(t) e^{i\omega_o t} dt \}. \qquad (2.49)$$

Then, substituting (2.44b) into (2.48) and applying the inverse Peterson-Knight transform, we obtain

$$S(\omega_o) = \frac{i}{\sqrt{2\pi}} \int_{-\infty}^{+\infty} A(\omega) \{ \int_{-\infty}^{o} e^{i(\omega_o - \omega)t} dt + \int_{o}^{\infty} e^{i(\omega_o - \omega)t} dt \} d\omega. \quad (2.50)$$

Then the results are

$$S(\omega_o) = \frac{2}{\pi} \int_{o}^{\infty} \frac{\omega A(\omega)}{\omega^2 - \omega_o^2} d\omega \quad (2.51a)$$

and also

$$A(\omega_o) \frac{2\omega_o}{\pi} \int_{o}^{\infty} \frac{S(\omega)}{\omega_o^2 - \omega^2} d\omega. \quad (2.51b)$$

Comparing Equation (2.51a) with (2.41) we have

$$n(\omega_o) = 1 + \frac{2}{\pi} \int_{o}^{\infty} \frac{\omega\, k(\omega)}{\omega_o^2 - \omega_o^2} d\omega \quad (2.52a)$$

$$k(\omega_o) = \frac{2\omega_o}{\pi} \int_{o}^{\infty} \frac{[n(\omega)-1]}{\omega_o^2 - \omega^2} d\omega, \quad (2.52b)$$

As we understand that the Fourier transform technique is equivalent to conventional Kramers-Kronig analysis, the advantage is in the ability to use the digital Fast Fourier Transform yielding equivalent results with much less computer time.

CHAPTER III

DESCRIPTION OF THE WEDGE-SHAPED CELL

An exploded view of the wedge-shaped absorption cell, cell holder, and transtage unit is shown in Fig. 2.

A rectangular aluminum base 18;

A rectangular aluminum standard 1 measuring 16.25 cm x 7.8 cm x 2.23 cm with a rectangular hole measuring 5.23 cm x 2.54 cm x 2.23 cm centered through, and mounted on base 18 as shown in Fig. 2;

Toggle clamps[12] 2' and 2" mounted on 1;

Spring plungers[13] 3' and 3" mounted in the heads of 2' and 2", respectively;

Two rectangular aluminum pieces 4' and 4", with two threaded holes in each for receiving threaded ball plungers[13] 8' and 8", and threaded ball plungers 9' and 9" are mounted on 1, respectively, with a slot 0.77 cm deep and 0.038 cm wide each block, and with 4' and 4" mounted on 1, as shown in Fig. 2;

Two stainless steel posts 5' and 5" mounted 2.05 cm and 2.3 cm from edges of standard 1, as shown in Fig. 2;

Four set screws 7' and 7", 8' and 8" are threaded through base 1, as shown in Fig. 2;

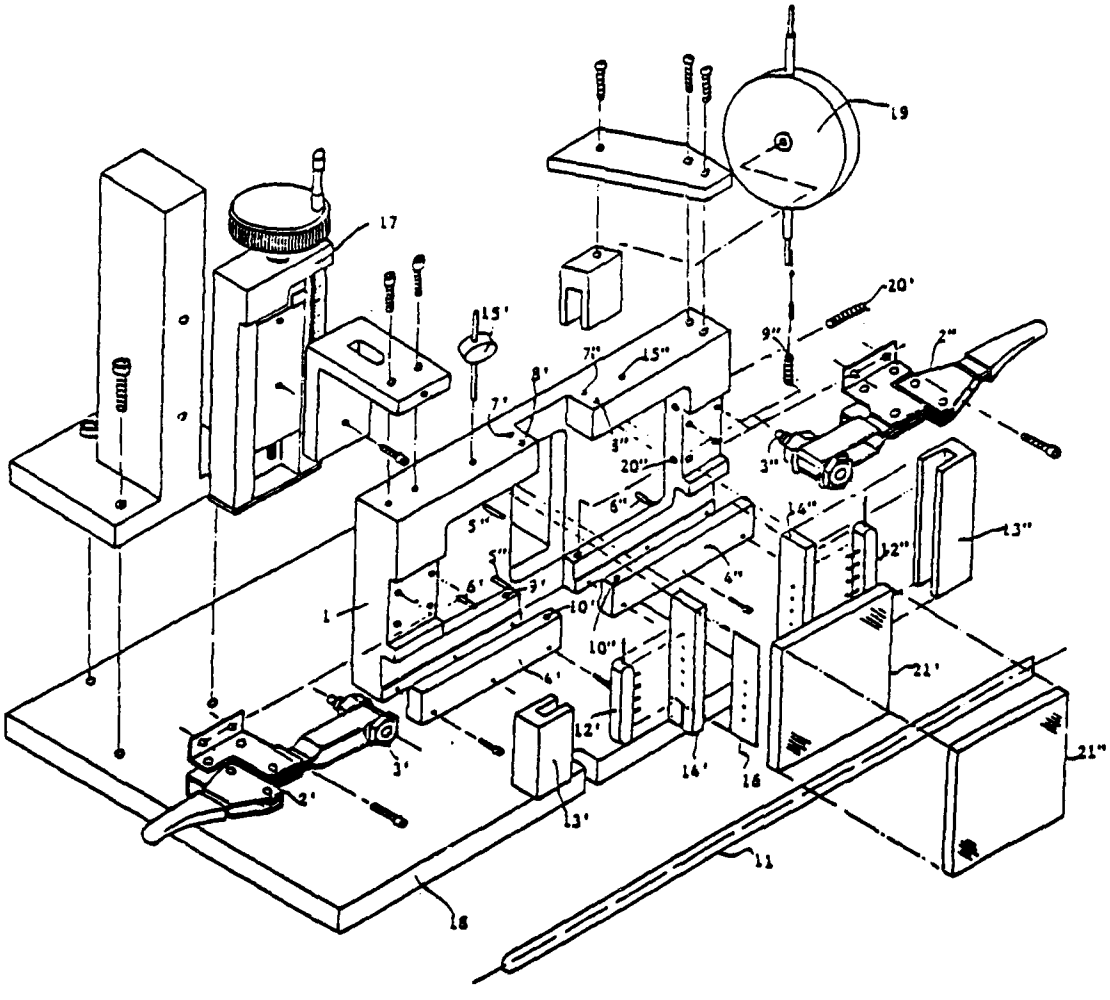

Fig. 2. An exploded drawing of components comprising a wedge-shaped cell unit for measuring the Lambert absorption coefficient of low and high absorbent liquids.

A segment of machine stainless steel feeler stock[14] 11 measuring about 30 cm x 1.2 cm and of a thickness depending on the absorption measurement;

Two manifolds[15] 12' and 12", with two aluminum U holders 13' and 13" through two teflon spacers 14' and 14", measuring 5.23 cm x 1.9 cm x 0.7 cm set on both sides of optically flat windows 21' and 21";

Two reducers[15] 15' and 15" connected between manifolds and syringes;

A rectangular stainless steel spacer 16 setting between 12" and 14" and against 5' and 5", as shown in Fig. 2.

A unislide translation stage[16] 17 with 3.81 cm movement mounted on an aluminum base 18; as shown in Fig. 2;

A dial-indicator[17] 19 mounted on 1, for measuring displacement between 1 and 18, as shown in Fig. 2; and

Two set screws 20' and 20" threaded through 1, as shown in Fig. 2.

The cell is assembled as follows. Place manifolds, teflon spacers, U holders, rectangular pieces, and reducers together in standard 1 as shown in Fig. 2. The manifolds and reducers are connected by shrinkable tubing. The bottom window 21' rests flat against the top surface of standard 1, the feeler stock 11 with a thin layer of silicon

vacuum grease on both surfaces, set between 21' and 21". Four set screws 7' and 7", 8' and 8" are set at the same plane surface perpendicular to base 1 then adjust the ball ends of ball plungers 8' and 8", 9' and 9" to contact the opposites of window 21", thus providing a resilient means for holding windows in place. Toggle clamps 2' and 2" are then closed so spring plungers 3' and 3" gently but resiliently contact points on the top surface of window 10". Finally, tighten the set screws 20' and 20", push the whole cell unit against the posts 5' and 5", and the wedge cell should be sealed and completely assembled.

CHAPTER IV

EXPERIMENTAL METHODS

The experimental procedure follows:

1. Assemble the wedge-shaped cell,
2. Determine the angle of wedge,
3. Measure the absorption spectrum in the visible and infrared spectral regions, and
4. Analyze the results.

Assemble the wedge-shaped cell

One main purpose of the project is to find a way to seal the wedge-cell and yet be able to vary the angle of the wedge. During the initial assembly silicon vacuum grease is applied along the thin end of the wedge and both sides of the feeler stock. Two teflon pieces on the left and right sides of the wedge are pushed against the windows. The silicon vacuum grease and teflon provide an adequate seal.

Also a very important consideration during the initial assembly is to choose the right size of feeler stock to be used since the thickness of the feeler stock is directly related to the accuracy of the measurement. It is understandable that the best data for transmittance measurements

requires the fractional spectral transmittance to be between 20 and 80 percent. As Equation (2.6) shows, this requires the value of product $\alpha(\upsilon)$ and x to be between 0.22 and 1.6. Since samples have very strong absorption bands in the infrared region, it demands that the wedge be very thin. In the case of a strong absorption band region, instead of the stainless steel feeler stock we used silicon vacuum grease as a spacer that reduced the maximum thickness of the wedge to approximately 1 μm. This technique has been used to successfully measure a Lambert absorption coefficient as high as 13000 cm^{-1}.

The determination of the wedge angle

Consider any sample holder consisting of two plane parallel plates with an inert spacer on one end to produce a very small triangular wedge of air. As we showed in Chapter II Eq. (2.3), when a radiation source is incident on the wedge, a set of fringes which are equidistant and parallel to the apex of the wedge angle can be found on the side of incidence.

To determine the angle of the wedge-cell, we measured the number of interference fringes Δm passing a detector as the cell was translated through the distance Δx, and then used Eq. (2.3) to calculate the angle β. The empty cell is placed in a holder that could be moved laterally along the ways parallel to the vertical axis. A plane mirror and two

spherical mirrors were employed to increase the relative separation of the inteference fringes, and the light is then incident on a photomultiplier detector which was fixed in position. A He-Ne laser was used as the incidence light source with a focusing lens to produce a focused light beam on the front surface of the air film at any arbitrary position A. Interference fringes were observed at A in reflection. When the wedge was slowly moved to some arbitrary position B a distance Δx from A, then m complete fringe maxima were observed by the photomultiplier, and recorded by an electronic counter. The differential thickness

d is given by

$$2\Delta dn\cos\theta' = \lambda m \qquad (4.1)$$

For an air film, n=1, and near normal incidence implies $\theta' \approx 0$ and $\cos' \approx 1$. So Eq. (3.1a) reduces to $2\Delta d = \lambda m$.

Thus, the angle β of the wedge is defined as

$$\tan\beta = \frac{\Delta d}{\Delta x}, \qquad (4.2)$$

and

$$\tan\beta = \frac{m\lambda}{2\Delta x}. \qquad (4.3)$$

The value used for the wedge angle was the average of the sum of five measurements.

The Measurement of Absorption Spectrum

After the cell was assembled and the wedge angle determined the sample liquid was injected into the wedge through one of the manifolds This procedure must be performed slowly and carefully, otherwise it will cause air bubbles within the cell or it will burst the seal causing leakage.

A Varian Cary-2300 Spectrophotometer and fused silica windows were employed in the spectral region between 12500 cm^{-1} and 3745 cm^{-1} by 1 nm increment, and a Perkin-Elmer 580B infrared Spectrophotometer and ZnSe windows in the region between 4000 cm^{-1} and 500 cm^{-1} with 1 cm^{-1} increment. Both instruments are double beam spectrophotometers capable of absorbance measurements. A longer time response was required during the absorbance measurement to reduce significant error in the strong absorption regions. The absorbance spectra were taken at four different positions of the cell with the displacement determined by the size of the beam and the magnitude of the absorbance. The size of the feeler stock was changed when necessary.

The imaginary parts of the complex refractive index was calculated by the average of the six combination subtractions from four measurements. If we define A_1 and

A_2, the absorbances at position x_1 and x_2 at wavenumber ν, then $k(\nu)$ can be defined as:

$$k(\nu) = - \frac{A_2 - A_1}{4\pi\nu \tan\beta (\log_{10} e)(x_2 - x_1)}. \qquad (4.4)$$

where β is the vertex angle of the wedge.

The Application of Kramers-Kronig Relations

After determining the imaginary parts of the complex refractive index, we applied Kramers-Kronig relations to calculate the real parts of the complex refractive index. As we discussed in Chapter 1, there will be a significant error when using the Kramers-Kronig relations for the limited range of calculation, because Eq. (2.52) indicates the results will depend on the amplitude of $k(\nu)$ at all spectral regions from zero to infinity. We use two methods to avoid this limitation.

First, we set k to be zero in the extended region above 12500 cm^{-1} to as high as possible, since the values of k are very small in that region.

Second, in the region 0 to 500 cm^{-1} the k values will be set in different ways depending on the amplitude of k at 500 cm^{-1}.. If k is small, then it will be set to zero from 500 cm^{-1} to 0 cm^{-1}. If k is larger in value, we set k as a linear variation from 500 cm^{-1} to 0, and the slope is defined by the value of k at 500 cm^{-1} divided by 500.

After we extended the wave-number region as described above, it provided more accurate results through Fast Fourier Transform calculations which are equivalent to the conventional Kramers-Kronig analyses.

Results

The results for water are illustrated in Fig. 2 and Fig. 4 and are in very good agreement with previous publications,[3,19,20] except that we found that there is a step existing at 3900 cm^{-1} wave-number region which had never been found in previous research. Fig. 2 shows that there are five absorption bands in the spectral region between 500 and 12500 cm^{-1}. In the infrared region, we observed the maximum value of $\alpha(\nu)$ at the center of the 3406 cm^{-1} absorption band to be 12263 per centimeter, with an uncertainty of ± 189 per centimeter. This band is due to the symmetrical stretching vibration. The natural dipole moment of the water molecule (directed along the axis bisecting the H-O-H angle) is modified in magnitude by this stretching. Also the water bending motion changes the magnitude of the dipole moment and this is observed at the maximum value of $\alpha(\nu)$=2710 cm^{-1} at the center of the 1642 cm^{-1} absorption band in the infrared spectrum.

The real and imaginary parts of the complex refractive index of ethyl alcohol, methyl alcohol, SF96, diesel fuel, fogoil, ethyl sulfide (DES), diethyl phthalate (DEP),

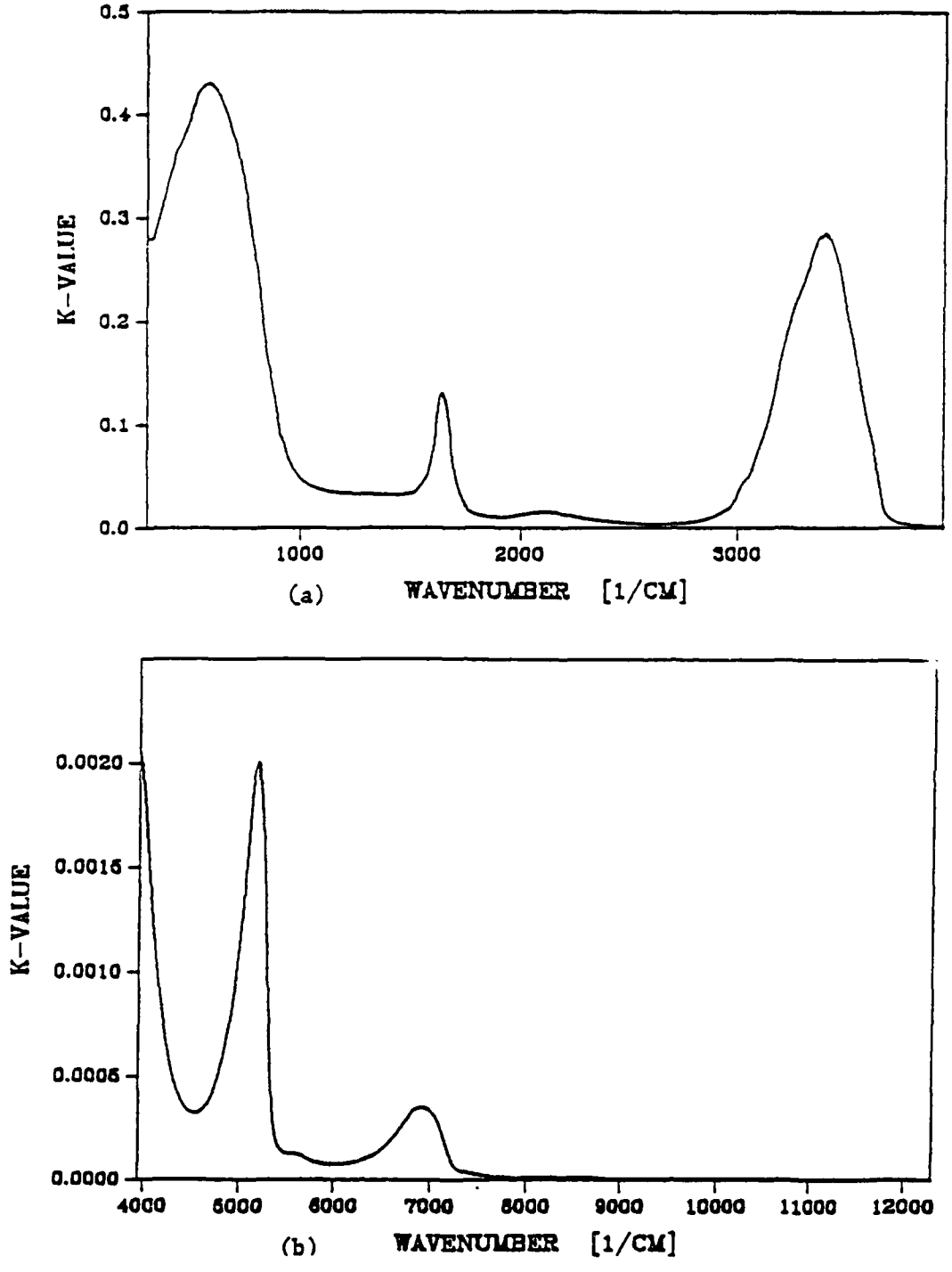

Fig. 3. Extinction coefficient k of water: (a) in the 500-3950 cm^{-1} wave-number region; (b) in the 3950-12500 cm^{-1} wave-number region.

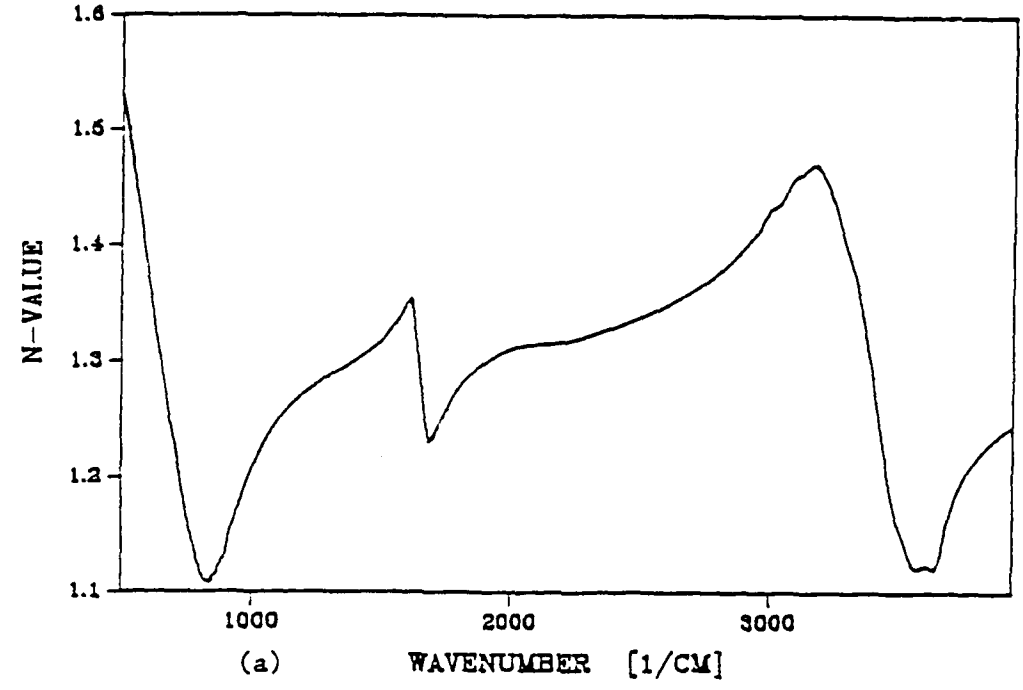

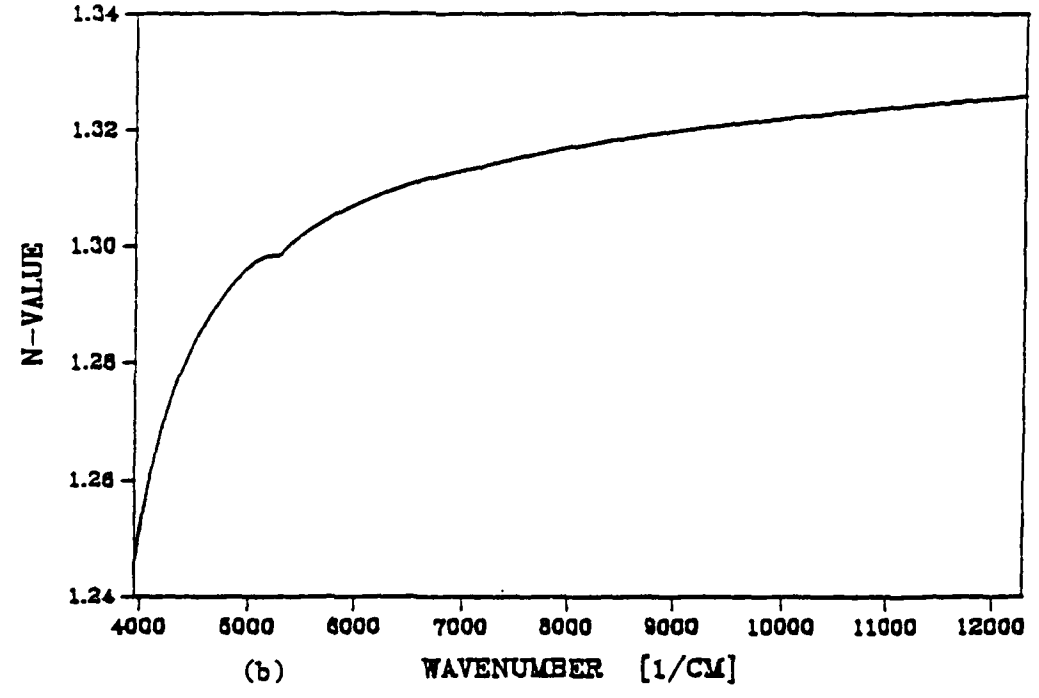

Fig. 4. Index of refraction n of water: (a) in the 500-3950 cm^{-1} wave-number region; (b) in the 3950-12500 cm^{-1} wave-number region.

dimethyl methylphosphonate (DMMP), diisopropylmethyl-phosphonate (DIMP), and glycerin are illustrated by Fig. 5 through Fig. 24. We used 6.5^{o} as an incident angle and apply Eq. (2.30) and Eq. (2.31) to calculate the reflection coefficient of SF96, DEP, DMMP, and DIMP. Comparing the calculated results of the reflection coefficients of these liquids with the results[21] from reflectivity measurements, show good agreement.

In the near infrared region, the absorption is due almost entirely to overtone and combination bands arising from changes in vibrational states, and they are much weaker than the fundamental bands which occur at lower frequencies.

It is important to know what uncertainties in $k(\nu)$ can be expected from uncertainties in the measured absorbance $A(\nu)$, the measured angle of wedge β, and the displacement of wedge Δx. Differentiation of Eq. (4.4) gives

$$\delta k = \frac{\Delta A}{A} + \frac{\Delta x}{x} + \frac{\Delta \tan\beta}{\tan\beta}. \qquad (4.5)$$

From the measured wedge angle, the maximum value of the uncertainty of $\Delta \tan\beta/\tan\beta$ is about 3 percent. The uncertainty of the dial-indicator is less than one percent. The uncertainty of absorbance A can be defined as followsing Fig. 24

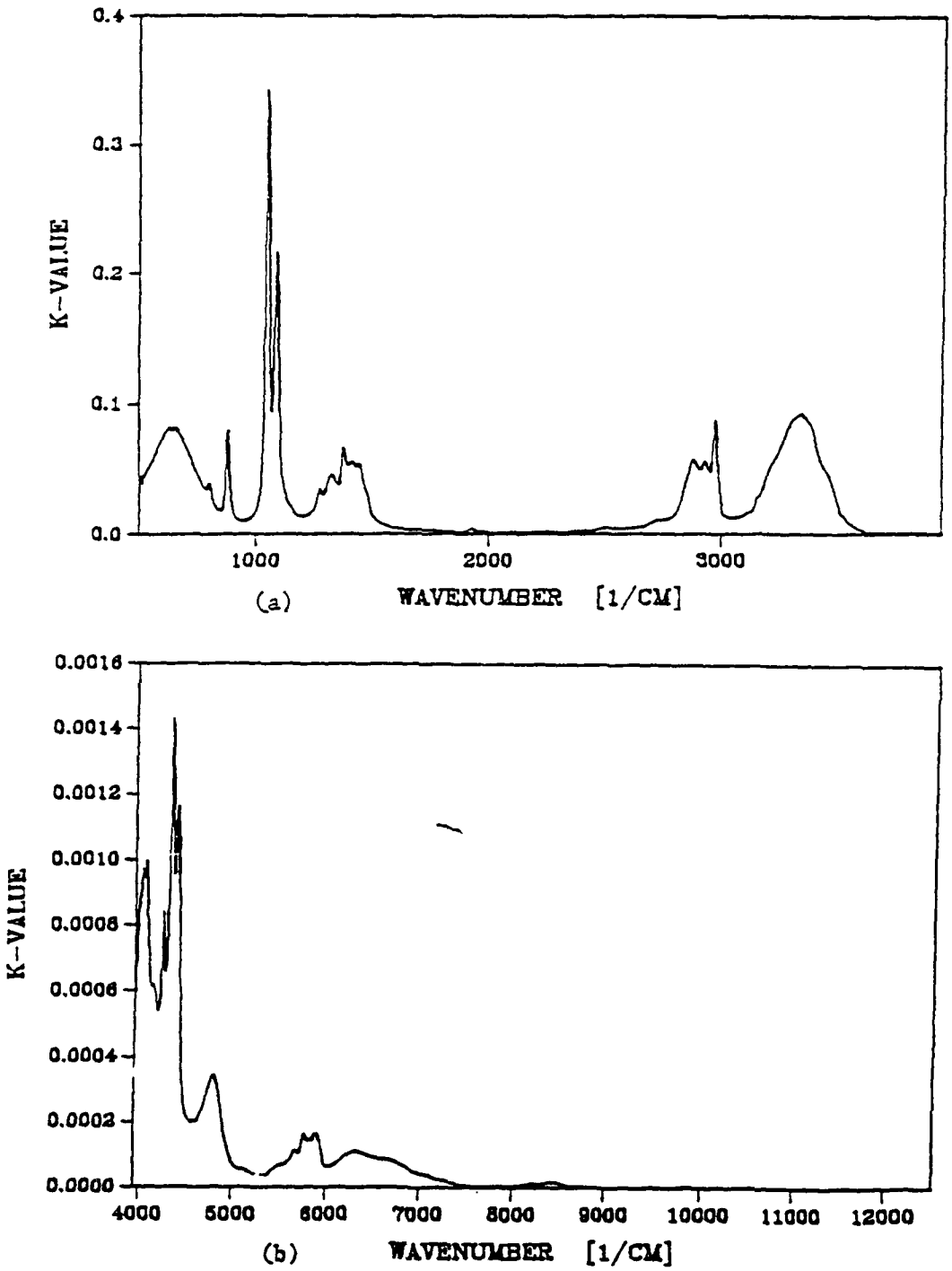

Fig. 5. Extinction coefficient k of ethyl alcohol: (a) in the 500-3950 cm^{-1} wave-number region; (b) in the 3950-12500 cm^{-1} wave number region.

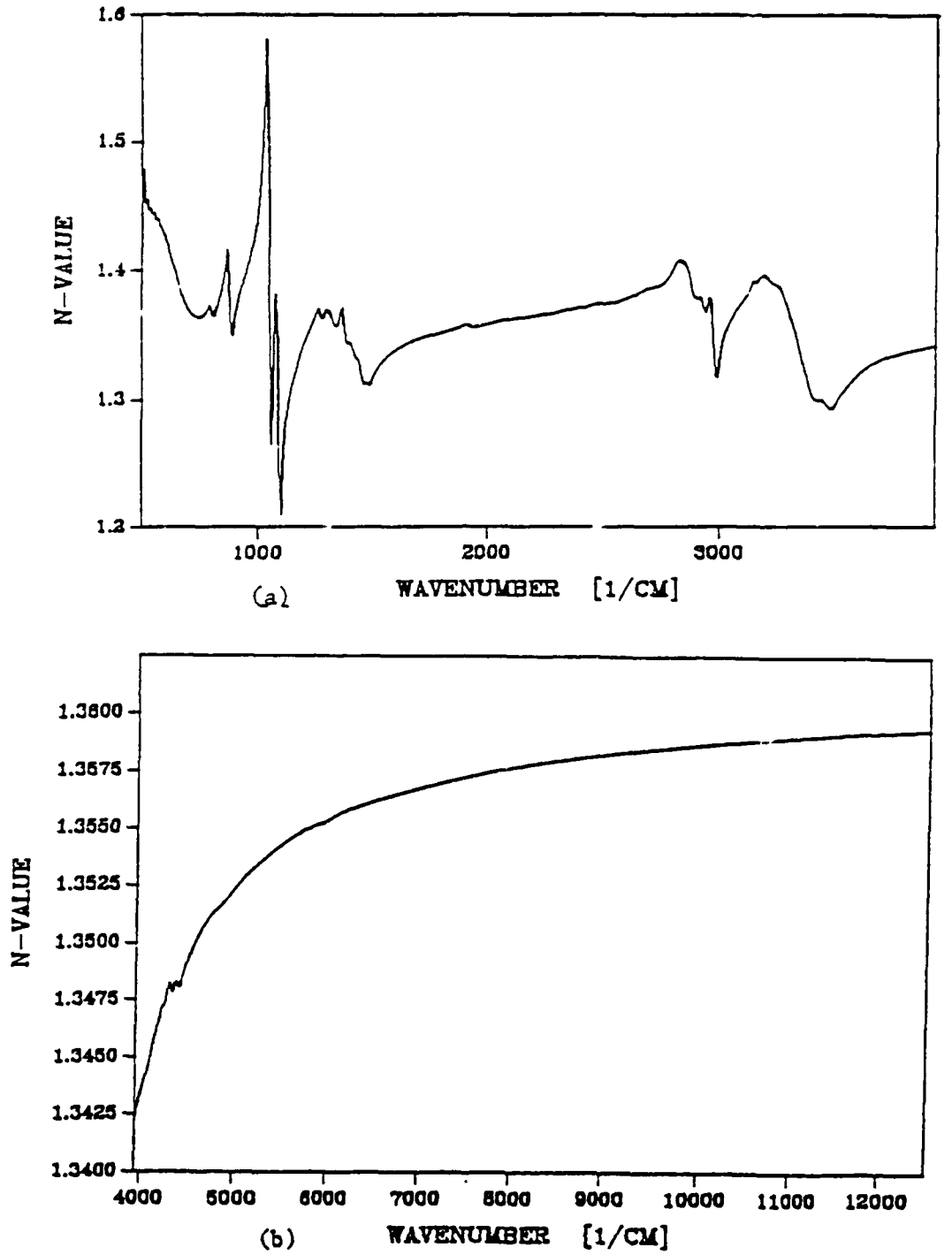

Fig. 6. Index of refraction n of ethyl alcohol: (a) in the 500-3950 cm^{-1} wave-number region; (b) in the 3950-12500 cm^{-1} wave-number region.

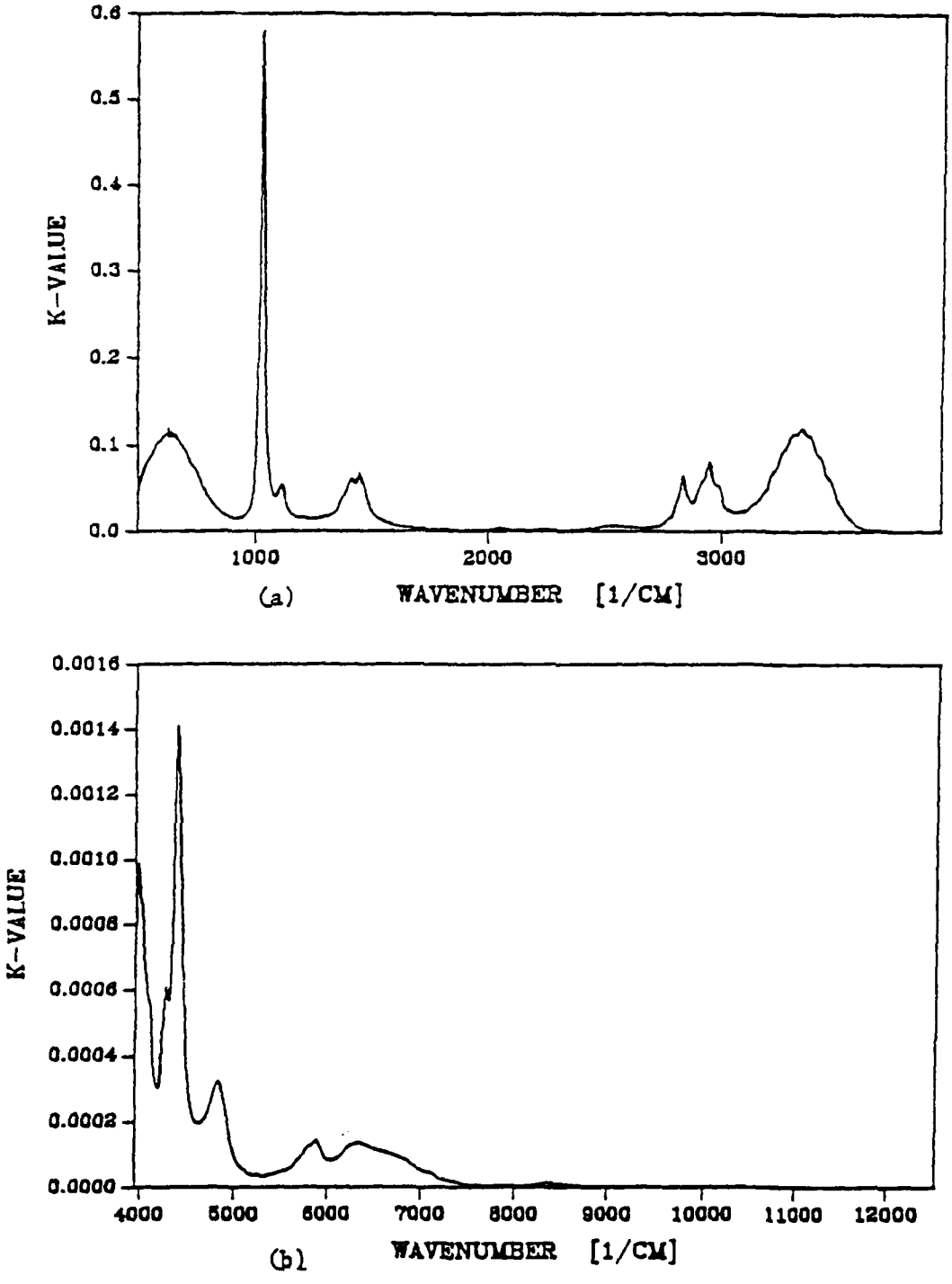

Fig. 7. Extinction coefficient k of methyl alcohol: (a) in the 500-3950 cm^{-1} wave-number region; (b) in the 3950-12500 cm^{-1} wave-number region.

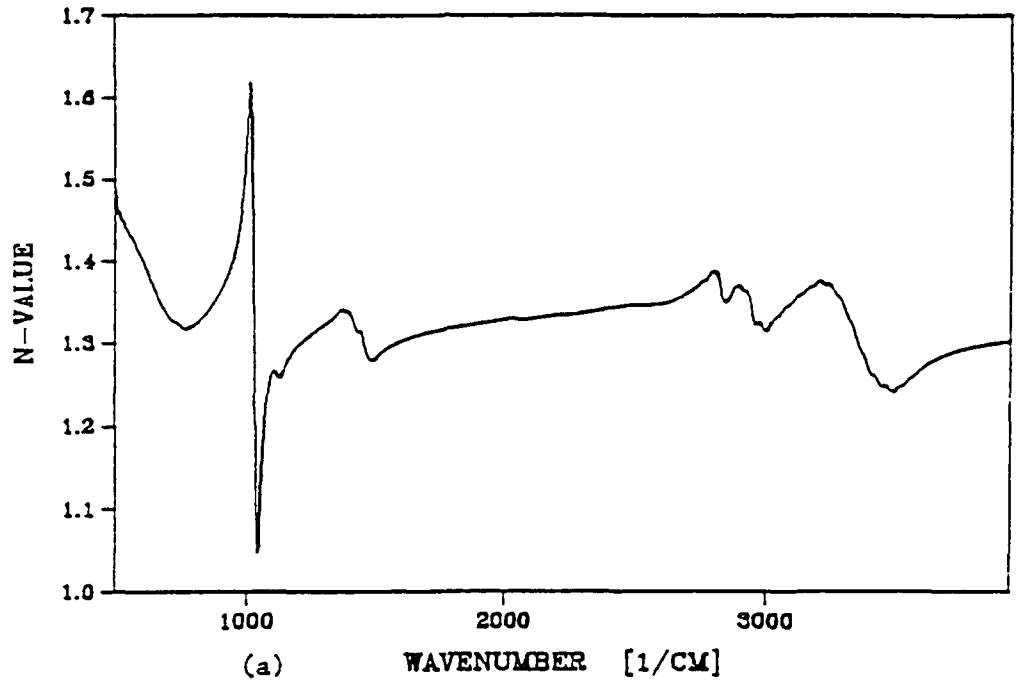

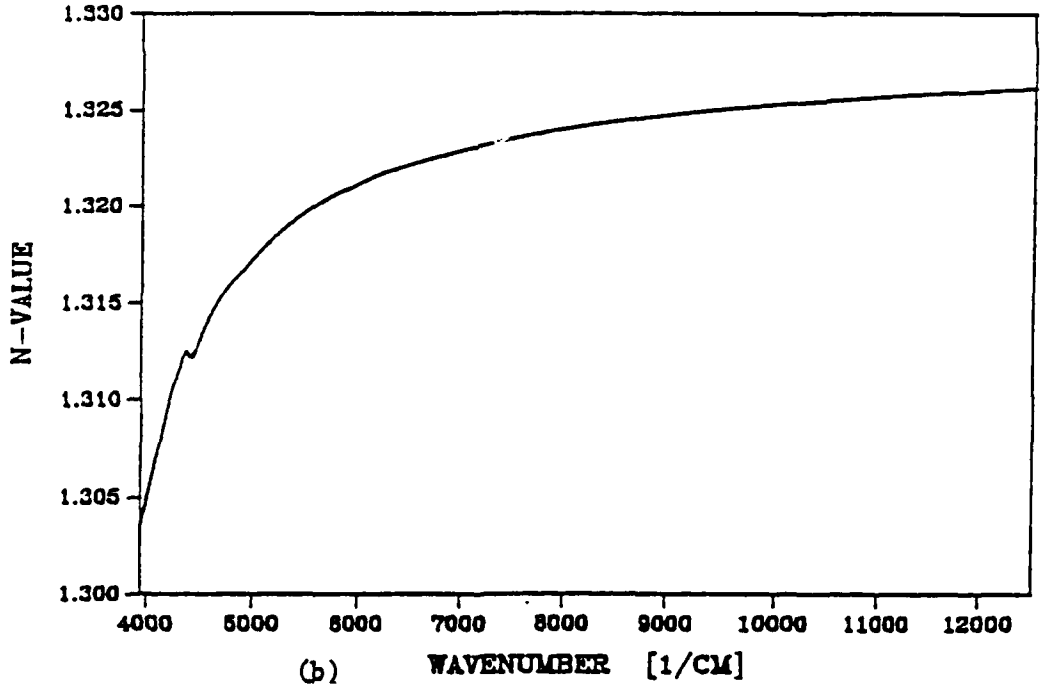

Fig. 8. Index of refraction n of methyl alcohol: (a) in the 500-3950 cm^{-1} wave-number region; (b) in the 3950-12500 cm^{-1} wave-number region.

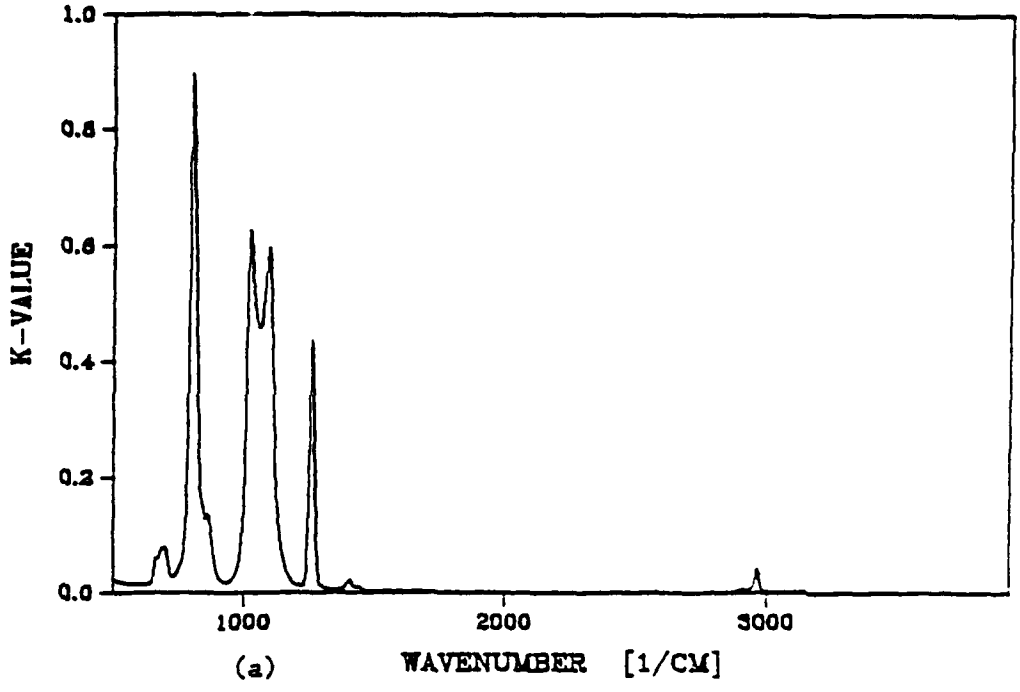

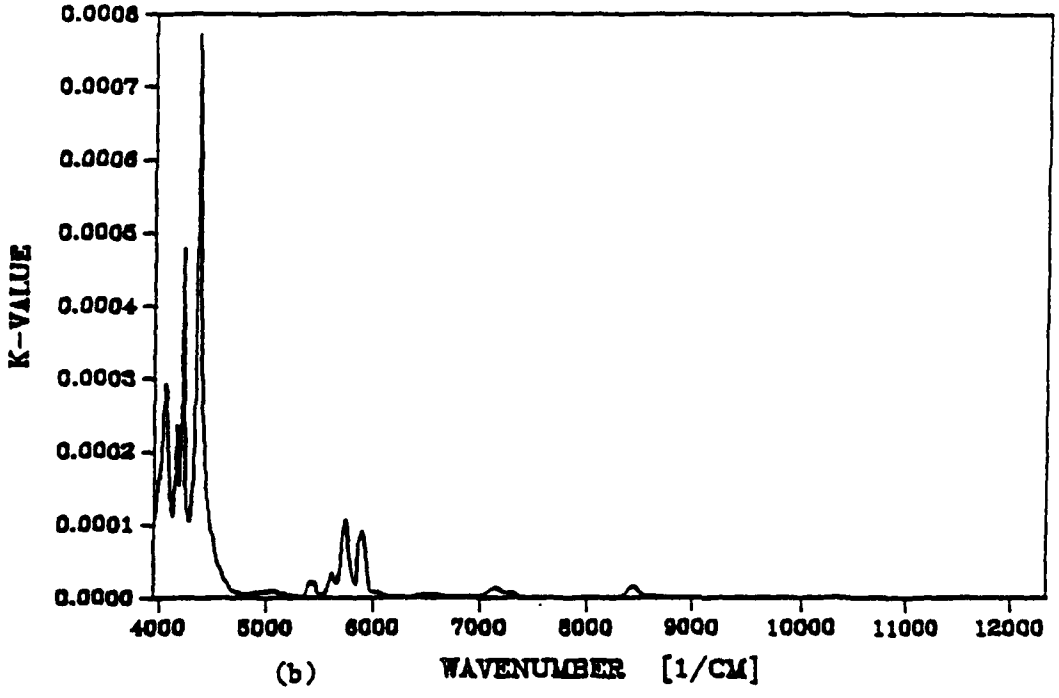

Fig. 9. Extinction coefficient k of SF96: (a) in the 500-3950 cm^{-1} wave-number region; (b) in the 3950-12500 cm^{-1} wave-number region.

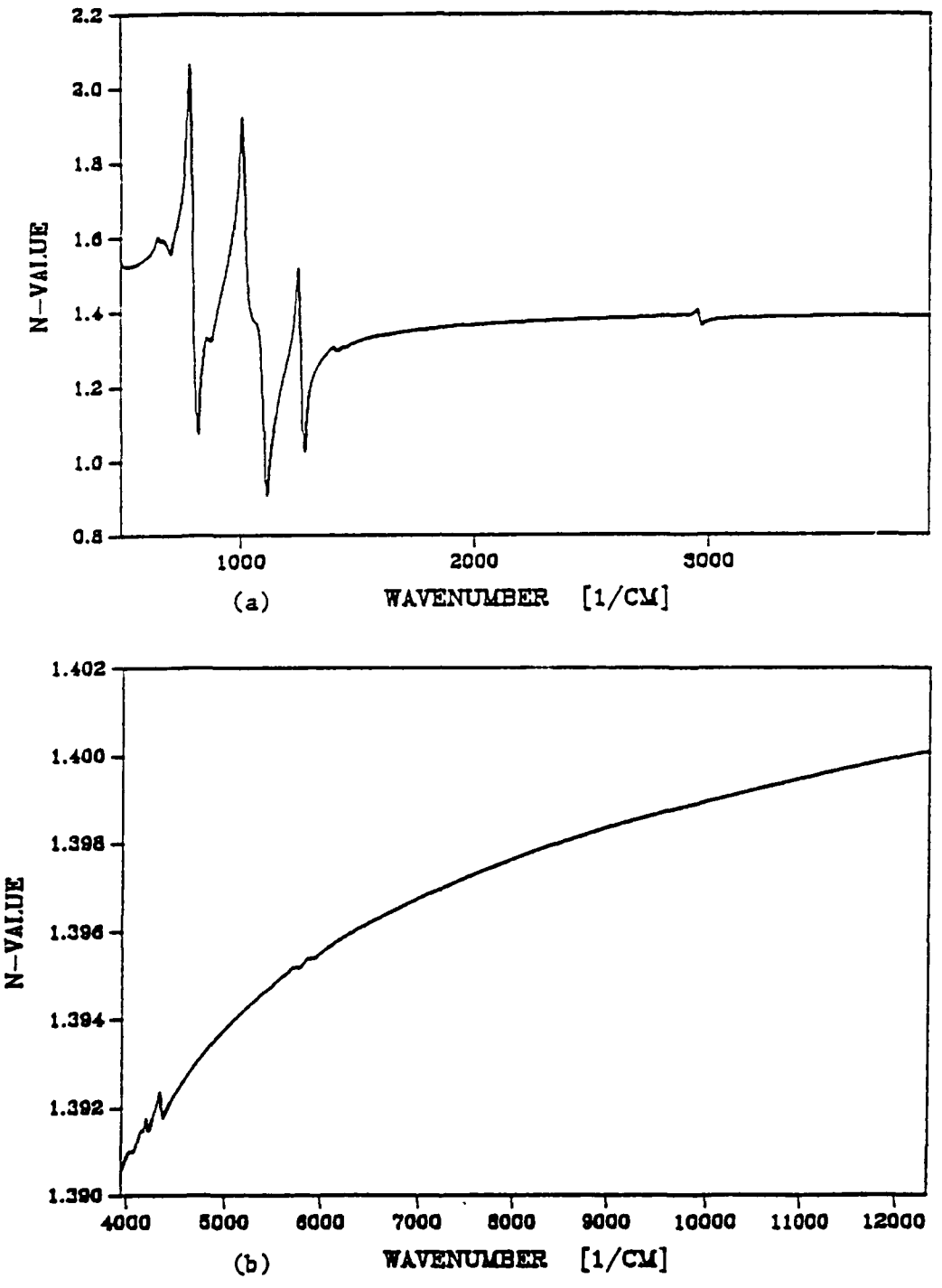

Fig. 10. Index of refraction n of SF96: (a) in the 500-3950 cm^{-1} wave-number region; (b) in the 3950-12500 cm^{-1} wave-number region.

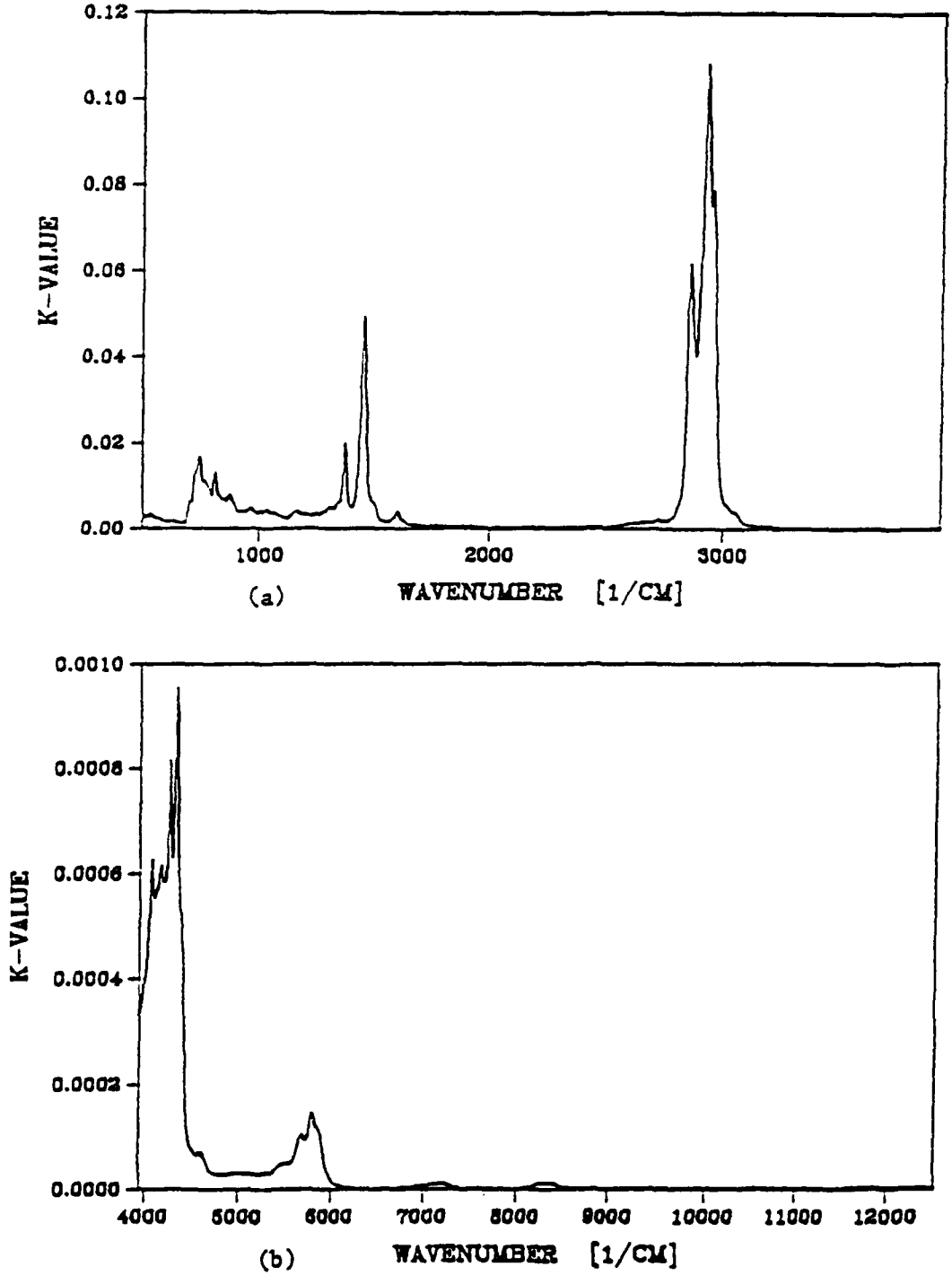

Fig. 11. Extinction coefficient k of diesel fuel: (a) in the 500-3950 cm^{-1} wave-number region; (b) in the 3950-12500 cm^{-1} wave-number region.

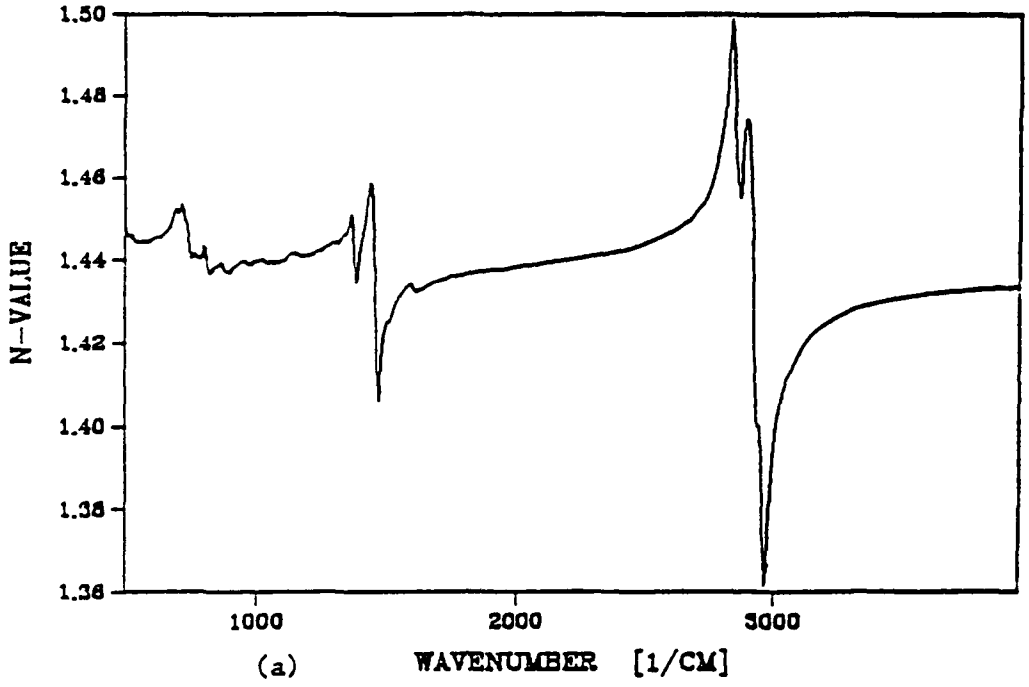

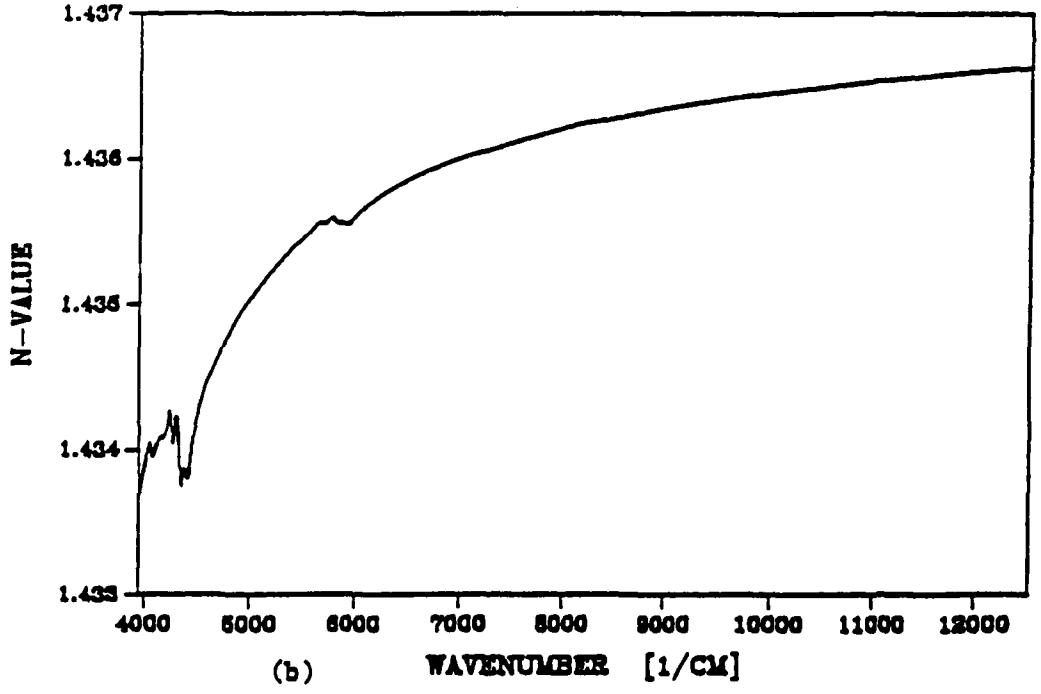

Fig. 12. Index of refraction n of diesel fuel: (a) in the 500-3950 cm^{-1} wave-number region; (b) in the 3950-12500 cm^{-1} wave-number region.

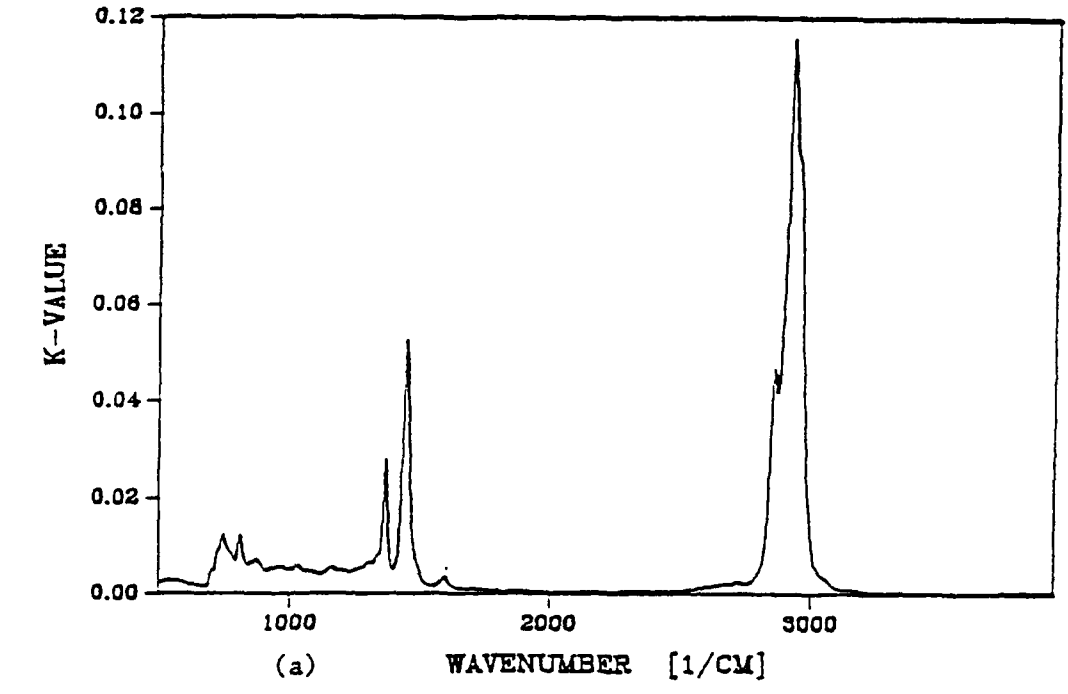

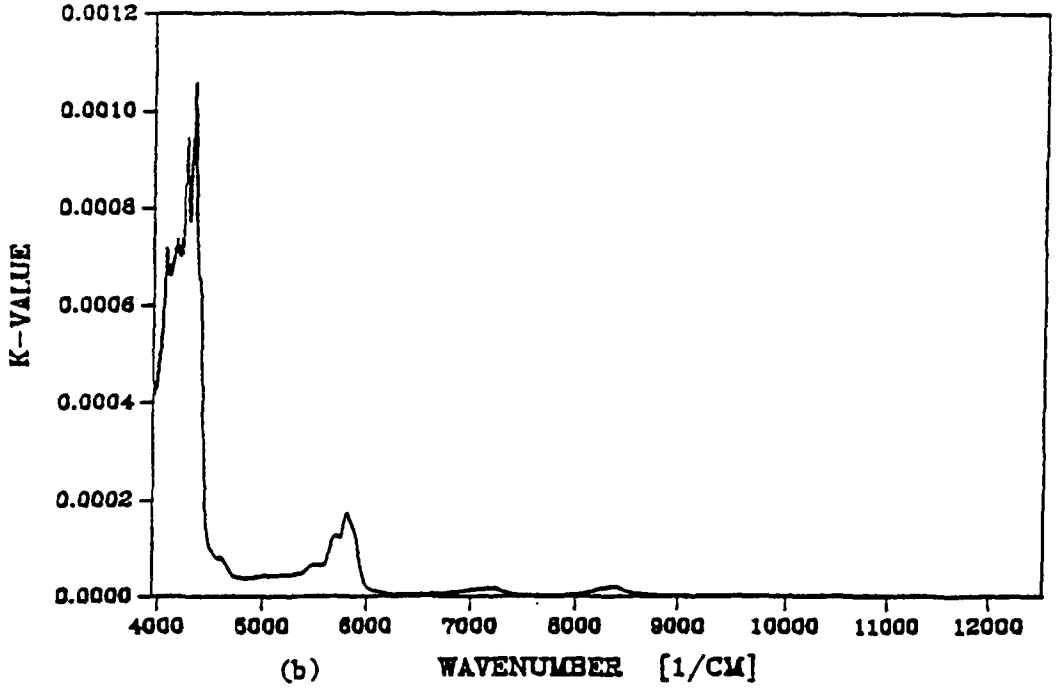

Fig. 13. Extinction coefficient k of fogoil: (a) in the 500-3950 cm^{-1} wave-number region; (b) in the 3950-12500 cm^{-1} wave-number region.

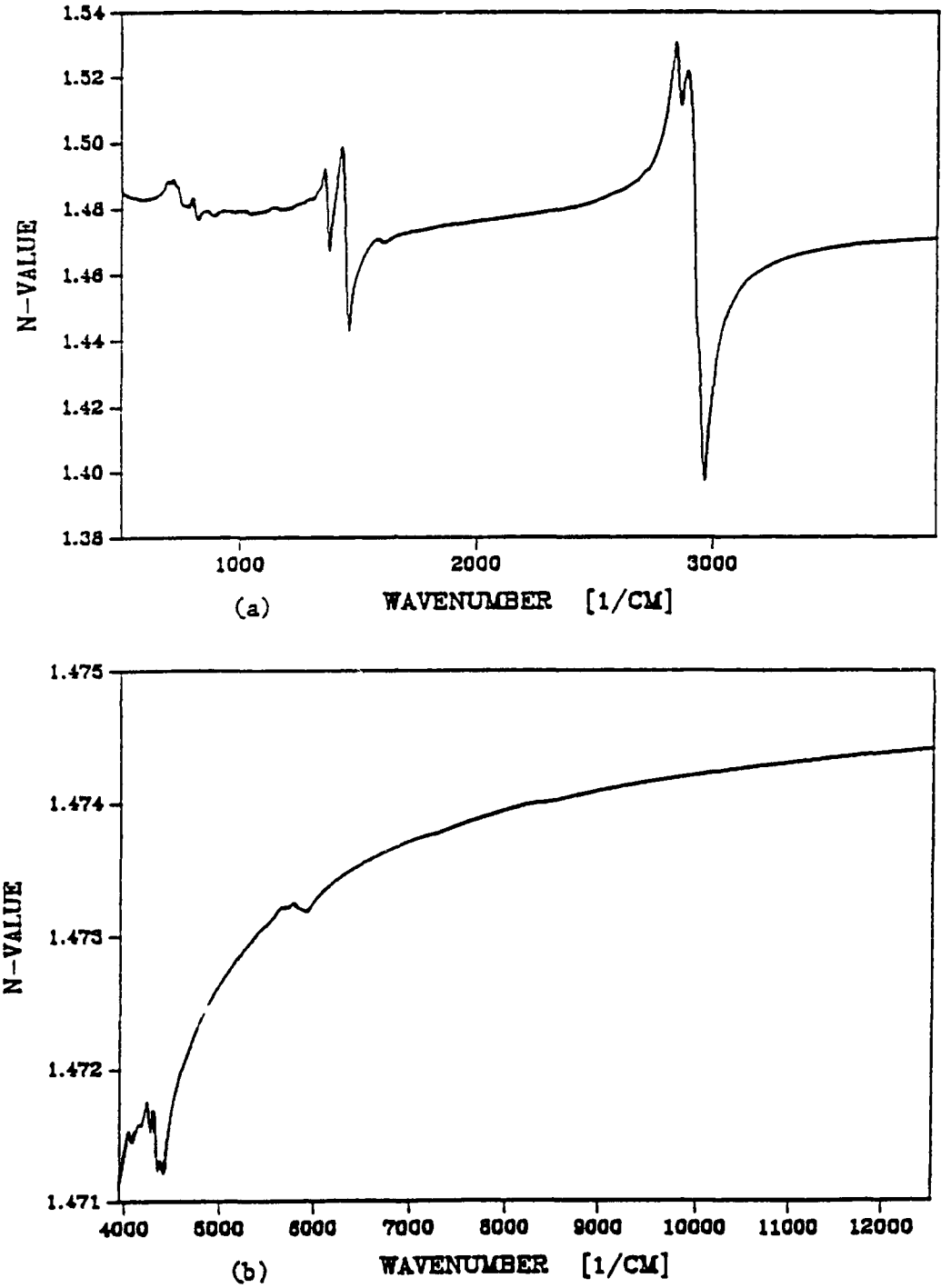

Fig. 14. Index of refraction n of fogoil: (a) in the 500-3950 cm^{-1} wave-number region; (b) in the 3950-12500 cm^{-1} wave-number region.

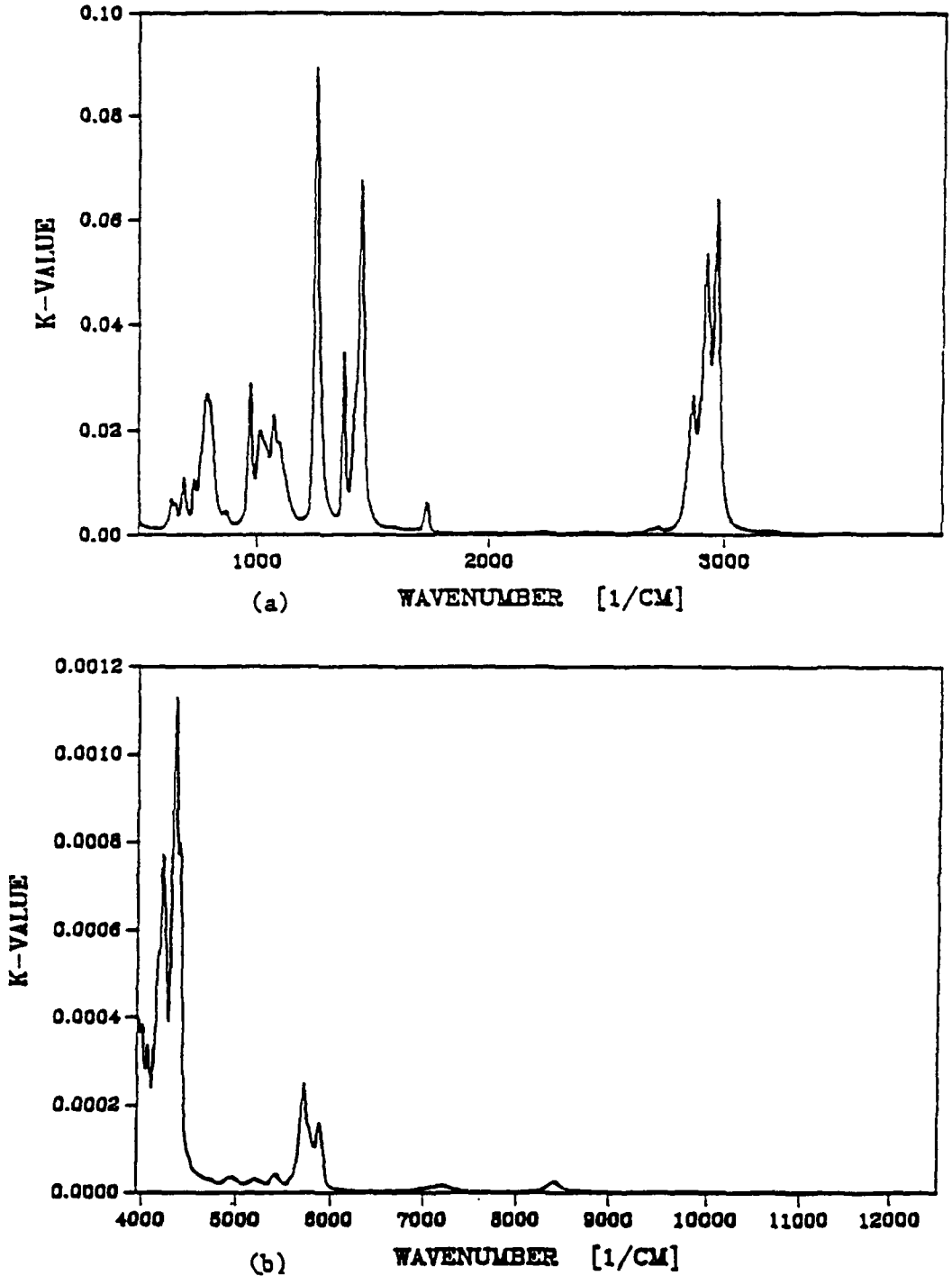

Fig. 15. Extinction coefficient k of ethyl sulfide: (a) in the 500-3950 cm^{-1} wave-number region; (b) in the 3950-12500 cm^{-1} wave-number region.

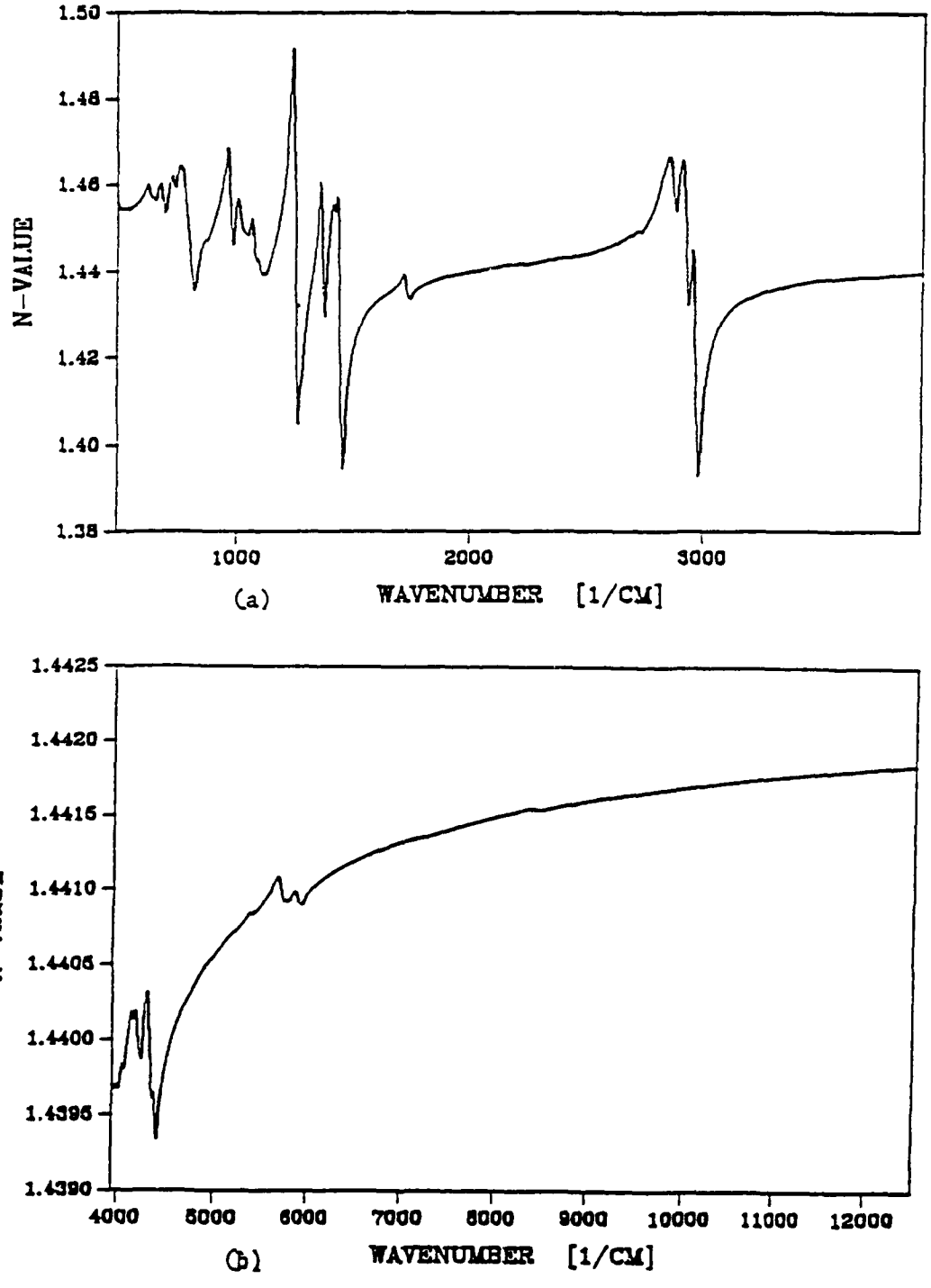

Fig. 16. Index of refraction n of ethyl sulfide: (a) in the 500-3950 cm^{-1} wave-number region; (b) in the 3950-12500 cm^{-1} wave-number region.

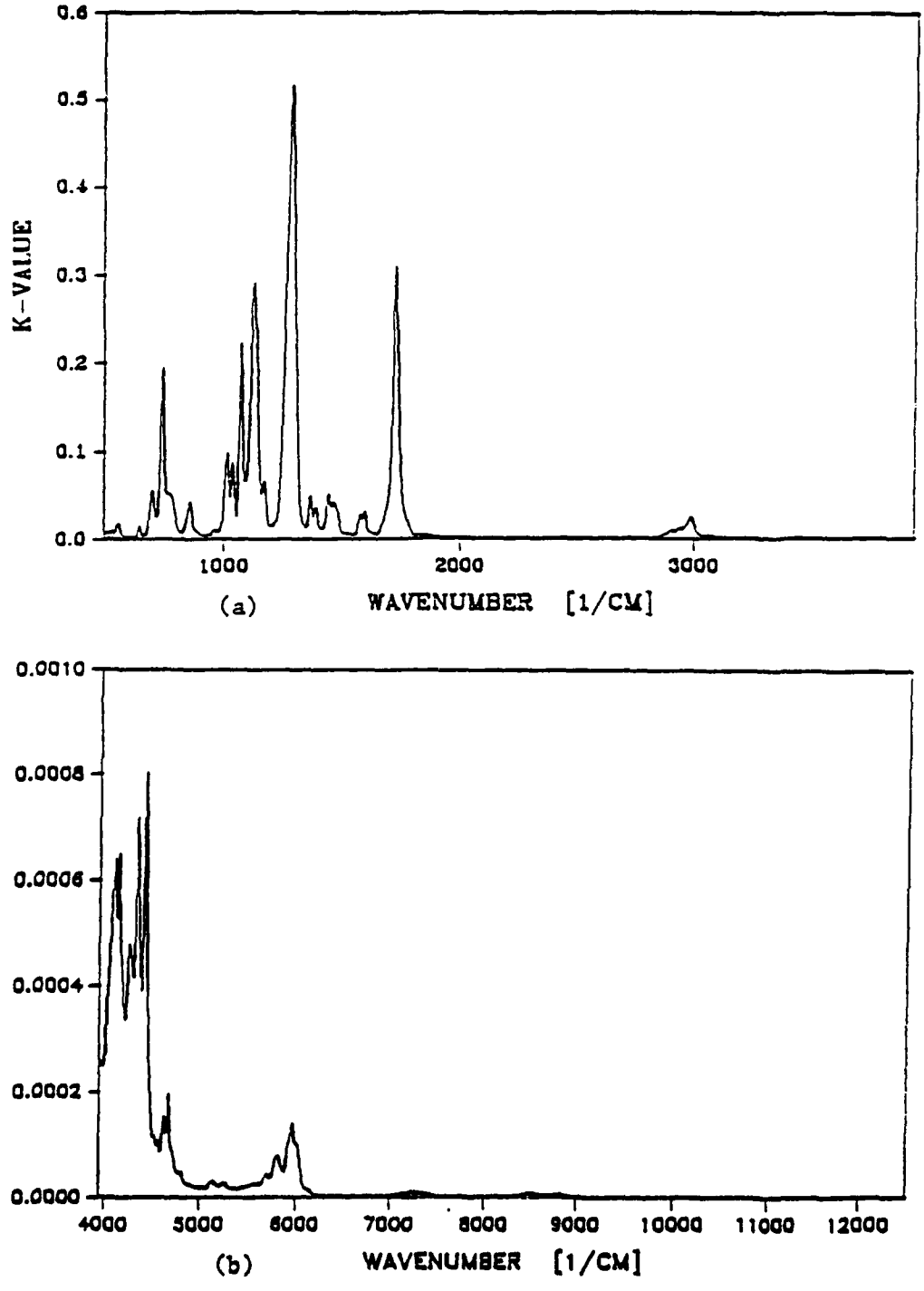

Fig. 17. Extinction coefficient k of diethyl phthalate: (a) in the 500-3950 cm^{-1} wave-number region; (b) in the 3950-12500 cm^{-1} wave-number region.

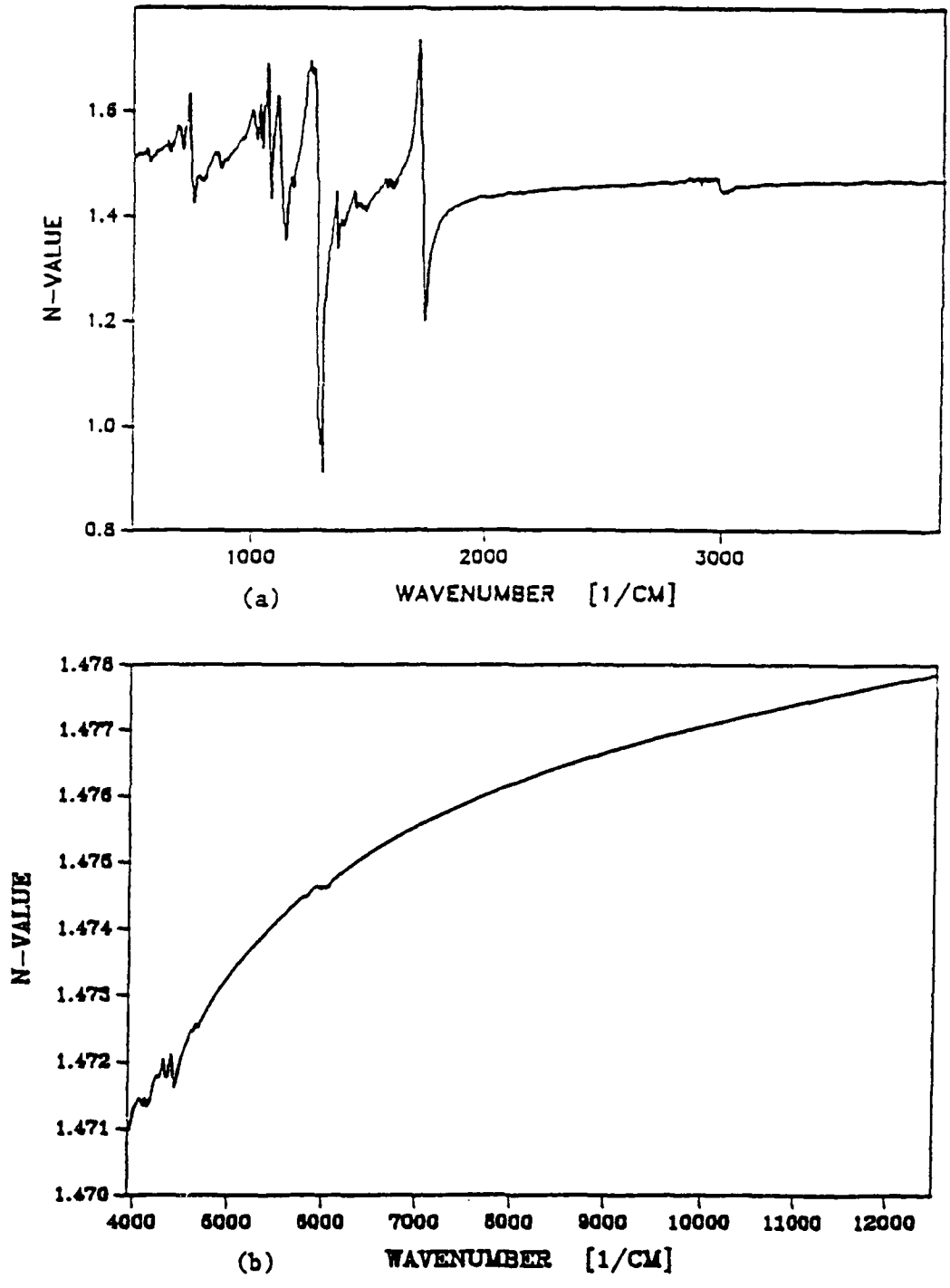

Fig. 18. Index of refraction n of diethyl phthalate: (a) in the 500-3950 cm^{-1} wave-number region; (b) in the 3950-12500 cm^{-1} wave-number region.

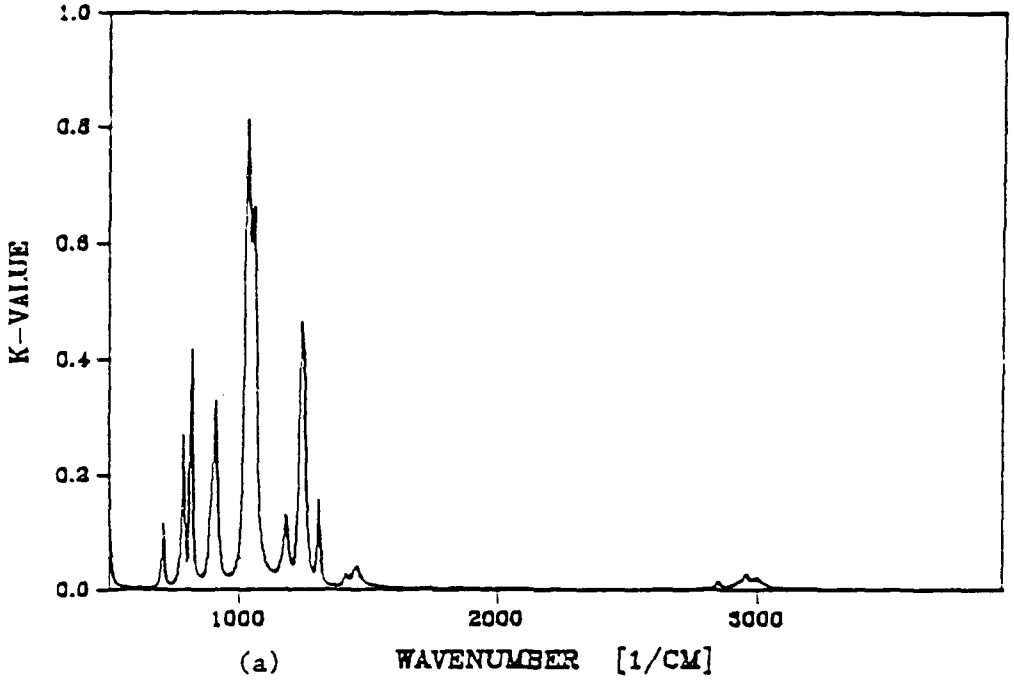

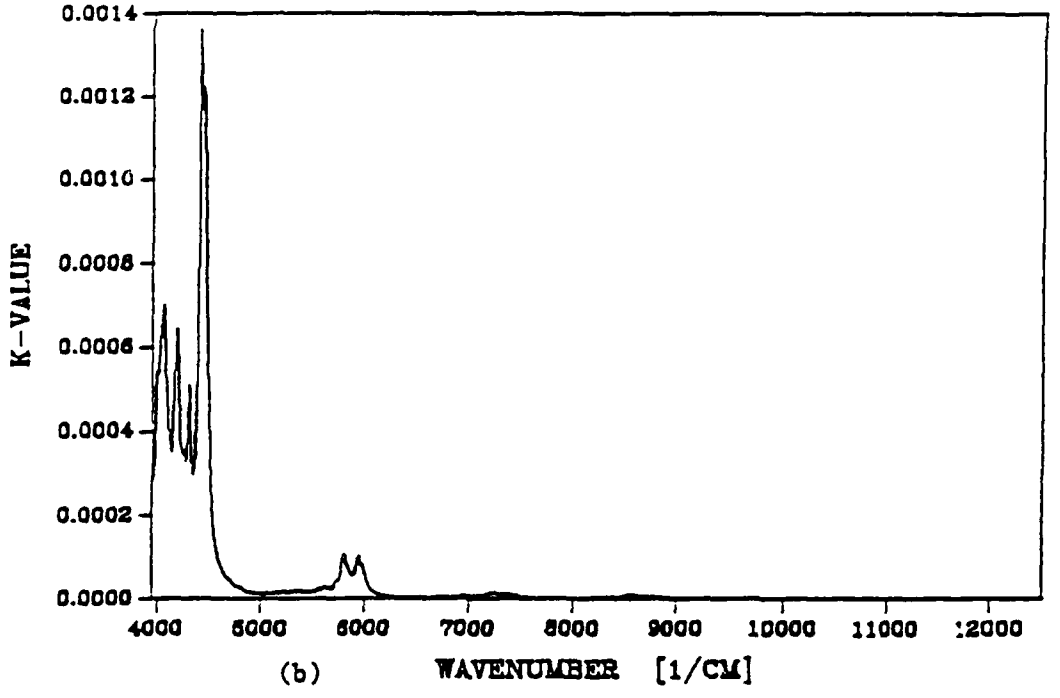

Fig. 19. Extinction coefficient k of dimethyl methylphosphonate: (a) in the 500-3950 cm^{-1} wave-number region; (b) in the 3950-12500 cm^{-1} wave-number region.

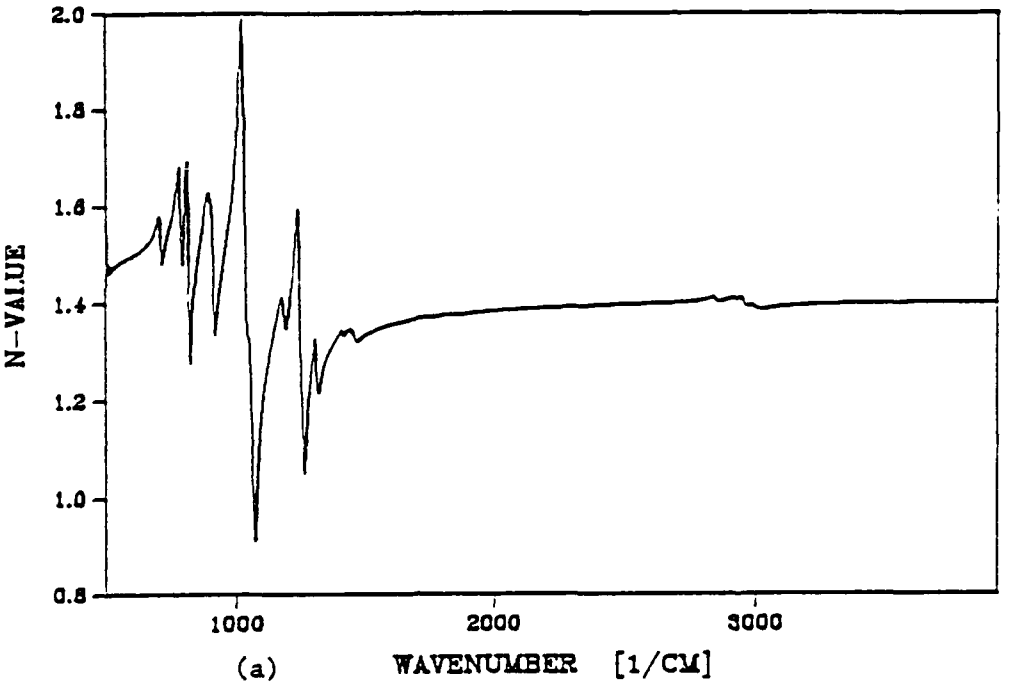

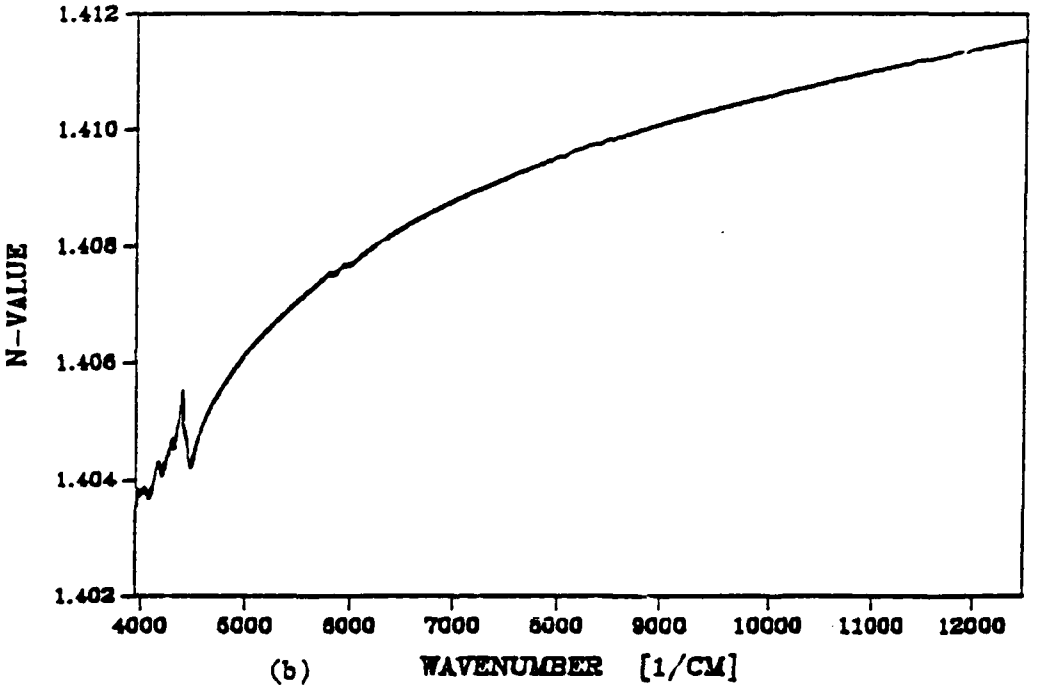

Fig. 20. Index of refraction n of dimethyl methylphosphonate: (a) in the 500-3950 cm^{-1} wave-number region; (b) in the 3950-12500 cm^{-1} wave-number region.

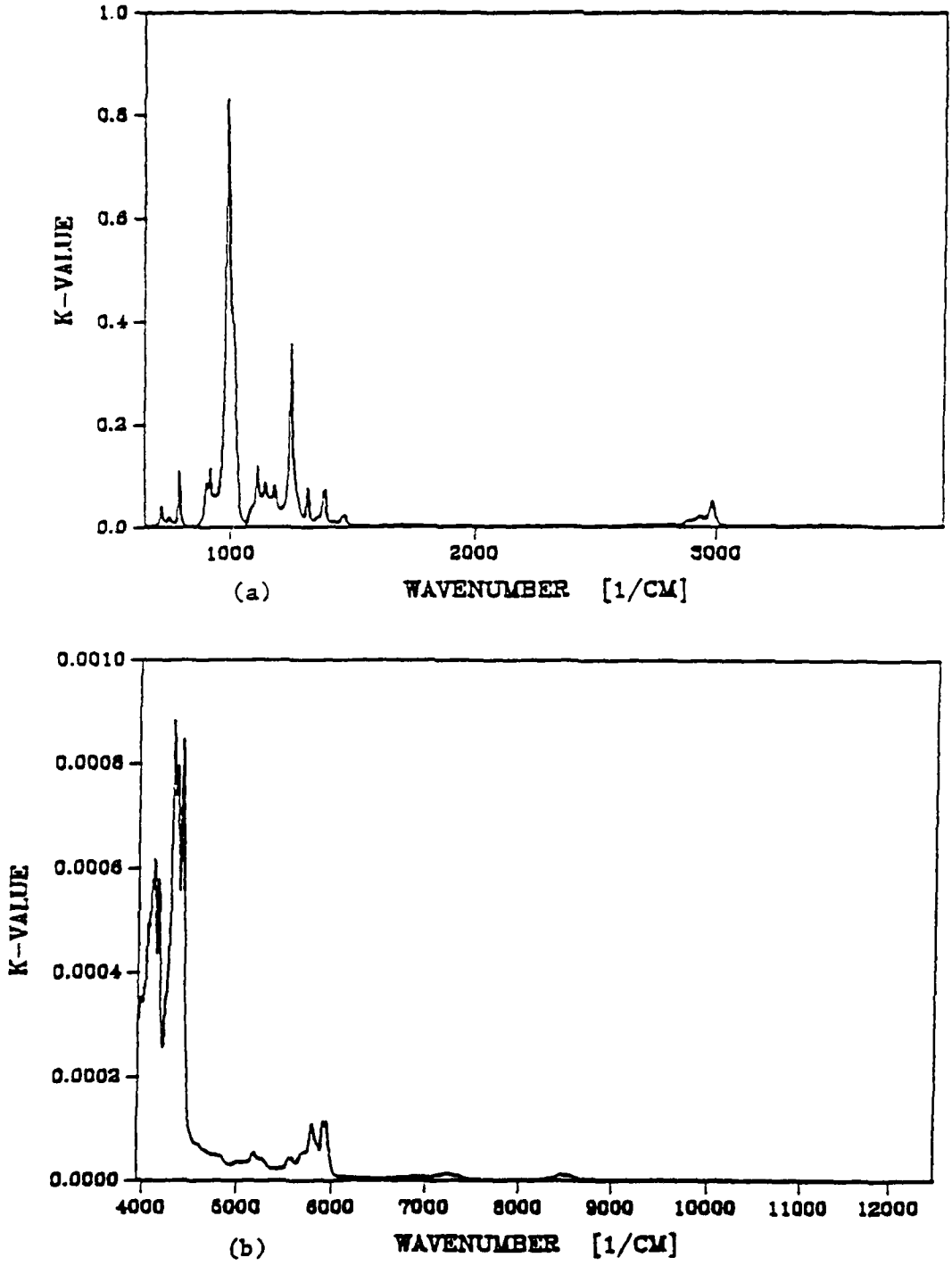

Fig. 21. Extinction coefficient k of diisopropylmethylphosphonate: (a) in the 500-3950 cm^{-1} wave-number region; (b) in the 3950-12500 cm^{-1} wave-number region.

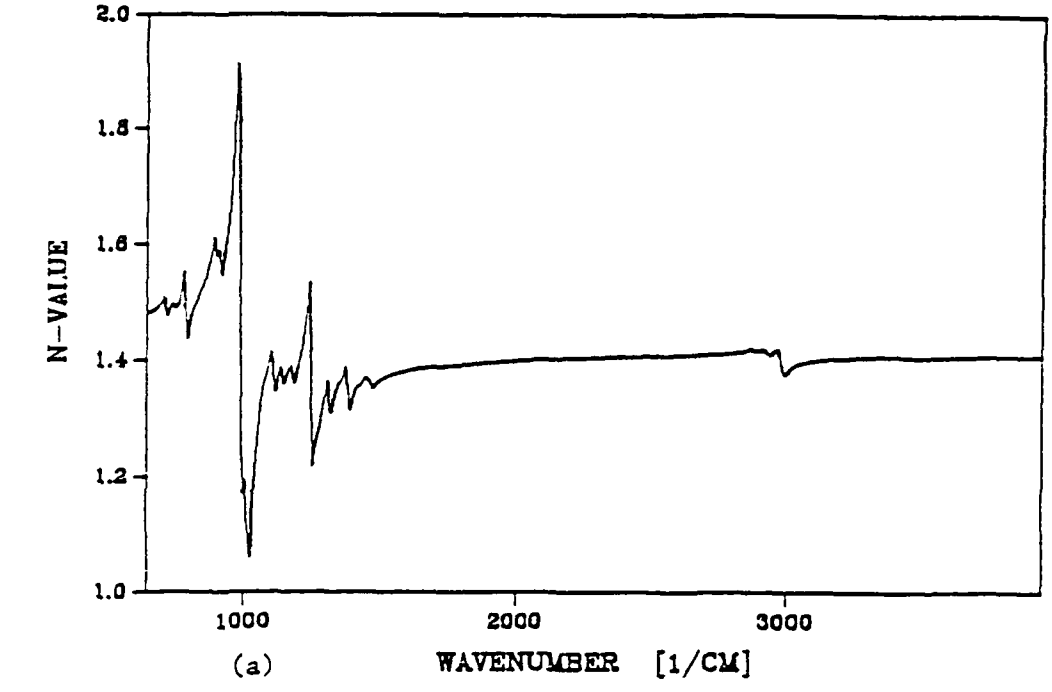

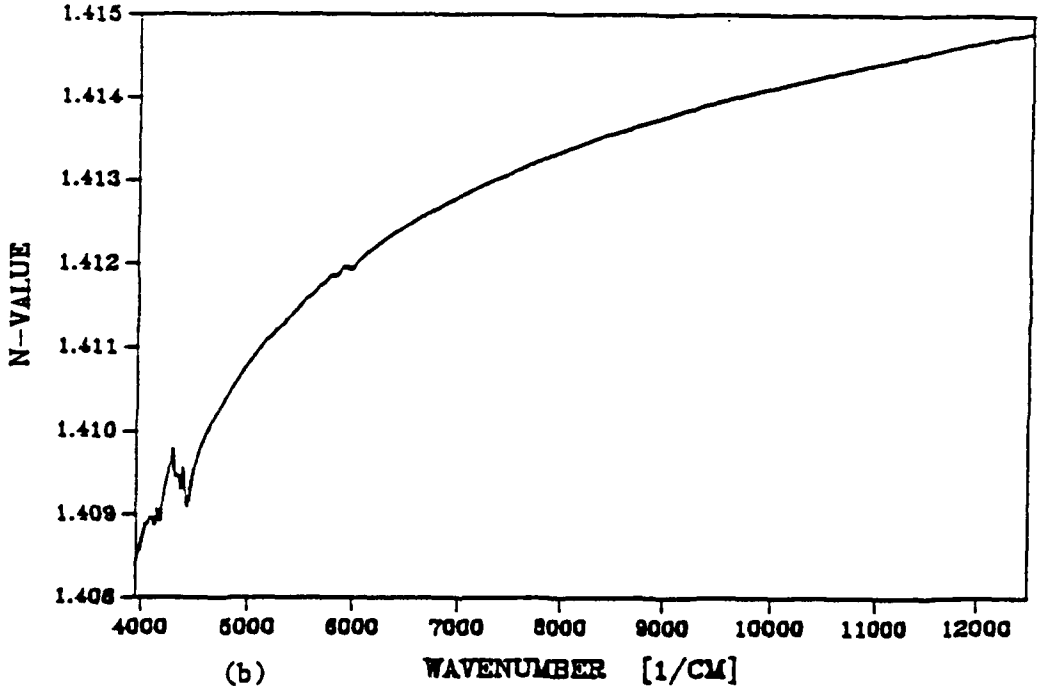

Fig. 22. Index of refraction n of diisopropylmethylphosphonate: (a) in the 500-3950 cm^{-1} wave-number region; (b) in the 3950-1250 cm^{-1} wave-number region.

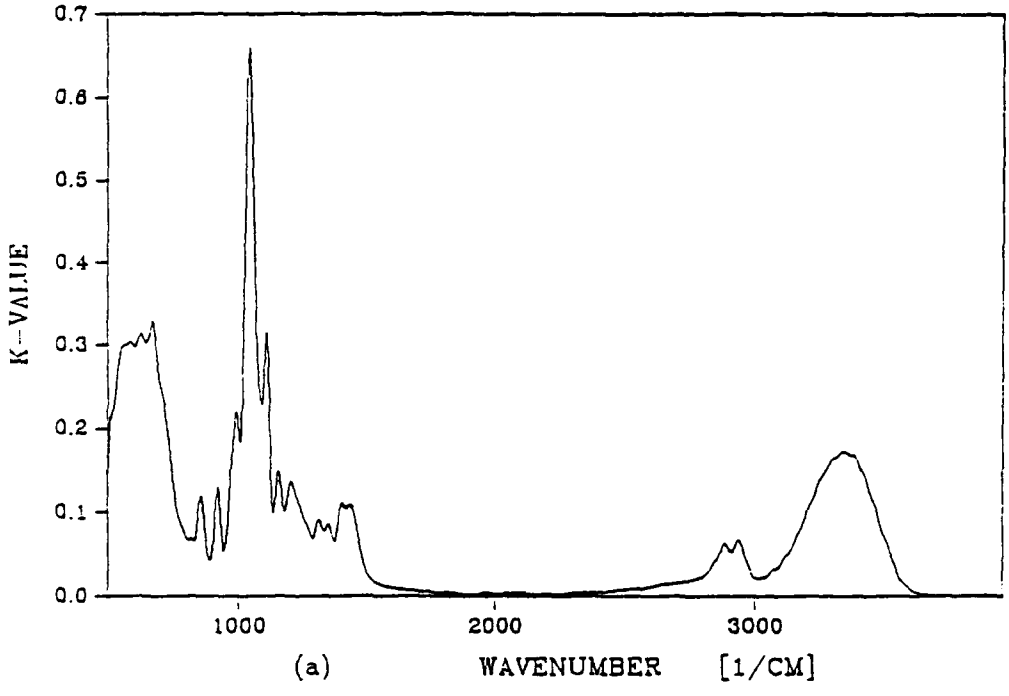

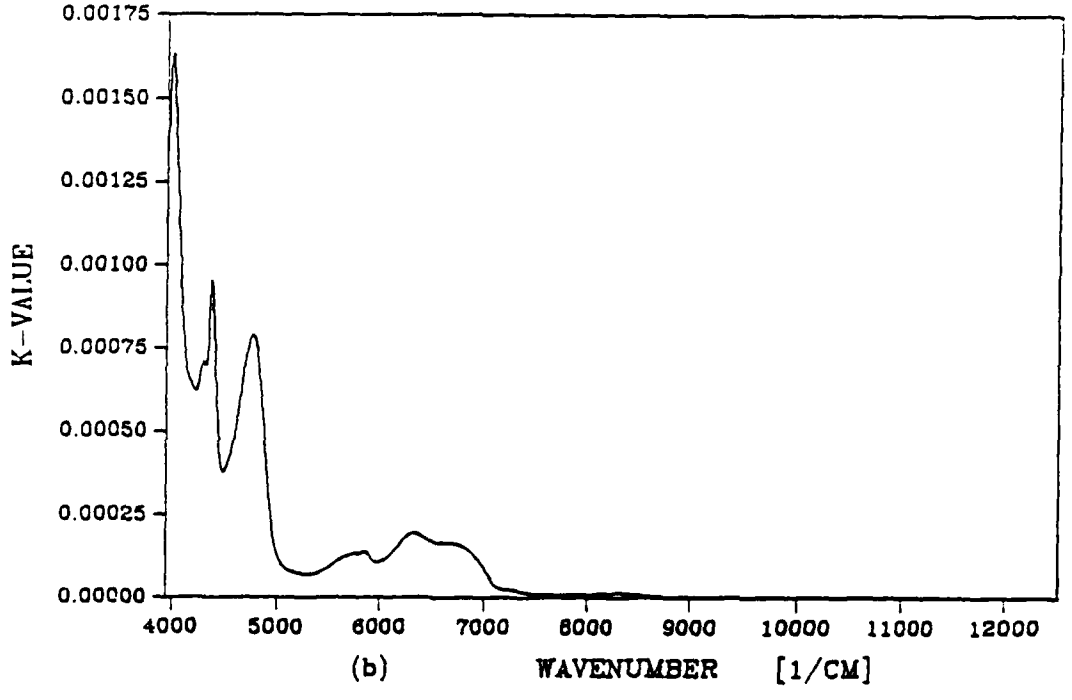

Fig. 23. Extinction coefficient k of glycerin: (a) in the 500-3950 cm^{-1} wave-number region; (b) in the 3950-12500 cm^{-1} wave-number region.

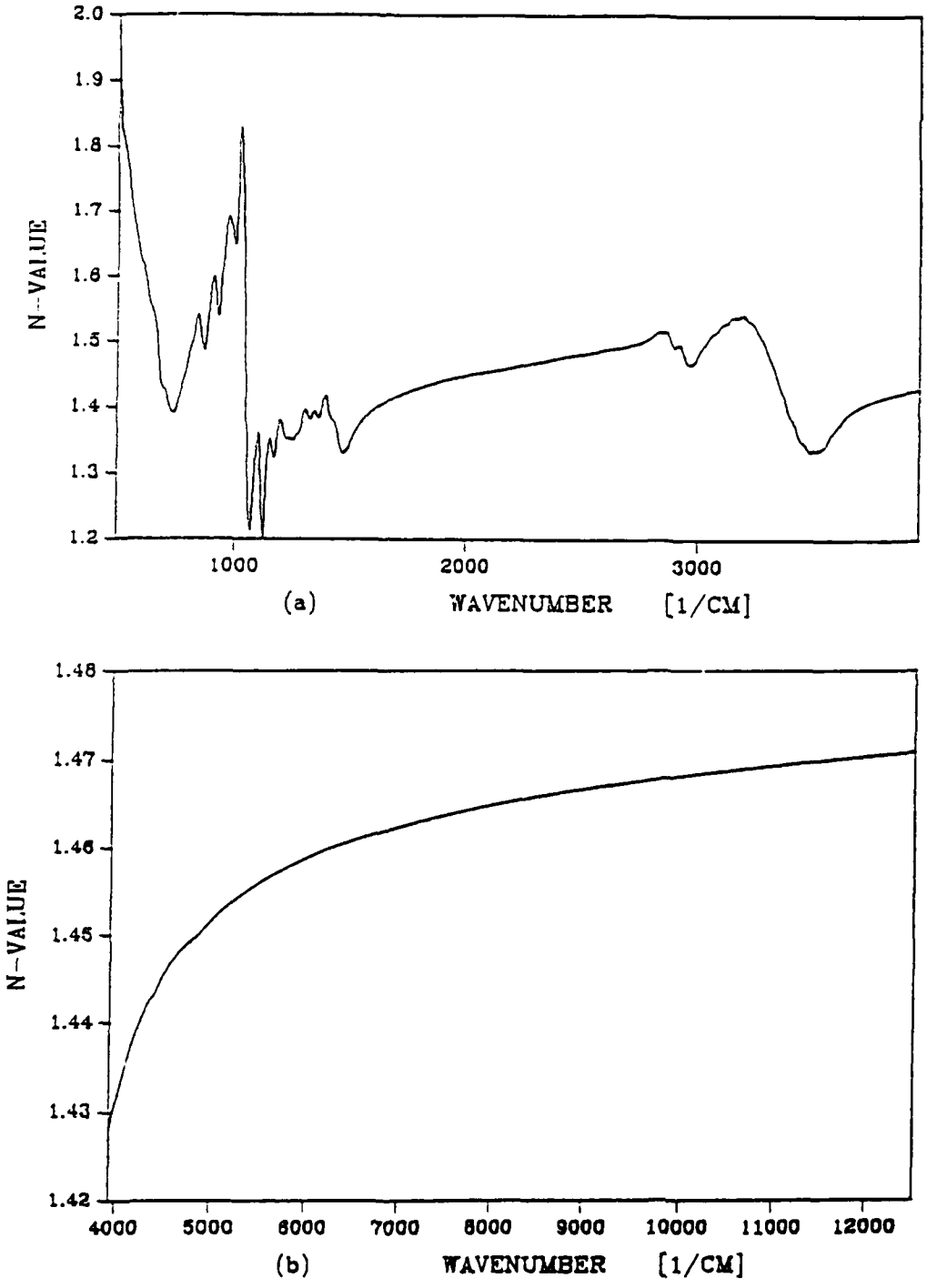

Fig. 24. Index of refraction n of glycerin: (a) in the 500-3950 cm^{-1} wave-number region; (b) in the 3950-12500 cm^{-1} wave-number region.

$$\Delta A = \log \frac{I_o - \Delta I}{I - \Delta I} - \log \frac{I_o}{I}$$

$$= \log \frac{1 - \Delta I/I_o}{1 - \Delta I/I} \qquad (4.6)$$

where I_o is the energy intensity of incident radiation source; I is the energy intensity of transmitted radiation source. The error ΔI will be small compared to I_o and for most values of the I, the ratio $\Delta I/I$ will also be small. The result of Eq. (4.6) is very close to zero. It also indicates that a large value of I_o and I will increase the accuracy. The uncertainty of measured $k(\nu)$ value can be expected to be less than four percent by Eq. (4.5). The experimental results show that the uncertainty of $k(\nu)$ at the absorption band region is less than five percent.

The complex refractive index, Lambert absorption coefficient, and reflection coefficient of eleven samples are listed in Table 1 through Table 11 by listing every twenty measurement points. WN is the wave-number with units of cm^{-1}; WL is the wavelength with units of μm, k is the imaginary part of the complex refractive index, n is the real part of the complex refractive index; LAL is the Lambert Absorption Coefficient with units of cm^{-1} and R is the reflection coefficient calculated from the Fresnel equations at normal incidence.

TABLE 1. WATER

THE COMPLEX REFRACTIVE INDEX, LAMBERT ABSORPTION COEFFICIENT, AND REFLECTION COEFFICIENT.

WN	WL	n	k	LAC	R
302.69	33.0370	2.0249	0.2830020	1076.462	0.122486
508.16	19.6789	1.5212	0.4006730	2558.583	0.066322
534.56	18.7068	1.4839	0.4185910	2811.897	0.064520
564.94	17.7011	1.4351	0.4273560	3033.889	0.060851
598.41	16.7109	1.3809	0.4293290	3228.497	0.056278
636.80	15.7036	1.3215	0.4176280	3341.944	0.049923
680.77	14.6893	1.2597	0.3942670	3372.874	0.042364
729.46	13.7088	1.1938	0.3546420	3250.875	0.033071
787.05	12.7057	1.1308	0.2791190	2760.574	0.020573
855.07	11.6950	1.1134	0.1621030	1741.811	0.008713
900.00	11.1111	1.1431	0.1005870	1137.612	0.006647
920.00	10.8696	1.1538	0.0851463	984.382	0.006652
940.00	10.6383	1.1681	0.0715050	844.645	0.007091
960.00	10.4167	1.1826	0.0613040	739.554	0.007782
980.00	10.2041	1.1961	0.0537024	661.347	0.008566
1000.00	10.0000	1.2081	0.0478981	601.905	0.009348
1020.00	9.8039	1.2190	0.0441750	566.222	0.010133
1040.00	9.6154	1.2287	0.0414152	541.256	0.010872
1060.00	9.4340	1.2367	0.0394339	525.273	0.011506
1080.00	9.2593	1.2445	0.0378846	514.158	0.012148
1100.00	9.0909	1.2514	0.0366934	507.213	0.012731
1120.00	8.9286	1.2566	0.0359114	505.429	0.013180
1140.00	8.7719	1.2622	0.0351849	504.047	0.013673
1160.00	8.6207	1.2676	0.0347630	506.740	0.014158
1180.00	8.4746	1.2720	0.0342641	508.079	0.014557
1200.00	8.3333	1.2757	0.0340121	512.890	0.014897
1220.00	8.1967	1.2789	0.0338111	518.357	0.015195
1240.00	8.0645	1.2820	0.0334315	520.940	0.015482
1260.00	7.9365	1.2852	0.0328852	520.692	0.015780
1280.00	7.8125	1.2883	0.0329544	530.070	0.016077
1300.00	7.6923	1.2914	0.0328899	537.299	0.016375
1320.00	7.5758	1.2939	0.0326285	541.229	0.016614
1340.00	7.4627	1.2965	0.0322709	543.408	0.016863
1360.00	7.3529	1.2985	0.0320224	547.271	0.017056
1380.00	7.2464	1.3005	0.0318269	551.929	0.017251
1400.00	7.1429	1.3021	0.0317010	557.713	0.017407
1420.00	7.0423	1.3045	0.0316394	564.581	0.017644
1440.00	6.9444	1.3065	0.0316813	573.291	0.017844
1460.00	6.8493	1.3089	0.0323195	592.963	0.018091
1480.00	6.7568	1.3113	0.0328717	611.355	0.018339

TABLE 1-Continued

WN	WL	n	k	LAC	R
1500.00	6.6667	1.3136	0.0337149	635.511	0.018581
1520.00	6.5789	1.3173	0.0351967	672.288	0.018975
1540.00	6.4935	1.3220	0.0394454	763.356	0.019513
1560.00	6.4103	1.3288	0.0454257	890.504	0.020307
1580.00	6.3291	1.3428	0.0537822	1067.838	0.021925
1600.00	6.2500	1.3475	0.0711197	1429.946	0.022810
1620.00	6.1728	1.3366	0.1109570	2258.809	0.022955
1640.00	6.0976	1.3022	0.1309120	2697.946	0.020398
1660.00	6.0241	1.2566	0.1213780	2531.966	0.015778
1680.00	5.9524	1.2395	0.0913958	1929.503	0.013081
1700.00	5.8824	1.2353	0.0539355	1152.215	0.011656
1720.00	5.8140	1.2481	0.0363531	785.742	0.012438
1740.00	5.7471	1.2611	0.0263557	576.280	0.013468
1760.00	5.6818	1.2705	0.0177008	391.485	0.014253
1780.00	5.6180	1.2750	0.0144768	323.819	0.014652
1800.00	5.5556	1.2839	0.0127447	288.278	0.015482
1820.00	5.4945	1.2891	0.0116556	266.573	0.015976
1840.00	5.4348	1.2937	0.0108311	250.438	0.016418
1860.00	5.3763	1.2978	0.0103660	242.289	0.016817
1880.00	5.3191	1.3008	0.0103220	243.855	0.017112
1900.00	5.2632	1.3037	0.0104246	248.899	0.017400
1920.00	5.2083	1.3072	0.0104934	253.179	0.017749
1940.00	5.1546	1.3101	0.0107615	262.352	0.018041
1960.00	5.1020	1.3120	0.0113594	279.783	0.018235
1980.00	5.0505	1.3135	0.0121867	303.222	0.018390
2000.00	5.0000	1.3149	0.0129053	324.346	0.018535
2020.00	4.9505	1.3163	0.0135342	343.553	0.018680
2040.00	4.9020	1.3177	0.0143427	367.681	0.018827
2060.00	4.8544	1.3182	0.0149986	388.265	0.018882
2080.00	4.8077	1.3186	0.0154910	404.905	0.018925
2100.00	4.7619	1.3196	0.0155787	411.112	0.019028
2120.00	4.7170	1.3131	0.0155141	413.307	0.018977
2140.00	4.6729	1.3191	0.0152405	409.848	0.018975
2160.00	4.6296	1.3186	0.0148102	401.999	0.018922
2180.00	4.5872	1.3187	0.0139804	382.989	0.018928
2200.00	4.5455	1.3192	0.0131462	363.440	0.018975
2220.00	4.5045	1.3197	0.0123182	343.645	0.019022
2240.00	4.4643	1.3207	0.0115147	324.124	0.019121
2260.00	4.4248	1.3217	0.0106517	302.508	0.019220
2280.00	4.3860	1.3222	0.0097809	280.237	0.019268
2300.00	4.3478	1.3232	0.0091268	263.790	0.019369
2320.00	4.3103	1.3237	0.0085439	249.089	0.019419
2340.00	4.2735	1.3251	0.0078621	231.187	0.019561
2360.00	4.2373	1.3266	0.0072743	215.731	0.019715
2380.00	4.2017	1.3285	0.0068132	203.768	0.019911
2400.00	4.1667	1.3304	0.0063886	192.675	0.020108
2420.00	4.1322	1.3323	0.0059844	181.990	0.020306
2440.00	4.0984	1.3337	0.0055570	170.388	0.020452

TABLE 1-Continued

WN	WL	n	k	LAC	R
2460.00	4.0650	1.3351	0.0051553	159.368	0.020599
2480.00	4.0323	1.3365	0.0049117	153.072	0.020746
2500.00	4.0000	1.3388	0.0046361	145.647	0.020988
2520.00	3.9683	1.3416	0.0043337	137.238	0.021285
2540.00	3.9370	1.3439	0.0040760	130.101	0.021530
2560.00	3.9063	1.3462	0.0039110	125.817	0.021776
2580.00	3.8760	1.3490	0.0037808	122.579	0.022077
2600.00	3.8462	1.3517	0.0036691	119.879	0.022368
2620.00	3.8168	1.3540	0.0035875	118.115	0.022617
2640.00	3.7879	1.3553	0.0036240	120.227	0.022758
2660.00	3.7594	1.3576	0.0037121	124.082	0.023009
2680.00	3.7313	1.3603	0.0038026	128.063	0.023305
2700.00	3.7037	1.3621	0.0039515	134.071	0.023502
2720.00	3.6765	1.3652	0.0042201	144.245	0.023844
2740.00	3.6496	1.3683	0.0045694	157.334	0.024188
2760.00	3.6232	1.3714	0.0050019	173.482	0.024533
2780.00	3.5971	1.3754	0.0054944	191.943	0.024981
2800.00	3.5714	1.3793	0.0061206	215.358	0.025420
2820.00	3.5461	1.3832	0.0069690	246.960	0.025862
2840.00	3.5211	1.3875	0.0079541	283.872	0.026353
2860.00	3.4965	1.3918	0.0091704	329.582	0.026848
2880.00	3.4722	1.3961	0.0106399	385.070	0.027347
2900.00	3.4483	1.4007	0.0124306	453.002	0.027885
2920.00	3.4247	1.4061	0.0146212	536.507	0.028522
2940.00	3.4014	1.4123	0.0173616	641.427	0.029262
2960.00	3.3784	1.4180	0.0196816	732.086	0.029948
2980.00	3.3557	1.4247	0.0258826	969.246	0.030790
3000.00	3.3333	1.4309	0.0350500	1321.354	0.031622
3020.00	3.3113	1.4379	0.0428926	1627.793	0.032553
3040.00	3.2895	1.4450	0.0476445	1820.104	0.033492
3060.00	3.2680	1.4527	0.0540482	2078.321	0.034536
3080.00	3.2468	1.4601	0.0655276	2536.208	0.035663
3100.00	3.2258	1.4664	0.0793249	3090.161	0.036756
3120.00	3.2051	1.4719	0.0920786	3610.133	0.037780
3140.00	3.1847	1.4781	0.1058070	4174.975	0.038974
3160.00	3.1646	1.4770	0.1232370	4893.708	0.039461
3180.00	3.1447	1.4756	0.1449720	5793.235	0.040200
3200.00	3.1250	1.4690	0.1655870	6658.649	0.040399
3220.00	3.1056	1.4633	0.1832550	7415.178	0.040684
3240.00	3.0864	1.4515	0.1989900	8101.886	0.040243
3260.00	3.0675	1.4326	0.2160660	8851.440	0.039205
3280.00	3.0488	1.4173	0.2267220	9344.959	0.038262
3300.00	3.0303	1.4066	0.2369390	9825.629	0.037871
3320.00	3.0120	1.3902	0.2486890	10375.393	0.037075
3340.00	2.9940	1.3745	0.2606180	10938.575	0.036482
3360.00	2.9762	1.3501	0.2739550	11567.204	0.035302
3380.00	2.9586	1.3230	0.2819500	11975.638	0.033570
3400.00	2.9412	1.2913	0.2854350	12196.399	0.031197

TABLE 1-Continued

WN	WL	n	k	LAC	R
3420.00	2.9240	1.2537	0.2825580	12143.492	0.027952
3440.00	2.9070	1.2107	0.2765400	11954.359	0.024351
3460.00	2.8902	1.1803	0.2636650	11464.060	0.021153
3480.00	2.8736	1.1526	0.2451480	10720.560	0.017765
3500.00	2.8571	1.1345	0.2230100	9808.492	0.014726
3520.00	2.8409	1.1100	0.2031740	8987.123	0.011880
3540.00	2.8249	1.0828	0.1853910	8247.110	0.009429
3560.00	2.8090	1.0902	0.1612540	7213.904	0.007768
3580.00	2.7933	1.0906	0.1355540	6098.250	0.006057
3600.00	2.7778	1.1090	0.1129330	5108.969	0.005523
3620.00	2.7624	1.1145	0.0959832	4366.301	0.004982
3640.00	2.7473	1.1122	0.0772541	3533.725	0.004154
3660.00	2.7322	1.1309	0.0490922	2257.894	0.004302
3680.00	2.7174	1.1499	0.0238816	1104.387	0.004984
3700.00	2.7027	1.1639	0.0124796	580.246	0.005770
3720.00	2.6882	1.1781	0.0081047	378.871	0.006700
3742.51	2.6720	1.1903	0.0054560	256.595	0.007556
3770.74	2.6520	1.2036	0.0039432	186.849	0.008538
3799.39	2.6320	1.2139	0.0031633	151.031	0.009335
3828.48	2.6120	1.2223	0.0026470	127.347	0.010007
3858.02	2.5920	1.2294	0.0023164	112.303	0.010593
3888.02	2.5720	1.2356	0.0021583	105.448	0.011104
3918.50	2.5520	1.2408	0.0020987	103.344	0.011552
3949.45	2.5320	1.2454	0.0020648	102.477	0.011944
3980.89	2.5120	1.2494	0.0019844	99.270	0.012294
4012.84	2.4920	1.2530	0.0018243	91.995	0.012609
4045.31	2.4720	1.2563	0.0015861	80.631	0.012901
4078.30	2.4520	1.2593	0.0013534	69.363	0.013175
4111.84	2.4320	1.2622	0.0011557	59.718	0.013435
4145.94	2.4120	1.2649	0.0009902	51.590	0.013678
4180.60	2.3920	1.2674	0.0008574	45.042	0.013905
4215.85	2.3720	1.2697	0.0007381	39.104	0.014118
4251.70	2.3520	1.2719	0.0006365	34.009	0.014320
4288.16	2.3320	1.2739	0.0005513	29.709	0.014511
4325.26	2.3120	1.2758	0.0004806	26.121	0.014690
4363.00	2.2920	1.2777	0.0004244	23.269	0.014862
4401.41	2.2720	1.2794	0.0003805	21.048	0.015025
4440.50	2.2520	1.2810	0.0003501	19.534	0.015180
4480.29	2.2320	1.2826	0.0003304	18.602	0.015327
4520.80	2.2120	1.2841	0.0003217	18.276	0.015468
4562.04	2.1920	1.2855	0.0003205	18.375	0.015604
4604.05	2.1720	1.2868	0.0003324	19.233	0.015732
4646.84	2.1520	1.2881	0.0003510	20.496	0.015855
4690.43	2.1320	1.2894	0.0003817	22.500	0.015975
4734.85	2.1120	1.2905	0.0004283	25.484	0.016089
4780.11	2.0920	1.2917	0.0004919	29.548	0.016199
4826.25	2.0720	1.2928	0.0005732	34.763	0.016305
4873.29	2.0520	1.2938	0.0006780	41.523	0.016407

TABLE 1-Continued

WN	WL	n	k	LAC	R
4921.26	2.0320	1.2948	0.0008087	50.010	0.016503
4970.18	2.0120	1.2957	0.0009765	60.987	0.016595
5020.08	1.9920	1.2966	0.0011980	75.572	0.016680
5070.99	1.9720	1.2974	0.0014773	94.138	0.016753
5122.95	1.9520	1.2979	0.0017851	114.920	0.016807
5175.98	1.9320	1.2982	0.0019970	129.893	0.016834
5230.13	1.9120	1.2982	0.0018492	121.533	0.016839
5285.41	1.8920	1.2984	0.0010691	71.007	0.016858
5341.88	1.8720	1.2995	0.0003351	22.497	0.016965
5399.57	1.8520	1.3006	0.0001674	11.360	0.017071
5458.52	1.8320	1.3015	0.0001326	9.096	0.017159
5518.76	1.8120	1.3023	0.0001267	8.789	0.017240
5580.36	1.7920	1.3030	0.0001252	8.782	0.017313
5643.34	1.7720	1.3037	0.0001166	8.272	0.017383
5707.76	1.7520	1.3044	0.0001000	7.172	0.017449
5773.67	1.7320	1.3050	0.0000862	6.252	0.017514
5841.12	1.7120	1.3057	0.0000785	5.766	0.017578
5910.17	1.6920	1.3063	0.0000743	5.519	0.017641
5980.86	1.6720	1.3069	0.0000737	5.542	0.017700
6053.27	1.6520	1.3075	0.0000747	5.682	0.017761
6127.45	1.6320	1.3081	0.0000785	6.046	0.017818
6203.47	1.6120	1.3087	0.0000842	6.564	0.017874
6281.41	1.5920	1.3092	0.0000934	7.369	0.017930
6361.32	1.5720	1.3097	0.0001083	8.657	0.017984
6443.30	1.5520	1.3103	0.0001288	10.426	0.018038
6527.42	1.5320	1.3108	0.0001603	13.146	0.018089
6613.76	1.5120	1.3113	0.0002034	16.903	0.018139
6702.41	1.4920	1.3118	0.0002601	21.910	0.018188
6793.48	1.4720	1.3122	0.0003223	27.511	0.018230
6887.05	1.4520	1.3126	0.0003523	30.492	0.018269
6983.24	1.4320	1.3129	0.0003368	29.552	0.018305
7082.15	1.4120	1.3133	0.0002705	24.069	0.018341
7183.91	1.3920	1.3137	0.0001311	11.831	0.018384
7288.63	1.3720	1.3142	0.0000504	4.619	0.018437
7396.45	1.3520	1.3147	0.0000358	3.324	0.018485
7507.51	1.3320	1.3152	0.0000259	2.442	0.018532
7621.95	1.3120	1.3156	0.0000171	1.634	0.018578
7739.94	1.2920	1.3160	0.0000133	1.290	0.018622
7861.64	1.2720	1.3165	0.0000113	1.119	0.018665
7987.22	1.2520	1.3169	0.0000117	1.175	0.018709
8116.88	1.2320	1.3173	0.0000126	1.289	0.018752
8250.83	1.2120	1.3177	0.0000125	1.294	0.018794
8389.26	1.1920	1.3182	0.0000146	1.544	0.018837
8532.42	1.1720	1.3186	0.0000140	1.505	0.018878
8680.56	1.1520	1.3190	0.0000127	1.390	0.018918
8833.92	1.1320	1.3194	0.0000069	0.769	0.018959
8992.81	1.1120	1.3198	0.0000052	0.585	0.019001
9157.51	1.0920	1.3202	0.0000044	0.508	0.019041

TABLE 1-Continued

WN	WL	n	k	LAC	R
9328.36	1.0720	1.3206	0.0000042	0.488	0.019082
9505.70	1.0520	1.3210	0.0000036	0.436	0.019123
9689.92	1.0320	1.3214	0.0000044	0.542	0.019165
9881.42	1.0120	1.3218	0.0000051	0.639	0.019205
10080.60	0.9920	1.3221	0.0000063	0.799	0.019246
10288.10	0.9720	1.3226	0.0000060	0.771	0.019287
10504.20	0.9520	1.3229	0.0000053	0.703	0.019328
10729.60	0.9320	1.3234	0.0000036	0.484	0.019370
10964.90	0.9120	1.3238	0.0000028	0.384	0.019412
11210.80	0.8920	1.3242	0.0000030	0.426	0.019454
11467.90	0.8720	1.3246	0.0000026	0.371	0.019497
11737.10	0.8520	1.3250	0.0000024	0.350	0.019541
12019.20	0.8320	1.3254	0.0000023	0.348	0.019585

```
FORTRAN STOP
$
```

TABLE 2. ETHYL ALCOHOL

THE COMPLEX REFRACTIVE INDEX, LAMBERT ABSORPTION COEFFICIENT, AND REFLECTION COEFFICIENT.

WN	WL	n	k	LAC	R
501.00	19.9601	1.4767	0.0325976	205.226	0.037208
520.00	19.2308	1.4538	0.0442105	288.894	0.034514
540.00	18.5185	1.4474	0.0508177	344.841	0.033830
560.00	17.8571	1.4409	0.0580617	408.590	0.033170
580.00	17.2414	1.4344	0.0664472	484.300	0.032557
600.00	16.6667	1.4267	0.0736704	555.462	0.031815
620.00	16.1290	1.4159	0.0801532	624.486	0.030699
640.00	15.6250	1.4027	0.0806231	648.409	0.029189
660.00	15.1515	1.3904	0.0812008	673.464	0.027799
680.00	14.7059	1.3796	0.0757914	647.648	0.026431
700.00	14.2857	1.3710	0.0683652	601.372	0.025291
720.00	13.8889	1.3651	0.0598786	541.769	0.024461
740.00	13.5135	1.3632	0.0507871	472.275	0.024069
760.00	13.1579	1.3640	0.0427053	407.854	0.024024
780.00	12.8205	1.3674	0.0357485	350.399	0.024304
800.00	12.5000	1.3708	0.0387096	389.151	0.024724
820.00	12.1951	1.3667	0.0249074	256.656	0.024112
840.00	11.9048	1.3794	0.0186035	196.374	0.025482
860.00	11.6279	1.3983	0.0199314	215.400	0.027644
880.00	11.3636	1.3948	0.0771127	852.744	0.028182
900.00	11.1111	1.3556	0.0238085	269.268	0.022887
920.00	10.8696	1.3771	0.0119129	137.726	0.025189
940.00	10.6383	1.3911	0.0099775	117.858	0.026768
960.00	10.4167	1.4043	0.0103118	124.399	0.028295
980.00	10.2041	1.4200	0.0121761	149.949	0.030149
1000.00	10.0000	1.4432	0.0175466	220.497	0.032952
1020.00	9.8039	1.4888	0.0346574	444.228	0.038765
1040.00	9.6154	1.5704	0.1819910	2378.445	0.053985
1060.00	9.4340	1.2709	0.1690760	2252.152	0.019663
1080.00	9.2593	1.3748	0.1503580	2040.611	0.028803
1100.00	9.0909	1.2176	0.1203550	1663.668	0.012536
1120.00	8.9286	1.2775	0.0343949	484.085	0.015073
1140.00	8.7719	1.3054	0.0237997	340.946	0.017658
1160.00	8.6207	1.3201	0.0181634	264.768	0.019092
1180.00	8.4746	1.3331	0.0138908	205.977	0.020416
1200.00	8.3333	1.3434	0.0136376	205.650	0.021512
1220.00	8.1967	1.3521	0.0145635	223.273	0.022444
1240.00	8.0645	1.3602	0.0168162	262.035	0.023340
1260.00	7.9365	1.3692	0.0238067	376.946	0.024377
1280.00	7.8125	1.3629	0.0334971	538.799	0.023783

TABLE 2-Continued

WN	WL	n	k	LAC	R
1300.00	7.6923	1.3687	0.0336290	549.373	0.024429
1320.00	7.5758	1.3652	0.0443850	736.241	0.024186
1340.00	7.4627	1.3562	0.0433923	730.680	0.023181
1360.00	7.3529	1.3643	0.0376985	644.277	0.023995
1380.00	7.2464	1.3573	0.0665300	1153.736	0.023747
1400.00	7.1429	1.3434	0.0528610	929.979	0.021976
1420.00	7.0423	1.3381	0.0553455	987.599	0.021464
1440.00	6.9444	1.3310	0.0515687	933.165	0.020641
1460.00	6.8493	1.3157	0.0490124	899.226	0.019026
1480.00	6.7568	1.3123	0.0323059	600.833	0.018437
1500.00	6.6667	1.3139	0.0173546	327.127	0.018459
1520.00	6.5789	1.3222	0.0112565	215.009	0.019269
1540.00	6.4935	1.3277	0.0081344	157.418	0.019834
1560.00	6.4103	1.3317	0.0065362	128.132	0.020243
1580.00	6.3291	1.3351	0.0051199	101.654	0.020597
1600.00	6.2500	1.3381	0.0045247	90.974	0.020911
1620.00	6.1728	1.3402	0.0038727	78.838	0.021137
1640.00	6.0976	1.3422	0.0034448	70.993	0.021352
1660.00	6.0241	1.3440	0.0030328	63.264	0.021541
1680.00	5.9524	1.3458	0.0028704	60.598	0.021736
1700.00	5.8824	1.3471	0.0027572	58.902	0.021871
1720.00	5.8140	1.3483	0.0026411	57.086	0.022000
1740.00	5.7471	1.3495	0.0025993	56.836	0.022126
1760.00	5.6818	1.3504	0.0028152	62.264	0.022223
1780.00	5.6180	1.3508	0.0023153	51.789	0.022269
1800.00	5.5556	1.3518	0.0017701	40.038	0.022374
1820.00	5.4945	1.3529	0.0015773	36.074	0.022500
1840.00	5.4348	1.3541	0.0013758	31.812	0.022626
1860.00	5.3763	1.3551	0.0014477	33.839	0.022733
1880.00	5.3191	1.3561	0.0015376	36.325	0.022842
1900.00	5.2632	1.3574	0.0020455	48.838	0.022985
1920.00	5.2083	1.3577	0.0041571	100.299	0.023016
1940.00	5.1546	1.3556	0.0026142	63.732	0.022790
1960.00	5.1020	1.3569	0.0016280	40.097	0.022928
1980.00	5.0505	1.3577	0.0014245	35.443	0.023016
2000.00	5.0000	1.3585	0.0009932	24.962	0.023103
2020.00	4.9505	1.3593	0.0008968	22.765	0.023197
2040.00	4.9020	1.3601	0.0008409	21.557	0.023284
2060.00	4.8544	1.3611	0.0009314	24.111	0.023391
2080.00	4.8077	1.3617	0.0012543	32.786	0.023454
2100.00	4.7619	1.3621	0.0012591	33.227	0.023500
2120.00	4.7170	1.3628	0.0015298	40.755	0.023579
2140.00	4.6729	1.3630	0.0017190	46.228	0.023594
2160.00	4.6296	1.3634	0.0013944	37.849	0.023641
2180.00	4.5872	1.3640	0.0013182	36.111	0.023706
2200.00	4.5455	1.3646	0.0013499	37.319	0.023779
2220.00	4.5045	1.3653	0.0013202	36.830	0.023853
2240.00	4.4643	1.3660	0.0015463	43.527	0.023930

TABLE 2-Continued

WN	WL	n	k	LAC	R
2260.00	4.4248	1.3659	0.0018688	53.075	0.023919
2280.00	4.3860	1.3666	0.0012919	37.016	0.023997
2300.00	4.3478	1.3675	0.0011644	33.653	0.024091
2320.00	4.3103	1.3684	0.0012272	35.777	0.024195
2340.00	4.2735	1.3691	0.0015901	46.759	0.024277
2360.00	4.2373	1.3698	0.0019139	56.760	0.024355
2380.00	4.2017	1.3705	0.0020560	61.492	0.024427
2400.00	4.1667	1.3712	0.0024540	74.011	0.024504
2420.00	4.1322	1.3713	0.0026926	81.884	0.024524
2440.00	4.0984	1.3724	0.0023508	72.079	0.024638
2460.00	4.0650	1.3736	0.0029647	91.648	0.024780
2480.00	4.0323	1.3741	0.0037744	117.627	0.024838
2500.00	4.0000	1.3745	0.0044355	139.346	0.024875
2520.00	3.9683	1.3748	0.0046044	145.808	0.024908
2540.00	3.9370	1.3750	0.0048650	155.284	0.024940
2560.00	3.9063	1.3754	0.0043478	139.869	0.024977
2580.00	3 8760	1.3767	0.0040911	132.637	0.025127
2600.00	3.8462	1.3781	0.0043107	140.841	0.025278
2620.00	3.8168	1.3794	0.0045930	151.219	0.025425
2640.00	3.7879	1.3807	0.0048879	162.157	0.025578
2660.00	3.7594	1.3826	0.0053048	177.321	0.025795
2680.00	3.7313	1.3849	0.0065333	220.028	0.026052
2700.00	3.7037	1.3862	0.0083553	283.488	0.026210
2720.00	3.6765	1.3873	0.0099135	338.850	0.026338
2740.00	3.6496	1.3882	0.0108056	372.057	0.026437
2760.00	3.6232	1.3901	0.0109092	378.366	0.026662
2780.00	3.5971	1.3938	0.0117530	410.585	0.027088
2800.00	3.5714	1.3993	0.0140050	492.778	0.027730
2820.00	3.5461	1.4066	0.0214639	760.620	0.028620
2840.00	3.5211	1.4077	0.0345963	1234.690	0.028876
2860.00	3.4965	1.4038	0.0469173	1686.199	0.028590
2880.00	3.4722	1.3889	0.0573767	2076.529	0.027069
2900.00	3.4483	1.3784	0.0516361	1881.747	0.025767
2920.00	3.4247	1.3783	0.0526446	1931.731	0.025783
2940.00	3.4014	1.3682	0.0510667	1886.666	0.024623
2960.00	3.3784	1.3784	0.0592414	2203.570	0.025920
2980.00	3.3557	1.3216	0.0687220	2573.487	0.020050
3000.00	3.3333	1.3314	0.0184503	695.560	0.020271
3020.00	3.3113	1.3498	0.0130239	494.263	0.022185
3040.00	3.2895	1.3591	0.0119129	455.094	0.023196
3060.00	3.2680	1.3662	0.0122084	469.451	0.023978
3080.00	3.2468	1.3718	0.0134532	520.698	0.024604
3100.00	3.2258	1.3770	0.0150731	587.184	0.025190
3120.00	3.2051	1.3820	0.0170814	669.712	0.025774
3140.00	3.1847	1.3917	0.0218196	860.967	0.026903
3160.00	3.1646	1.3918	0.0290014	1151.638	0.026974
3180.00	3.1447	1.3964	0.0367791	1469.732	0.027587
3200.00	3.1250	1.3956	0.0476526	1916.225	0.027650

TABLE 2-Continued

WN	WL	n	k	LAC	R
3220.00	3.1056	1.3914	0.0551397	2231.157	0.027306
3240.00	3.0864	1.3889	0.0606960	2471.240	0.027133
3260.00	3.0675	1.3867	0.0692514	2836.978	0.027067
3280.00	3.0488	1.3792	0.0798698	3292.049	0.026500
3300.00	3.0303	1.3685	0.0865286	3588.257	0.025509
3320.00	3.0120	1.3567	0.0897469	3744.272	0.024328
3340.00	2.9940	1.3443	0.0924216	3879.090	0.023085
3360.00	2.9762	1.3299	0.0901739	3807.413	0.021512
3380.00	2.9586	1.3172	0.0855158	3632.227	0.020071
3400.00	2.9412	1.3041	0.0747929	3195.576	0.018458
3420.00	2.9240	1.2993	0.0612742	2633.381	0.017638
3440.00	2.9070	1.2992	0.0518877	2243.018	0.017431
3460.00	2.8902	1.2974	0.0462307	2010.094	0.017158
3480.00	2.8736	1.2933	0.0379172	1658.156	0.016625
3500.00	2.8571	1.2932	0.0256359	1127.526	0.016467
3520.00	2.8409	1.2991	0.0159688	706.358	0.016975
3540.00	2.8249	1.3045	0.0119581	531.956	0.017489
3560.00	2.8090	1.3088	0.0081257	363.514	0.017900
3580.00	2.7933	1.3130	0.0053812	242.085	0.018315
3600.00	2.7778	1.3168	0.0034365	155.465	0.018704
3620.00	2.7624	1.3202	0.0022303	101.457	0.019051
3640.00	2.7473	1.3232	0.0014556	66.580	0.019353
3660.00	2.7322	1.3258	0.0008853	40.715	0.019625
3680.00	2.7174	1.3281	0.0006789	31.395	0.019864
3700.00	2.7027	1.3300	0.0005954	27.684	0.020060
3720.00	2.6882	1.3316	0.0005575	26.063	0.020230
3740.00	2.6738	1.3330	0.0005586	26.254	0.020378
3759.40	2.6600	1.3343	0.0005062	23.915	0.020505
3787.88	2.6400	1.3358	0.0004520	21.515	0.020669
3816.79	2.6200	1.3372	0.0004159	19.948	0.020815
3846.15	2.6000	1.3385	0.0004075	19.695	0.020952
3875.97	2.5800	1.3396	0.0003656	17.809	0.021068
3906.25	2.5600	1.3407	0.0003598	17.662	0.021191
3937.01	2.5400	1.3418	0.0004918	24.329	0.021301
3968.25	2.5200	1.3427	0.0007179	35.801	0.021394
4000.00	2.5000	1.3432	0.0008896	44.714	0.021458
4032.26	2.4800	1.3438	0.0009656	48.927	0.021514
4065.04	2.4600	1.3442	0.0009887	50.507	0.021560
4098.36	2.4400	1.3447	0.0006956	35.824	0.021613
4132.23	2.4200	1.3454	0.0006175	32.067	0.021687
4166.67	2.4000	1.3460	0.0005951	31.161	0.021748
4201.68	2.3800	1.3466	0.0005450	28.777	0.021816
4237.29	2.3600	1.3472	0.0007320	38.978	0.021881
4273.50	2.3400	1.3474	0.0006729	36.139	0.021907
4310.34	2.3200	1.3482	0.0009476	51.329	0.021987
4347.83	2.3000	1.3479	0.0012859	70.255	0.021952
4385.96	2.2800	1.3483	0.0010619	58.528	0.021996
4424.78	2.2600	1.3481	0.0008609	47.867	0.021974

TABLE 2-Continued

WN	WL	n	k	LAC	R
4464.29	2.2400	1.3486	0.0003267	18.325	0.022032
4504.50	2.2200	1.3492	0.0002283	12.925	0.022095
4545.45	2.2000	1.3496	0.0002036	11.632	0.022139
4587.16	2.1800	1.3500	0.0002000	11.528	0.022183
4629.63	2.1600	1.3504	0.0002036	11.845	0.022224
4672.90	2.1400	1.3507	0.0002301	13.509	0.022257
4716.98	2.1200	1.3510	0.0002708	16.049	0.022287
4761.90	2.1000	1.3512	0.0003177	19.014	0.022316
4807.69	2.0800	1.3514	0.0003436	20.758	0.022337
4854.37	2.0600	1.3516	0.0002932	17.889	0.022356
4901.96	2.0400	1.3518	0.0001982	12.210	0.022379
4950.50	2.0200	1.3521	0.0001223	7.607	0.022406
5000.00	2.0000	1.3523	0.0000780	4.900	0.022434
5050.50	1.9800	1.3526	0.0000584	3.704	0.022461
5102.04	1.9600	1.3528	0.0000537	3.440	0.022489
5154.64	1.9400	1.3531	0.0000508	3.294	0.022515
5208.33	1.9200	1.3533	0.0000433	2.832	0.022535
5263.16	1.9000	1.3535	0.0000381	2.517	0.022561
5319.15	1.8800	1.3537	0.0000362	2.418	0.022580
5376.34	1.8600	1.3539	0.0000400	2.699	0.022606
5434.78	1.8400	1.3541	0.0000544	3.717	0.022625
5494.51	1.8200	1.3542	0.0000664	4.585	0.022642
5555.56	1.8000	1.3544	0.0000714	4.987	0.022662
5617.98	1.7800	1.3546	0.0000855	6.033	0.022681
5681.82	1.7600	1.3548	0.0001121	8.001	0.022697
5747.13	1.7400	1.3549	0.0001401	10.116	0.022715
5813.95	1.7200	1.3550	0.0001428	10.431	0.022725
5882.35	1.7000	1.3552	0.0001595	11.791	0.022743
5952.38	1.6800	1.3552	0.0001241	9.283	0.022747
6024.10	1.6600	1.3554	0.0000631	4.777	0.022769
6097.56	1.6400	1.3556	0.0000687	5.264	0.022784
6172.84	1.6200	1.3557	0.0000850	6.596	0.022801
6250.00	1.6000	1.3558	0.0001029	8.084	0.022816
6329.11	1.5800	1.3560	0.0001109	8.818	0.022827
6410.26	1.5600	1.3561	0.0001022	8.231	0.022838
6493.51	1.5400	1.3561	0.0000926	7.559	0.022848
6578.95	1.5200	1.3563	0.0000885	7.316	0.022864
6666.67	1.5000	1.3564	0.0000846	7.090	0.022873
6756.76	1.4800	1.3565	0.0000757	6.425	0.022887
6849.31	1.4600	1.3566	0.0000636	5.477	0.022898
6944.44	1.4400	1.3567	0.0000479	4.181	0.022910
7042.25	1.4200	1.3568	0.0000387	3.423	0.022922
7142.86	1.4000	1.3569	0.0000297	2.662	0.022930
7246.38	1.3800	1.3570	0.0000235	2.136	0.022945
7352.94	1.3600	1.3571	0.0000150	1.390	0.022954
7462.69	1.3400	1.3572	0.0000054	0.510	0.022965
7575.76	1.3200	1.3573	0.0000034	0.323	0.022977
7692.31	1.3000	1.3574	0.0000030	0.295	0.022989

TABLE 2-Continued

WN	WL	n	k	LAC	R
7812.50	1.2800	1.3575	0.0000037	0.367	0.022998
7936.51	1.2600	1.3576	0.0000049	0.488	0.023007
8064.52	1.2400	1.3577	0.0000067	0.684	0.023018
8196.72	1.2200	1.3578	0.0000113	1.166	0.023029
8333.33	1.2000	1.3579	0.0000128	1.341	0.023036
8474.58	1.1800	1.3579	0.0000174	1.850	0.023045
8620.69	1.1600	1.3580	0.0000062	0.669	0.023054
8771.93	1.1400	1.3581	0.0000036	0.393	0.023064
8928.57	1.1200	1.3582	0.0000006	0.071	0.023074
9090.91	1.1000	1.3583	0.0000008	0.092	0.023081
9259.26	1.0800	1.3584	0.0000008	0.089	0.023091
9433.96	1.0600	1.3585	0.0000011	0.129	0.023100
9615.38	1.0400	1.3585	0.0000012	0.150	0.023106
9803.92	1.0200	1.3586	0.0000016	0.194	0.023115
10000.00	1.0000	1.3587	0.0000013	0.169	0.023122
10204.10	0.9800	1.3587	0.0000007	0.091	0.023130
10416.70	0.9600	1.3588	0.0000004	0.053	0.023139
10638.30	0.9400	1.3589	0.0000004	0.055	0.023147
10869.60	0.9200	1.3589	0.0000006	0.081	0.023153
11111.10	0.9000	1.3590	0.0000007	0.095	0.023161
11363.60	0.8800	1.3591	0.0000001	0.021	0.023168
11627.90	0.8600	1.3591	0.0000003	0.046	0.023176
11904.80	0.8400	1.3592	0.0000005	0.069	0.023183
12195.10	0.8200	1.3593	0.0000004	0.066	0.023191
12500.00	0.8000	1.3593	0.0000006	0.096	0.023197
12820.50	0.7800	1.3594	0.0000007	0.111	0.023203
13157.90	0.7600	1.3595	0.0000007	0.111	0.023211
13513.50	0.7400	1.3595	0.0000005	0.087	0.023218
13888.90	0.7200	1.3596	0.0000011	0.187	0.023225
14285.70	0.7000	1.3597	0.0000011	0.192	0.023232
14705.90	0.6800	1.3597	0.0000012	0.214	0.023238
15151.50	0.6600	1.3598	0.0000013	0.251	0.023245
15625.00	0.6400	1.3598	0.0000011	0.217	0.023252
16129.00	0.6200	1.3599	0.0000007	0.151	0.023259
16666.70	0.6000	1.3600	0.0000005	0.100	0.023266
17241.40	0.5800	1.3600	0.0000002	0.053	0.023273
17857.10	0.5600	1.3601	0.0000000	0.010	0.023280
18518.50	0.5400	1.3602	0.0000002	0.056	0.023287
19230.80	0.5200	1.3602	0.0000004	0.103	0.023294
20000.00	0.5000	1.3603	0.0000005	0.129	0.023301
20833.30	0.4800	1.3604	0.0000004	0.099	0.023309
21739.10	0.4600	1.3604	0.0000001	0.029	0.023316
22727.30	0.4400	1.3605	0.0000000	0.006	0.023324
23809.50	0.4200	1.3606	0.0000001	0.021	0.023332
25000.00	0.4000	1.3606	0.0000001	0.017	0.023340
26315.80	0.3800	1.3607	0.0000000	0.011	0.023349
27777.80	0.3600	1.3608	0.0000001	0.019	0.023359
29411.80	0.3400	1.3609	0.0000002	0.073	0.023369

TABLE 2-Continued

WN	WL	n	k	LAC	R
31250.00	0.3200	1.3610	0.0000001	0.047	0.023380
33333.30	0.3000	1.3611	0.0000002	0.094	0.023393
35714.30	0.2800	1.3613	0.0000254	11.406	0.023407
38461.50	0.2600	1.3614	0.0000201	9.735	0.023423
41666.70	0.2400	1.3616	0.0000904	47.314	0.023445
45454.50	0.2200	1.3617	0.0001369	78.220	0.023457

TABLE 3. METHYL ALCOHOL

THE COMPLEX REFRACTIVE INDEX, LAMBERT ABSORPTION COEFFICIENT, AND REFLECTION COEFFICIENT.

WN	WL	n	k	LAC	R
501.00	19.9601	1.4851	0.0597325	376.061	0.038656
520.00	19.2308	1.4589	0.0653928	427.310	0.035518
540.00	18.5185	1.4423	0.0791971	537.419	0.033813
560.00	17.8571	1.4308	0.0884773	622.630	0.032693
580.00	17.2414	1.4199	0.0994601	724.914	0.031750
600.00	16.6667	1.4059	0.1051930	793.137	0.030319
620.00	16.1290	1.3910	0.1120410	872.928	0.028870
640.00	15.6250	1.3745	0.1122020	902.382	0.027049
660.00	15.1515	1.3593	0.1106800	917.958	0.025341
680.00	14.7059	1.3438	0.1032620	882.387	0.023417
700.00	14.2857	1.3345	0.0952094	837.506	0.022158
720.00	13.8889	1.3259	0.0833996	754.582	0.020890
740.00	13.5135	1.3229	0.0745310	693.072	0.020336
760.00	13.1579	1.3173	0.0641244	612.416	0.019497
780.00	12.8205	1.3188	0.0496458	486.617	0.019348
800.00	12.5000	1.3222	0.0408703	410.873	0.019555
820.00	12.1951	1.3276	0.0324905	334.796	0.019997
840.00	11.9048	1.3345	0.0260457	274.932	0.020657
860.00	11.6279	1.3426	0.0205907	222.525	0.021463
880.00	11.3636	1.3521	0.0173633	192.010	0.022458
900.00	11.1111	1.3631	0.0151996	171.903	0.023647
920.00	10.8696	1.3760	0.0149717	173.089	0.025079
940.00	10.6383	1.3916	0.0160247	189.290	0.026857
960.00	10.4167	1.4148	0.0196042	236.500	0.029566
980.00	10.2041	1.4532	0.0289555	356.588	0.034268
1000.00	10.0000	1.5344	0.0744723	935.847	0.045279
1020.00	9.8039	1.5851	0.3515310	4505.818	0.068458
1040.00	9.6154	1.0473	0.3478670	4546.283	0.028580
1060.00	9.4340	1.1597	0.0682629	909.286	0.006462
1080.00	9.2593	1.2342	0.0405682	550.579	0.011317
1100.00	9.0909	1.2670	0.0478800	661.846	0.014312
1120.00	8.9286	1.2594	0.0503270	708.319	0.013670
1140.00	8.7719	1.2652	0.0259062	371.123	0.013835
1160.00	8.6207	1.2805	0.0184453	268.877	0.015196
1180.00	8.4746	1.2912	0.0162840	241.464	0.016207
1200.00	8.3333	1.2983	0.0159402	240.373	0.016898
1220.00	8.1967	1.3042	0.0150969	231.450	0.017469
1240.00	8.0645	1.3093	0.0148830	231.911	0.017981
1260.00	7.9365	1.3141	0.0146682	232.251	0.018463
1280.00	7.8125	1.3189	0.0157290	253.000	0.018957

TABLE 3-Continued

WN	WL	n	k	LAC	R
1300.00	7.6923	1.3230	0.0168078	274.577	0.019388
1320.00	7.5758	1.3276	0.0185703	308.037	0.019867
1340.00	7.4627	1.3328	0.0212473	357.782	0.020429
1360.00	7.3529	1.3401	0.0286154	489.045	0.021267
1380.00	7.2464	1.3390	0.0404401	701.296	0.021303
1400.00	7.1429	1.3353	0.0518201	911.667	0.021093
1420.00	7.0423	1.3203	0.0608246	1085.369	0.019729
1440.00	6.9444	1.3136	0.0568268	1028.314	0.018963
1460.00	6.8493	1.2922	0.0622233	1141.605	0.016977
1480.00	6.7568	1.2792	0.0435456	809.871	0.015363
1500.00	6.6667	1.2808	0.0255235	481.107	0.015282
1520.00	6.5789	1.2879	0.0176907	337.908	0.015897
1540.00	6.4935	1.2932	0.0136297	263.765	0.016378
1560.00	6.4103	1.2968	0.0110640	216.894	0.016719
1580.00	6.3291	1.2999	0.0088380	175.477	0.017017
1600.00	6.2500	1.3026	0.0073774	148.331	0.017278
1620.00	6.1728	1.3051	0.0059530	121.188	0.017529
1640.00	6.0976	1.3073	0.0051657	106.459	0.017746
1660.00	6.0241	1.3092	0.0043520	90.782	0.017933
1680.00	5.9524	1.3112	0.0038688	81.677	0.018128
1700.00	5.8824	1.3126	0.0033603	71.785	0.018270
1720.00	5.8140	1.3141	0.0029252	63.226	0.018425
1740.00	5.7471	1.3155	0.0026760	58.511	0.018566
1760.00	5.6818	1.3168	0.0023431	51.822	0.018696
1780.00	5.6180	1.3178	0.0021800	48.762	0.018805
1800.00	5.5556	1.3190	0.0018868	42.679	0.018925
1820.00	5.4945	1.3201	0.0017776	40.654	0.019039
1840.00	5.4348	1.3210	0.0015649	36.184	0.019131
1860.00	5.3763	1.3221	0.0014677	34.305	0.019240
1880.00	5.3191	1.3230	0.0013439	31.750	0.019339
1900.00	5.2632	1.3239	0.0012406	29.621	0.019431
1920.00	5.2083	1.3248	0.0011925	28.773	0.019522
1940.00	5.1546	1.3259	0.0011028	26.884	0.019628
1960.00	5.1020	1.3268	0.0011244	27.694	0.019723
1980.00	5.0505	1.3278	0.0011719	29.159	0.019829
2000.00	5.0000	1.3290	0.0016053	40.346	0.019960
2020.00	4.9505	1.3301	0.0025083	63.671	0.020066
2040.00	4.9020	1.3297	0.0044534	114.165	0.020028
2060.00	4.8544	1.3280	0.0035277	91.319	0.019852
2080.00	4.8077	1.3286	0.0019878	51.958	0.019910
2100.00	4.7619	1.3297	0.0013635	35.982	0.020024
2120.00	4.7170	1.3307	0.0011946	31.824	0.020137
2140.00	4.6729	1.3317	0.0011834	31.824	0.020238
2160.00	4.6296	1.3325	0.0012118	32.892	0.020324
2180.00	4.5872	1.3334	0.0014224	38.966	0.020415
2200.00	4.5455	1.3342	0.0017567	48.566	0.020495
2220.00	4.5045	1.3345	0.0021275	59.351	0.020529
2240.00	4.4643	1.3346	0.0020775	58.478	0.020540

TABLE 3-Continued

WN	WL	n	k	LAC	R
2260.00	4.4248	1.3351	0.0016364	46.475	0.020595
2280.00	4.3860	1.3359	0.0013035	37.348	0.020677
2300.00	4.3478	1.3367	0.0010703	30.935	0.020768
2320.00	4.3103	1.3379	0.0009943	28.988	0.020887
2340.00	4.2735	1.3389	0.0010468	30.781	0.020998
2360.00	4.2373	1.3400	0.0011385	33.763	0.021112
2380.00	4.2017	1.3412	0.0014266	42.667	0.021240
2400.00	4.1667	1.3425	0.0018817	56.750	0.021375
2420.00	4.1322	1.3434	0.0026512	80.625	0.021478
2440.00	4.0984	1.3442	0.0032580	99.896	0.021560
2460.00	4.0650	1.3452	0.0037925	117.240	0.021673
2480.00	4.0323	1.3463	0.0048509	151.177	0.021783
2500.00	4.0000	1.3465	0.0063619	199.864	0.021813
2520.00	3.9683	1.3459	0.0070848	224.356	0.021747
2540.00	3.9370	1.3456	0.0065686	209.659	0.021718
2560.00	3.9063	1.3463	0.0059558	191.599	0.021786
2580.00	3.8760	1.3474	0.0058736	190.429	0.021911
2600.00	3.8462	1.3480	0.0059586	194.682	0.021978
2620.00	3.8168	1.3488	0.0050378	165.863	0.022058
2640.00	3.7879	1.3509	0.0041920	139.070	0.022283
2660.00	3.7594	1.3534	0.0039009	130.392	0.022558
2680.00	3.7313	1.3564	0.0039872	134.282	0.022874
2700.00	3.7037	1.3598	0.0045194	153.339	0.023247
2720.00	3.6765	1.3639	0.0055860	190.933	0.023700
2740.00	3.6496	1.3687	0.0076445	263.213	0.024236
2760.00	3.6232	1.3746	0.0121778	422.365	0.024917
2780.00	3.5971	1.3788	0.0169423	591.871	0.025412
2800.00	3.5714	1.3869	0.0297751	1047.662	0.026423
2820.00	3.5461	1.3839	0.0506963	1796.533	0.026372
2840.00	3.5211	1.3522	0.0550731	1965.476	0.022955
2860.00	3.4965	1.3530	0.0363688	1307.088	0.022735
2880.00	3.4722	1.3663	0.0355701	1287.323	0.024188
2900.00	3.4483	1.3686	0.0514070	1873.398	0.024682
2920.00	3.4247	1.3620	0.0602812	2211.946	0.024124
2940.00	3.4014	1.3471	0.0786782	2906.776	0.022973
2960.00	3.3784	1.3218	0.0598631	2226.695	0.019861
2980.00	3.3557	1.3217	0.0529112	1981.407	0.019706
3000.00	3.3333	1.3143	0.0354270	1338.566	0.018676
3020.00	3.3113	1.3256	0.0251151	953.129	0.019720
3040.00	3.2896	1.3325	0.0231057	882.679	0.020418
3060.00	3.2680	1.3397	0.0209386	805.154	0.021158
3080.00	3.2468	1.3457	0.0228957	886.165	0.021810
3100.00	3.2258	1.3513	0.0234277	912.644	0.022419
3120.00	3.2051	1.3575	0.0278447	1091.709	0.023130
3140.00	3.1847	1.3614	0.0316286	1248.014	0.023601
3160.00	3.1646	1.3671	0.0375717	1491.962	0.024296
3180.00	3.1447	1.3701	0.0450040	1798.408	0.024737
3200.00	3.1250	1.3764	0.0553791	2226.926	0.025621

TABLE 3-Continued

WN	WL	n	k	LAC	R
3220.00	3.1056	1.3714	0.0682834	2763.000	0.025335
3240.00	3.0864	1.3711	0.0775644	3158.038	0.025533
3260.00	3.0675	1.3625	0.0919696	3767.661	0.025023
3280.00	3.0488	1.3541	0.0983896	4055.393	0.024335
3300.00	3.0303	1.3430	0.1108050	4594.975	0.023613
3320.00	3.0120	1.3274	0.1130480	4716.402	0.022097
3340.00	2.9940	1.3143	0.1188450	4988.124	0.021021
3360.00	2.9762	1.2940	0.1154550	4874.857	0.018913
3380.00	2.9586	1.2820	0.1105550	4695.750	0.017580
3400.00	2.9412	1.2645	0.1015310	4337.979	0.015623
3420.00	2.9240	1.2590	0.0881010	3786.316	0.014648
3440.00	2.9070	1.2496	0.0796555	3443.373	0.013536
3460.00	2.8902	1.2471	0.0640387	2784.380	0.012896
3480.00	2.8736	1.2433	0.0569714	2491.415	0.012398
3500.00	2.8571	1.2411	0.0394990	1737.257	0.011880
3520.00	2.8409	1.2477	0.0303738	1343.543	0.012324
3540.00	2.8249	1.2508	0.0216979	965.230	0.012512
3560.00	2.8090	1.2573	0.0150992	675.482	0.013034
3580.00	2.7933	1.2615	0.0105511	474.669	0.013394
3600.00	2.7778	1.2673	0.0062577	283.093	0.013906
3620.00	2.7624	1.2722	0.0040446	183.988	0.014352
3640.00	2.7473	1.2765	0.0024782	113.356	0.014753
3660.00	2.7322	1.2803	0.0014436	66.397	0.015113
3680.00	2.7174	1.2837	0.0009430	43.606	0.015433
3700.00	2.7027	1.2865	0.0007193	33.446	0.015702
3720.00	2.6882	1.2888	0.0006032	28.197	0.015924
3740.00	2.6738	1.2909	0.0004923	23.139	0.016121
3760.00	2.6596	1.2927	0.0004007	18.934	0.016299
3780.00	2.6455	1.2943	0.0003371	16.012	0.016453
3800.00	2.6316	1.2958	0.0002864	13.676	0.016599
3828.48	2.6120	1.2977	0.0002912	14.008	0.016788
3858.02	2.5920	1.2994	0.0005680	27.538	0.016951
3888.02	2.5720	1.3007	0.0003940	19.252	0.017086
3918.50	2.5520	1.3023	0.0004931	24.281	0.017236
3949.45	2.5320	1.3034	0.0007715	38.289	0.017353
3980.89	2.5120	1.3042	0.0009821	49.127	0.017434
4012.84	2.4920	1.3050	0.0008729	44.019	0.017513
4045.31	2.4720	1.3059	0.0007065	35.913	0.017595
4078.30	2.4520	1.3067	0.0005984	30.666	0.017682
4111.84	2.4320	1.3075	0.0005236	27.056	0.017760
4145.94	2.4120	1.3083	0.0003630	18.910	0.017839
4180.60	2.3920	1.3091	0.0003059	16.073	0.017922
4215.85	2.3720	1.3100	0.0003299	17.479	0.018008
4251.70	2.3520	1.3107	0.0005364	28.662	0.018077
4288.16	2.3320	1.3112	0.0005924	31.920	0.018126
4325.26	2.3120	1.3119	0.0006242	33.925	0.018199
4363.00	2.2920	1.3124	0.0010448	57.285	0.018254
4401.41	2.2720	1.3123	0.0013872	76.728	0.018242

TABLE 3-Continued

WN	WL	n	k	LAC	R
4440.50	2.2520	1.3123	0.0008833	49.289	0.018237
4480.29	2.2320	1.3128	0.0004540	25.563	0.018293
4520.80	2.2120	1.3134	0.0002891	16.425	0.018354
4562.04	2.1920	1.3139	0.0002147	12.307	0.018406
4604.05	2.1720	1.3144	0.0001954	11.307	0.018457
4646.84	2.1520	1.3149	0.0001945	11.360	0.018505
4690.43	2.1320	1.3153	0.0002113	12.452	0.018547
4734.85	2.1120	1.3157	0.0002448	14.563	0.018585
4780.11	2.0920	1.3160	0.0002911	17.484	0.018619
4826.25	2.0720	1.3163	0.0003214	19.491	0.018646
4873.29	2.0520	1.3165	0.0002897	17.741	0.018671
4921.26	2.0320	1.3168	0.0002078	12.850	0.018699
4970.18	2.0120	1.3171	0.0001289	8.051	0.018729
5020.08	1.9920	1.3174	0.0000865	5.458	0.018760
5070.99	1.9720	1.3177	0.0000611	3.892	0.018795
5122.95	1.9520	1.3180	0.0000491	3.160	0.018824
5175.98	1.9320	1.3183	0.0000378	2.462	0.018853
5230.13	1.9120	1.3186	0.0000386	2.539	0.018881
5285.41	1.8920	1.3189	0.0000339	2.249	0.018908
5341.88	1.8720	1.3191	0.0000348	2.339	0.018932
5399.57	1.8520	1.3193	0.0000395	2.680	0.018958
5458.52	1.8320	1.3196	0.0000443	3.037	0.018983
5518.76	1.8120	1.3198	0.0000499	3.458	0.019006
5580.36	1.7920	1.3200	0.0000556	3.898	0.019029
5643.34	1.7720	1.3202	0.0000689	4.885	0.019050
5707.76	1.7520	1.3204	0.0000890	6.386	0.019069
5773.67	1.7320	1.3206	0.0001185	8.600	0.019091
5841.12	1.7120	1.3208	0.0001303	9.567	0.019108
5910.17	1.6920	1.3209	0.0001354	10.057	0.019122
5980.86	1.6720	1.3211	0.0000909	6.833	0.019138
6053.27	1.6520	1.3213	0.0000802	6.102	0.019161
6127.45	1.6320	1.3215	0.0000909	6.995	0.019181
6203.47	1.6120	1.3217	0.0001135	8.846	0.019198
6281.41	1.5920	1.3218	0.0001331	10.507	0.019213
6361.32	1.5720	1.3219	0.0001358	10.858	0.019224
6443.30	1.5520	1.3221	0.0001260	10.204	0.019238
6527.42	1.5320	1.3222	0.0001152	9.447	0.019254
6613.76	1.5120	1.3224	0.0001085	9.021	0.019268
6702.41	1.4920	1.3225	0.0001008	8.491	0.019280
6793.48	1.4720	1.3226	0.0000904	7.718	0.019293
6887.05	1.4520	1.3227	0.0000752	6.507	0.019307
6983.24	1.4320	1.3229	0.0000574	5.033	0.019323
7082.15	1.4120	1.3230	0.0000460	4.095	0.019334
7183.91	1.3920	1.3232	0.0000285	2.577	0.019350
7288.63	1.3720	1.3233	0.0000204	1.870	0.019364
7396.45	1.3520	1.3234	0.0000147	1.365	0.019378
7507.51	1.3320	1.3235	0.0000067	0.633	0.019390
7621.95	1.3120	1.3237	0.0000048	0.459	0.019403

TABLE 3-Continued

WN	WL	n	k	LAC	R
7739.94	1.2920	1.3238	0.0000044	0.432	0.019414
7861.64	1.2720	1.3239	0.0000052	0.515	0.019427
7987.22	1.2520	1.3240	0.0000063	0.628	0.019439
8116.88	1.2320	1.3242	0.0000060	0.612	0.019452
8250.83	1.2120	1.3243	0.0000098	1.020	0.019464
8389.26	1.1920	1.3244	0.0000141	1.488	0.019475
8532.42	1.1720	1.3245	0.0000096	1.032	0.019484
8680.56	1.1520	1.3246	0.0000060	0.658	0.019496
8833.92	1.1320	1.3247	0.0000029	0.323	0.019506
8992.81	1.1120	1.3248	0.0000018	0.208	0.019515
9157.51	1.0920	1.3249	0.0000019	0.218	0.019526
9328.36	1.0720	1.3250	0.0000022	0.253	0.019536
9505.70	1.0520	1.3251	0.0000024	0.287	0.019547
9689.92	1.0320	1.3252	0.0000025	0.301	0.019557
9881.42	1.0120	1.3252	0.0000026	0.318	0.019565
10080.60	0.9920	1.3253	0.0000022	0.272	0.019575
10288.10	0.9720	1.3254	0.0000015	0.200	0.019584
10504.20	0.9520	1.3255	0.0000012	0.156	0.019593
10729.60	0.9320	1.3256	0.0000013	0.172	0.019603
10964.90	0.9120	1.3257	0.0000015	0.212	0.019611
11210.80	0.8920	1.3258	0.0000010	0.139	0.019620
11467.90	0.8720	1.3259	0.0000006	0.084	0.019628
11737.10	0.8520	1.3260	0.0000005	0.074	0.019639
12019.20	0.8320	1.3260	0.0000005	0.071	0.019646
12315.30	0.8120	1.3261	0.0000004	0.069	0.019655
12626.30	0.7920	1.3262	0.0000002	0.038	0.019663
12953.40	0.7720	1.3263	0.0000003	0.041	0.019671
13297.90	0.7520	1.3264	0.0000002	0.038	0.019680
13661.20	0.7320	1.3264	0.0000003	0.046	0.019689
14044.90	0.7120	1.3265	0.0000002	0.044	0.019697
14450.90	0.6920	1.3266	0.0000003	0.051	0.019704
14881.00	0.6720	1.3267	0.0000003	0.049	0.019713
15337.40	0.6520	1.3267	0.0000004	0.079	0.019721
15822.80	0.6320	1.3268	0.0000005	0.106	0.019729
16339.90	0.6120	1.3269	0.0000005	0.109	0.019737
16891.90	0.5920	1.3270	0.0000006	0.120	0.019745
17482.50	0.5720	1.3271	0.0000006	0.137	0.019754
18115.90	0.5520	1.3271	0.0000007	0.161	0.019762
18797.00	0.5320	1.3272	0.0000007	0.163	0.019771
19531.30	0.5120	1.3273	0.0000007	0.162	0.019779
20325.20	0.4920	1.3274	0.0000006	0.164	0.019788
21186.40	0.4720	1.3275	0.0000005	0.140	0.019797
22123.90	0.4520	1.3276	0.0000005	0.149	0.019806
23148.10	0.4320	1.3277	0.0000006	0.163	0.019816
24271.80	0.4120	1.3278	0.0000007	0.218	0.019826
25510.20	0.3920	1.3279	0.0000010	0.321	0.019836
26881.70	0.3720	1.3280	0.0000014	0.478	0.019847
28409.10	0.3520	1.3281	0.0000020	0.728	0.019859

TABLE 3-Continued

WN	WL	n	k	LAC	R
30120.50	0.3320	1.3282	0.0000030	1.126	0.019872
32051.30	0.3120	1.3283	0.0000036	1.463	0.019885
34246.60	0.2920	1.3285	0.0000075	3.231	0.019901
36764.70	0.2720	1.3286	0.0000208	9.624	0.019918
39682.50	0.2520	1.3289	0.0000269	13.420	0.019940
43103.40	0.2320	1.3291	0.0000892	48.312	0.019963
47169.80	0.2120	1.3293	0.0001082	64.154	0.019983

TABLE 4. SF96

THE COMPLEX REFRACTIVE INDEX, LAMBERT ABSORPTION COEFFICIENT, AND REFLECTION COEFFICIENT.

WN	WL	n	k	LAC	R
501.00	19.9601	1.5415	0.0230116	144.875	0.045474
520.00	19.2308	1.5223	0.0199854	130.595	0.042943
540.00	18.5185	1.5229	0.0171470	116.357	0.043003
560.00	17.8571	1.5274	0.0154602	108.796	0.043586
580.00	17.2414	1.5341	0.0145499	106.047	0.044454
600.00	16.6667	1.5432	0.0146418	110.397	0.045650
620.00	16.1290	1.5543	0.0155933	121.490	0.047130
640.00	15.6250	1.5721	0.0158996	127.872	0.049515
660.00	15.1515	1.6030	0.0497583	412.686	0.054008
680.00	14.7059	1.5925	0.0675967	577.623	0.052872
700.00	14.2857	1.5722	0.0809607	712.168	0.050432
720.00	13.8889	1.5810	0.0297691	269.344	0.050793
740.00	13.5135	1.6465	0.0308537	286.912	0.059803
760.00	13.1579	1.7275	0.0500747	478.236	0.071459
780.00	12.8205	1.9445	0.1512790	1482.802	0.105250
800.00	12.5000	1.7634	0.8693580	8739.740	0.159501
820.00	12.1951	1.0935	0.5088630	5243.540	0.057670
840.00	11.9048	1.2391	0.1619460	1709.462	0.016549
860.00	11.6279	1.3318	0.1314450	1420.537	0.023352
880.00	11.3636	1.3234	0.0925253	1023.182	0.020931
900.00	11.1111	1.3828	0.0331095	374.460	0.026001
920.00	10.8696	1.4446	0.0192997	223.125	0.033141
940.00	10.6383	1.5018	0.0173357	204.776	0.040271
960.00	10.4167	1.5674	0.0252991	305.201	0.048929
980.00	10.2041	1.6590	0.0497192	612.294	0.061755
1000.00	10.0000	1.8257	0.1404620	1765.098	0.087644
1020.00	9.8039	1.7345	0.6137410	7866.747	0.116647
1040.00	9.6154	1.4227	0.5270510	6888.043	0.074252
1060.00	9.4340	1.3747	0.4587470	6110.672	0.059975
1080.00	9.2593	1.3445	0.5138900	6974.351	0.066444
1100.00	9.0909	1.0636	0.5731940	7923.265	0.072507
1120.00	8.9286	0.9486	0.2046480	2880.285	0.011600
1140.00	8.7719	1.0751	0.0933754	1337.665	0.003329
1160.00	8.6207	1.1510	0.0423881	617.891	0.005315
1180.00	8.4746	1.2143	0.0220567	327.064	0.009468
1200.00	8.3333	1.2680	0.0133432	201.211	0.013994
1220.00	8.1967	1.3276	0.0129569	198.642	0.019840
1240.00	8.0645	1.4634	0.0592214	922.806	0.035947
1260.00	7.9365	1.2925	0.4363780	6909.447	0.050675
1280.00	7.8125	1.0639	0.0766128	1232.313	0.002333

TABLE 4-Continued

WN	WL	n	k	LAC	R
1300.00	7.6923	1.1981	0.0117679	192.244	0.008148
1320.00	7.5758	1.2406	0.0074808	124.089	0.011540
1340.00	7.4627	1.2649	0.0061588	103.707	0.013683
1360.00	7.3529	1.2820	0.0063388	108.331	0.015282
1380.00	7.2464	1.2961	0.0077329	134.101	0.016643
1400.00	7.1429	1.3059	0.0187739	330.288	0.017662
1420.00	7.0423	1.2958	0.0162559	290.074	0.016649
1440.00	6.9444	1.3064	0.0099567	180.173	0.017665
1460.00	6.8493	1.3096	0.0058247	106.865	0.017977
1480.00	6.7568	1.3172	0.0045284	84.220	0.018741
1500.00	6.6667	1.3224	0.0038735	73.014	0.019271
1520.00	6.5789	1.3269	0.0037018	70.707	0.019737
1540.00	6.4935	1.3308	0.0037454	72.483	0.020150
1560.00	6.4103	1.3342	0.0038200	74.886	0.020500
1580.00	6.3291	1.3373	0.0042701	84.782	0.020831
1600.00	6.2500	1.3391	0.0047506	95.516	0.021016
1620.00	6.1728	1.3408	0.0040057	81.546	0.021203
1640.00	6.0976	1.3430	0.0035233	72.611	0.021432
1660.00	6.0241	1.3451	0.0029582	61.708	0.021653
1680.00	5.9524	1.3472	0.0027225	57.475	0.021885
1700.00	5.8824	1.3491	0.0025640	54.774	0.022085
1720.00	5.8140	1.3507	0.0025321	54.728	0.022263
1740.00	5.7471	1.3523	0.0021597	47.223	0.022428
1760.00	5.6818	1.3539	0.0021250	46.999	0.022602
1780.00	5.6180	1.3550	0.0020468	45.784	0.022723
1800.00	5.5556	1.3562	0.0014826	33.536	0.022850
1820.00	5.4945	1.3576	0.0009753	22.305	0.023012
1840.00	5.4348	1.3593	0.0006637	15.346	0.023190
1860.00	5.3763	1.3608	0.0006738	15.749	0.023362
1880.00	5.3191	1.3622	0.0007919	18.709	0.023510
1900.00	5.2632	1.3635	0.0009322	22.258	0.023652
1920.00	5.2083	1.3647	0.0014199	34.258	0.023784
1940.00	5.1546	1.3653	0.0022384	54.569	0.023855
1960.00	5.1020	1.3650	0.0019592	48.256	0.023821
1980.00	5.0505	1.3657	0.0010508	26.145	0.023901
2000.00	5.0000	1.3668	0.0007778	19.548	0.024022
2020.00	4.9505	1.3679	0.0004549	11.548	0.024145
2040.00	4.9020	1.3692	0.0007705	19.753	0.024287
2060.00	4.8544	1.3694	0.0010598	27.434	0.024309
2080.00	4.8077	1.3700	0.0007690	20.099	0.024374
2100.00	4.7619	1.3707	0.0005904	15.579	0.024456
2120.00	4.7170	1.3715	0.0005567	14.832	0.024537
2140.00	4.6729	1.3720	0.0005006	13.462	0.024601
2160.00	4.6296	1.3727	0.0003517	9.547	0.024672
2180.00	4.5872	1.3734	0.0002957	8.100	0.024751
2200.00	4.5455	1.3740	0.0003195	8.833	0.024817
2220.00	4.5045	1.3745	0.0002718	7.581	0.024880
2240.00	4.4643	1.3751	0.0002507	7.057	0.024941

TABLE 4-Continued

WN	WL	n	k	LA	R
2260.00	4.4248	1.3756	0.0001972	5.602	0.025002
2280.00	4.3860	1.3762	0.0002141	6.134	0.025061
2300.00	4.3478	1.3766	0.0001412	4.082	0.025114
2320.00	4.3103	1.3772	0.0001255	3.658	0.025176
2340.00	4.2735	1.3776	0.0001144	3.364	0.025227
2360.00	4.2373	1.3782	0.0000829	2.457	0.025285
2380.00	4.2017	1.3786	0.0000957	2.862	0.025334
2400.00	4.1667	1.3791	0.0000499	1.504	0.025389
2420.00	4.1322	1.3795	0.0000958	2.914	0.025439
2440.00	4.0984	1.3800	0.0000527	1.617	0.025489
2460.00	4.0650	1.3805	0.0001132	3.499	0.025544
2480.00	4.0323	1.3809	0.0001537	4.789	0.025596
2500.00	4.0000	1.3811	0.0004858	15.261	0.025619
2520.00	3.9683	1.3814	0.0001399	4.431	0.025647
2540.00	3.9370	1.3819	0.0000780	2.491	0.025706
2560.00	3.9063	1.3823	0.0000982	3.160	0.025752
2580.00	3.8760	1.3828	0.0000633	2.052	0.025804
2600.00	3.8462	1.3832	0.0001235	4.036	0.025853
2620.00	3.8168	1.3836	0.0001130	3.720	0.025904
2640.00	3.7879	1.3841	0.0002745	9.107	0.025962
2660.00	3.7594	1.3844	0.0004747	15.866	0.025988
2680.00	3.7313	1.3847	0.0003403	11.461	0.026022
2700.00	3.7037	1.3852	0.0002959	10.038	0.026077
2720.00	3.6765	1.3857	0.0002849	9.737	0.026140
2740.00	3.6496	1.3863	0.0003681	12.674	0.026208
2760.00	3.6232	1.3871	0.0005064	17.562	0.026293
2780.00	3.5971	1.3879	0.0011190	39.093	0.026386
2800.00	3.5714	1.3879	0.0017778	62.554	0.026392
2820.00	3.5461	1.3882	0.0017821	63.153	0.026419
2840.00	3.5211	1.3889	0.0018471	65.921	0.026500
2860.00	3.4965	1.3900	0.0020667	74.277	0.026631
2880.00	3.4722	1.3918	0.0031431	113.754	0.026832
2900.00	3.4483	1.3924	0.0070412	256.597	0.026905
2920.00	3.4247	1.3912	0.0051079	187.426	0.026773
2940.00	3.4014	1.3988	0.0071750	265.081	0.027649
2960.00	3.3784	1.3884	0.0402845	1498.441	0.026724
2980.00	3.3557	1.3678	0.0077239	289.243	0.024138
3000.00	3.3333	1.3758	0.0032838	123.798	0.025021
3020.00	3.3113	1.3791	0.0020579	78.100	0.025397
3040.00	3.2895	1.3809	0.0018460	70.522	0.025600
3060.00	3.2680	1.3818	0.0017546	67.469	0.025701
3080.00	3.2468	1.3825	0.0015612	60.426	0.025777
3100.00	3.2258	1.3830	0.0014858	57.882	0.025831
3120.00	3.2051	1.3833	0.0012834	50.317	0.025861
3140.00	3.1847	1.3836	0.0009549	37.677	0.025901
3160.00	3.1646	1.3841	0.0006994	27.772	0.025952
3180.00	3.1447	1.3845	0.0005808	23.209	0.026001
3200.00	3.1250	1.3849	0.0004748	19.093	0.026042

TABLE 4-Continued

WN	WL	n	k	LAC	R
3220.00	3.1056	1.3852	0.0004243	17.170	0.026082
3240.00	3.0864	1.3855	0.0003473	14.141	0.026113
3260.00	3.0675	1.3858	0.0002928	11.997	0.026150
3280.00	3.0488	1.3861	0.0002676	11.030	0.026179
3300.00	3.0303	1.3863	0.0002289	9.492	0.026210
3320.00	3.0120	1.3866	0.0002274	9.485	0.026236
3340.00	2.9940	1.3868	0.0001945	8.165	0.026260
3360.00	2.9762	1.3870	0.0001731	7.309	0.026283
3380.00	2.9586	1.3872	0.0001168	4.963	0.026308
3400.00	2.9412	1.3874	0.0001026	4.384	0.026335
3420.00	2.9240	1.3876	0.0000919	3.949	0.026359
3440.00	2.9070	1.3879	0.0001000	4.323	0.026385
3460.00	2.8902	1.3881	0.0001251	5.441	0.026406
3480.00	2.8736	1.3882	0.0001282	5.605	0.026428
3500.00	2.8571	1.3884	0.0001534	6.749	0.026449
3520.00	2.8409	1.3886	0.0001738	7.689	0.026470
3540.00	2.8249	1.3888	0.0002101	9.346	0.026492
3560.00	2.8090	1.3890	0.0002786	12.462	0.026516
3580.00	2.7933	1.3892	0.0004316	19.416	0.026533
3600.00	2.7778	1.3892	0.0004995	22.595	0.026536
3620.00	2.7624	1.3893	0.0005168	23.507	0.026553
3640.00	2.7473	1.3894	0.0006831	31.245	0.026558
3660.00	2.7322	1.3894	0.0005834	26.832	0.026559
3680.00	2.7174	1.3897	0.0006736	31.150	0.026590
3700.00	2.7027	1.3896	0.0009668	44.950	0.026580
3720.00	2.6882	1.3894	0.0008619	40.293	0.026559
3740.00	2.6738	1.3895	0.0007356	34.570	0.026572
3760.00	2.6596	1.3895	0.0008619	40.725	0.026571
3780.00	2.6455	1.3893	0.0007229	34.340	0.026549
3800.00	2.6316	1.3894	0.0004007	19.133	0.026557
3828.48	2.6120	1.3897	0.0002995	14.411	0.026593
3858.02	2.5920	1.3898	0.0001613	7.821	0.026610
3888.02	2.5720	1.3901	0.0001123	5.486	0.026642
3918.50	2.5520	1.3903	0.0001007	4.961	0.026665
3949.45	2.5320	1.3905	0.0001057	5.248	0.026690
3980.89	2.5120	1.3907	0.0001402	7.012	0.026711
4012.84	2.4920	1.3909	0.0001795	9.053	0.026729
4045.31	2.4720	1.3910	0.0002839	14.433	0.026742
4078.30	2.4520	1.3910	0.0002137	10.951	0.026744
4111.84	2.4320	1.3912	0.0001165	6.018	0.026766
4145.94	2.4120	1.3915	0.0001616	8.417	0.026794
4180.60	2.3920	1.3915	0.0001735	9.113	0.026801
4215.85	2.3720	1.3916	0.0004750	25.167	0.026816
4251.70	2.3520	1.3916	0.0001359	7.259	0.026814
4288.16	2.3320	1.3919	0.0001099	5.922	0.026846
4325.26	2.3120	1.3922	0.0002113	11.484	0.026882
4363.00	2.2920	1.3920	0.0007647	41.924	0.026855
4401.41	2.2720	1.3919	0.0002701	14.941	0.026845

TABLE 4-Continued

WN	WL	n	k	LAC	R
4440.50	2.2520	1.3921	0.0001443	8.052	0.026868
4480.29	2.2320	1.3923	0.0000941	5.299	0.026887
4520.80	2.2120	1.3924	0.0000717	4.074	0.026904
4562.04	2.1920	1.3926	0.0000436	2.498	0.026921
4604.05	2.1720	1.3927	0.0000273	1.581	0.026936
4646.84	2.1520	1.3928	0.0000179	1.046	0.026953
4690.43	2.1320	1.3930	0.0000100	0.590	0.026968
4734.85	2.1120	1.3931	0.0000073	0.434	0.026984
4780.11	2.0920	1.3932	0.0000058	0.346	0.026998
4826.25	2.0720	1.3934	0.0000051	0.307	0.027012
4873.29	2.0520	1.3935	0.0000060	0.369	0.027026
4921.26	2.0320	1.3936	0.0000082	0.509	0.027040
4970.18	2.0120	1.3937	0.0000092	0.577	0.027054
5020.08	1.9920	1.3938	0.0000110	0.696	0.027066
5070.99	1.9720	1.3939	0.0000105	0.666	0.027080
5122.95	1.9520	1.3941	0.0000064	0.415	0.027092
5175.98	1.9320	1.3942	0.0000056	0.363	0.027105
5230.13	1.9120	1.3943	0.0000039	0.258	0.027118
5285.41	1.8920	1.3944	0.0000023	0.154	0.027132
5341.88	1.8720	1.3945	0.0000023	0.152	0.027145
5399.57	1.8520	1.3946	0.0000226	1.534	0.027158
5458.52	1.8320	1.3947	0.0000181	1.244	0.027168
5518.76	1.8120	1.3948	0.0000044	0.304	0.027182
5580.36	1.7920	1.3950	0.0000207	1.450	0.027197
5643.34	1.7720	1.3951	0.0000216	1.532	0.027208
5707.76	1.7520	1.3952	0.0000818	5.869	0.027223
5773.67	1.7320	1.3952	0.0000622	4.511	0.027223
5841.12	1.7120	1.3954	0.0000314	2.304	0.027243
5910.17	1.6920	1.3954	0.0000838	6.225	0.027247
5980.86	1.6720	1.3955	0.0000089	0.669	0.027258
6053.27	1.6520	1.3956	0.0000080	0.607	0.027272
6127.45	1.6320	1.3957	0.0000030	0.232	0.027284
6203.47	1.6120	1.3958	0.0000012	0.095	0.027296
6281.41	1.5920	1.3959	0.0000010	0.076	0.027309
6361.32	1.5720	1.3960	0.0000018	0.145	0.027321
6443.30	1.5520	1.3961	0.0000050	0.404	0.027333
6527.42	1.5320	1.3962	0.0000056	0.457	0.027344
6613.76	1.5120	1.3963	0.0000044	0.362	0.027355
6702.41	1.4920	1.3964	0.0000016	0.132	0.027367
6793.48	1.4720	1.3965	0.0000015	0.127	0.027379
6887.05	1.4520	1.3967	0.0000015	0.130	0.027391
6983.24	1.4320	1.3967	0.0000036	0.313	0.027402
7082.15	1.4120	1.3969	0.0000095	0.845	0.027415
7183.91	1.3920	1.3969	0.0000116	1.051	0.027424
7288.63	1.3720	1.3970	0.0000072	0.655	0.027436
7396.45	1.3520	1.3971	0.0000011	0.107	0.027448
7507.51	1.3320	1.3972	0.0000007	0.063	0.027459
7621.95	1.3120	1.3973	0.0000004	0.036	0.027471

TABLE 4-Continued

WN	WL	n	k	LAC	R
7739.94	1.2920	1.3974	0.0000005	0.046	0.027483
7861.64	1.2720	1.3975	0.0000006	0.058	0.027494
7987.22	1.2520	1.3976	0.0000008	0.079	0.027506
8116.88	1.2320	1.3978	0.0000004	0.037	0.027518
8250.83	1.2120	1.3979	0.0000012	0.126	0.027530
8389.26	1.1920	1.3980	0.0000109	1.150	0.027542
8532.42	1.1720	1.3980	0.0000045	0.486	0.027552
8680.56	1.1520	1.3982	0.0000027	0.292	0.027564
8833.92	1.1320	1.3983	0.0000003	0.032	0.027576
8992.81	1.1120	1.3984	0.0000006	0.069	0.027588
9157.51	1.0920	1.3985	0.0000005	0.061	0.027601
9328.36	1.0720	1.3986	0.0000010	0.120	0.027613
9505.70	1.0520	1.3987	0.0000007	0.090	0.027625
9689.92	1.0320	1.3988	0.0000007	0.088	0.027638
9881.42	1.0120	1.3989	0.0000005	0.068	0.027650
10080.60	0.9920	1.3990	0.0000007	0.083	0.027663
10288.10	0.9720	1.3991	0.0000009	0.111	0.027676
10504.20	0.9520	1.3992	0.0000009	0.114	0.027689
10729.60	0.9320	1.3994	0.0000010	0.129	0.027703
10964.90	0.9120	1.3995	0.0000005	0.068	0.027717
11210.80	0.8920	1.3996	0.0000012	0.171	0.027730
11467.90	0.8720	1.3997	0.0000013	0.193	0.027745
11737.10	0.8520	1.3998	0.0000014	0.208	0.027759
12019.20	0.8320	1.4000	0.0000017	0.251	0.027774
12315.30	0.8120	1.4001	0.0000009	0.144	0.027789

TABLE 5. DIESEL FUEL

THE COMPLEX REFRACTIVE INDEX, LAMBERT ABSORPTION COEFFICIENT, AND REFLECTION COEFFICIENT.

WN	WL	n	k	LAC	R
501.00	19.9601	1.4479	0.0030147	18.980	0.033480
520.00	19.2308	1.4458	0.0027692	18.095	0.033226
540.00	18.5185	1.4444	0.0033380	22.651	0.033058
560.00	17.8571	1.4444	0.0024204	17.033	0.033047
580.00	17.2414	1.4442	0.0020706	15.092	0.033034
600.00	16.6667	1.4448	0.0015633	11.787	0.033096
620.00	16.1290	1.4455	0.0017220	13.416	0.033185
640.00	15.6250	1.4457	0.0015164	12.196	0.033215
660.00	15.1515	1.4471	0.0013375	11.093	0.033383
680.00	14.7059	1.4496	0.0012988	11.099	0.033686
700.00	14.2857	1.4518	0.0061748	54.316	0.033959
720.00	13.8889	1.4529	0.0114216	103.340	0.034108
740.00	13.5135	1.4467	0.0163399	151.947	0.033378
760.00	13.1579	1.4411	0.0108301	103.432	0.032673
780.00	12.8205	1.4403	0.0099617	97.642	0.032572
800.00	12.5000	1.4432	0.0089751	90.227	0.032924
820.00	12.1951	1.4366	0.0095909	98.829	0.032126
840.00	11.9048	1.4383	0.0068292	72.088	0.032321
860.00	11.6279	1.4391	0.0064551	69.761	0.032420
880.00	11.3636	1.4371	0.0071809	79.409	0.032180
900.00	11.1111	1.4370	0.0045442	51.394	0.032156
920.00	10.8696	1.4386	0.0038081	44.026	0.032347
940.00	10.6383	1.4395	0.0039253	46.367	0.032464
960.00	10.4167	1.4396	0.0047641	57.473	0.032478
980.00	10.2041	1.4389	0.0037210	45.824	0.032386
1000.00	10.0000	1.4399	0.0038234	48.046	0.032503
1020.00	9.8039	1.4400	0.0040972	52.517	0.032526
1040.00	9.6154	1.4391	0.0041072	53.677	0.032408
1060.00	9.4340	1.4395	0.0037222	49.581	0.032455
1080.00	9.2593	1.4395	0.0030882	41.912	0.032455
1100.00	9.0909	1.4400	0.0026595	36.762	0.032514
1120.00	8.9286	1.4410	0.0022788	32.073	0.032635
1140.00	8.7719	1.4417	0.0031817	45.579	0.032726
1160.00	8.6207	1.4412	0.0040512	59.054	0.032668
1180.00	8.4746	1.4409	0.0032693	48.479	0.032628
1200.00	8.3333	1.4412	0.0032712	49.329	0.032662
1220.00	8.1967	1.4417	0.0029728	45.575	0.032725
1240.00	8.0645	1.4423	0.0032743	51.022	0.032804
1260.00	7.9365	1.4430	0.0032382	51.272	0.032883
1280.00	7.8125	1.4436	0.0037523	60.355	0.032960

TABLE 5-Continued

WN	WL	n	k	LAC	R
1300.00	7.6923	1.4443	0.0048038	78.476	0.033050
1320.00	7.5758	1.4445	0.0046899	77.794	0.033073
1340.00	7.4627	1.4462	0.0059542	100.262	0.033283
1360.00	7.3529	1.4499	0.0085521	146.158	0.033738
1380.00	7.2464	1.4381	0.0183129	317.575	0.032337
1400.00	7.1429	1.4415	0.0048773	85.806	0.032705
1420.00	7.0423	1.4494	0.0064198	114.557	0.033672
1440.00	6.9444	1.4586	0.0206507	373.686	0.034855
1460.00	6.8493	1.4316	0.0494562	907.368	0.031901
1480.00	6.7568	1.4135	0.0096718	179.879	0.029368
1500.00	6.6667	1.4242	0.0060089	113.265	0.030630
1520.00	6.5789	1.4262	0.0031733	60.613	0.030862
1540.00	6.4935	1.4298	0.0017911	34.662	0.031287
1560.00	6.4103	1.4319	0.0015509	30.402	0.031543
1580.00	6.3291	1.4336	0.0020566	40.834	0.031745
1600.00	6.2500	1.4340	0.0038212	76.829	0.031799
1620.00	6.1728	1.4324	0.0023731	48.310	0.031603
1640.00	6.0976	1.4331	0.0015857	32.680	0.031683
1660.00	6.0241	1.4340	0.0009149	19.084	0.031789
1680.00	5.9524	1.4346	0.0008677	18.319	0.031870
1700.00	5.8824	1.4350	0.0007932	16.945	0.031916
1720.00	5.8140	1.4354	0.0006138	13.268	0.031956
1740.00	5.7471	1.4360	0.0005551	12.137	0.032032
1760.00	5.6818	1.4361	0.0007148	15.809	0.032051
1780.00	5.6180	1.4363	0.0006426	14.375	0.032075
1800.00	5.5556	1.4365	0.0005268	11.915	0.032100
1820.00	5.4945	1.4369	0.0004735	10.829	0.032138
1840.00	5.4348	1.4371	0.0004879	11.282	0.032168
1860.00	5.3763	1.4373	0.0005049	11.801	0.032190
1880.00	5.3191	1.4375	0.0005191	12.263	0.032220
1900.00	5.2632	1.4377	0.0006470	15.447	0.032234
1920.00	5.2083	1.4376	0.0006003	14.483	0.032228
1940.00	5.1546	1.4377	0.0004581	11.168	0.032244
1960.00	5.1020	1.4380	0.0002742	6.754	0.032272
1980.00	5.0505	1.4382	0.0002554	6.355	0.032303
2000.00	5.0000	1.4385	0.0002497	6.276	0.032333
2020.00	4.9505	1.4387	0.0003401	8.632	0.032356
2040.00	4.9020	1.4388	0.0003321	8.513	0.032368
2060.00	4.8544	1.4389	0.0003158	8.175	0.032389
2080.00	4.8077	1.4391	0.0002831	7.399	0.032408
2100.00	4.7619	1.4393	0.0002856	7.538	0.032433
2120.00	4.7170	1.4395	0.0002946	7.847	0.032453
2140.00	4.6729	1.4397	0.0003139	8.440	0.032480
2160.00	4.6296	1.4398	0.0003790	10.286	0.032495
2180.00	4.5872	1.4400	0.0003630	9.943	0.032515
2200.00	4.5455	1.4401	0.0003929	10.863	0.032534
2220.00	4.5045	1.4403	0.0003625	10.112	0.032556
2240.00	4.4643	1.4405	0.0003986	11.220	0.032581

TABLE 5-Continued

WN	WL	n	k	LAC	R
2260.00	4.4248	1.4407	0.0003977	11.296	0.032603
2280.00	4.3860	1.4409	0.0004529	12.975	0.032632
2300.00	4.3478	1.4411	0.0004887	14.126	0.032651
2320.00	4.3103	1.4413	0.0005185	15.117	0.032677
2340.00	4.2735	1.4414	0.0005352	15.737	0.032694
2360.00	4.2373	1.4417	0.0004896	14.521	0.032725
2380.00	4.2017	1.4419	0.0005370	16.060	0.032754
2400.00	4.1667	1.4422	0.0005250	15.833	0.032784
2420.00	4.1322	1.4425	0.0005383	16.369	0.032816
2440.00	4.0984	1.4427	0.0004768	14.620	0.032851
2460.00	4.0650	1.4431	0.0004714	14.572	0.032900
2480.00	4.0323	1.4435	0.0004707	14.668	0.032945
2500.00	4.0000	1.4440	0.0004872	15.306	0.033006
2520.00	3.9683	1.4445	0.0005840	18.495	0.033063
2540.00	3.9370	1.4450	0.0006393	20.404	0.033126
2560.00	3.9063	1.4456	0.0007842	25.227	0.033198
2580.00	3.8760	1.4462	0.0009774	31.688	0.033271
2600.00	3.8462	1.4467	0.0012124	39.613	0.033338
2620.00	3.8168	1.4473	0.0012943	42.612	0.033409
2640.00	3.7879	1.4481	0.0013833	45.890	0.033506
2660.00	3.7594	1.4490	0.0015998	53.475	0.033612
2680.00	3.7313	1.4499	0.0016055	54.070	0.033720
2700.00	3.7037	1.4513	0.0015374	52.164	0.033894
2720.00	3.6765	1.4530	0.0020394	69.708	0.034108
2740.00	3.6496	1.4545	0.0019010	65.457	0.034289
2760.00	3.6232	1.4577	0.0017694	61.368	0.034678
2780.00	3.5971	1.4620	0.0023680	82.726	0.035217
2800.00	3.5714	1.4683	0.0040399	142.147	0.035994
2820.00	3.5461	1.4778	0.0069110	244.905	0.037194
2840.00	3.5211	1.4976	0.0273567	976.319	0.039809
2860.00	3.4965	1.4674	0.0607507	2183.369	0.036465
2880.00	3.4722	1.4591	0.0408991	1480.185	0.035119
2900.00	3.4483	1.4743	0.0602807	2196.778	0.037315
2920.00	3.4247	1.4476	0.1052390	3861.619	0.035223
2940.00	3.4014	1.4000	0.0764492	2824.426	0.028758
2960.00	3.3784	1.3668	0.0644863	2398.662	0.024739
2980.00	3.3557	1.3778	0.0145548	545.045	0.025282
3000.00	3.3333	1.3964	0.0064228	242.133	0.027365
3020.00	3.3113	1.4050	0.0050948	193.351	0.028363
3040.00	3.2895	1.4101	0.0040061	153.042	0.028962
3060.00	3.2680	1.4130	0.0032466	124.841	0.029293
3080.00	3.2468	1.4156	0.0018775	72.669	0.029596
3100.00	3.2258	1.4181	0.0011412	44.455	0.029902
3120.00	3.2051	1.4202	0.0008453	33.143	0.030145
3140.00	3.1847	1.4218	0.0007694	30.360	0.030338
3160.00	3.1646	1.4231	0.0007405	29.404	0.030484
3180.00	3.1447	1.4240	0.0006988	27.926	0.030601
3200.00	3.1250	1.4248	0.0005725	23.020	0.030696

TABLE 5-Continued

WN	WL	n	k	LAC	R
3220.00	3.1056	1.4256	0.0004230	17.116	0.030790
3240.00	3.0864	1.4263	0.0003370	13.721	0.030875
3260.00	3.0675	1.4270	0.0002796	11.455	0.030952
3280.00	3.0488	1.4275	0.0002610	10.758	0.031019
3300.00	3.0303	1.4280	0.0002405	9.975	0.031079
3320.00	3.0120	1.4285	0.0002402	10.019	0.031133
3340.00	2.9940	1.4289	0.0002355	9.885	0.031180
3360.00	2.9762	1.4292	0.0002302	9.722	0.031223
3380.00	2.9586	1.4296	0.0002177	9.247	0.031261
3400.00	2.9412	1.4299	0.0002011	8.593	0.031297
3420.00	2.9240	1.4301	0.0002104	9.041	0.031331
3440.00	2.9070	1.4304	0.0001991	8.608	0.031359
3460.00	2.8902	1.4306	0.0001809	7.863	0.031388
3480.00	2.8736	1.4308	0.0001782	7.794	0.031414
3500.00	2.8571	1.4311	0.0001421	6.252	0.031439
3520.00	2.8409	1.4313	0.0001298	5.742	0.031466
3540.00	2.8249	1.4315	0.0001274	5.667	0.031491
3560.00	2.8090	1.4317	0.0001415	6.331	0.031513
3580.00	2.7933	1.4318	0.0001486	6.683	0.031535
3600.00	2.7778	1.4320	0.0001906	8.625	0.031555
3620.00	2.7624	1.4321	0.0002232	10.155	0.031569
3640.00	2.7473	1.4323	0.0002164	9.898	0.031584
3660.00	2.7322	1.4324	0.0002143	9.858	0.031599
3680.00	2.7174	1.4325	0.0002206	10.202	0.031614
3700.00	2.7027	1.4326	0.0002284	10.621	0.031628
3720.00	2.6882	1.4327	0.0002322	10.853	0.031642
3740.00	2.6738	1.4328	0.0002510	11.798	0.031654
3760.00	2.6596	1.4329	0.0002556	12.079	0.031665
3780.00	2.6455	1.4330	0.0002700	12.825	0.031677
3800.00	2.6316	1.4331	0.0002803	13.383	0.031688
3820.00	2.6178	1.4332	0.0002961	14.213	0.031698
3840.00	2.6042	1.4333	0.0003038	14.659	0.031707
3860.00	2.5907	1.4334	0.0003055	14.816	0.031716
3880.00	2.5773	1.4334	0.0003188	15.544	0.031725
3900.00	2.5641	1.4335	0.0003205	15.707	0.031733
3920.00	2.5510	1.4336	0.0003316	16.336	0.031742
3940.00	2.5381	1.4336	0.0003311	16.395	0.031750
3960.00	2.5253	1.4337	0.0003409	16.966	0.031760
3980.00	2.5126	1.4338	0.0003619	18.099	0.031770
4000.00	2.5000	1.4339	0.0003950	19.857	0.031778
4032.26	2.4800	1.4340	0.0004483	22.714	0.031792
4065.04	2.4600	1.4340	0.0006180	31.570	0.031796
4098.36	2.4400	1.4340	0.0005541	28.539	0.031792
4132.23	2.4200	1.4340	0.0005704	29.619	0.031799
4166.67	2.4000	1.4341	0.0006141	32.156	0.031804
4201.68	2.3800	1.4341	0.0005847	30.871	0.031808
4237.29	2.3600	1.4342	0.0006385	33.997	0.031823
4273.50	2.3400	1.4340	0.0007446	39.989	0.031798

TABLE 5-Continued

WN	WL	n	k	LAC	R
4310.34	2.3200	1.4342	0.0007267	39.363	0.031820
4347.83	2.3000	1.4338	0.0007861	42.948	0.031765
4385.96	2.2800	1.4339	0.0005214	28.735	0.031778
4424.78	2.2600	1.4338	0.0002559	14.229	0.031774
4464.29	2.2400	1.4341	0.0001049	5.885	0.031802
4504.50	2.2200	1.4342	0.0000783	4.431	0.031822
4545.45	2.2000	1.4344	0.0000670	3.828	0.031836
4587.16	2.1800	1.4345	0.0000687	3.961	0.031848
4629.63	2.1600	1.4345	0.0000652	3.792	0.031856
4672.90	2.1400	1.4346	0.0000497	2.920	0.031865
4716.98	2.1200	1.4347	0.0000322	1.907	0.031874
4761.90	2.1000	1.4347	0.0000292	1.746	0.031883
4807.69	2.0800	1.4348	0.0000277	1.673	0.031891
4854.37	2.0600	1.4349	0.0000278	1.697	0.031899
4901.96	2.0400	1.4349	0.0000294	1.810	0.031906
4950.50	2.0200	1.4350	0.0000315	1.962	0.031913
5000.00	2.0000	1.4350	0.0000320	2.010	0.031919
5050.50	1.9800	1.4351	0.0000302	1.914	0.031925
5102.04	1.9600	1.4351	0.0000300	1.923	0.031931
5154.64	1.9400	1.4352	0.0000297	1.922	0.031937
5208.33	1.9200	1.4352	0.0000304	1.989	0.031942
5263.16	1.9000	1.4353	0.0000307	2.030	0.031948
5319.15	1.8800	1.4353	0.0000318	2.125	0.031953
5376.34	1.8600	1.4354	0.0000329	2.221	0.031959
5434.78	1.8400	1.4354	0.0000432	2.949	0.031964
5494.51	1.8200	1.4355	0.0000484	3.342	0.031968
5555.56	1.8000	1.4355	0.0000495	3.453	0.031973
5617.98	1.7800	1.4355	0.0000630	4.450	0.031980
5681.82	1.7600	1.4356	0.0001032	7.371	0.031981
5747.13	1.7400	1.4356	0.0000995	7.183	0.031985
5813.95	1.7200	1.4356	0.0001404	10.255	0.031982
5882.35	1.7000	1.4356	0.0001078	7.968	0.031980
5952.38	1.6800	1.4356	0.0000439	3.284	0.031982
6024.10	1.6600	1.4356	0.0000140	1.059	0.031989
6097.56	1.6400	1.4357	0.0000070	0.536	0.031995
6172.84	1.6200	1.4357	0.0000025	0.194	0.032000
6250.00	1.6000	1.4358	0.0000009	0.069	0.032005
6329.11	1.5800	1.4358	0.0000002	0.019	0.032009
6410.26	1.5600	1.4358	0.0000002	0.017	0.032013
6493.51	1.5400	1.4359	0.0000004	0.031	0.032017
6578.95	1.5200	1.4359	0.0000008	0.068	0.032020
6666.67	1.5000	1.4359	0.0000018	0.153	0.032024
6756.76	1.4800	1.4359	0.0000029	0.245	0.032027
6849.31	1.4600	1.4360	0.0000043	0.366	0.032031
6944.44	1.4400	1.4360	0.0000071	0.621	0.032034
7042.25	1.4200	1.4360	0.0000093	0.819	0.032037
7142.86	1.4000	1.4360	0.0000108	0.973	0.032039
7246.38	1.3800	1.4361	0.0000102	0.930	0.032041

TABLE 5-Continued

WN	WL	n	k	LAC	R
7352.94	1.3600	1.4361	0.0000027	0.249	0.032044
7462.69	1.3400	1.4361	0.0000010	0.092	0.032048
7575.76	1.3200	1.4361	0.0000014	0.134	0.032051
7692.31	1.3000	1.4362	0.0000013	0.124	0.032054
7812.50	1.2800	1.4362	0.0000010	0.096	0.032056
7936.51	1.2600	1.4362	0.0000003	0.030	0.032059
8064.52	1.2400	1.4362	0.0000017	0.174	0.032062
8196.72	1.2200	1.4363	0.0000091	0.940	0.032065
8333.33	1.2000	1.4363	0.0000126	1.322	0.032067
8474.58	1.1800	1.4363	0.0000068	0.726	0.032068
8620.69	1.1600	1.4363	0.0000020	0.213	0.032071
8771.93	1.1400	1.4363	0.0000006	0.071	0.032073
8928.57	1.1200	1.4363	0.0000020	0.225	0.032076
9090.91	1.1000	1.4364	0.0000023	0.257	0.032078
9259.26	1.0800	1.4364	0.0000022	0.257	0.032081
9433.96	1.0600	1.4364	0.0000021	0.244	0.032083
9615.38	1.0400	1.4364	0.0000021	0.254	0.032085
9803.92	1.0200	1.4364	0.0000021	0.259	0.032088
10000.00	1.0000	1.4365	0.0000023	0.293	0.032090
10204.10	0.9800	1.4365	0.0000026	0.328	0.032092
10416.70	0.9600	1.4365	0.0000025	0.323	0.032094
10638.30	0.9400	1.4365	0.0000022	0.288	0.032096
10869.60	0.9200	1.4365	0.0000017	0.237	0.032098
11111.10	0.9000	1.4365	0.0000022	0.313	0.032100
11363.60	0.8800	1.4366	0.0000026	0.368	0.032103
11627.90	0.8600	1.4366	0.0000027	0.401	0.032105
11904.80	0.8400	1.4366	0.0000028	0.420	0.032107
12195.10	0.8200	1.4366	0.0000029	0.439	0.032109
12500.00	0.8000	1.4366	0.0000018	0.289	0.032111
12820.50	0.7800	1.4366	0.0000005	0.087	0.032113
13157.90	0.7600	1.4367	0.0000005	0.081	0.032115
13513.50	0.7400	1.4367	0.0000015	0.250	0.032117
13888.90	0.7200	1.4367	0.0000017	0.302	0.032119
14285.70	0.7000	1.4367	0.0000016	0.279	0.032121
14705.90	0.6800	1.4367	0.0000014	0.251	0.032123
15151.50	0.6600	1.4368	0.0000010	0.196	0.032126
15625.00	0.6400	1.4368	0.0000007	0.135	0.032128
16129.00	0.6200	1.4368	0.0000005	0.094	0.032130
16666.70	0.6000	1.4368	0.0000001	0.016	0.032132
17241.40	0.5800	1.4368	0.0000007	0.149	0.032135
17857.10	0.5600	1.4369	0.0000018	0.397	0.032138
18518.50	0.5400	1.4369	0.0000033	0.777	0.032140
19230.80	0.5200	1.4369	0.0000053	1.281	0.032143
20000.00	0.5000	1.4369	0.0000070	1.756	0.032146
20833.30	0.4800	1.4369	0.0000087	2.290	0.032149
21739.10	0.4600	1.4370	0.0000110	3.012	0.032152
22727.30	0.4400	1.4370	0.0000155	4.439	0.032156
23809.50	0.4200	1.4370	0.0000277	8.290	0.032161

TABLE 5-Continued

WN	WL	n	k	LAC	R
25000.00	0.4000	1.4371	0.0000584	18.334	0.032167
26315.80	0.3800	1.4371	0.0001645	54.403	0.032167
27777.80	0.3600	1.4370	0.0002375	82.896	0.032160

TABLE 6. FOGOIL

THE COMPLEX REFRACTIVE INDEX, LAMBERT ABSORPTION COEFFICIENT, AND REFLECTION COEFFICIENT.

WN	WL	n	k	LAC	R
501.00	19.9601	1.4859	0.0023289	14.662	0.038200
520.00	19.2308	1.4841	0.0027177	17.759	0.037979
540.00	18.5185	1.4833	0.0028578	19.393	0.037880
560.00	17.8571	1.4830	0.0027731	19.515	0.037843
580.00	17.2414	1.4828	0.0025769	18.782	0.037810
600.00	16.6667	1.4828	0.0022263	16.786	0.037816
620.00	16.1290	1.4832	0.0019733	15.374	0.037867
640.00	15.6250	1.4837	0.0018651	15.000	0.037923
660.00	15.1515	1.4845	0.0016566	13.740	0.038024
680.00	14.7059	1.4861	0.0015341	13.109	0.038231
700.00	14.2857	1.4881	0.0047445	41.735	0.038493
720.00	13.8889	1.4889	0.0077508	70.128	0.038591
740.00	13.5135	1.4863	0.0109809	102.113	0.038276
760.00	13.1579	1.4810	0.0099437	94.966	0.037606
780.00	12.8205	1.4805	0.0082571	80.934	0.037529
800.00	12.5000	1.4834	0.0085497	85.951	0.037905
820.00	12.1951	1.4768	0.0095999	98.922	0.037071
840.00	11.9048	1.4788	0.0059437	62.740	0.037322
860.00	11.6279	1.4794	0.0065722	71.027	0.037389
880.00	11.3636	1.4781	0.0069163	76.483	0.037233
900.00	11.1111	1.4780	0.0050077	56.636	0.037213
920.00	10.8696	1.4793	0.0049988	57.791	0.037381
940.00	10.6383	1.4795	0.0055181	65.182	0.037397
960.00	10.4167	1.4793	0.0056664	68.358	0.037374
980.00	10.2041	1.4787	0.0052355	64.475	0.037302
1000.00	10.0000	1.4793	0.0050922	63.990	0.037379
1020.00	9.8039	1.4795	0.0055014	70.515	0.037404
1040.00	9.6154	1.4783	0.0054512	71.241	0.037251
1060.00	9.4340	1.4788	0.0047494	63.263	0.037311
1080.00	9.2593	1.4790	0.0046186	62.683	0.037332
1100.00	9.0909	1.4792	0.0041993	58.047	0.037359
1120.00	8.9286	1.4799	0.0040685	57.261	0.037446
1140.00	8.7719	1.4805	0.0045959	65.839	0.037533
1160.00	8.6207	1.4801	0.0054987	80.155	0.037482
1180.00	8.4746	1.4797	0.0048866	72.460	0.037423
1200.00	8.3333	1.4801	0.0046753	70.502	0.037479
1220.00	8.1967	1.4805	0.0044490	68.207	0.037523
1240.00	8.0645	1.4813	0.0046583	72.587	0.037632
1260.00	7.9365	1.4819	0.0051739	81.922	0.037699
1280.00	7.8125	1.4824	0.0054296	87.335	0.037765

TABLE 6-Continued

WN	WL	n	k	LAC	R
1300.00	7.6923	1.4831	0.0063763	104.164	0.037863
1320.00	7.5758	1.4837	0.0064148	106.407	0.037930
1340.00	7.4627	1.4858	0.0078978	132.990	0.038207
1360.00	7.3529	1.4912	0.0124609	212.960	0.038906
1380.00	7.2464	1.4723	0.0253748	440.039	0.036593
1400.00	7.1429	1.4772	0.0051017	89.755	0.037116
1420.00	7.0423	1.4878	0.0069659	124.301	0.038458
1440.00	6.9444	1.4986	0.0258967	468.616	0.039930
1460.00	6.8493	1.4632	0.0521098	956.053	0.035798
1480.00	6.7568	1.4485	0.0129752	241.316	0.033581
1500.00	6.6667	1.4585	0.0057269	107.949	0.034785
1520.00	6.5789	1.4629	0.0027702	52.914	0.035327
1540.00	6.4935	1.4665	0.0017511	33.887	0.035767
1560.00	6.4103	1.4689	0.0015700	30.778	0.036066
1580.00	6.3291	1.4705	0.0022943	45.552	0.036273
1600.00	6.2500	1.4707	0.0035714	71.807	0.036300
1620.00	6.1728	1.4697	0.0021681	44.136	0.036177
1640.00	6.0976	1.4706	0.0013118	27.034	0.036288
1660.00	6.0241	1.4716	0.0010237	21.354	0.036411
1680.00	5.9524	1.4723	0.0009815	20.721	0.036490
1700.00	5.8824	1.4728	0.0010433	22.287	0.036552
1720.00	5.8140	1.4730	0.0009941	21.486	0.036583
1740.00	5.7471	1.4733	0.0009780	21.384	0.036622
1760.00	5.6818	1.4735	0.0008233	18.210	0.036651
1780.00	5.6180	1.4738	0.0007137	15.963	0.036686
1800.00	5.5556	1.4741	0.0005870	13.279	0.036724
1820.00	5.4945	1.4745	0.0005238	11.980	0.036769
1840.00	5.4348	1.4748	0.0005573	12.886	0.036807
1860.00	5.3763	1.4750	0.0005942	13.888	0.036835
1880.00	5.3191	1.4752	0.0006319	14.929	0.036858
1900.00	5.2632	1.4753	0.0006415	15.317	0.036875
1920.00	5.2083	1.4754	0.0005798	13.988	0.036886
1940.00	5.1546	1.4756	0.0004726	11.520	0.036910
1960.00	5.1020	1.4759	0.0003705	9.125	0.036941
1980.00	5.0505	1.4761	0.0003505	8.722	0.036972
2000.00	5.0000	1.4763	0.0003573	8.981	0.037001
2020.00	4.9505	1.4766	0.0003952	10.032	0.037028
2040.00	4.9020	1.4767	0.0004154	10.650	0.037047
2060.00	4.8544	1.4769	0.0003975	10.289	0.037069
2080.00	4.8077	1.4771	0.0003902	10.199	0.037093
2100.00	4.7619	1.4773	0.0003913	10.327	0.037118
2120.00	4.7170	1.4775	0.0004074	10.855	0.037143
2140.00	4.6729	1.4777	0.0004307	11.584	0.037168
2160.00	4.6296	1.4778	0.0004730	12.840	0.037190
2180.00	4.5872	1.4780	0.0004922	13.482	0.037212
2200.00	4.5455	1.4782	0.0004968	13.735	0.037234
2220.00	4.5045	1.4784	0.0005028	14.026	0.037259
2240.00	4.4643	1.4786	0.0005138	14.464	0.037285

TABLE 6-Continued

WN	WL	n	k	LAC	R
2260.00	4.4248	1.4788	0.0005376	15.268	0.037313
2280.00	4.3860	1.4790	0.0005793	16.598	0.037340
2300.00	4.3478	1.4792	0.0006116	17.676	0.037366
2320.00	4.3103	1.4795	0.0006393	18.639	0.037392
2340.00	4.2735	1.4797	0.0006466	19.012	0.037419
2360.00	4.2373	1.4799	0.0006530	19.365	0.037452
2380.00	4.2017	1.4802	0.0006796	20.325	0.037485
2400.00	4.1667	1.4805	0.0007042	21.238	0.037519
2420.00	4.1322	1.4807	0.0006948	21.128	0.037554
2440.00	4.0984	1.4811	0.0006676	20.471	0.037596
2460.00	4.0650	1.4815	0.0006631	20.497	0.037645
2480.00	4.0323	1.4819	0.0006723	20.953	0.037698
2500.00	4.0000	1.4824	0.0007014	22.035	0.037760
2520.00	3.9683	1.4829	0.0007829	24.791	0.037827
2540.00	3.9370	1.4835	0.0008839	28.212	0.037898
2560.00	3.9063	1.4841	0.0010355	33.311	0.037977
2580.00	3.8760	1.4847	0.0012781	41.436	0.038056
2600.00	3.8462	1.4853	0.0015073	49.247	0.038127
2620.00	3.8168	1.4859	0.0016377	53.919	0.038207
2640.00	3.7879	1.4867	0.0017494	58.035	0.038307
2660.00	3.7594	1.4876	0.0020124	67.267	0.038427
2680.00	3.7313	1.4885	0.0020441	68.841	0.038535
2700.00	3.7037	1.4899	0.0020102	68.203	0.038718
2720.00	3.6765	1.4916	0.0025511	87.197	0.038928
2740.00	3.6496	1.4931	0.0022405	77.146	0.039123
2760.00	3.6232	1.4964	0.0021067	73.066	0.039536
2780.00	3.5971	1.5008	0.0027660	96.630	0.040098
2800.00	3.5714	1.5066	0.0042746	150.406	0.040853
2820.00	3.5461	1.5163	0.0081088	287.352	0.042108
2840.00	3.5211	1.5297	0.0242585	865.749	0.043933
2860.00	3.4965	1.5151	0.0469273	1686.559	0.042273
2880.00	3.4722	1.5183	0.0463188	1676.331	0.042682
2900.00	3.4483	1.5203	0.0739816	2696.073	0.043448
2920.00	3.4247	1.4867	0.1138500	4177.589	0.040324
2940.00	3.4014	1.4373	0.0931763	3442.411	0.033607
2960.00	3.3784	1.4002	0.0690243	2567.459	0.028607
2980.00	3.3557	1.4101	0.0235112	880.442	0.029041
3000.00	3.3333	1.4249	0.0095116	358.579	0.030719
3020.00	3.3113	1.4373	0.0050851	192.981	0.032198
3040.00	3.2895	1.4440	0.0036603	139.832	0.033005
3060.00	3.2680	1.4481	0.0029357	112.889	0.033507
3080.00	3.2468	1.4511	0.0018293	70.803	0.033877
3100.00	3.2258	1.4540	0.0011491	44.766	0.034229
3120.00	3.2051	1.4563	0.0009327	36.569	0.034514
3140.00	3.1847	1.4581	0.0008786	34.668	0.034731
3160.00	3.1646	1.4594	0.0008797	34.931	0.034898
3180.00	3.1447	1.4605	0.0008295	33.148	0.035028
3200.00	3.1250	1.4614	0.0006954	27.964	0.035140

TABLE 6-Continued

WN	WL	n	k	LAC	R
3220.00	3.1056	1.4623	0.0005432	21.979	0.035245
3240.00	3.0864	1.4631	0.0004416	17.979	0.035344
3260.00	3.0675	1.4638	0.0003873	15.864	0.035432
3280.00	3.0488	1.4644	0.0003562	14.681	0.035509
3300.00	3.0303	1.4649	0.0003425	14.205	0.035577
3320.00	3.0120	1.4654	0.0003351	13.979	0.035638
3340.00	2.9940	1.4659	0.0003348	14.050	0.035691
3360.00	2.9762	1.4662	0.0003207	13.541	0.035739
3380.00	2.9586	1.4666	0.0003060	12.998	0.035783
3400.00	2.9412	1.4669	0.0002858	12.210	0.035824
3420.00	2.9240	1.4672	0.0002696	11.587	0.035862
3440.00	2.9070	1.4675	0.0002545	11.003	0.035898
3460.00	2.8902	1.4678	0.0002436	10.594	0.035931
3480.00	2.8736	1.4680	0.0002365	10.340	0.035962
3500.00	2.8571	1.4683	0.0002184	9.608	0.035991
3520.00	2.8409	1.4685	0.0002123	9.393	0.036019
3540.00	2.8249	1.4687	0.0002065	9.185	0.036046
3560.00	2.8090	1.4689	0.0002082	9.315	0.036072
3580.00	2.7933	1.4691	0.0002121	9.543	0.036097
3600.00	2.7778	1.4693	0.0002425	10.969	0.036119
3620.00	2.7624	1.4694	0.0002623	11.930	0.036137
3640.00	2.7473	1.4696	0.0002625	12.006	0.036155
3660.00	2.7322	1.4697	0.0002668	12.269	0.036173
3680.00	2.7174	1.4699	0.0002776	12.838	0.036191
3700.00	2.7027	1.4700	0.0002902	13.491	0.036207
3720.00	2.6882	1.4701	0.0003013	14.086	0.036223
3740.00	2.6738	1.4702	0.0003189	14.987	0.036237
3760.00	2.6596	1.4703	0.0003340	15.782	0.036251
3780.00	2.6455	1.4704	0.0003553	16.875	0.036264
3800.00	2.6316	1.4705	0.0003698	17.659	0.036275
3820.00	2.6178	1.4706	0.0003887	18.661	0.036286
3840.00	2.6042	1.4707	0.0003935	18.987	0.036295
3860.00	2.5907	1.4708	0.0004009	19.447	0.036306
3880.00	2.5773	1.4709	0.0004069	19.839	0.036315
3900.00	2.5641	1.4709	0.0004083	20.008	0.036325
3920.00	2.5510	1.4710	0.0004103	20.212	0.036334
3940.00	2.5381	1.4711	0.0004118	20.388	0.036345
3960.00	2.5253	1.4712	0.0004230	21.048	0.036355
3980.00	2.5126	1.4713	0.0004359	21.799	0.036366
4000.00	2.5000	1.4714	0.0004717	23.711	0.036378
4032.26	2.4800	1.4715	0.0005558	28.163	0.036394
4065.04	2.4600	1.4715	0.0007174	36.645	0.036393
4098.36	2.4400	1.4715	0.0006608	34.032	0.036394
4132.23	2.4200	1.4716	0.0006889	35.771	0.036402
4166.67	2.4000	1.4716	0.0007362	38.547	0.036405
4201.68	2.3800	1.4716	0.0007013	37.029	0.036411
4237.29	2.3600	1.4717	0.0008082	43.034	0.036426
4273.50	2.3400	1.4715	0.0008742	46.949	0.036399

TABLE 6-Continued

WN	WL	n	k	LAC	R
4310.34	2.3200	1.4717	0.0008981	48.648	0.036419
4347.83	2.3000	1.4713	0.0008921	48.741	0.036364
4385.96	2.2800	1.4713	0.0006463	35.619	0.036370
4424.78	2.2600	1.4713	0.0003217	17.888	0.036364
4464.29	2.2400	1.4715	0.0001270	7.123	0.036398
4504.50	2.2200	1.4717	0.0000941	5.326	0.036422
4545.45	2.2000	1.4718	0.0000819	4.681	0.036439
4587.16	2.1800	1.4720	0.0000802	4.621	0.036453
4629.63	2.1600	1.4720	0.0000722	4.202	0.036464
4672.90	2.1400	1.4721	0.0000558	3.277	0.036474
4716.98	2.1200	1.4722	0.0000406	2.408	0.036485
4761.90	2.1000	1.4723	0.0000386	2.307	0.036496
4807.69	2.0800	1.4724	0.0000372	2.248	0.036505
4854.37	2.0600	1.4725	0.0000374	2.284	0.036514
4901.96	2.0400	1.4725	0.0000389	2.398	0.036523
4950.50	2.0200	1.4726	0.0000408	2.539	0.036530
5000.00	2.0000	1.4726	0.0000419	2.631	0.036538
5050.50	1.9800	1.4727	0.0000418	2.650	0.036545
5102.04	1.9600	1.4728	0.0000422	2.705	0.036552
5154.64	1.9400	1.4728	0.0000427	2.764	0.036558
5208.33	1.9200	1.4729	0.0000438	2.865	0.036565
5263.16	1.9000	1.4729	0.0000449	2.967	0.036571
5319.15	1.8800	1.4730	0.0000463	3.096	0.036577
5376.34	1.8600	1.4730	0.0000489	3.306	0.036584
5434.78	1.8400	1.4731	0.0000599	4.090	0.036590
5494.51	1.8200	1.4731	0.0000648	4.471	0.036594
5555.56	1.8000	1.4731	0.0000636	4.438	0.036600
5617.98	1.7800	1.4732	0.0000802	5.658	0.036608
5681.82	1.7600	1.4732	0.0001245	8.890	0.036610
5747.13	1.7400	1.4732	0.0001262	9.114	0.036613
5813.95	1.7200	1.4732	0.0001695	12.382	0.036610
5882.35	1.7000	1.4732	0.0001305	9.649	0.036606
5952.38	1.6800	1.4732	0.0000463	3.462	0.036609
6024.10	1.6600	1.4733	0.0000161	1.218	0.036618
6097.56	1.6400	1.4733	0.0000102	0.781	0.036625
6172.84	1.6200	1.4734	0.0000064	0.494	0.036631
6250.00	1.6000	1.4734	0.0000046	0.362	0.036636
6329.11	1.5800	1.4735	0.0000040	0.318	0.036641
6410.26	1.5600	1.4735	0.0000036	0.290	0.036646
6493.51	1.5400	1.4735	0.0000042	0.341	0.036650
6578.95	1.5200	1.4736	0.0000049	0.404	0.036655
6666.67	1.5000	1.4736	0.0000063	0.528	0.036659
6756.76	1.4800	1.4736	0.0000076	0.643	0.036663
6849.31	1.4600	1.4737	0.0000089	0.764	0.036667
6944.44	1.4400	1.4737	0.0000118	1.034	0.036670
7042.25	1.4200	1.4737	0.0000143	1.265	0.036674
7142.86	1.4000	1.4738	0.0000165	1.477	0.036677
7246.38	1.3800	1.4738	0.0000160	1.457	0.036679

TABLE 6-Continued

WN	WL	n	k	LAC	R
7352.94	1.3600	1.4738	0.0000069	0.635	0.036682
7462.69	1.3400	1.4738	0.0000022	0.209	0.036686
7575.76	1.3200	1.4739	0.0000018	0.171	0.036690
7692.31	1.3000	1.4739	0.0000022	0.212	0.036693
7812.50	1.2800	1.4739	0.0000025	0.243	0.036697
7936.51	1.2600	1.4739	0.0000038	0.379	0.036700
8064.52	1.2400	1.4740	0.0000067	0.677	0.036703
8196.72	1.2200	1.4740	0.0000141	1.455	0.036706
8333.33	1.2000	1.4740	0.0000195	2.042	0.036708
8474.58	1.1800	1.4740	0.0000127	1.354	0.036709
8620.69	1.1600	1.4740	0.0000062	0.673	0.036713
8771.93	1.1400	1.4741	0.0000035	0.390	0.036716
8928.57	1.1200	1.4741	0.0000013	0.151	0.036719
9090.91	1.1000	1.4741	0.0000011	0.123	0.036722
9259.26	1.0800	1.4741	0.0000011	0.125	0.036724
9433.96	1.0600	1.4742	0.0000014	0.162	0.036727
9615.38	1.0400	1.4742	0.0000014	0.166	0.036730
9803.92	1.0200	1.4742	0.0000013	0.158	0.036732
10000.00	1.0000	1.4742	0.0000011	0.141	0.036735
10204.10	0.9800	1.4742	0.0000010	0.128	0.036738
10416.70	0.9600	1.4743	0.0000010	0.137	0.036740
10638.30	0.9400	1.4743	0.0000014	0.183	0.036743
10869.60	0.9200	1.4743	0.0000020	0.267	0.036745
11111.10	0.9000	1.4743	0.0000014	0.189	0.036747
11363.60	0.8800	1.4743	0.0000010	0.144	0.036750
11627.90	0.8600	1.4744	0.0000007	0.100	0.036752
11904.80	0.8400	1.4744	0.0000006	0.097	0.036755
12195.10	0.8200	1.4744	0.0000006	0.097	0.036757
12500.00	0.8000	1.4744	0.0000010	0.155	0.036760
12820.50	0.7800	1.4744	0.0000014	0.227	0.036762
13157.90	0.7600	1.4745	0.0000013	0.219	0.036765
13513.50	0.7400	1.4745	0.0000014	0.239	0.036767
13888.90	0.7200	1.4745	0.0000015	0.258	0.036769
14285.70	0.7000	1.4745	0.0000016	0.283	0.036772
14705.90	0.6800	1.4745	0.0000017	0.310	0.036774
15151.50	0.6600	1.4746	0.0000019	0.361	0.036777
15625.00	0.6400	1.4746	0.0000018	0.349	0.036779
16129.00	0.6200	1.4746	0.0000016	0.333	0.036782
16666.70	0.6000	1.4746	0.0000016	0.341	0.036785
17241.40	0.5800	1.4746	0.0000016	0.353	0.036787
17857.10	0.5600	1.4747	0.0000018	0.394	0.036790
18518.50	0.5400	1.4747	0.0000019	0.446	0.036793
19230.80	0.5200	1.4747	0.0000022	0.524	0.036796
20000.00	0.5000	1.4747	0.0000027	0.680	0.036800
20833.30	0.4800	1.4748	0.0000038	0.988	0.036803
21739.10	0.4600	1.4748	0.0000052	1.416	0.036808
22727.30	0.4400	1.4748	0.0000125	3.578	0.036812
23809.50	0.4200	1.4749	0.0000162	4.855	0.036819

TABLE 6-Continued

WN	WL	n	k	LAC	R
25000.00	0.4000	1.4750	0.0000665	20.878	0.036828
26315.80	0.3800	1.4750	0.0001679	55.508	0.036827
27777.80	0.3600	1.4749	0.0002791	97.421	0.036819

TABLE 7. ETHYL SULFIDE

THE COMPLEX REFRACTIVE INDEX, LAMBERT ABSORPTION COEFFICIENT, AND REFLECTION COEFFICIENT.

WN	WL	n	k	LAC	R
501.00	19.9601	1.4558	0.0023182	14.595	0.034445
520.00	19.2308	1.4542	0.0018279	11.944	0.034247
540.00	18.5185	1.4543	0.0014876	10.094	0.034260
560.00	17.8571	1.4548	0.0013877	9.766	0.034326
580.00	17.2414	1.4554	0.0013157	9.589	0.034400
600.00	16.6667	1.4567	0.0013104	9.880	0.034564
620.00	16.1290	1.4589	0.0023238	18.105	0.034826
640.00	15.6250	1.4577	0.0068616	55.185	0.034688
660.00	15.1515	1.4561	0.0054828	45.473	0.034484
680.00	14.7059	1.4601	0.0062683	53.564	0.034987
700.00	14.2857	1.4535	0.0079498	69.930	0.034179
720.00	13.8889	1.4595	0.0041282	37.351	0.034901
740.00	13.5135	1.4600	0.0104649	97.314	0.034978
760.00	13.1579	1.4642	0.0128188	122.425	0.035517
780.00	12.8205	1.4610	0.0237840	233.125	0.035183
800.00	12.5000	1.4470	0.0258208	259.579	0.033477
820.00	12.1951	1.4363	0.0163123	168.089	0.032111
840.00	11.9048	1.4414	0.0048365	51.053	0.032689
860.00	11.6279	1.4465	0.0043185	46.670	0.033316
880.00	11.3636	1.4478	0.0035598	39.365	0.033473
900.00	11.1111	1.4508	0.0021164	23.936	0.033838
920.00	10.8696	1.4546	0.0021650	25.030	0.034305
940.00	10.6383	1.4595	0.0034492	40.743	0.034904
960.00	10.4167	1.4684	0.0111646	134.687	0.036033
980.00	10.2041	1.4462	0.0229086	282.120	0.033359
1000.00	10.0000	1.4552	0.0120000	150.796	0.034398
1020.00	9.8039	1.4516	0.0198382	254.280	0.034000
1040.00	9.6154	1.4485	0.0172659	225.648	0.033598
1060.00	9.4340	1.4511	0.0157314	209.548	0.033911
1080.00	9.2593	1.4433	0.0207773	281.983	0.032988
1100.00	9.0909	1.4409	0.0173719	240.132	0.032674
1120.00	8.9286	1.4393	0.0116691	164.235	0.032452
1140.00	8.7719	1.4411	0.0066309	94.992	0.032659
1160.00	8.6207	1.4455	0.0039231	57.187	0.033195
1180.00	8.4746	1.4504	0.0028975	42.965	0.033788
1200.00	8.3333	1.4565	0.0031009	46.761	0.034534
1220.00	8.1967	1.4677	0.0049407	75.745	0.035919
1240.00	8.0645	1.4902	0.0278963	434.689	0.038874
1260.00	7.9365	1.4240	0.0827384	1310.049	0.031719
1280.00	7.8125	1.4133	0.0238162	383.083	0.029426

TABLE 7-Continued

WN	WL	n	k	LAC	R
1300.00	7.6923	1.4252	0.0076032	124.207	0.030743
1320.00	7.5758	1.4348	0.0044121	73.187	0.031889
1340.00	7.4627	1.4428	0.0036314	61.149	0.032864
1360.00	7.3529	1.4561	0.0082884	141.651	0.034496
1380.00	7.2464	1.4341	0.0295169	511.870	0.031953
1400.00	7.1429	1.4448	0.0088750	156.136	0.033117
1420.00	7.0423	1.4554	0.0213942	381.763	0.034474
1440.00	6.9444	1.4569	0.0400644	724.988	0.034834
1460.00	6.8493	1.4006	0.0499082	915.661	0.028267
1480.00	6.7568	1.4074	0.0082491	153.419	0.028651
1500.00	6.6667	1.4191	0.0036840	69.442	0.030011
1520.00	6.5789	1.4244	0.0023270	44.448	0.030644
1540.00	6.4935	1.4276	0.0017311	33.500	0.031028
1560.00	6.4103	1.4299	0.0015142	29.683	0.031301
1580.00	6.3291	1.4314	0.0015569	30.912	0.031481
1600.00	6.2500	1.4327	0.0014546	29.246	0.031632
1620.00	6.1728	1.4335	0.0012283	25.005	0.031735
1640.00	6.0976	1.4345	0.0011413	23.520	0.031849
1660.00	6.0241	1.4353	0.0010837	22.606	0.031945
1680.00	5.9524	1.4361	0.0010959	23.137	0.032047
1700.00	5.8824	1.4372	0.0011556	24.688	0.032176
1720.00	5.8140	1.4391	0.0036330	78.525	0.032406
1740.00	5.7471	1.4338	0.0044309	96.884	0.031771
1760.00	5.6818	1.4348	0.0008738	19.325	0.031893
1780.00	5.6180	1.4361	0.0004885	10.927	0.032045
1800.00	5.5556	1.4368	0.0004114	9.306	0.032131
1820.00	5.4945	1.4373	0.0003285	7.512	0.032188
1840.00	5.4348	1.4377	0.0002653	6.133	0.032242
1860.00	5.3763	1.4381	0.0001943	4.542	0.032292
1880.00	5.3191	1.4385	0.0002283	5.394	0.032337
1900.00	5.2632	1.4388	0.0002176	5.197	0.032374
1920.00	5.2083	1.4391	0.0002685	6.478	0.032413
1940.00	5.1546	1.4393	0.0003440	8.386	0.032437
1960.00	5.1020	1.4395	0.0003119	7.681	0.032459
1980.00	5.0505	1.4398	0.0003014	7.499	0.032488
2000.00	5.0000	1.4400	0.0003480	8.746	0.032516
2020.00	4.9505	1.4400	0.0003871	9.826	0.032522
2040.00	4.9020	1.4403	0.0002362	6.056	0.032548
2060.00	4.8544	1.4405	0.0003018	7.812	0.032579
2080.00	4.8077	1.4406	0.0002719	7.107	0.032593
2100.00	4.7619	1.4409	0.0002438	6.434	0.032624
2120.00	4.7170	1.4410	0.0002828	7.533	0.032643
2140.00	4.6729	1.4413	0.0003378	9.083	0.032674
2160.00	4.6296	1.4413	0.0004511	12.245	0.032681
2180.00	4.5872	1.4415	0.0003942	10.798	0.032700
2200.00	4.5455	1.4417	0.0004425	12.233	0.032725
2220.00	4.5045	1.4418	0.0006470	18.049	0.032735
2240.00	4.4643	1.4417	0.0005755	16.199	0.032722

TABLE 7-Continued

WN	WL	n	k	LAC	R
2260.00	4.4248	1.4418	0.0003736	10.609	0.032732
2280.00	4.3860	1.4420	0.0002836	8.127	0.032767
2300.00	4.3478	1.4423	0.0002456	7.099	0.032792
2320.00	4.3103	1.4425	0.0002561	7.467	0.032827
2340.00	4.2735	1.4427	0.0004389	12.907	0.032847
2360.00	4.2373	1.4428	0.0003235	9.593	0.032855
2380.00	4.2017	1.4431	0.0003568	10.670	0.032895
2400.00	4.1667	1.4433	0.0005286	15.942	0.032922
2420.00	4.1322	1.4432	0.0006542	19.894	0.032901
2440.00	4.0984	1.4434	0.0004191	12.851	0.032934
2460.00	4.0650	1.4436	0.0004630	14.314	0.032960
2480.00	4.0323	1.4438	0.0004344	13.536	0.032979
2500.00	4.0000	1.4440	0.0003847	12.086	0.033009
2520.00	3.9683	1.4443	0.0003558	11.266	0.033037
2540.00	3.9370	1.4446	0.0002619	8.360	0.033076
2560.00	3.9063	1.4449	0.0002518	8.101	0.033119
2580.00	3.8760	1.4454	0.0002331	7.557	0.033170
2600.00	3.8462	1.4458	0.0002755	9.001	0.033221
2620.00	3.8168	1.4463	0.0002804	9.231	0.033280
2640.00	3.7879	1.4469	0.0003465	11.494	0.033351
2660.00	3.7594	1.4475	0.0004983	16.656	0.033433
2680.00	3.7313	1.4482	0.0008787	29.592	0.033517
2700.00	3.7037	1.4487	0.0010972	37.228	0.033571
2720.00	3.6765	1.4494	0.0014549	49.731	0.033660
2740.00	3.6496	1.4497	0.0010871	37.431	0.033705
2760.00	3.6232	1.4515	0.0008268	28.675	0.033918
2780.00	3.5971	1.4537	0.0011005	38.444	0.034187
2800.00	3.5714	1.4567	0.0018487	65.049	0.034558
2820.00	3.5461	1.4610	0.0044055	156.118	0.035096
2840.00	3.5211	1.4651	0.0100153	357.431	0.035619
2860.00	3.4965	1.4655	0.0212515	763.775	0.035716
2880.00	3.4722	1.4543	0.0222748	806.151	0.034337
2900.00	3.4483	1.4640	0.0244698	891.740	0.035560
2920.00	3.4247	1.4578	0.0498258	1828.298	0.035089
2940.00	3.4014	1.4332	0.0345339	1275.859	0.031891
2960.00	3.3784	1.4404	0.0552872	2056.488	0.033061
2980.00	3.3557	1.3935	0.0315246	1180.526	0.027193
3000.00	3.3333	1.4077	0.0074604	281.251	0.028686
3020.00	3.3113	1.4181	0.0030250	114.800	0.029900
3040.00	3.2895	1.4231	0.0019859	75.866	0.030493
3060.00	3.2680	1.4263	0.0014708	56.556	0.030865
3080.00	3.2468	1.4283	0.0011696	45.270	0.031115
3100.00	3.2258	1.4299	0.0009217	35.906	0.031304
3120.00	3.2051	1.4312	0.0007883	30.906	0.031458
3140.00	3.1847	1.4322	0.0007854	30.989	0.031579
3160.00	3.1646	1.4329	0.0007864	31.226	0.031666
3180.00	3.1447	1.4335	0.0007534	30.107	0.031738
3200.00	3.1250	1.4340	0.0007150	28.753	0.031791

TABLE 7-Continued

WN	WL	n	k	LAC	R
3220.00	3.1056	1.4344	0.0005616	22.723	0.031840
3240.00	3.0864	1.4348	0.0004137	16.843	0.031893
3260.00	3.0675	1.4353	0.0003678	15.067	0.031948
3280.00	3.0488	1.4356	0.0003352	13.816	0.031988
3300.00	3.0303	1.4359	0.0003343	13.862	0.032028
3320.00	3.0120	1.4362	0.0003035	12.660	0.032056
3340.00	2.9940	1.4364	0.0002683	11.259	0.032085
3360.00	2.9762	1.4366	0.0001957	8.265	0.032111
3380.00	2.9586	1.4369	0.0001552	6.593	0.032142
3400.00	2.9412	1.4371	0.0001344	5.742	0.032170
3420.00	2.9240	1.4373	0.0001422	6.111	0.032197
3440.00	2.9070	1.4375	0.0001578	6.821	0.032218
3460.00	2.8902	1.4377	0.0001672	7.270	0.032238
3480.00	2.8736	1.4378	0.0001804	7.890	0.032257
3500.00	2.8571	1.4380	0.0002011	8.846	0.032273
3520.00	2.8409	1.4381	0.0002167	9.585	0.032286
3540.00	2.8249	1.4382	0.0002103	9.354	0.032300
3560.00	2.8090	1.4383	0.0002233	9.989	0.032313
3580.00	2.7933	1.4384	0.0002192	9.863	0.032325
3600.00	2.7778	1.4385	0.0002389	10.809	0.032338
3620.00	2.7624	1.4386	0.0002630	11.966	0.032345
3640.00	2.7473	1.4386	0.0002488	11.382	0.032354
3660.00	2.7322	1.4387	0.0002470	11.359	0.032363
3680.00	2.7174	1.4388	0.0002434	11.254	0.032371
3700.00	2.7027	1.4388	0.0002415	11.227	0.032378
3720.00	2.6882	1.4389	0.0002223	10.391	0.032385
3740.00	2.6738	1.4390	0.0001964	9.232	0.032392
3760.00	2.6596	1.4390	0.0001556	7.352	0.032399
3780.00	2.6455	1.4391	0.0001201	5.703	0.032411
3800.00	2.6316	1.4392	0.0000977	4.664	0.032424
3820.00	2.6178	1.4393	0.0001135	5.451	0.032438
3840.00	2.6042	1.4394	0.0001501	7.242	0.032447
3860.00	2.5907	1.4395	0.0001569	7.611	0.032458
3880.00	2.5773	1.4396	0.0002070	10.091	0.032468
3900.00	2.5641	1.4396	0.0002730	13.378	0.032475
3920.00	2.5510	1.4397	0.0003106	15.300	0.032476
3940.00	2.5381	1.4397	0.0003478	17.218	0.032481
3960.00	2.5253	1.4397	0.0003939	19.603	0.032480
3980.00	2.5126	1.4397	0.0003703	18.521	0.032479
4000.00	2.5000	1.4397	0.0003844	19.324	0.032481
4032.26	2.4800	1.4397	0.0002850	14.441	0.032486
4065.04	2.4600	1.4398	0.0003373	17.229	0.032497
4098.36	2.4400	1.4399	0.0002469	12.714	0.032511
4132.23	2.4200	1.4401	0.0003166	16.441	0.032531
4166.67	2.4000	1.4402	0.0005380	28.170	0.032537
4201.68	2.3800	1.4402	0.0006650	35.112	0.032540
4237.29	2.3600	1.4399	0.0006842	36.429	0.032506
4273.50	2.3400	1.4400	0.0004019	21.582	0.032516

TABLE 7-Continued

WN	WL	n	k	LAC	R
4310.34	2.3200	1.4403	0.0006858	37.145	0.032556
4347.83	2.3000	1.4399	0.0011282	61.641	0.032504
4385.96	2.2800	1.4396	0.0007799	42.983	0.032474
4424.78	2.2600	1.4393	0.0004313	23.980	0.032438
4464.29	2.2400	1.4397	0.0001229	6.894	0.032476
4504.50	2.2200	1.4398	0.0000834	4.723	0.032498
4545.45	2.2000	1.4400	0.0000546	3.116	0.032512
4587.16	2.1800	1.4401	0.0000468	2.698	0.032524
4629.63	2.1600	1.4401	0.0000394	2.294	0.032534
4672.90	2.1400	1.4402	0.0000336	1.973	0.032542
4716.98	2.1200	1.4403	0.0000307	1.823	0.032550
4761.90	2.1000	1.4403	0.0000262	1.565	0.032557
4807.69	2.0800	1.4404	0.0000210	1.267	0.032563
4854.37	2.0600	1.4404	0.0000241	1.470	0.032571
4901.96	2.0400	1.4405	0.0000319	1.966	0.032576
4950.50	2.0200	1.4405	0.0000359	2.234	0.032581
5000.00	2.0000	1.4406	0.0000304	1.910	0.032585
5050.50	1.9800	1.4406	0.0000214	1.356	0.032590
5102.04	1.9600	1.4406	0.0000200	1.284	0.032596
5154.64	1.9400	1.4407	0.0000259	1.677	0.032601
5208.33	1.9200	1.4407	0.0000329	2.154	0.032605
5263.16	1.9000	1.4407	0.0000259	1.711	0.032609
5319.15	1.8800	1.4408	0.0000198	1.321	0.032614
5376.34	1.8600	1.4408	0.0000345	2.330	0.032620
5434.78	1.8400	1.4408	0.0000400	2.730	0.032621
5494.51	1.8200	1.4409	0.0000218	1.504	0.032626
5555.56	1.8000	1.4410	0.0000245	1.709	0.032634
5617.98	1.7800	1.4410	0.0000485	3.425	0.032642
5681.82	1.7600	1.4411	0.0001785	12.747	0.032649
5747.13	1.7400	1.4409	0.0001757	12.688	0.032629
5813.95	1.7200	1.4409	0.0001070	7.818	0.032631
5882.35	1.7000	1.4410	0.0001597	11.803	0.032634
5952.38	1.6800	1.4409	0.0000500	3.738	0.032628
6024.10	1.6600	1.4410	0.0000113	0.855	0.032638
6097.56	1.6400	1.4410	0.0000081	0.620	0.032644
6172.84	1.6200	1.4411	0.0000059	0.458	0.032648
6250.00	1.6000	1.4411	0.0000033	0.262	0.032652
6329.11	1.5800	1.4411	0.0000025	0.196	0.032656
6410.26	1.5600	1.4412	0.0000029	0.233	0.032659
6493.51	1.5400	1.4412	0.0000035	0.283	0.032662
6578.95	1.5200	1.4412	0.0000031	0.255	0.032666
6666.67	1.5000	1.4412	0.0000044	0.371	0.032669
6756.76	1.4800	1.4413	0.0000065	0.550	0.032671
6849.31	1.4600	1.4413	0.0000056	0.485	0.032674
6944.44	1.4400	1.4413	0.0000095	0.826	0.032677
7042.25	1.4200	1.4413	0.0000110	0.971	0.032679
7142.86	1.4000	1.4413	0.0000155	1.388	0.032682
7246.38	1.3800	1.4414	0.0000152	1.386	0.032683

TABLE 7-Continued

WN	WL	n	k	LAC	R
7352.94	1.3600	1.4414	0.0000082	0.755	0.032685
7462.69	1.3400	1.4414	0.0000019	0.174	0.032688
7575.76	1.3200	1.4414	0.0000015	0.141	0.032690
7692.31	1.3000	1.4414	0.0000015	0.148	0.032693
7812.50	1.2800	1.4415	0.0000016	0.161	0.032695
7936.51	1.2600	1.4415	0.0000020	0.204	0.032698
8064.52	1.2400	1.4415	0.0000023	0.233	0.032700
8196.72	1.2200	1.4415	0.0000052	0.539	0.032703
8333.33	1.2000	1.4415	0.0000154	1.613	0.032706
8474.58	1.1800	1.4415	0.0000175	1.863	0.032705
8620.69	1.1600	1.4416	0.0000058	0.627	0.032707
8771.93	1.1400	1.4416	0.0000035	0.389	0.032709
8928.57	1.1200	1.4416	0.0000013	0.142	0.032712
9090.91	1.1000	1.4416	0.0000011	0.127	0.032714
9259.26	1.0800	1.4416	0.0000011	0.128	0.032716
9433.96	1.0600	1.4416	0.0000012	0.145	0.032718
9615.38	1.0400	1.4417	0.0000013	0.156	0.032720
9803.92	1.0200	1.4417	0.0000015	0.179	0.032722
10000.00	1.0000	1.4417	0.0000012	0.151	0.032724
10204.10	0.9800	1.4417	0.0000009	0.119	0.032725
10416.70	0.9600	1.4417	0.0000009	0.122	0.032727
10638.30	0.9400	1.4417	0.0000010	0.139	0.032729
10869.60	0.9200	1.4418	0.0000017	0.235	0.032731
11111.10	0.9000	1.4418	0.0000016	0.222	0.032733
11363.60	0.8800	1.4418	0.0000008	0.121	0.032735
11627.90	0.8600	1.4418	0.0000007	0.095	0.032736
11904.80	0.8400	1.4418	0.0000006	0.089	0.032738
12195.10	0.8200	1.4418	0.0000005	0.077	0.032740
12500.00	0.8000	1.4418	0.0000003	0.042	0.032742
12820.50	0.7800	1.4419	0.0000002	0.028	0.032744
13157.90	0.7600	1.4419	0.0000002	0.027	0.032745
13513.50	0.7400	1.4419	0.0000008	0.137	0.032747
13888.90	0.7200	1.4419	0.0000008	0.141	0.032749
14285.70	0.7000	1.4419	0.0000008	0.151	0.032751
14705.90	0.6800	1.4419	0.0000009	0.167	0.032752
15151.50	0.6600	1.4419	0.0000010	0.186	0.032754
15625.00	0.6400	1.4420	0.0000011	0.210	0.032756
16129.00	0.6200	1.4420	0.0000010	0.206	0.032758
16666.70	0.6000	1.4420	0.0000010	0.216	0.032760
17241.40	0.5800	1.4420	0.0000010	0.221	0.032761
17857.10	0.5600	1.4420	0.0000010	0.230	0.032763
18518.50	0.5400	1.4420	0.0000010	0.225	0.032765
19230.80	0.5200	1.4421	0.0000010	0.234	0.032767
20000.00	0.5000	1.4421	0.0000009	0.238	0.032769
20833.30	0.4800	1.4421	0.0000010	0.267	0.032772
21739.10	0.4600	1.4421	0.0000011	0.306	0.032774
22727.30	0.4400	1.4421	0.0000013	0.357	0.032776
23809.50	0.4200	1.4421	0.0000014	0.412	0.032779

TABLE 7-Continued

WN	WL	n	k	LAC	R
25000.00	0.4000	1.4422	0.0000017	0.519	0.032781
26315.80	0.3800	1.4422	0.0000021	0.683	0.032784
27777.80	0.3600	1.4422	0.0000027	0.958	0.032788
29411.80	0.3400	1.4423	0.0000043	1.597	0.032791
31250.00	0.3200	1.4423	0.0000076	2.993	0.032796
33333.30	0.3000	1.4423	0.0000169	7.080	0.032802
35714.30	0.2800	1.4424	0.0000932	41.815	0.032807

TABLE 8. DIETHYL PHTHALATE

THE COMPLEX REFRACTIVE INDEX, LAMBERT ABSORPTION COEFFICIENT, AND REFLECTION COEFFICIENT.

WN	WL	n	k	LAC	R
501.00	19.9601	1.5115	0.0055487	34.934	0.041483
520.00	19.2308	1.5184	0.0078417	51.242	0.042381
540.00	18.5185	1.5168	0.0078933	53.563	0.042174
560.00	17.8571	1.5211	0.0185386	130.459	0.042775
580.00	17.2414	1.5115	0.0042048	30.646	0.041481
600.00	16.6667	1.5256	0.0022154	16.704	0.043310
620.00	16.1290	1.5271	0.0018739	14.599	0.043506
640.00	15.6250	1.5347	0.0038552	31.006	0.044503
660.00	15.1515	1.5278	0.0061848	51.296	0.043602
680.00	14.7059	1.5526	0.0061184	52.282	0.046871
700.00	14.2857	1.5664	0.0514088	452.215	0.049089
720.00	13.8889	1.5579	0.0246208	222.764	0.047660
740.00	13.5135	1.6191	0.1475480	1372.066	0.058862
760.00	13.1579	1.4463	0.0589015	562.535	0.033844
780.00	12.8205	1.4770	0.0506161	496.127	0.037486
800.00	12.5000	1.4679	0.0271952	273.396	0.036063
820.00	12.1951	1.4938	0.0076484	78.812	0.039217
840.00	11.9048	1.5186	0.0138609	146.312	0.042427
860.00	11.6279	1.5134	0.0415177	448.685	0.041986
880.00	11.3636	1.4979	0.0126952	140.389	0.039756
900.00	11.1111	1.5108	0.0065355	73.915	0.041395
920.00	10.8696	1.5226	0.0035200	40.695	0.042920
940.00	10.6383	1.5324	0.0041168	48.629	0.044201
960.00	10.4167	1.5488	0.0096700	116.656	0.046375
980.00	10.2041	1.5618	0.0079230	97.573	0.048101
1000.00	10.0000	1.5947	0.0332868	418.294	0.052688
1020.00	9.8039	1.5500	0.0898935	1152.228	0.047704
1040.00	9.6154	1.5825	0.0869546	1136.412	0.051951
1060.00	9.4340	1.6451	0.0451140	600.934	0.059753
1080.00	9.2593	1.4318	0.1571610	2132.939	0.035557
1100.00	9.0909	1.5775	0.0730776	1010.152	0.050963
1120.00	8.9286	1.5621	0.2624810	3694.246	0.058019
1140.00	8.7719	1.3675	0.2173460	3113.626	0.032252
1160.00	8.6207	1.4511	0.0510602	744.304	0.034290
1180.00	8.4746	1.4546	0.0421175	624.532	0.034584
1200.00	8.3333	1.5174	0.0144019	217.176	0.042274
1220.00	8.1967	1.5765	0.0200434	307.285	0.050123
1240.00	8.0645	1.6735	0.0868160	1352.793	0.064449
1260.00	7.9365	1.6791	0.2682010	4246.595	0.073537
1280.00	7.8125	1.5674	0.4884130	7856.101	0.082062

TABLE 8-Continued

WN	WL	n	k	LAC	R
1300.00	7.6923	0.9644	0.3208740	5241.888	0.026308
1320.00	7.5758	1.2466	0.0525923	872.381	0.012590
1340.00	7.4627	1.3463	0.0154290	259.808	0.021826
1360.00	7.3529	1.4345	0.0315480	539.164	0.032016
1380.00	7.2464	1.3801	0.0263453	456.869	0.025623
1400.00	7.1429	1.3885	0.0235630	414.542	0.026551
1420.00	7.0423	1.4130	0.0112778	201.244	0.029316
1440.00	6.9444	1.4490	0.0378272	684.505	0.033844
1460.00	6.8493	1.4238	0.0366791	672.948	0.030794
1480.00	6.7568	1.4129	0.0363346	675.759	0.029503
1500.00	6.6667	1.4197	0.0095558	180.123	0.030100
1520.00	6.5789	1.4362	0.0057097	109.060	0.032064
1540.00	6.4935	1.4468	0.0049426	95.650	0.033349
1560.00	6.4103	1.4577	0.0055800	109.389	0.034687
1580.00	6.3291	1.4634	0.0286978	569.791	0.035518
1600.00	6.2500	1.4608	0.0315529	634.409	0.035223
1620.00	6.1728	1.4652	0.0085230	173.507	0.035622
1640.00	6.0976	1.4822	0.0051097	105.305	0.037742
1660.00	6.0241	1.5031	0.0079687	166.229	0.040407
1680.00	5.9524	1.5329	0.0240718	508.192	0.044351
1700.00	5.8824	1.5984	0.0498677	1065.315	0.053385
1720.00	5.8140	1.7204	0.2448230	5291.643	0.077597
1740.00	5.7471	1.2749	0.1850640	4046.514	0.021081
1760.00	5.6818	1.3019	0.0402992	891.290	0.017502
1780.00	5.6180	1.3562	0.0186780	417.792	0.022915
1800.00	5.5556	1.3867	0.0060603	137.081	0.026258
1820.00	5.4945	1.4022	0.0040597	92.850	0.028036
1840.00	5.4348	1.4119	0.0039762	91.938	0.029168
1860.00	5.3763	1.4165	0.0039094	91.375	0.029709
1880.00	5.3191	1.4211	0.0025904	61.198	0.030252
1900.00	5.2632	1.4268	0.0019827	47.338	0.030931
1920.00	5.2083	1.4301	0.0020275	48.918	0.031326
1940.00	5.1546	1.4334	0.0023633	57.615	0.031722
1960.00	5.1020	1.4363	0.0025292	62.295	0.032072
1980.00	5.0505	1.4387	0.0026538	66.031	0.032362
2000.00	5.0000	1.4359	0.0018446	46.360	0.032023
2020.00	4.9505	1.4379	0.0011982	30.416	0.032264
2040.00	4.9020	1.4396	0.0008535	21.880	0.032470
2060.00	4.8544	1.4396	0.0008456	21.891	0.032470
2080.00	4.8077	1.4436	0.0010574	27.639	0.032955
2100.00	4.7619	1.4440	0.0011032	29.113	0.033004
2120.00	4.7170	1.4444	0.0014023	37.359	0.033053
2140.00	4.6729	1.4456	0.0016023	43.090	0.033199
2160.00	4.6296	1.4464	0.0010613	28.807	0.033296
2180.00	4.5872	1.4485	0.0006713	18.389	0.033553
2200.00	4.5455	1.4481	0.0006977	19.290	0.033504
2220.00	4.5045	1.4501	0.0007582	21.151	0.033748
2240.00	4.4643	1.4497	0.0009871	27.786	0.033699

TABLE 8-Continued

WN	WL	n	k	LAC	R
2260.00	4.4248	1.4517	0.0009917	28.165	0.033944
2280.00	4.3860	1.4533	0.0009053	25.939	0.034141
2300.00	4.3478	1.4521	0.0008859	25.605	0.033993
2320.00	4.3103	1.4525	0.0008236	24.013	0.034042
2340.00	4.2735	1.4533	0.0010086	29.658	0.034141
2360.00	4.2373	1.4521	0.0009223	27.351	0.033993
2380.00	4.2017	1.4529	0.0011522	34.459	0.034092
2400.00	4.1667	1.4553	0.0012532	37.796	0.034387
2420.00	4.1322	1.4557	0.0011831	35.980	0.034436
2440.00	4.0984	1.4549	0.0007662	23.493	0.034337
2460.00	4.0650	1.4569	0.0006632	20.500	0.034583
2480.00	4.0323	1.4565	0.0006132	19.110	0.034534
2500.00	4.0000	1.4581	0.0006583	20.681	0.034731
2520.00	3.9683	1.4585	0.0007101	22.486	0.034781
2540.00	3.9370	1.4577	0.0007998	25.529	0.034682
2560.00	3.9063	1.4585	0.0009489	30.525	0.034781
2580.00	3.8760	1.4589	0.0010070	32.647	0.034830
2600.00	3.8462	1.4597	0.0008446	27.594	0.034929
2620.00	3.8168	1.4613	0.0006713	22.103	0.035127
2640.00	3.7879	1.4585	0.0005234	17.365	0.034781
2660.00	3.7594	1.4601	0.0005307	17.741	0.034978
2680.00	3.7313	1.4625	0.0004576	15.410	0.035275
2700.00	3.7037	1.4617	0.0004215	14.302	0.035176
2720.00	3.6765	1.4629	0.0007287	24.907	0.035325
2740.00	3.6496	1.4653	0.0010012	34.472	0.035623
2760.00	3.6232	1.4645	0.0009937	34.465	0.035523
2780.00	3.5971	1.4625	0.0009574	33.448	0.035275
2800.00	3.5714	1.4645	0.0009863	34.704	0.035523
2820.00	3.5461	1.4684	0.0014936	52.928	0.036009
2840.00	3.5211	1.4672	0.0018356	65.508	0.035859
2860.00	3.4965	1.4728	0.0032258	115.936	0.036559
2880.00	3.4722	1.4664	0.0057660	208.676	0.035765
2900.00	3.4483	1.4754	0.0097039	353.635	0.036898
2920.00	3.4247	1.4687	0.0081587	299.374	0.036056
2940.00	3.4014	1.4710	0.0125331	463.037	0.036357
2960.00	3.3784	1.4686	0.0138578	515.461	0.036064
2980.00	3.3557	1.4618	0.0236727	886.490	0.035278
3000.00	3.3333	1.4449	0.0149917	565.174	0.033150
3020.00	3.3113	1.4500	0.0049396	187.462	0.033740
3040.00	3.2895	1.4509	0.0030943	118.206	0.033848
3060.00	3.2680	1.4593	0.0034591	133.013	0.034881
3080.00	3.2468	1.4581	0.0032498	125.781	0.034733
3100.00	3.2258	1.4561	0.0019072	74.296	0.034485
3120.00	3.2051	1.4601	0.0013013	51.020	0.034979
3140.00	3.1847	1.4593	0.0010065	39.716	0.034880
3160.00	3.1646	1.4621	0.0009416	37.390	0.035226
3180.00	3.1447	1.4629	0.0009040	36.124	0.035325
3200.00	3.1250	1.4625	0.0007360	29.597	0.035275

TABLE 8-Continued

WN	WL	n	k	LAC	R
3220.00	3.1056	1.4601	0.0005548	22.450	0.034978
3240.00	3.0864	1.4629	0.0004286	17.451	0.035325
3260.00	3.0675	1.4633	0.0003505	14.360	0.035374
3280.00	3.0488	1.4637	0.0003076	12.680	0.035424
3300.00	3.0303	1.4629	0.0003372	13.985	0.035325
3320.00	3.0120	1.4629	0.0003681	15.357	0.035325
3340.00	2.9940	1.4649	0.0003137	13.169	0.035573
3360.00	2.9762	1.4657	0.0002797	11.809	0.035672
3380.00	2.9586	1.4653	0.0003215	13.657	0.035623
3400.00	2.9412	1.4661	0.0005336	22.800	0.035722
3420.00	2.9240	1.4653	0.0012339	53.028	0.035623
3440.00	2.9070	1.4657	0.0015111	65.321	0.035673
3460.00	2.8902	1.4653	0.0008988	39.080	0.035623
3480.00	2.8736	1.4665	0.0004331	18.940	0.035772
3500.00	2.8571	1.4665	0.0002944	12.949	0.035772
3520.00	2.8409	1.4649	0.0003176	14.050	0.035573
3540.00	2.8249	1.4661	0.0004161	18.511	0.035722
3560.00	2.8090	1.4672	0.0004497	20.117	0.035859
3580.00	2.7933	1.4680	0.0003357	15.103	0.035959
3600.00	2.7778	1.4688	0.0003128	14.151	0.036058
3620.00	2.7624	1.4692	0.0004267	19.411	0.036108
3640.00	2.7473	1.4665	0.0004974	22.752	0.035772
3660.00	2.7322	1.4669	0.0004187	19.259	0.035822
3680.00	2.7174	1.4661	0.0003489	16.137	0.035722
3700.00	2.7027	1.4680	0.0002276	10.583	0.035958
3720.00	2.6882	1.4692	0.0001724	8.059	0.036108
3740.00	2.6738	1.4676	0.0002060	9.683	0.035909
3760.00	2.6596	1.4688	0.0002845	13.443	0.036058
3780.00	2.6455	1.4665	0.0002372	11.268	0.035772
3800.00	2.6316	1.4672	0.0001896	9.053	0.035859
3820.00	2.6178	1.4684	0.0001803	8.653	0.036008
3840.00	2.6042	1.4653	0.0001891	9.126	0.035623
3860.00	2.5907	1.4680	0.0002061	9.998	0.035958
3880.00	2.5773	1.4700	0.0001890	9.215	0.036208
3900.00	2.5641	1.4692	0.0001668	8.176	0.036108
3920.00	2.5510	1.4684	0.0001875	9.234	0.036008
3940.00	2.5381	1.4676	0.0002392	11.842	0.035909
3960.00	2.5253	1.4661	0.0002575	12.812	0.035722
3980.00	2.5126	1.4661	0.0002494	12.476	0.035722
4000.00	2.5000	1.4712	0.0002584	12.990	0.036358
4016.06	2.4900	1.4713	0.0003195	16.126	0.036371
4032.26	2.4800	1.4713	0.0003917	19.846	0.036376
4048.58	2.4700	1.4714	0.0004335	22.057	0.036384
4065.04	2.4600	1.4715	0.0005019	25.641	0.036389
4081.63	2.4500	1.4715	0.0005822	29.861	0.036389
4098.36	2.4400	1.4714	0.0006374	32.826	0.036384
4115.23	2.4300	1.4713	0.0005812	30.054	0.036376
4132.23	2.4200	1.4715	0.0005522	28.677	0.036390

TABLE 8-Continued

WN	WL	n	k	LAC	R
4149.38	2.4100	1.4714	0.0006344	33.081	0.036378
4166.67	2.4000	1.4714	0.0004908	25.697	0.036379
4184.10	2.3900	1.4714	0.0004322	22.723	0.036384
4201.68	2.3800	1.4715	0.0003530	18.639	0.036396
4219.41	2.3700	1.4716	0.0003382	17.930	0.036413
4237.29	2.3600	1.4717	0.0003863	20.569	0.036425
4255.32	2.3500	1.4718	0.0004619	24.698	0.036431
4273.50	2.3400	1.4718	0.0004740	25.452	0.036430
4291.85	2.3300	1.4718	0.0004430	23.892	0.036434
4310.34	2.3200	1.4719	0.0004178	22.628	0.036448
4329.00	2.3100	1.4720	0.0005919	32.201	0.036463
4347.83	2.3000	1.4718	0.0006987	38.172	0.036436
4366.81	2.2900	1.4718	0.0005134	28.175	0.036430
4385.96	2.2800	1.4719	0.0003972	21.889	0.036444
4405.29	2.2700	1.4721	0.0005016	27.766	0.036469
4424.78	2.2600	1.4720	0.0007927	44.078	0.036451
4444.44	2.2500	1.4716	0.0005285	29.517	0.036410
4464.29	2.2400	1.4717	0.0002760	15.481	0.036425
4484.31	2.2300	1.4719	0.0001736	9.781	0.036441
4504.50	2.2200	1.4720	0.0001200	6.795	0.036459
4524.89	2.2100	1.4721	0.0001193	6.782	0.036473
4545.45	2.2000	1.4722	0.0000985	5.625	0.036483
4566.21	2.1900	1.4723	0.0001089	6.248	0.036493
4587.16	2.1800	1.4723	0.0000868	5.002	0.036501
4608.29	2.1700	1.4725	0.0001152	6.670	0.036514
4629.63	2.1600	1.4725	0.0001538	8.947	0.036516
4651.16	2.1500	1.4725	0.0001259	7.360	0.036524
4672.90	2.1400	1.4725	0.0001980	11.626	0.036526
4694.84	2.1300	1.4725	0.0001102	6.502	0.036526
4716.98	2.1200	1.4726	0.0000865	5.130	0.036535
4739.34	2.1100	1.4727	0.0000636	3.787	0.036541
4761.90	2.1000	1.4727	0.0000474	2.837	0.036550
4784.69	2.0900	1.4728	0.0000453	2.726	0.036559
4807.69	2.0800	1.4729	0.0000475	2.867	0.036565
4830.92	2.0700	1.4729	0.0000352	2.137	0.036571
4854.37	2.0600	1.4730	0.0000279	1.700	0.036579
4878.05	2.0500	1.4730	0.0000251	1.537	0.036585
4901.96	2.0400	1.4731	0.0000239	1.473	0.036593
4926.11	2.0300	1.4731	0.0000217	1.345	0.036599
4950.50	2.0200	1.4732	0.0000196	1.221	0.036605
4975.12	2.0100	1.4732	0.0000194	1.216	0.036611
5000.00	2.0000	1.4733	0.0000194	1.219	0.036618
5025.13	1.9900	1.4733	0.0000196	1.236	0.036624
5050.50	1.9800	1.4734	0.0000182	1.154	0.036630
5076.14	1.9700	1.4734	0.0000185	1.179	0.036636
5102.04	1.9600	1.4735	0.0000257	1.648	0.036643
5128.21	1.9500	1.4735	0.0000318	2.048	0.036648
5154.64	1.9400	1.4736	0.0000288	1.865	0.036653

TABLE 8-Continued

WN	WL	n	k	LAC	R
5181.35	1.9300	1.4736	0.0000227	1.477	0.036658
5208.33	1.9200	1.4736	0.0000213	1.395	0.036664
5235.60	1.9100	1.4737	0.0000265	1.745	0.036670
5263.16	1.9000	1.4737	0.0000276	1.824	0.036675
5291.01	1.8900	1.4738	0.0000201	1.338	0.036680
5319.15	1.8800	1.4738	0.0000170	1.135	0.036685
5347.59	1.8700	1.4739	0.0000164	1.105	0.036691
5376.34	1.8600	1.4739	0.0000159	1.075	0.036698
5405.41	1.8500	1.4740	0.0000162	1.098	0.036703
5434.78	1.8400	1.4740	0.0000186	1.272	0.036709
5464.48	1.8300	1.4740	0.0000212	1.455	0.036714
5494.51	1.8200	1.4741	0.0000220	1.520	0.036719
5524.86	1.8100	1.4741	0.0000242	1.678	0.036724
5555.56	1.8000	1.4742	0.0000263	1.838	0.036730
5586.59	1.7900	1.4742	0.0000270	1.893	0.036735
5617.98	1.7800	1.4743	0.0000236	1.669	0.036740
5649.72	1.7700	1.4743	0.0000291	2.063	0.036747
5681.82	1.7600	1.4743	0.0000432	3.087	0.036752
5714.29	1.7500	1.4744	0.0000386	2.770	0.036755
5747.13	1.7400	1.4744	0.0000430	3.107	0.036763
5780.35	1.7300	1.4745	0.0000724	5.259	0.036767
5813.95	1.7200	1.4745	0.0000784	5.727	0.036769
5847.95	1.7100	1.4745	0.0000568	4.176	0.036773
5882.35	1.7000	1.4746	0.0000514	3.798	0.036780
5917.16	1.6900	1.4746	0.0001004	7.467	0.036787
5952.38	1.6800	1.4746	0.0001342	10.038	0.036788
5988.02	1.6700	1.4746	0.0001140	8.581	0.036784
6024.10	1.6600	1.4746	0.0000997	7.548	0.036787
6060.61	1.6500	1.4746	0.0000424	3.226	0.036789
6097.56	1.6400	1.4747	0.0000187	1.431	0.036797
6134.97	1.6300	1.4748	0.0000160	1.231	0.036804
6172.84	1.6200	1.4748	0.0000114	0.881	0.036809
6211.18	1.6100	1.4748	0.0000056	0.441	0.036814
6250.00	1.6000	1.4749	0.0000046	0.360	0.036820
6289.31	1.5900	1.4749	0.0000029	0.232	0.036825
6329.11	1.5800	1.4750	0.0000022	0.179	0.036830
6369.43	1.5700	1.4750	0.0000018	0.140	0.036835
6410.26	1.5600	1.4751	0.0000015	0.124	0.036840
6451.61	1.5500	1.4751	0.0000014	0.113	0.036846
6493.51	1.5400	1.4751	0.0000012	0.100	0.036851
6535.95	1.5300	1.4752	0.0000014	0.114	0.036856
6578.95	1.5200	1.4752	0.0000020	0.161	0.036861
6622.52	1.5100	1.4753	0.0000020	0.169	0.036864
6666.67	1.5000	1.4753	0.0000022	0.183	0.036869
6711.41	1.4900	1.4753	0.0000024	0.206	0.036874
6756.76	1.4800	1.4754	0.0000028	0.237	0.036879
6802.72	1.4700	1.4754	0.0000033	0.279	0.036883
6849.31	1.4600	1.4754	0.0000037	0.317	0.036888

TABLE 8-Continued

WN	WL	n	k	LAC	R
6896.55	1.4500	1.4755	0.0000041	0.354	0.036893
6944.44	1.4400	1.4755	0.0000041	0.357	0.036897
6993.01	1.4300	1.4756	0.0000046	0.404	0.036902
7042.25	1.4200	1.4756	0.0000056	0.498	0.036907
7092.20	1.4100	1.4756	0.0000070	0.627	0.036911
7142.86	1.4000	1.4757	0.0000089	0.802	0.036916
7194.24	1.3900	1.4757	0.0000104	0.942	0.036919
7246.38	1.3800	1.4757	0.0000104	0.946	0.036923
7299.27	1.3700	1.4758	0.0000093	0.853	0.036928
7352.94	1.3600	1.4758	0.0000075	0.689	0.036932
7407.41	1.3500	1.4758	0.0000053	0.495	0.036937
7462.69	1.3400	1.4759	0.0000023	0.220	0.036941
7518.80	1.3300	1.4759	0.0000013	0.127	0.036946
7575.76	1.3200	1.4759	0.0000011	0.105	0.036951
7633.59	1.3100	1.4760	0.0000011	0.109	0.036955
7692.31	1.3000	1.4760	0.0000010	0.101	0.036960
7751.94	1.2900	1.4760	0.0000010	0.102	0.036963
7812.50	1.2800	1.4761	0.0000008	0.077	0.036968
7874.02	1.2700	1.4761	0.0000008	0.077	0.036973
7936.51	1.2600	1.4761	0.0000008	0.084	0.036977
8000.00	1.2500	1.4762	0.0000009	0.088	0.036982
8064.52	1.2400	1.4762	0.0000010	0.103	0.036986
8130.08	1.2300	1.4763	0.0000010	0.100	0.036991
8196.72	1.2200	1.4763	0.0000012	0.119	0.036995
8264.46	1.2100	1.4763	0.0000018	0.188	0.037000
8333.33	1.2000	1.4764	0.0000031	0.327	0.037005
8403.36	1.1900	1.4764	0.0000053	0.561	0.037009
8474.58	1.1800	1.4764	0.0000099	1.059	0.037012
8547.01	1.1700	1.4765	0.0000075	0.803	0.037017
8620.69	1.1600	1.4765	0.0000054	0.583	0.037021
8695.65	1.1500	1.4765	0.0000042	0.460	0.037026
8771.93	1.1400	1.4766	0.0000067	0.740	0.037030
8849.56	1.1300	1.4766	0.0000060	0.671	0.037034
8928.57	1.1200	1.4766	0.0000027	0.298	0.037039
9009.01	1.1100	1.4767	0.0000012	0.131	0.037044
9090.91	1.1000	1.4767	0.0000007	0.082	0.037047
9174.31	1.0900	1.4768	0.0000005	0.059	0.037052
9259.26	1.0800	1.4768	0.0000005	0.055	0.037057
9345.79	1.0700	1.4768	0.0000004	0.049	0.037061
9433.96	1.0600	1.4769	0.0000004	0.044	0.037066
9523.81	1.0500	1.4769	0.0000005	0.057	0.037070
9615.38	1.0400	1.4769	0.0000007	0.079	0.037075
9708.74	1.0300	1.4770	0.0000007	0.080	0.037080
9803.92	1.0200	1.4770	0.0000007	0.086	0.037084
9900.99	1.0100	1.4770	0.0000007	0.082	0.037089
10000.00	1.0000	1.4771	0.0000005	0.066	0.037094
10101.00	0.9900	1.4771	0.0000005	0.063	0.037098
10204.10	0.9800	1.4771	0.0000004	0.052	0.037103

TABLE 8-Continued

WN	WL	n	k	LAC	R
10309.30	0.9700	1.4772	0.0000004	0.046	0.037108
10416.70	0.9600	1.4772	0.0000004	0.047	0.037113
10526.30	0.9500	1.4773	0.0000003	0.043	0.037118
10638.30	0.9400	1.4773	0.0000003	0.045	0.037122
10752.70	0.9300	1.4773	0.0000003	0.047	0.037127
10869.60	0.9200	1.4774	0.0000004	0.055	0.037132
10989.00	0.9100	1.4774	0.0000006	0.084	0.037137
11111.10	0.9000	1.4775	0.0000007	0.103	0.037142
11236.00	0.8900	1.4775	0.0000004	0.061	0.037147
11363.60	0.8800	1.4775	0.0000002	0.034	0.037152
11494.30	0.8700	1.4776	0.0000004	0.064	0.037157
11627.90	0.8600	1.4776	0.0000004	0.052	0.037162
11764.70	0.8500	1.4777	0.0000002	0.030	0.037167
11904.80	0.8400	1.4777	0.0000002	0.027	0.037172
12048.20	0.8300	1.4777	0.0000001	0.011	0.037177
12195.10	0.8200	1.4778	0.0000000	0.007	0.037183
12345.70	0.8100	1.4778	0.0000000	0.003	0.037188

TABLE 9. DIMETHYL METHYLPHOSPHONATE

THE COMPLEX REFRACTIVE INDEX, LAMBERT ABSORPTION COEFFICIENT, AND REFLECTION COEFFICIENT.

WN	WL	n	k	LAC	R
501.00	19.9601	1.5603	0.0324601	204.361	0.048046
520.00	19.2308	1.4665	0.0233041	152.281	0.035852
540.00	18.5185	1.4790	0.0085166	57.793	0.037347
560.00	17.8571	1.4867	0.0052887	37.217	0.038311
580.00	17.2414	1.4927	0.0044844	32.684	0.039077
600.00	16.6667	1.4985	0.0038840	29.284	0.039810
620.00	16.1290	1.5048	0.0035167	27.399	0.040612
640.00	15.6250	1.5127	0.0029518	23.739	0.041629
660.00	15.1515	1.5232	0.0040174	33.319	0.042998
680.00	14.7059	1.5388	0.0062580	53.476	0.045041
700.00	14.2857	1.5721	0.0293050	257.780	0.049591
720.00	13.8889	1.4879	0.0426149	385.571	0.038741
740.00	13.5135	1.5431	0.0104306	96.995	0.045624
760.00	13.1579	1.5899	0.0184048	175.774	0.051921
780.00	12.8205	1.6746	0.1094940	1073.235	0.065181
800.00	12.5000	1.5115	0.0669914	673.471	0.042155
820.00	12.1951	1.5024	0.4166050	4292.875	0.066186
840.00	11.9048	1.4175	0.0365437	385.746	0.030042
860.00	11.6279	1.5078	0.0231356	250.028	0.041086
880.00	11.3636	1.5928	0.0483335	534.491	0.052599
900.00	11.1111	1.6142	0.1860000	2103.610	0.059957
920.00	10.8696	1.3452	0.2464270	2848.958	0.032352
940.00	10.6383	1.4300	0.0421724	498.157	0.031606
960.00	10.4167	1.5161	0.0242248	292.241	0.042169
980.00	10.2041	1.5964	0.0292351	360.032	0.052878
1000.00	10.0000	1.7263	0.0633458	796.027	0.071466
1020.00	9.8039	1.9795	0.3519270	4510.894	0.120351
1040.00	9.6154	1.3975	0.7200310	9410.104	0.107947
1060.00	9.4340	1.1570	0.6619420	8817.301	0.090912
1080.00	9.2593	0.9958	0.1394930	1893.154	0.004866
1100.00	9.0909	1.1854	0.0576505	796.903	0.007888
1120.00	8.9286	1.2677	0.0372771	524.650	0.014201
1140.00	8.7719	1.3259	0.0304021	435.530	0.019804
1160.00	8.6207	1.3800	0.0429955	626.745	0.025807
1180.00	8.4746	1.4084	0.1121710	1663.307	0.030853
1200.00	8.3333	1.3651	0.0618108	932.085	0.024491
1220.00	8.1967	1.4796	0.0600817	921.111	0.037977
1240.00	8.0645	1.5675	0.3553740	5537.544	0.066739
1260.00	7.9365	1.1041	0.3564500	5643.896	0.030278
1280.00	7.8125	1.1818	0.0507086	815.646	0.007479

TABLE 9-Continued

WN	WL	n	k	LAC	R
1300.00	7.6923	1.2949	0.0381687	623.535	0.016780
1320.00	7.5758	1.2209	0.1014950	1683.559	0.011953
1340.00	7.4627	1.2607	0.0145663	245.281	0.013336
1360.00	7.3529	1.2943	0.0083505	142.712	0.016467
1380.00	7.2464	1.3156	0.0066538	115.388	0.018582
1400.00	7.1429	1.3329	0.0092335	162.444	0.020373
1420.00	7.0423	1.3401	0.0280369	500.297	0.021268
1440.00	6.9444	1.3461	0.0220559	399.114	0.021850
1460.00	6.8493	1.3412	0.0399875	733.647	0.021523
1480.00	6.7568	1.3226	0.0238649	443.845	0.019399
1500.00	6.6667	1.3316	0.0119069	224.440	0.020254
1520.00	6.5789	1.3391	0.0084515	161.432	0.021029
1540.00	6.4935	1.3439	0.0064252	124.342	0.021531
1560.00	6.4103	1.3489	0.0052289	102.505	0.022066
1580.00	6.3291	1.3522	0.0045081	89.507	0.022420
1600.00	6.2500	1.3557	0.0036611	73.611	0.022802
1620.00	6.1728	1.3585	0.0030132	61.341	0.023106
1640.00	6.0976	1.3611	0.0024778	51.065	0.023396
1660.00	6.0241	1.3638	0.0017688	36.897	0.023684
1680.00	5.9524	1.3665	0.0013328	28.136	0.023987
1700.00	5.8824	1.3692	0.0013234	28.272	0.024287
1720.00	5.8140	1.3720	0.0019903	43.019	0.024592
1740.00	5.7471	1.3726	0.0040965	89.573	0.024666
1760.00	5.6818	1.3728	0.0028971	64.074	0.024683
1780.00	5.6180	1.3742	0.0021171	47.355	0.024839
1800.00	5.5556	1.3767	0.0018706	42.311	0.025124
1820.00	5.4945	1.3777	0.0033995	77.749	0.025236
1840.00	5.4348	1.3782	0.0040577	93.823	0.025292
1860.00	5.3763	1.3773	0.0033562	78.445	0.025189
1880.00	5.3191	1.3783	0.0021992	51.956	0.025301
1900.00	5.2632	1.3794	0.0013403	32.000	0.025428
1920.00	5.2083	1.3810	0.0009100	21.955	0.025611
1940.00	5.1546	1.3825	0.0011192	27.285	0.025775
1960.00	5.1020	1.3832	0.0016774	41.314	0.025856
1980.00	5.0505	1.3835	0.0013323	33.149	0.025891
2000.00	5.0000	1.3847	0.0008698	21.861	0.026020
2020.00	4.9505	1.3856	0.0011995	30.449	0.026130
2040.00	4.9020	1.3862	0.0010313	26.437	0.026197
2060.00	4.8544	1.3870	0.0011384	29.470	0.026289
2080.00	4.8077	1.3875	0.0012410	32.437	0.026347
2100.00	4.7619	1.3881	0.0011549	30.478	0.026411
2120.00	4.7170	1.3887	0.0011459	30.528	0.026480
2140.00	4.6729	1.3889	0.0011467	30.838	0.026504
2160.00	4.6296	1.3895	0.0006293	17.081	0.026567
2180.00	4.5872	1.3904	0.0004189	11.475	0.026672
2200.00	4.5455	1.3912	0.0007567	20.920	0.026769
2220.00	4.5045	1.3914	0.0010159	28.342	0.026784
2240.00	4.4643	1.3915	0.0008492	23.905	0.026800

TABLE 9-Continued

WN	WL	n	k	LAC	R
2260.00	4.4248	1.3921	0.0004972	14.119	0.026865
2280.00	4.3860	1.3927	0.0004214	12.074	0.026933
2300.00	4.3478	1.3933	0.0004896	14.149	0.027003
2320.00	4.3103	1.3936	0.0006282	18.316	0.027038
2340.00	4.2735	1.3939	0.0004924	14.479	0.027071
2360.00	4.2373	1.3943	0.0003565	10.572	0.027124
2380.00	4.2017	1.3948	0.0002646	7.914	0.027180
2400.00	4.1667	1.3953	0.0002312	6.972	0.027240
2420.00	4.1322	1.3959	0.0002755	8.379	0.027301
2440.00	4.0984	1.3963	0.0003302	10.123	0.027356
2460.00	4.0650	1.3969	0.0004272	13.208	0.027414
2480.00	4.0323	1.3972	0.0006547	20.404	0.027452
2500.00	4.0000	1.3974	0.0006584	20.686	0.027477
2520.00	3.9683	1.3977	0.0005038	15.954	0.027510
2540.00	3.9370	1.3982	0.0003707	11.833	0.027571
2560.00	3.9063	1.3988	0.0003958	12.732	0.027634
2580.00	3.8760	1.3993	0.0004646	15.062	0.027696
2600.00	3.8462	1.3999	0.0006984	22.820	0.027764
2620.00	3.8168	1.4000	0.0011199	36.870	0.027779
2640.00	3.7879	1.4001	0.0009607	31.870	0.027785
2660.00	3.7594	1.4005	0.0006588	22.020	0.027831
2680.00	3.7313	1.4011	0.0005485	18.473	0.027904
2700.00	3.7037	1.4017	0.0005437	18.447	0.027977
2720.00	3.6765	1.4024	0.0006073	20.758	0.028057
2740.00	3.6496	1.4031	0.0006601	22.728	0.028139
2760.00	3.6232	1.4040	0.0007362	25.534	0.028247
2780.00	3.5971	1.4052	0.0009547	33.353	0.028382
2800.00	3.5714	1.4068	0.0013701	48.208	0.028563
2820.00	3.5461	1.4091	0.0024431	86.576	0.028832
2840.00	3.5211	1.4136	0.0075775	270.430	0.029374
2860.00	3.4965	1.4014	0.0111383	400.309	0.027960
2880.00	3.4722	1.4057	0.0055510	200.899	0.028448
2900.00	3.4483	1.4092	0.0079797	290.800	0.028861
2920.00	3.4247	1.4110	0.0129677	475.834	0.029089
2940.00	3.4014	1.4101	0.0172569	637.558	0.029006
2960.00	3.3784	1.3959	0.0265408	987.224	0.027423
2980.00	3.3557	1.3961	0.0172321	645.304	0.027382
3000.00	3.3333	1.3895	0.0189660	715.001	0.026634
3020.00	3.3113	1.3868	0.0117227	444.882	0.026285
3040.00	3.2895	1.3879	0.0065562	250.460	0.026390
3060.00	3.2680	1.3907	0.0041937	161.261	0.026706
3080.00	3.2468	1.3921	0.0033666	130.303	0.026874
3100.00	3.2258	1.3932	0.0026680	103.933	0.026990
3120.00	3.2051	1.3940	0.0020624	80.862	0.027092
3140.00	3.1847	1.3949	0.0016103	63.540	0.027184
3160.00	3.1646	1.3956	0.0013017	51.689	0.027268
3180.00	3.1447	1.3962	0.0010928	43.668	0.027340
3200.00	3.1250	1.3967	0.0009525	38.301	0.027402

TABLE 9-Continued

WN	WL	n	k	LAC	R
3220.00	3.1056	1.3972	0.0008485	34.332	0.027455
3240.00	3.0864	1.3976	0.0007355	29.947	0.027499
3260.00	3.0675	1.3980	0.0006227	25.511	0.027546
3280.00	3.0488	1.3984	0.0005904	24.336	0.027590
3300.00	3.0303	1.3987	0.0005820	24.136	0.027622
3320.00	3.0120	1.3989	0.0004794	20.001	0.027652
3340.00	2.9940	1.3992	0.0004111	17.257	0.027689
3360.00	2.9762	1.3995	0.0003876	16.365	0.027725
3380.00	2.9586	1.3999	0.0003979	16.903	0.027761
3400.00	2.9412	1.4001	0.0004483	19.155	0.027794
3420.00	2.9240	1.4004	0.0005183	22.273	0.027822
3440.00	2.9070	1.4006	0.0006038	26.103	0.027845
3460.00	2.8902	1.4007	0.0007057	30.685	0.027859
3480.00	2.8736	1.4008	0.0007128	31.170	0.027866
3500.00	2.8571	1.4009	0.0007038	30.953	0.027881
3520.00	2.8409	1.4010	0.0007403	32.748	0.027890
3540.00	2.8249	1.4010	0.0006914	30.757	0.027889
3560.00	2.8090	1.4010	0.0005141	22.998	0.027897
3580.00	2.7933	1.4012	0.0003504	15.763	0.027919
3600.00	2.7778	1.4014	0.0002717	12.293	0.027945
3620.00	2.7624	1.4016	0.0002488	11.318	0.027967
3640.00	2.7473	1.4018	0.0002403	10.991	0.027984
3660.00	2.7322	1.4019	0.0001903	8.752	0.028001
3680.00	2.7174	1.4021	0.0001561	7.220	0.028021
3700.00	2.7027	1.4023	0.0001690	7.857	0.028044
3720.00	2.6882	1.4024	0.0002211	10.336	0.028060
3740.00	2.6738	1.4025	0.0002675	12.574	0.028072
3755.16	2.6630	1.4026	0.0002220	10.476	0.028083
3769.32	2.6530	1.4028	0.0001732	8.205	0.028102
3783.58	2.6430	1.4029	0.0002139	10.172	0.028118
3797.95	2.6330	1.4031	0.0002445	11.668	0.028133
3812.43	2.6230	1.4032	0.0004723	22.628	0.028151
3827.02	2.6130	1.4030	0.0006520	31.357	0.028128
3841.72	2.6030	1.4029	0.0005139	24.811	0.028117
3856.54	2.5930	1.4031	0.0003136	15.200	0.028141
3871.47	2.5830	1.4034	0.0003904	18.991	0.028171
3886.51	2.5730	1.4033	0.0006658	32.517	0.028166
3901.68	2.5630	1.4032	0.0006386	31.313	0.028143
3916.96	2.5530	1.4032	0.0004704	23.152	0.028146
3932.36	2.5430	1.4033	0.0003182	15.724	0.028162
3947.89	2.5330	1.4034	0.0002825	14.016	0.028176
3963.54	2.5230	1.4037	0.0003128	15.580	0.028202
3979.31	2.5130	1.4038	0.0004406	22.031	0.028222
3995.21	2.5030	1.4037	0.0005407	27.149	0.028211
4011.23	2.4930	1.4038	0.0005499	27.721	0.028222
4027.39	2.4830	1.4039	0.0006154	31.146	0.028225
4043.67	2.4730	1.4038	0.0006664	33.862	0.028221
4060.09	2.4630	1.4038	0.0006946	35.440	0.028220

TABLE 9-Continued

WN	WL	n	k	LAC	R
4076.64	2.4530	1.4037	0.0005793	29.676	0.028204
4093.33	2.4430	1.4038	0.0004522	23.259	0.028222
4110.15	2.4330	1.4039	0.0003805	19.651	0.028226
4127.12	2.4230	1.4041	0.0003525	18.279	0.028252
4144.22	2.4130	1.4041	0.0003895	20.282	0.028259
4161.46	2.4030	1.4043	0.0004953	25.899	0.028280
4178.85	2.3930	1.4042	0.0006108	32.076	0.028270
4196.39	2.3830	1.4041	0.0006169	32.533	0.028259
4214.08	2.3730	1.4041	0.0004275	22.637	0.028259
4231.91	2.3630	1.4043	0.0003437	18.276	0.028272
4249.89	2.3530	1.4044	0.0003573	19.083	0.028291
4268.03	2.3430	1.4045	0.0003308	17.741	0.028301
4286.33	2.3330	1.4046	0.0003727	20.073	0.028312
4304.78	2.3230	1.4046	0.0005108	27.630	0.028315
4323.39	2.3130	1.4047	0.0003516	19.100	0.028319
4342.16	2.3030	1.4048	0.0002994	16.339	0.028337
4361.10	2.2930	1.4050	0.0003400	18.635	0.028356
4380.20	2.2830	1.4053	0.0004785	26.339	0.028388
4399.47	2.2730	1.4055	0.0010656	58.910	0.028414
4418.91	2.2630	1.4049	0.0012134	67.379	0.028341
4438.53	2.2530	1.4047	0.0012137	67.697	0.028325
4458.31	2.2430	1.4043	0.0010410	58.323	0.028282
4478.28	2.2330	1.4043	0.0006808	38.310	0.028273
4498.43	2.2230	1.4044	0.0004188	23.677	0.028284
4518.75	2.2130	1.4045	0.0002647	15.028	0.028303
4539.26	2.2030	1.4047	0.0001825	10.412	0.028320
4559.96	2.1930	1.4048	0.0001326	7.598	0.028337
4580.85	2.1830	1.4049	0.0001039	5.982	0.028349
4601.93	2.1730	1.4050	0.0000867	5.016	0.028359
4623.21	2.1630	1.4051	0.0000740	4.301	0.028366
4644.68	2.1530	1.4051	0.0000593	3.461	0.028372
4666.36	2.1430	1.4052	0.0000506	2.968	0.028386
4688.23	2.1330	1.4054	0.0000465	2.742	0.028400
4710.32	2.1230	1.4054	0.0000421	2.493	0.028404
4732.61	2.1130	1.4054	0.0000344	2.045	0.028407
4755.11	2.1030	1.4055	0.0000306	1.830	0.028422
4777.83	2.0930	1.4056	0.0000292	1.751	0.028429
4800.77	2.0830	1.4056	0.0000276	1.666	0.028432
4823.93	2.0730	1.4058	0.0000224	1.359	0.028446
4847.31	2.0630	1.4057	0.0000179	1.090	0.028445
4870.92	2.0530	1.4059	0.0000159	0.973	0.028461
4894.76	2.0430	1.4059	0.0000152	0.938	0.028459
4918.84	2.0330	1.4060	0.0000143	0.884	0.028474
4943.15	2.0230	1.4060	0.0000129	0.801	0.028476
4967.71	2.0130	1.4061	0.0000123	0.770	0.028483
4992.51	2.0030	1.4062	0.0000118	0.740	0.028495
5017.56	1.9930	1.4062	0.0000116	0.731	0.028496
5042.86	1.9830	1.4062	0.0000120	0.762	0.028501

TABLE 9-Continued

WN	WL	n	k	LAC	R
5068.42	1.9730	1.4063	0 0000126	0.803	0.028511
5094.24	1.9630	1.4064	0.0000137	0.878	0.028521
5120.33	1.9530	1.4064	0.0000143	0.921	0.028525
5146.68	1.9430	1.4065	0.0000154	0.994	0.028529
5173.31	1.9330	1.4065	0.0000161	1.044	0.028534
5200.21	1.9230	1.4066	0.0000196	1.280	0.028539
5227.39	1.9130	1.4066	0.0000171	1.121	0.028546
5254.86	1.9030	1.4067	0.0000151	1.000	0.028553
5282.62	1.8930	1.4067	0.0000180	1.193	0.028561
5310.67	1.8830	1.4068	0.0000191	1.272	0.028568
5339.03	1.8730	1.4068	0.0000178	1.191	0.028571
5367.69	1.8630	1.4068	0.0000189	1.274	0.028572
5396.65	1.8530	1.4069	0.0000161	1.089	0.028581
5425.94	1.8430	1.4070	0.0000159	1.085	0.028590
5455.54	1.8330	1.4070	0.0000159	1.093	0.028590
5485.46	1.8230	1.4071	0.0000174	1.196	0.028601
5515.72	1.8130	1.4071	0.0000191	1.324	0.028603
5546.31	1.8030	1.4072	0.0000249	1.738	0.028612
5577.24	1.7930	1.4072	0.0000227	1.589	0.028613
5608.52	1.7830	1.4073	0.0000293	2.064	0.028624
5640.16	1.7730	1.4073	0.0000269	1.908	0.028627
5672.15	1.7630	1.4073	0.0000243	1.732	0.028629
5704.51	1.7530	1.4074	0.0000362	2.593	0.028640
5737.23	1.7430	1.4075	0.0000441	3.179	0.028647
5770.34	1.7330	1.4076	0.0000705	5.113	0.028656
5803.83	1.7230	1.4075	0.0001033	7.533	0.028655
5837.71	1.7130	1.4076	0.0000807	5.917	0.028658
5871.99	1.7030	1.4076	0.0000578	4.264	0.028663
5906.67	1.6930	1.4077	0.0000615	4.562	0.028668
5941.77	1.6830	1.4077	0.0001018	7.603	0.028668
5977.29	1.6730	1.4077	0.0000827	6.215	0.028670
6013.23	1.6630	1.4077	0.0000542	4.093	0.028677
6049.61	1.6530	1.4078	0.0000260	1.975	0.028679
6086.43	1.6430	1.4078	0.0000166	1.271	0.028687
6123.70	1.6330	1.4079	0.0000121	0.928	0.028692
6161.43	1.6230	1.4079	0.0000089	0.688	0.028700
6199.63	1.6130	1.4079	0.0000063	0.493	0.028700
6238.30	1.6030	1.4080	0.0000046	0.364	0.028710
6377.55	1.5680	1.4082	0.0000022	0.180	0.028729
6418.49	1.5580	1.4082	0.0000020	0.160	0.028736
6459.95	1.5480	1.4083	0.0000021	0.168	0.028742
6501.95	1.5380	1.4083	0.0000021	0.169	0.028745
6544.50	1.5280	1.4083	0.0000021	0.170	0.028746
6587.62	1.5180	1.4084	0.0000024	0.198	0.028756
6631.30	1.5080	1.4084	0.0000033	0.275	0.028758
6675.57	1.4980	1.4085	0.0000040	0.338	0.028767
6720.43	1.4880	1.4085	0.0000043	0.361	0.028767
6765.90	1.4780	1.4086	0.0000033	0.284	0.028775

TABLE 9-Continued

WN	WL	n	k	LAC	R
6811.99	1.4680	1.4086	0.0000037	0.313	0.028782
6858.71	1.4580	1.4087	0.0000042	0.362	0.028788
6906.08	1.4480	1.4087	0.0000062	0.536	0.028793
6954.10	1.4380	1.4088	0.0000083	0.724	0.028797
7002.80	1.4280	1.4088	0.0000075	0.660	0.028799
7052.19	1.4180	1.4088	0.0000073	0.649	0.028803
7102.27	1.4080	1.4089	0.0000072	0.639	0.028812
7153.08	1.3980	1.4089	0.0000103	0.922	0.028812
7204.61	1.3880	1.4090	0.0000140	1.266	0.028821
7256.89	1.3780	1.4090	0.0000141	1.290	0.028825
7309.94	1.3680	1.4090	0.0000111	1.021	0.028828
7363.77	1.3580	1.4091	0.0000115	1.065	0.028832
7418.40	1.3480	1.4091	0.0000089	0.833	0.028838
7473.84	1.3380	1.4092	0.0000059	0.558	0.028845
7530.12	1.3280	1.4092	0.0000022	0.206	0.028847
7587.25	1.3180	1.4092	0.0000013	0.127	0.028853
7645.26	1.3080	1.4093	0.0000009	0.090	0.028857
7704.16	1.2980	1.4093	0.0000009	0.084	0.028865
7763.98	1.2880	1.4094	0.0000008	0.080	0.028869
7824.73	1.2780	1.4094	0.0000009	0.088	0.028874
7886.44	1.2680	1.4095	0.0000008	0.081	0.028880
7949.13	1.2580	1.4095	0.0000010	0.099	0.028882
8012.82	1.2480	1.4095	0.0000011	0.108	0.028887
8077.54	1.2380	1.4096	0.0000011	0.116	0.028892
8143.32	1.2280	1.4096	0.0000011	0.118	0.028900
8210.18	1.2180	1.4097	0.0000013	0.131	0.028904
8278.15	1.2080	1.4097	0.0000019	0.194	0.028909
8347.25	1.1980	1.4098	0.0000029	0.304	0.028913
8417.51	1.1880	1.4098	0.0000049	0.513	0.028915
8488.96	1.1780	1.4098	0.0000085	0.908	0.028924
8561.64	1.1680	1.4099	0.0000116	1.249	0.028928
8635.58	1.1580	1.4099	0.0000069	0.744	0.028932
8710.80	1.1480	1.4100	0.0000047	0.516	0.028938
8787.35	1.1380	1.4100	0.0000041	0.458	0.028941
8865.25	1.1280	1.4100	0.0000026	0.294	0.028946
8944.54	1.1180	1.4101	0.0000012	0.140	0.028949
9025.27	1.1080	1.4101	0.0000007	0.084	0.028954
9107.47	1.0980	1.4102	0.0000005	0.057	0.028960
9191.18	1.0880	1.4102	0.0000005	0.056	0.028969
9276.44	1.0780	1.4102	0.0000005	0.057	0.028970
9363.30	1.0680	1.4103	0.0000005	0.055	0.028975
9451.80	1.0580	1.4103	0.0000005	0.058	0.028980
9541.98	1.0480	1.4104	0.0000005	0.062	0.028988
9633.91	1.0380	1.4104	0.0000006	0.070	0.028990
9727.63	1.0280	1.4105	0.0000007	0.084	0.028997
9823.18	1.0180	1.4105	0.0000008	0.093	0.029001
9920.63	1.0080	1.4106	0.0000009	0.117	0.029009
10020.00	0.9980	1.4106	0.0000008	0.098	0.029012

TABLE 9-Continued

WN	WL	n	k	LAC	R
10121.50	0.9880	1.4106	0.0000005	0.061	0.029017
10224.90	0.9780	1.4107	0.0000004	0.053	0.029025
10330.60	0.9680	1.4107	0.0000004	0.051	0.029027
10438.40	0.9580	1.4108	0.0000003	0.044	0.029033
10548.50	0.9480	1.4108	0.0000003	0.041	0.029040
10661.00	0.9380	1.4109	0.0000002	0.021	0.029044
10775.90	0.9280	1.4109	0.0000002	0.027	0.029050
10893.20	0.9180	1.4110	0.0000003	0.048	0.029057
11013.20	0.9080	1.4110	0.0000006	0.081	0.029060
11135.90	0.8980	1.4111	0.0000010	0.142	0.029067
11261.30	0.8880	1.4111	0.0000008	0.113	0.029074
11389.50	0.8780	1.4112	0.0000005	0.078	0.029080
11520.70	0.8680	1.4112	0.0000005	0.076	0.029084
11655.00	0.8580	1.4113	0.0000004	0.053	0.029090
11792.50	0.8480	1.4113	0.0000003	0.041	0.029097
11933.20	0.8380	1.4114	0.0000002	0.036	0.029102
12077.30	0.8280	1.4114	0.0000002	0.034	0.029110
12224.90	0.8180	1.4115	0.0000002	0.031	0.029115
12376.20	0.8080	1.4115	0.0000003	0.040	0.029122

TABLE 10. DIISOPROPYLMETHYLPHOSPHONATE

THE COMPLEX REFRACTIVE INDEX, LAMBERT ABSORPTION COEFFICIENT, AND REFLECTION COEFFICIENT.

WN	WL	n	k	LAC	R
651.00	15.3610	1.4831	0.0047656	38.986	0.037856
670.00	14.9254	1.4840	0.0027008	22.739	0.037972
690.00	14.4928	1.4913	0.0032839	28.474	0.038886
710.00	14.0845	1.5060	0.0150391	134.181	0.040804
730.00	13.6986	1.4815	0.0125731	115.339	0.037671
750.00	13.3333	1.4945	0.0212185	199.980	0.039373
770.00	12.9870	1.5046	0.0081480	78.841	0.040606
790.00	12.6582	1.5229	0.1020530	1013.124	0.044516
810.00	12.3457	1.4697	0.0071116	72.387	0.036172
830.00	12.0482	1.5008	0.0004607	4.805	0.040101
850.00	11.7647	1.5233	0.0017220	18.394	0.043007
870.00	11.4943	1.5526	0.0057214	62.550	0.046866
890.00	11.2360	1.5965	0.0299671	335.154	0.052902
910.00	10 9890	1.5865	0.0822053	940.050	0.052379
930.00	10.7527	1.5767	0.0617611	721.785	0.050642
950.00	10.5263	1.6593	0.0683720	816.229	0.062092
970.00	10.3093	1.8577	0.2083280	2539.389	0.094892
990.00	10.1010	1.4495	0.8281530	10302.809	0.132801
1010.00	9.9010	1.1747	0.4026410	5110.334	0.039384
1030.00	9.7087	1.0833	0.1233900	1597.081	0.005088
1050.00	9.5238	1.2580	0.0135269	178.483	0.013088
1070.00	9.3458	1.3484	0.0146749	197.319	0.022051
1090.00	9.1743	1.3867	0.0407834	558.624	0.026536
1110.00	9.0090	1.3747	0.1179970	1645.901	0.027294
1130.00	8.8496	1.3762	0.0598935	850.488	0.025679
1150.00	8.6957	1.3632	0.0621215	897.738	0.024300
1170.00	8.5470	1.3884	0.0607154	892.678	0.027076
1190.00	8.4034	1.3688	0.0432712	647.077	0.024570
1210.00	8.2645	1.4168	0.0361335	549.421	0.029963
1230.00	8.1301	1.4903	0.0905859	1400.153	0.040036
1250.00	8.0000	1.2196	0.2384850	3746.114	0.021090
1270.00	7.8740	1.2737	0.0651710	1040.083	0.015301
1290.00	7.7519	1.3196	0.0226461	367.107	0.019082
1310.00	7.6336	1.3553	0.0702065	1155.736	0.023622
1330.00	7.5188	1.3347	0.0125575	209.877	0.020583
1350.00	7.4074	1.3618	0.0184987	313.823	0.023529
1370.00	7.2993	1.3875	0.0377128	649.261	0.026589
1390.00	7.1942	1.3153	0.0414105	723.328	0.018860
1410.00	7.0922	1.3495	0.0086507	153.278	0.022137
1430.00	6.9930	1.3592	0.0092588	166.379	0.023195

TABLE 10-Continued

WN	WL	n	k	LAC	R
1450.00	6.8966	1.3703	0.0168387	306.822	0.024457
1470.00	6.8027	1.3548	0.0232628	429.724	0.022799
1490.00	6.7114	1.3611	0.0046729	87.496	0.023397
1510.00	6.6225	1.3681	0.0028829	54.703	0.024168
1530.00	6.5359	1.3727	0.0023015	44.251	0.024678
1550.00	6.4516	1.3762	0.0021092	41.083	0.025068
1570.00	6.3694	1.3792	0.0022063	43.530	0.025406
1590.00	6.2893	1.3815	0.0023289	46.532	0.025663
1610.00	6.2112	1.3837	0.0024839	50.254	0.025914
1630.00	6.1350	1.3855	0.0030463	62.398	0.026119
1650.00	6.0606	1.3867	0.0033752	69.983	0.026255
1670.00	5.9880	1.3880	0.0033395	70.083	0.026396
1690.00	5.9172	1.3896	0.0041031	87.139	0.026582
1710.00	5.8480	1.3894	0.0045886	98.602	0.026562
1730.00	5.7803	1.3896	0.0046177	100.388	0.026587
1750.00	5.7143	1.3904	0.0038082	83.747	0.026675
1770.00	5.6497	1.3902	0.0036481	81.142	0.026655
1790.00	5.5866	1.3913	0.0023811	53.559	0.026772
1810.00	5.5249	1.3924	0.0020497	46.621	0.026898
1830.00	5.4645	1.3934	0.0016383	37.676	0.027020
1850.00	5.4054	1.3946	0.0016326	37.955	0.027155
1870.00	5.3476	1.3953	0.0017935	42.146	0.027236
1890.00	5.2910	1.3959	0.0017936	42.598	0.027303
1910.00	5.2356	1.3965	0.0016020	38.451	0.027370
1930.00	5.1813	1.3971	0.0015539	37.687	0.027448
1950.00	5.1282	1.3978	0.0013922	34.116	0.027521
1970.00	5.0761	1.3984	0.0013368	33.093	0.027591
1990.00	5.0251	1.3991	0.0012387	30.975	0.027669
2010.00	4.9751	1.3998	0.0013132	33.170	0.027754
2030.00	4.9261	1.4003	0.0014948	38.132	0.027810
2050.00	4.8780	1.4008	0.0014578	37.555	0.027869
2070.00	4.8309	1.4013	0.0015830	41.177	0.027933
2090.00	4.7847	1.4019	0.0018376	48.262	0.027996
2110.00	4.7393	1.4020	0.0020312	53.858	0.028005
2130.00	4.6948	1.4022	0.0019437	52.025	0.028035
2150.00	4.6512	1.4026	0.0018330	49.523	0.028079
2170.00	4.6083	1.4031	0.0018212	49.663	0.028134
2190.00	4.5662	1.4035	0.0019665	54.120	0.028182
2210.00	4.5249	1.4038	0.0020502	56.939	0.028221
2230.00	4.4843	1.4041	0.0021013	58.884	0.028258
2250.00	4.4444	1.4045	0.0023149	65.453	0.028305
2270.00	4.4053	1.4047	0.0024419	69.657	0.028321
2290.00	4.3668	1.4049	0.0026294	75.665	0.028352
2310.00	4.3290	1.4048	0.0027950	81.134	0.028336
2330.00	4.2918	1.4049	0.0024949	73.048	0.028352
2350.00	4.2553	1.4052	0.0023311	68.841	0.028386
2370.00	4.2194	1.4056	0.0024151	71.927	0.028435
2390.00	4.1841	1.4057	0.0026367	79.189	0.028438

TABLE 10-Continued

WN	WL	n	k	LAC	R
2410.00	4.1494	1.4057	0.0025440	77.046	0.028438
2430.00	4.1152	1.4058	0.0022907	69.951	0.028457
2450.00	4.0816	1.4063	0.0020498	63.110	0.028506
2470.00	4.0486	1.4067	0.0020818	64.617	0.028555
2490.00	4.0161	1.4070	0.0021077	65.950	0.028589
2510.00	3.9841	1.4073	0.0021991	69.362	0.028627
2530.00	3.9526	1.4075	0.0021816	69.359	0.028649
2550.00	3.9216	1.4079	0.0021972	70.406	0.028703
2570.00	3.8911	1.4082	0.0022713	73.354	0.028730
2590.00	3.8610	1.4086	0.0023228	75.601	0.028778
2610.00	3.8314	1.4089	0.0025188	82.612	0.028817
2630.00	3.8023	1.4093	0.0027221	89.964	0.028856
2650.00	3.7736	1.4093	0.0029735	99.021	0.028860
2670.00	3.7453	1.4096	0.0027015	90.640	0.028899
2690.00	3.7175	1.4101	0.0029359	99.243	0.028960
2710.00	3.6900	1.4104	0.0031156	106.100	0.028996
2730.00	3.6630	1.4108	0.0034471	118.257	0.029041
2750.00	3.6364	1.4109	0.0032565	112.538	0.029052
2770.00	3.6101	1.4117	0.0031050	108.080	0.029139
2790.00	3.5842	1.4127	0.0032259	113.099	0.029257
2810.00	3.5587	1.4139	0.0037532	132.532	0.029401
2830.00	3.5336	1.4148	0.0043376	154.257	0.029508
2850.00	3.5088	1.4169	0.0048567	173.938	0.029762
2870.00	3.4843	1.4210	0.0094357	340.302	0.030250
2890.00	3.4602	1.4176	0.0125002	453.967	0.029858
2910.00	3.4364	1.4182	0.0152242	556.721	0.029949
2930.00	3.4130	1.4144	0.0226755	834.900	0.029547
2950.00	3.3898	1.4120	0.0156159	578.894	0.029215
2970.00	3.3670	1.4204	0.0351444	1311.664	0.030378
2990.00	3.3445	1.3772	0.0319928	1202.080	0.025358
3010.00	3.3223	1.3835	0.0075031	283.805	0.025896
3030.00	3.3003	1.3923	0.0032718	124.577	0.026895
3050.00	3.2787	1.3961	0.0024213	92.803	0.027328
3070.00	3.2573	1.3984	0.0019510	75.266	0.027589
3090.00	3.2362	1.3999	0.0016949	65.813	0.027772
3110.00	3.2154	1.4012	0.0015178	59.319	0.027913
3130.00	3.1949	1.4021	0.0014495	57.012	0.028025
3150.00	3.1746	1.4029	0.0014117	55.882	0.028117
3170.00	3.1546	1.4036	0.0014633	58.291	0.028197
3190.00	3.1348	1.4041	0.0015761	63.182	0.028258
3210.00	3.1153	1.4045	0.0016101	64.950	0.028300
3230.00	3.0960	1.4048	0.0015877	64.445	0.028339
3250.00	3.0769	1.4052	0.0015139	61.829	0.028381
3270.00	3.0581	1.4056	0.0014823	60.912	0.028433
3290.00	3.0395	1.4061	0.0015367	63.530	0.028483
3310.00	3.0211	1.4065	0.0016406	68.239	0.028535
3330.00	3.0030	1.4070	0.0018644	78.017	0.028587
3350.00	2.9851	1.4074	0.0022585	95.078	0.028637

TABLE 10-Continued

WN	WL	n	k	LAC	R
3370.00	2.9674	1.4077	0.0028796	121.948	0.028674
3390.00	2.9499	1.4076	0.0037033	157.761	0.028669
3410.00	2.9326	1.4070	0.0044180	189.319	0.028595
3430.00	2.9155	1.4060	0.0046004	198.288	0.028479
3450.00	2.8986	1.4052	0.0041008	177.788	0.028382
3470.00	2.8818	1.4048	0.0035239	153.660	0.028336
3490.00	2.8653	1.4047	0.0028352	124.345	0.028329
3510.00	2.8490	1.4050	0.0024395	107.601	0.028360
3530.00	2.8329	1.4051	0.0023308	103.394	0.028368
3550.00	2.8169	1.4049	0.0020394	90.978	0.028345
3570.00	2.8011	1.4049	0.0014797	66.384	0.028350
3590.00	2.7855	1.4052	0.0010482	47.290	0.028385
3610.00	2.7701	1.4056	0.0008003	36.303	0.028427
3630.00	2.7548	1.4059	0.0006823	31.126	0.028462
3650.00	2.7397	1.4061	0.0005699	26.138	0.028485
3670.00	2.7248	1.4063	0.0004382	20.208	0.028515
3690.00	2.7100	1.4066	0.0003626	16.816	0.028540
3710.00	2.6954	1.4068	0.0002677	12.480	0.028571
3730.00	2.6810	1.4070	0.0002636	12.357	0.028597
3750.00	2.6667	1.4072	0.0002372	11.178	0.028620
3770.00	2.6525	1.4075	0.0002178	10.318	0.028646
3790.00	2.6385	1.4077	0.0003084	14.688	0.028672
3810.98	2.6240	1.4077	0.0003977	19.047	0.028673
3840.25	2.6040	1.4079	0.0003479	16.791	0.028696
3869.97	2.5840	1.4081	0.0004049	19.692	0.028717
3900.16	2.5640	1.4082	0.0003898	19.104	0.028730
3930.82	2.5440	1.4083	0.0003218	15.896	0.028741
3961.97	2.5240	1.4085	0.0003271	16.284	0.028766
3993.61	2.5040	1.4086	0.0003434	17.234	0.028783
4025.76	2.4840	1.4088	0.0003794	19.191	0.028805
4058.44	2.4640	1.4089	0.0004904	25.011	0.028814
4091.65	2.4440	1.4090	0.0005774	29.687	0.028821
4125.41	2.4240	1.4089	0.0005254	27.240	0.028811
4159.73	2.4040	1.4090	0.0005762	30.120	0.028831
4194.63	2.3840	1.4091	0.0002807	14.795	0.028834
4230.12	2.3640	1.4094	0.0003097	16.463	0.028871
4266.21	2.3440	1.4096	0.0004165	22.328	0.028893
4302.93	2.3240	1.4098	0.0007847	42.432	0.028915
4340.28	2.3040	1.4095	0.0007435	40.549	0.028880
4378.28	2.2840	1.4094	0.0005722	31.483	0.028868
4416.96	2.2640	1.4092	0.0008082	44.862	0.028853
4456.33	2.2440	1.4092	0.0002437	13.649	0.028853
4496.40	2.2240	1.4095	0.0001048	5.924	0.028887
4537.21	2.2040	1.4097	0.0000787	4.485	0.028910
4578.75	2.1840	1.4099	0.0000712	4.098	0.028928
4621.07	2.1640	1.4100	0.0000641	3.723	0.028943
4664.18	2.1440	1.4101	0.0000579	3.392	0.028956
4708.10	2.1240	1.4102	0.0000528	3.125	0.028970

TABLE 10-Continued

WN	WL	n	k	LAC	R
4752.85	2.1040	1.4103	0.0000501	2.990	0.028981
4798.46	2.0840	1.4104	0.0000489	2.951	0.028993
4844.96	2.0640	1.4105	0.0000460	2.798	0.029004
4892.37	2.0440	1.4106	0.0000330	2.028	0.029015
4940.71	2.0240	1.4107	0.0000300	1.861	0.029026
4990.02	2.0040	1.4108	0.0000351	2.199	0.029037
5040.32	1.9840	1.4109	0.0000355	2.248	0.029047
5091.65	1.9640	1.4110	0.0000358	2.289	0.029057
5144.03	1.9440	1.4111	0.0000414	2.673	0.029067
5197.51	1.9240	1.4111	0.0000499	3.260	0.029074
5252.10	1.9040	1.4112	0.0000420	2.772	0.029083
5307.86	1.8840	1.4113	0.0000329	2.193	0.029092
5364.81	1.8640	1.4114	0.0000222	1.496	0.029102
5422.99	1.8440	1.4114	0.0000222	1.515	0.029112
5482.46	1.8240	1.4115	0.0000241	1.657	0.029121
5543.24	1.8040	1.4116	0.0000453	3.154	0.029130
5605.38	1.7840	1.4117	0.0000361	2.545	0.029138
5668.93	1.7640	1.4118	0.0000502	3.573	0.029148
5733.94	1.7440	1.4118	0.0000568	4.094	0.029157
5800.46	1.7240	1.4119	0.0001043	7.606	0.029160
5868.54	1.7040	1.4119	0.0000592	4.364	0.029168
5938.24	1.6840	1.4120	0.0001129	8.424	0.029172
6009.62	1.6640	1.4120	0.0000210	1.583	0.029175
6082.73	1.6440	1.4121	0.0000076	0.582	0.029187
6157.64	1.6240	1.4122	0.0000080	0.620	0.029197
6253.91	1.5990	1.4123	0.0000055	0.432	0.029208
6333.12	1.5790	1.4123	0.0000049	0.392	0.029215
6414.37	1.5590	1.4124	0.0000046	0.371	0.029223
6497.73	1.5390	1.4125	0.0000042	0.340	0.029232
6583.28	1.5190	1.4125	0.0000047	0.388	0.029239
6671.11	1.4990	1.4126	0.0000064	0.539	0.029247
6761.33	1.4790	1.4127	0.0000063	0.539	0.029255
6854.01	1.4590	1.4127	0.0000081	0.694	0.029262
6949.27	1.4390	1.4128	0.0000077	0.675	0.029269
7047.22	1.4190	1.4128	0.0000077	0.682	0.029277
7147.96	1.3990	1.4129	0.0000117	1.049	0.029284
7251.63	1.3790	1.4130	0.0000135	1.232	0.029290
7358.35	1.3590	1.4130	0.0000092	0.852	0.029297
7468.26	1.3390	1.4131	0.0000021	0.201	0.029304
7581.50	1.3190	1.4131	0.0000015	0.141	0.029312
7698.23	1.2990	1.4132	0.0000014	0.133	0.029319
7818.61	1.2790	1.4133	0.0000013	0.125	0.029326
7942.81	1.2590	1.4133	0.0000015	0.153	0.029334
8071.02	1.2390	1.4134	0.0000021	0.209	0.029341
8203.45	1.2190	1.4135	0.0000025	0.260	0.029348
8340.28	1.1990	1.4135	0.0000058	0.610	0.029356
8481.76	1.1790	1.4136	0.0000121	1.291	0.029362
8628.13	1.1590	1.4136	0.0000058	0.628	0.029369

TABLE 10-Continued

WN	WL	n	k	LAC	R
8779.63	1.1390	1.4137	0.0000038	0.416	0.029376
8936.55	1.1190	1.4138	0.0000013	0.145	0.029384
9099.18	1.0990	1.4138	0.0000011	0.124	0.029391
9267.84	1.0790	1.4139	0.0000011	0.126	0.029399
9442.87	1.0590	1.4139	0.0000011	0.129	0.029406
9624.64	1.0390	1.4140	0.0000011	0.128	0.029413
9813.54	1.0190	1.4141	0.0000012	0.143	0.029420
10010.00	0.9990	1.4141	0.0000012	0.150	0.029428
10214.50	0.9790	1.4142	0.0000009	0.112	0.029435
10427.50	0.9590	1.4143	0.0000008	0.104	0.029443
10649.60	0.9390	1.4143	0.0000008	0.108	0.029450
10881.40	0.9190	1.4144	0.0000008	0.116	0.029459
11123.50	0.8990	1.4145	0.0000013	0.176	0.029466
11376.60	0.8790	1.4145	0.0000007	0.103	0.029474
11641.40	0.8590	1.4146	0.0000005	0.071	0.029482
11919.00	0.8390	1.4147	0.0000004	0.062	0.029491
12210.00	0.8190	1.4147	0.0000003	0.052	0.029499

TABLE 11. GLYCERIN

THE COMPLEX REFRACTIVE INDEX, LAMBERT ABSORPTION COEFFICIENT, AND REFLECTION COEFFICIENT.

WN	WL	n	k	LAC	R
500.00	20.0000	1.9790	0.1668370	1048.268	0.110790
519.00	19.2678	1.8234	0.2180950	1422.404	0.090471
539.00	18.5529	1.7826	0.2690170	1822.126	0.087630
559.00	17.8891	1.7129	0.2992480	2102.098	0.080247
579.00	17.2712	1.6682	0.3018710	2196.392	0.074559
599.00	16.6945	1.6271	0.2998030	2256.694	0.069102
619.00	16.1551	1.6056	0.3070250	2388.220	0.066978
639.00	15.6495	1.5609	0.3078350	2471.888	0.061530
659.00	15.1745	1.5390	0.3084620	2554.447	0.058952
679.00	14.7275	1.4707	0.3246530	2770.123	0.052649
699.00	14.3062	1.4270	0.2573870	2260.860	0.041728
719.00	13.9082	1.4080	0.2266450	2047.788	0.037234
739.00	13.5318	1.3901	0.1744400	1619.945	0.031794
759.00	13.1752	1.4026	0.1187640	1132.756	0.030443
779.00	12.8370	1.4349	0.0870755	852.400	0.033141
799.00	12.5156	1.4652	0.0693012	695.821	0.036373
819.00	12.2100	1.4965	0.0686708	706.750	0.040278
839.00	11.9190	1.5362	0.0778424	820.707	0.045602
859.00	11.6414	1.5099	0.1198840	1294.089	0.043451
879.00	11.3766	1.4999	0.0555708	613.826	0.040464
899.00	11.1235	1.5747	0.0520695	588.238	0.050207
919.00	10.8814	1.5827	0.1266730	1462.882	0.053180
939.00	10.6496	1.5631	0.0585936	691.394	0.048767
959.00	10.4275	1.6603	0.0821125	989.550	0.062499
979.00	10.2145	1.6834	0.1804650	2220.167	0.069075
999.00	10.0100	1.6487	0.2120630	2662.197	0.065976
1019.00	9.8135	1.8053	0.2666250	3414.168	0.090615
1039.00	9.6246	1.6367	0.6357850	8301.101	0.110056
1059.00	9.4429	1.2468	0.5067700	6743.987	0.059891
1079.00	9.2678	1.2627	0.2553950	3462.930	0.025887
1099.00	9.0992	1.3612	0.2577940	3560.249	0.034905
1119.00	8.9366	1.2116	0.2561090	3601.346	0.022265
1139.00	8.7796	1.3131	0.1005490	1439.168	0.020171
1159.00	8.6281	1.3377	0.1496420	2179.450	0.024868
1179.00	8.4818	1.3467	0.1008290	1493.857	0.023634
1199.00	8.3403	1.3782	0.1297200	1954.501	0.028180
1219.00	8.2034	1.3526	0.1274870	1952.898	0.025329
1239.00	8.0710	1.3514	0.1109830	1727.976	0.024503
1259.00	7.9428	1.3549	0.0903916	1430.091	0.024146
1279.00	7.8186	1.3643	0.0759635	1220.915	0.024750

TABLE 11-Continued

WN	WL	n	k	LAC	R
1299.00	7.6982	1.3923	0.0731190	1193.574	0.027796
1319.00	7.5815	1.3855	0.0906598	1502.690	0.027515
1339.00	7.4683	1.3896	0.0767817	1291.957	0.027587
1359.00	7.3584	1.3853	0.0838354	1431.716	0.027296
1379.00	7.2516	1.4020	0.0656619	1137.857	0.028737
1399.00	7.1480	1.4126	0.1026980	1805.467	0.030999
1419.00	7.0472	1.3818	0.1057760	1886.164	0.027610
1439.00	6.9493	1.3684	0.1086800	1965.261	0.026243
1459.00	6.8540	1.3341	0.0903928	1657.292	0.021956
1479.00	6.7613	1.3336	0.0534600	993.590	0.020953
1499.00	6.6711	1.3464	0.0291245	548.618	0.021946
1519.00	6.5833	1.3622	0.0196554	375.189	0.023576
1539.00	6.4977	1.3736	0.0152318	294.578	0.024818
1559.00	6.4144	1.3823	0.0126284	247.403	0.025783
1579.00	6.3331	1.3895	0.0107525	213.354	0.026586
1599.00	6.2539	1.3954	0.0095140	191.170	0.027263
1619.00	6.1767	1.4005	0.0084256	171.418	0.027847
1639.00	6.1013	1.4050	0.0075886	156.296	0.028372
1659.00	6.0277	1.4090	0.0068473	142.749	0.028833
1679.00	5.9559	1.4127	0.0061905	130.613	0.029263
1699.00	5.8858	1.4160	0.0056641	120.931	0.029658
1719.00	5.8173	1.4191	0.0051652	111.577	0.030024
1739.00	5.7504	1.4220	0.0047849	104.563	0.030364
1759.00	5.6850	1.4247	0.0043738	96.680	0.030681
1779.00	5.6211	1.4273	0.0040499	90.538	0.030987
1799.00	5.5586	1.4296	0.0037159	84.006	0.031271
1819.00	5.4975	1.4321	0.0034831	79.617	0.031562
1839.00	5.4377	1.4341	0.0034263	79.180	0.031811
1859.00	5.3792	1.4362	0.0031288	73.091	0.032057
1879.00	5.3220	1.4383	0.0030865	72.880	0.032311
1899.00	5.2659	1.4401	0.0030829	73.568	0.032537
1919.00	5.2110	1.4420	0.0031535	76.046	0.032758
1939.00	5.1573	1.4436	0.0032368	78.868	0.032958
1959.00	5.1046	1.4451	0.0034551	85.056	0.033138
1979.00	5.0531	1.4463	0.0033279	82.762	0.033280
1999.00	5.0025	1.4479	0.0029863	75.017	0.033478
2019.00	4.9529	1.4495	0.0031379	79.613	0.033679
2039.00	4.9044	1.4510	0.0033226	85.135	0.033860
2059.00	4.8567	1.4521	0.0036937	95.572	0.033997
2079.00	4.8100	1.4530	0.0035805	93.542	0.034112
2099.00	4.7642	1.4542	0.0034392	90.716	0.034254
2119.00	4.7192	1.4554	0.0032130	85.555	0.034399
2139.00	4.6751	1.4567	0.0031536	84.767	0.034557
2159.00	4.6318	1.4578	0.0028872	78.333	0.034690
2179.00	4.5893	1.4593	0.0026171	71.662	0.034876
2199.00	4.5475	1.4607	0.0025769	71.208	0.035052
2219.00	4.5065	1.4622	0.0025921	72.280	0.035241
2239.00	4.4663	1.4636	0.0027363	76.988	0.035408

TABLE 11-Continued

WN	WL	n	k	LAC	R
2259.00	4.4267	1.4651	0.0028239	80.162	0.035595
2279.00	4.3879	1.4564	0.0032149	92.070	0.035761
2299.00	4.3497	1.4676	0.0034019	98.281	0.035911
2319.00	4.3122	1.4688	0.0036844	107.368	0.036062
2339.00	4.2753	1.4700	0.0036776	108.093	0.036211
2359.00	4.2391	1.4716	0.0038725	114.798	0.036406
2379.00	4.2034	1.4730	0.0041912	125.298	0.036583
2399.00	4.1684	1.4745	0.0046224	139.351	0.036780
2419.00	4.1339	1.4760	0.0052493	159.568	0.036963
2439.00	4.1000	1.4774	0.0060141	184.327	0.037143
2459.00	4.0667	1.4785	0.0069261	214.021	0.037282
2479.00	4.0339	1.4795	0.0075539	235.319	0.037405
2499.00	4.0016	1.4805	0.0081547	256.086	0.037531
2519.00	3.9698	1.4815	0.0085429	270.424	0.037657
2539.00	3.9386	1.4827	0.0088485	282.320	0.037812
2559.00	3.9078	1.4842	0.0091620	294.627	0.038002
2579.00	3.8775	1.4860	0.0098039	317.731	0.038234
2599.00	3.8476	1.4878	0.0109139	356.448	0.038462
2619.00	3.8183	1.4892	0.0123100	405.138	0.038651
2639.00	3.7893	1.4902	0.0136510	452.703	0.038775
2659.00	3.7608	1.4910	0.0144163	481.706	0.038886
2679.00	3.7327	1.4923	0.0149843	504.451	0.039051
2699.00	3.7051	1.4942	0.0156348	530.280	0.039291
2719.00	3.6778	1.4962	0.0168793	576.731	0.039558
2739.00	3.6510	1.4980	0.0181961	626.297	0.039792
2759.00	3.6245	1.5002	0.0193872	672.166	0.040089
2779.00	3.5984	1.5031	0.0209348	731.084	0.040458
2799.00	3.5727	1.5067	0.0226509	796.706	0.040933
2819.00	3.5474	1.5123	0.0274869	973.712	0.041702
2839.00	3.5224	1.5163	0.0376638	1343.691	0.042316
2859.00	3.4977	1.5151	0.0462985	1663.378	0.042271
2879.00	3.4734	1.5071	0.0621211	2247.453	0.041497
2899.00	3.4495	1.4916	0.0559236	2037.292	0.039412
2919.00	3.4258	1.4966	0.0578873	2123.378	0.040077
2939.00	3.4025	1.4784	0.0668647	2469.485	0.037958
2959.00	3.3795	1.4649	0.0488354	1815.890	0.035950
2979.00	3.3568	1.4677	0.0320314	1199.102	0.036078
2999.00	3.3344	1.4815	0.0212430	800.575	0.037717
3019.00	3.3124	1.4929	0.0211947	804.082	0.039169
3039.00	3.2906	1.5028	0.0226175	863.744	0.040432
3059.00	3.2690	1.5124	0.0289094	1111.293	0.041725
3079.00	3.2478	1.5164	0.0335047	1296.359	0.042279
3099.00	3.2268	1.5260	0.0398692	1552.634	0.043602
3119.00	3.2062	1.5295	0.0497024	1948.061	0.044187
3139.00	3.1857	1.5363	0.0579813	2287.121	0.045206
3159.00	3.1656	1.5385	0.0724196	2874.853	0.045772
3179.00	3.1456	1.5401	0.0833830	3331.025	0.046244
3199.00	3.1260	1.5396	0.1018880	4095.879	0.046678

TABLE 11-Continued

WN	WL	n	k	LAC	R
3219.00	3.1066	1.5319	0.1149530	4649.981	0.046100
3239.00	3.0874	1.5262	0.1308720	5326.814	0.045946
3259.00	3.0684	1.5118	0.1437430	5886.823	0.044646
3279.00	3.0497	1.4997	0.1548950	6382.469	0.043635
3299.00	3.0312	1.4803	0.1646400	6825.391	0.041721
3319.00	3.0130	1.4638	0.1687220	7037.021	0.039938
3339.00	2.9949	1.4422	0.1721160	7221.835	0.037564
3359.00	2.9771	1.4228	0.1687840	7124.447	0.035136
3379.00	2.9595	1.4047	0.1679560	7131.709	0.033037
3399.00	2.9420	1.3833	0.1554490	6639.708	0.029993
3419.00	2.9248	1.3684	0.1472680	6327.285	0.027958
3439.00	2.9078	1.3497	0.1281430	5537.796	0.025049
3459.00	2.8910	1.3441	0.1112110	4834.017	0.023742
3479.00	2.8744	1.3331	0.0916797	4008.090	0.021894
3499.00	2.8580	1.3361	0.0711436	3128.165	0.021609
3519.00	2.8417	1.3355	0.0549494	2429.921	0.021180
3539.00	2.8257	1.3401	0.0387135	1721.682	0.021386
3559.00	2.8098	1.3489	0.0218690	978.063	0.022146
3579.00	2.7941	1.3614	0.0147212	662.087	0.023461
3599.00	2.7785	1.3701	0.0090224	408.052	0.024403
3619.00	2.7632	1.3787	0.0051416	233.828	0.025347
3639.00	2.7480	1.3863	0.0030840	141.030	0.026204
3659.00	2.7330	1.3925	0.0020875	95.983	0.026917
3679.00	2.7181	1.3976	0.0016284	75.281	0.027504
3699.00	2.7034	1.4019	0.0013690	63.635	0.028003
3719.00	2.6889	1.4056	0.0012402	57.959	0.028426
3739.00	2.6745	1.4088	0.0011752	55.220	0.028796
3759.00	2.6603	1.4115	0.0010698	50.533	0.029116
3779.00	2.6462	1.4140	0.0009708	46.104	0.029416
3799.00	2.6323	1.4163	0.0009976	47.626	0.029683
3819.00	2.6185	1.4183	0.0009611	46.122	0.029923
3839.00	2.6048	1.4202	0.0009814	47.345	0.030144
3859.00	2.5913	1.4219	0.0009831	47.672	0.030345
3879.00	2.5780	1.4235	0.0009994	48.717	0.030535
3899.00	2.5648	1.4250	0.0010538	51.634	0.030713
3919.00	2.5517	1.4263	0.0011794	58.081	0.030876
3939.00	2.5387	1.4275	0.0012945	64.076	0.031016
3959.00	2.5259	1.4287	0.0013766	68.487	0.031153
3979.00	2.5132	1.4296	0.0015486	77.435	0.031271
3999.00	2.5006	1.4304	0.0016330	82.063	0.031366
4030.63	2.4810	1.4316	0.0014683	74.368	0.031505
4063.39	2.4610	1.4329	0.0011862	60.571	0.031658
4096.68	2.4410	1.4342	0.0009086	46.777	0.031817
4130.52	2.4210	1.4356	0.0007335	38.075	0.031982
4164.93	2.4010	1.4369	0.0006648	34.794	0.032138
4199.92	2.3810	1.4380	0.0006406	33.811	0.032282
4235.49	2.3610	1.4391	0.0006203	33.018	0.032415
4271.68	2.3410	1.4402	0.0006578	35.309	0.032542

TABLE 11-Continued

WN	WL	n	k	LAC	R
4308.49	2.3210	1.4411	0.0007100	38.439	0.032657
4345.94	2.3010	1.4421	0.0007340	40.087	0.032770
4384.04	2.2810	1.4428	0.0009561	52.671	0.032852
4422.82	2.2610	1.4433	0.0006822	37.914	0.032920
4462.29	2.2410	1.4442	0.0004168	23.371	0.033029
4502.48	2.2210	1.4451	0.0003789	21.439	0.033140
4543.39	2.2010	1.4459	0.0004095	23.378	0.033240
4585.05	2.1810	1.4467	0.0004621	26.625	0.033334
4627.49	2.1610	1.4474	0.0005434	31.597	0.033416
4670.71	2.1410	1.4480	0.0006389	37.502	0.033492
4714.76	2.1210	1.4486	0.0007315	43.339	0.033560
4759.64	2.1010	1.4490	0.0007879	47.127	0.033616
4805.38	2.0810	1.4494	0.0007633	46.090	0.033662
4852.01	2.0610	1.4498	0.0006242	38.058	0.033710
4899.56	2.0410	1.4503	0.0004139	25.481	0.033769
4948.05	2.0210	1.4509	0.0002369	14.733	0.033842
4997.50	2.0010	1.4515	0.0001388	8.716	0.033920
5047.96	1.9810	1.4521	0.0000991	6.285	0.033988
5099.44	1.9610	1.4526	0.0000828	5.303	0.034059
5151.98	1.9410	1.4531	0.0000760	4.920	0.034121
5205.62	1.9210	1.4536	0.0000730	4.773	0.034181
5260.39	1.9010	1.4541	0.0000690	4.561	0.034241
5316.32	1.8810	1.4546	0.0000680	4.542	0.034298
5373.46	1.8610	1.4550	0.0000732	4.942	0.034351
5431.83	1.8410	1.4555	0.0000809	5.524	0.034407
5491.49	1.8210	1.4559	0.0000901	6.217	0.034460
5552.47	1.8010	1.4563	0.0001037	7.238	0.034510
5614.82	1.7810	1.4567	0.0001167	8.236	0.034557
5678.59	1.7610	1.4571	0.0001268	9.045	0.034603
5743.83	1.7410	1.4574	0.0001327	9.581	0.034649
5810.58	1.7210	1.4578	0.0001347	9.836	0.034694
5878.89	1.7010	1.4581	0.0001372	10.135	0.034735
5948.84	1.6810	1.4585	0.0001064	7.951	0.034779
6020.47	1.6610	1.4589	0.0001102	8.339	0.034826
6093.85	1.6410	1.4592	0.0001266	9.696	0.034871
6169.03	1.6210	1.4596	0.0001509	11.700	0.034911
6246.10	1.6010	1.4599	0.0001794	14.084	0.034949
6325.11	1.5810	1.4602	0.0001942	15.432	0.034985
6406.15	1.5610	1.4604	0.0001848	14.879	0.035021
6489.29	1.5410	1.4607	0.0001700	13.866	0.035057
6574.62	1.5210	1.4611	0.0001649	13.625	0.035096
6662.23	1.5010	1.4613	0.0001646	13.784	0.035132
6752.19	1.4810	1.4616	0.0001597	13.547	0.035164
6844.63	1.4610	1.4619	0.0001453	12.496	0.035200
6939.63	1.4410	1.4622	0.0001182	10.311	0.035233
7037.30	1.4210	1.4624	0.0000710	6.277	0.035266
7137.76	1.4010	1.4627	0.0000299	2.678	0.035304
7241.13	1.3810	1.4631	0.0000232	2.109	0.035344

TABLE 11-Continued

WN	WL	n	k	LAC	R
7347.54	1.3610	1.4633	0.0000181	1.672	0.035378
7457.12	1.3410	1.4636	0.0000115	1.073	0.035415
7570.02	1.3210	1.4639	0.0000083	0.791	0.035450
7686.40	1.3010	1.4642	0.0000081	0.783	0.035484
7806.40	1.2810	1.4645	0.0000094	0.920	0.035519
7930.21	1.2610	1.4647	0.0000101	1.003	0.035553
8058.02	1.2410	1.4650	0.0000108	1.098	0.035585
8190.01	1.2210	1.4653	0.0000135	1.388	0.035621
8326.39	1.2010	1.4655	0.0000150	1.571	0.035652
8467.40	1.1810	1.4658	0.0000102	1.088	0.035685
8613.26	1.1610	1.4661	0.0000059	0.637	0.035716
8764.24	1.1410	1.4663	0.0000040	0.439	0.035750
8920.61	1.1210	1.4666	0.0000032	0.355	0.035782
9082.65	1.1010	1.4668	0.0000035	0.399	0.035815
9250.69	1.0810	1.4671	0.0000035	0.408	0.035847
9425.07	1.0610	1.4674	0.0000039	0.458	0.035878
9606.15	1.0410	1.4676	0.0000039	0.465	0.035910
9794.32	1.0210	1.4679	0.0000043	0.534	0.035943
9990.01	1.0010	1.4681	0.0000043	0.545	0.035975
10193.70	0.9810	1.4684	0.0000038	0.482	0.036007
10405.80	0.9610	1.4687	0.0000026	0.345	0.036040
10627.00	0.9410	1.4689	0.0000022	0.297	0.036072
10857.80	0.9210	1.4692	0.0000025	0.336	0.036105
11098.80	0.9010	1.4695	0.0000020	0.276	0.036140
11350.70	0.8810	1.4697	0.0000015	0.215	0.036173
11614.40	0.8610	1.4700	0.0000013	0.196	0.036207
11890.60	0.8410	1.4703	0.0000010	0.152	0.036242
12180.30	0.8210	1.4706	0.0000008	0.130	0.036278
12484.40	0.8010	1.4709	0.0000007	0.109	0.036314

CHAPTER V

CONCLUSION

We have measured the Lambert absorption coefficient of eleven liquids in the 500-12500 cm^{-1} region. Thus we determined both real and imaginary parts of the complex refractive index. The dielectric function and the complex reflectance can be calculated using the complex refractive index. The experimental results for several liquids are in very good agreement with previous research from the literature. The maximum value of the Lambert absorption coefficient of water is 12263 cm^{-1} with an uncertainty of ± 189 per centimeter at the wavenumber of 3406 cm^{-1}. The minimum value of the Lambert absorption coefficient of Diesel fuel is 1.01 cm^{-1} with an uncertainty of ± 0.05 per centimeter at the wave-number of 7092 cm^{-1}. This work represents a marked improvement in knowledge of the complex refractive index of the eleven liquids. The computation program of Kramers-Kronig relation gives us the value of the real part of the complex refractive index.

Together we designed, constructed, and tested a wedge-shaped absorption cell that is extremely versatile. By use of the cell one can easily and accurately measure the

Lambert absorption coefficient of low or highly absorbent liquids. The provision of a variable apex angle permits cell parameters to be optimized for any given sample. The cell can be used to measure absorption from any liquid sample in any spectral region because the wedge cell is designed to be able to seal and several different sets of windows are freely interchangeable.

REFERENCES

1. J. Faharenfort, Spectrochimica Acta. 17, 700 (1961).
2. R.P. Bauman, Absorption Spectroscopy (John Wiley & Sons Inc., 1962), pp. 186-188.
3. C.W. Robertson and D. Williams, J. Opt. Soc. Am. 61, 1316 (1971).
4. I.L. Tyler, G. Taylor, and M.R. Querry, Applied Optics, 17, 960 (1978).
5. M. Born and E. Wolf, Principles of Optics (Pergamon Press, 1970), pp. 281-288.
6. P. Bonguer, Essai d' optique sur la gradation de la lumiere, 1729.
7. J.H. Lambert, Photometria, sive de mensura et gradibus luminis, colorum, et umbrae, 1760.
8. A. Beer, Ann. Physik. Chem. (2) 86, 48 (1952).
9. James Clerk Maxwell, A Dynamical Theory of the Electromagnetic Field, in W.D. Niven (ed.), "The Scientific Papers of James Clerk Maxwel," Vol. I, Cambridge Univrsity Press, London, (1890).
10. J.D. Jackson, Classical Electrodynamics (Wiley, New York, 1975), p. 218.
11. T.S. Robinson, Proc. Phys. Soc. (London) B65, 910 (1952).

12. Manufactured by De-Sta-Co., Divison, Dover Corp., Detroit, Michigan, 48203.

13. Manufactured by Vlier Engineering Corp., Burbank, California, 91505.

14. Manufactured by Eastern Industries Corp., Rocky Hill, Connecticut, 06067.

15. Manufactured by Small Parts, Inc., Miami, Florida.

16. Manufactured by Two-Six, Inc., Saxonburg, Pennsylvania.

17. Manufactured by Danforth 3-D, Inc., Independence, Missouri.

18. Manufactured by Velmex, Inc., Bloomfield, New York.

19. G.M. Hale and M.R. Querry, Applied Optics, 12, 555 (1973).

20. A.N. Rusk, D. Williams, and M.R. Querry, J. Opt. Soc. 61, 895 (1971).

21. M.R. Querry, W.P. Roach, D.L. Striley, and C.T. Heese, "Optical Properties of Powders, Liquids, and Metals in the Infrared, Visible, and Ultraviolet Spectral Regions", Proceedings of the 1986 CRDC Scientific Conference on Obscuration and Aerosol Research, Ronald H. Kohl, editor, p.

VITA

Shengshan Weng was born in Shanghai, China on April 2, 1960. He was graduated from Hu-Guang High School in Shanghai in July, 1978. In the fall of 1978, he entered undergraduate study in semiconductor physics at Fudan University, Shanghai, China.

After he graduated from Fudan University in July 1982, he worked as an assistant engineer at the 21st Transistor Factory, Shanghai. He came to the United States in December 1982. In the fall of 1985, he attended the University of Missouri-Kansas City to continue his graduate work in physics. He has been a research assistant in physics at the University of Missouri-Kansas City since January 1986. Upon completion of his Master Science degree, Mr. Weng plans to continue his education in physics. He has presented part of his research at the 34th Midwest Solid State Conference in St. Louis.

II. ATTENUATED TOTAL REFLECTION

a. INTRODUCTION

Reflection measurements from liquids has always been a complicated procedure, especially from liquids with a high vapor pressure. In addition, the surface tension creating the miniscus effect produces a sample surface with a slight curvature. One solution to this problem is the technique of attenuated total reflection, ATR.

The ATR technique replaces the air-sample boundary with a boundary between a material which is optically dense and the sample. The largest distinct advantage is the ability to seal the sample to avoid lose due to evaporation. In addition, the boundary between the two materials is well defined. The ability to perform reflection measurements on a liquid provides complimentary information to the transmission measurements of Chapter 1. Once the reflection measurements have been performed the complex refractive index can be computed in several ways. The techniques of Querry and Avery, discussed in Chapters 3 and 4 can be applied to directly determine the optical constants. If the optically dense material permits the measurement of the reflection coefficients for a wide spectral range the technique Kramers-Kronig analysis can be employed. In the following discussion the techniques of Querry and Avery will only be used to determine the optical constants for the sample liquids.

Querry's Method

The complete description of Querry's method is given in Chapter 3 and only a brief non-mathematical discussion will follow. The essence of the technique is to determine the reflection coefficients for both polarization states, s and p, and then to treat the corresponding Fresnel equations as two equations in two unknowns, namely n and k. The solution to this problem has been worked out in detail[1] and the pertinent equations are given in Chapter 3. Although the equations are for an air-sample boundary the compensation for the window material, ZnSe here, can be performed in a straight forward manner.

The main difficulty in this technique is the need for an extremely accurate determination of the reflection coefficients. The results from Chapter 3 indicate a variation of 2% in the reflection coefficients can produce errors in the complex refractive index of well over 30%. The other problem arises from the fact the experiment is much more sensitive to the liquid sample for conditions of internal reflection. If the index of refraction of the sample increases to be large than the window material the advantage of internal reflection is lost and less information is carried away with the reflected light.

Avery's Method

Avery's method originally was to measure the reflection coefficient at a minimum of two angles of incidence and to graphically present the iso-reflectance curves in the n-k plane. The intersection of the isoreflectance curves would then provide the complex refractive index. Again a complete discussion of the technique is provided in Chapter 4 and we will only review the method here.

The graphical method proves to be extremely tedious and prone to error since the angle of intersection of the isoreflectance curves tends to be acute. A direct solution has been obtained by Fahrenfort and Visser[2]. The pertinent equations are given in Chapter 4. The equations have been coded and the effect of the ZnSe prism has been compensated for. The main difficulty here is the need for extreme accuracy in the reflection coefficients prior to the determination of the complex refractive index.

Both techniques, Querry's or Avery's, are valid techniques to determine the complex refractive index of the sample material. The error associated with Avery's method is smaller than the error for Querry's method under conditions in which the angle of incidence is well known and the extinction coefficient is small. For cases in which the angle of incidence can be in error the polarization method appears to provide better complex refractive indices. Although, comparitively Avery's technique is prone to less error than Querry's method both are susceptible to large uncertainties in the complex refarctive index.

b. ERROR ANALYSIS

The details of the error analysis are left to the individual chaptes on each of the techniques. Reiterating the conclusions of the error analysis in Chaps. 3 and 4, the accuracy of the experimental reflection coefficients must be less than 1%. Due to this restriction no data was analyzed from the use of the CO_2 laser. The refletion coefficients determined with this light source proved to be too noisy to continue with evaluation of the reflection coefficients. The reader is referred to appendix 2.2 where Zhiqin Huang's master thesis is provided. The data presented in this thesis was obtained using a Perkin-Elmer IR model 580 spectrophotometer. These results indicate the cell which has been developed does function properly and the computer codes supplied in the appendices of the thesis are accurate.

c. DESCRIPTION OF THE EQUIPMENT

Fig. 2.1 provides a three dimensional blow up image of the ATR cell. The cell was modeled extensively after a previous cell developed at CRDEC[3]. The cell is composed of two distinct subassemblies, the ZnSe prism mount and the Al prism mount.

ZnSe Prism Mount

The Znse prism mount comprises:

a rectangular stainless steel sample chamber 1 dimensioned to fit either the 30°-60°-90° ZnSe prism or the 40°-50°-90° prism with an o-ring groove to provide the seal;

a rectangular stainless steel sample chamber 2 dimensioned to fiteither the 30°-60°-90° ZnSe prism or the 40°-50°-90° prism with an o-ring groove to provide the seal and with two threaded holes to fix chamber 1 to chamber 2;

teflon o-rings 3' and 3'' sized to fit the grooves of chambers 1 and 2;

teflon seal plates 4' and 4'' to seal the back of chambers 1 and 2;

stainless steel pressure plates 5' and 5'' with holes to fill the cells with the sample liquid via tubing reducers;

a ZnSe prism 6 either a 40°-50°-90° or a 30°-60°-90°;

teflon spacer 7 to protect front surface of prism 6 from scratches, apertures are unique to choice of prism 6;

stainless steel pressure plate 8 to press ZnSe prism 6 against o-ring seals 3, plate 8 is unique to choice of prism 6;

stainless steel base plate to mount the ZnSe subassembly to the Unislide translator;

Unislide translator 10 to accurately position the ZnSe prism for data acquisition.

Al Prism Mount

45°-45°-90° prism 12 with two sides Al and IR coated;

stainless steel angular plate 13 to rotate the Al prism to provide desired angle of incidence;

stainless steel angular scale 14'and 14'' to accurately determine the angular position of prism 12;

stainless steel hold down plates 15' and 15'' to clamp angular scale 14'.

Both subassemblies are positioned on base plate 11 which is then fixed to plate 19.

Before assembly the components of the cell are cleaned in either acetone, methyl alcohol, or ethyl alcohol in an ultrasonic cleaner. The cell is the assembled as follows. Mount Unislide translator 10 onto base plate 11. Place o-rings 3' and 3'' into o-ring grooves in sample chambers 1 and 2, respecitvely. Join sample chamber 1 to sample chamber 2 via threaded holes in 2. Bolt combined sample chambers to base plate 9. Place prism 6 into area between sample chambers 1 and 2. Bolt pressure plate 8 with teflon spacer 7 to from of sample chambers 1 and 2. Bolt base plate 9 to Unislide. Bolt pressure plates 5' and 5'' with seals 4' and 4'' in position to samples chambers 1 and 2, respectively.

Mount angular scale 14' to angular plate 13 and position on base plate 11. Position angular vernier 14'' on base plate 11 and clamp in position with clamps 15' and 15''. Place Al prism 12 into position on angular plate 13.

The cell is initially aligned using a HeNe laser reflected from the hypotenuse of the Al prism and the two ZnSe prism sides viewable when plates 5' and 5'' are removed. The computed angle between these normals assure correct alignment of the system. At this position the angle of incidence on the hypotenuse of the ZnSe prism is 0° and therefore the angle of incidence at the sample chambers are the angles of the two prisms directly. Adjustment of the Al prism will allow for +/- 10° degrees from normal at the hypotenuse with the application of Snell's law to determine the angle of incidence at the sample chambers.

Once the cell is aligned it is placed in the path of the CO_2 laser and is adjusted both horizontally and vertically to maximize the signal at the pyroelectric detector. The pressure plate 8 provides a natural aperture to block any light from striking any of the sample chamber sides except where the chamber is physically located.

d. ACQUISITION OF DATA

After alignment of the ATR device the following procedure is employed to obtain the reflection coefficients for the sample material being studied.

1. With the sample holder empty the intensity of the CO_2 laser is determined as a function of wavelength, I_o.
2. The CO_2 laser is tuned to the appropriate line and the dither stabilizer is activated.
3. The sample and reference lock-in amplifiers are adjusted with respect to phase, amplitude, and time constant.
4. The operating parameters are input into the computer to be stored with the data.
5. The sample and reference lock-ins and the power meter are read and the data stored to disk.
6. The procedure 2 thru 5 is repeated for all wavelengths available from the CO_2 laser.
7. After I_o is obtained one of the sample chambers is filled with the sample liquid.
8. The procedure 2 thru 5 is repeated for all wavelengths available from the CO_2 laser.
9. The reflection coefficients are determined as a function of wavelength.
10. The reflection coefficients are input into either the program QUERRY or AVERY and the complex refractive index is determined.

Using the above procedure data was obtained for water with the CO_2 laser as the light source. We do not present the data here due to the extreme noise which is present. Attempts at determining the complex refractive index from the experimental data resulted in no wavelengths at which the computation could be carried out.

e. CONCLUSION

The ATR device described here has been shown to provide accurate values for water and SF-96 when used in conjunction with the Perkin-Elmer instrument. The error present when using the CO_2 laser continues to be a mystery. The noise has plagued all aspects of this project. The results from the Perkin-Elmer instrument indicate the accuracy at which the complex refractive index can be determined with this unit.

[1]Marvin R. Querry, J. Opt. Soc. Amer., 59, 876 (1969)

[2]J. Fahrenfort and W.M. Visser, Spectorchimica Acta, 18, 1103 1962

[3]Merrill Milham, private communication

f. APPENDIX 2.1

Construction Drawings of ATR Cell

f. Appendix 2.1

Construction Drawings of the ATR Cell

Two dimensional construction drawings for the ATR device. The three dimensional expanded drawing numerically identifies the items listed below.

1. Stainless steel chamber 1
2. Stainless steel chamber 2
3. Teflon O-ring seals
4. Teflon flat seal
5. Stainless steel sealing plate with sample introduction holes
6. ZnSe prism
7. Teflon spacer
8. Stainless steel pressure plate and limiting aperture
9. Base plate for mounting ZnSe prism subassembly
10. Unislide for positioning ZnSe prism
11. Base plate for mounting Unislide, ZnSe prism subassembly, and Al prism subassembly
12. 45 degree right angle Al prism
13. Angular plate to position Al prism
14. Angular indicator
15. Clamps for angle indicator 14
16. Polarizer mounting plate
17. Polarizer assembly
18. Polarizer wire grid - used only in Perkin-Elmer
19. Main assembly base plate

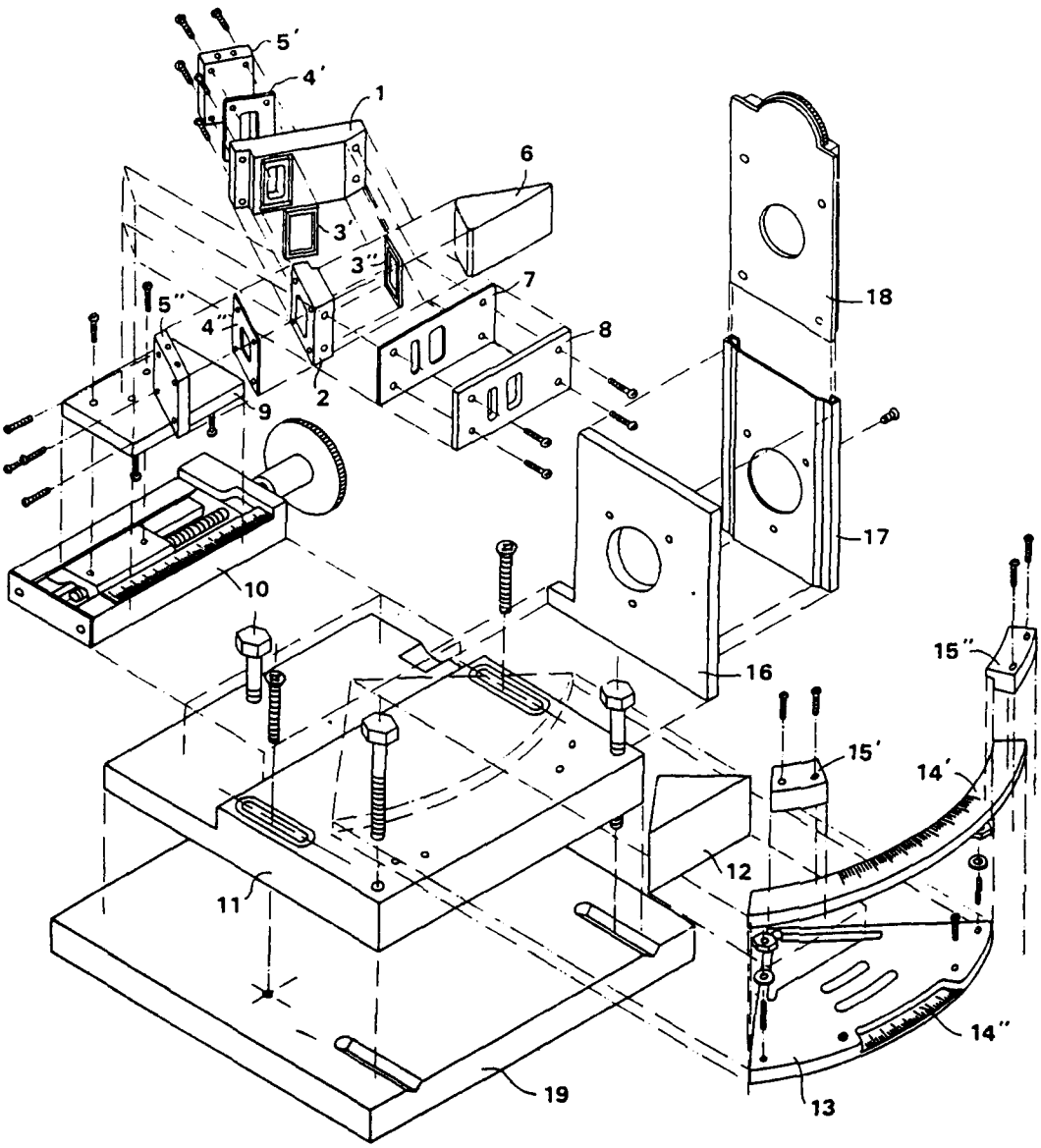

FIG. 2.1 Exploded view of the attenuated total reflection device.

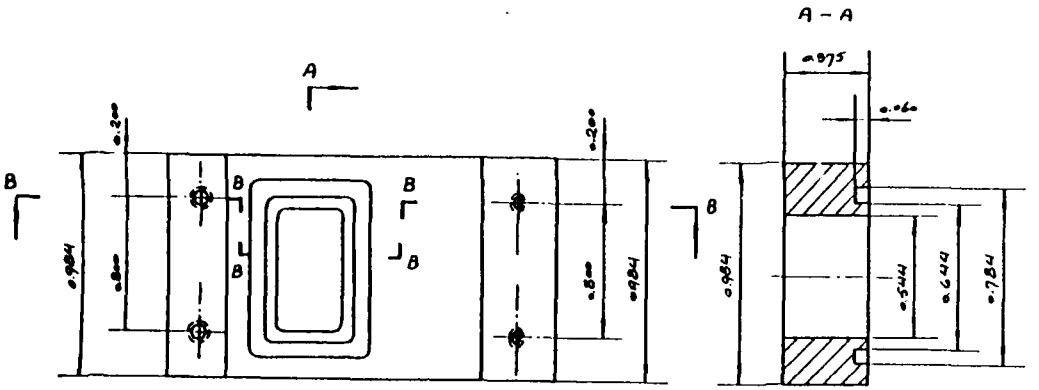

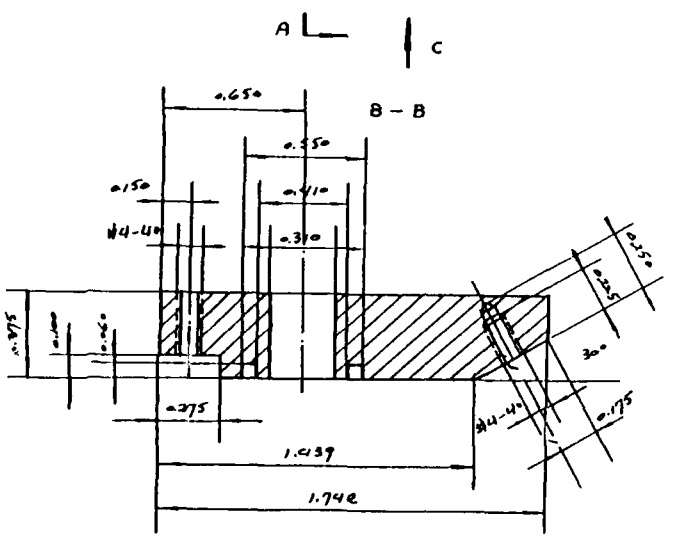

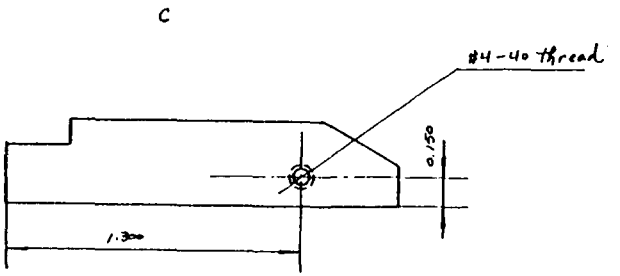

ITEM# - 1

MATERIAL - STAINLESS STEEL

PRISM - 30-60-90

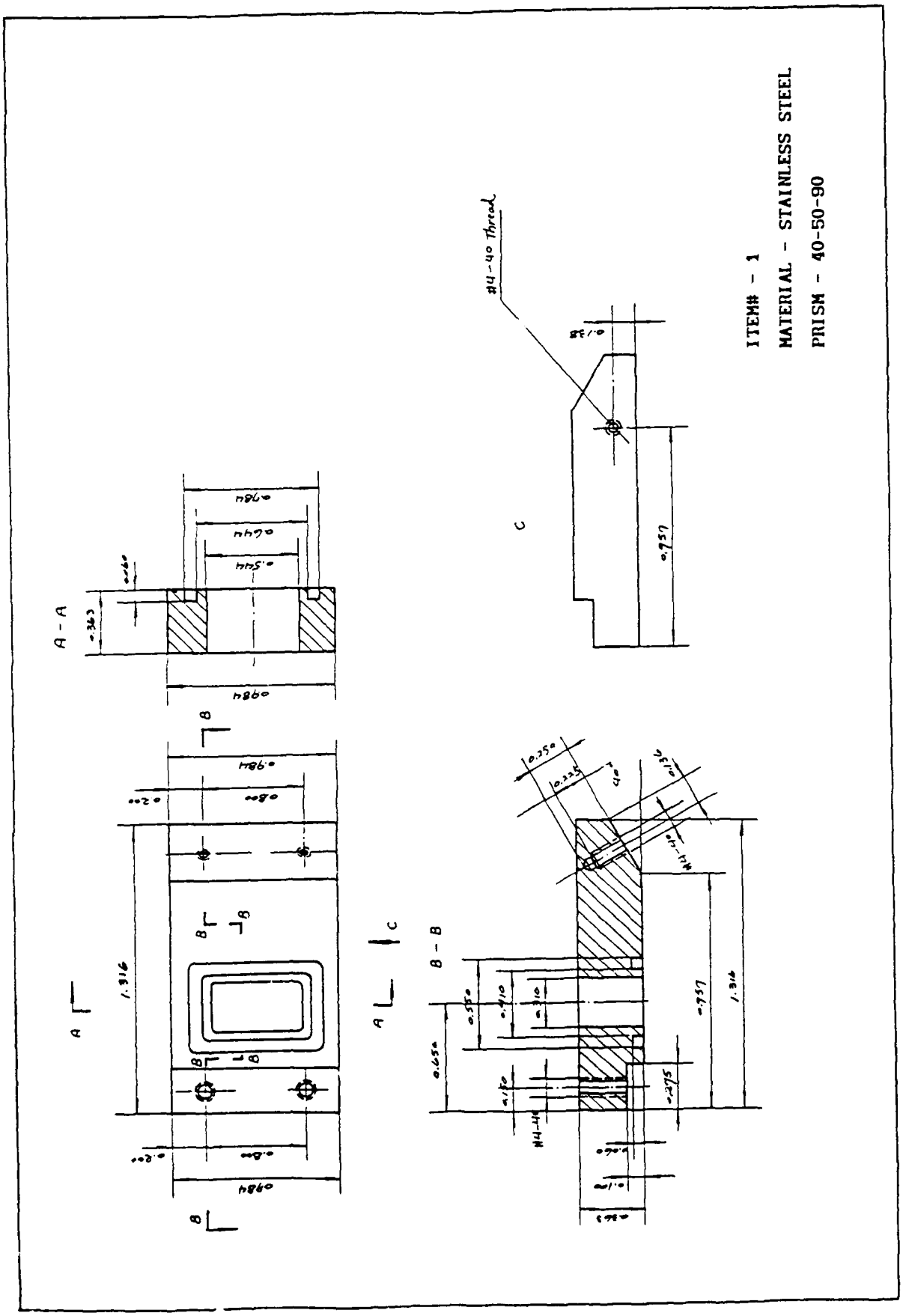
ITEM# - 1
MATERIAL - STAINLESS STEEL
PRISM - 40-50-90
#4-40 Thread
A - A
B - B
C

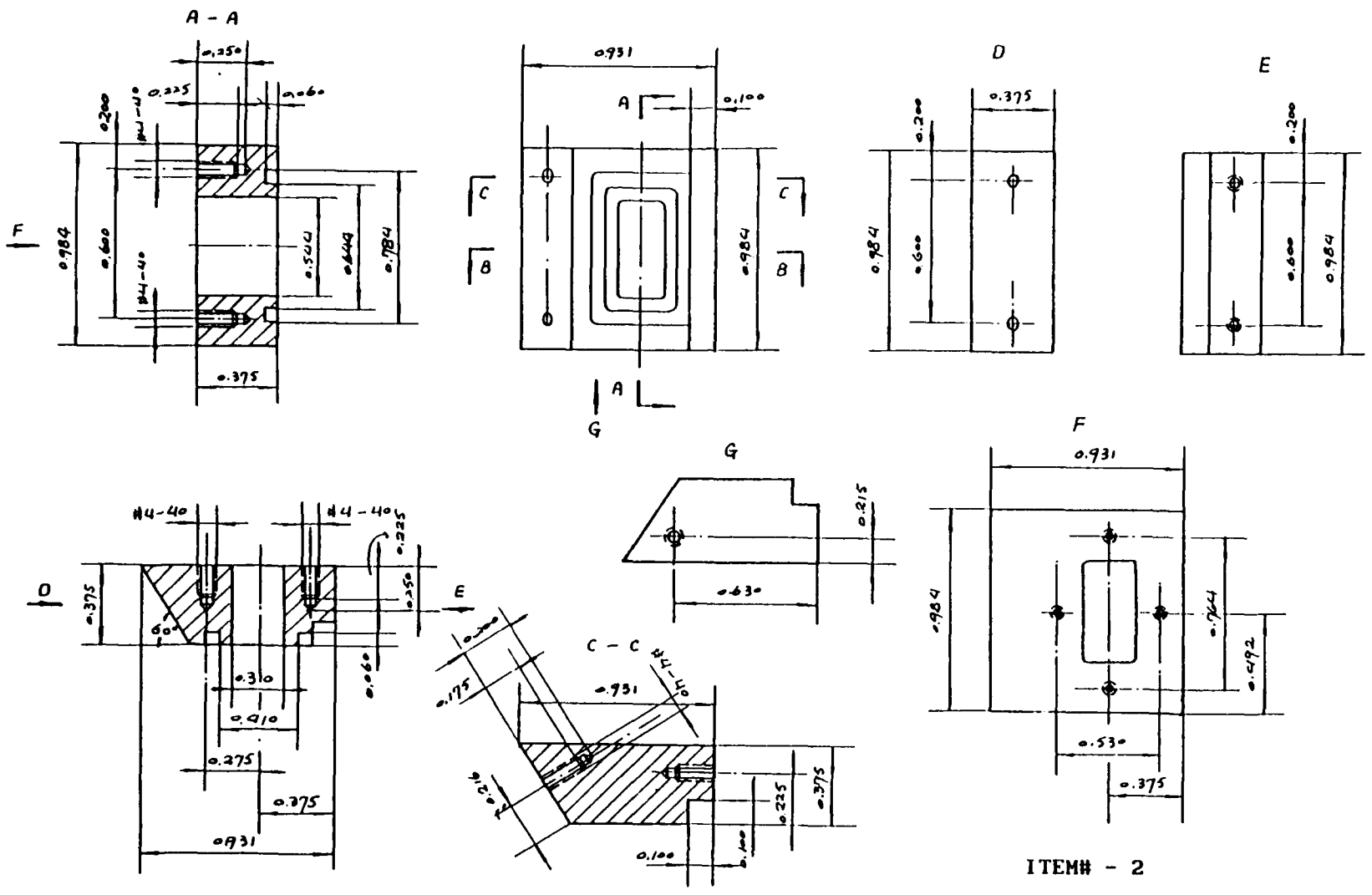

ITEM# - 2

MATERIAL - STAINLESS STEEL

PRISM - 30-60-90

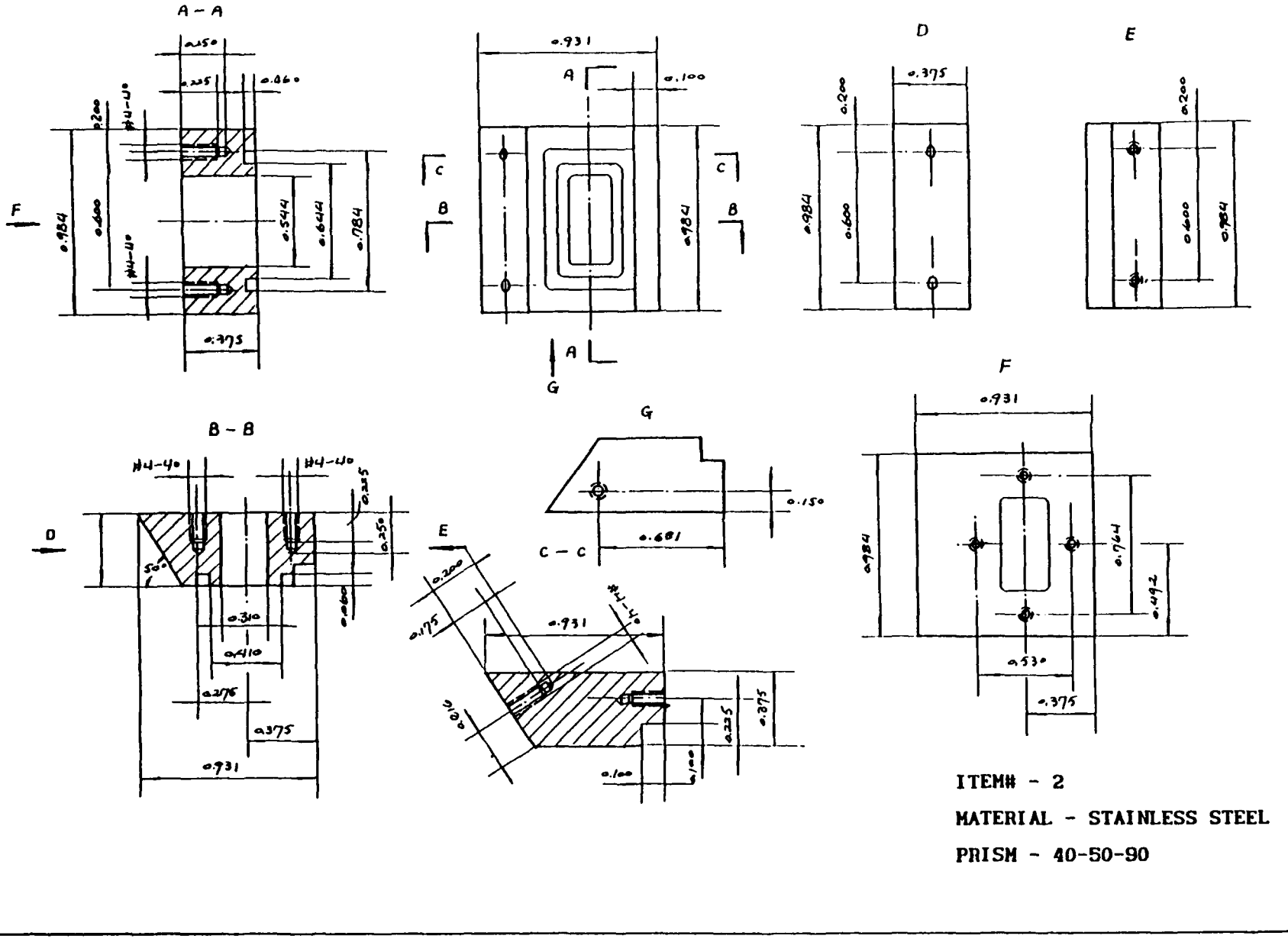

ITEM# - 2

MATERIAL - STAINLESS STEEL

PRISM - 40-50-90

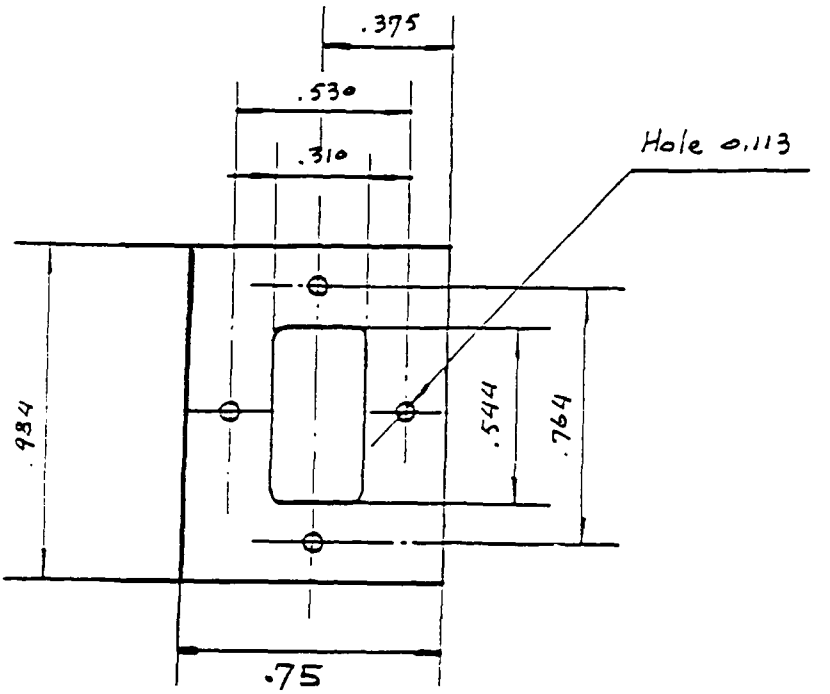

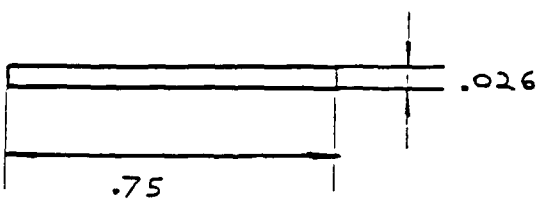

ITEM# - 4' 4"

MATERIAL - TEFLON

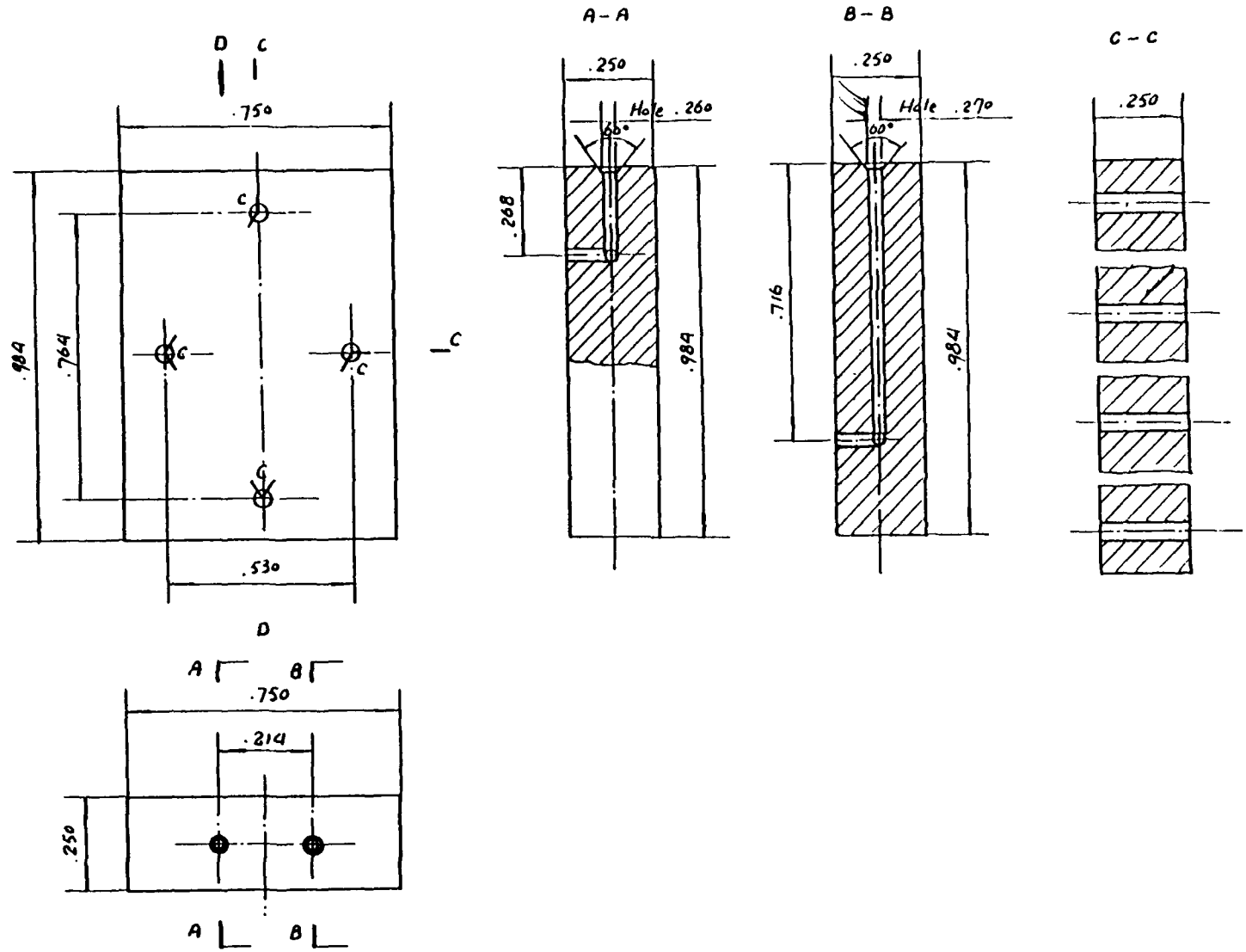

247

ITEM# - 5' 5"

MATERIAL - STAINLESS STEEL

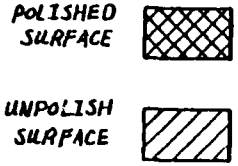

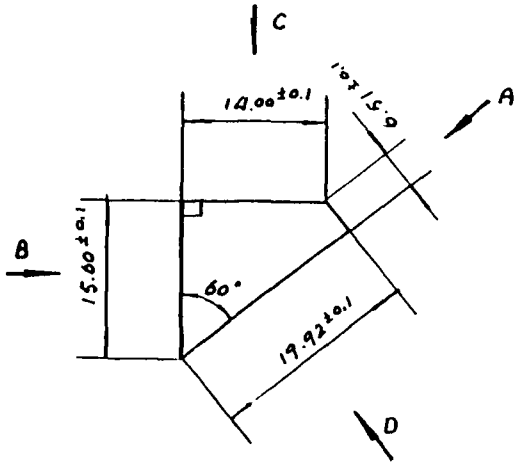

Angular Dimensions ;
Anglar Tolerance ± 5'
Common Plane (normals) ± 5'
material : $Zn Se$
No Depolarization or Birefringence

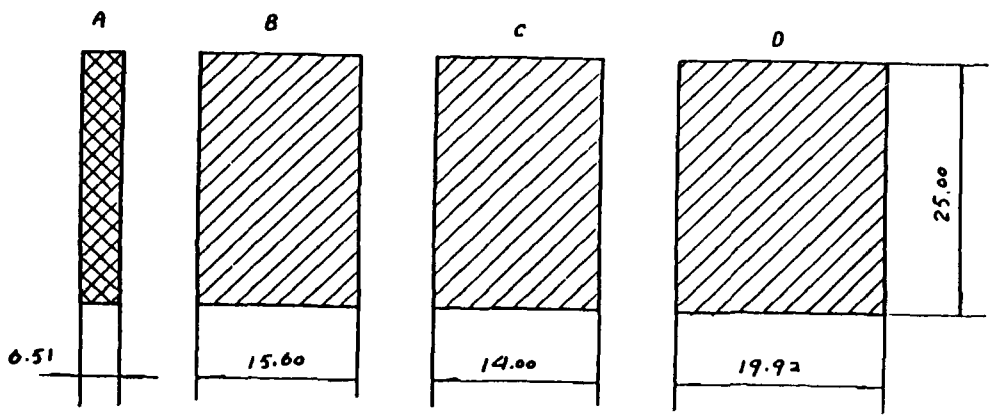

ITEM# - 6

MATERIAL - ZINC SELENIDE

PRISM - 30-60-90

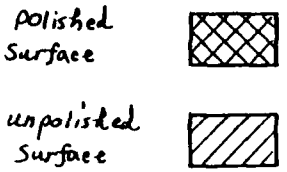

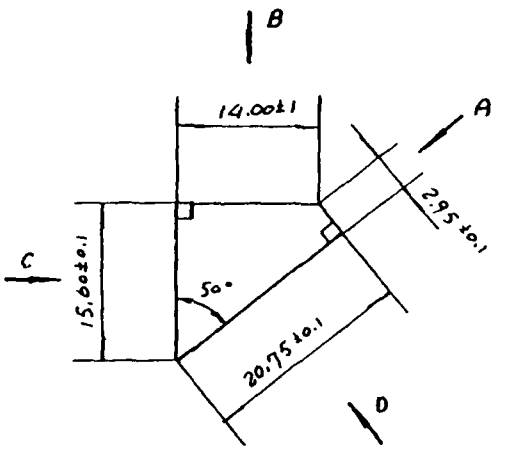

Angular Dimensions
Angles 90°, 50°, 90°
Angles tolerence ±5'
Common plane (normals) ±5'
Polish : Scrate - Dig 20-10
matrial : ZnSe
No Depolarization or Birefringence

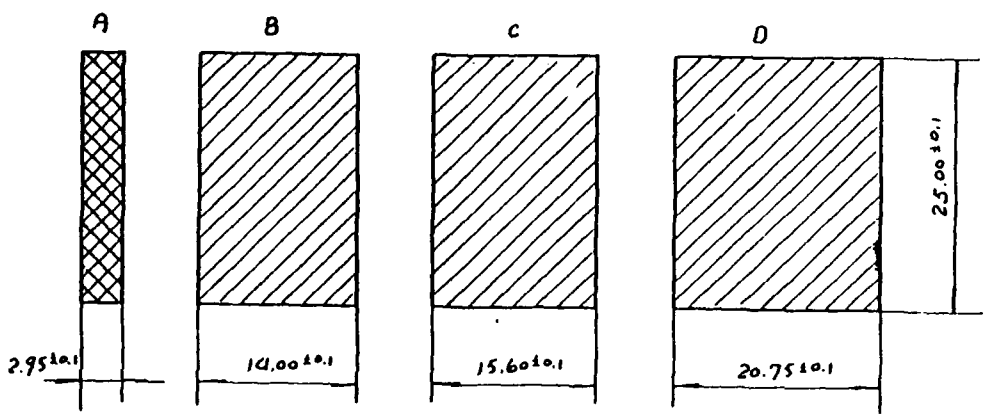

ITEM# - 6

MATERIAL - ZINC SELENIDE

PRISM - 40-50-90

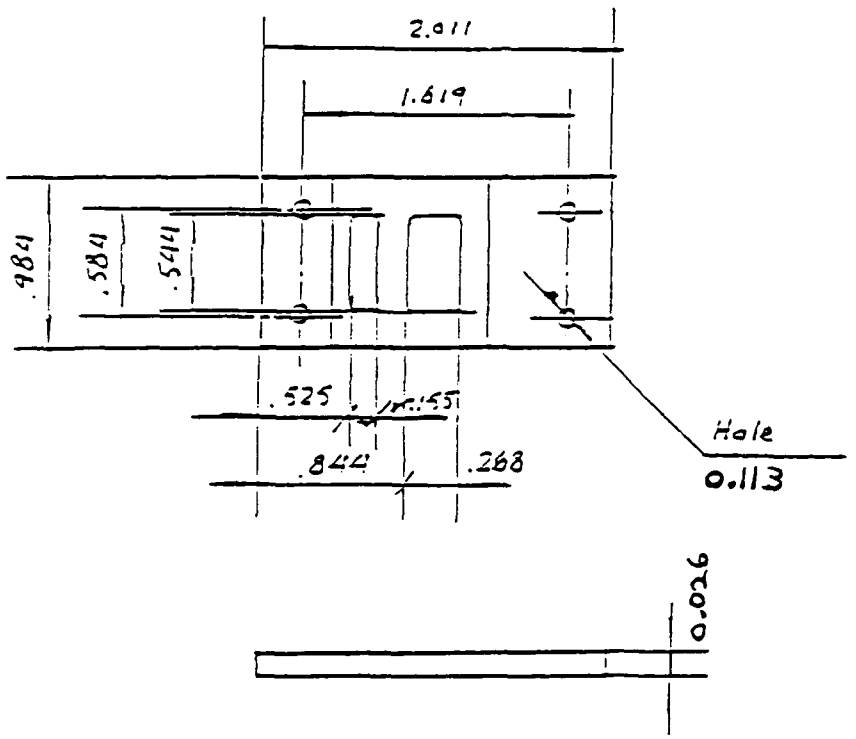

ITEM# - 7

MATERIAL - TEFLON

PRISM - 30-60-90

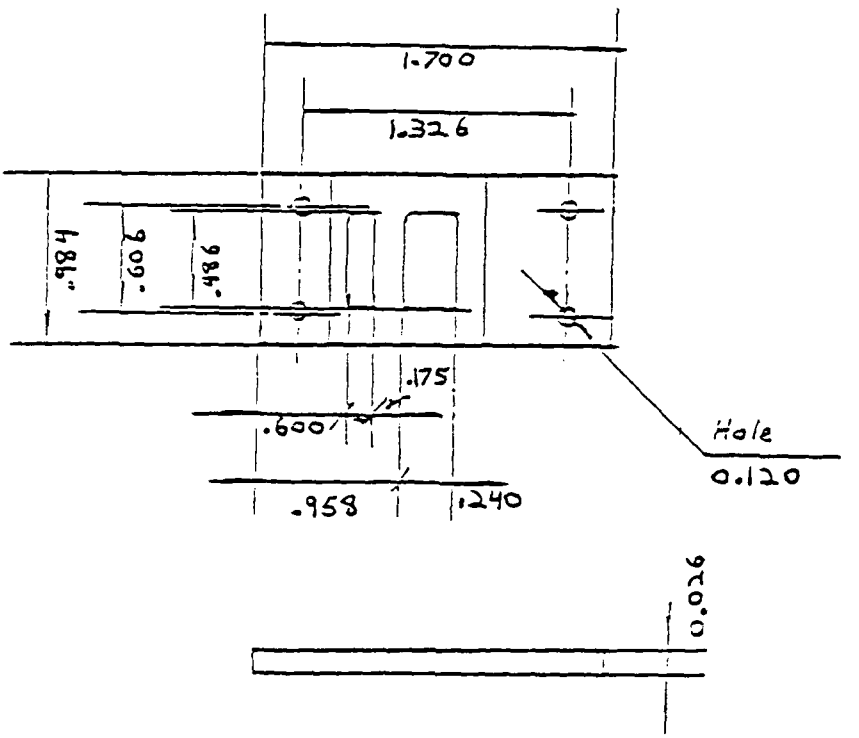

ITEM# - 7

MATERIAL - TEFLON

PRISM - 40-50-90

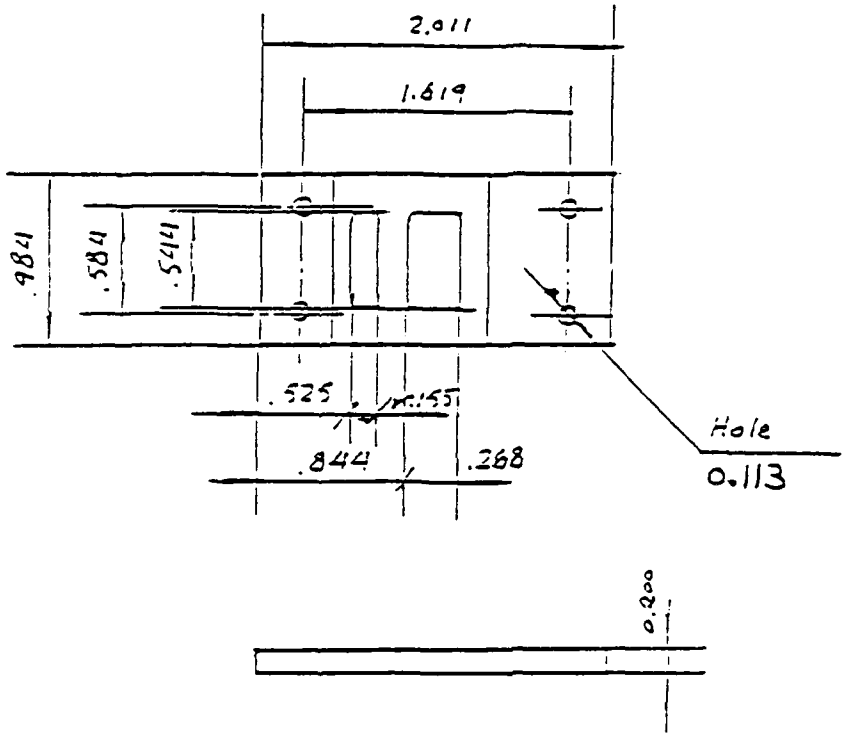

ITEM# - 8

MATERIAL - STAINLESS STEEL

PRISM - 30-60-90

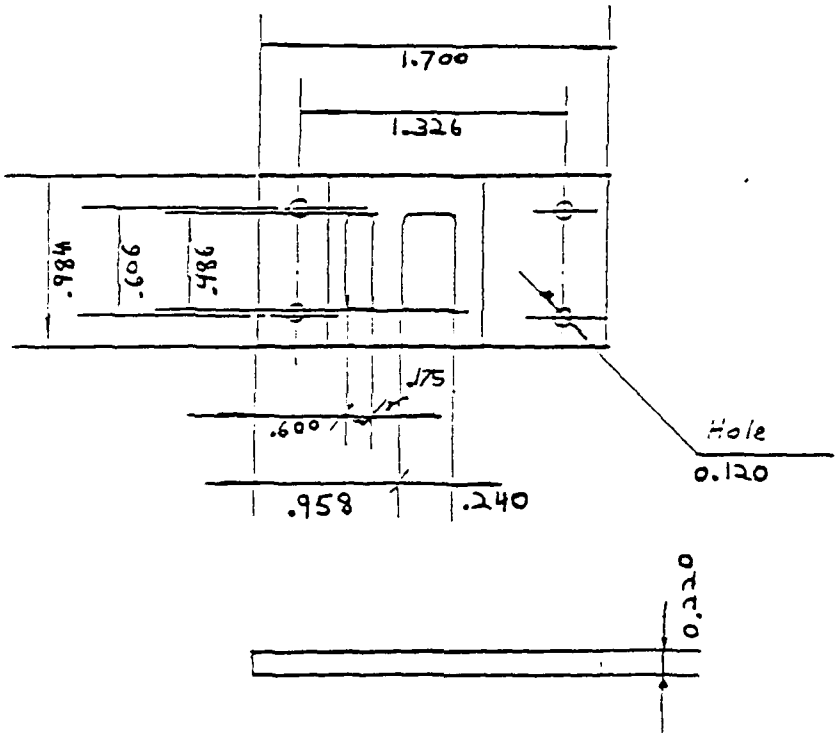

ITEM# - 8

MATERIAL - STAINLESS STEEL

PRISM - 40-50-90

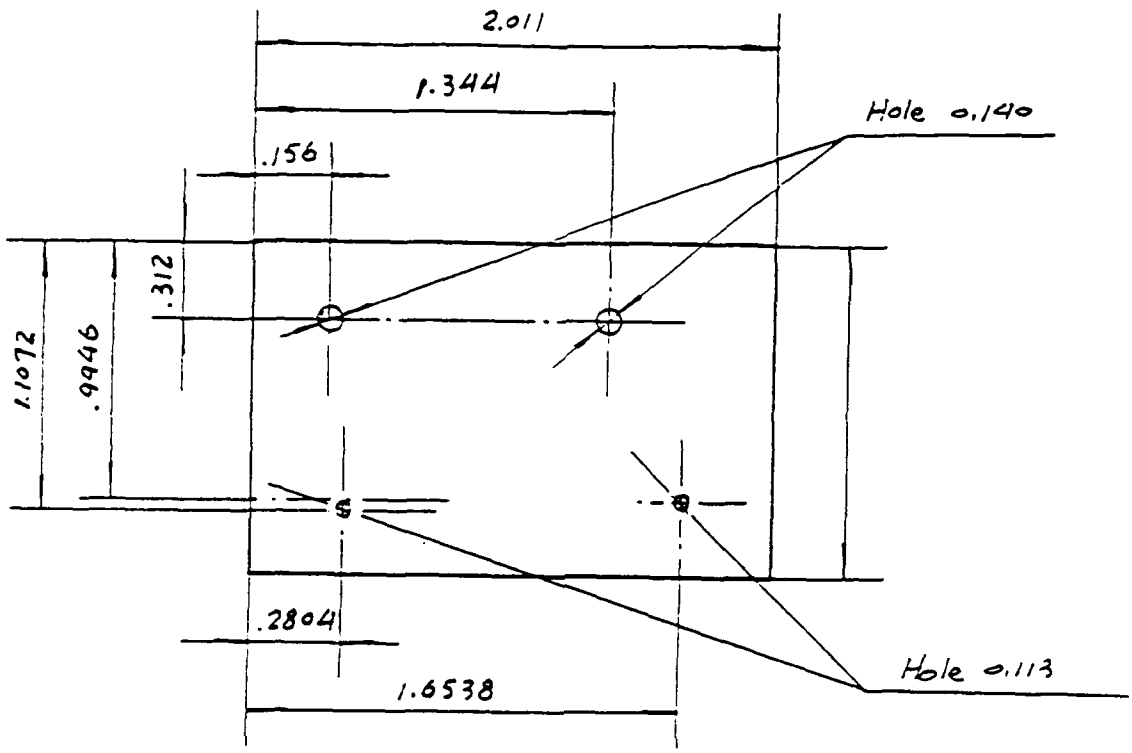

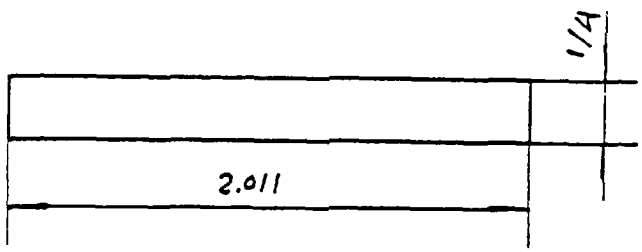

ITEM# - 9

MATERIAL - STAINLESS STEEL

PRISM - 30-60-90

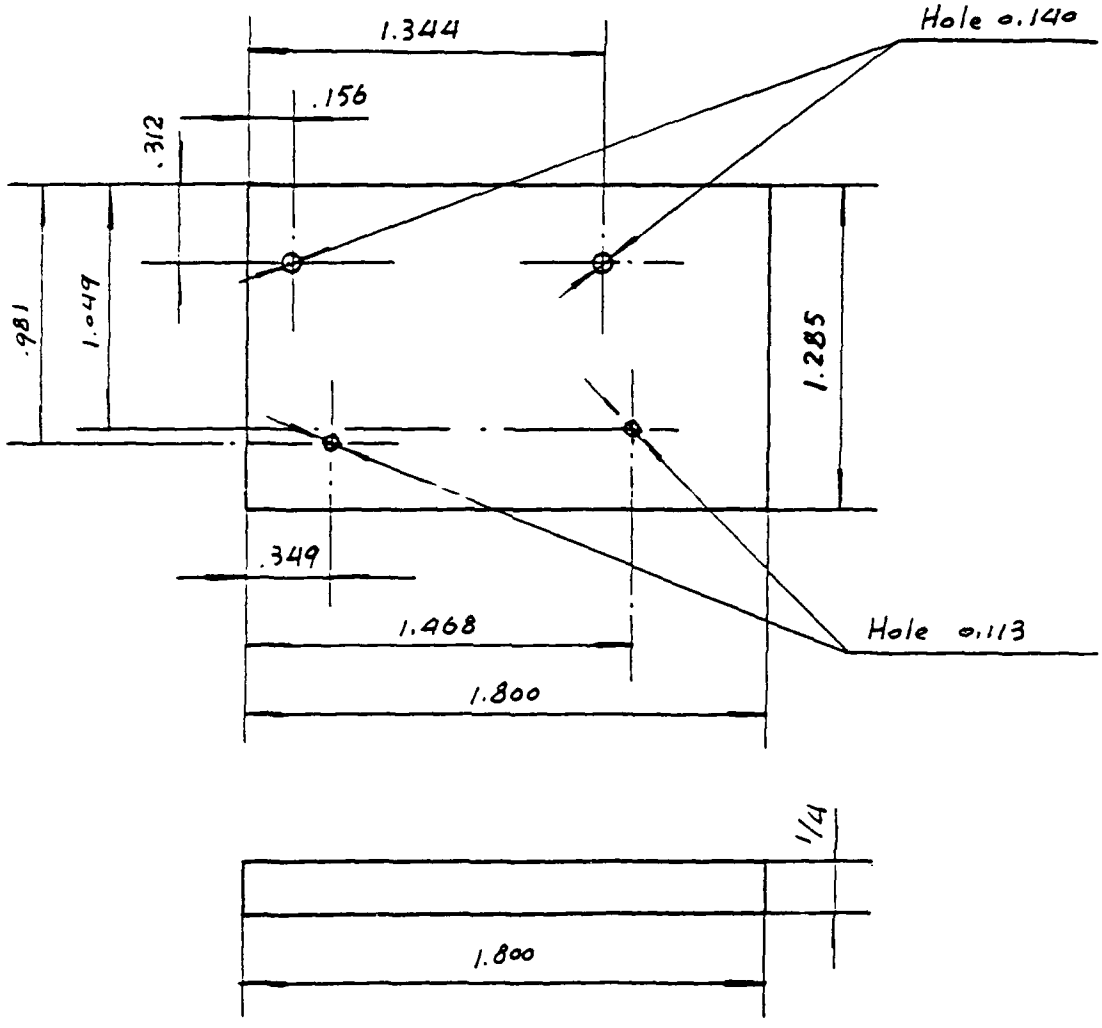

ITEM# - 9

MATERIAL - STAINLESS STEEL

PRISM - 40-50-90

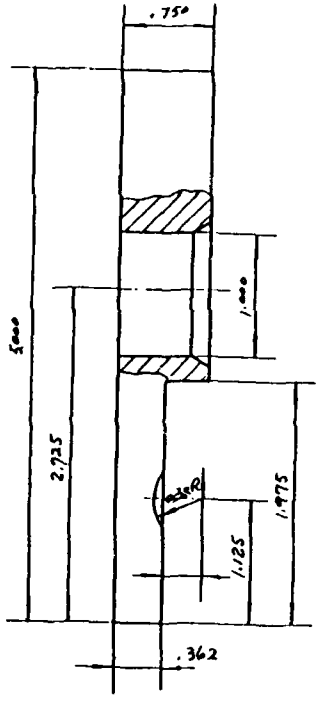

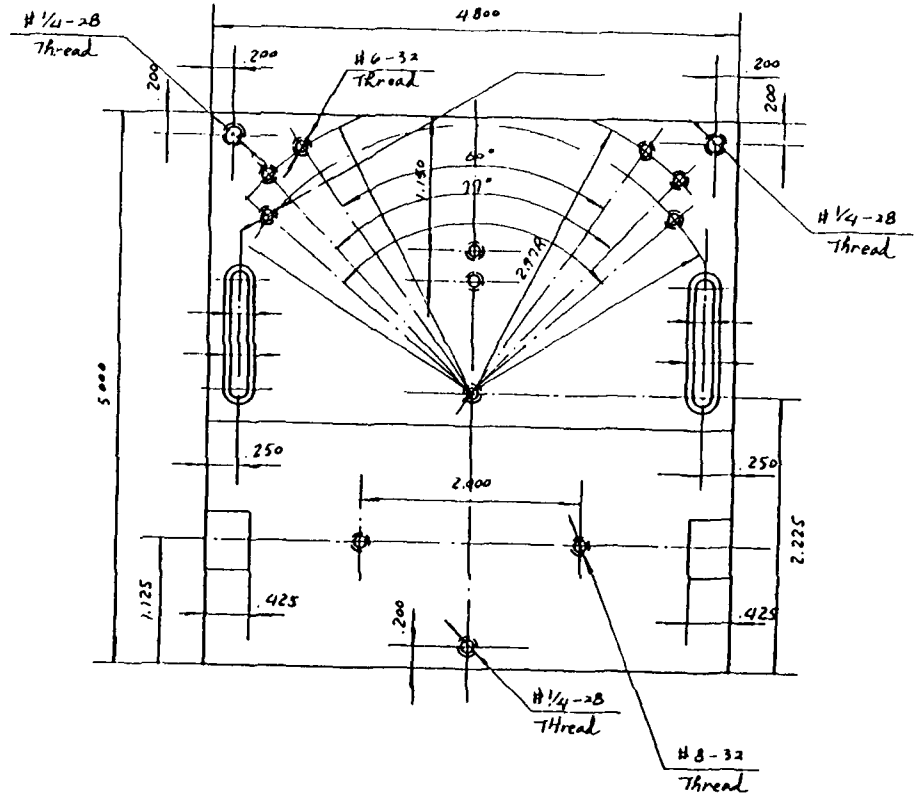

ITEM# - 11

MATERIAL - STAINLESS STEEL

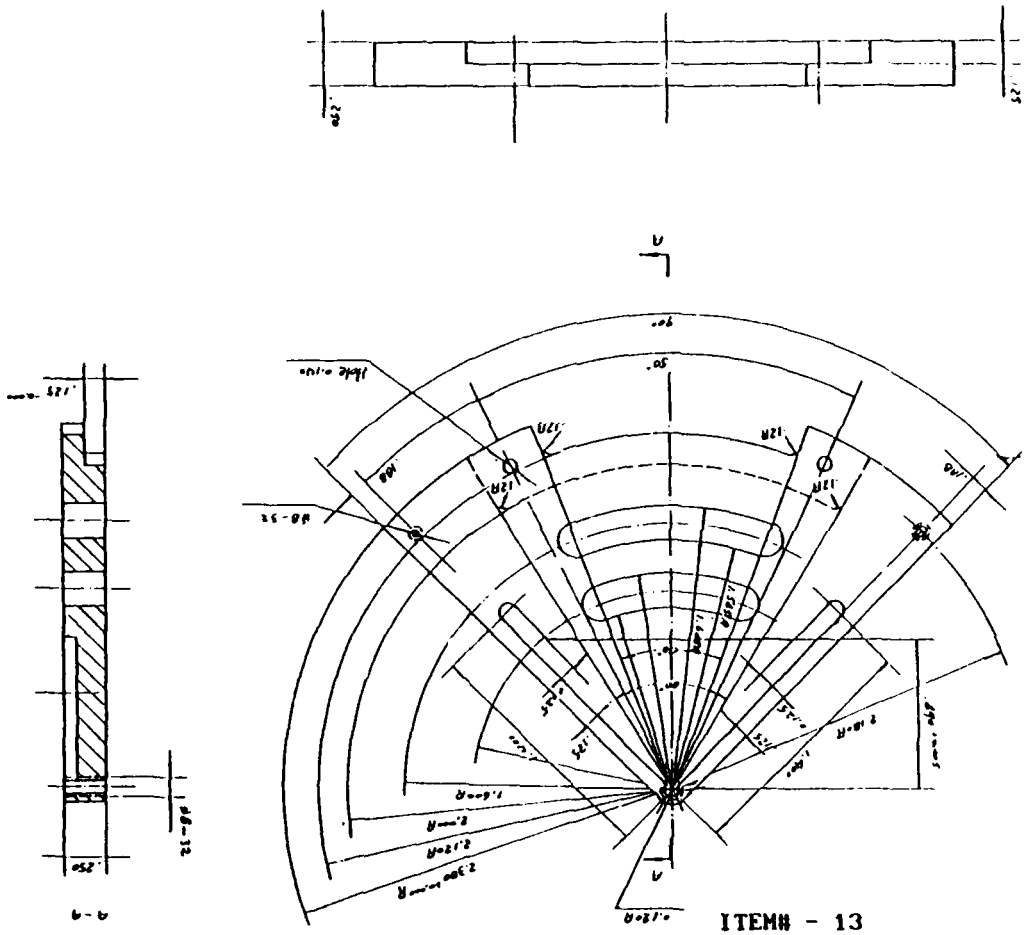

ITEM# - 13

MATERIAL - STAINLESS STEEL

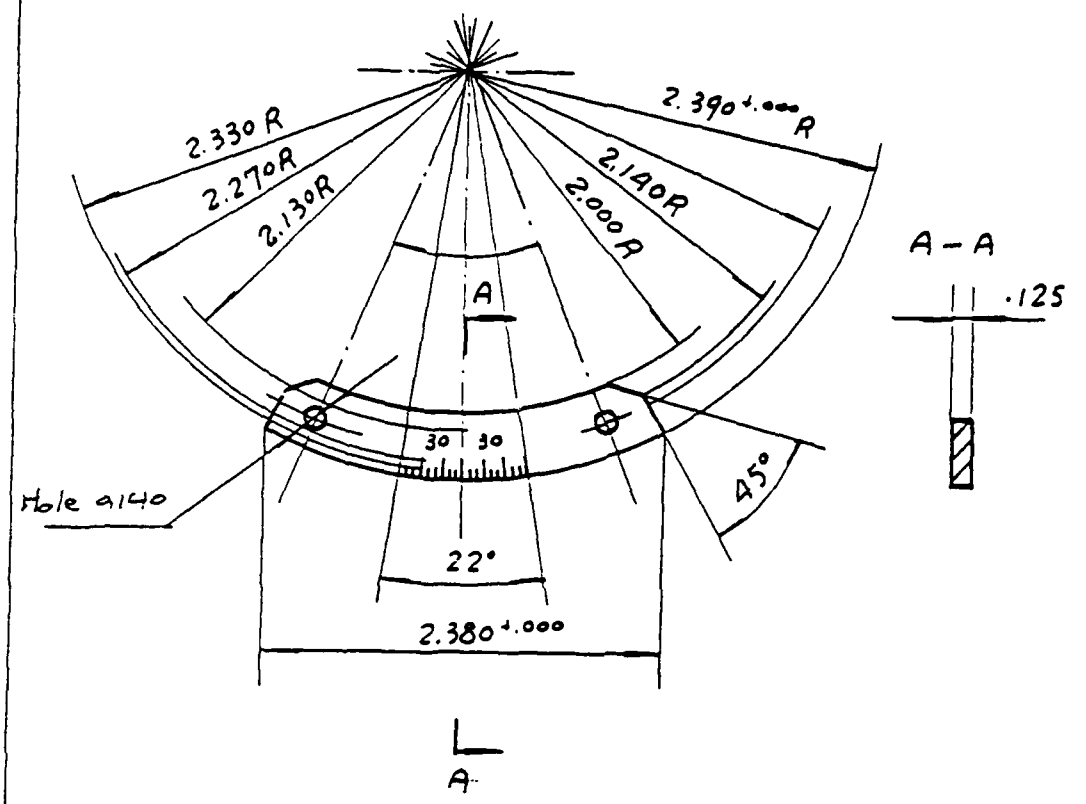

MILL NUMBERS (1/8 HIGH)
AND SCALE LINES
(1 LINE PER 54.999 MIN.)

ITEM# - 14"

MATERIAL - STAINLESS STEEL

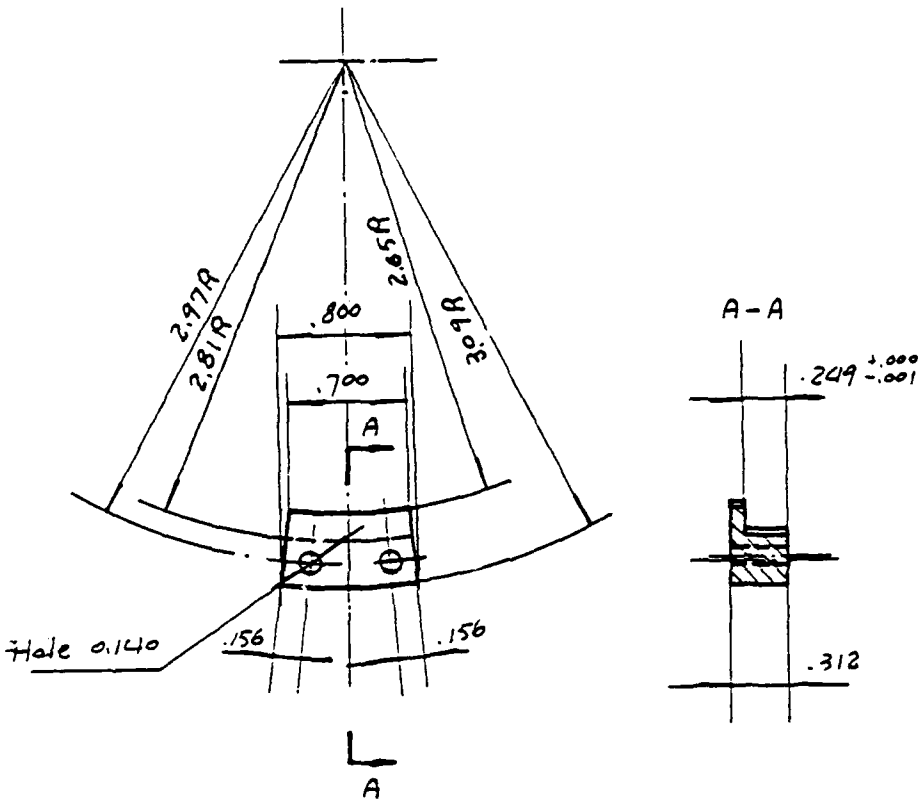

ITEM# - 15' 15"

MATERIAL - STAINLESS STEEL

Blank

g. APPENDIX 2.2

Zhiqin Huang's Thesis

g. Appendix 2.2

Zhiqin Huang's Thesis

Master's thesis of Zhiqin Huang using the ATR device to determine the complex refractive index of water and SF-96. The cell was used in conjunction with a Perkin-Elmer 580B spectrophotometer.

ATTENUATED TOTAL REFLECTION APPLIED TO LIQUIDS

A THESIS IN
Physics
Presented to the Faculty of the University
of Missouri-Kansas City in partial fulfillment of
the requirement of the degree

MASTER OF SCIENCE

by
ZHIQIN HUANG
B.S., Harbin Institute of Technology

Kansas City, Missouri
1988

This thesis has been renumbered tc correspond with numbering in this contract report.

ATTENUATED TOTAL REFLECTION APPLIED TO LIQUIDS

Zhiqin Huang, Master of Science

University of Missouri-Kansas City, 1988

ABSTRACT

The attenuated total reflection technique (ATR) applied to two liquid samples, water and SF96, is introduced in this paper. The details of the basic theory of ATR associated with the two approaches (the angle and polarization methods), the equipment set up, the measurement procedure, the experimental results and the error analysis are given in the paper.

This abstract of 56 words is approved as to form and content.

David M. Wieliczka

David M. Wieliczka, Ph.D.

The undersigned, appointed by the Associate Vice Chancellor for Graduate Studies, have examined a thesis entitled "Attenuated Total Reflection Applied To Liquids", presented by Zhiqin Huang, a candidate for the degree of Master of Science and hereby certify that in their opinion it is worthy of acceptance.

David M. Wieliczka — Aug 19, 1988

David M. Wieliczka, Ph.D. — Date

Department of Physics

Marvin R. Querry — 19 Aug. 1988

Marvin R. Querry, Ph.D. — Date

Department of Physics

John R. Urani — Aug 19, 1988

John R. Urani, Ph.D. — Date

Department of Physics

TABLE OF CONTENTS

LIST OF ILLUSTRATIONS

LIST OF TABLE

ACKNOWLEDGEMENTS

I would like to gratefully thank my advisor Dr. David M. Wieliczka for his guidance and help. Without his encouragement, constant support and advice, I could not imagine this thesis work would be done. Valuable encouragements and discussions were also received from Dr. Marvin R. Querry and Dr. John R. Urani and other faculty members of the Physics Department at the University of Missouri-Kansas City.

I also thank Lewis A. Meloan for his great contribution in constructing the experimental instruments.

I would also like to thank my wife for her help.

FORWARD

The purpose of this paper is to give an analysis of the technique of attenuated total reflection (ATR) which can be used to obtain the complex refractive index of liquids.

The paper is divided into five chapters, Introduction; Basic Theory of ATR; Equipment Setup and Measurement; Error Analysis and Appendices. Athough.the paper provides the details of how to determine the complex refractive index of liquids, using the ATR technique, the emphasis is on the analysis of the method. The results of the measurements and the final result of the calculations are at the end of Chapter 3 while the computer programs are in the appendices.

The Introduction discusses the theory critical to internal reflection. In Basic Theory of ATR, two techniques used to compute the complex refractive index are introduced. The details of performing the measurements are presented in Equipment Setup and Measurement. Athough the Error Analysis is short, it is the core of the paper.

CHAPTER I

INTRODUCTION

Two techniques are often used to determine the complex refractive index of a material, transmission or reflection measurement. The method of transmission is usually limited to materials with weak absorption. This limitation arises from the impractically thin sample needed for strongly absorbing materials and also the accuracy necessary in the measurement of the cell thickness to minimize the error introduced in the calculated absorption coefficient. The reason is that the energy from a general light source is totally absorbed in a sample material with a large absorption index, and therefore the transmitted intensity is too small to measure.

Reflection measurements at an air-sample boundary have problems with materials with high vapor pressure and the menuscus effect if liquids are studied. A general problem with reflection is that it normally fails for substances showing weak absorption. This limits the applicability of the technique.

The attenuated total reflection technique (ATR) is quite powerful in that it avoids the problems of the above two methods.

ATR was developed more than twenty years ago by

J.Fahrenfort [1], and uses, instead of an air interface, the interface between the sample and an optically dense dielectric. If the refractive index of the optically dense dielectric is larger than that of the sample, total reflection can be achieved. In ATR, the incident electromagnetic wave first penetrates the interface into the sample medium, then is reflected back into the incident medium. If the absorption index k of the sample medium is not equal to zero, an attenuation occurs in the sample. It is this attenuation which provides the sample information to the reflected wave.

An advantage of ATR is that it employs a good interface, and no vapor and has no meniscus effects. The most important advantage of ATR is the sensitivity of the reflected intensity as a function of the sample complex refractive index and the incident angle. The first feature is obviously important to the measurement, and the second makes it easy to use this technique on weakly or strongly absorbing materials. In short, the ATR method can work on materials which have strong absorption or even on opaque materials, and also on materials with weak absorption.

The effect of an interface between two dielectric transparent materials on an incident electromagnetic wave can be determined by examining the electromagnetic boundary conditions. Applying these boundary conditions leads to four equations which relate the magnitude of the reflected and transmitted electric field to the incident electric field. These equations are known as

the Fresnel equations. The ratio of reflected to incident electrical field magnitudes are given in Equations 1-1 and 1-2 for s and p polarization. The polarization states s and p indicate the plane of the electric field being perpendicular or parallel to the plane of incidence, respectively,

$$r_s = \frac{(n_i + jk_i)\cos\phi_i - (n_t + jk_t)\cos\phi_t}{(n_i + jk_i)\cos\phi_i + (n_t + jk_t)\cos\phi_t} \quad , \qquad 1\text{-}1$$

$$r_p = \frac{(n_t + jk_t)\cos\phi_i - (n_i + jk_i)\cos\phi_t}{(n_t + jk_t)\cos\phi_i + (n_i + jk_i)\cos\phi_t} \quad . \qquad 1\text{-}2$$

Here n and k are refraction and absorption indices, and ϕ_i and ϕ_t are incident and transmitted angles respectively. Note that the refractive index here is complex.

The fundamental consideration necessary for the ATR technique is that the incident light reaches the interface at an angle adjacent to the critical angle, and also equal to or larger than the critical angle. The theory of internal reflection explains the ATR process. First assume the absorption index of the sample is zero, and that the incident angle is equal to or great than the critical angle. Then the electromagnetic wave will be totally reflected and no energy is lost in the sample medium. This can be proved from Fresnel's equations.

Figure 1 shows the relationship of the incident, transmitted and reflected beam on the boundary.

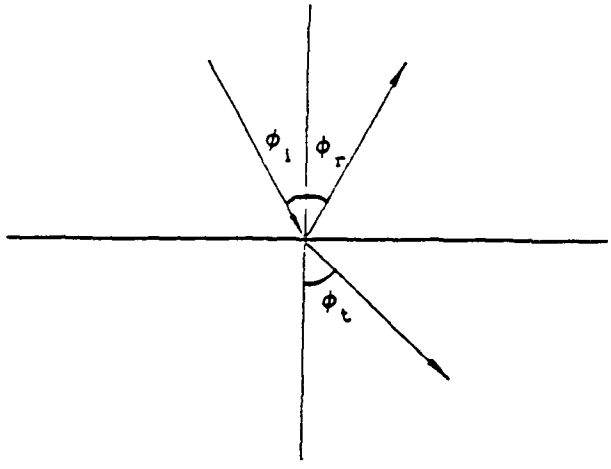

Fig.1--Diagram of the incident, transmitted and reflected beam on the boundary

Setting k=0 in equations 1-1 and 1-2, we have:

$$r_s = \frac{n_i \cdot \cos\phi_i - n_t \cdot \cos\phi_t}{n_i \cdot \cos\phi_i + n_t \cdot \cos\phi_t} \quad , \qquad 1\text{-}3$$

$$r_p = \frac{n_t \cdot \cos\phi_i - n_i \cdot \cos\phi_t}{n_t \cdot \cos\phi_i + n_i \cdot \cos\phi_t} \quad . \qquad 1\text{-}4$$

From Snell's law,

$$n_i \cdot \sin\phi_i = n_t \cdot \sin\phi_t \quad , \qquad 1\text{-}5$$

we find

$$\cos\phi_t = \pm \sqrt{1-\left[\frac{n_i}{n_t}\right]^2 \cdot \sin\phi_i} \quad . \qquad 1\text{-}6$$

When the angle ϕ_i is larger than the critical angle ϕ_c, $\cos\phi_t$ becomes an imaginary number, and can be written as

$$\cos\phi_t = \pm j \frac{n_i}{n_t} \sqrt{\sin\phi_i - \left[\frac{n_t}{n_i}\right]^2} \quad . \qquad 1\text{-}7$$

The negative sign is not meaningful here, because the wave cannot be infinite in the second medium. We finally have that

$$\cos\phi_t = j \frac{n_i}{n_t} \sqrt{\sin_i\phi - \left[\frac{n_t}{n_i}\right]^2} \quad . \qquad 1\text{-}8$$

Substituting this result into Equations 1-3 and 1-4, we have:

$$R_s = r_s \cdot r_s^* = 1 \ , \qquad R_p = r_p \cdot r_p^* = 1 \qquad 1\text{-}9$$

This indicates that the incident beam is totally reflected. However, it is not true that the wave does not travel into the sample medium. In fact,only the average flow into the medium is equal to zero. This can be seen from the following argument.

Refering to Fig.1, the general form of an electromagnetic

wave E field can be written as shown in Equation 1-10. The subscript t in Equation 1-11 indicates the wave is in the transmitted medium. In x-y coordinates, we have Equations 1-12 and 1-13;

$$E = E \cdot e^{j(n \cdot r - \omega \cdot t)} \qquad 1\text{-}10$$

$$E_t = E \cdot e^{j(n_t \cdot r - \omega \cdot t)} \qquad 1\text{-}11$$

$$= E \cdot e^{j\,[N_t(\cos\phi_t\, i + \sin\phi_t\, j)\cdot(xi+yj) - \omega \cdot t]} \qquad 1\text{-}12$$

$$= E \cdot e^{j\,[N_t(x\cdot\cos\phi_t + y\cdot\sin\phi_t) - \omega \cdot t]} \qquad 1\text{-}13$$

Using the relationship of Equation 1-5 and Equation 1-8 in Equation 1-13, we obtain:

$$E_t = E\, e^{-N_i[\sin^2\phi_i - (N_t/N_i)^2]^{1/2}\cdot x + j(N_i \cdot y \cdot \sin\phi_i + \omega \cdot t)} \qquad 1\text{-}14$$

$$= E\, e^{-\beta \cdot x + j(d \cdot y + \omega \cdot t)} \qquad 1\text{-}15$$

where

$$\beta = N_i[\sin^2\phi_i - (N_t/N_i)^2]^{1/2} \quad \text{and} \quad d = N_i \cdot \sin\phi_i \qquad 1\text{-}16$$

In the x direction, E_t will be attenuated. The distance the

wave is transmitted into the second medium depends on β. However, β is a function of the incident angle ϕ_i . For instance, when $\phi_i=\phi_c$ (ϕ_c=the critical angle), we have sin $\phi_t=1$ and $\sin\phi_i=N_t/N_i$, so that $\beta=0$ and E_t will not be attenuated. Therefore adjustment of the incident angle can control the depth of the wave transmitted into the second medium. Although E is attenuated in the second medium, there is no discipation there because the absorption index k is zero. All energy is reflected back into the first medium. The equations used above are time dependent. If we time average these equations, we find no energy lost in the second material. The average flow into the second material will be zero.

This can be shown by considering the normal component of the Poynting vector:

$$S\cdot n=\frac{c}{8\pi}Re\{n\cdot(E_t\times H_t^*)\} \qquad 1\text{-}17$$

since

$$H_t=\frac{c}{\mu\cdot\omega}(N_t\times E_t) \qquad 1\text{-}18$$

so

$$S\cdot n=\frac{c^2}{8\pi\mu\cdot\omega}Re\{(n\cdot N_t)|E_t|^2\} \qquad 1\text{-}19$$

where

$$n\cdot N=N\cdot\cos\phi_t \qquad 1\text{-}20$$

When $\phi_i\geq\phi_c$ then $\cos\phi_t$ is pure imaginary and therefore $S\cdot n=0$. This indicates the time average of the Poynting Vector is zero in the second medium indicating no energy is transmitted. The same result

was obtained in Equation 1-9 which shows a reflection coefficient of 1. The electromagnetic wave does flow across the surface but it also flows back again.

If the refractive index N_t is not real, as assumed in the equations above, but is complex, then R in Equation 1-9, will no longer equal one (details in the next chapter). The imaginary part of N_t is related to the Lambert absorption coefficient. Due to the imaginary part of N_t energy is discipated in the transmitted medium. This can be represented by the equations below, namely

$$R_s = r_s \cdot r_s^* < 1 \quad \text{and} \quad R_p = r_p \cdot r_p^* < 1 \ . \qquad 1\text{-}21$$

The discipation of the energy and the reflected intensity are a function of the incident angle. Also R_s and R_p have different responses to n_t and k_t ($N_t = n_t + j\ k_t$). These facts can be used to solve for n_t and k_t provided R_s , R_p and ϕ_i are known.

The degree of sensitivity of the ATR technique is very important in determining n_t and k_t accurately. The degree of sensitivity is related to the distance the wave travels into the second medium. In fact, the incident angle ϕ_i is the dominating factor in controling the depth the wave travels into the second medium. Determining the best angle or the relationship of the angle to the degree of sensitivity becomes quite important.

From the equation below,

$$\beta = N_1 [\sin^2 \phi_i - (N_t / N_1)]^{1/2} \ , \qquad 1\text{-}22$$

we can see that the closer the incident angle ϕ_1 is to the critical angle the deeper the wave travels into the sample. As the wave travels deeper into the sample medium, more information about the complex refractive index is brought out by the reflected light. But if the wave is transmitted into the second medium too deeply, the reflected wave becomes too weak to be detected. Combining these two factors, our purpose is to find the best condition to perform the measurements.

First consider the relationship of the degree of sensitivity to the incident angle ϕ_1. As an example, the derivative of R_s with respect to the absorption index k, $\delta R_s/\delta k$ is calculated for water and shown in Fig 2. From the figure it can be seen that the sensitivity of the reflection coefficient R to the absorption index k, ($\delta R/\delta k$), does have a peak which is located around the critical angle. When the refractive index n changes as the wave number changes (X-axis), the peak moves as the critical angle varies. The larger the value of $\delta R/\delta k$, the more accurately the complex refractive index can be obtained from the measurement. The most sensitive region is located adjacent to the critical angle.

Fig 3 shows $\delta R/\delta n$ as a function of the incident angle and the imaginary part of the complex refractive index, K. It can be seen that n is very sensititve to the incident angle ϕ_1 and to k.

For most samples we must perform the measurement several times to find the best incident angle ϕ_1 in order to obtain the

maximum degree of sensitivity for n_t and k_t. Sometimes under the maximum degree of sensitivity the reflected light is too weak to be detected so that we must trade off some sensitivity for reflected intensity.

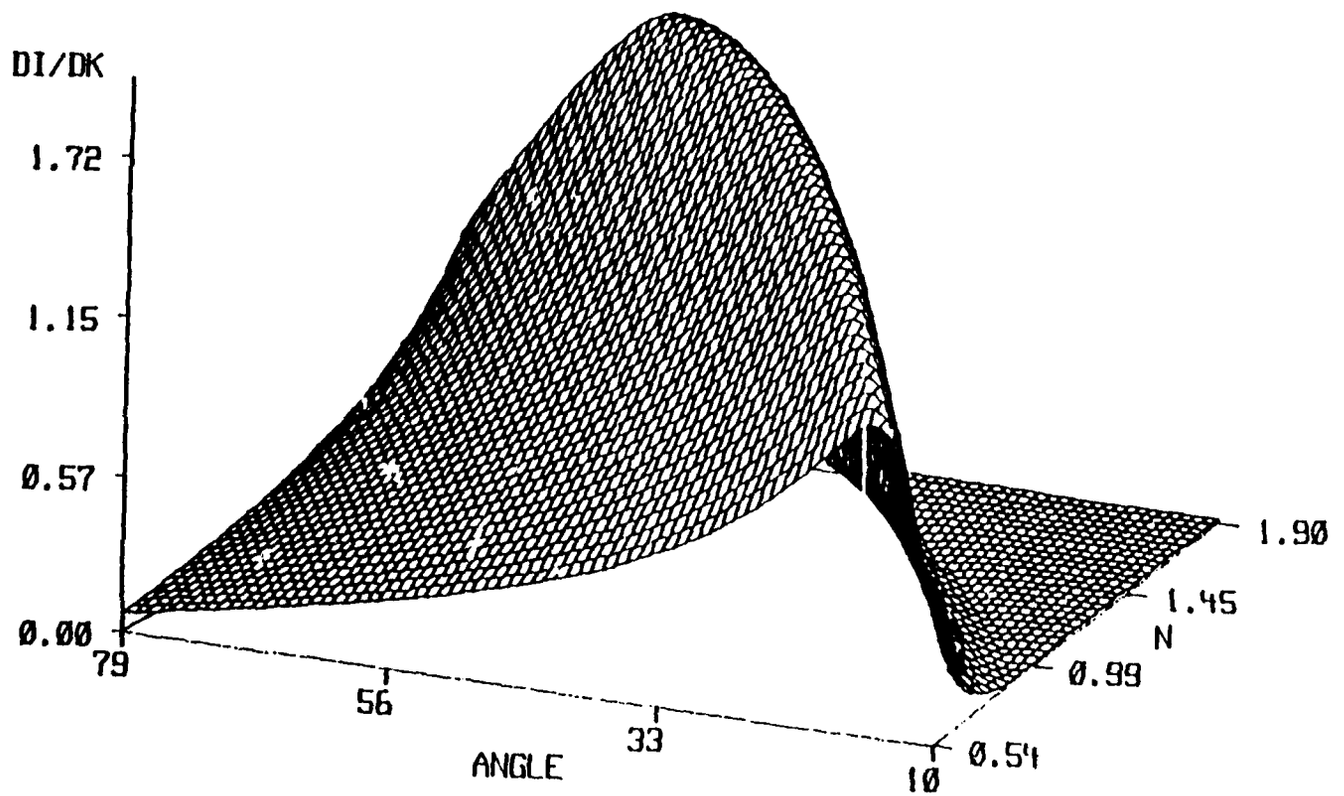

Fig.2--The relationship of the degree of sensitivity to the incident angle ϕ_1 and the refractive index n.

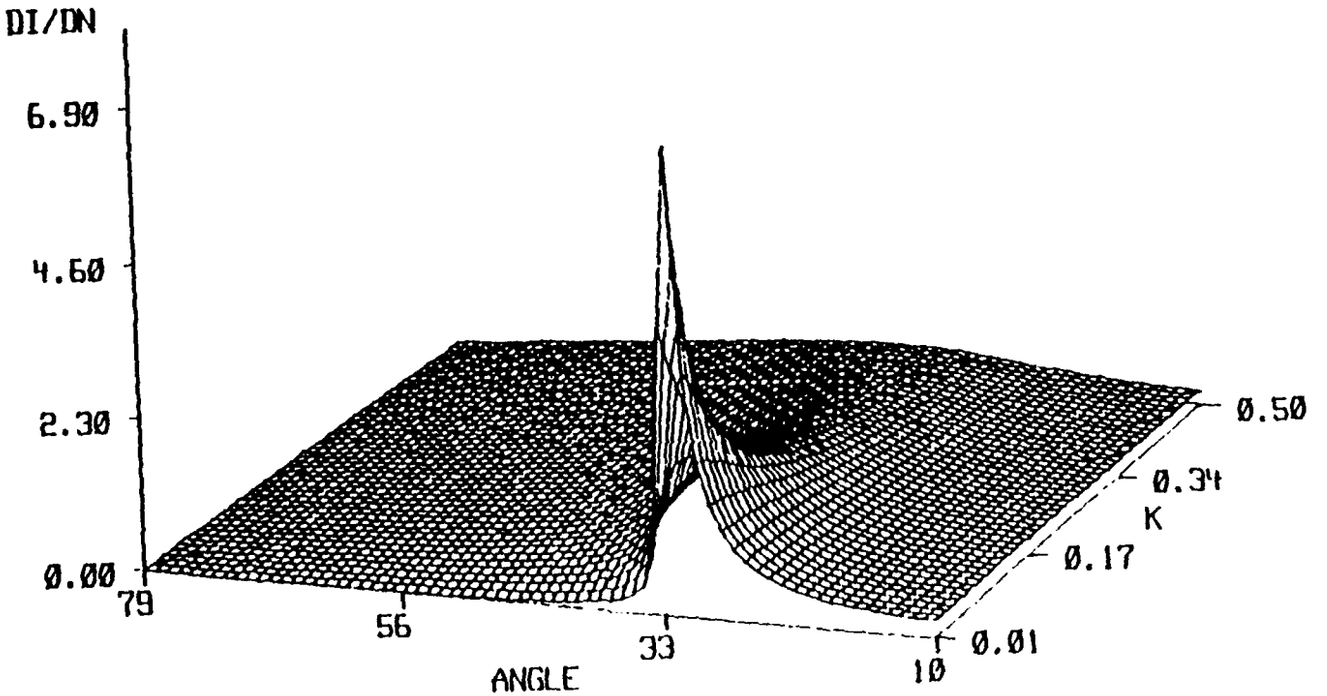

Fig.3--The relationship of the degree of sensitivity to the incident angle ϕ_1 and the absorption index k.

CHAPTER II

BASIC THEORY OF ATR

From the Fresnel equations, only three parameters need be used to determine the indices n_t and k_t. They are R_s, R_p and ϕ_i where R_s and R_p can be obtained from the measurement of the intensity of reflected light. The incident angle ϕ_i is to be chosen to satisfy the best measuring conditions.

To obtain the indices we can fix ϕ_i and take measurement R_s and R_p or change the incident angle ϕ_i from ϕ_{i1} to ϕ_{i2} and take two measurements $R_s(\phi_1)$ and $R_s(\phi_2)$ or $R_p(\phi_1)$ and $R_p(\phi_2)$.

Starting with fixed angle ϕ_i and performing the measurements of R_s and R_p, n_t and k_t can be determined from the Fresnel equations, a system of two equations with two unknowns.

The Fresnel equations can be written as,

$$r_s = \frac{N_i \cdot \cos\phi_i - (N_t^2 - N_t^2 \cdot \sin^2\phi_i)^{1/2}}{N_i \cdot \cos\phi_i + (N_t^2 - N_t^2 \cdot \sin^2\phi_i)^{1/2}} , \qquad 2\text{-}1$$

$$r_p = \frac{N_t \cdot \cos\phi_i - N_i \cdot (N_t^2 - N_i^2 \cdot \sin^2\phi_i)^{1/2}}{N_t \cdot \cos\phi_i - N_i \cdot (N_t^2 - N_i^2 \cdot \sin^2\phi_i)^{1/2}} . \qquad 2\text{-}2$$

Where

$$N_i = n_i + jk_i \quad \text{and} \quad N_t = n_t + jk_t \ . \qquad 2\text{-}3$$

Let

$$N + jK = \left[\frac{N_t}{N_i}\right]^2 = \left[\frac{n_t + jk_t}{n_i + jk_i}\right]^2 \ , \qquad 2\text{-}4$$

then 2-1 and 2-2 become:

$$r_s = \frac{\cos\phi_i - (N + jK - \sin\phi_i)^{1/2}}{\cos\phi_i + (N + jK - \sin\phi_i)^{1/2}} \qquad 2\text{-}5$$

$$r_p = \frac{(N + jK)\cdot\cos\phi_i - (N + jK - \sin\phi_i)^{1/2}}{(N + jK)\cdot\cos\phi_i + (N + jK - \sin\phi_i)^{1/2}} \ . \qquad 2\text{-}6$$

To obtain R_s and R_p,

let

$$(N + jK - \sin\phi_i)^{1/2} = P + jQ \ . \qquad 2\text{-}7$$

Then

$$R_s = r_s \cdot r_s^* = \frac{\cos^2\phi_i - 2\cdot P\cdot\cos\phi_i + P^2 + Q^2}{\cos^2\phi_i + 2\cdot P\cdot\cos\phi_i + P^2 + Q^2} \qquad 2\text{-}8$$

and

$$R_p = r_p \cdot r_p^* = \frac{\cos\phi_1\{(P^2+Q^2)-2\cdot(P^2+Q^2)\cdot\sin^2\phi_1+4\cdot P^2\sin^2\phi_1+\sin^4\phi_1\}+}{\cos\phi_1\{(P^2+Q^2)-2\cdot(P^2+Q^2)\cdot\sin^2\phi_1+4\cdot P^2\sin^2\phi_1+\sin^4\phi_1\}+}$$

$$\frac{P^2+Q^2-2\cdot(P^2+Q^2+\sin\phi_1)\cdot P\cdot\cos\phi_1}{P^2+Q^2+2\cdot(P^2+Q^2+\sin\phi_1)\cdot P\cdot\cos\phi_1} \qquad 2\text{-}9$$

By letting $P^2+Q^2=U$, we can cancel Q from both equations.

Then

$$R_s = \frac{\cos^2\phi_1-2\cdot P\cdot\cos\phi_1+P^2+Q^2}{\cos^2\phi_1+2\cdot P\cdot\cos\phi_1+P^2+Q^2} \qquad 2\text{-}10$$

and

$$R_p = \frac{(U-\sin^2\phi_1)+4\cdot P^2\sin^2\phi_1\cdot\cos^2\phi_1+U-2\cdot(U+\cos^2\phi_1)\cdot P\cdot\cos\phi_1}{(U-\sin^2\phi_1)+4\cdot P^2\sin^2\phi_1\cdot\cos^2\phi_1+U+2\cdot(U+\cos^2\phi_1)\cdot P\cdot\cos\phi_1} \quad . \qquad 2\text{-}11$$

Rearranging the equations above and solving for U and P, we have:

$$P = -\frac{(1-R_p)\cdot A-2\cdot(1+R_p)\cdot\sin^2\phi_1\cdot\cos^2\phi_1-2\cdot(1-R_p)\cdot A\cdot\cos^2\phi_1+}{(A^2+4\cdot\sin^2\phi_1)(1-R_p)\cdot\cos^2\phi_1-2\cdot(1+R_p)\cdot A\cdot}$$

$$\frac{2\cdot(1+R_p)\cdot\cos^2\phi_1}{\cos\phi_1} \qquad 2\text{-}12$$

and,

$$U = A \cdot P - \cos^2\phi_i \quad , \tag{2-13}$$

where

$$A = \frac{2 \cdot (1 + R_s)}{1 - R_s} \cos\phi_i \tag{2-14}$$

After obtaining P and U, we can determine Q,

$$Q = \pm \sqrt{U^2 - P^2} \tag{2-15}$$

Since

$$P + j\,Q = \sqrt{N + j\,K - \sin^2\phi_i} \tag{2-16}$$

and $N \geq \sin^2\phi_i$ and $K \geq 0$ (in the range of interest) then P and Q have the same sign. But $U \geq 0$, and from equations 2-7 and 2-13 we know P is larger than zero, thus we have,

$$Q = \sqrt{U^2 - P^2} \tag{2-17}$$

From Equation 2-4 we obtain

$$N = \frac{a \cdot x + b \cdot y}{a^2 + b^2} \quad \text{and} \quad K = \frac{a \cdot y + b \cdot x}{a^2 + b^2} \tag{2-18}$$

where

$$a = n_i^2 - k_i^2 \quad , \qquad b = 2 \cdot n_i \cdot k_i \tag{2-19}$$

$$x = n_t^2 - k_t^2 \quad \text{and} \quad y = 2 \cdot n_t \cdot k_t \tag{2-20}$$

Finally we have:

$$n_t = \{ [x + (x^2 + y^2)^{1/2}]/2\}^{1/2} \qquad 2\text{-}21$$

$$k_t = \frac{y}{2 \cdot n_t} \qquad 2\text{-}22$$

The computer program using this method is given in Appendix A.

The second technique used to determine the indices n and k is to measure the reflectance at two different incident angles but with the same polarization state. We then have two equations $R_s(\phi_1)$ and $R_s(\phi_2)$ which can be used to solve for n_t and k_t. The derivation of these two equations is similar to the previous one and the details of the derivation can be found in [2]. The computer program for using this second method is in Appendix B.

The first method is easy to implement if the incident angle cannot be changed easily and for certain k values (this will be discussed later). If the measurement conditions allow a change of the incident angle, the second method has the advantage. If the incident angle is selective, it is easy to obtain the best measurement conditions. The error associated with the second method, applied to most liquids, is smaller than that for the first method. This will also be discussed in the error analysis section.

The previous discussion of the Fresnel equations applied to the ATR technique indicates a need for polarized light in performing the experiments. Two polarizers are employed to

accomplish this. One polarizer is placed before the cell to define the polarization state of the incident beam. A second is placed after the cell to reduce both the effect of the ZnSe prism on the polarization state and the leakage of the polarizers. Since no optical system is perfect, we must examine the efficiency of the polarizers and the response of the Perkin-Elmer spectrophotometer (580B) to polarized light.

We denote the efficiency of the first and second polarizers P_1 and P_2, respectively and leakages L_1 and L_2. The light in the Perkin-Elmer can be resolved into two polarization components, vertical V and horizontal H. Theoretically, H and V should be the same, or very close, but because of the response of the grating, detector, light source and the mirrors, the polarization state of the light varies as a function of wavelength. Therefore we must compensate for the distortion. The distortion produced by each element will not be considered but we will consider the distortion produced by the entire optical system as a whole. Then V and H can be obtained by employing several measurements with no ATR cell. To obtain the factors P, L, V and H, the polarizers are positioned in different combinations. For instance, if one polarizer is positioned to pass the vertical state and the other is positioned to pass the horizontal state we then have

$$\frac{P_1 \cdot L_2 \cdot V + L_1 \cdot P_2 \cdot H}{P \cdot V_r + P \cdot H_r} = I \ . \qquad 2\text{-}23$$

Since we have eight unknown variables, eight different

combinations are used to obtain the eight equations. We list seven below:

$$\frac{P_1 \cdot V + L_1 \cdot H}{V_r + H_r} = I_1 \qquad 2\text{-}24$$

$$\frac{L_1 \cdot V + P_1 \cdot H}{V_r + H_r} = I_2 \qquad 2\text{-}25$$

$$\frac{P_1 \cdot P_2 \cdot V + L_1 \cdot L_2 \cdot H}{P_2 \cdot V_r + L_2 \cdot H_r} = I_3 \qquad 2\text{-}26$$

$$\frac{L_1 \cdot L_2 \cdot V + P_1 \cdot P_2 \cdot H}{L_2 \cdot V_r + P_2 \cdot H_r} = I_4 \qquad 2\text{-}27$$

$$\frac{P_1 \cdot L_2 \cdot V + L_1 \cdot P_2 \cdot H}{L_2 \cdot V_r + P_2 \cdot H_r} = I_5 \qquad 2\text{-}28$$

$$\frac{L_1 \cdot P_2 \cdot V + P_1 \cdot L_2 \cdot H}{P_2 \cdot V_r + L_2 \cdot H_r} = I_6 \qquad 2\text{-}29$$

$$\frac{V + H}{V_r + H_r} = I_7 \qquad 2\text{-}30$$

A double beam scan, sample beam and reference beam, is used here and it gives the smallest error in the measurements. In our experimental set up both sample beam and reference beam pass through the internal polarizer but only the sample beam passes through the external polarizer in front of the prism (details of set-up in the next chapter). The denominators are representative of the reference beam in the reference channel and the numerators are representative of the sample beam in the sample channel. The subscripts 1 and 2 indicate the polarizer positioned before and

after the cell respectively.

Unfortunately, of the seven equations above only five of them are independent. Therefore we cannot solve for the eight unknowns. Experimentally, it was found that the two polarizers are essentially identical. We can then assume that P_1 equals P_2 and L_1 equals L_2. The beam in the reference channel can be treated as one unknown. Based on these assumptions, we have

$$P \cdot L \frac{V+H}{P \cdot V_r + L \cdot H_r} = I_1 \qquad 2\text{-}31$$

$$\frac{P \cdot V + L \cdot H}{P \cdot V_r + L \cdot H_r} = I_2 \qquad 2\text{-}32$$

$$\frac{P \cdot V + L \cdot H}{V_r + H_r} = I_3 \qquad 2\text{-}33$$

$$\frac{L \cdot V + P \cdot H}{V_r + H_r} = I_4 \qquad 2\text{-}34$$

$$\frac{V+H}{V_r + H_r} = I_5 \qquad 2\text{-}35$$

These equations are obtained by dividing the sample beam intensity by the reference beam intensity. Equation 2-31 represents both polarizers in the beam with the transmission axes perpendicular to each other. Equation 2-32 indicates only the internal polarizer in the beam. Equation 2-33 and 2-34 are for one

polarizer in front of the prism, but one allows the vertical state to pass the cell while the other allows the horizontal state to pass. Notice there is no polarizer in the reference channel at this time. Equation 2-35 assumes no polarizer in the beam.

Because we will continue to use a double beam scan through the entire experiment, we make some substitution to create new variables related to the primary unknowns in order to reduce the number of the variables.

The new unknowns are X and Y. They are,

$$X = \frac{V}{H_r + V_r} \qquad 2\text{-}36$$

$$Y = \frac{H}{H_r + V_r} \qquad 2\text{-}37$$

Performing algebraic operations on Equations 2-31, 2-32, 2-33 and 2-34, we obtain,

$$\gamma = P \cdot L = \frac{I_1 \cdot I_3}{I_2 \cdot I_4} \qquad 1\text{-}38$$

With X, Y and γ, we then solve these equations and wethen have,

$$P = 1/2\left\{ \frac{I_3+I_4}{I_5} + \left[\left(\frac{I_2+I_4}{I_5}\right) - 4\cdot\gamma\right] \right\} , \qquad 2\text{-}39$$

$$L = \gamma / P , \qquad 2\text{-}40$$

$$X = \frac{\gamma\cdot I_5 - P\cdot I_4}{\gamma - P\cdot P} , \qquad 2\text{-}41$$

$$Y = I_5 - \gamma . \qquad 2\text{-}42$$

The above equations were solved by computer. The resulting values for P, L, X and Y are presented in Fig.4. Here the top curve is pass (P). Leak (L) is the bottom one. X has a minimum value of 0.7% and Y has a maximum value of 0.56%.

From the figure it can be seen that the polarizers are quite good, but the beam of the Pekin-Elmer spectrophotometer is distorted through the scan region. The detailed calculation of the error of using these results is given in the error analysis chapter.

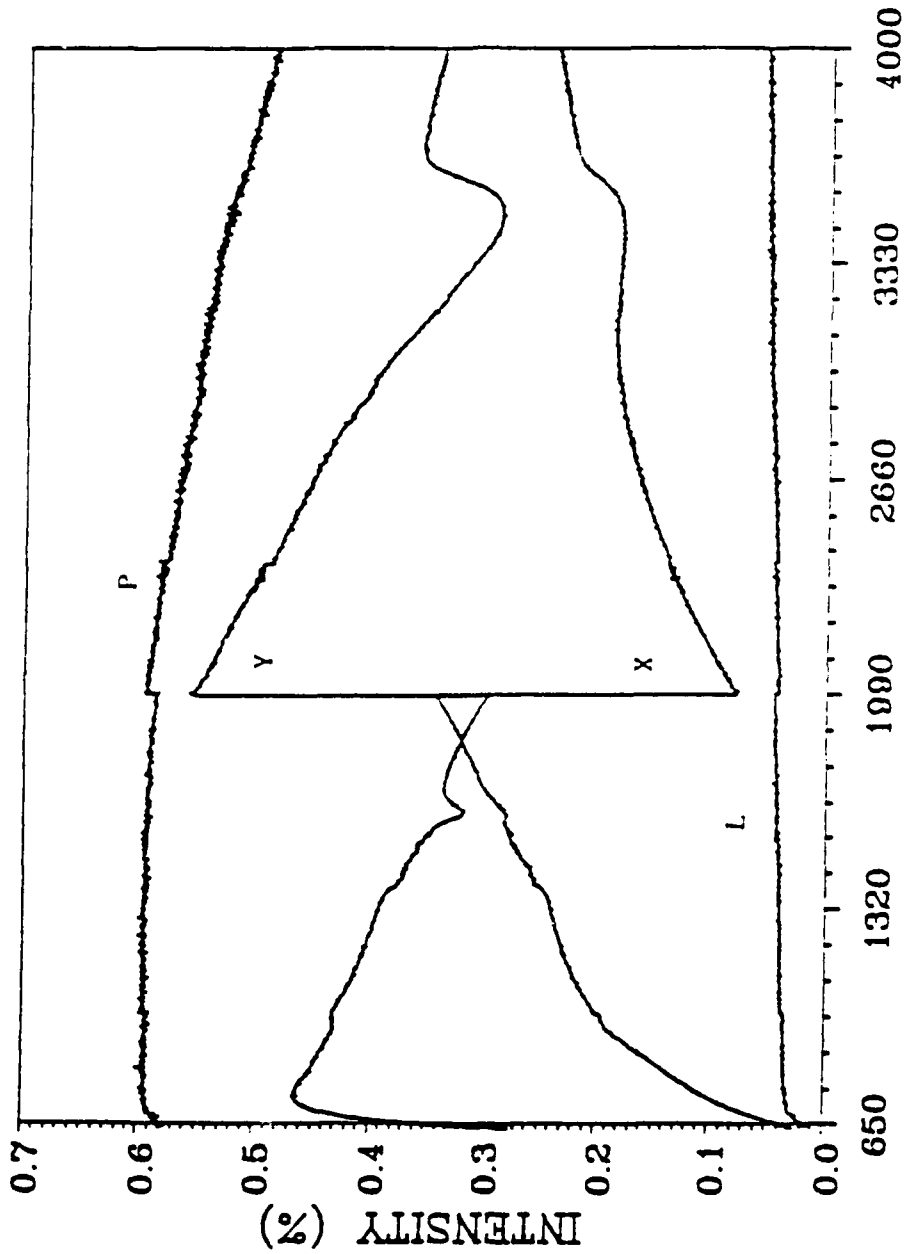

Fig. 4--The pass and leak of the polarizers and the distortion of the polarized vertical and horizontal beam.

CHAPTER III

EXPERIMENT SET UP AND MEASUREMENT

The internal reflectance accessory was installed in the sample compartment of the Perkin-Elmer Infrared Spectrophotometer (model 580B) as in Fig 5. Radiation from the light source enters the compartment and passes the first polarizer in front of the cell. After reflection by the mirror prism M, the light is incident on the sample prism S. The beam then reaches the empty cell (cell 1) and then is reflected back to the other surface (F_2) of the mirror prism from the sample-ZnSe cell (cell 2) interface. The reflected wave finally passes through the second polarizer and reaches the detector.

The internal reflectance accessory (dashed line in Fig 5) is presented in detail in Fig 6.

The sample prism unit and the mirror prism must be cleaned both before and after each measurement. First the sample prism unit of the internal reflectance accessory was removed from the internal reflectance accessory and disassembled. The unit is first placed in acetone and then placed in the tank of an ultrasonic cleaner . After ten to fifteen minutes of ultrasonic cleaning the unit is dried in air, the cell is reassembled and then reinstalled in the accessory. After use with the SF96 sample, the cell first was cleaned in normal detergent to wash off the oil before

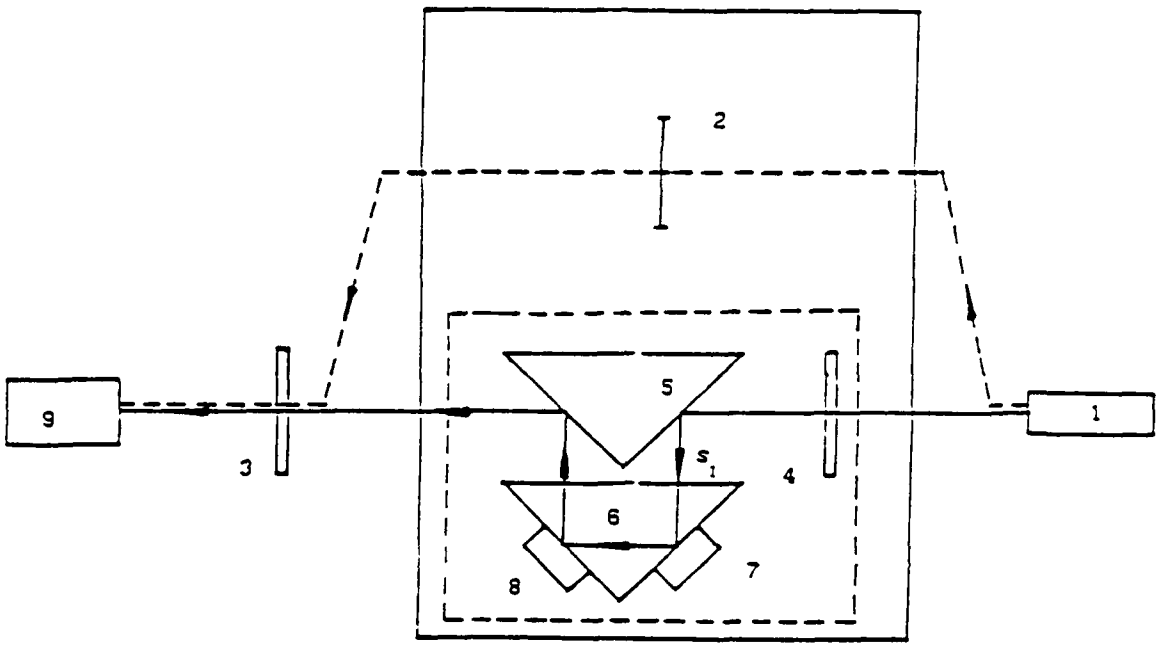

Fig.5--The internal reflectance accessory installation in the spectrophotometer and schematic of the sample and reference beam. 1.source 2.attenuator 3.external polarizer 4.internal polarizer 5.mirror prism 6.ZnSe prism 7.cell 1 8.cell 2 9.detector

Fig.6--Assembly diagram of the internal reflectance accessory.

1. Stainless steel plate -- sample chamber 1 (cell 1)
2. Stainless steel plate -- sample chamber 2 (cell 2)
3'-3". Teflon O-ring
4'-4". Teflon seal
5'-5". Stainless steel sealing plate with holes to inject sample fluid
6. ZnSe prism either 30-60-90 or 40-50-90
7. Teflon spacer
8. Stainless steel sealing plate with optical limiting apertures
9. Baseplate for mounting ZnSe prism subassembly on
10. Unislide for prism translation
11. Baseplate to mount unislide, ZnSe prism and mirrored prism subassemblies
12. 45^{0} right angle mirrored prism
13. Baseplate to mount mirrored prism
14'-14". Angle indicator to adjust angle of incidence
15'-15". Clamps for angle indicator
16. Plate for mounting polarizer assembly
17. Polarizer assembly
18. Polarizer wire grid
19. Baseplate for entire assembly

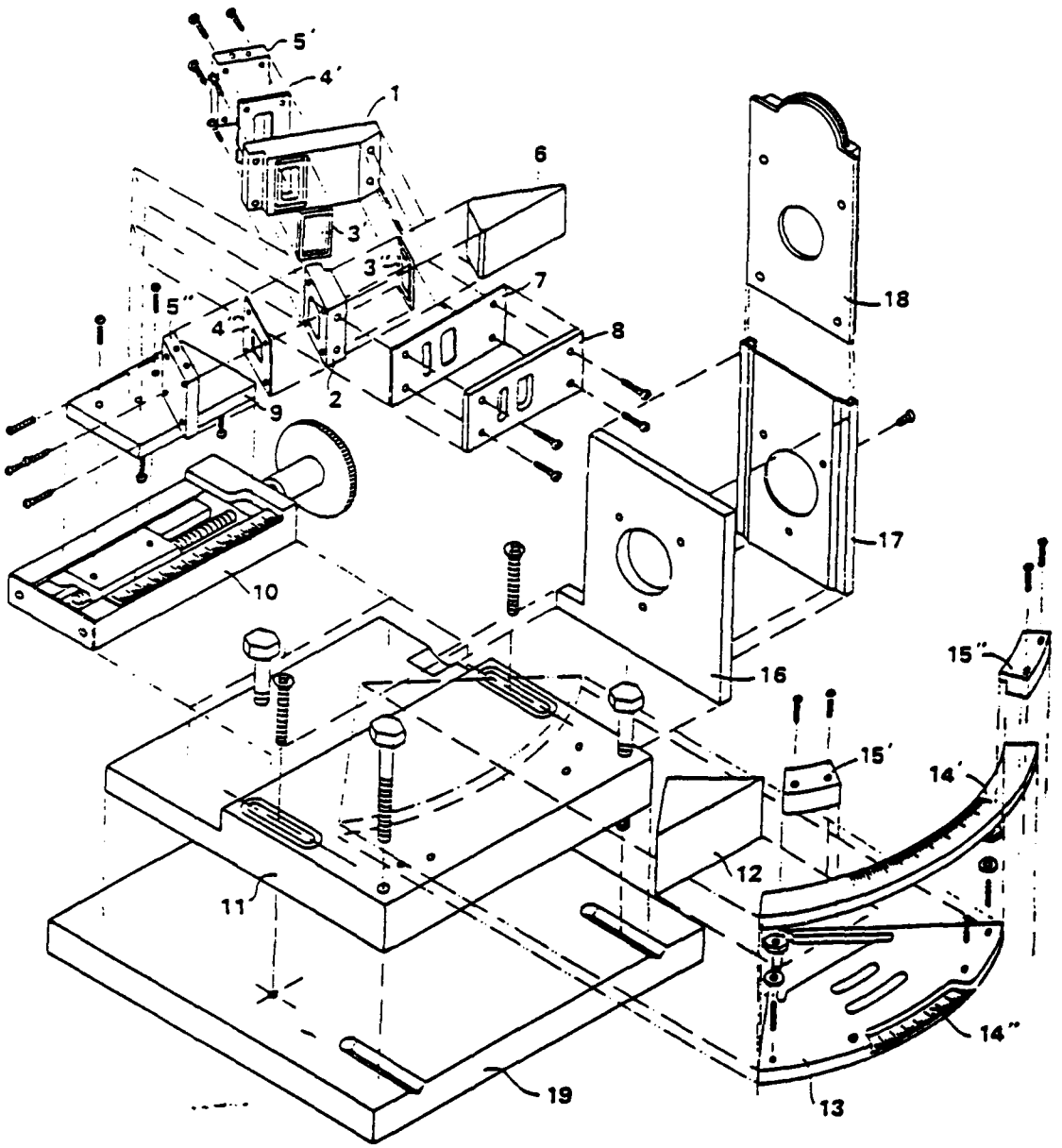
5'
4'
1
6
3'
3"
7
5"
4"
8
2
9
18
10
17
16
15"
15'
14'
12
11
14"
19
13

performing the above procedure.

The internal reflectance accessory must be aligned before use. The relative position between the sample and mirror prism must be set in alignment in order to obtain the desired angle of incidence at the ZnSe-sample cell interface.

Usually the beam which travels into sample prism must be perpendicular to the sample prism surface. For this condition the incident beam has an incident angle at the ZnSe-sample interface equal to the sample prism angle between the front surface S_1 and the empty cell (cell 2).

We use a prism spectrometer and a Helium-Neon laser to perform the alignment. The internal reflectance accessory is placed on the rotating table of the prism-spectrometer and the beam of the laser is adjusted to be incident on the back window of the cell of the ZnSe prism thus producing a reflected beam. By rotating the table of the prism-spectrometer the laser beam can be reflected back on itself [Fig 7]. This indicates that the incident beam is perpendicular to the surface of the prism. The angular reading from the prism-spectrometer is made and then the table is rotated again until the angular reading in the telescope is equal to the alignment angle. At this time, the mirror prism holder is adjusted until the laser beam is reflected back upon itself (Fig 8).

The alignment angle φ is obtained from $\varphi = \pi - \alpha$. Here α is the sample prism angle between the front surface S_1 of the sample

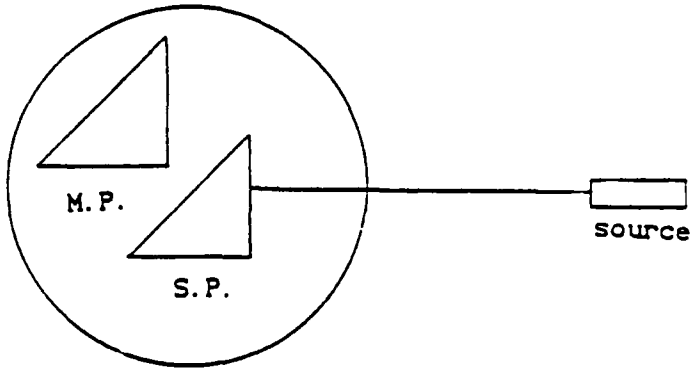

Fig.7--First position of the alignment of the prisms on the table of the prism spectrometer.

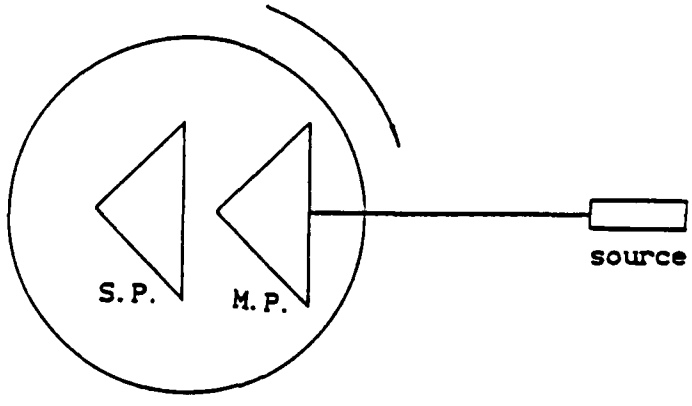

Fig.8--Second position of the alignment of the prisms on the table of the prism spectrometer.

prism and the surface on which the laser is incident when the alignment is performed. The angle φ (φ=90-α) is the incident angle on the ZnSe-sample interface. This angle will be identified as the normal' incident angle, because the light travels into the prism perpendicular the sample prism front surface S_1.

When the alignment angle is obtained, the light travels into the sample prism perpendicular to the surface S_1. Sometimes a small adjustment of the alignment angle is necessary to obtain a good incident angle on the ZnSe-sample interface or to achieve two different incident angle scans on one prism. This can be implemented by adjusting the vernier on the mirror prism holder. At this time the incident angle is not the normal incident angle. In our experiment, this angle is usually less than 10 degrees (restriction comes from the cell and the front panel). One thing has to be mentioned, this auxiliary angle can not be directly added to the incident angle because the refractive index n of ZnSe is about 2.4.

Internal reflection intensities, I_s and I_p, for radiant flux linearly polarized perpendicular and parallel, respectively to the plane of incidence, are obtained at the selected angle of incidence. The ratios of I_s and I_p to the incident beam I_0 give the reflection coefficients R_s and R_p .

After the internal reflectance accessory was installed in the sample compartment of the 580B spectrophotometer, the three screws on baseplate 11 of the internal reflectance accessory are

adjusted in order to level the baseplate. The baseplate 11 is then translated horizontally on baseplate 19 so that the light is incident on the window of the ZnSe prism. Since our measurements are performed via the double beam scan and the scan result is given by the ratio of the sample beam intensity to the reference beam intensity. an adjustable attenuator (Fig.5) is installed in the reference beam to achieve the ideal detector response. In our experiments, we adjusted the attenuator to obtain a ratio of sample to reference beam of 60% of full scale. We find in our experiments that if a higher percentage (reducing the intensity of the reference beam) than 60% is used, the ratio of the noise to signal is increased and a lower percentage reduces the sensitivity of the measurements.

After finishing these adjustments on the internal reflectance accessory in the compartment, two screws on baseplate 19 are tightened to lock baseplate 11 and then the compartment is closed.

The compartment was purged with air from a dryer for thirty minutes after each opening of the door of the compartment of the 580B. This is to minimize water vapor and CO_2 in the atmosphere of the spectrometer.

To obtain R_s and R_p five scans were performed. Both the polarizers were oriented to pass the s polarization component while performing the scan on the empty cell and the cell with the liquid. These two scans are then repeated with both polarizers

oriented to pass the p polarization component. finally, a zero intensity scan is performed to obtain detector zero response.

In the actual experiment both polarizers were set to pass the s polarization component first. The settings of the 580B were maximum resolution 2.3, relative noise 0.15 and scan time 32 minutes. A spectrum scan with both sample cells 1 and 2 empty was obtained in a scan time of about 30 minutes. Then the door of the compartment was opened and the polarizers were rotated 90 degrees to pass the p polarization component. After the compartment door was closed, the compartment was purged again for about 30 minutes. Then the above process was repeated with the same equipment settings to obtain the p component empty cell spectrum. The door to the compartment was then opened, sample cell 2 (Fig 5) of the internal reflectance accessory was filled with the liquid and the compartment door was closed. After about a 30 minute wait for purging the p spectrum for the liquid was obtained by use of the same 580B settings as in the empty cell scan. Finally, the polarizers were rotated back to pass the s component to obtain the s spectrum for the liquid.

To perform the measurements for the angle method the same procedure was applied as in the measurements of thes state above. The s state measurements were performed on a 30-60-90 prism and a 40-50-90 prism, respectively. The reflectances with incident angles 30 and 40 degrees were obtained.

The zero intensity I_0 scan was performed with the sample

beam totally blocked. Subtracting I_0 from the results of four scans above, we can compensate for the effect of the background output.

The empty cell scan constitutes the case of total internal reflection so the ratio of the spectrum for the liquid to the empty cell spectrum provides the ratio of internal reflection coefficient R_s (or R_p) to internal total reflection coefficients R_e R_s/R_e or R_p/R_e (reference last section). By knowing the refractive indices of the ZnSe n and k [6], the empty cell reflection coefficient R_e can be obtained by calculating Fresnel's equations.

The experimental results for R_s/R_e and R_p/R_e are presented in Fig. 9 through 11. Figure 9 shows the results (R_s/R_e--solid line and R_p/R_e--dotted line) of the polarization method with a water sample and 40 degree incident angle. In Figures 10 and 11, the angle method was employed with water and SF96 as the samples, respectively. The incident angles for water are 30 (dotted line) and 40 (solid line) degrees, and for SF96 are 30 (dotted line)and 38 (solid line) degrees. Notice the incident angle, 38 degrees, here is not a normal incident angle. It is the normal incident angle 30 degrees plus the auxiliary angle 8 degrees, so that the actual incident angle has to be calculated by Snell's law using the complex refractive index of the ZnSe prism.

The final results for the complex refractive index of water and SF96 are obtained by applying the angle method. The

polarization method will be dealt in the next chapter. The results are presented in Figures 12 through 15. Fig.12 is the refractive index of water, Fig.13 is the absorption index of water, Fig.14 is the refractive index of SF96 and Fig.15 is the absorption index of SF96.

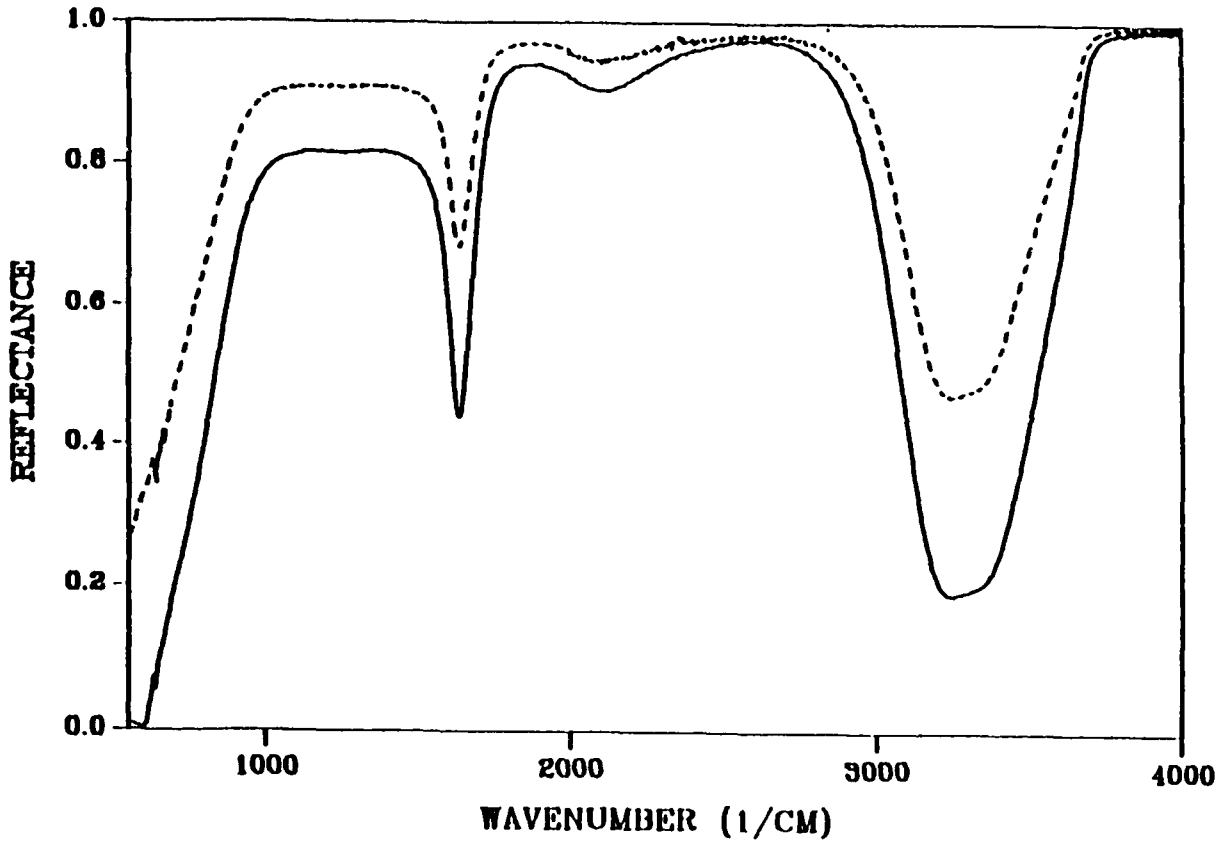

Fig. 9--Vertical (dotted line) and horizontal (solid line) reflectance with water sample.

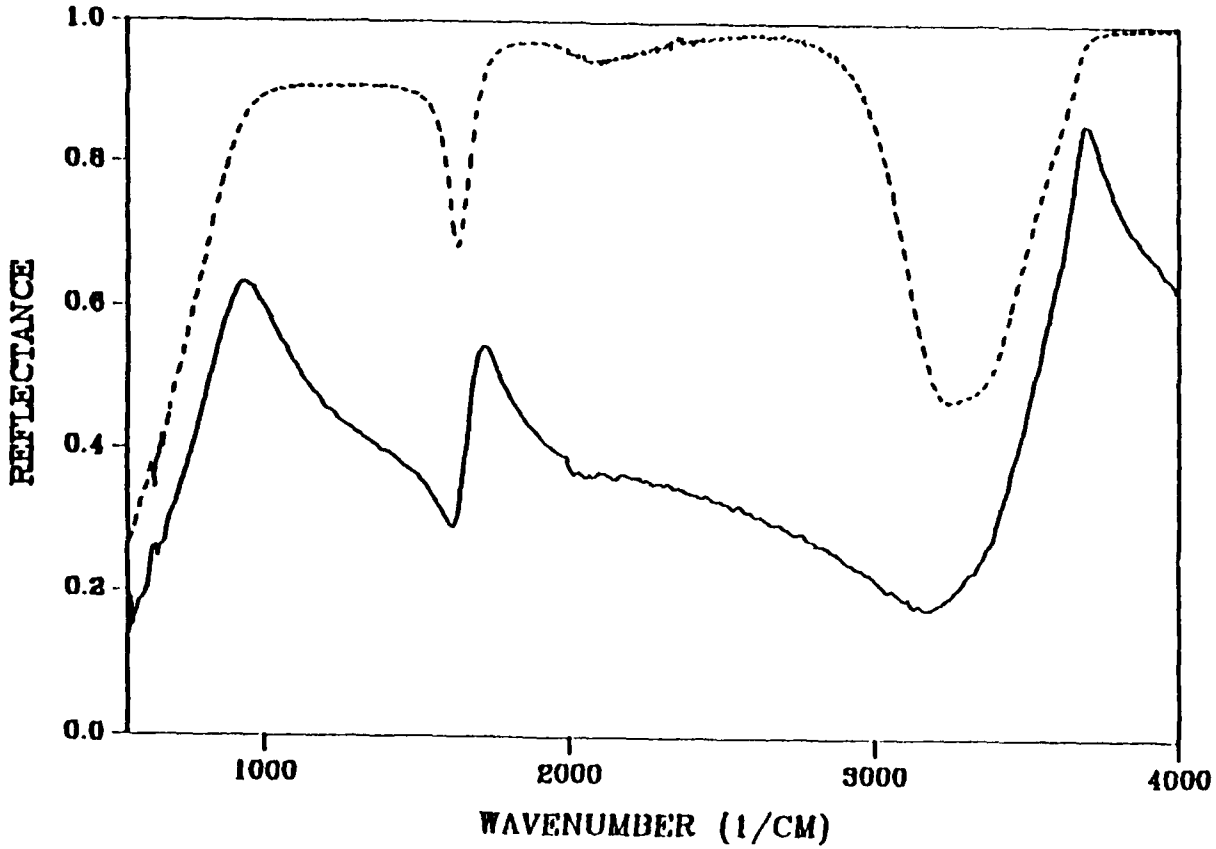

Fig. 10--Vertical reflectance with water sample at incident angle 30 degrees (solid line) and 40 degrees (dotted line).

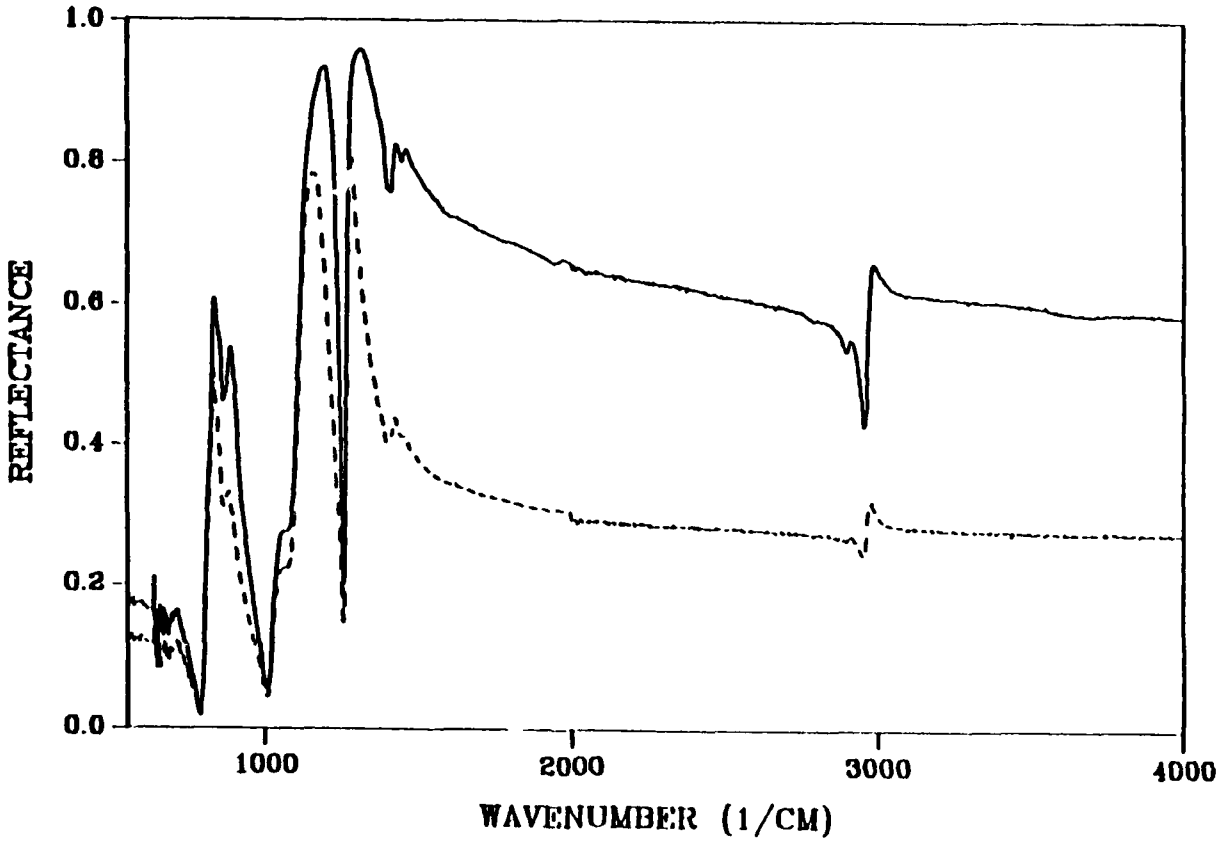

Fig.11--Vertical reflectance with sample SF96 at incident angle 30 degrees (dotted line) and 40 degrees (solid line).

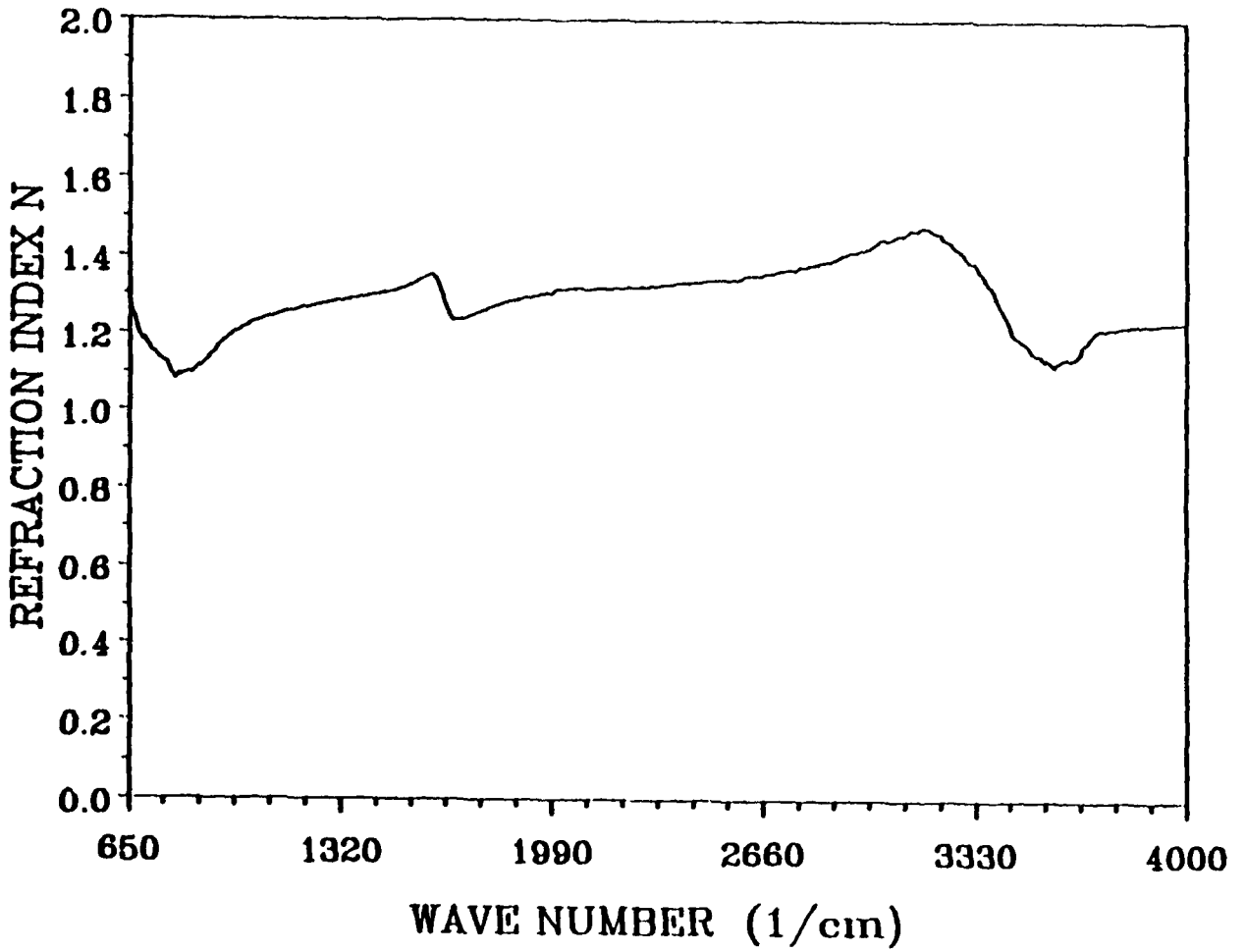

Fig. 12--The refractive index of water.

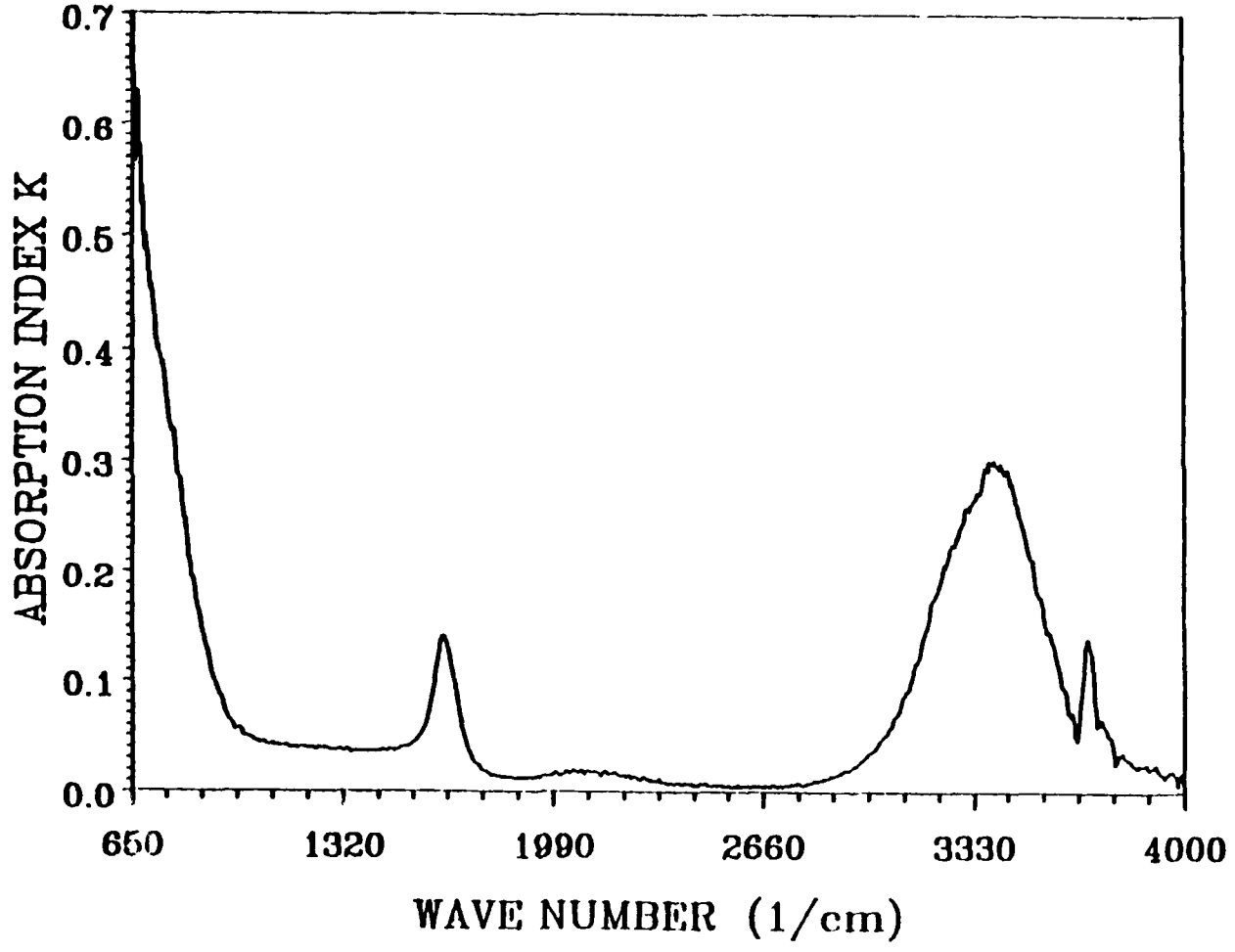

Fig. 13--The absorption index of water.

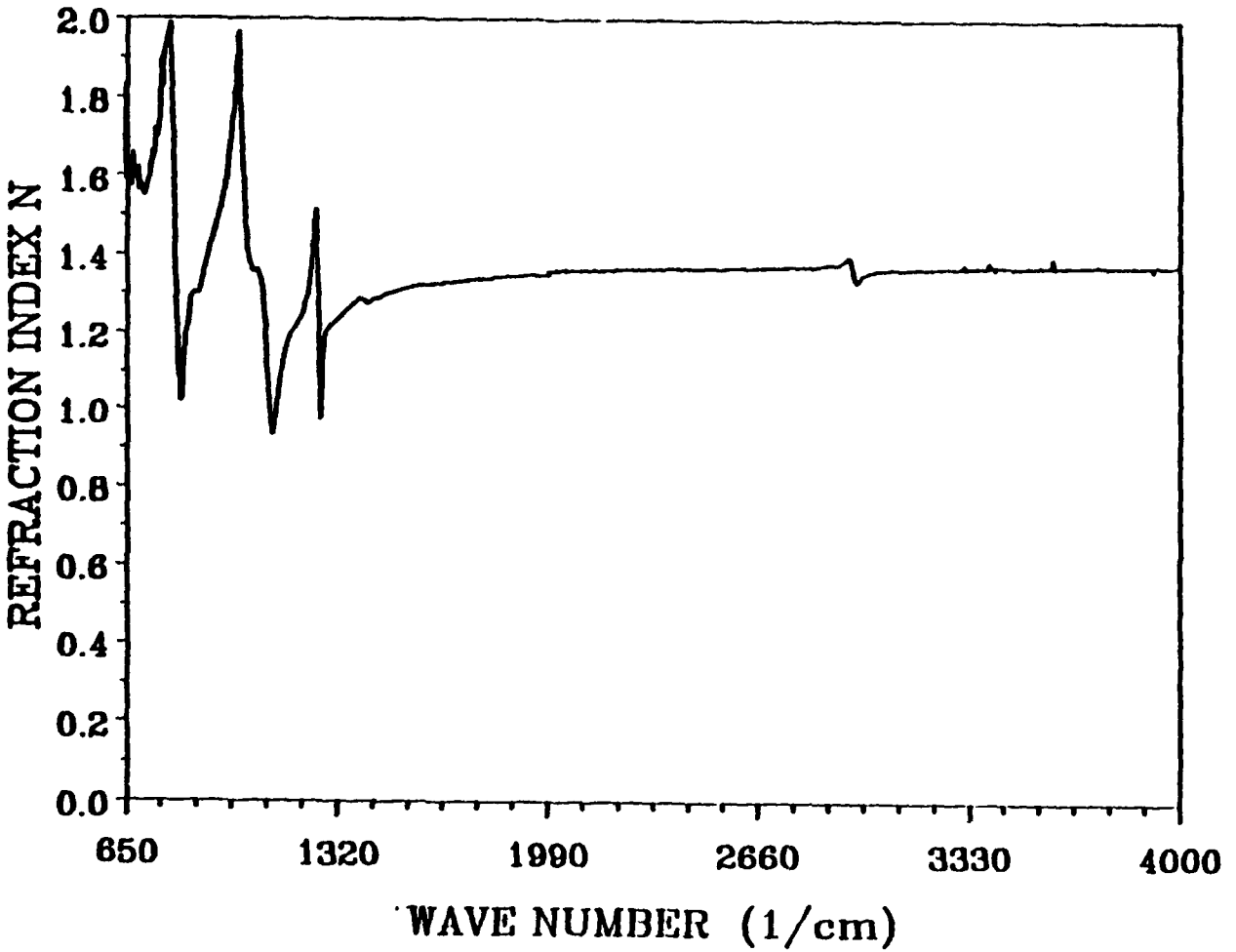

Fig. 14--The refractive index of SF96.

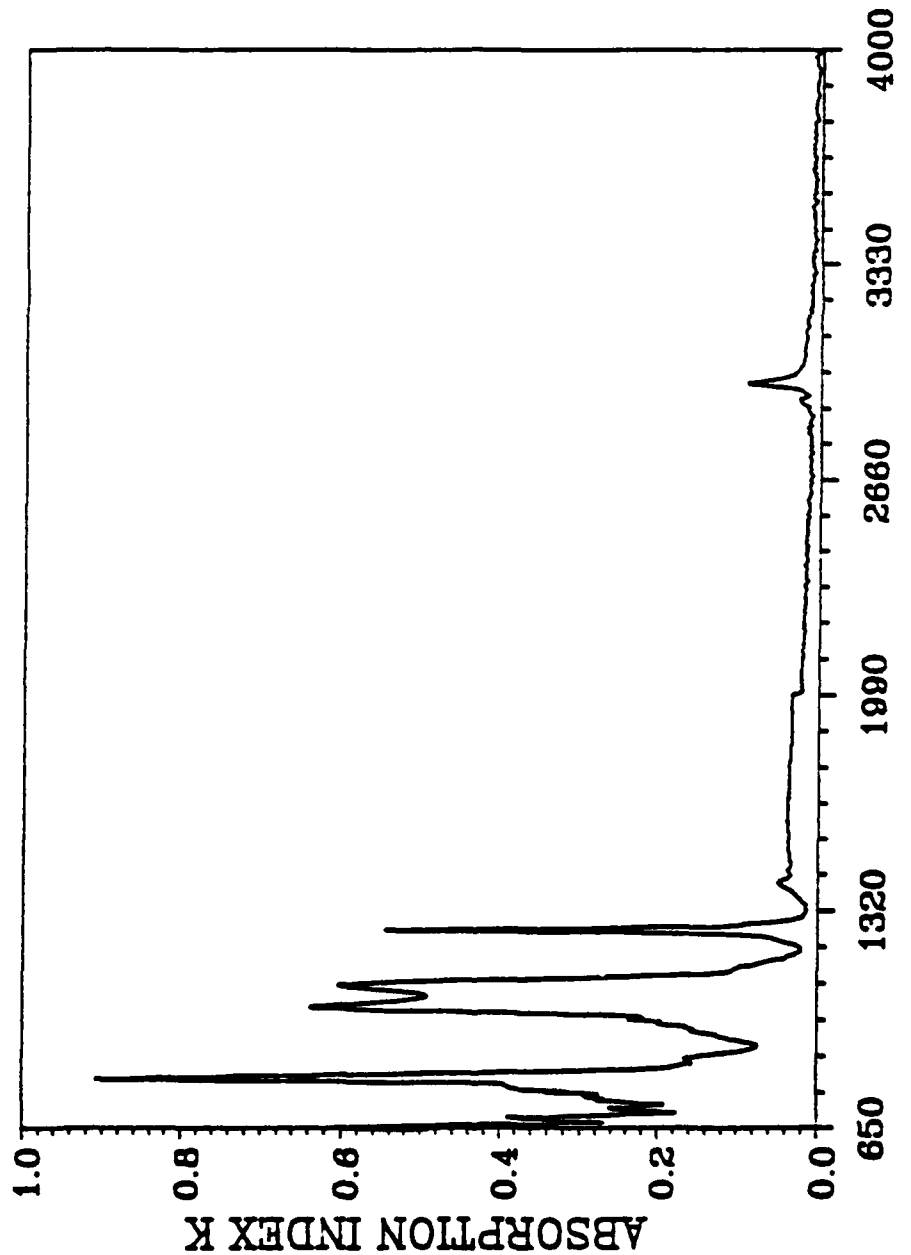

Fig. 15--The absorption index of SF96.

CHAPTER IV

ERROR ANALYSIS

This section deals with the error analysis associated with both the measurements and the calculations.

From previous chapters we know that the vertical and horizontal components of the incident beam vary with wave number and that the polarizers are not perfect. For instance, when the polarizer is oriented to pass the s polarization component, a small portion of the p component also passes the polarizer. After considering the two effects above and ignoring some unimportant effects (i.e. the s and p components of the internal total reflection in the ZnSe are not equal, etc,(discussed later)), we obtained the ratio of the measured intensity with the liquid in the cell to that with the empty cell, as follows:

$$\frac{I_s}{I_{se}} = \frac{P^2 \cdot V \cdot R_s + L^2 \cdot H \cdot R_p}{P^2 \cdot V \cdot R_{se} + L \cdot H \cdot R_{pe}} \qquad 4\text{-}1$$

here I_s is the intensity measured with the liquid in the cell for s polarization state, and I_{se} is the intensity measured with the cell empty. R_s and R_p are respectively s and p polarization state reflection coefficients with the liquid in the cell. R_{se} and R_{pe} are respectively s and p state reflection coefficients with the empty cell. Parameters P, L, V, and H are the same as before.

The figure below shows the relationship of the beams in the measurements.

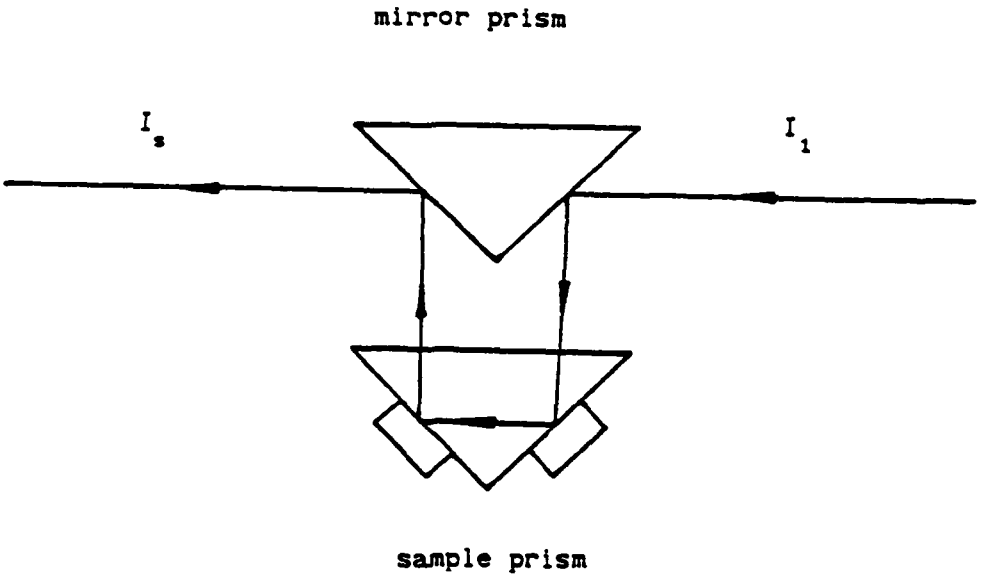

Fig.16--The diagram of beam routine in the internal reflection accessory.

From Fig. 16, we have:

$$I_s = I_1 \cdot R_2 \cdot T_3 \cdot R_4 \cdot R_s \cdot T_6 \cdot R_7 \quad , \qquad 4\text{-}2$$

but only R_s is the reflection coefficient reflected from the ZnSe-sample interface. We would like to cancel R_2 , T_3 , R_4 , T_6 and

R_6 to accomplish this another measurement with the empty cell is

taken yielding,

$$I_{se}=I_1 \cdot R_2 \cdot T_3 \cdot R_4 \cdot \mathbb{R}_{se} \cdot T_6 \cdot R_7 \quad , \qquad 4\text{-}3$$

Then we have,

$$\frac{I_s}{I_{se}} = \frac{\mathbb{R}_s}{\mathbb{R}_{se}} \quad , \qquad 4\text{-}4$$

so that

$$\mathbb{R}_s = \frac{I_s}{I_{se}} \mathbb{R}_{se} \quad . \qquad 4\text{-}5$$

But the problem is not so simple. I_s is obtained under the assumption that the polarizers are ideal. If the polarizer is not ideal then a portion of the orthogonal polarization state will be transmitted. Then I_s becomes

$$I_s=I_{1s} \cdot R_{2s} \cdot T_{3s} \cdot R_{4s} \cdot \mathbb{R}_s \cdot T_{6s} \cdot R_{7s} \cdot P^2 \cdot V + I_{1p} \cdot R_{2p} \cdot T_{3p} \cdot R_{4p} \cdot \mathbb{R}_p \cdot T_{6p} \cdot R_{7p} \cdot L^2 \cdot H \qquad 4\text{-}6$$

and I_{se} is given by

$$I_{se}=I_{1s} \cdot R_{2s} \cdot T_{3s} \cdot R_{4s} \cdot \mathbb{R}_{se} \cdot T_{6s} \cdot R_{7s} \cdot P^2 \cdot V + I_{1p} \cdot R_{2p} \cdot T_{3p} \cdot R_{4p} \cdot \mathbb{R}_{pe} \cdot T_{6p} \cdot R_{7p} \cdot L^2 \cdot H. \qquad 4\text{-}7$$

In these two equations we assume the polarizers are oriented to pass the s polarization component and the second term is due to the orthogonal polarization state, the p component. In this case, R_{1s} and T_{1s} can not be simply cancelled, Equation 4-4 then appears as,

$$\frac{I_o}{I_{oe}} = \frac{R_s \cdot P^2 \cdot V \cdot \prod_{i=n} R_{is} \cdot T_{is} + R_p \cdot L^2 \cdot H \cdot \prod_{i=n} R_{ip} \cdot T_{ip}}{R_{se} \cdot P^2 \cdot V \cdot \prod_{i=n} R_{is} \cdot T_{is} + R_p \cdot L^2 \cdot H \cdot \prod_{i=n} R_{ip} \cdot T_{ip}} \quad . \quad 4\text{-}8$$

Now, there are two choices. The first is to perform a step by step calculation to solve the above equation while the other is to use an approximation to simplify Equation 4-8. The first choice seems more accurate at first glance, but this may not be true. First we can compute R_i ,and T_i only from the data which was obtained from prior experiments of measuring the complex refractive index of the prism. The error associated with this data can not be avoided. Second, the calculation necessary to compute R_i and T_i creates more errors, which we will see later.

In order to see if we can simplify this equation, we first must estimate the errors introduced by the approximations.

The purpose of the approximation is an attempt to remove the second term of the denominator and numerator in Equation 4-8. Then Equation 4-8 will become,

$$\frac{I_o}{I_{oe}} = \frac{R_{2s} \cdot T_{3s} \cdot R_{4s} \cdot R_s \cdot T_{6s} \cdot R_{7s} \cdot P^2 \cdot V}{R_{2s} \cdot T_{3s} \cdot R_{4s} \cdot R_{se} \cdot T_{6s} \cdot R_{7s} \cdot P^2 \cdot V} = \frac{R_s}{R_{se}} \quad . \quad 4\text{-}9$$

Equation 4-9 is the same result as that of Equation 4-4. We next calculate the errors created by using Equation 4-9 instead of Equation 4-8. The following calculations assume that the ZnSe absorption coefficient is zero, $K \approx 0$, $R_{is} \approx R_{ip}$; $T_{is} \approx T_{ip}$. These assumptions are reasonable in most of the experimental spectral

ranges and, if later calculation proves the second term is much less than the first, the assumption of $R_{is} = R_{ip}$ and $T_{is} = T_{ip}$ becomes more reasonable. We can then estimate the error of using equation 4-9 instead of equation 4-8.

After cancelling R_{is}, R_{ip}, T_{is} and T_{ip}, we have,

$$\frac{I_o}{I} = \frac{P^2 \cdot V \cdot R_s + L^2 \cdot H \cdot R_p}{P^2 \cdot V \cdot R_{se} + L^2 \cdot H \cdot R_{pe}} = \frac{R_s + \gamma \cdot R_p}{R_{se} + \gamma \cdot R_{pe}} \quad , \qquad 4\text{-}10$$

where,

$$\gamma = \frac{L^2 \cdot H}{P^2 \cdot V} \quad . \qquad 4\text{-}11$$

Then the error from using Equation 4-9 instead of Equation 4-4 is

$$\mathcal{E} = \left| \frac{\dfrac{R_s + \gamma \cdot R_p}{R_{se} + \gamma \cdot R_{pe}} - \dfrac{R_s}{R_{se}}}{\dfrac{R_s + \gamma \cdot R_p}{R_{se} + \gamma \cdot R_{pe}}} \right| \qquad 4\text{-}12$$

$$= \frac{\gamma \cdot (R_p \cdot R_{se} - R_s \cdot R_{pe})}{R_{se} \cdot (R_s + \gamma \cdot R_p)} \quad . \qquad 4\text{-}13$$

Taking a close look at γ, it is found that γ is different for different polarization states. For the p component passed by the polarizers (R_p / R_{pe}), we have,

$$\gamma = \frac{L^2 \cdot V}{P^2 \cdot H} \quad . \qquad 4\text{-}14$$

From now on, we use γ_s and γ_p to identify the two cases. Since V and H vary with wavenumber so that $\gamma_s \neq \gamma_p$ and because γ_s and γ_p are not constants over the whole range of the experimental spectrum, the errors $\mathcal{E}_s$ and $\mathcal{E}_p$ are functions of wavenumber. Exact values of $\mathcal{E}_s$ and $\mathcal{E}_p$, for the water sample, are shown in Fig 17 and Fig 18.

From the Fig 17 and Fig 18 we can see that the vertical polarization state V and horizontal polarization state H are distorted, but the errors are kept small in the entire range. This is because the leakage of the polarizers is less than ten percent. Employing two polarizers in the experiment reduces the leakage to less than one percent.

The errors introduced by the Perkin-Elmer Infared Spectrophotometer (580B) itself can be found from its specifications. Some of the specifications related to our analysis are given in Table 1.

From the table we can see that the abscissa accuracy is quite high. This small error has only a subtle influence on the complex refractive index value shifting with wave number because the wave number never appears in the calculation equations. The ordinate accuracy and the stray light together form a 0.5% error of full scale in most spectral ranges we are interested.

Combining the errors of the polarized light, the polarizers

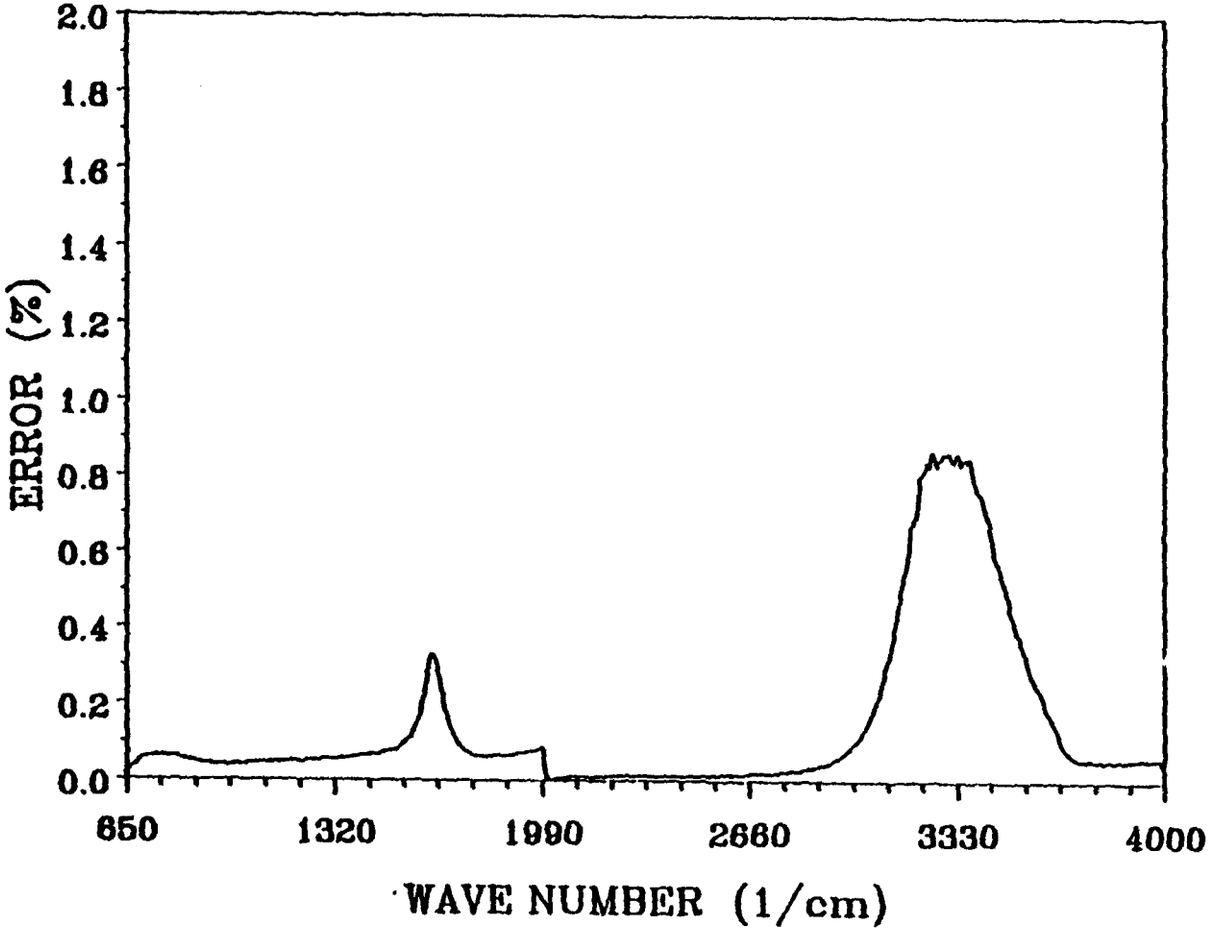

Fig. 17--The error associated with employing approximation on the vertical reflectance calculation.

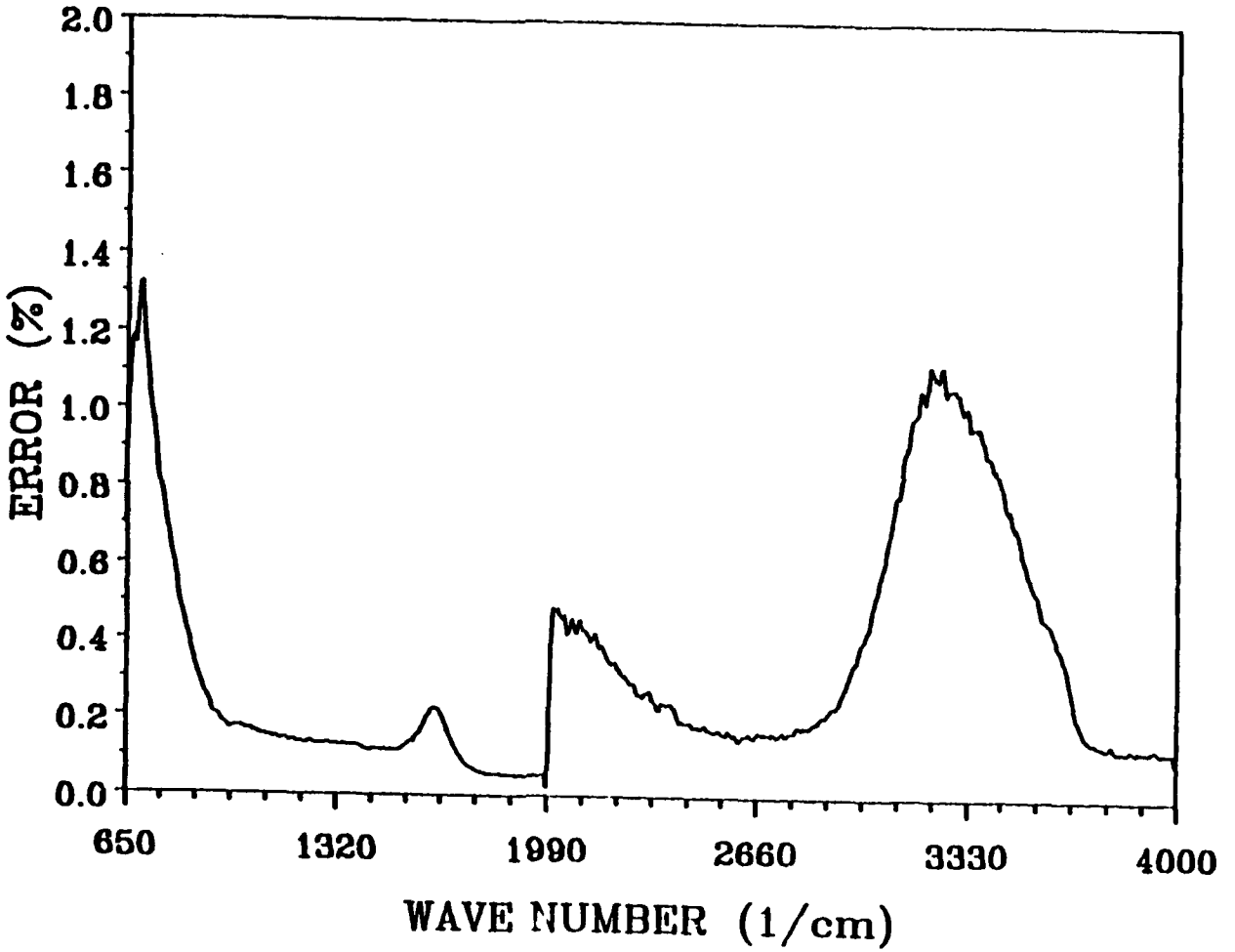

Fig. 18--The error associated with employing approximation on the horizontal reflectance calculation.

Table 1--The specifications of Perkin-Elmer Infared Spectrophotometer (580)

Table 2

abscissa accuracy:	±1.5 cm^{-1} decreasing linearly to ±1 cm^{-1}	4000 to 3500 cm^{-1}.
	±1 cm^{-1} over the range 3500 to 200 cm^{-1}.	
	±1 cm^{-1} decreasing linearly to ±0.5 cm^{-1} from	2000 to 1450 cm^{-1}.
	±0.5 cm^{-1} over the range 1450 to 180 cm^{-1}.	
ordinate accuracy:	±0.2%T	4000 to 700 cm^{-1}.
	±0.5%T	700 to 180 cm^{-1}.
stray light:	less than 0.1%	4000 to 2000 cm^{-1}.
	less than 0.2%	2000 to 1000 cm^{-1}.
	less than 0.3%	1000 to 750 cm^{-1}.
	less than 0.4%	750 to 400 cm^{-1}.

and the infared spectrophotometer, the error in most spectral ranges is less than 1% , and in isolated regions 2% .We will see later that a 2% error will introduce a large error in later calculations. Notice here that we did not consider the effect of the aging of the equipment which may enlarge the errors given in the table.

The experimental data has unavoidable errors associated with it. These errors will be " amplified " in the final data calculations. In the worst case, the errors from the experimental measurements can render the calculations invalid.

There are two techniques to obtain two equations for calculating the indices as we mentioned before. For ease of discussion, the technique with two different polarization components s and p as incident beams is called the polarization method and the one with two different incident angles is called the angle method. The polarization method is very straight forward to apply to the ATR technique because the incident angle cannot be easily changed. Although the angle method is difficult to perform, it does provide the means of achieving the maximum sensitivity. The question is which method gives the smallest error or has the more accurate result.

The method to estimate the error introduced by the calculation is to use two groups of reflection coeffecients. One group includes R_s and R_p which obtained in the non-error measurements and the other includes $R_s + \delta R_s$ and $R_p - \delta R_p$ which are

obtained by an assumption that a small error exists in the measurements. In the expressions, $R_s + \delta R_s$ and $R_p - \delta R_p$, one has the plus sign and the other is the minus in order to calculate the maximum errors. Computing the complex refractive index n and k using the program we developed in the previous chapters and the two groups of the reflection coefficients, we obtained two groups of complex refractive indices. Then comparing the results of the complex refractive index created by the two groups of reflection coeficients we finally have the error associated with the calculation.

We use n and k to indicate the results of the calculation when R_s and R_p are used, and n' and k' to indicate the results of the calculation when $R_s + \delta R_s$ and $R_p - \delta R_p$ are used. The error is then computed by the following equations,

$$\varepsilon_k = \left| \frac{k - k'}{k} \right| \quad \text{and} \quad \varepsilon_n = \left| \frac{n - n'}{n} \right| . \qquad 4\text{-}15$$

The results computed by employing the above methods are presented in Figures 19 through 23.

Fig 19 shows the results of the polarization method at an incident beam angle of 40 degrees. It can be seen that the error in k (dotted line) increases when k is smaller than 0.3. Notice that when k is less than 0.01, the program does not work since the reflection coefficients have one percent errors. The solid line shows the errors of the refractive index. Fig 20 shows the errors

employing the angle method at incident beam angles 30 and 40 degrees, respectively. The small window on the top shows that the errors increase as k (dotted line) becomes larger, but the error is much smaller than the polarization method in the small k range. The solid line shows the errors of the refractive index n. Fig. 21 shows the errors of the polarization method at an incident beam angle of 30 degrees. Both errors of the refractive index (solid line) and absorption index are smaller than that of using the polarization method. The top window gives detail in small k range.

In the same way as for errors associated with the refractive coefficient, we assume that there is a small incident angle error. Using the same method and two incident angles, ϕ_i and $\phi_i + \delta\phi_i$ determined the errors coming from the calculations. Since we use two different angles for the angle method, our assumptions of incident angles in computing the errors associated with the angle method calculation are ϕ_{1i}, ϕ_{2i}, $\phi_{1i} + \delta\phi_{1i}$, and $\phi_{2i} - \delta\phi_{2i}$.

Fig 22 and 23 show the errors associated with calculations due to the errors in the incident angles. The Fig 22 shows errors introduced by the polarization method when the incident beam angle has a variation one degree. The Fig 23 presents the calculation errors by employing the angle method with the incident angles at 30 and 40 degrees and both having a variation of one degree. In both of the figures the solid line presents errors of the refractive index and the dotted line denotes errors of the absorption index again.

Comparing Fig.19 and Fig.21, we find that varying the incident angle from 40 degrees to 30 degrees can reduce the errors of computed complex refractive index. It proves the discussion in Chapter I that proper selection of the incedent angle is very important to the ATR techniqe.

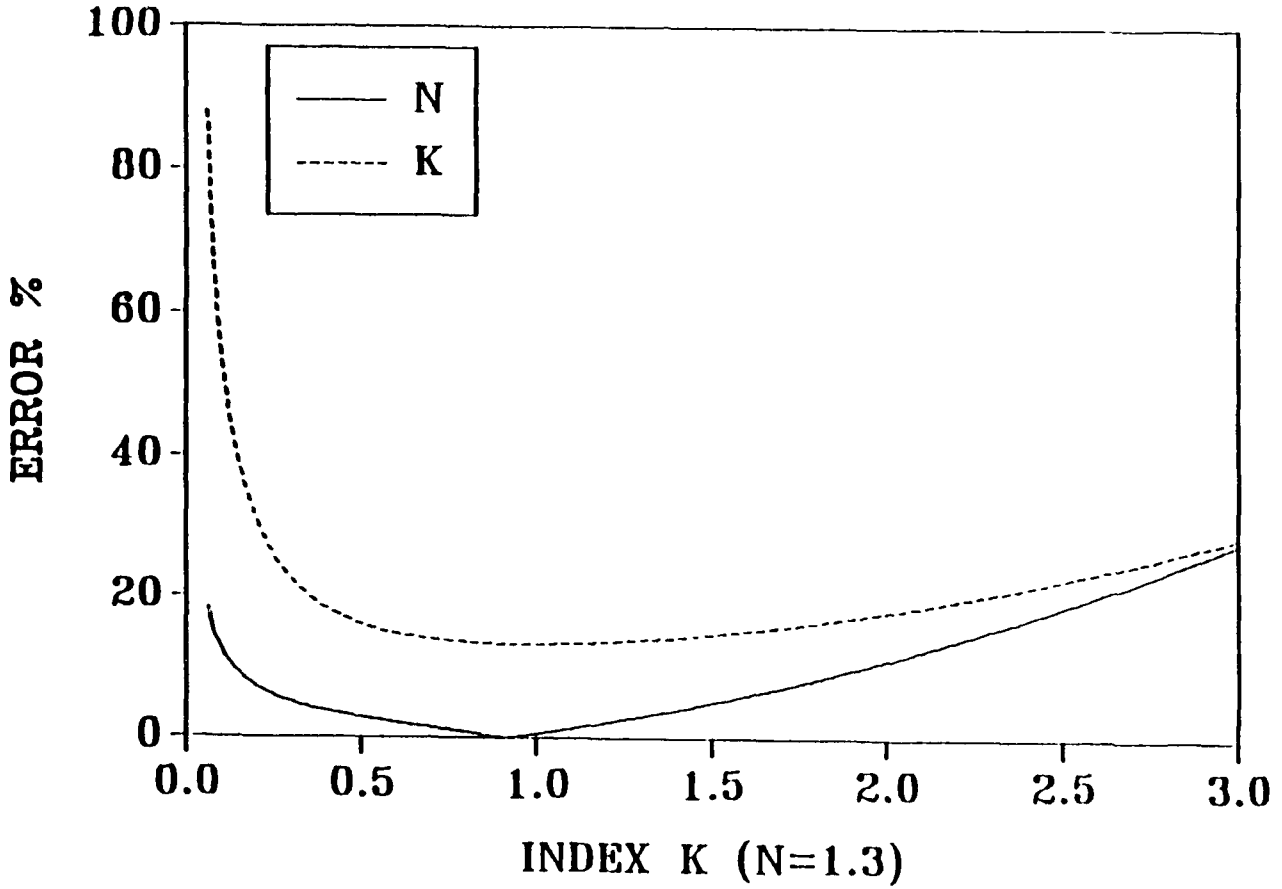

Fig. 19--The error of computed complex refractive index in use of polarization method associated with one percent error on the reflectance and different absorption index value. The incident angle is 40 degrees.

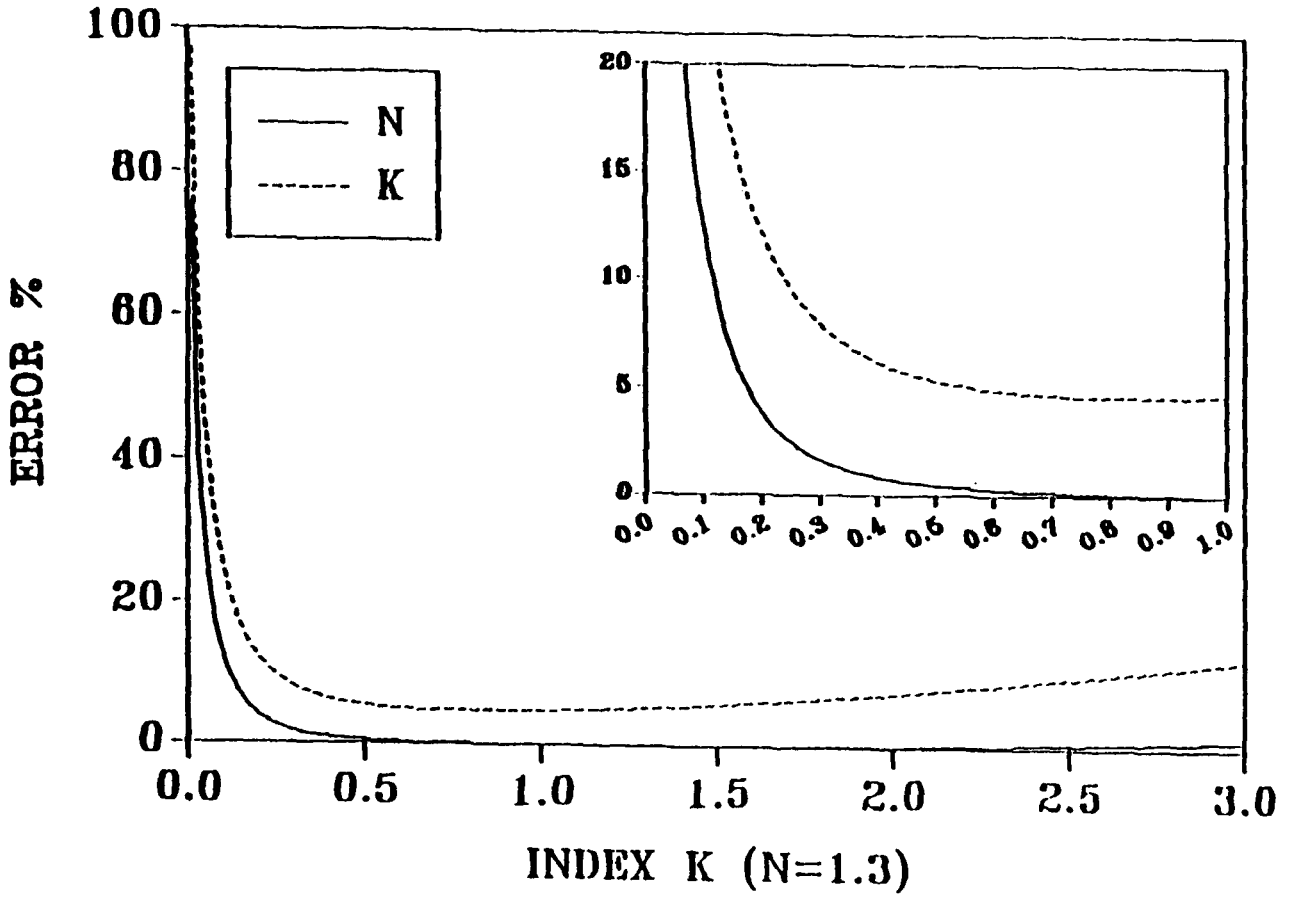

Fig.20--The error of computed complex refractive index in use of the angle method associated with one degree error on the incident angles and different absorption index value. The incident angles are 30 and 40 degrees.

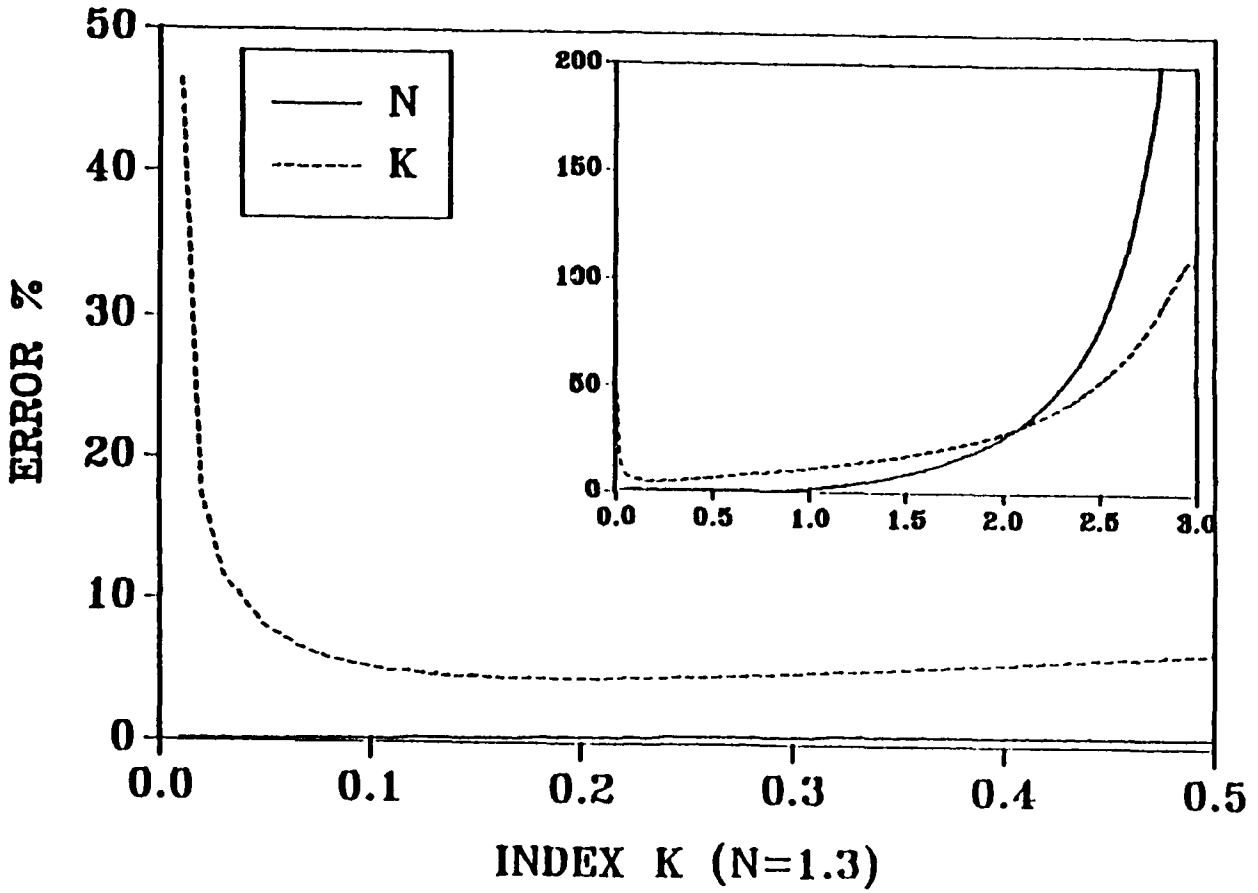

Fig.21--The error of computed complex refractive index in use of polarization method associated with one percent error on the reflectance and different absorption index value. The incident angle is 30 degrees.

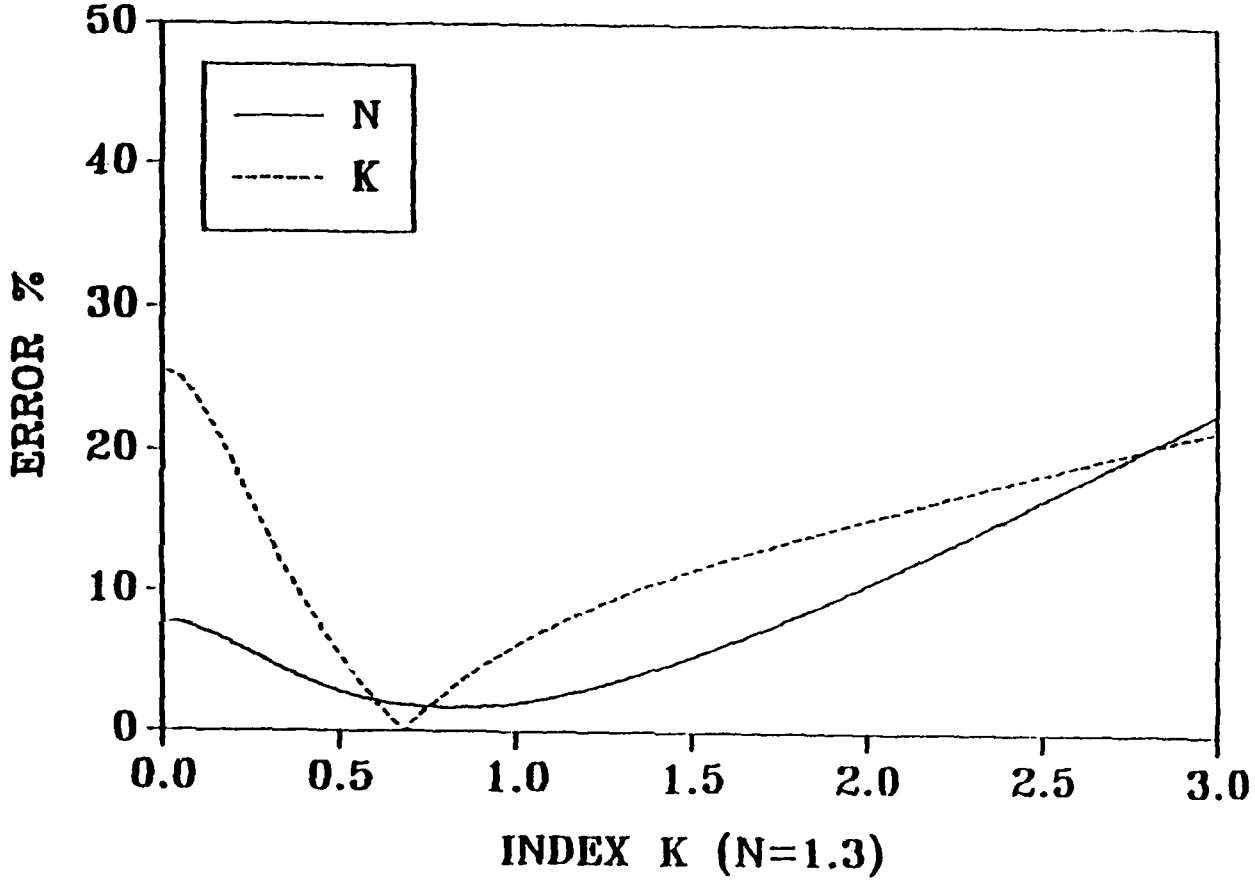

Fig. 22--The error of computed complex refractive index in use of polarization method associated with one degree error on the incident angle and different absorption index value. The incident angle is 40 degrees.

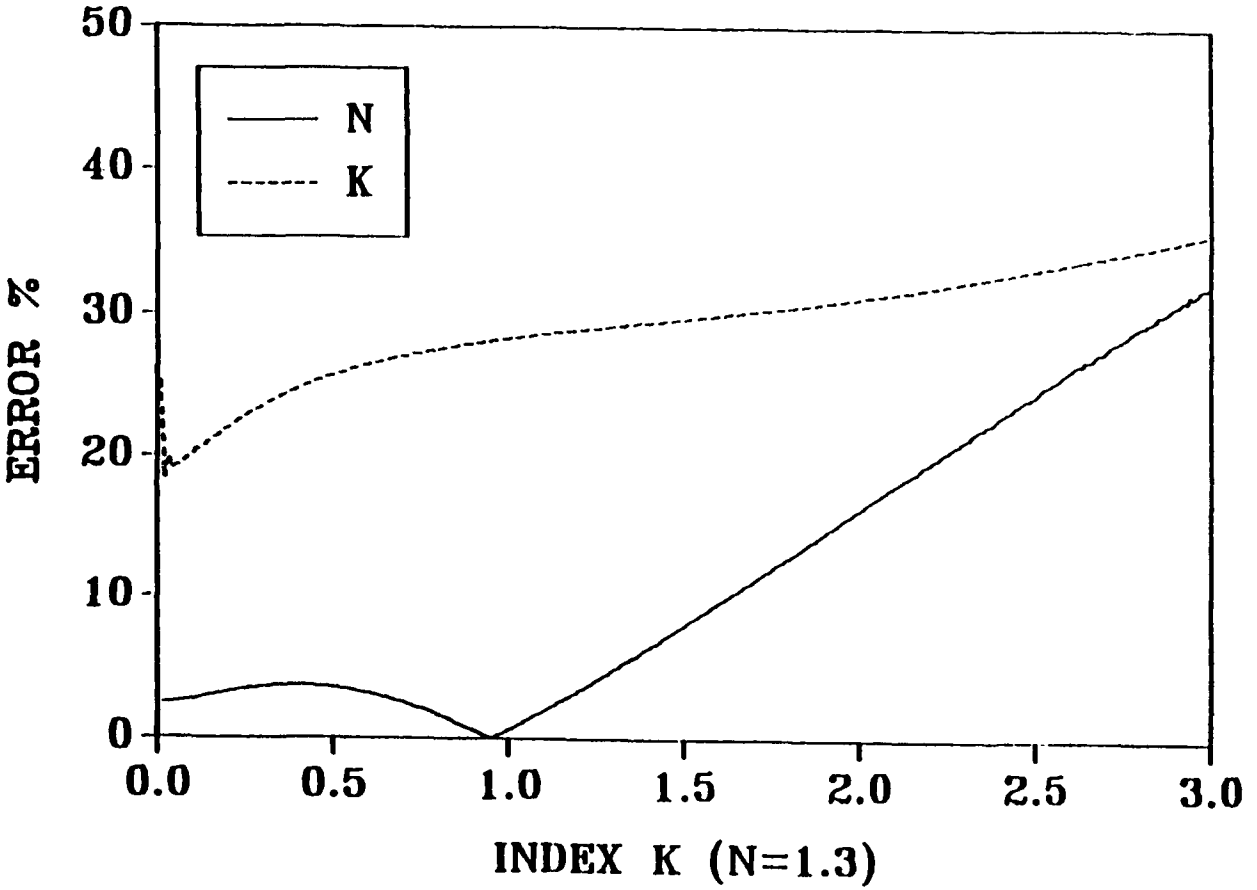

Fig.23--The error of computed complex refractive index in use of the angle method associated with one degree error on the incident angle and different absorption index value. The incident angle is 30 and 40 degrees.

CHAPTER V

CONCLUSION

Experimental results of the complex refractive index $n+jk$ for water and SF96 are presented in Figures 12 to 15 in Chapter II. The error associated with n is less than 2% . In the most of the region, the error associated with k is less than 10% (reference Chapter IV).

To obtain good measurements, properly setting up the internal reflection accessory and equipment is important. Two things are emphasized here. First in order to obtain the polarized light, the leakage of the polarizers and the response of the components of the instruments to the polarized light must be considered. The two polarizers were used in our experiments to reduce the measurement errors and then the mathematical approximations can be implemented (reference Chapter IV). Second the error in the incident angle increases the calculation errors. In our experiments, we did alignment of the internal reflection accesory, but there is no way to examine the alignment between the spectrophotometer (580) and the internal reflection accessory. Hopefully, it will be improved in later experiments.

Experimental results given in this paper were obtained by employing the angle method. The polarization method was

impractical because the absorption coefficient k of water and SF96 were too small (less than 0.02) in the part of the experimental region, 550-4000 cm^{-1}. Since the measurement errors can only be kept under 2%, the computational errors are more than 100%, which renders the calculation impractical (reference chapter IV).

Comparing the two methods, the angle method has a smaller error in the range with small absorption index , and the polarization method has the smaller error in the range with large absorption index. Usually the other two factors , incident angle and polarized light, have to be considered. The angle method requires two incident angles, and the polarization method requires two polarization states, so that the experimental conditions should be considered. This includes the errors associated with setting up, the features of the equipment, and even the speed of taking the data.

APPENDICES

APPENDIX A
PROGRAM OF THE POLARIZATION METHOD

```
C*************************************************************************
C     THIS PROGRAM IS TO COMPUTE THE COMPLEX REFRACTIVE INDEX USING THE
C     POLARIZATION METHOD. THE DETAIL DERIVATION OF THE METHOD IS IN CHAPTER 2.
C*************************************************************************
C*************************************************************************
C     RS AND RP ARE THE REFLECTANCES OBTAINED FROM THE MEASUREMENTS. ANI AND
C     AKI ARE THE COMPLEX REFRACTIVE INDICES OF THE ZNSE PRISM. 'ANGLE' IS THE
C     INCIDENT ANGLE. THE FIRST PART OF THE PROGRAM IS TO READ IN THE DATA.
C*************************************************************************
      IMPLICIT REAL*8(A-H,O-Z)
      DIMENSION ANI(3500),AKI(3500),ANT(3500),AKT(3500),
     1RP(3500),RS(3500),WN(3500),WN1(3500)
      DATA PI/3.1415927D0/, E1/0.0/,E2/0.01/
      DO 200 I=1,N
      READ (53,10) WN(I),RS(I),RP(I)
  10  FORMAT(3E18.8)
      READ (17,30) WN1(I),ANI(I),AKI(I)
  30  FORMAT(3E20.10)
  200 CONTINUE
      TYPE 6
  6   FORMAT('    INPUT THE ANGLE   :',$)
      ACCEPT *, ANGLE
      ANGLE=ANGLE*PI/180.0D0
      B=DSIN(ANGLE)
      A=DCOS(ANGLE)
      DO 201 I=1,N,INC
C*************************************************************************
C     CALCULATION OF THE REFLECTION COEFFICIENTS RSE AND RPE WITH EMPTY
C     CELL. THE SAME METHOD AS IN CHAPTER 2, BUT REVERSE.
C*************************************************************************
      A1=ANI(I)**2-AKI(I)**2
      B1=2.0D0*ANI(I)*AKI(I)
      BAS=A1**2+B1**2
      ANE1=A1/BAS
      AKE1=-B1/BAS
      PE1=ANE1-B**2
      PE=SQRT((PE1+SQRT(PE1**2+AKE1**2))/2.0D0)
      QE=AKE1/(2.0D0*PE)
      AMID1=PE**2+QE**2
      RSE=(AMID1-2.0D0*A*PE+A**2)/(AMID1+2.0D0*A*PE+A**2)
      AMID2=A**2*((AMID1-B**2)**2+4.0D0*(B*PE)**2)+AMID1
      RPEIN=2.0D0*A*(AMID1+B**2)*PE
      RPE=(AMID2-RPEIN)/(AMID2+RPEIN)
C*************************************************************************
C     CONCEL THE EMPTY CELL EFFECT AND OBTAIN ACTUAL REFLECTANCES RS AND RP.
C*************************************************************************
      RS(I)=RS(I)*RSE
      RP(I)=RP(I)*RPE
C*************************************************************************
C     USING THE EQUATIONS IN CHAPTER 2 TO COMPUTE THE ANT (n) AND AKT (k). HERE
c     D IS A; A1 IS a AND B1 IS b; P, Q, X AND Y ARE THE SAME AS IN THE CHAPTER
c     2.
C*************************************************************************
      C1=1.0D0-RP(I)
      C2=1.0D0+RP(I)
      C3=1.0D0-RS(I)
      C4=1.0D0+RS(I)
      D=2.0D0*A*C4/C3
      E=A**2*C1*(D**2+4.0D0*B**2)-2.0D0*D*A*C2
```

```
      F=C1*D+2.0D0*C2*A**3-2.0D0*A*B**2*C2-2.0D0*D*C1*A**2
      P=-F/E
      U=D*P-A**2
      T=U-P**2
C*****************************************************************************
C     IN CASE THE EXPERIMENTAL VALUES ARE BAD VALUES, PROGRAM BRANCH TO THE END
C*****************************************************************************
      IF(T.LT.0.0) GOTO 201
      Q=SQRT(T)
      AN1=P**2-Q**2+B**2
      AK1=2.0D0*P*Q
      Y=B1*AN1+A1*AK1
      X=A1*AN1-B1*AK1
      ANT(I)=SQRT((X+SQRT(X**2+Y**2))/2.0D0)
      AKT(I)=Y/(2.0D0*ANT(I))
      WRITE(99,99) WN(I),ANT(I),AKT(I)
C*****************************************************************************
C     COUNTER HERE IS TO SEE HOW MANY POITES ARE CALCULATED
C*****************************************************************************
      L=L+1
 99   FORMAT(3E18.8)
 201  CONTINUE
      WRITE(5,*)L
      STOP
      END
```

APPENDIX B
PROGRAM OF THE ANGLE METHOD

```
C*************************************************************************
C     THIS PROGRAM IS TO COMPUTE THE COMPLEX REFRACTIVE INDEX USING THE ANGLE
C     METHOD. THE DETAIL DISCUSSION OF THE DERIVATION IS IN [2].
C*************************************************************************
C*************************************************************************
C     AIS1 AND AIS2 ARE REFLECTANCES OBTAINED FROM THE MEASUREMENTS. CC AND DD
C     ARE THE COMPLEX REFRACTIVE INDICES OF THE ZNSE. PRISM. ANGLE1 AND ANGLE2
C     ARE THE INCIDENT ANGLES. THE FIRST PART OF THE PROGRAM IS READ IN THE DATA
C*************************************************************************
      DIMENSION WN(4000),AIS1(4000),AIS2(4000),WN1(4000),CC(4000)
     1, DD(4000)
      TYPE 5
   5  FORMAT('   INPUT NUMBER OF DATA,ANGLE1,ANGLE2 :' , $)
      ACCEPT *,NCOUNT,ANGLE1,ANGLE2
      DO 20 I=1, NCOUNT
      READ(54,*) WN(I),AIS1(I),AIS2(I)
      READ(17,*) WN1(I),CC(I),DD(I)
  10  FORMAT(3E18.8)
  20  CONTINUE
      ANGLE1=ANGLE1*3.141592654/180.0
      ANGLE2=ANGLE2*3.141592654/180.0
      COA=COS(ANGLE1)
      COB=COS(ANGLE2)
      DO 100 I=1,NCOUNY
C*************************************************************************
C     CALCULATION OF A,B,C AND D IN [2].
C*************************************************************************
      A1=(1.0-AIS1(I))**4/AIS1(I)
      B1=(1.0+AIS1(I))**2*COA**4
      C1=((1.0-AIS1(I))*COA)**2
      D1=AIS1(I)*COA**4
      A2=(1.0-AIS2(I))**4/AIS2(I)
      B2=(1.0+AIS2(I))**2*COB**4
      C2=((1.0-AIS2(I))*COB)**2
      D2=AIS2(I)*COB**4
      G=C1*D2-C2*D1
C*************************************************************************
C     CALCULATION OF P AND Q IN [2].
C*************************************************************************
      P=(A1*D2-A2*D1)/G
      Q=(B1*D2-B2*D1)/G
C*************************************************************************
C     CALCULATION OF X, Y AND Z IN [2].
C*************************************************************************
      X=0.25*(A1-C1*P+0.25*D1*P**2)
      Y=4.0*(-B1+C1*Q-0.5*D1*P*Q)
      Z=16.0*D1*Q**2
C*************************************************************************
C     CALCULATION OF M, u and w IN [2].
C*************************************************************************
      AM=(-Y-SQRT(Y**2-4.0*X*Z))/(2.0*X)
      U=Q-P*AM/16.0
      W1=(AM-U**2)
      W=SQRT(W1)
C*************************************************************************
C     CALCULATION OF THE COMPLEX REFRACTIVE INDEX n AND k.
C*************************************************************************
      E=U-1.0
      AK1=(E+SQRT(E**2+W**2))/W
      AN=SQRT(W/(2.0*AK1))*CC(I)
      AK=AN*AK1
      WRITE(MM,10) WN(I),AN,AK
```

```
C*****************************************************************************
C     COMPUTE THE POINTS CALCULATED.
C*****************************************************************************
      L=L+1
  100 CONTINUE
      WRITE(5,*) L
      STOP
      END
```

REFERENCES

1. J. Fahrenfort, Spectrochim. Acta 17, 698 (1961).
2. J. Fahrenfort and W. M. Visser, Spectrochim. Acta 18, 1103 (1962).
3. J. A. Stratton, Electromagnetic Theory, 1st ed. (McGraw-Hill, New York, London, 1941).
4. J. D. Jackson, Classical Electrodynamics, (Wiley, New York, 1975).
5. W. N. Hansen, Spectrochim. Acta, 21, 815 (1965).
6. Marvin R. Querry, (Private, communication).

VITA

Zhiqin Huang was born in Beijing, China in 1953. He graduated from the Subsidiary School of the Peking University. From 1969 to 1978 he was working in the garage in the Five Lake Farm as a technician. He studied in the Harbin Institute of Technology from 1978 to 1982, and earned his B.S.degree in electrical engineering in 1982. After that, he was a teacher in the University of Science and Technology at Harbin, 1982 through 1985. In August of 1985, he came as a graduate student, as well as teaching assistant in the Physics Department at the University of Missouri-Kansas City, and also a graduate student in the Electrical Engineering Department at the University of Missouri-Columbia, since 1987.

III. Querry's Method

a. INTRODUCTION

Employing the Fresnel equations one can obtain the refractive index of a material provided the reflection coefficients are known at either two angles of incidence or for two polarization states. Querry's method employs the measurement of the reflection coefficients for two polarization states at the same angle of incidence.[1] We have included the solution from Querry's paper below.

From the Fresnel equations one can obtain two relationships for n and k, as given in Eqs. 3.1 and 3.2.

$$n = \left\{ \frac{1}{2} \left[-P^2+Q^2+ \sin^2\theta + \left(\left(P^2-Q^2-\sin^2\theta \right)^2 +4P^2Q^2 \right)^{1/2} \right] \right\}^{1/2} \qquad (3.1)$$

and

$$nk = QP. \qquad (3.2)$$

Where Q and P are given by Eqs. 3.3 and 3.4 as

$$Q = \frac{\left[(F - G)(\sin\theta)(\cot 2\theta) \right]}{\left[GF + (1 - F^2)\cos^2\theta - 1 \right]} \qquad (3.3)$$

and

$$P^2 = -Q^2 - 2FQ\cos\theta - \cos^2\theta. \qquad (3.4)$$

The quantities F and G in Eqs. 3.3 and 3.4 are given by

$$F = \frac{\left(R_{\perp} + 1 \right)}{\left(R_{\parallel} + 1 \right)} \qquad (3.5)$$

and

$$G = \frac{\left(R_{\parallel} + 1 \right)}{\left(R_{\perp} + 1 \right)} . \qquad (3.6)$$

Notice that F and G are dependent only on $R_{\perp}$ and $R_{\parallel}$. Values for n and k can then be determined by computing in order F, G, Q, P, n, and k.

This technique is applied to solids by measuring the reflectances $R_{\perp}$ and $R_{\parallel}$ for several angles of incidence. The refractive index computed for each angle of incidence is then used to determine a mean and standard deviation for the given angle. The computer program is listed in appendix 3.1 of this section. We then have:

$$\bar{n} = \frac{\Sigma\, n_i}{l} \qquad \bar{k} = \frac{\Sigma\, k_i}{l} , \qquad (3.7)$$

and

$$\sigma_n = \left\{ (l-1)^{-1} \sum [n_i - \bar{n}]^2 \right\}^{1/2} , \qquad (3.8)$$

and

$$\sigma_k = \left\{ (l-1)^{-1} \sum [k_i - \bar{k}]^2 \right\}^{1/2} . \qquad (3.9)$$

The standard deviation as given in Eqs. 3.8 and 3.9 should provide a reasonable estimate of the uncertainty of the complex refractive index as determined with this technique.

b. Error Analysis

The error in the complex refractive index cannot be estimated through the use of the theory of the propragation of error since the Fresnel equations cannot be explicitly solved for n and k. To examine the error associated with the Querry method we can estimate the error by 1) compute the reflection coefficients from known n and k values, 2) modify the reflection coefficients by a fractional percent, 3) recompute n and k from the modified reflection coefficients, 4) and compare the recomputed n and k values to the original values. The reflection coefficients R_s and R_p are presented in Figs. 3.1 - 3.6 for $\theta = 10^\circ$, 30°, and 60°, respectively. Notice the large increase in R for either polarization state as the refractive index, n, becomes greater than 2. Also the reflection coefficients stay below 30% for most of the range of values of the complex refractive index with the exception of $\theta = 60^\circ$. If we can measure the absolute reflection to within 2% we are modifiying the isoreflectance curves by an appreciable amount. Due to the changes in R as a function of n and k it is obvious the error in both n and k will be a strong function of these values. We therefore have plotted in the following figures the fractional uncertainty in n and k versus both n and k in a three dimensional plot. The three parameters, R_s, R_p, and θ were individually adjusted by 2% for each of the discussions below.

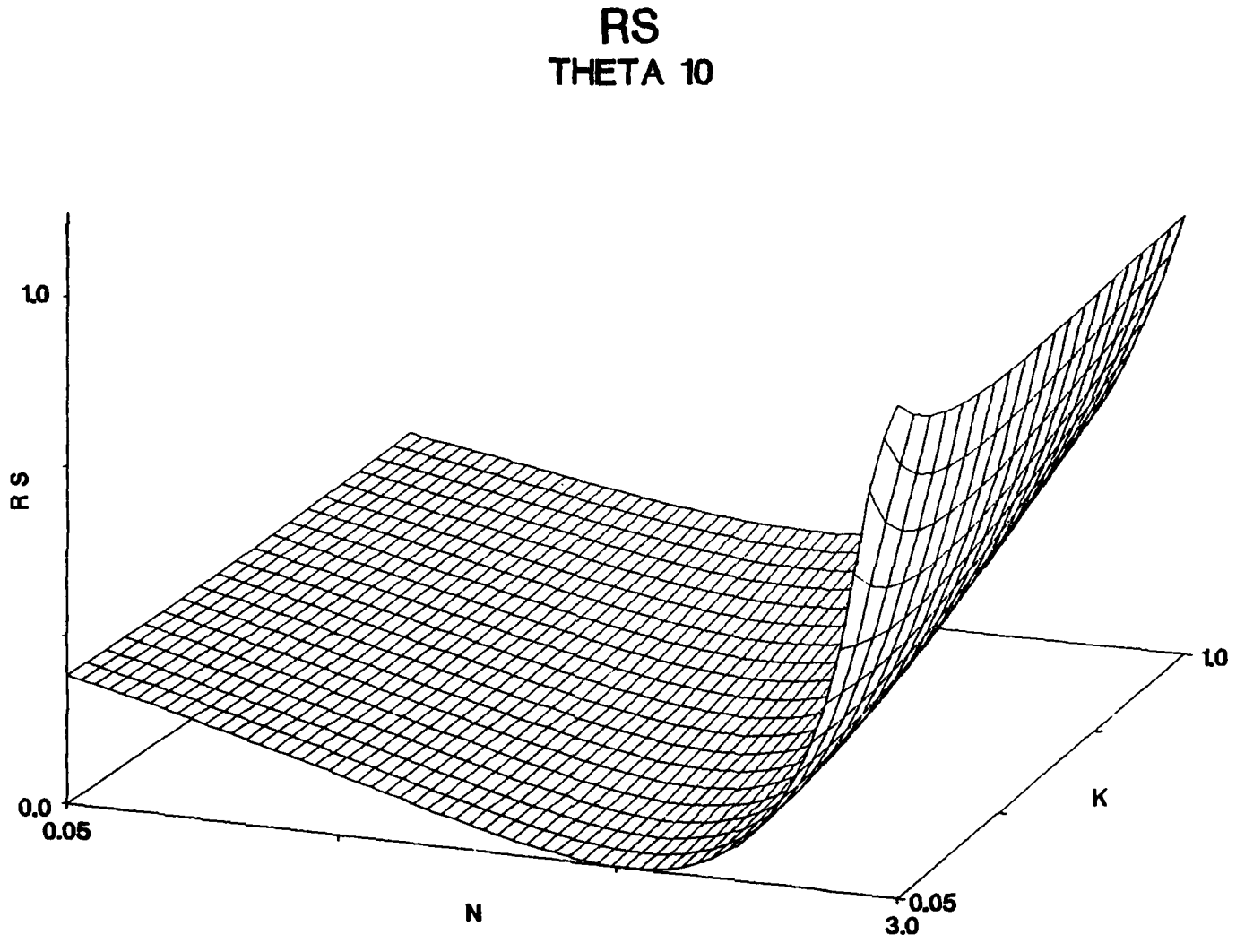

FIG. 3.1 Reflection coefficient for E perpendicular to the plane of incidence and an angle of incidence of $\theta = 10^{\circ}$.

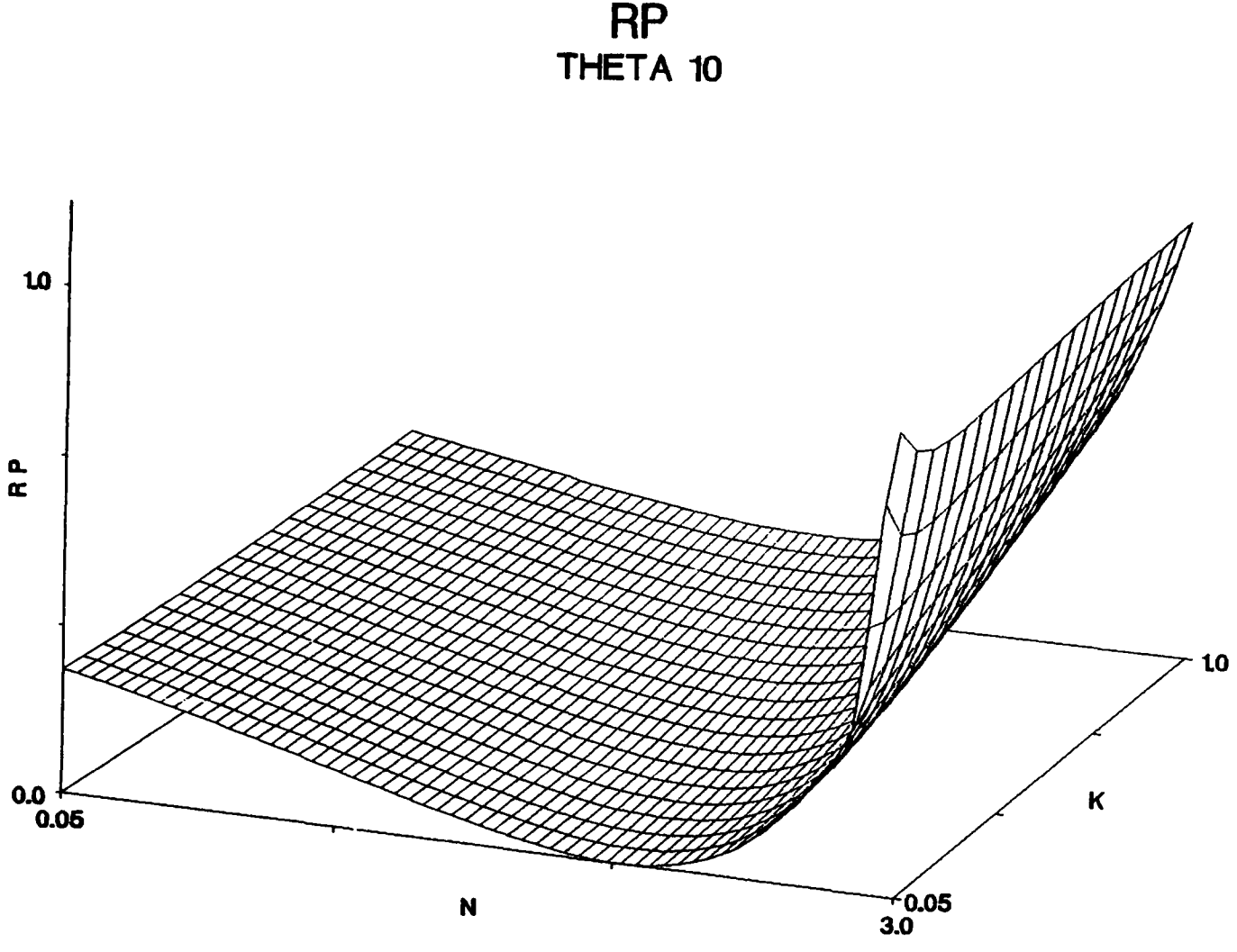

FIG. 3.2 Reflection coefficient for E parallel to the plane of incidence and an angle of incidence of $\theta = 10^{\circ}$

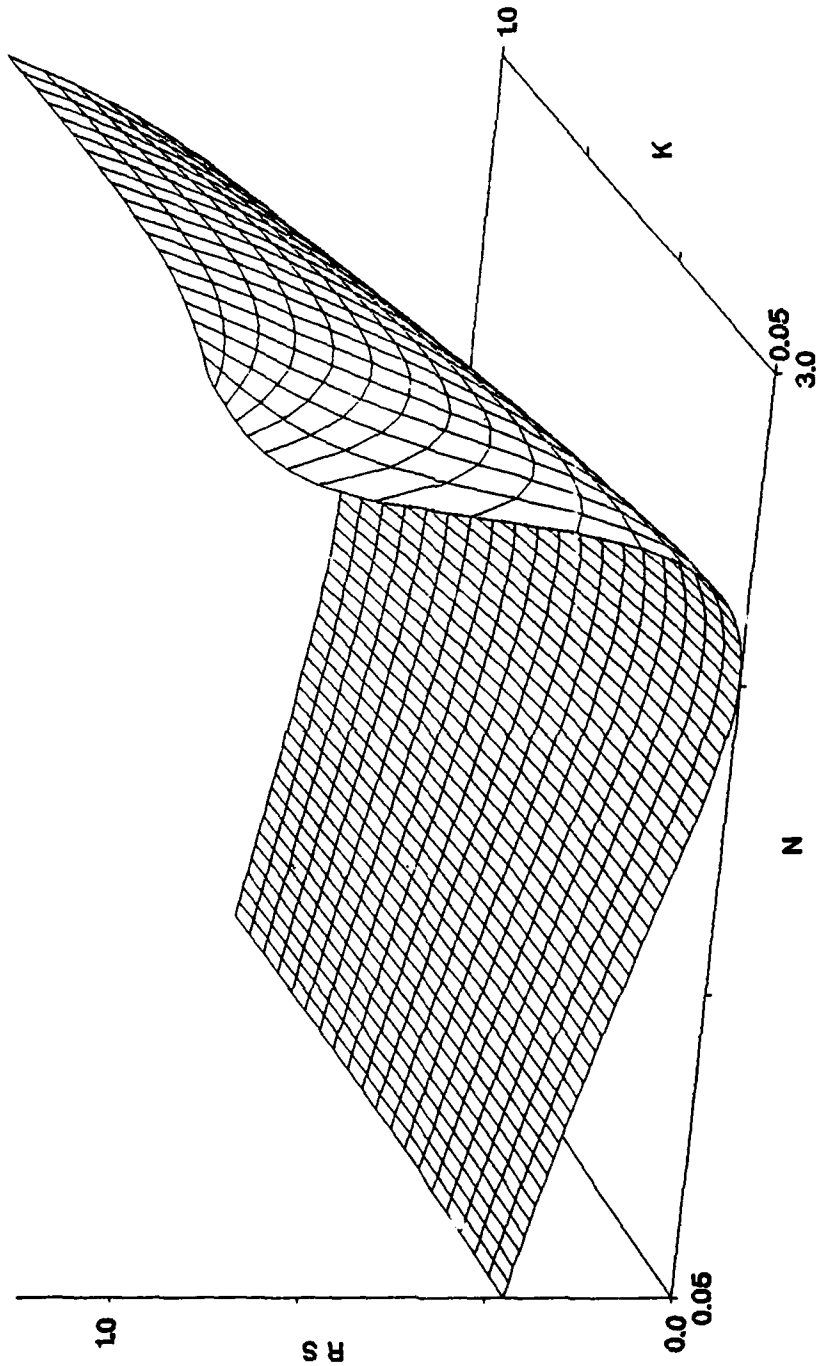

FIG. 3.3 Same as Fig. 3.1 but with $\theta = 30°$.

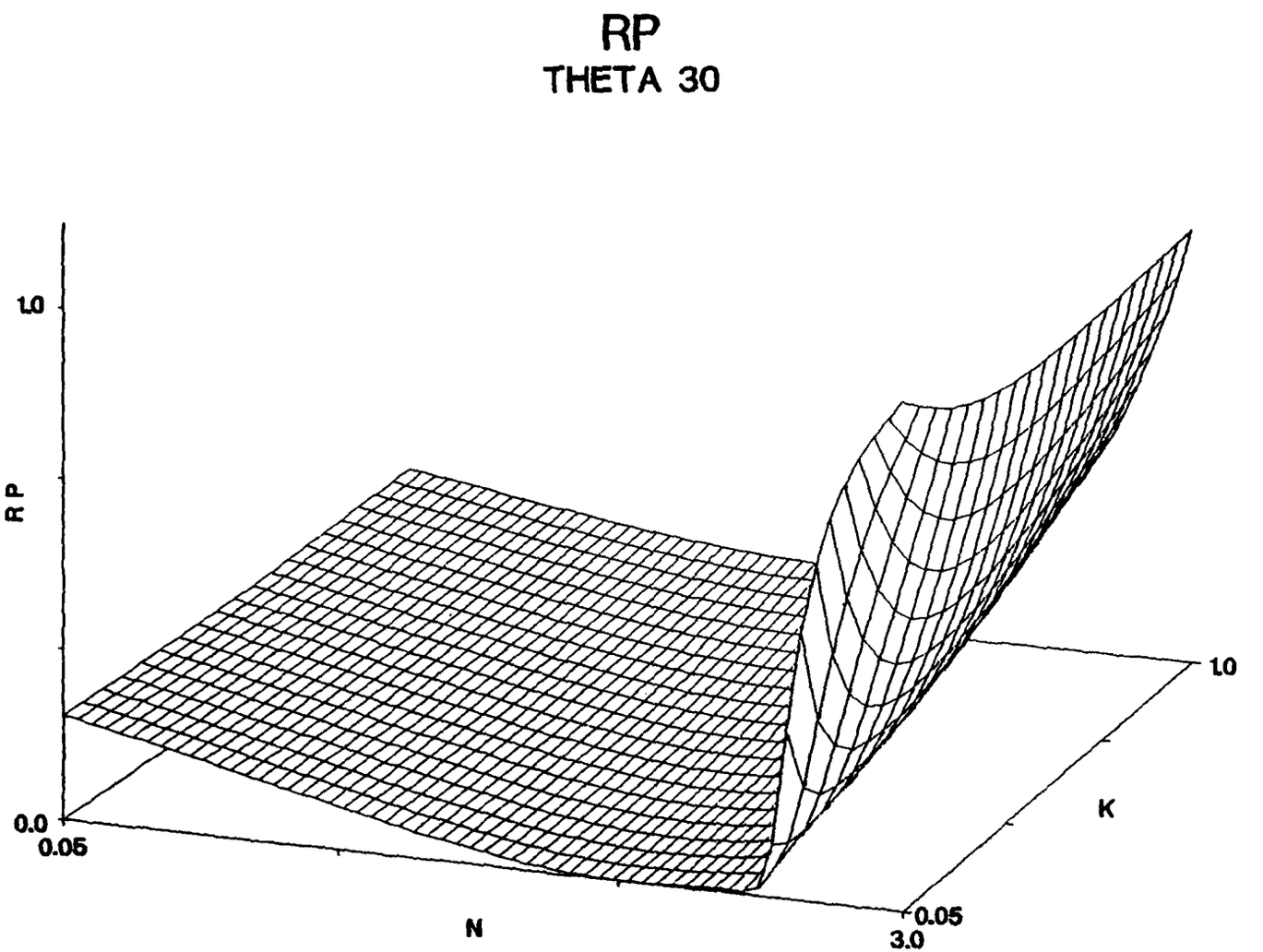

FIG. 3.4 Same as Fig. 3.2 but with $\theta = 30^{\circ}$.

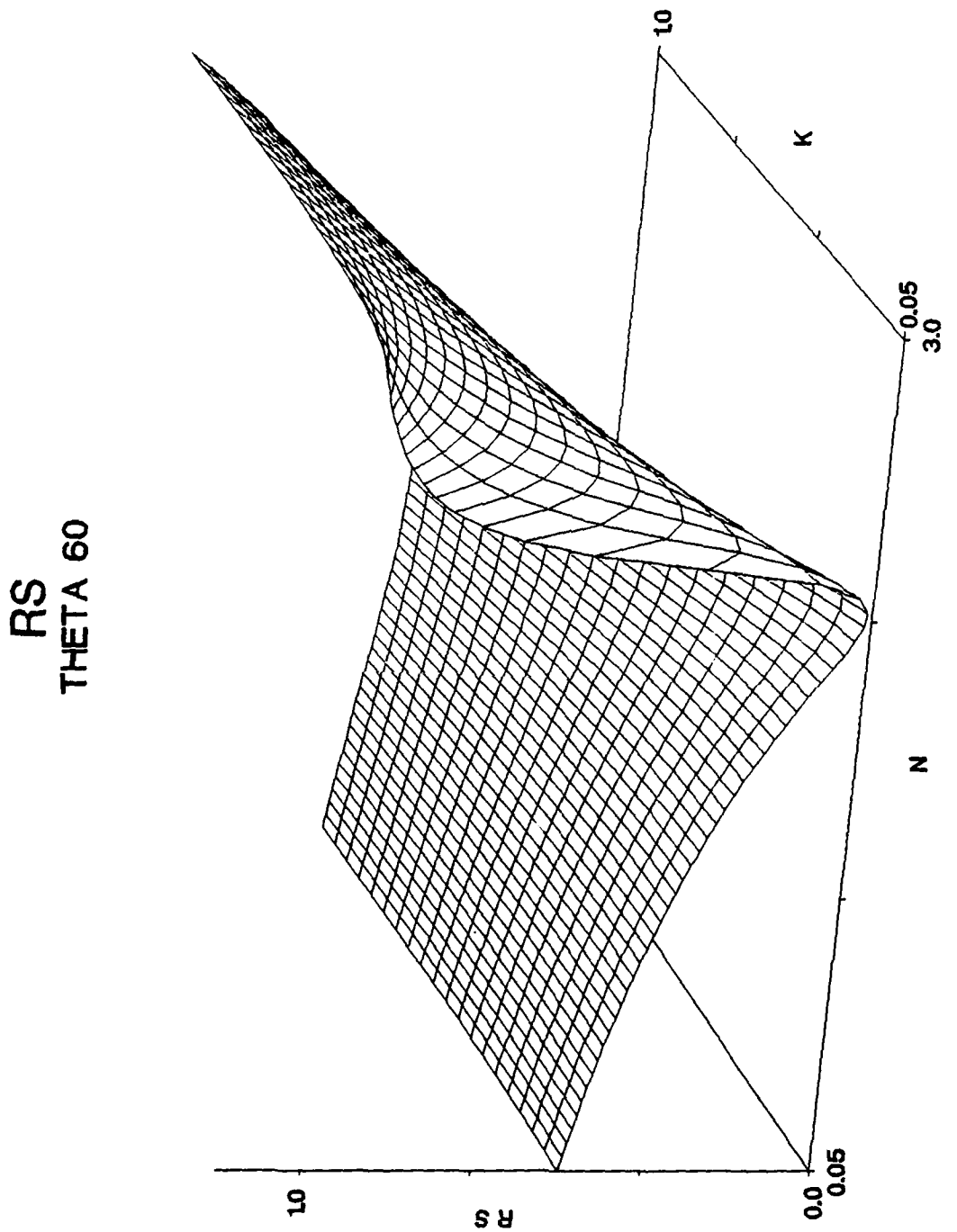

FIG. 3.5 Same as Fig. 3.1 but with $\theta = 60°$.

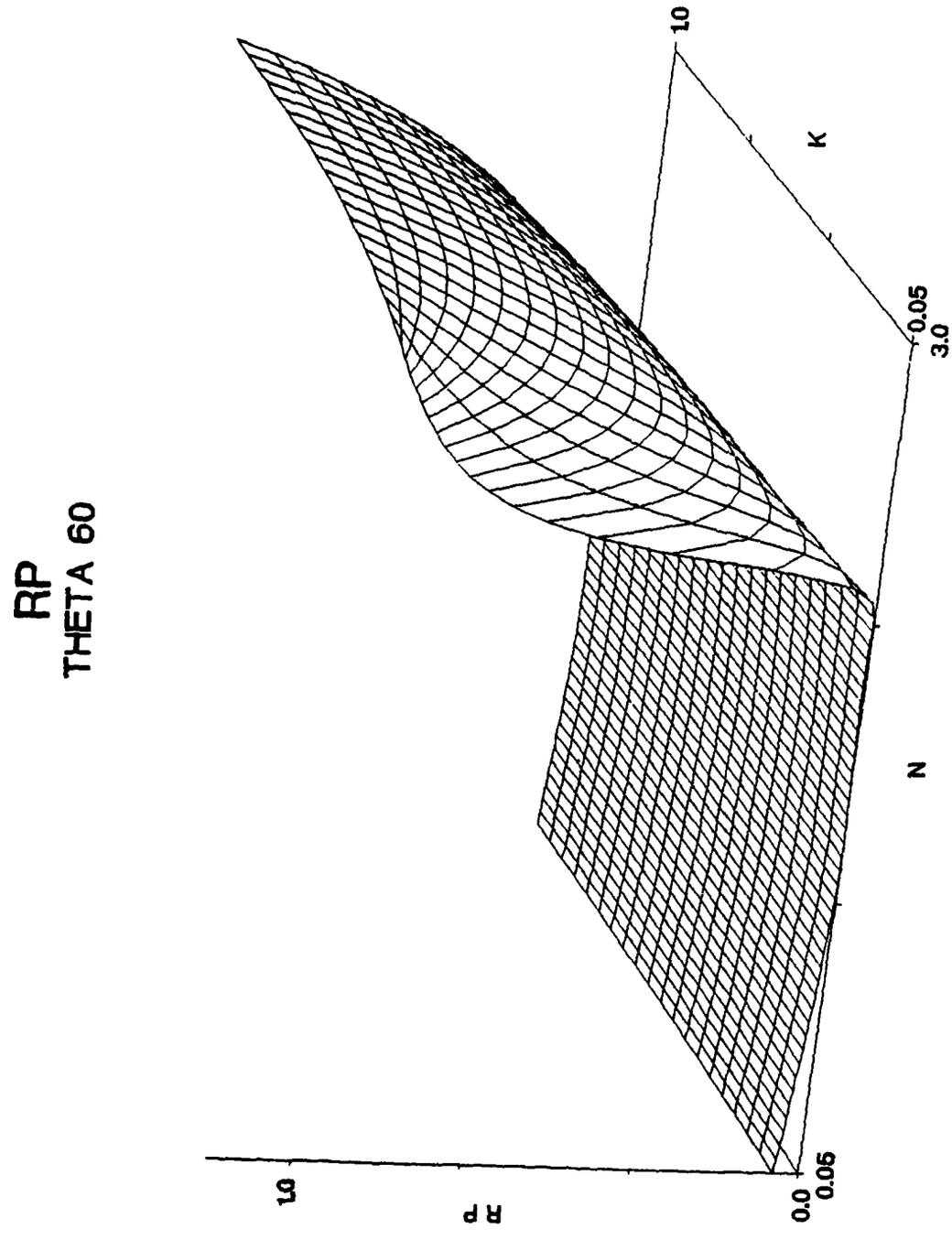

FIG. 3.6 Same as Fig. 3.2 but with $\theta = 60°$.

VARIATION IN R_s

In Figs. 3.7 - 3.9 we present the fractional uncertainty in n for a variation of R_s by 2%, and in Figs. 3.10 - 3.12 the corresponding uncertainty in k. The angles of incidence are 10°, 30°, and 60°, respectively. The surface regions which are blank are representative of the inability to compute the complex refractive index at these values, i.e. the variation of 2% provides an error of n and k of infinity. From the figures we can identify several conditions necessary for the accurate determination of the optical constants. For n less than 2, the uncertainty in n is reduced as the angle of incidence is increased. There is a limit to the angle of incidence, at too large of an angle the region below n = 1 cannot be solved except for large k values. For n greater than 3 smaller, angles appear to provide a more accurate determination of the real part of the refractive index. From Figs. 3.10 - 3.12 the error in k is greater than 100% for all regions except for large n where the error becomes less but is still extremely large. These results indicate the uncertainty in R_s must be less than 2% in order to obtain accurate values for the refractive index.

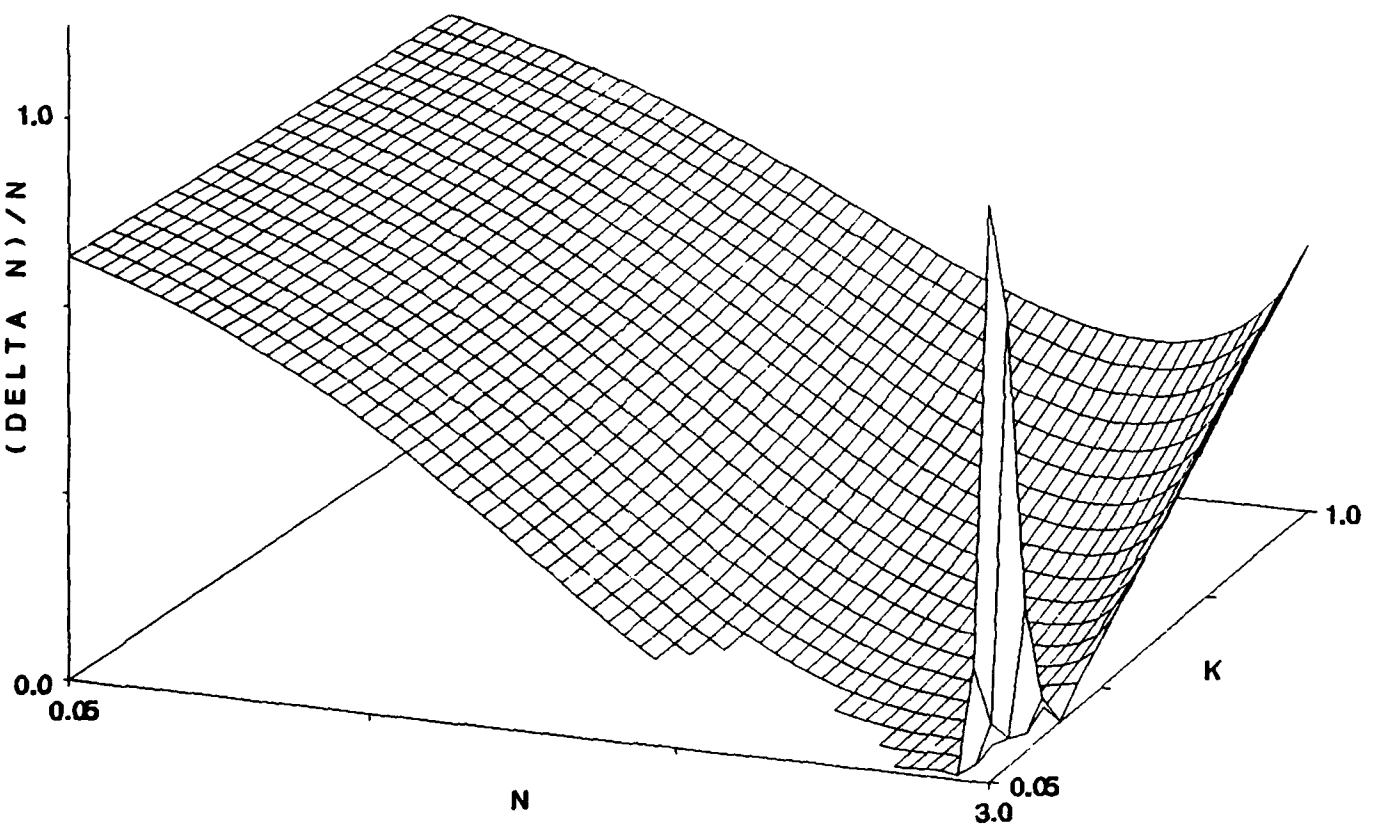

FIG. 3.7 Fractional error in n, $\Delta n/n$, increasing R_s by 2% at angle of incidence of 10°.

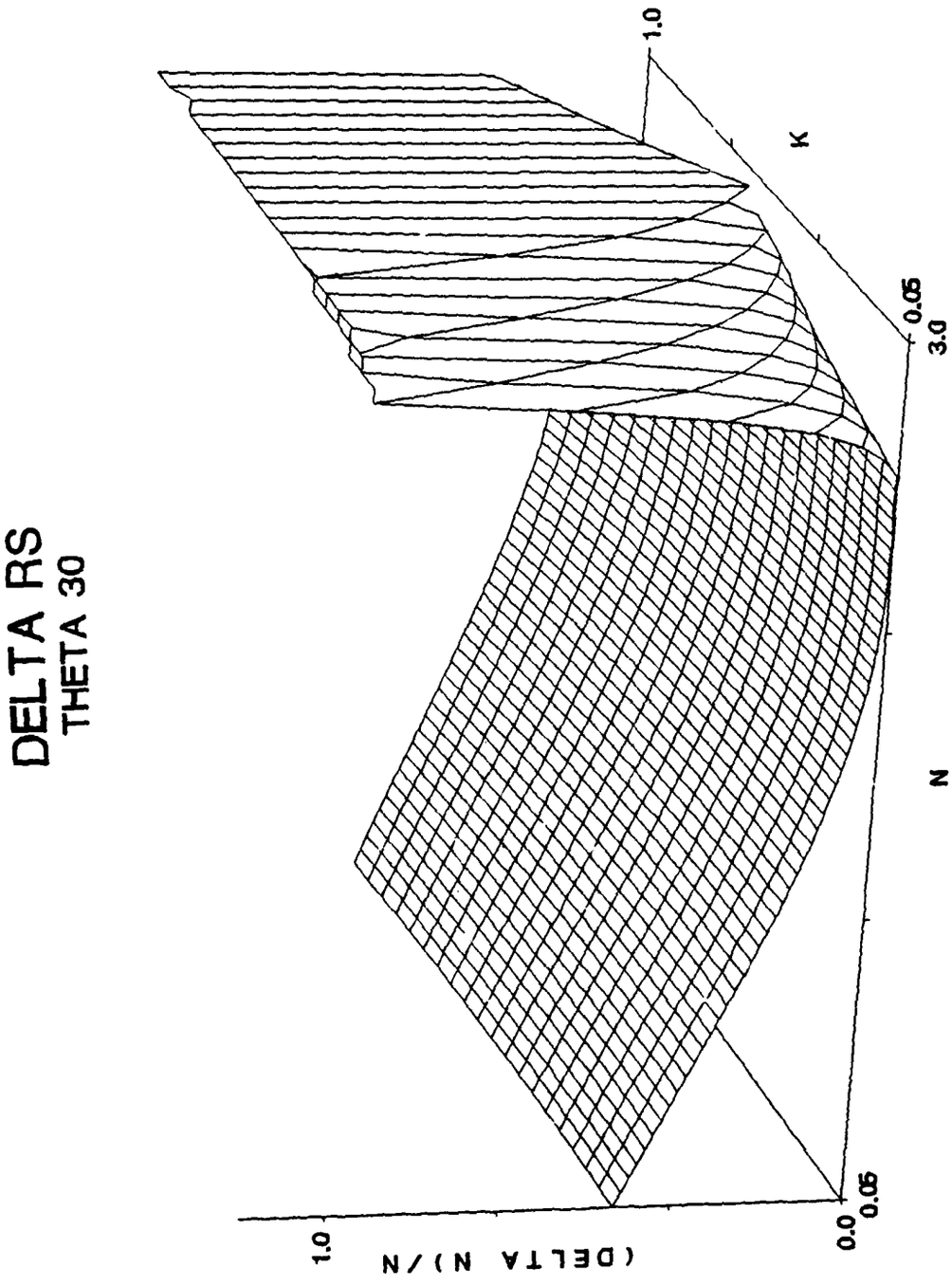

FIG. 3.8 Same as Fig. 3.7 but with $\theta = 30°$.

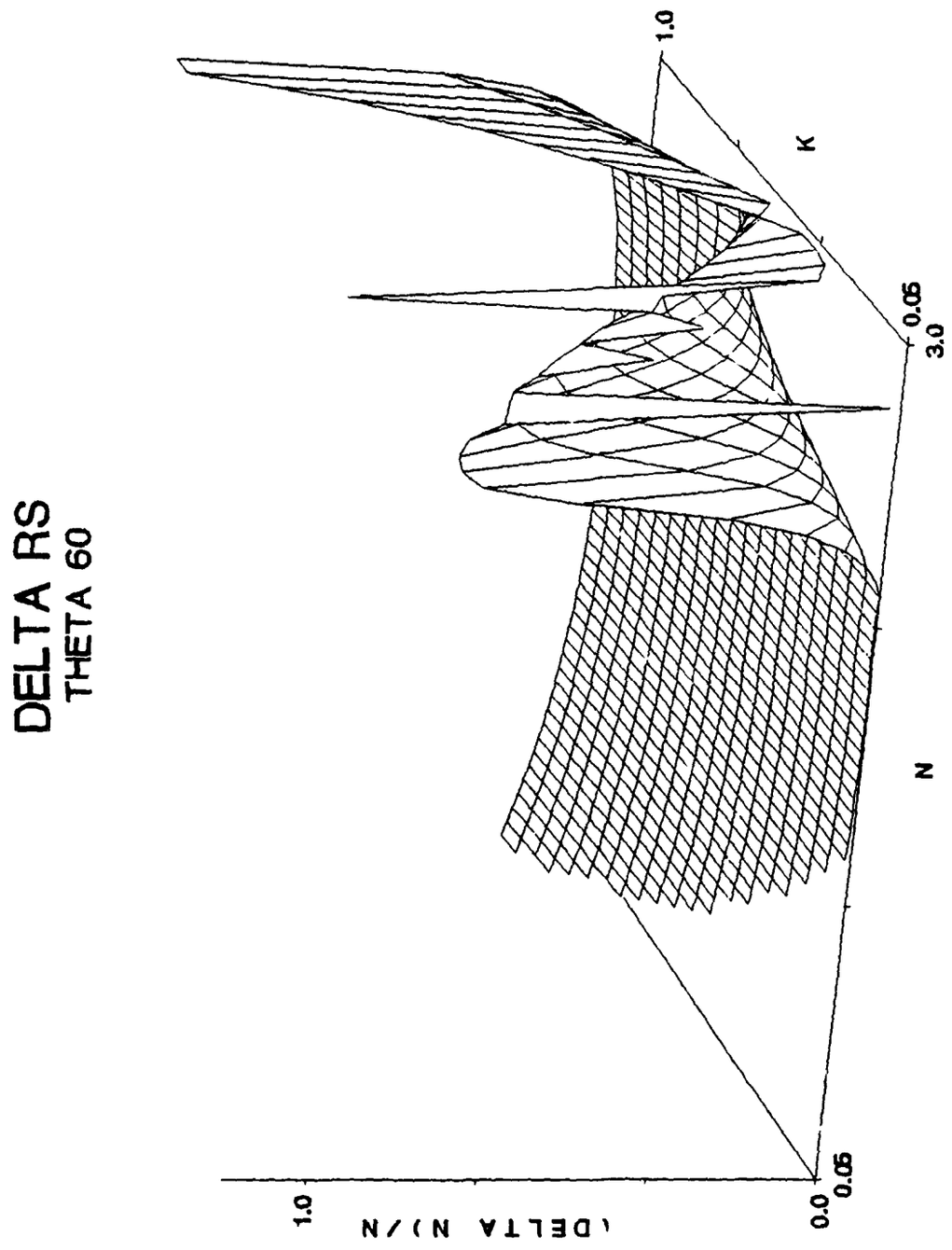

FIG. 3.9 Same as Fig. 3.7 but with $\theta = 60^{\circ}$.

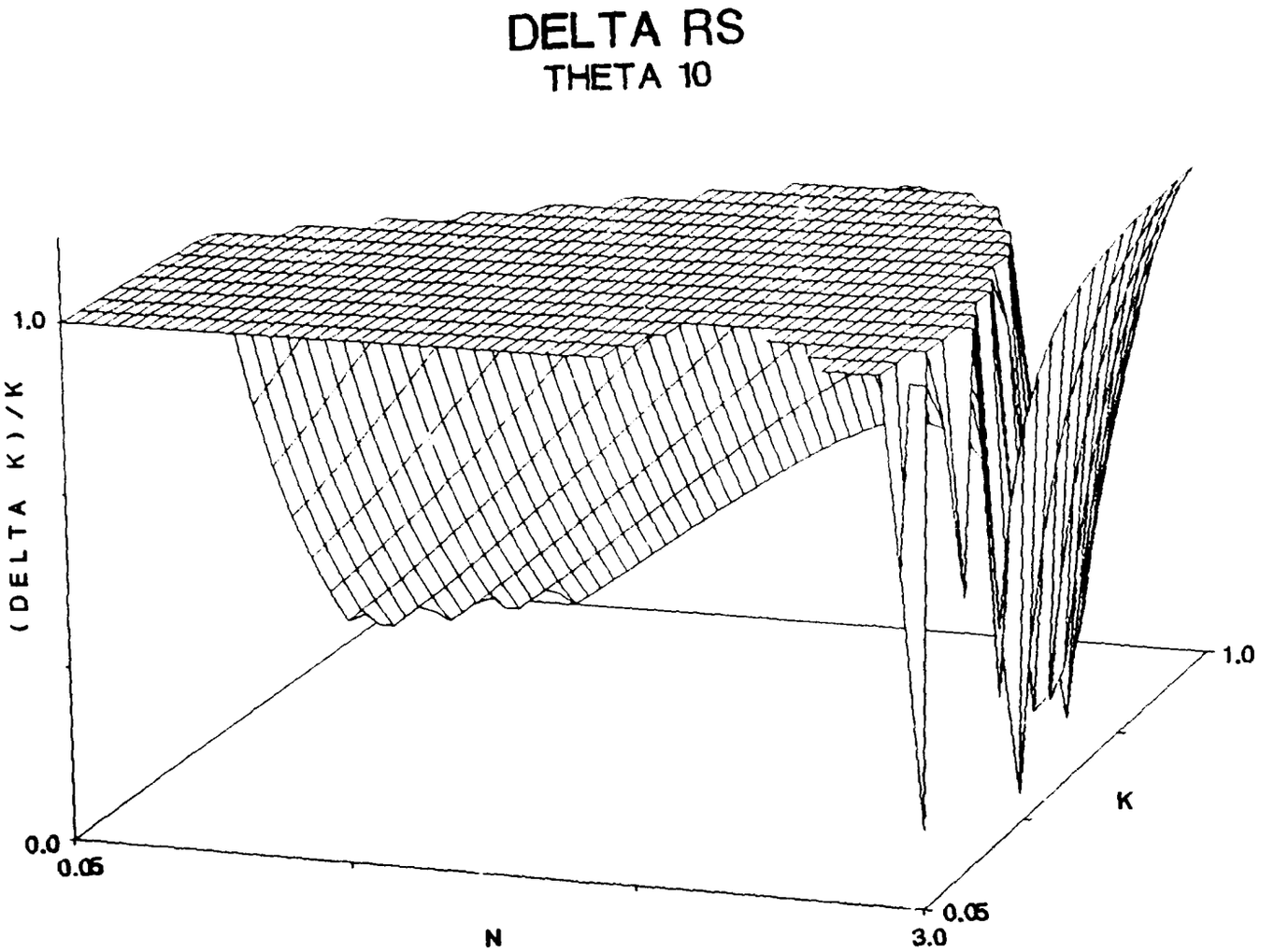

FIG. 3.10 Fractional error in k, $\Delta k/k$, increasing R_s by 2% at an angle of incidence of 10°.

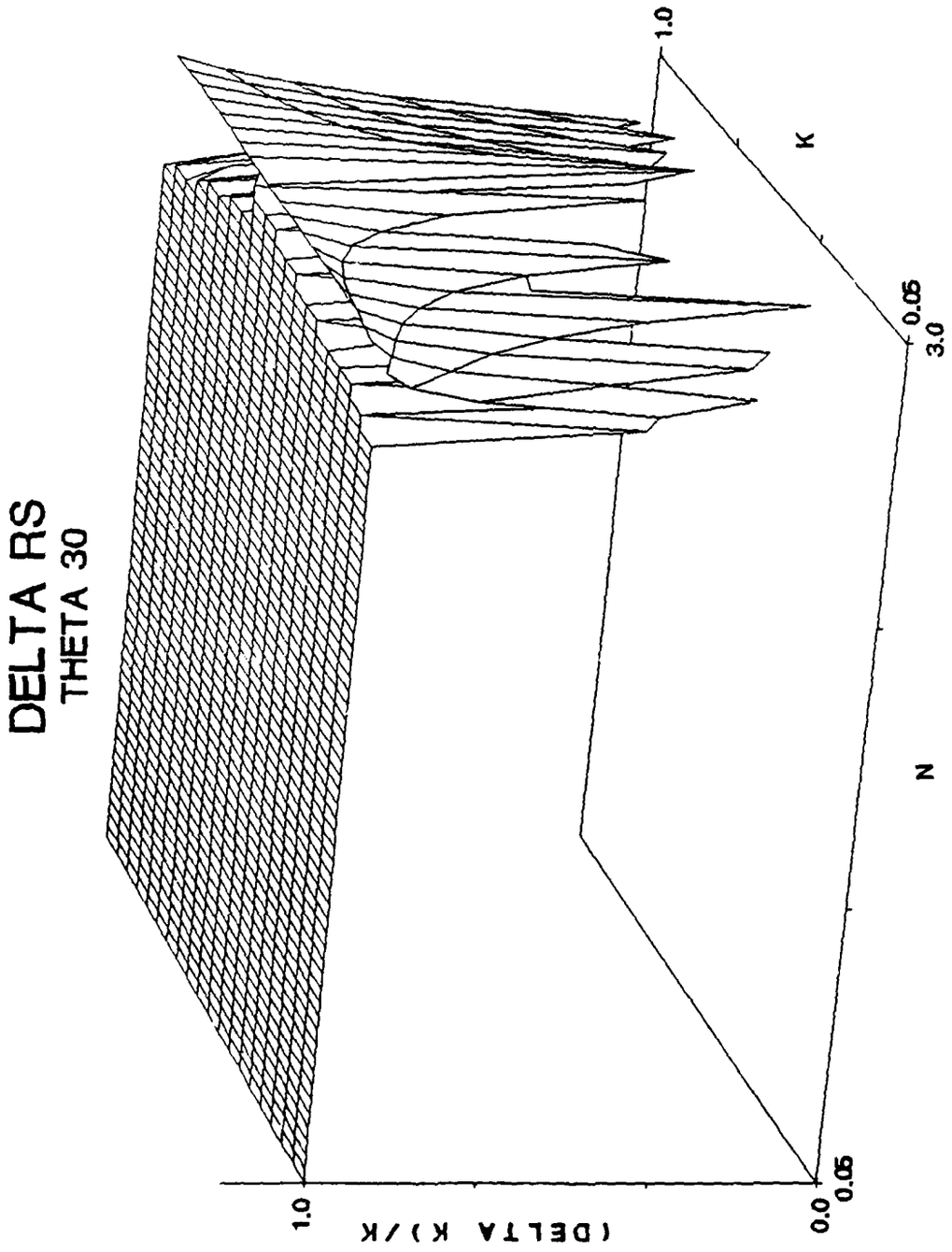

FIG. 3.11 Same as Fig. 3.10 but with $\theta = 30°$.

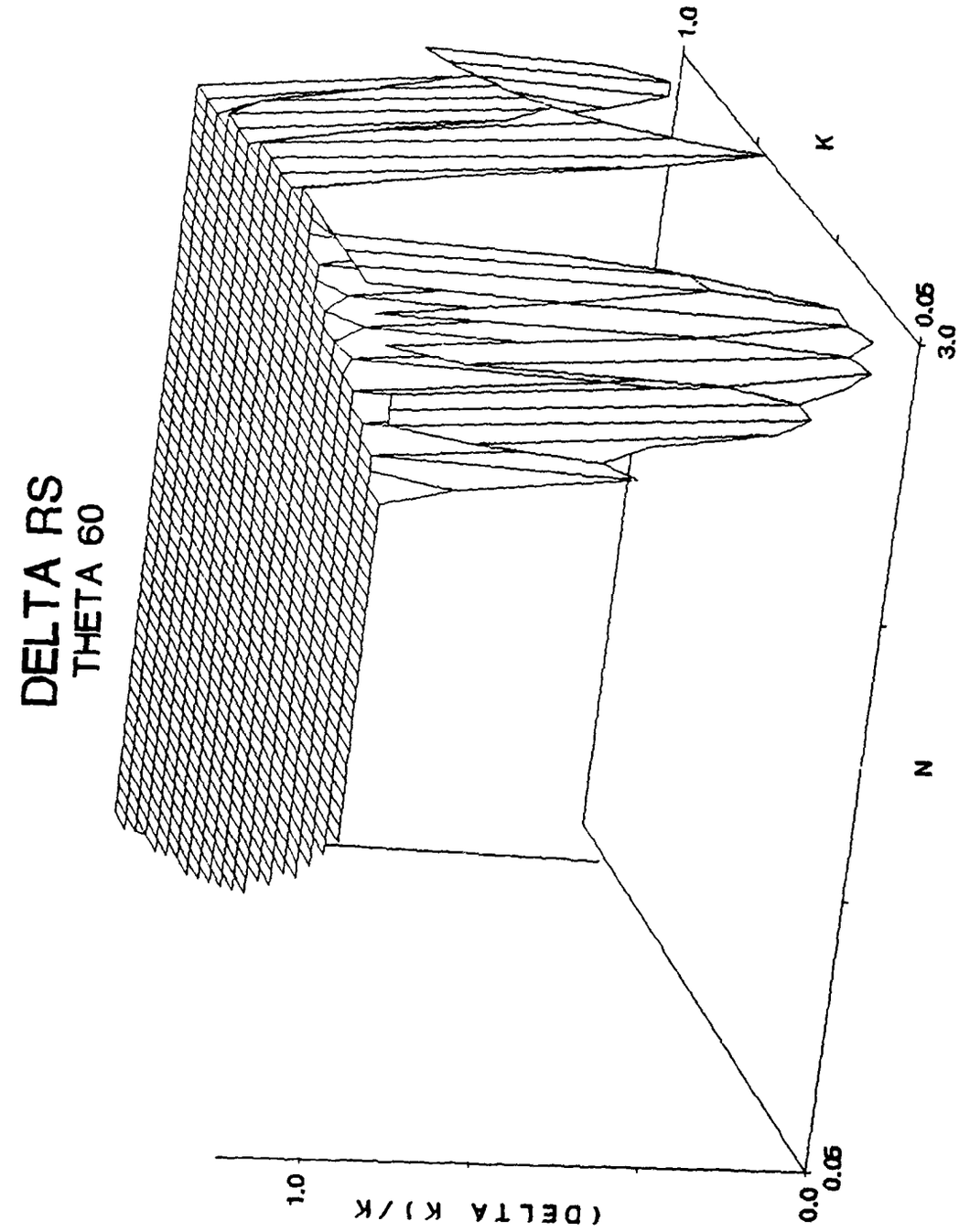

FIG. 3.12 Same as Fig. 3.10 but with $\theta = 60°$.

VARIATION IN R_p

The fractional uncertainty in the complex refractive index is presented in Figs. 3.13 - 3.18 associated with a 2% modification of R_p. From Figs. 3.13 - 3.15 similar conditions as presented in the previous section must be met to provide accurate values for n. For n less than 2, a greater angle of incidence provides less error in the determination of n. For n greater than 2 the error is reduced at angles between 10° and 30°. Figs. 3.16 - 3.18 again indicate the fractional error in k is extremely large even for an uncertainty in R_p of 2%. These results indicate the need to measure the reflection coefficients to an uncertainty of much less than 2%.

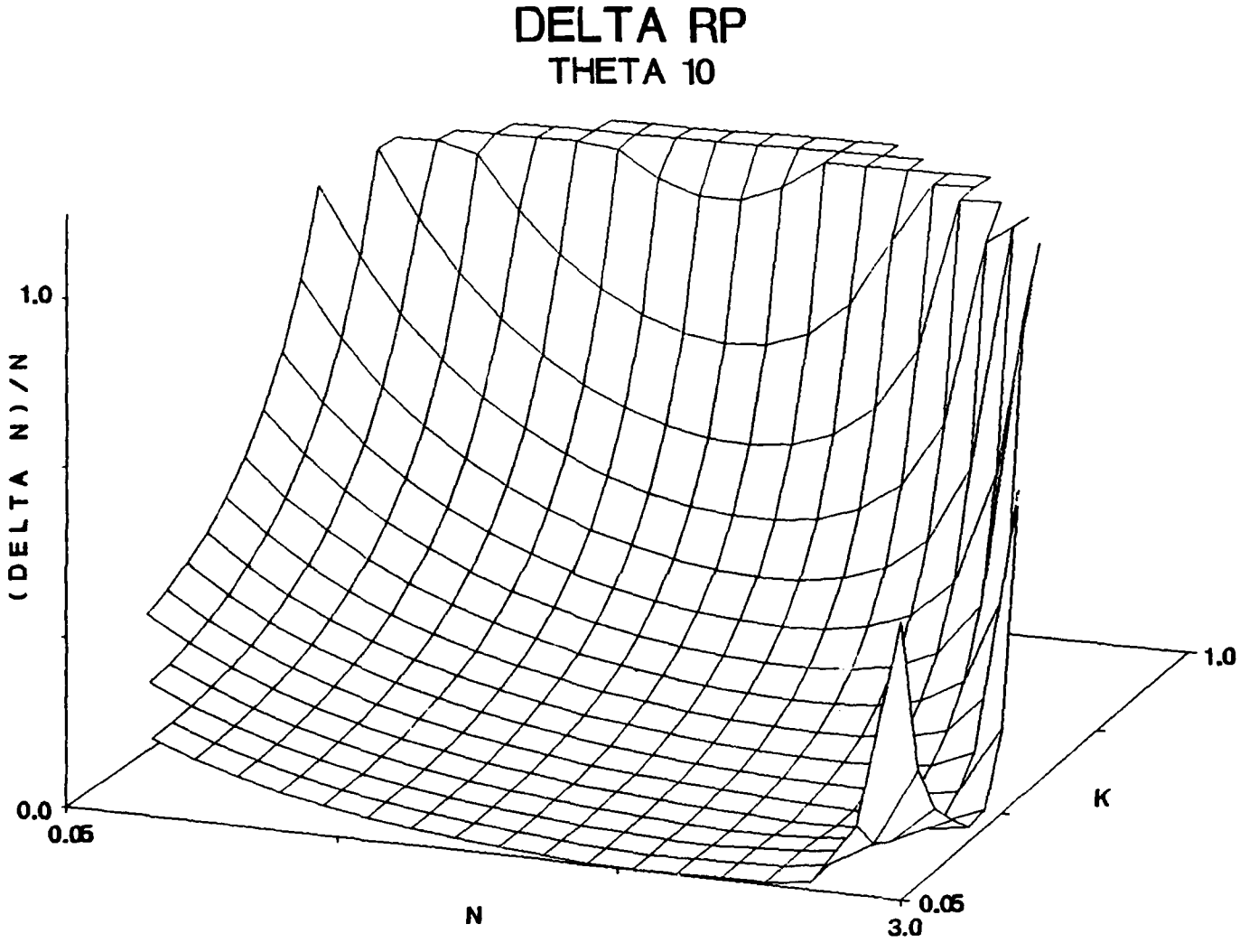

FIG. 3.13 Fractional error in n, $\Delta n/n$, increasing R_p by 2% at an angle of incidence of 10°.

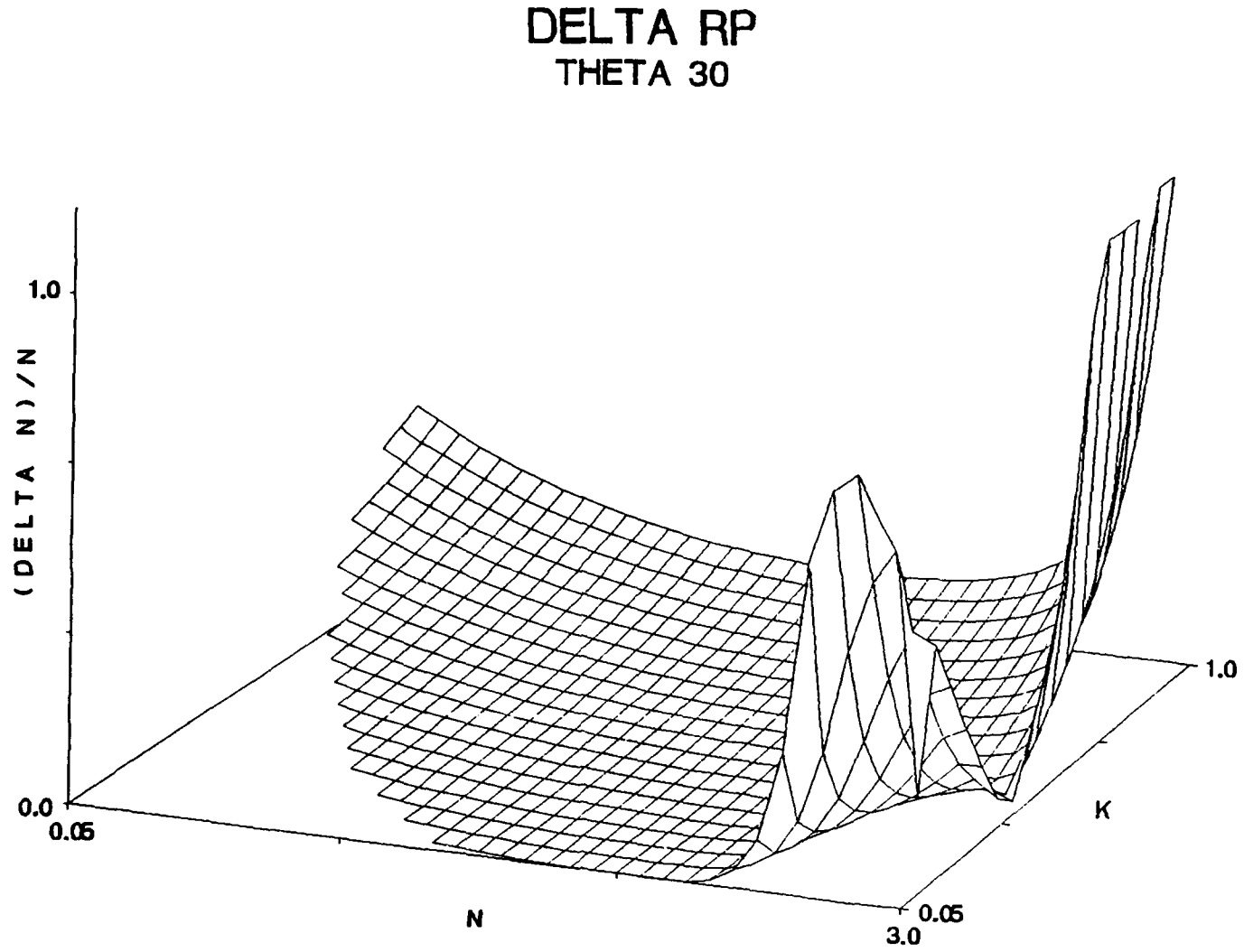

FIG. 3.14 Same as Fig. 3.13 but with $\theta = 30°$.

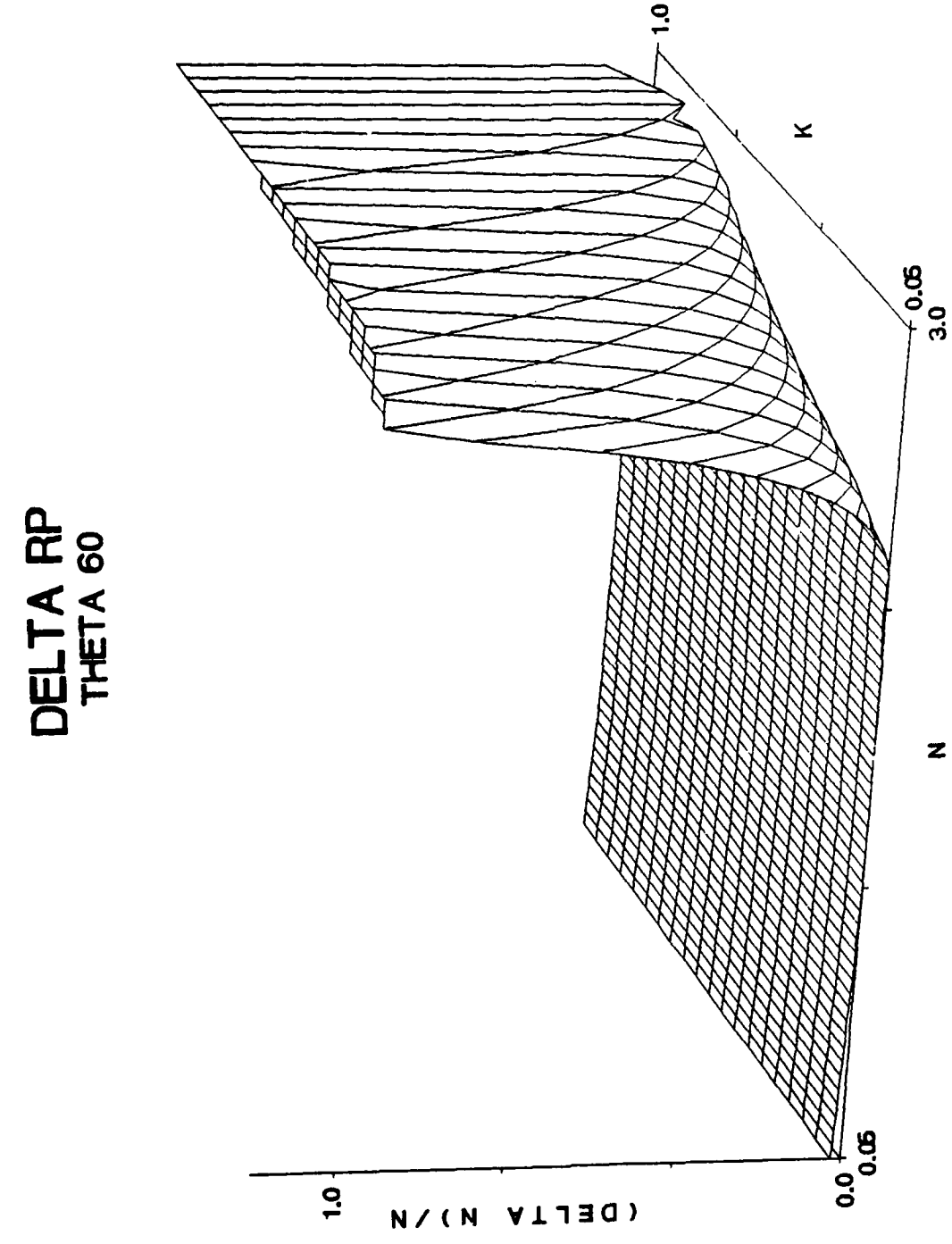

FIG. 3.15 Same as Fig. 3.13 but with $\theta = 60°$.

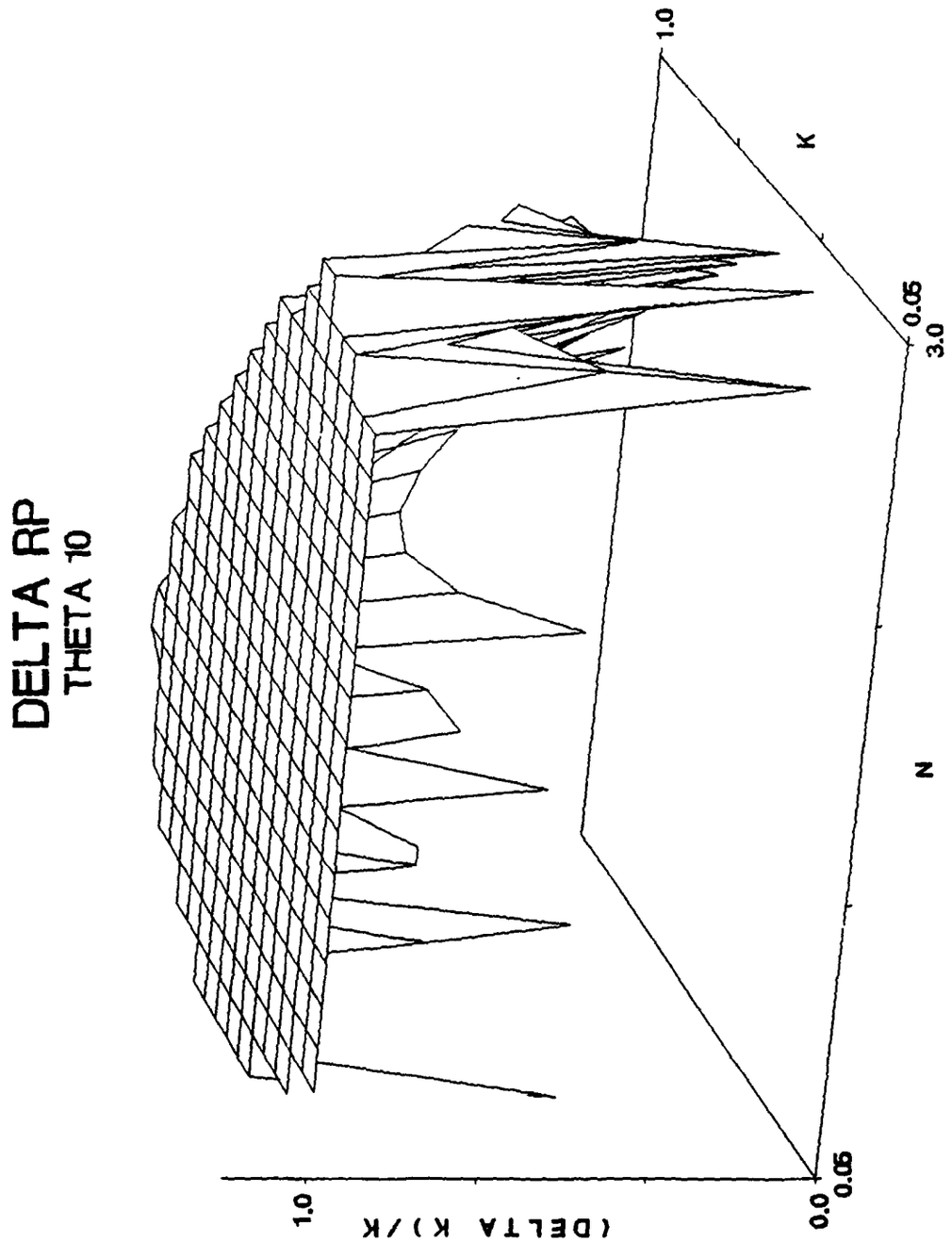

FIG. 3.16 Fractional error in k, $\Delta k/k$, increasing R_p by 2% at an angle of incidence of 10°.

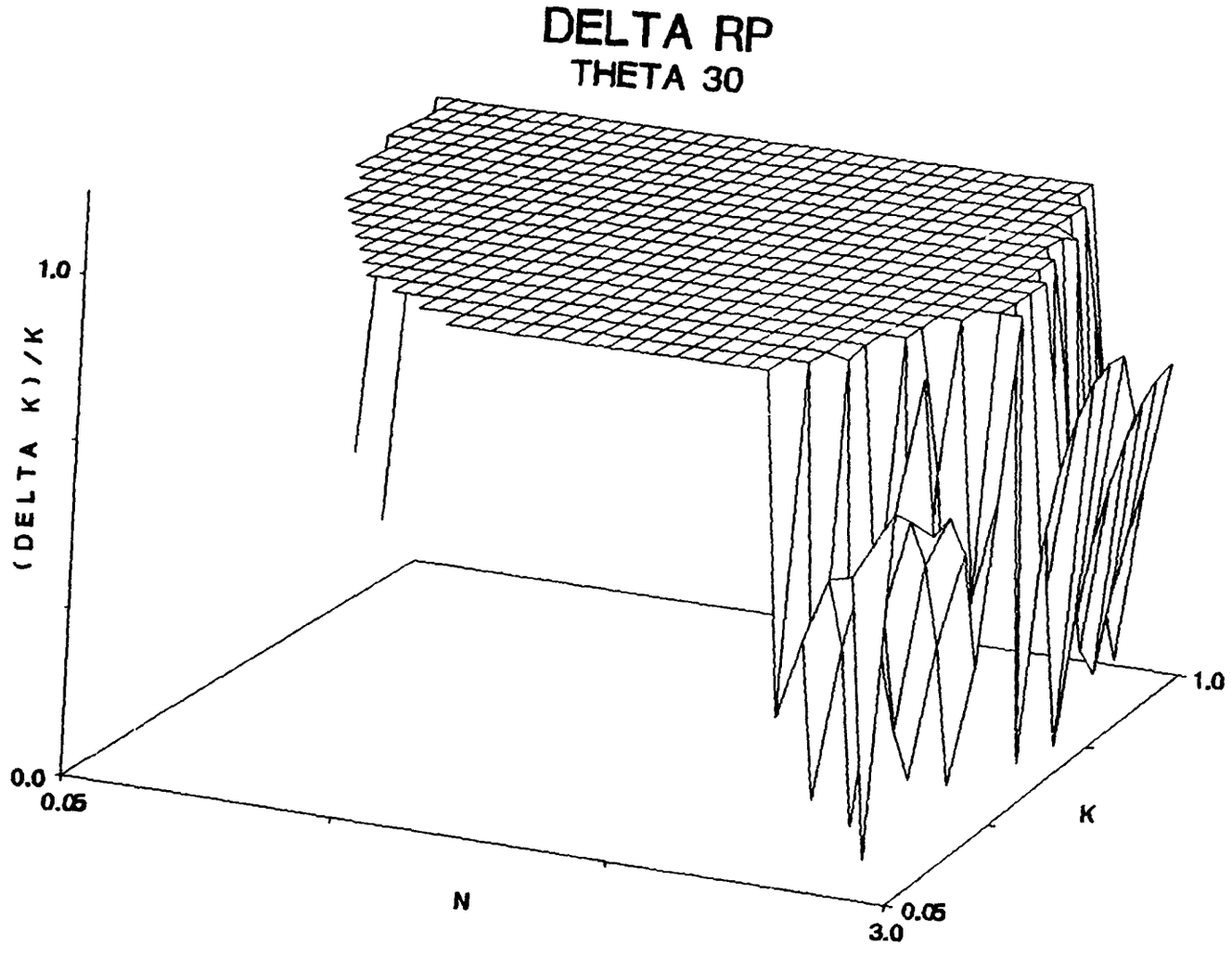

FIG. 3.17 Same as Fig. 3.16 but with $\theta = 30°$.

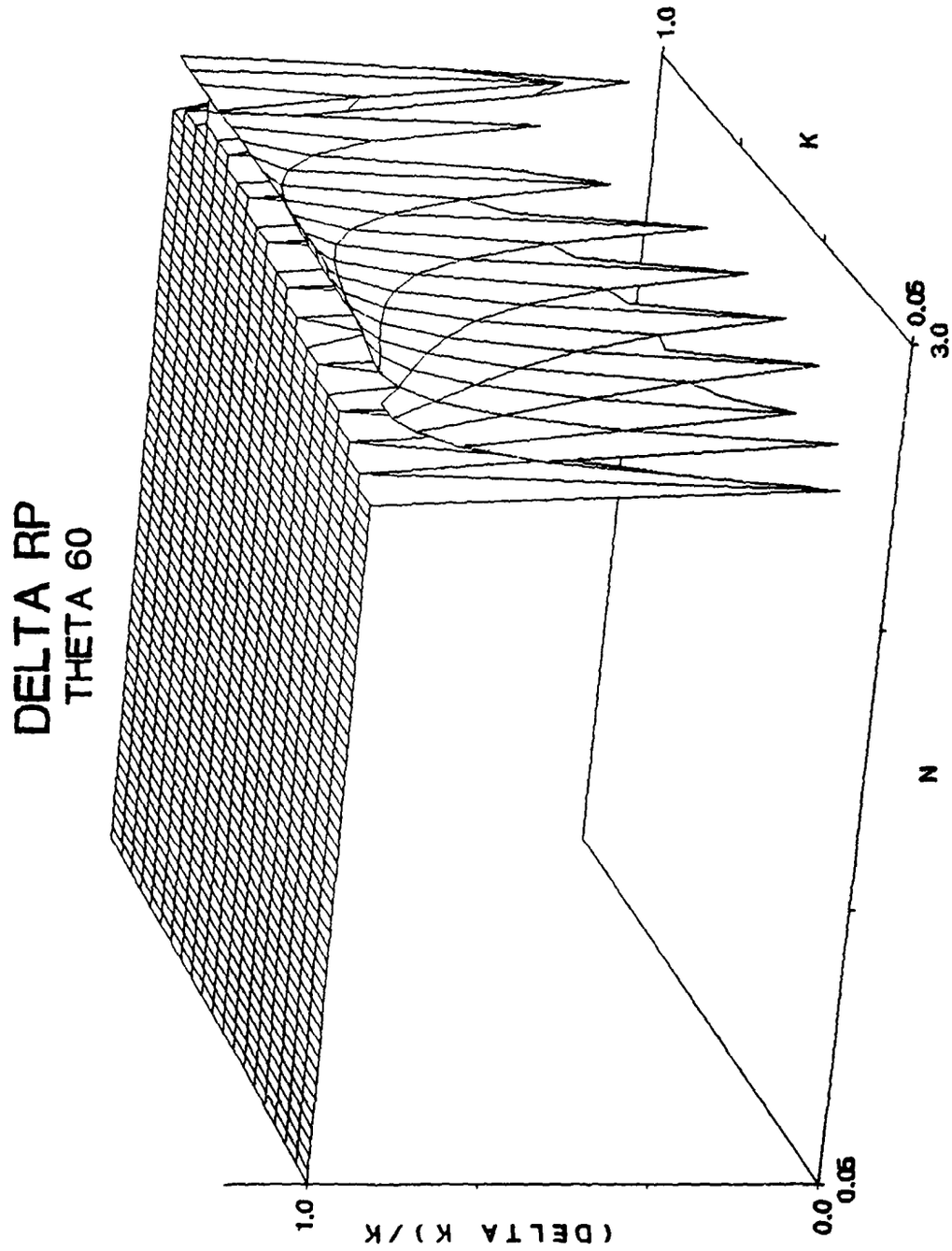

FIG. 3.18 Same as Fig. 3.16 but with $\theta = 60°$.

VARIATION IN θ

The last parameter to obtain any uncertainty is θ. The uncertainty in the complex refractive index associated with the variation in θ is presented in Figs. 3.19 - 3.24. The same conditions as discussed previously appear. The larger angle of incidence leads to a smaller uncertainty in n. Accurate values of k can be obtained at intermediate angles of incidence, considerable error is associated with both the small, less than 10° and at large angles, greater than 60°. Considerable structure appears in Fig. 3.24, indicating the regions of great sensitivity in determining k.

The final conclusion of these simulations indicate the need for extreme accuracy in determining the reflection coefficients. The application of Querry's method is very sensitive to minutefluctuations in these values.

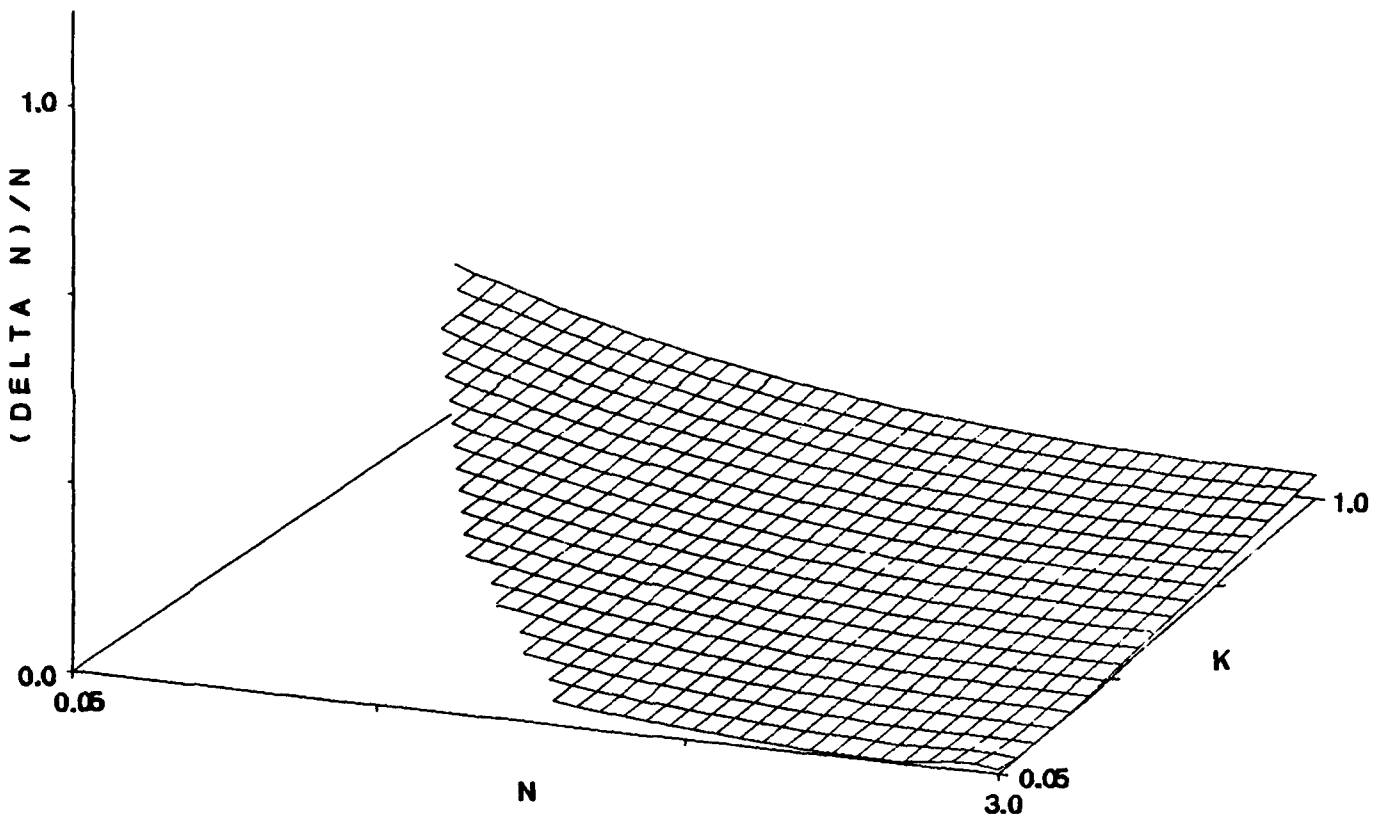

FIG. 3.19 Fractional error in n, $\Delta n/n$, increasing θ by 2% at an angle of incidence of 10°.

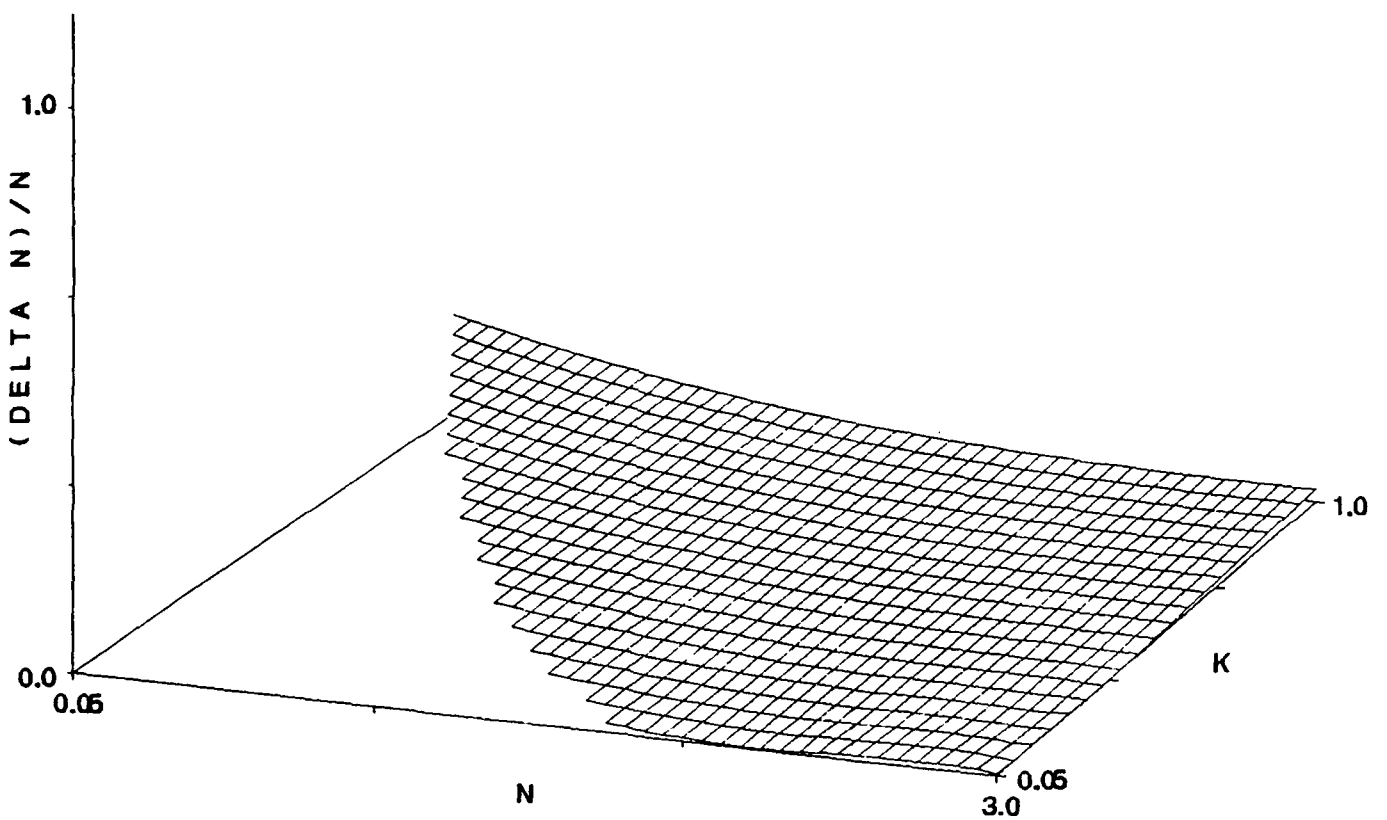

FIG. 3.20 Same as Fig. 3.19 but with $\theta = 30^{\circ}$

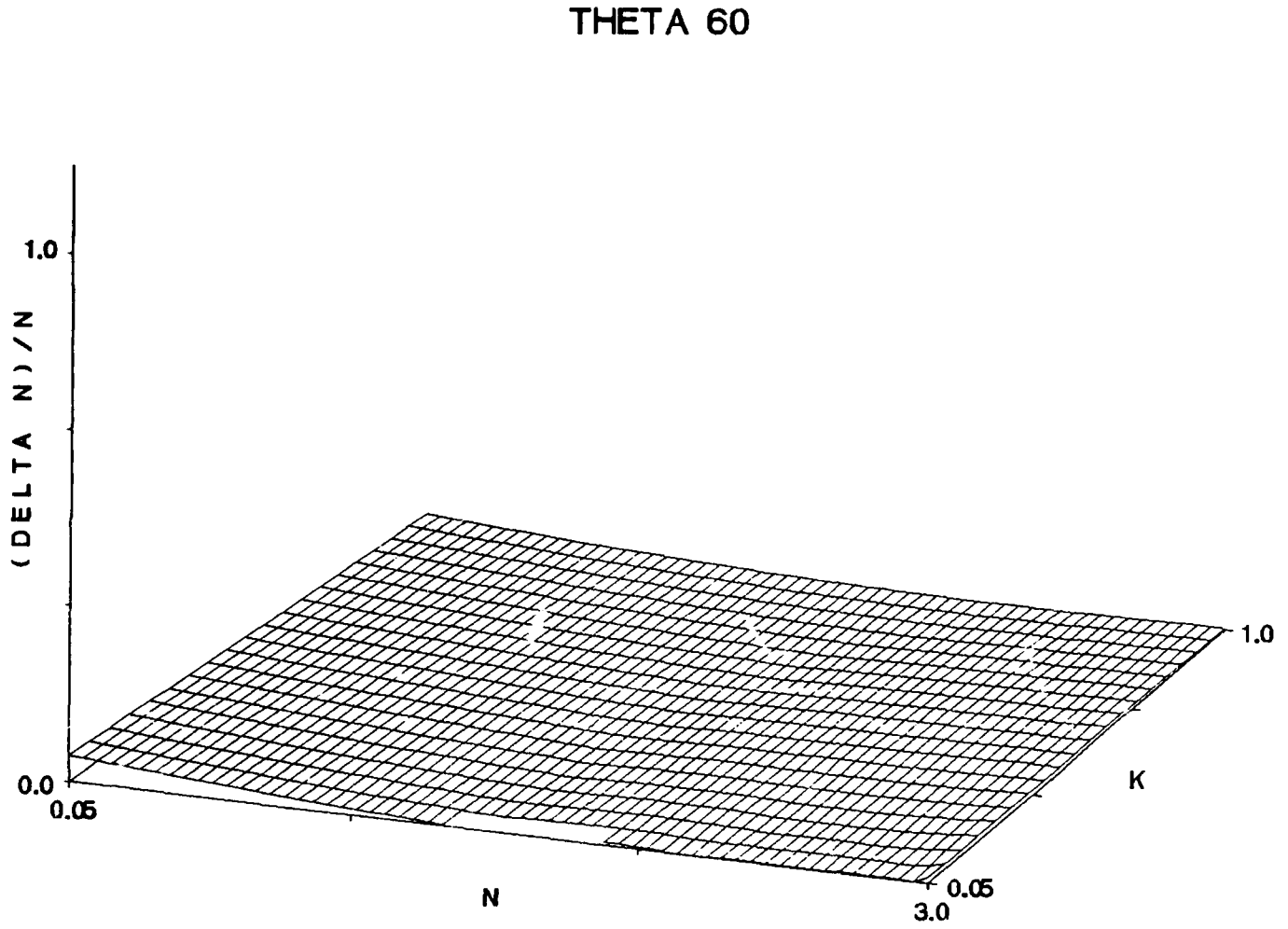

FIG. 3.21 Same as Fig. 3.19 but with $\theta = 60°$.

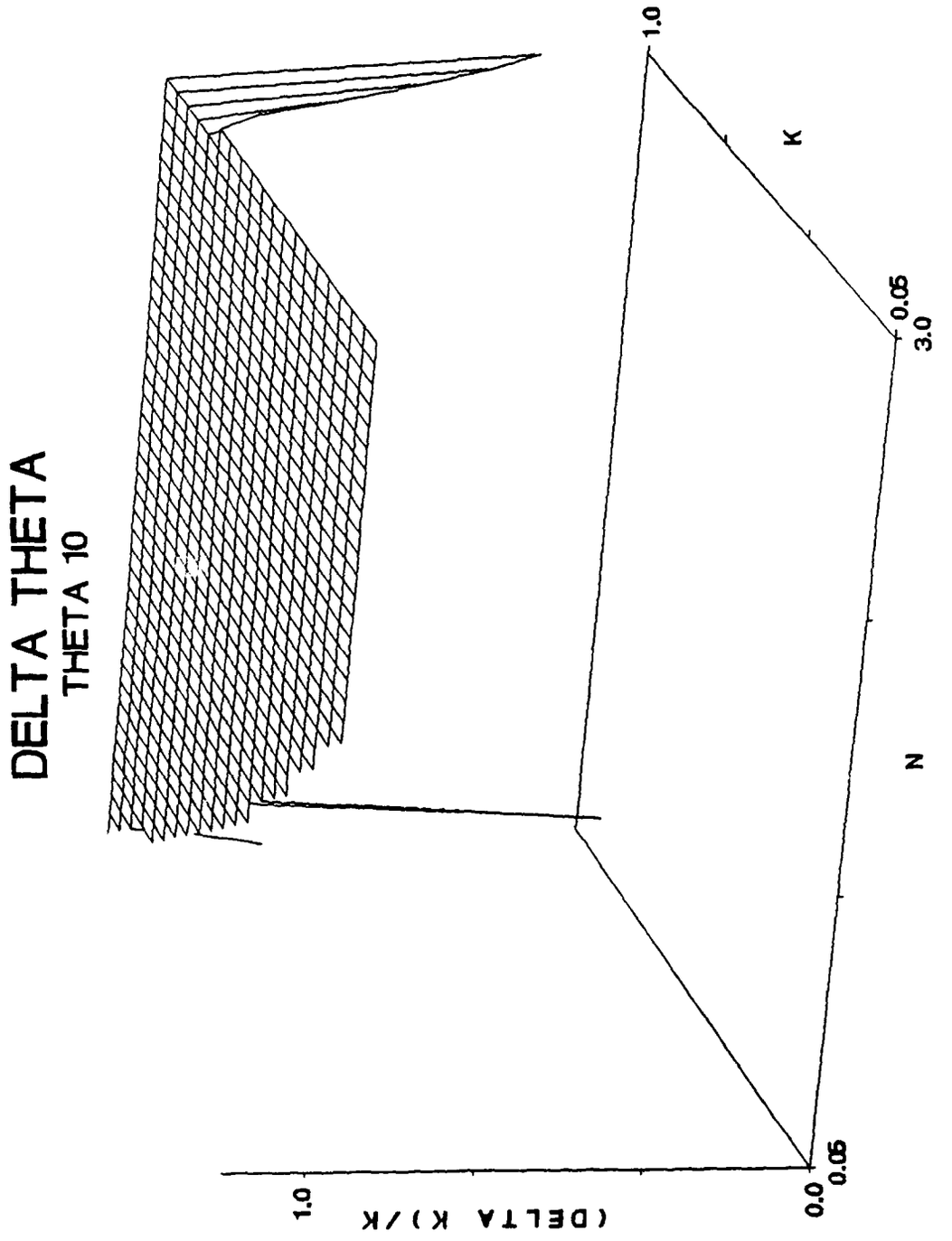

FIG. 3.22 Fractional error in k, $\Delta k/k$, increasing θ by 2% at an angle of incidence of 10°.

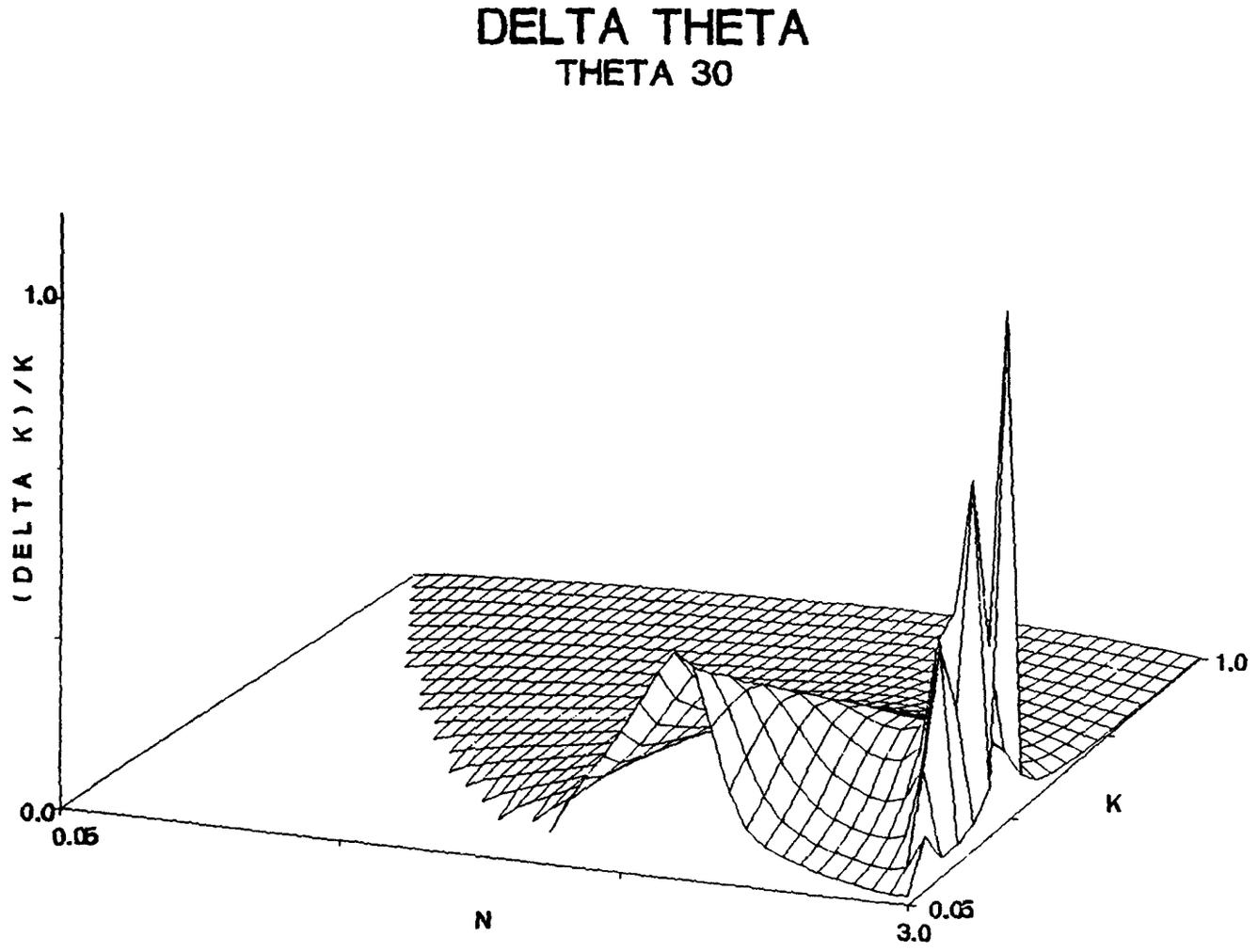

FIG. 3.23 Same as Fig. 3.22 but with $\theta = 30°$.

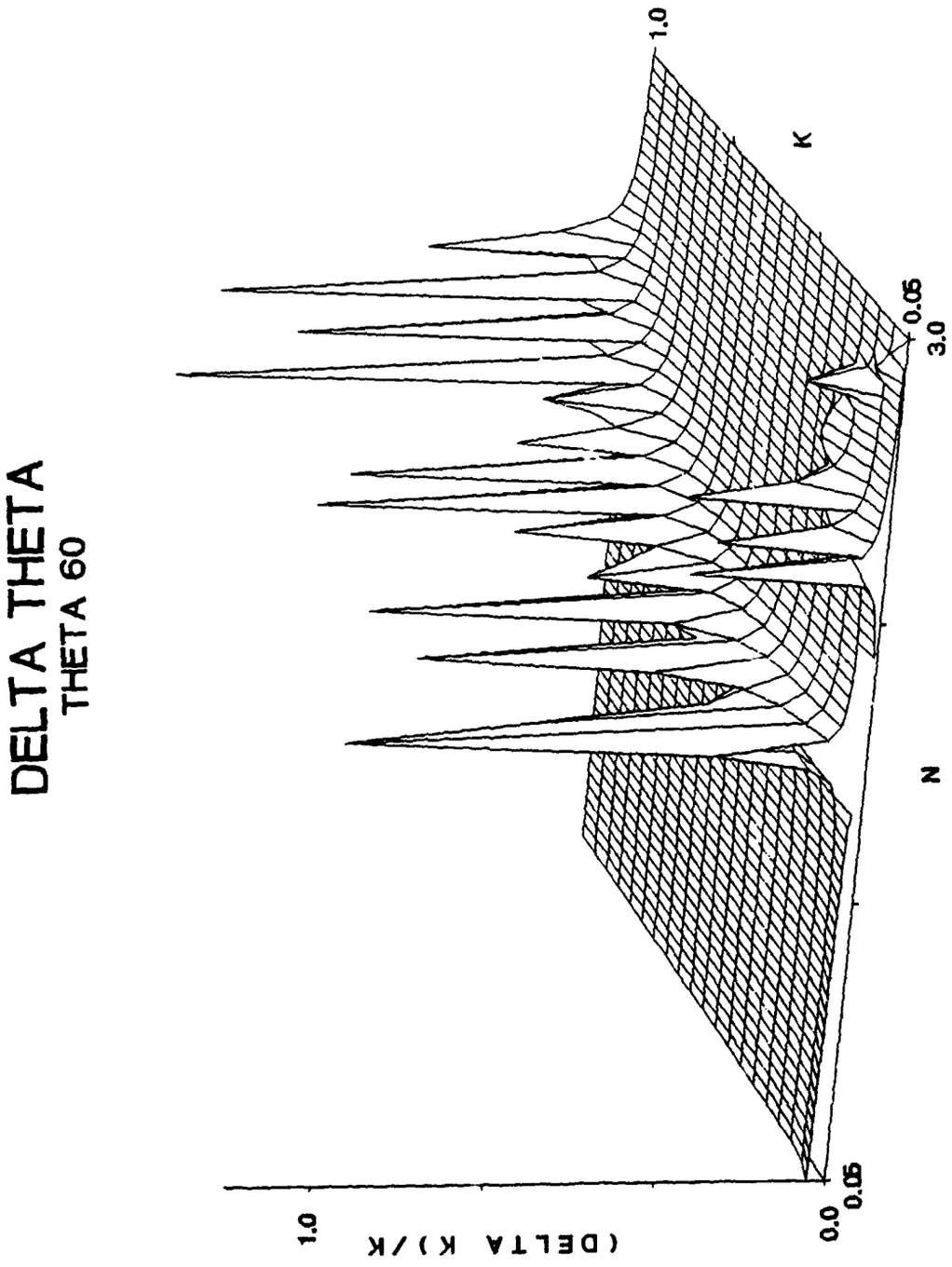

FIG. 3.24 Same as Fig. 3.22 but with $\theta = 60°$.

c. DESCRIPTION OF EQUIPMENT

The equipment employed in the acquisition of the reflection coefficients is comprised of two major components, the polarizer and the sample mount. The polarizer was a Cleveland Crystals Model 1600 IR polarizer mounted in a custom built frame. The polarizer was able to be rotated to any desirable angle and was calibrated by locating the extinction points from the output of the polarized CO_2 laser. Construction drawings are currently being prepared and will be submitted when available.

The sample mount was custom built allowing for a continuous variation of the angle of incidence and for accurate positioning of the sample surface. The sample was mounted on a gimble and translation stage. The gimble allowed for tilting of the sample to place the surface normal in a horizontal plane coincident with the IR light. The translation stage allowed the surface to be placed coincident with the axis of rotation of the table. The alignment procedure invovled an iterative process in which the sample tilt was adjusted to bring the light coincident with the detector, the angle of incidence was changed and the sample translated to again bring the light coincident with the detector. The tilt was adjusted if necessary and the procedure repeated until adjustments were minimal. Again construction drawings are being prepared and will be forwarded when available.

d. ACQUISITION OF DATA

All data was acquired under computer control using the program listed in appendix 3.2, AMENU. The data was reduced and n and k was determined by the program QUERRY, in appendix 3.1. The data necessary to obtain the reflection coefficients was obtained using the following procedure:

1. Polarizer adjusted to provide either R_s or R_p.
2. With the sample holder empty the intensity of the CO_2 laser was determined as a function of wavelength, I_0.
3. The sample was mounted and its position adjusted to provide an accurate determination of the angle of incidence.
4. The CO_2 laser was tuned to the appropriate line and the dither stabilizer unit was activated.
5. The sample and reference lock-in amplifiers were adjusted with respect ot phase, amplitude, and time constant.
6. The operating parameters were input into the computer to be stored with the data.
7. The amplitudes of the lock-ins were read and the data stored to disk.
8. For each wavelength several angles of incidence were used providing a variety of reflection coefficients.
9. The procedure from step 4 was repeated until all possible wavelengths had been measured.
10. After obtaining the raw data the files were reduced and a master file containing wavelenght, angle of incidence, R_s, and R_p was created for each sample.
11. The reflection coefficients were then input into the computer program QUERRY for determination of n and k.

Table 3.1 provides a listing of representative data prior to the determination of the reflection coefficients. Notice that several angles of incidence are associated with each wavelength of incident light.

TABLE 3.1

Raw data for Querry's method

Wavelength (μm)	Angle (degrees)	Sample Lock-in (V)	Reference Lock-in (V)	Power Meter (W)
10.741	16.95	1.164E-02	1.037E-01	2.13
10.741	37.05	1.475E-02	1.014E-01	2.13
10.741	41.00	1.609E-02	1.021E-01	2.14
10.741	45.00	1.827E-02	1.005E-01	2.13
10.741	51.10	2.877E-02	9.878E-02	2.14
10.741	57.10	3.837E-02	9.907E-02	2.14
10.741	61.10	4.216E-02	9.964E-02	2.14
10.741	66.90	5.410E-02	9.831E-02	2.14
10.696	17.00	4.543E-02	7.271E-02	2.08
10.696	16.90	4.453E-02	7.354E-02	2.08
10.696	22.85	6.136E-02	1.488E-01	2.08
10.696	37.10	3.506E-02	1.522E-01	2.08
10.696	41.00	3.697E-02	1.541E-01	2.08
10.696	44.85	1.126E-01	1.575E-01	2.07
10.696	51.10	5.466E-02	1.570E-01	2.08
10.696	57.10	6.973E-02	1.593E-01	2.07
10.696	61.00	7.512E-02	1.606E-01	2.07
10.696	67.00	1.273E-01	1.635E-01	2.08
10.632	16.90	2.978E-01	4.998E-01	1.12
10.632	22.85	3.137E-02	2.151E-01	1.11
10.632	37.10	6.759E-02	2.177E-01	1.11
10.632	41.05	4.204E-02	2.197E-01	1.10
10.632	45.00	4.925E-02	2.213E-01	1.10
10.632	50.95	4.164E-02	2.243E-01	1.10
10.632	50.95	1.196E-01	2.245E-01	1.09
10.632	61.10	1.258E-01	2.242E-01	1.09
10.632	67.00	1.587E-01	2.236E-01	1.10
10.571	17.75	3.690E-02	1.853E-01	3.51
10.571	22.95	2.832E-02	1.865E-01	3.53
10.571	36.90	4.732E-02	1.849E-01	3.52
10.571	41.05	3.314E-02	1.859E-01	3.53
10.571	45.05	3.767E-02	1.857E-01	3.53
10.571	51.00	3.748E-02	1.860E-01	3.54
10.571	56.90	9.222E-02	1.855E-01	3.54
10.571	61.00	1.065E-01	1.858E-01	3.55
10.571	67.00	1.070E-01	1.850E-01	3.54

The data from Table 3.1 is then reduced using the I_0 which had been measured prior to the sample insertion. In Table 3.2 we present the reflection coefficient, with the plane of polarization perpendicular to the plane of incidence, as a function of wavelength and angle of incidence. The results for a wavelength of 10.741 are shown in Fig. 3.25. The power meter readings from Table 3.1 are not used in the computation since they do not provide the sensitivity necessary and are not as accurate as the measurements from the pyroelectric detectors, they are simply measured for completeness.

Similar data for each sample was obtained for the other polarization state, R_p, and the data was reduced. After both sets of data were obtained the files were merged and read into the program to determine the complex refractive index. One difficulty which arose while reducing the data was with the expression given in Eq. 3.4. This quantity must always be positive in order to provide the square root needed in computing k given by Eq. 3.2. However, due to the noise in the reflection coefficients this requirement was not always met and several data points were discarded reducing the final dataset for the complex refractive index to approximately 20 points.

TABLE 3.2

Analyzed data for Querry's method

Wavelength (μm)	Angle (Degrees)	R_S
10.741	16.95	2.440E-02
10.741	37.05	3.161E-02
10.741	41.00	3.423E-02
10.741	45.00	3.949E-02
10.741	51.10	6.327E-02
10.741	57.10	8.412E-02
10.741	61.10	9.192E-02
10.741	66.90	1.195E-01
10.696	17.00	6.173E-02
10.696	16.90	5.983E-02
10.696	22.85	4.076E-02
10.696	37.10	2.276E-02
10.696	41.00	2.370E-02
10.696	44.85	7.064E-02
10.696	51.10	3.439E-02
10.696	57.10	4.324E-02
10.696	61.00	4.622E-02
10.696	67.00	7.691E-02
10.632	16.90	1.194E-01
10.632	22.85	2.922E-02
10.632	37.10	6.219E-02
10.632	41.05	3.834E-02
10.632	45.00	4.459E-02
10.632	50.95	3.720E-02
10.632	50.95	1.067E-01
10.632	61.10	1.124E-01
10.632	67.00	1.422E-01
10.571	17.75	5.074E-02
10.571	22.95	3.868E-02
10.571	36.90	6.521E-02
10.571	41.05	4.541E-02
10.571	45.05	5.169E-02
10.571	51.00	5.133E-02
10.571	56.90	1.266E-01
10.571	61.00	1.461E-01
10.571	67.00	1.474E-01

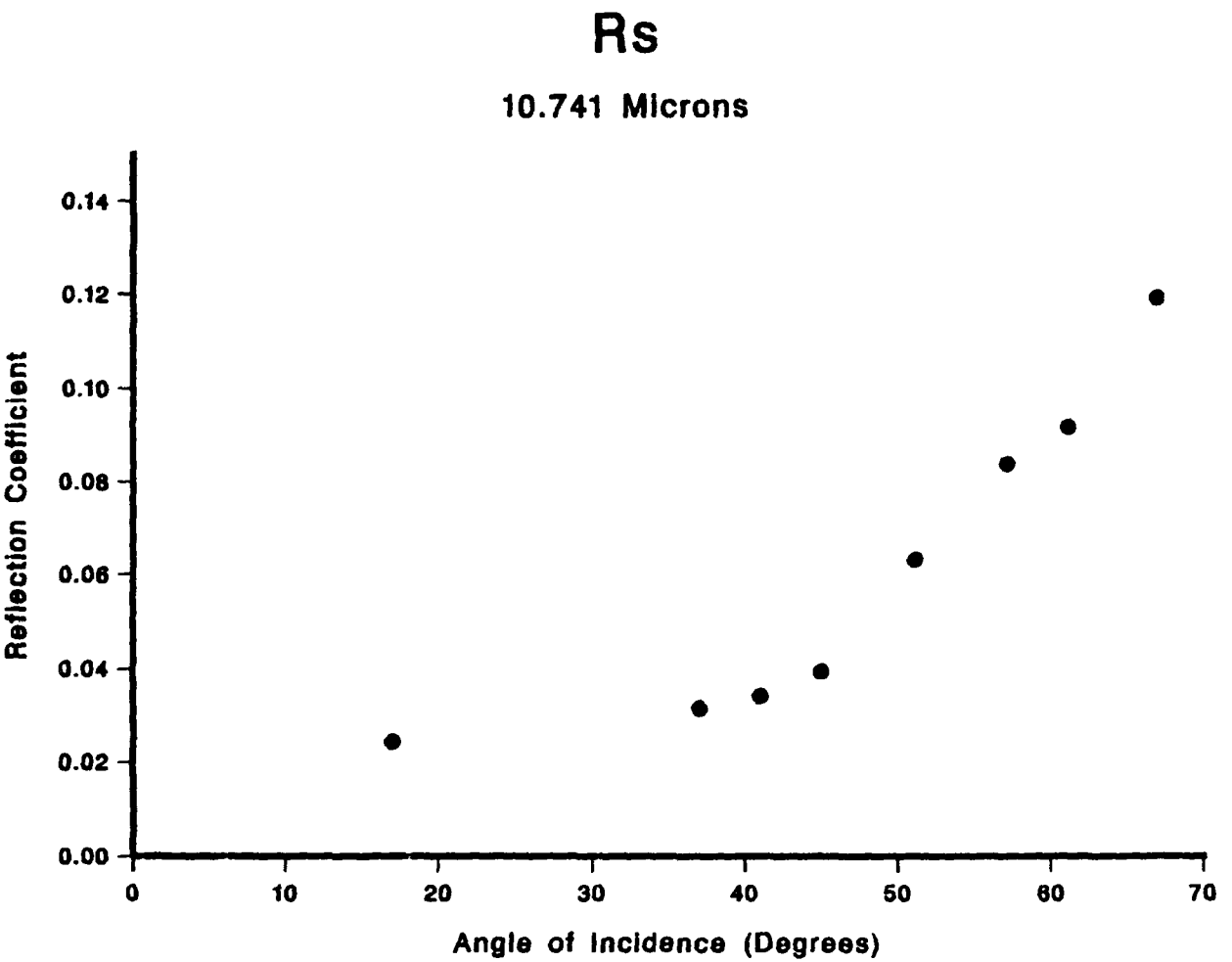

FIG. 3.25 Experimental reflection coefficients with E perpendicular to the plane of incidence at several angles.

e. RESULTS

The results obtained using the procedure set forth in the previous section are presented here in both tabular and graphical format. The complex refractive index as determined using Querry's method is compared to that determined from near normal reflection measurements and Kramers-Kronig analysis.[2]

The complex refractive index for Illite is presented in Table 3.3 and in Figs. 3.26 and 3.27. The table gives n and k as a function of wavelength and wavenumber. The standard deviation for each, n and k, is given in columns 4 and 5. The last column represents the number of pairs of the reflection coefficients have been used in determining the complex refractive index. If only one pair was employed the corresponding standard deviation was set equal to 0. The figures represent n and k as functions of wavenumber only with the error bars +/- one standard deviation from the calculated value for either n or k. The fact the complex refractive index is almost constant for both n and k and that the error bars are large indicate a need for a more accurate determination of the reflection coefficients. The sparseness of the data points as determined by Querry's method also are an indication of the large error in the reflection coefficients.

The complex refractive index for Kaolin is presented in Table 3.4 (the format is the same as in Table 3.3)and in Figs. 3.28 and 3.29 . The results are not much different from that for illite. Again the indication is that the reflection coefficients are poorly determined.

The complex refractive index for Montmorillinite is presented in Table 3.5 and in Figs. 3.30 and 3.31. The close agreement in k between 920 and 1000 cm^{-1} is not from an accurate determination of the refractive index but is purely coincidental.

TABLE 3.3

Complex Refractive Index for Illite

ν (cm^{-1})	λ (μm)	n	k	Δn	Δk	n_T
940.56	10.6320	0.913	0.176	0.099	0.106	3.000
945.98	10.5710	1.017	0.195	0.368	0.016	2.000
947.78	10.5510	1.017	0.255	0.243	0.126	4.000
951.20	10.5130	1.209	0.236	0.309	0.120	3.000
952.93	10.4940	1.139	0.263	0.140	0.113	3.000
975.90	10.2470	0.974	0.291	0.203	0.115	4.000
977.23	10.2330	1.229	0.158	0.482	0.133	3.000
978.47	10.2200	1.079	0.146	0.000	0.000	1.000
982.13	10.1820	0.879	0.158	0.202	0.042	3.000
983.19	10.1710	1.130	0.163	0.649	0.062	2.000
984.35	10.1590	0.971	0.167	0.295	0.116	3.000
985.42	10.1480	0.946	0.235	0.215	0.155	4.000
1037.45	9.6390	0.945	0.356	0.158	0.157	3.000
1041.34	9.6030	1.868	0.454	0.425	0.143	4.000
1043.19	9.5860	0.888	0.295	0.396	0.174	7.000
1045.04	9.5690	1.203	0.350	0.403	0.199	5.000
1046.90	9.5520	0.301	0.016	0.000	0.000	1.000
1048.66	9.5360	1.357	0.287	0.486	0.171	5.000

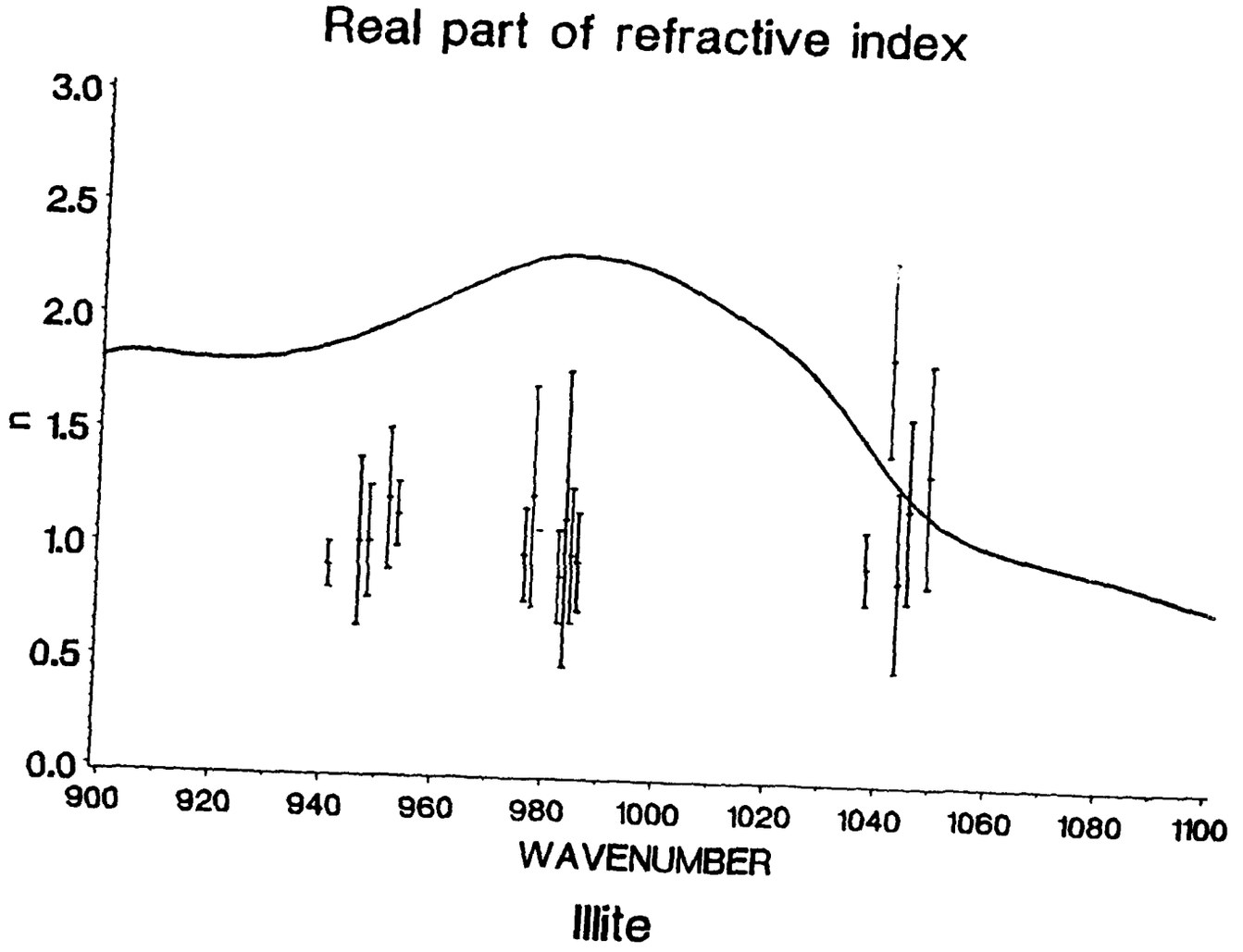

FIG. 3.26 Refractive index for Illite in the spectral region 900 to 1100 cm^{-1}. The laser data is represented by the symbols with the error bars representing +/- one standard deviation. The solid line is from Querry.

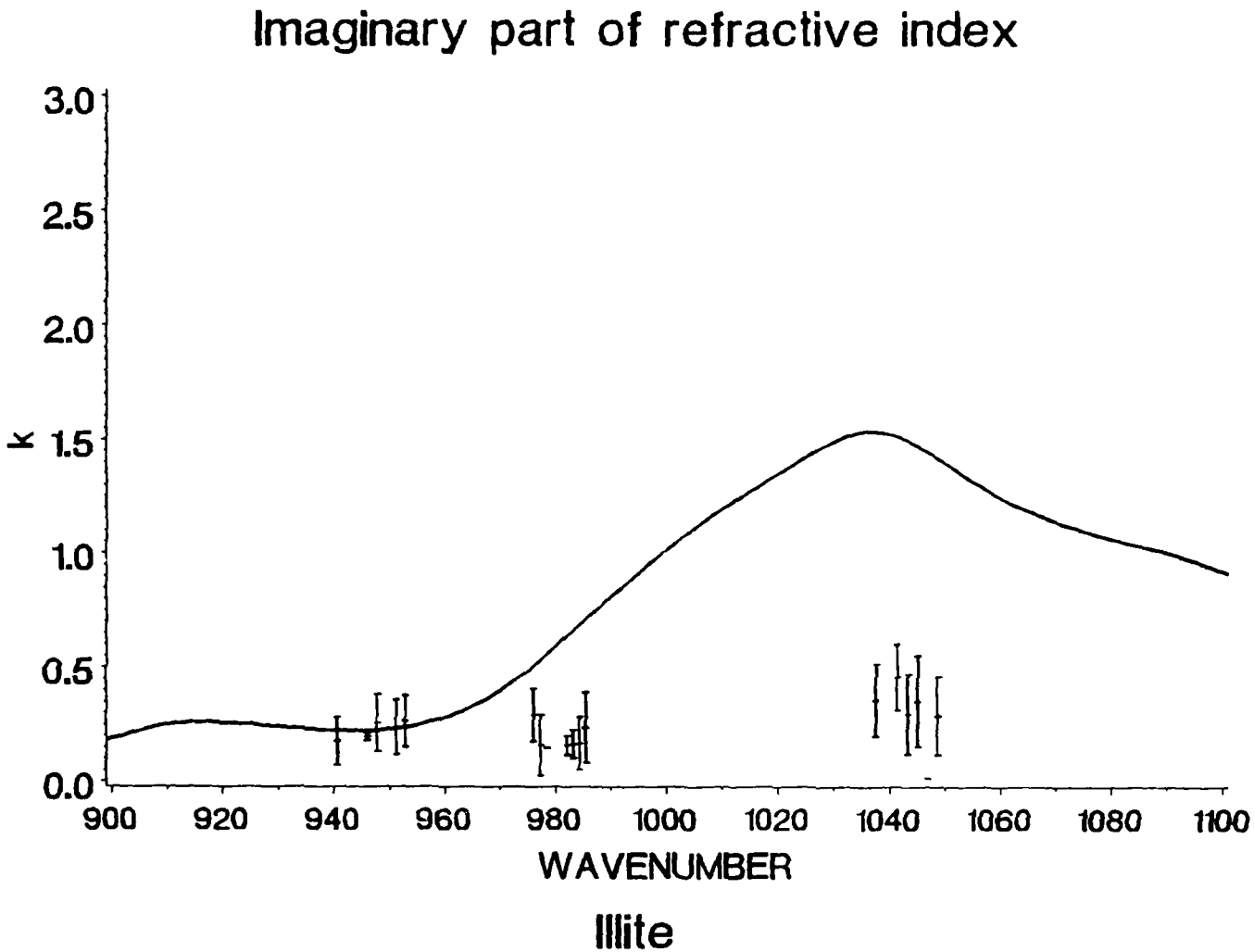

FIG. 3.27 Extinction coefficient for Illite in the spectral region 900 to 1100 cm^{-1}. The laser data is represented by the symbols with the error bars representing +/- one standard deviation. The solid line is from Querry.

TABLE 3.4

Complex refractive index for kaolin

ν (cm^{-1})	λ (μm)	n	k	Δn	Δk	n_T
931.01	10.7410	1.268	0.442	0.362	0.067	4.000
932.92	10.7190	1.565	0.297	0.786	0.205	3.000
940.56	10.6320	0.957	0.073	0.041	0.040	3.000
945.98	10.5710	1.384	0.267	0.557	0.155	5.000
947.78	10.5510	1.284	0.547	0.349	0.125	7.000
951.20	10.5130	0.994	0.396	0.125	0.098	4.000
952.93	10.4940	1.050	0.196	0.466	0.029	3.000
971.91	10.2890	1.090	0.384	0.324	0.150	6.000
975.90	10.2470	1.046	0.276	0.831	0.106	3.000
977.23	10.2330	1.485	0.300	1.227	0.231	2.000
978.47	10.2200	1.230	0.344	0.282	0.090	3.000
980.87	10.1950	1.486	0.582	0.496	0.205	5.000
982.13	10.1820	1.326	0.234	0.897	0.125	4.000
983.19	10.1710	1.096	0.315	0.559	0.154	5.000
984.35	10.1590	0.959	0.383	0.670	0.206	5.000
985.42	10.1480	1.059	0.194	0.239	0.093	3.000
1043.19	9.5860	1.074	0.635	0.640	0.314	6.000
1048.66	9.5360	1.288	0.457	1.292	0.414	4.000
1050.53	9.5190	0.677	0.242	0.094	0.150	4.000
1052.19	9.5040	0.265	0.033	0.000	0.000	1.000
1053.96	9.4880	0.279	0.055	0.017	0.073	2.000

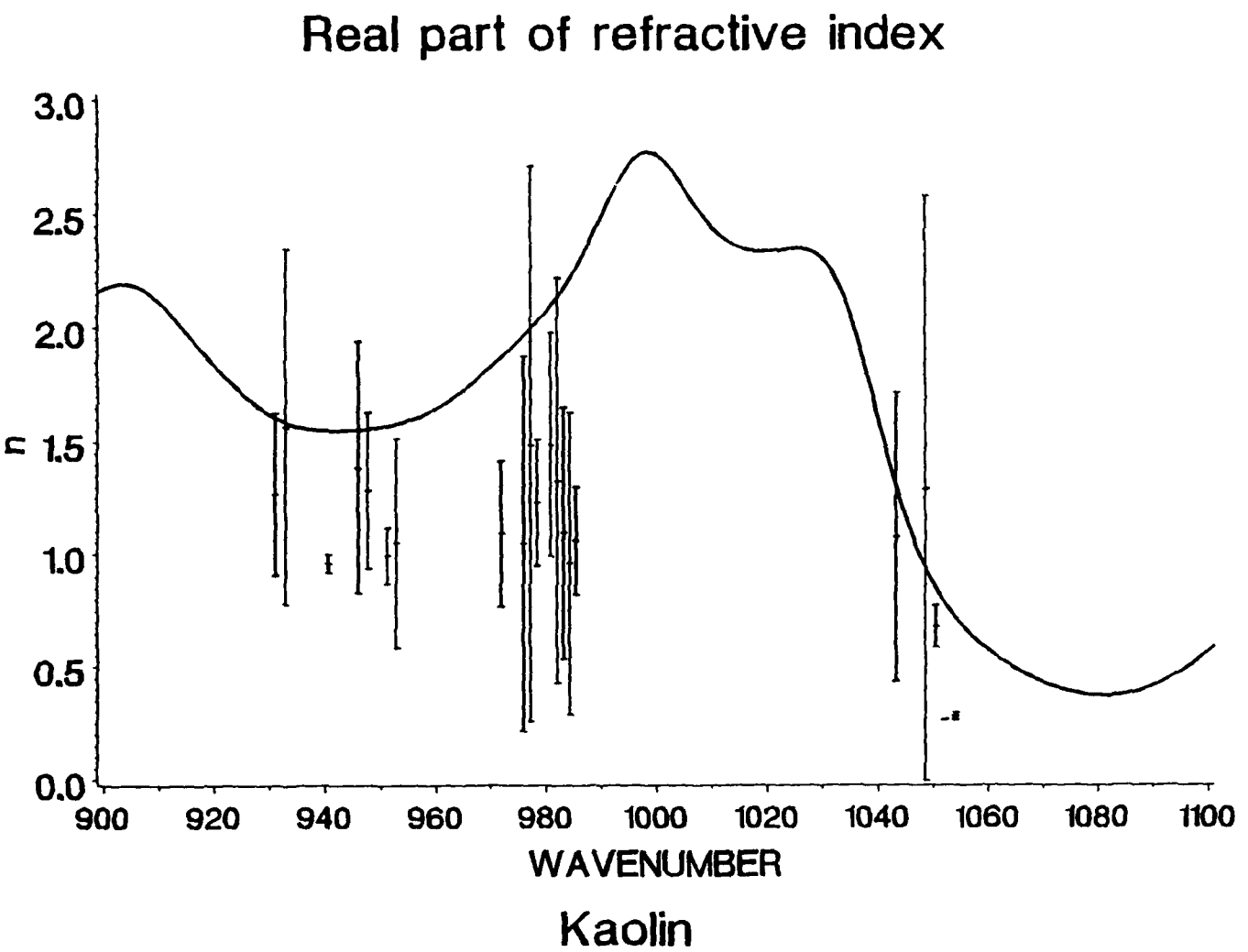

FIG. 3.28 Refractive index for Kaolin in the spectral region 900 to 1100 cm^{-1}. The laser data is represented by the symbols with the error bars representing +/- one standard deviation. The solid line is from Querry.

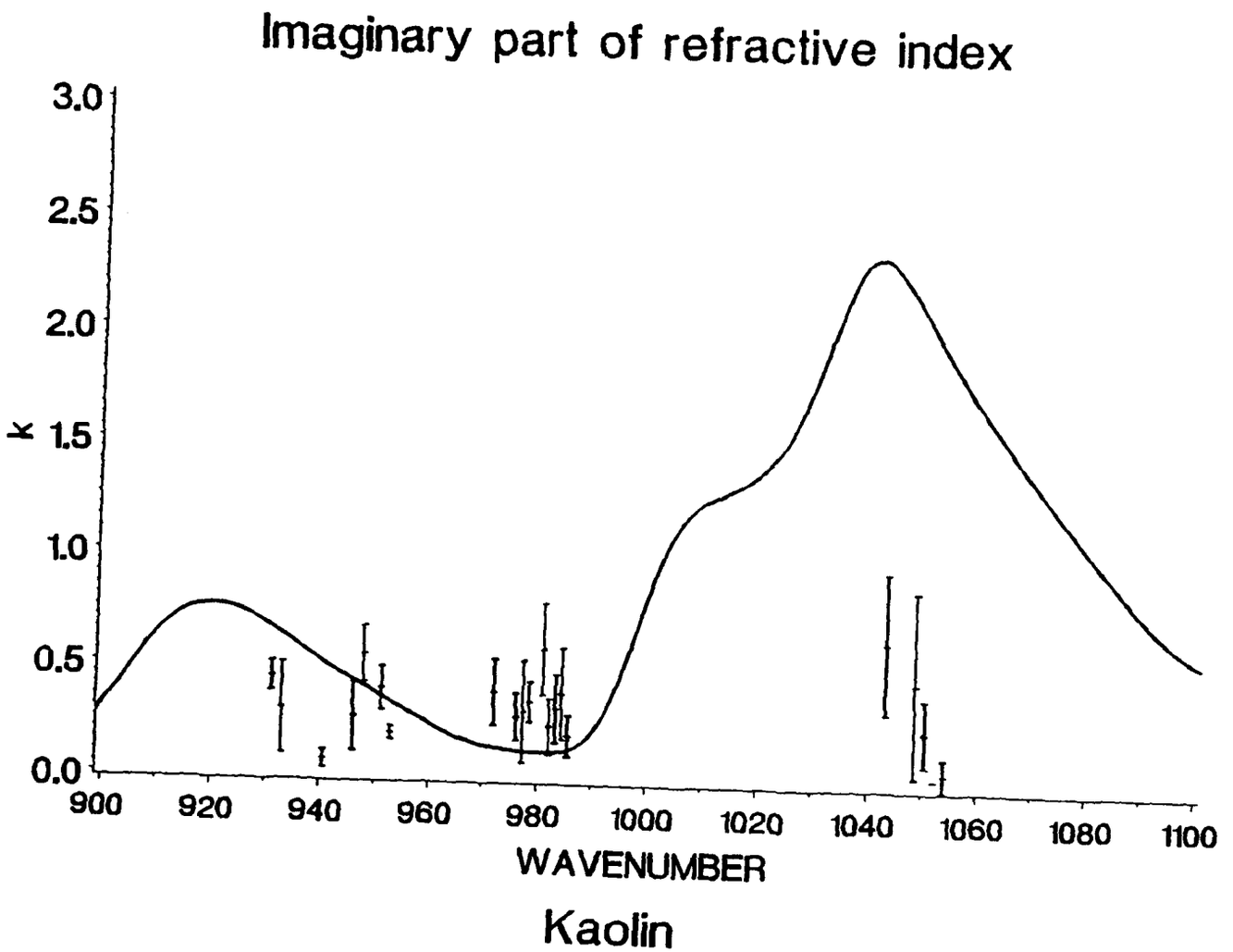

FIG. 3.29 Extinction coefficient for Kaolin in the spectral region 900 to 1100 cm^{-1}. The laser data is represented by the symbols with the error bars representing +/- one standard deviation. The solid line is from Querry.

TABLE 3.5

Complex refractive index for montmorillinite

ν (cm^{-1})	λ (μm)	n	k	Δn	Δk	n_T
931.01	10.7410	1.169	0.222	0.411	0.054	2.000
932.92	10.7190	1.079	0.232	0.319	0.058	3.000
940.56	10.6320	0.928	0.125	0.000	0.000	1.000
945.98	10.5710	1.086	0.158	0.095	0.009	3.000
947.78	10.5510	1.158	0.282	0.022	0.150	2.000
949.49	10.5320	1.011	0.229	0.217	0.092	2.000
951.20	10.5130	1.270	0.497	0.360	0.248	4.000
952.93	10.4940	0.950	0.247	0.235	0.082	4.000
975.90	10.2470	1.133	0.323	0.000	0.000	1.000
978.47	10.2200	1.118	0.263	0.151	0.080	3.000
980.87	10.1950	0.929	0.408	0.348	0.130	6.000
982.13	10.1820	1.022	0.100	0.138	0.028	2.000
983.19	10.1710	1.297	0.302	0.111	0.203	3.000
985.42	10.1480	1.108	0.264	0.431	0.116	4.000
1035.52	9.6570	1.167	0.317	0.340	0.164	5.000
1037.45	9.6390	1.198	0.495	0.325	0.154	6.000

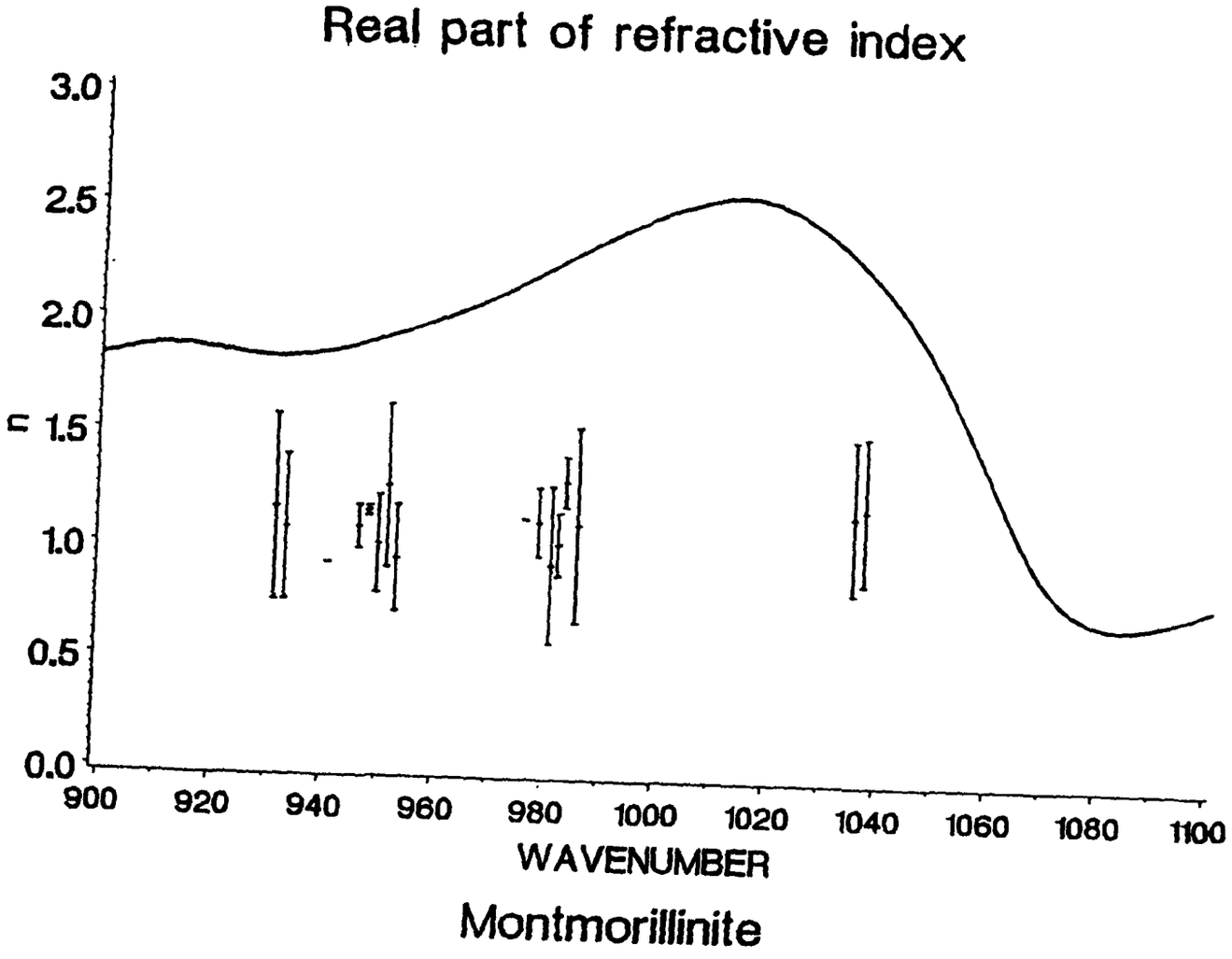

FIG. 3.30 Refractive index for Montmorillinite in the spectral region 900 to 1100 cm^{-1}. The laser data is represented by the symbols with the error bars representing +/- one standard deviation. The solid line is from Querry.

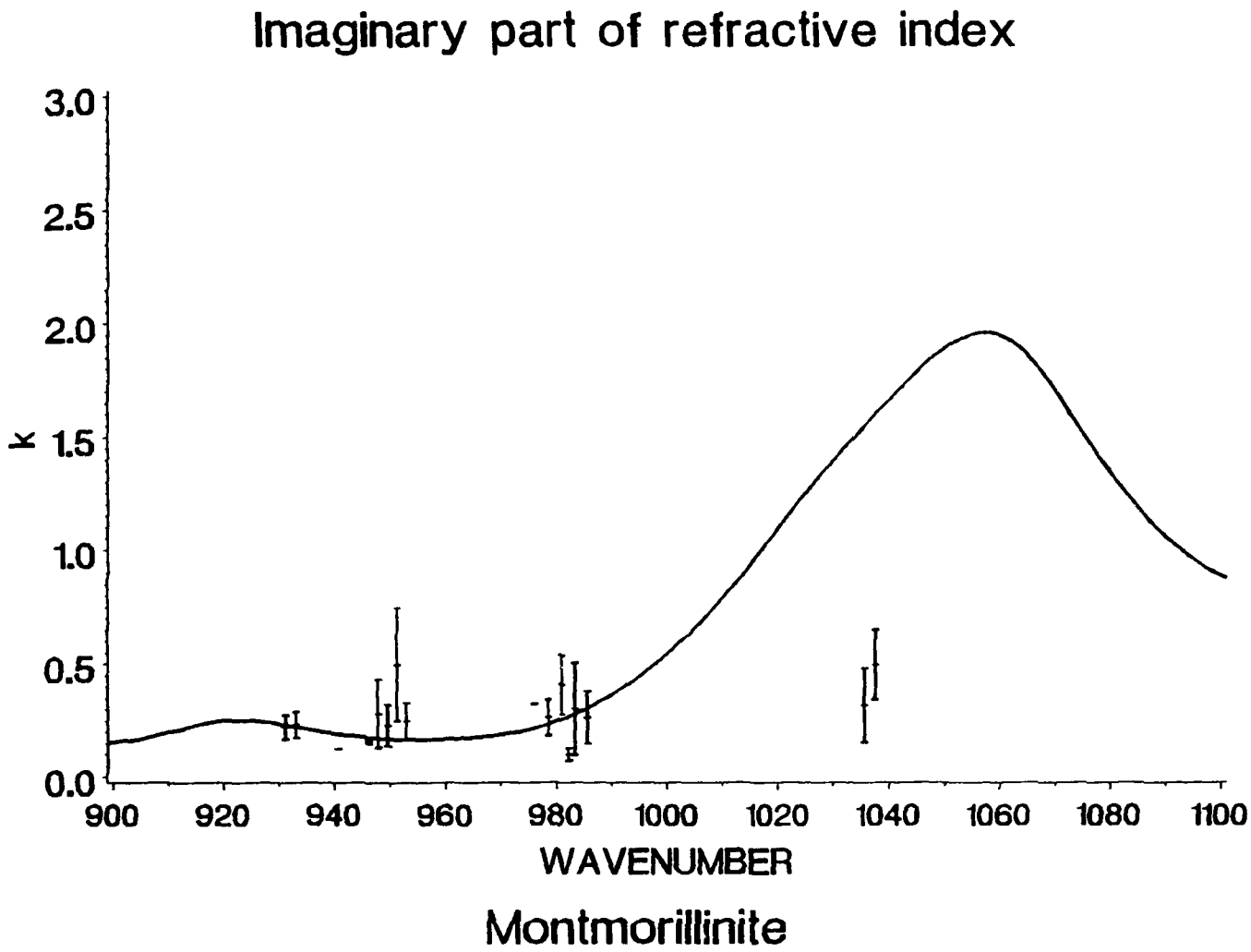

FIG. 3.31 Extinction coefficient for Montmorillinite in the spectral region 900 to 1100 cm^{-1}. The laser data is represented by the symbols with the error bars representing +/- one standard deviation. The solid line is from Querry.

f. CONCLUSION

The results presented are indicative of the technique proposed by Querry[1]. The graphs of the fractional uncertainty in n and k show that the complex refractive index is very sensitive to accurate determinations of the reflection coefficients and the angle of incidence. The samples in this section for which the optical constants were determined were pressed pellets. Although, every precaution was made to provide a good surface the inherent roughness of the surface leads to a diffuse reflection from the sample surface and therefore a large uncertainty in the reflection coefficients. From Figs. 3.10 - 3.18 it is seen that even a 2% change in the reflection coefficient can produce a 100% error in the complex refractive index. Since the surface roughness is inherent in these samples it is unlikely the results can be improved to match those obtained by Kramers-Kronig analysis. One possibility is to measure the reflectance from the pellet and then coat the surface with aluminum and measure the reflectance from this aluminized surface. If the aluminum film is thin enough the underlying roughness will be carried over to the aluminum surface. A comparison of the reflection coefficients from this roughened aluminum surface can then be made to a smooth surface and the corresponding reflection coefficients of the clay sample could be adjusted appropriately. The technique is extremely sensitive to the experimentally measured quantities but it is felt the uncertainty in these values can be reduced to appropriate values for smooth surfaces.

[1]Marvin R. Querry, "Direct Solution of the Generalized Fresnel Reflectance Equations," J. Optical Society of Amer., 59, 876, 1969.

[2]Marvin R. Querry, private communication

Blank

g. APPENDIX 3.1

Program Querry

g. Appendix 3.1

Program QUERRY

```
      PROGRAM QUERRY
C*************************************************************************
C
C WRITTEN MAY 10, 1988 BY DAVID WIELICZKA
C
C
C PROGRAM POLAR EMPLOYS QUERRY'S METHOD IN DETERMINING THE COMPLEX
C REFRACTIVE INDEX.  THE INPUT PARAMETERS ARE WAVELENGTH, ANGLE OF
C INCIDENCE, REFLECTION WITH E PERP. TO PLANE OF INCIDENCE, REFLECTION
C WITH E PARALLEL TO PLANE OF INCIDENCE.
C
C MARVIN R. QUERRY, J. OPTICAL SOC. AMER.,59, 876-877, 1969
C*************************************************************************

C*************************************************************************
C
C VARIABLE LIST
C
C BRN-REAL PART OF COMPLEX REFRACTIVE INDEX EQN. 5 FROM QUERRY'S PAPER
C COMK-IMAGINARY PART OF THE COMPLEX REFRACTIVE INDEX EQN. 4 FROM QUERRY'S
C PAPER
C CONVERT-CONVERSION FACTOR FROM DEGREES TO RADIANS
C CTHETA-COSINE OF THE ANGLE OF INCIDENCE
C F- EQN. 6A FROM QUERRY'S PAPER
C FINALK-AVERAGE K VALUE FOR ALL ANGLES OF INCIDENCE FOR A GIVEN WAVELENGTH
C FINALN-AVERAGE N VALUE FOR ALL ANGLES OF INCIDENCE FOR A GIVEN WAVELENGTH
C G-EQN. 7A FROM QUERRY'S PAPER
C IFLAG-FLAG USED TO MONITOR IF THE READ HAS REACHED THE END OF THE
C  DATA  FILE
C JCNT-INCREMENTAL NUMBER OF EXPERIMENTAL DATA VALUES FOR A GIVEN WAVELENGTH
C NP-NUMBER OF EXPERIMENTAL DATA VALUES FOR A GIVEN WAVELENGTH
C P2-EQUATION 6 FROM QUERRY'S PAPER
C Q-EQUATION  7 FROM QUERRY'S PAPER
C RP-EXPERIMENTAL REFLECTION COEF. FOR E PAR. TO PLANE OF INCIDENCE
C RPT-TEMPORARY STORAGE FOR RP
C RS-EXPERIMENTAL REFLECTION COEF. FOR E PERP. TO PLANE OF INCIDENCE
C RST-TEMPORARY STORAGE FOR RS
C SIGMAK-STANDARD DEVIATION FOR IMAGINARY PART OF COMPLEX REFRACTIVE INDEX
C SIGMAN-STANDARD DEVIATION FOR REAL PART OF COMPLEX REFRACTIVE INDEX
C SNP-NUMBER OF N AND K VALUES USED IN DETERMINING SUMK2,SUMN2,TOTALK, AND
C TOTALN
C STHETA-SINE OF THE ANGLE OF INCIDENCE
C SUMK2-SUM OF THE SQUARE OF THE IMAG. PART OF THE COMPLEX REFRACTIVE INDEX
C FOR A GIVEN WAVELENGTH
C SUMN2-SUM OF THE SQUARE OF THE REAL PART OF THE COMPLEX REFRACTIVE INDEX
C FOR A GIVEN WAVELENGTH
C THETA- ANGLE OF INCIDENCE
C THETAT-TEMPORARY STORAGE FOR THE ANGLE OF INCIDENCE
```

```
C TTHETA-TANGENT OF THE ANGLE OF INCIDENCE
C T2THETA-TANGENT OF TWICE THE ANGLE OF INCIDENCE
C TOTALK-SUM OF THE IMAG. PART OF THE COMPLEX REFRACTIVE INDEX FOR A GIVEN
C  WAVELENGTH
C TOTALN-SUM OF THE REAL PART OF THE COMPLEX REFRACTIVE INDEX FOR A GIVEN
C  WAVELENGTH
C WAVE-WAVELENGTH FOR ASSOCIATED WITH EXPERIMENTAL DATA
C WAVET-TEMPORARY STORAGE FOR WAVELENGTH
C
C**************************************************************************
      PARAMETER (CONVERT=3.14159/180.)
      IMPLICIT REAL*4 (A-H),(O-Z)
      IMPLICIT INTEGER (I-N)
      DIMENSION WAVE(50),THETA(50),RS(50),RP(50)
C*********************
C SET COUNT FOR GIVEN WAVELENGTH TO 1
C*********************
      JCNT=1
C*********************
C SET FLAG FOR MONITORING THE END OF FILE TO 1
C*********************
      IFLAG=1
C*********************
C READ IN A SET OF DATA VALUES
C*********************
C 1      READ(100,*,END=9000) WAVE(JCNT),RS(JCNT),RP(JCNT)
 1     READ(100,*,END=9000) WAVE(JCNT),THETA(JCNT),RS(JCNT),RP(JCNT)
C*********************
C IF JCNT=1 INCREMENT JCNT AND READ IN ANOTHER DATA VALUE
C
C IF JCNT IS NOT EQUAL TO 1 CHECK WAVELENGTH
C IF NEW WAVELENGTH IS EQUAL TO PREVIOUS WAVELENGTH FROM FIRST READ THEN
C READ IN A NEW DATA VALUE.
C IF NEW WAVELENGTH IS NOT EQUAL TO PREVIOUS WAVELENGTH THEN TERMINATE READ
C AND CALCULATE COMPLEX REFRACTIVE INDEX FOR THIS WAVELENGTH
C*********************
      IF (JCNT.EQ.1) THEN
  JCNT=JCNT+1
  GOTO 1
      ELSEIF (WAVE(JCNT).EQ.WAVE(1)) THEN
  JCNT=JCNT+1
  GOTO 1
      ENDIF
C*********************
C STORE THE DATA VALUES FROM THE LAST READ WHICH ARE FOR A DIFFERENT
C WAVELENGTH THEN THE OTHER VALUES IN TEMPORARY STORAGE
C*********************
      WAVET=WAVE(JCNT)
      THETAT=THETA(JCNT)
      RST=RS(JCNT)
      RPT=RP(JCNT)
C*********************
C SET FLAG TO -1
C THIS WILL BE CHECKED TO SHOW THE DATA FILE HAS MORE VALUES TO READ
```

```
C*********************
      IFLAG=-1
C*********************
C SET COUNT FOR LOOP FOR A GIVEN WAVELENGTH
C*********************
9000  NP=JCNT-1
C*********************
C ZERO VARIABLES USED IN DETERMINING THE AVERAGE COMPLEX REFRACTIVE INDEX
C AND THE STANDARD DEVIATION OF THE COMPLEX REFRACTIVE INDEX
C*********************
      TOTALN=0.0
      TOTALK=0.0
      SUMN2=0.0
      SUMK2=0.0
      SNP=0.0
C*********************
C BEGIN TO LOOP THRU DATA FOR A GIVEN WAVELENGTH AND DETEMINE COMPLEX
C REFRACTIVE INDEX FOR EACH ANGLE OF INCIDENCE
C STORE COMPELX REFRACTIVE INDEX FOR EACH ANGLE IN FILE FOR110.DAT
C*********************
      DO 1000 I=1,NP
C*********************
C THE FOLLOWING EQUATIONS ARE FROM QUERRY'S PAPER
C*********************
      STHETA=SIN(THETA(I)*CONVERT)
      CTHETA=COS(THETA(I)*CONVERT)
      TTHETA=TAN(THETA(I)*CONVERT)
      T2THETA=TAN(2.0*THETA(I)*CONVERT)
      G=(RP(I)+1.0)/(RP(I)-1.0)
      F=(RS(I)+1.0)/(RS(I)-1.0)
      Q=(F-G)*STHETA/T2THETA
      Q=Q/(G*F+(1.0-F**2)*CTHETA**2-1.0)
      P2=-1.0*(Q**2+2.0*F*Q*CTHETA+CTHETA**2)
C*********************
C IF P2 IS NEGATIVE THEN THE RESULT IS NOT PHYSICAL AND THE DATA POINT IS NOT
C USED IN DETERMINING THE AVERAGE COMPLEX REFRACTIVE INDEX
C*********************
      IF (P2.LT.0.0) GOTO 1000
C*********************
C CALCULATE THE REAL PART OF THE COMPLEX REFRACTIVE INDEX
C*********************
      BRN=SQRT(0.5*(Q**2-P2+STHETA**2+SQRT((P2-Q**2-STHETA**2)**2
     1+4.0*P2*Q**2)))
C*********************
C CALCULATE THE IMAGINARY PART OF THE COMPLEX REFRACTIVE INDEX
C*********************
      COMK=Q*SQRT(P2)/BRN
C*********************
C STORE INDIVIDUAL COMPLEX REFRACTIVE INDEX VALUES
C*********************
      WRITE(110,*) WAVE(I),THETA(I),BRN,COMK
C*********************
C SUM THE N,K VALUES AND THE N^2 AND K^2 VALUES
C*********************
```

```
      TOTALN=TOTALN+BRN
      TOTALK=TOTALK+COMK
      SUMN2=SUMN2+BRN**2
      SUMK2=SUMK2+COMK**2
C*********************
C INCREMENT THE COUNTER MONITORING THE NUMBER OF POINTS INCLUDED IN THE
C SUMMATION
C*********************
      SNP=SNP+1.0

1000  CONTINUE
C*********************
C DETERMINE THE AVERAGE N AND K VALUES
C*********************
 IF (SNP.EQ.0) THEN
 SNP=1.0
 ENDIF
      FINALN=TOTALN/SNP
      FINALK=TOTALK/SNP
C*********************
C DETERMINE THE STANDARD DEVIATION FOR THE ABOVE N AND K VALUES
C*********************
       SIGMAN=SQRT((SUMN2-SNP*FINALN**2)/(SNP))
       SIGMAK=SQRT((SUMK2-SNP*FINALK**2)/(SNP))
C*********************
C STORE THE COMPLEX REFRACTIVE INDEX AND STD IN FILE FOR101
C*********************
      WRITE(101,*) WAVE(1),FINALN,FINALK,SIGMAN,SIGMAK,SNP
C*********************
C REPLACE THE DATA VALUES IN TEMPORARY STORAGE INTO ARRAY ELEMENT 1
C FOR EACH VARIABLE TYPE
C*********************
      WAVE(1)=WAVET
      THETA(1)=THETAT
      RS(1)=RST
      RP(1)=RPT
C*********************
C SET ARRAY COUNTER TO 2
C*********************
      JCNT=2
C*********************
C CHECK FLAG MONITORING END OF FILE
C IF IFLAG IS -1 THEN SET IFLAG TO 0 AND READ IN MORE DATA
C IF IFLAG IS NOT -1 THEN END PROGRAM
C*********************
      IF (IFLAG.EQ.-1) THEN
  IFLAG=0
  GOTO 1
      ENDIF

999   END
```

Blank

h. APPENDIX 3.2

Program AMENU

h. Appendix 3.2

Program AMENU

```
10 'NAME:  Data Acquisition And Control (DAAC)
20 '       HEADER for BASICA
30 '
40 'FILE NAME:  DACHDR.BAS
50 '
60 'DOS DEVICE NAME:  DAAC
70 '
80 'RESERVED FUNCTION NAMES:
90 '          AINM, AINS, AINSC, AOUM, AOUS,
100 '          BINM, BINS, BITINS, BITOUS, BOUM, BOUS,
110 '          CINM, CINS, CSET, DELAY
120 'RESERVED DEF SEG VALUE NAME:  DSEG
130 '
140 'NAMES DEFINED AND USED BY HEADER:
150 '          ADAPT%, AI, COUNT, FOUND%,
160 '          HNAME$, SG%, STAT%
170 '
180 '
190 'When using the BASICA Interpreter, this header
200 'must be executed before any function calls are
210 'made that access the DAAC adapter.  It initializes
220 'a number of variables for each function call.  These
230 'variables are reserved and should not be used except
240 'to access the DAAC adapter.  This routine also does a
250 'DEF SEG to the segment where the DAAC Device Driver
260 '(DAC.COM) is loaded.  If you execute a DEF SEG to
270 'access other hardware, you must DEF SEG to the segment
280 'of the DAAC Device Driver before any subsequent
290 'calls to access the DAAC adapter.
300 '
310 '
320 FOUND% = 0
330 SG% = &H2E
340 'Start searching the interrupt vectors until you find
350 'one that points to the DAAC device driver.
360 'Do a DEF SEG to that segment.
370 WHILE ((SG% <= &H3E) AND (FOUND% = 0))
380       DEF SEG = 0
390       DSEG = PEEK(SG%) + PEEK(SG% + 1) * 256
400       DEF SEG = DSEG
410       HNAME$=""
420       FOR AI=10 TO 17
430                 HNAME$ = HNAME$ + CHR$(PEEK(AI))
440       NEXT AI
450       IF HNAME$ = "DAAC    " AND PEEK(18) + PEEK(19) <> 0 THEN FOUND% = 1
460       SG% = SG% + 4
470 WEND
```

```
480 IF FOUND% = 0 THEN PRINT "ERROR: DEVICE DRIVER DAC.COM NOT FOUND" : END
490 'Now initialize all function name variables for calls
500 'to access the device driver.
510 AINM        = PEEK(&H13) * 256 + PEEK(&H12)
520 AINS        = PEEK(&H15) * 256 + PEEK(&H14)
530 AINSC       = PEEK(&H17) * 256 + PEEK(&H16)
540 AOUM        = PEEK(&H19) * 256 + PEEK(&H18)
550 AOUS        = PEEK(&H1B) * 256 + PEEK(&H1A)
560 BINM        = PEEK(&H1D) * 256 + PEEK(&H1C)
570 BINS        = PEEK(&H1F) * 256 + PEEK(&H1E)
580 BITINS      = PEEK(&H21) * 256 + PEEK(&H20)
590 BITOUS      = PEEK(&H23) * 256 + PEEK(&H22)
600 BOUM        = PEEK(&H25) * 256 + PEEK(&H24)
610 BOUS        = PEEK(&H27) * 256 + PEEK(&H26)
620 CINM        = PEEK(&H29) * 256 + PEEK(&H28)
630 CINS        = PEEK(&H2B) * 256 + PEEK(&H2A)
640 CSET        = PEEK(&H2D) * 256 + PEEK(&H2C)
650 DELAY       = PEEK(&H2F) * 256 + PEEK(&H2E)
660 'Finally, execute any call to re-initialize the
670 'device driver from any former invocation of BASIC.
680 ADAPT% = 0
690 COUNT = 1
700 STAT% = 0
710 CALL DELAY (ADAPT%, COUNT, STAT%)
720 '
730 'End of DAAC BASICA Header
740 '
1000 REM PROGRAM AMENU.BAS
1001 REM THIS PROGRAM ACQUIRES DATA FROM THE LOCK-IN AMPLIFIERS
1002 REM AND THE POWER METER AND STORES IT ON DISK IN THE FILE
1003 REM NAMED AT THE BEGINNING OF EXECUTION
1004 REM WRITTEN BY DAVID WIELICZKA
1005 REM SUPPORTED BY CRDEC UNDER CONTRACT DAAA-15-85-K-0013
1010 REM $DYNAMIC
1020 OPTION BASE 1
1030 DEFSNG A-H
1040 DEFINT I-N
1050 DEFDBL T-Z
1060 DEFSTR O-S
1061 '*************************PARAMETER LIST*****************************
1062 B - ARRAY OF DIMENSION 7 TO STORE SCAN PARAMETERS
1063 B(1) - WAVELENGTH IN MICRONS
1064 B(2) - ANGLE IN DEGREES
1065 B(3) - SAMPLE LOCK-IN SCALE
1066 B(4) - REFERENCE LOCK-IN SCALE
1067 B(5) - POWER METER SCALE
1068 B(6) - LOCK-IN TIME CONSTANT
1069 B(7) - NUMBER OF A/D CONVERSIONS TO AVERAGE
1070 IDTA - ARRAY OF LENGTH 600 TO STORE A/D CONVERSIONS IN
1071 O - ARRAY OF LENGTH 12 FOR MENU LABELS
1072 Q - ARRAY OF LENGTH 2 FOR FILENAME AND COMMENT
1074 '*********************************************************************
1075 DIM Q(2),B(7),O(12),IDTA(600)
1080 O(1)="FILENAME FOR RAW DATA: "
```

```
1090 O(2)="COMMENT: "
1100 O(3)="WAVELENGTH IN MICRONS: "
1110 O(4)="ANGLE IN DEGREES: "
1120 O(5)="SAMPLE LOCK-IN SCALE: "
1130 O(6)="REFERENCE LOCK-IN SCALE: "
1140 O(7)="POWER METER SCALE: "
1150 O(8)="TIME CONSTANT: "
1160 O(9)="NUMBER OF A/D AVERAGES: "
1170 O(10)="ACQUIRE DATA"
1180 O(11)="A/D CONVERSION CHECK"
1190 O(12)="EXIT"
     'DISPLAY MENU ON SCREEN
1200 CLS:LOCATE 1,1
1210 FOR I=1 TO 2
1220 PRINT "(";CHR$(64+I);") ";O(I);Q(I)
1230 NEXT I
1240 FOR I=3 TO 9
1250 PRINT "(";CHR$(64+I);") ";O(I);B(I-2)
1260 NEXT I
1270 FOR I=10 TO 12
1280 PRINT "(";CHR$(64+I);") ";O(I)
1290 NEXT I
1300 PRINT "PRESS THE APPROPRIATE KEY TO CONTINUE!!"
1310 P=INKEY$:IF P="" THEN 1310
1320 A=ASC(P)-64 'SUBSTRACT ASCII OFFSET FOR 'A'
1330 IF A<1 GOTO 1310 'RETURN TO INKEY IF INCORRECT KEY DEPRESSED
1340 IF A<3 GOTO 1390 'INPUT A STRING VARIABLE
1350 IF A<10 GOTO 1530 'INPUT A NUMERIC VARIABLE
1360 IF A>12 GOTO 1310 'RETURN TO INKEY IF INCORRECT KEY DEPRESSED
1370 A=A-9
1380 ON A GOTO 2000,3000,3290
1390 REM INPUT A STRING VARIABLE
1400 ON A GOTO 1410,1450
1410 PRINT O(A);
1420 INPUT Q(A)
1430 OPEN Q(A) FOR OUTPUT AS #1:PRINT #1,DATE$:CLOSE #1
1440 GOTO 1200
1450 IF Q(1)<>"" THEN GOTO 1480 'SEE IF A FILENAME HAS BEEN INPUT
1460 IF Q(1)="" THEN LOCATE 22,1:PRINT "DATA FILE NOT CREATED
1461 '     STRIKE ANY KEY TO CONTINUE!!"
1470 P=INKEY$:IF P="" THEN 1470 ELSE GOTO 1200
1480 OPEN Q(1) FOR APPEND AS #1 'WRITE COMMENT TO DISK
1490 PRINT O(A);
1500 INPUT Q(A)
1510 PRINT #1,Q(A):CLOSE #1
1520 GOTO 1200
1530 REM INPUT A REAL VARIABLE
1540 PRINT O(A);
1550 INPUT B(A-2)
1560 GOTO 1200
2000 REM ACQUIRE DATA
2005 'TEST ALL SCAN PARAMETERS FOR INPUT
2010 FOR J=1 TO 2
2020 IF Q(J)="" THEN LOCATE 23,1:PRINT "NOT ALL STRINGS ARE INPUT
```

```
2021 'STRIKE ANY KEY TO CONTINUE":GOTO 2080
2030 NEXT J
2040 FOR J=1 TO 7
2050 IF B(J)=0 THEN LOCATE 23,1:PRINT "NOT ALL SCAN PARAMETERS ARE INPUT
2051 'STRIKE ANY KEY TO CONTINUE":GOTO 2080
2060 NEXT J
2070 GOTO 2090
2080 P=INKEY$:IF P="" THEN GOTO 2080 ELSE GOTO 1200
2090 CLS
2095 'INITIALIZE VARIABLES FOR A/D CONVERSION
2100 IADAPT=0' ALL CALLS ARE TO DAC ADAPTER 0
2110 IDEVICE=9' DEVICE IS 9 FOR A/D CALLS
2120 ICHANLO=0' SCAN BEGINNING WITH CHANNEL 0 - SAMPLE LOCKIN, 1-REF. LOCKIN
2130 ICHANHI=2' SCAN TO CHANNEL 2-POWER METER
2140 ICTRL=0
2150 IMODE=0
2160 ISTOR=0
2170 COUNT=B(7)' NUMBER OF A/D TO ACQUIRE
2180 ICT=CINT(B(7))
2190 IF B(6)<1! THEN CRATE=2!*(1/B(6)) ' RATE IS TWICE THE TIME CONSTANT
2200 IF B(6)>=1! THEN CRATE = 2! ' MINIMUM RATE IS 2 READS PER SECOND
2210 ISTAT=0
2220 IX=0:IY=0
2230 C1=0:C2=0:C3=0
2240 OPEN Q(1) FOR APPEND AS #1
2245 'WRITE SCAN PARAMETERS TO DISK
2250 FOR I=1 TO 7
2260 PRINT #1,B(I);
2270 NEXT I
2280 PRINT #1,
2290 FLAG=1
2300 CALL AINSC(IADAPT,IDEVICE,ICHANLO,ICHANHI,ICTRL,IMODE,ISTOR,COUNT,CRATE,
2301 'IDTA(1),ISTAT)
2310 IF ISTAT<>0 THEN PRINT "A/D CONVERSION ERROR";ISTAT:END
2320 IF FLAG=1 THEN FLAG=0:GOTO 2300
2325 'SEPARATE A/D CHANNELS
2330 FOR J=1 TO ICT
2340 C1=C1+CSNG(IDTA((3*J)-2))
2350 C2=C2+CSNG(IDTA((3*J)-1))
2360 C3=C3+CSNG(IDTA(3*J))
2370 NEXT J
2380 C1=C1/B(7)
2390 C2=C2/B(7)
2400 C3=C3/B(7)
2405 'WRITE A/D CONVERSION TO DISK
2410 PRINT #1,C1,C2,C3
2420 CLOSE #1
2430 GOTO 1200
3000 REM CHECK A/D
3010 CLS
3020 IADAPT=0' ALL CALLS ARE TO DAC ADAPTER 0
3030 IDEVICE=9' DEVICE IS 9 FOR A/D CALLS
3040 ICHANLO=0' SCAN BEGINNING WITH CHANNEL 0 - SAMPLE LOCKIN, 1-REF. LOCKIN
3050 ICHANHI=2' SCAN TO CHANNEL 2-POWER METER
```

```
3060 ICTRL=0
3070 ISTOR=0
3080 ISTAT=0
3090 IMODE=0
3100 COUNT=2
3110 CRATE=1
3120 CALL AINSC(IADAPT, IDEVICE, ICHANLO, ICHANHI, ICTRL, IMODE, ISTOR, COUNT, CRATE,
3121 'IDTA(1), ISTAT)
3130 IF ISTAT<>0 THEN PRINT "A/D CONVERSION ERROR"; ISTAT: END
3140 C1=C1+CSNG(IDTA(1))
3150 C2=C2+CSNG(IDTA(2))
3160 C3=C3+CSNG(IDTA(3))
3170 C1=(C1-2048!)*B(3)/2048!
3180 C2=(C2-2048!)*B(4)/2048!
3190 C3=(C3-2048!)*B(5)/2048!
3200 REM CLS
3210 PRINT "SAMPLE LOCK-IN SHOULD READ: "; C1
3220 PRINT
3230 PRINT "REFERENCE LOCK-IN SHOULD READ: "; C2
3240 PRINT
3250 PRINT "POWER METER SHOULD READ: "; C3
3260 LOCATE 10, 10: PRINT "PRESS ANY KEY TO CONTINUE!!"
3270 S=INKEY$: IF S="" THEN 3270
3280 GOTO 1200
3290 END
```

IV. AVERY'S METHOD

a. INTRODUCTION

The reflection coefficients are functions of n, k, θ, and polarization state. The previous chapter discussed the technique of determining n and k by measuring the reflection coefficients for one angle of incidence but for two polarization states, Querry's method. The approach examined here relies on a determination of the reflection coefficients for one polarization state but at two angles of incidence, Avery's technique.[1]

Avery's technique involves the graphical representation of the isoreflectance curves in the n vs. k plane. For two angles of incidence, and therefore two reflection coefficients, the intersection of the isoreflectance curves provides the complex refractive index at that wavelength. Fig. 4.1a shows three isoreflectance curves for $\theta = 10^\circ$, 30°, and 60° with the reflection coefficients being 0.571, 0.618, and 0.768, respectively. Fig. 4.1b provides an expanded view of the point of intersection. For computed values the intersection is truly a point, but the uncertainty in measured reflection coefficients will produce three points of intersection for the three isoreflectance curves. If the error in the measured reflection coefficients is to large, the isoreflectance curves may not even intersect.

Since this process must be repeated for each wavelength the complex refractive index is to be determined an application over a broad spectral range is not feasable. In a paper by J. Fahrenfort and W.M. Visser[2] an explicit solution for n and k was obtained using the reflection coefficient for light polarized perpendicular to the plane of incidence and for two angles. The pertinent equations have been reprinted below. Beginning with the Fresnel equation for R_s we have

$$r_s = \frac{-(n'^2 - \sin^2\theta)^{1/2} + \cos\theta}{(n'^2 - \sin^2\theta)^{1/2} + \cos\theta}, \qquad (4.1)$$

where $n' = n + ik$, n is the refractive index and k is the extinction coefficient, and θ is the angle of incidence. Hence:

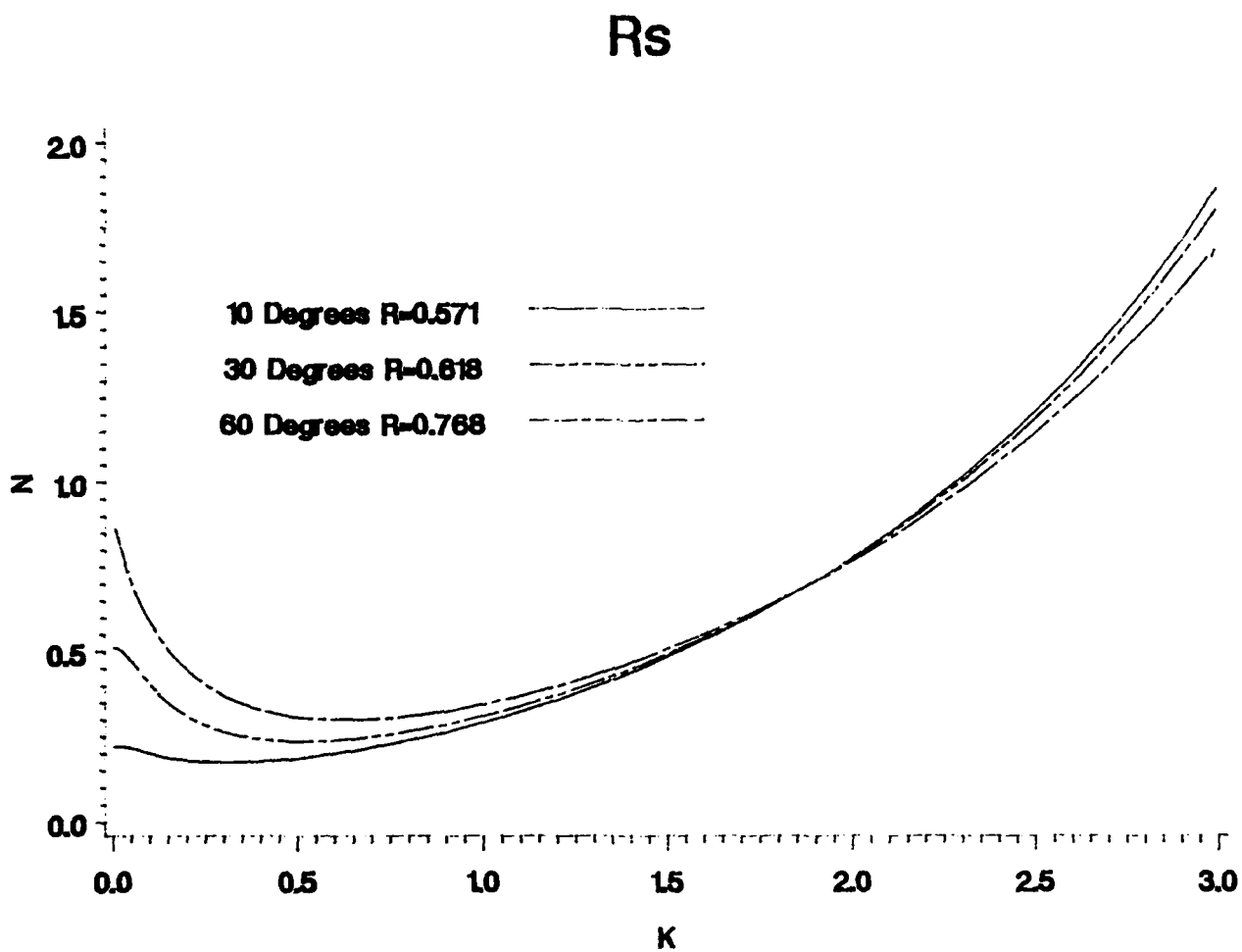

FIG. 4.1a Isoreflectance curves in the n-k plane at three angles of incidence. Solid line 10°, R_s = 0.571, double dash line 30°, R_s = 0.618, single dash line 60°, R_s = 0.768.

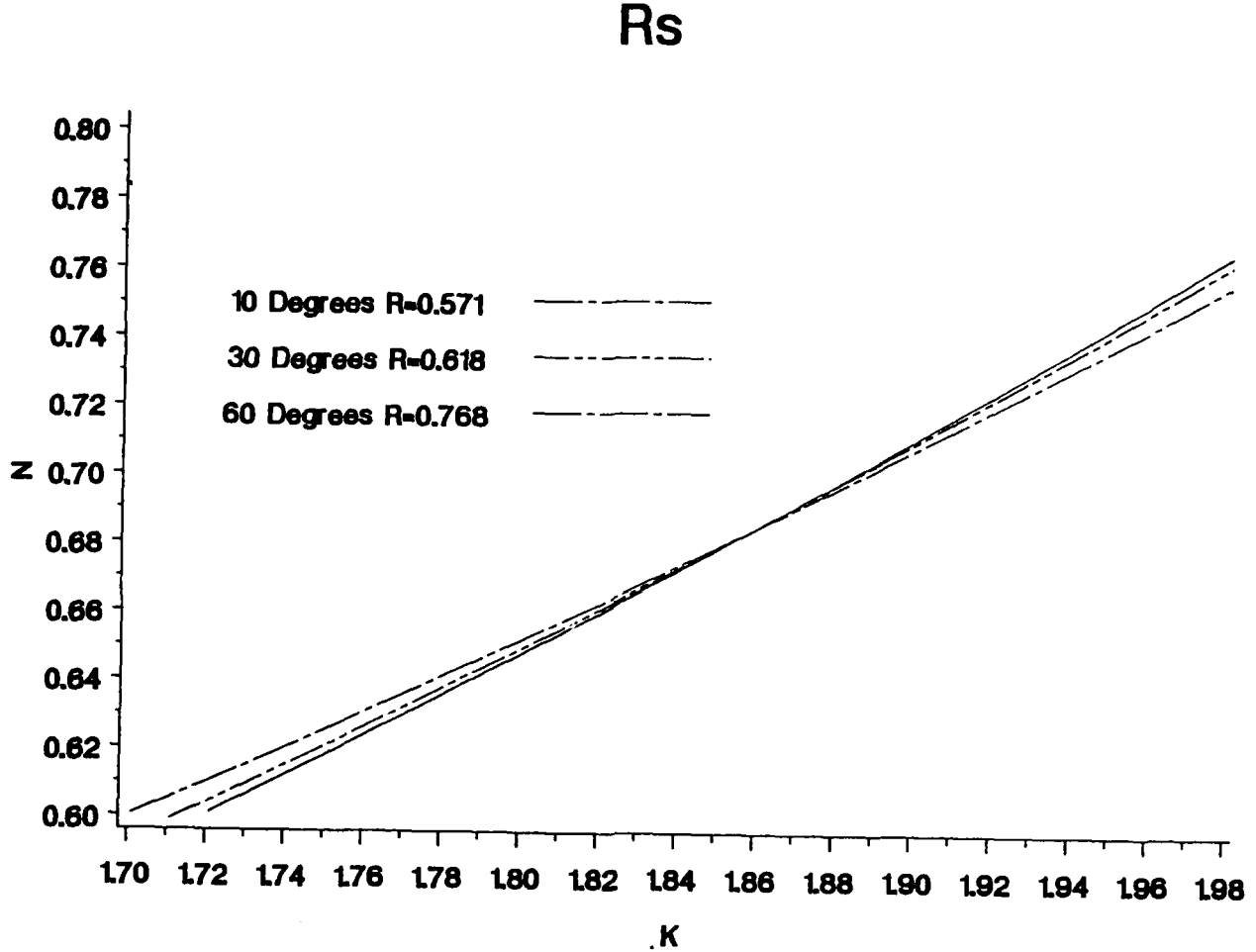

FIG. 4.1b Expanded scale of FIG. 4.1a showing the point of intersection of the three isoreflectance curves.

$$-\frac{1+\left[(1+r_s)/(1-r_s)\right]^2}{1-\left[(1+r_s)/(1-r_s)\right]^2} = \frac{1+\rho^2\, e^{2i\phi}}{2\rho\, e^{i\phi}} = \frac{n'^2-\sin\theta+\cos^2\theta}{1-n'^2} \,. \qquad (4.2)$$

Splitting Eq. 4.2 into real and imaginary components, and substituting

$$1 - n'^2 + k^2 = u \qquad\qquad n\,k = w \qquad (4.3)$$

we have:

$$\cos\phi = \frac{2\,u\cos^2\theta - (u^2+w^2)}{u^2+w^2} \cdot \frac{2\rho}{1+\rho^2} \,, \qquad (4.4)$$

$$\sin\phi = \frac{-2\,w\cos^2\theta}{u^2+w^2} \cdot \frac{2\rho}{(\rho^2-1)} \,. \qquad (4.5)$$

Now substitute $u^2 + w^2 = M$ and $\rho^2 = R$, and square and add Eqs. 4.4 and 4.5 to obtain:

$$-\frac{1}{4} A M^2 + 4 B M - 4 C u M - 16 D u^2 = 0 \qquad (4.6)$$

where

$$A = \frac{(1-R)^4}{R} \,, \qquad (4.7)$$

$$B = (1+R)^2 \cos^4\theta \,, \qquad (4.8)$$

$$C = (1-R)^2 \cos^2\theta \,, \qquad (4.9)$$

$$D = R\cos^4\theta \,. \qquad (4.10)$$

Where R in Eqs. 4.7 thru 4.10 is the measured reflection coefficient for the angle of incidence, θ. Measurement of the reflecting power R at two angles of incidence θ_1 and θ_2 yields two sets of coefficients for Eq. 4.6. Elimination of the term in u^2 and division by M yields

$$u = -\frac{1}{16} P M + Q , \tag{4.11}$$

with

$$P = \frac{A_1 D_2 - A_2 D_1}{C_1 D_2 - C_2 D_1} , \tag{4.12}$$

$$Q = \frac{B_1 D_2 - B_2 D_1}{C_1 D_2 - C_2 D_1} , \tag{4.13}$$

Substituting u from Eq. 4.11 into Eq. 4.6 we obtain a quadratic equation in M with only the solution

$$M = \frac{- Y - \left[Y^2 - 4 X Z \right]^{1/2}}{2 X} \tag{4.14}$$

with

$$X = \frac{1}{4} \left[A_1 - C_1 P + \frac{1}{4} D_1 P^2 \right] , \tag{4.15}$$

$$Y = 4 \left[-B_1 + C_1 Q - \frac{1}{2} D_1 P Q \right] , \tag{4.16}$$

$$Z = 16 D_1 Q^2 . \tag{4.17}$$

From Eq. 4.3 we have

$$w = [M - u^2]^{1/2} = 2 k/n \tag{4.18}$$

and then

$$n = \left\{ \frac{w}{2\kappa} \right\} , \tag{4.19}$$

$$k = n\kappa , \tag{4.20}$$

where

$$\kappa = \frac{-(1 - u) + [(1 - u)^2 + w^2]^{1/2}}{w} . \tag{4.21}$$

The complex refractive index can then be computed by calculating in order A, B, C, D, P, Q, X, Y, Z, M, u, w, κ, and finally n and k. The computer program developed to perform these computations, AVERY, is given in appendix 4.1.

This technique was applied by measuring the reflection coeficient R_s at several angles of incidence and then using all possible unique combinations of these pairs to determine a set of n and k values. From this set the mean and standard deviation were determined using the defination:

$$\bar{n} = \frac{\Sigma\, n_i}{l} \qquad \bar{k} = \frac{\Sigma\, k_i}{l} , \tag{4.22}$$

and

$$\sigma_n = \left\{ (l-1)^{-1} \sum [n_i - \bar{n}\,]^2 \right\}^{1/2} , \tag{4.23}$$

and

$$\sigma_k = \left\{ (l-1)^{-1} \sum [k_i - \bar{k}\,]^2 \right\}^{1/2} . \tag{4.24}$$

b. ERROR ANALYSIS

The technique of propagation of error could be used on the equations of the previous section but the resulting form would be extremely difficult to understand. In addition, a computer code would be necessary to provide any numerical output. To simplify this process the uncertainty in the complex refractive index will again be estimated as in the previous chapter; 1) Compute R_s for a region of n-k space and at two angles of incidence, 2) Modify the resulting R_s values by a fractional percent, 3) recompute n and k from the modified R_s and 4) compare the recomputed values to the original n and k values. The two angles of incidence are 10° and 60°, the reflection coefficients are shown in Figs. 3.1 and 3.5 of the previous chapter. The reflection coefficient and the angle of incidence will be modified by 2% in determining the uncertainty in n and k.

VARIATION IN R_s at 10°

Figs. 4.2 - 4.5 present the fractional error in n and k, respectively for a variation of +/- 2% in R_s. In Fig 4.2 the fractional error for values of n less than 1 cannot be determined even with the small variation in R_s of +2%. For most of the n - k plane that is examined the error is relatively small for small k but grows as k nears 1. In Fig. 4.3 the error is shown to be smaller for a reduction in R_s by 2%. Also, the only region in which the error could not be determined is for large n values, near 3. The error is below ~25% for this variation. Figs. 4.4 and 4.5 indicate the error in k for the same modifications of R_s and indicate the error in determining k is much larger than that of determining n. The error in k is minimized for larger values of n, n greater than 2. For both n and k an increase in the reflection coefficient appears to introduce more error in the final values of n and k than a reduction in this value.

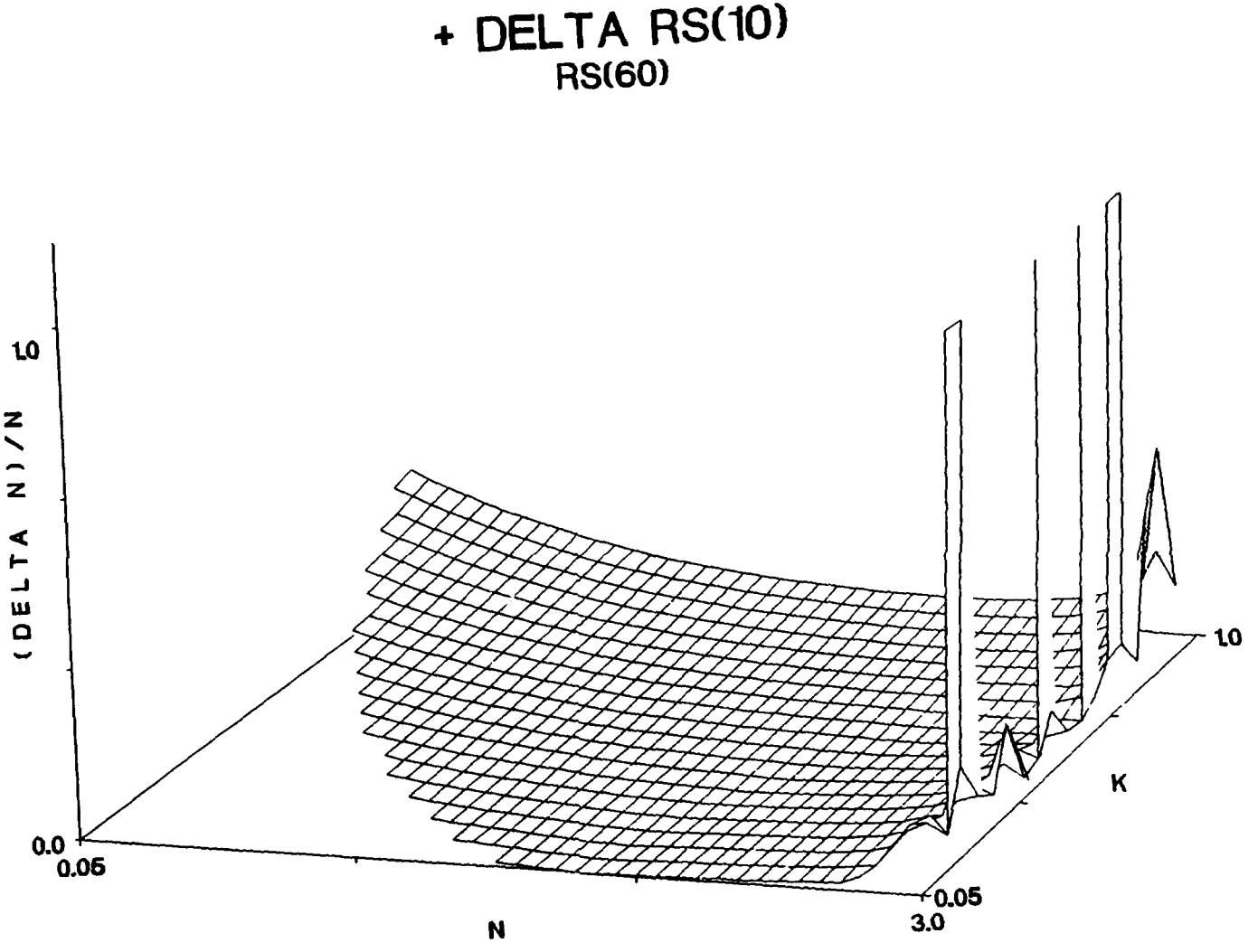

FIG. 4.2 Fractional error in n, $\Delta n/n$, with R_s varied upward by 2% at $\theta = 10^{\circ}$.

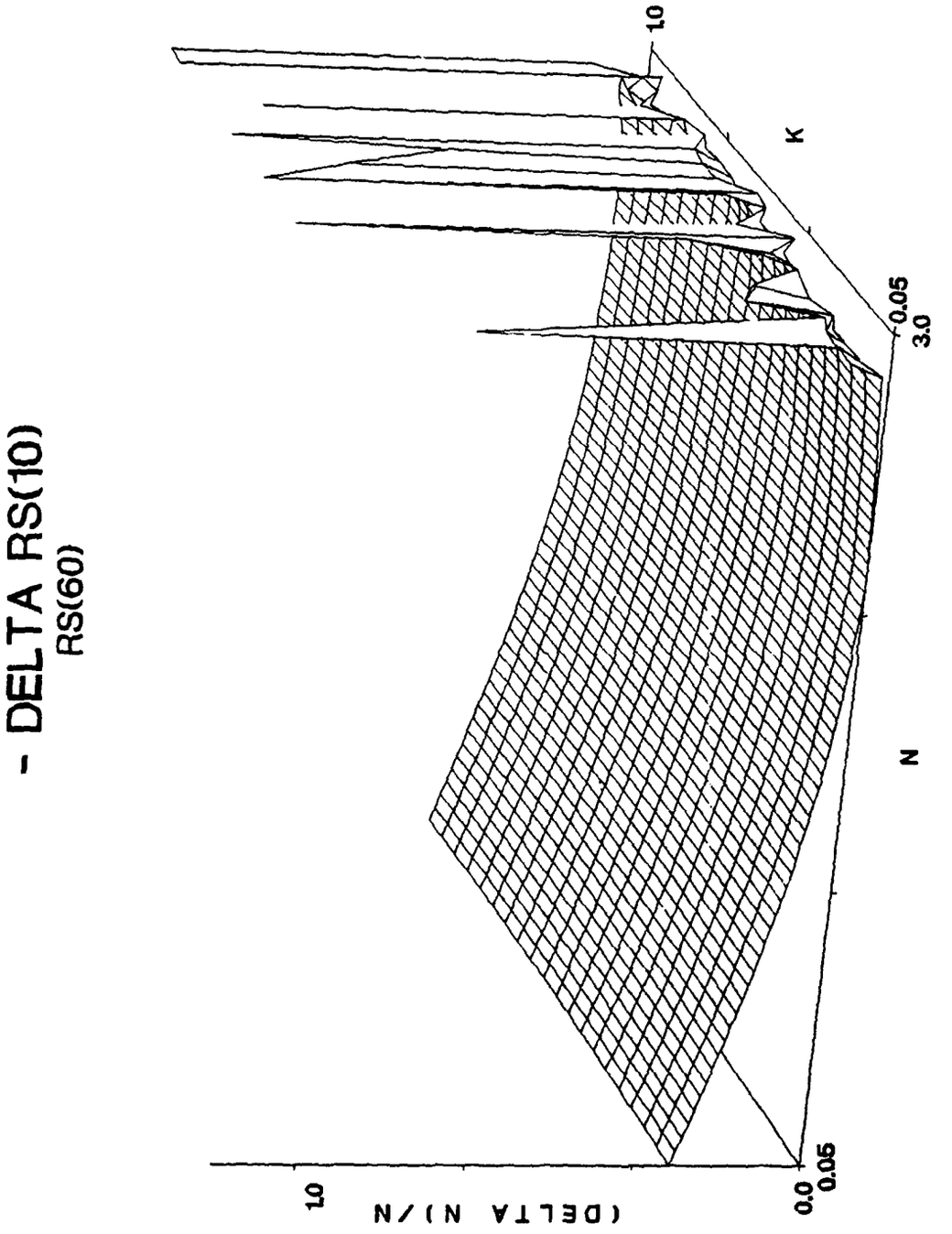

FIG. 4.3 Fractional error in n, $\Delta n/n$, with R_s varied downward by 2% at $\theta = 10^{\circ}$.

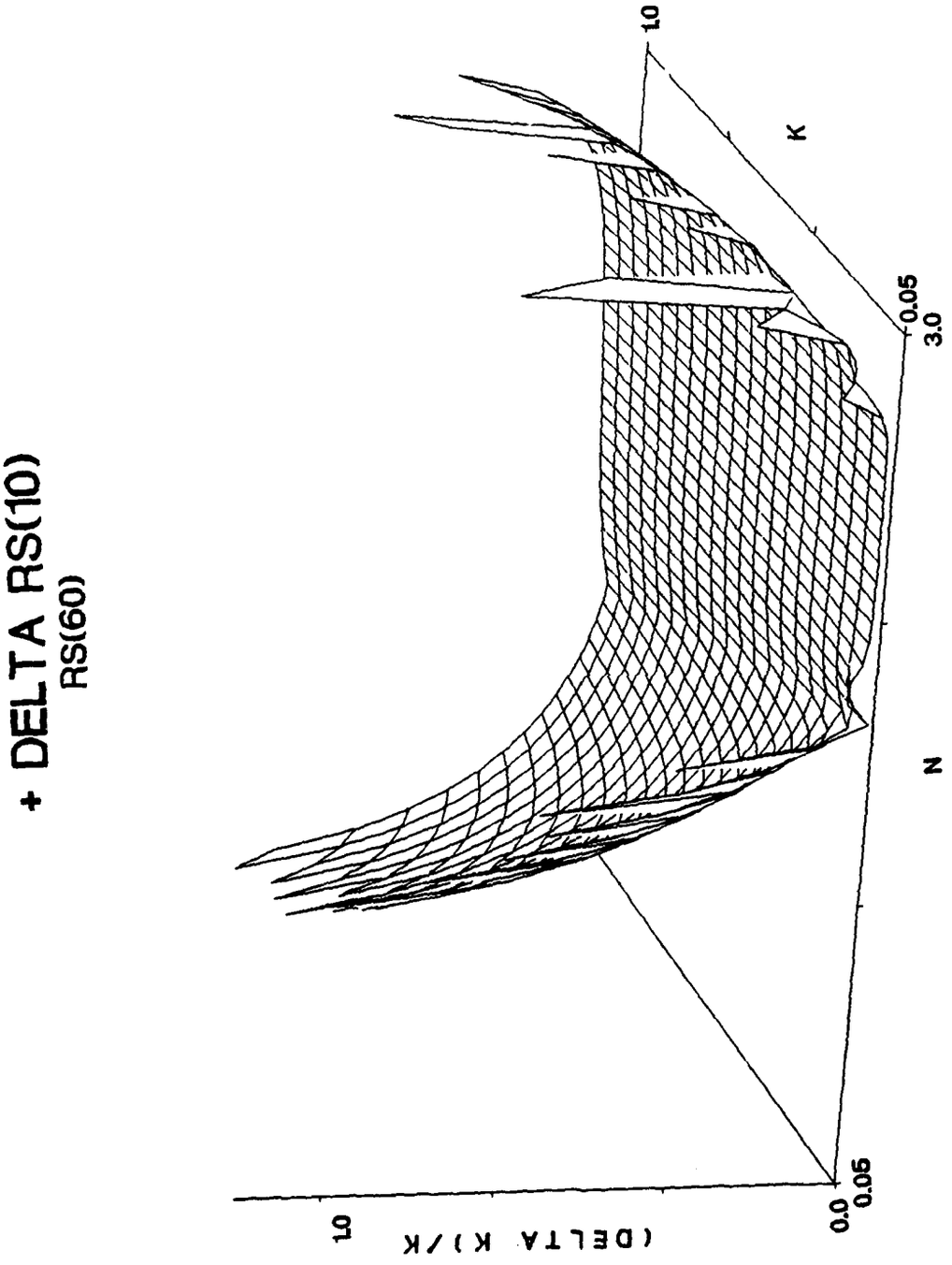

FIG. 4.4 Fractional error in k, $\Delta k/k$, with R_s varied upward by 2% at $\theta = 10^{\circ}$.

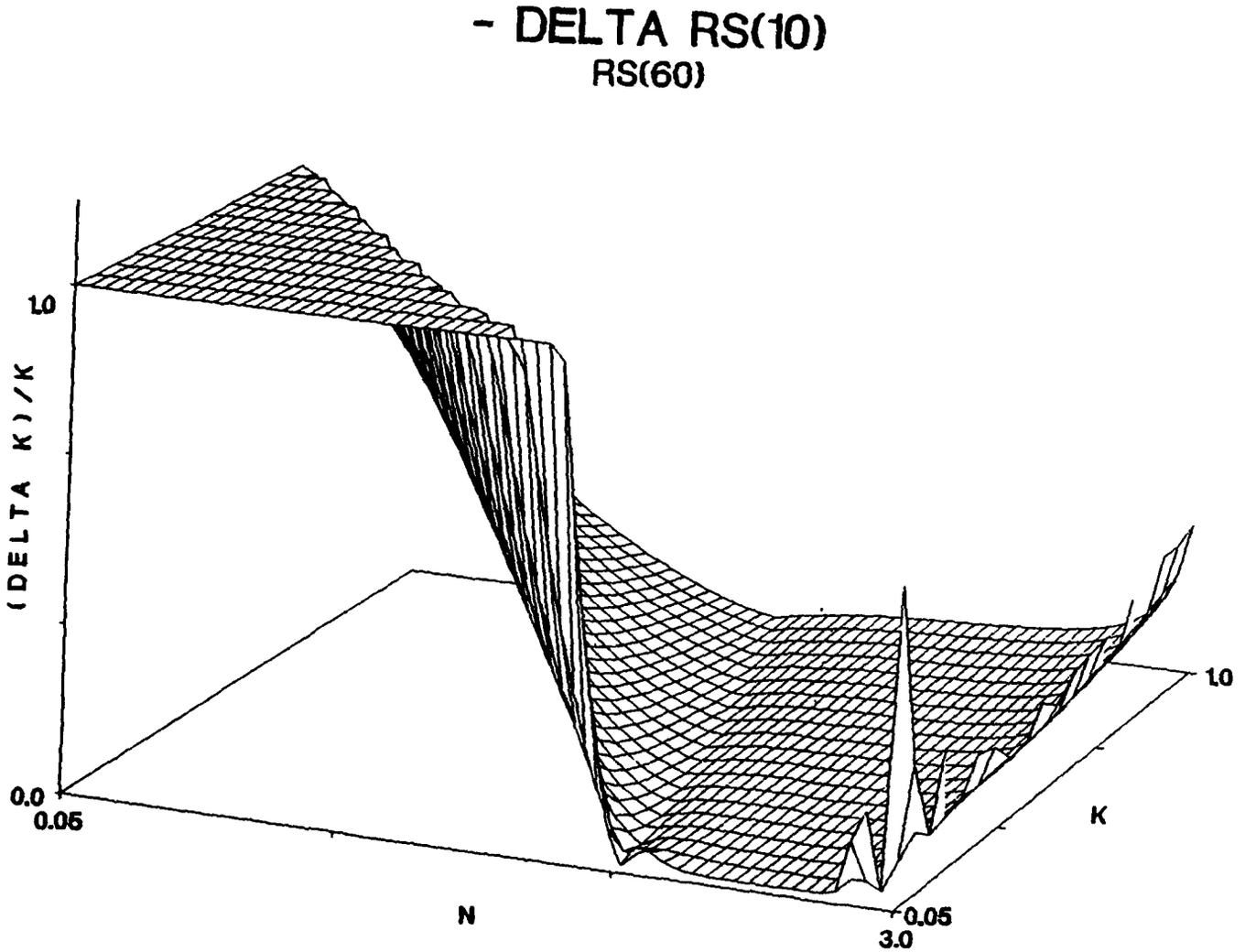

FIG. 4.5 Fractional error in k, $\Delta k/k$, with R_e varied downward by 2% at $\theta = 10^{\circ}$.

VARIATION IN R_s at 60°

Figs. 4.6 - 4.9 show the fractional error in n and k for a variation in the reflection coefficient at 60° angle of incidence. The results are qualitatively the same as for 10° except the error is larger and the entire surface can now be determined for an increase in R_s as opposed to a decrease in R_s. Again the error in n is minimized for values above 2. Figs. 4.8 and 4.9 indicate the error in k dramatically increases as the angle of incidence increases. The region of the n-k plane for which a small error in k exists has been reduced significantly. For values below n equal 2 and k less than 0.5, the error is above 100%.

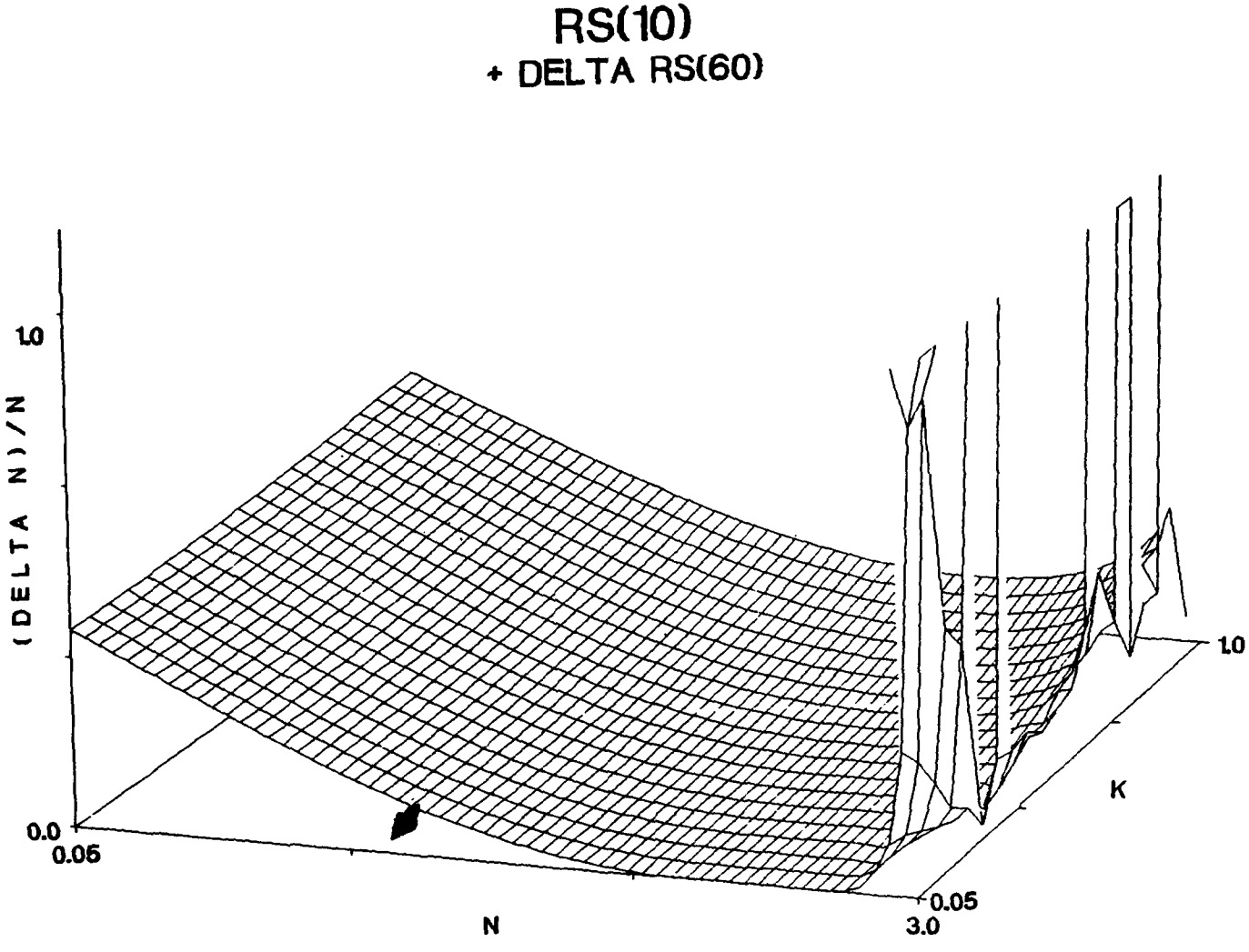

FIG. 4.6 Fractional error in n, $\Delta n/n$, with R_s varied upward by 2% at $\theta = 60^\circ$.

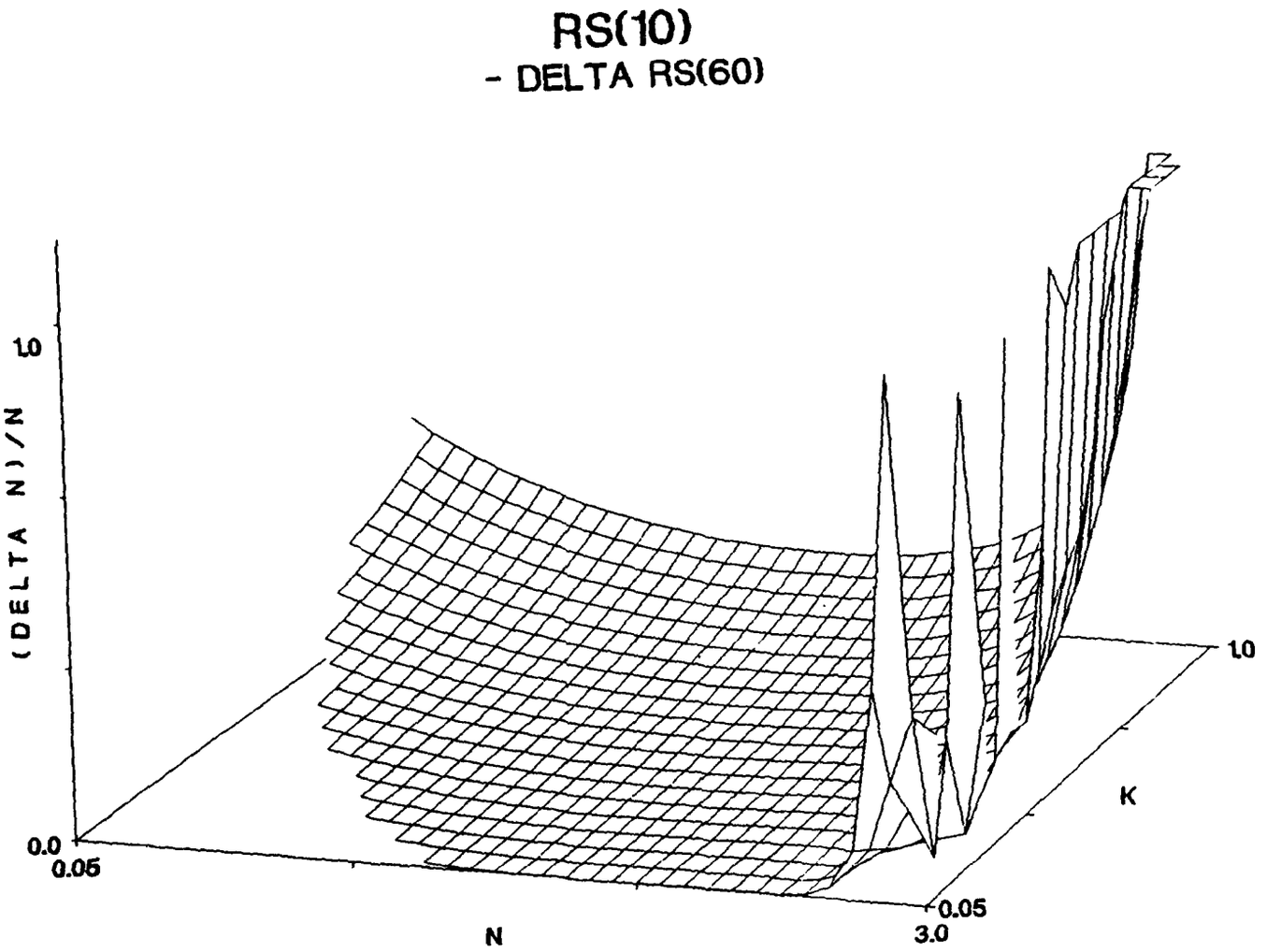

FIG. 4.7 Fractional error in n, $\Delta n/n$, with R_s varied downward by 2% at $\theta = 60^{\circ}$.

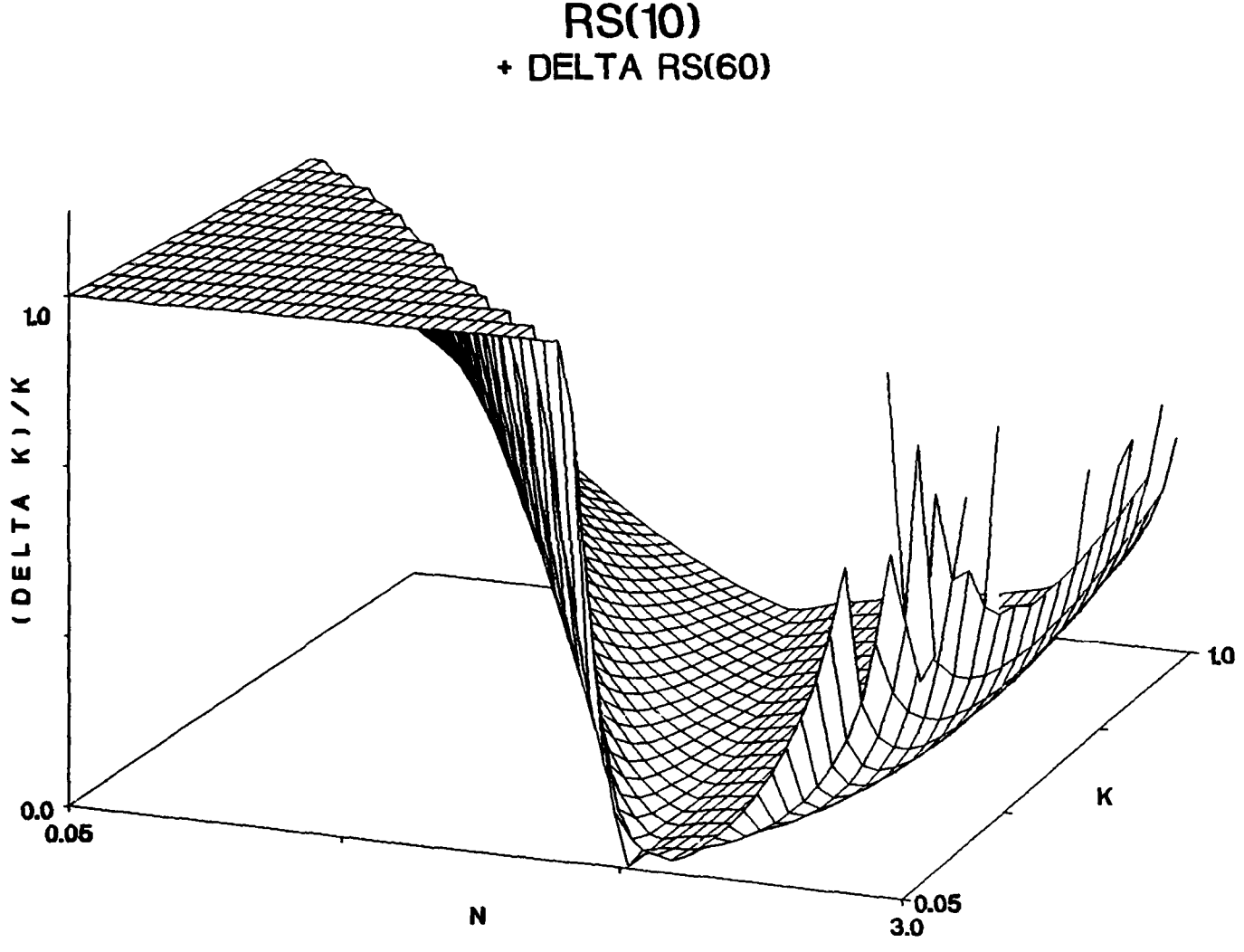

FIG. 4.8 Fractional error in k, $\Delta k/k$, with R_s varied upward by 2% at $\theta = 60^\circ$.

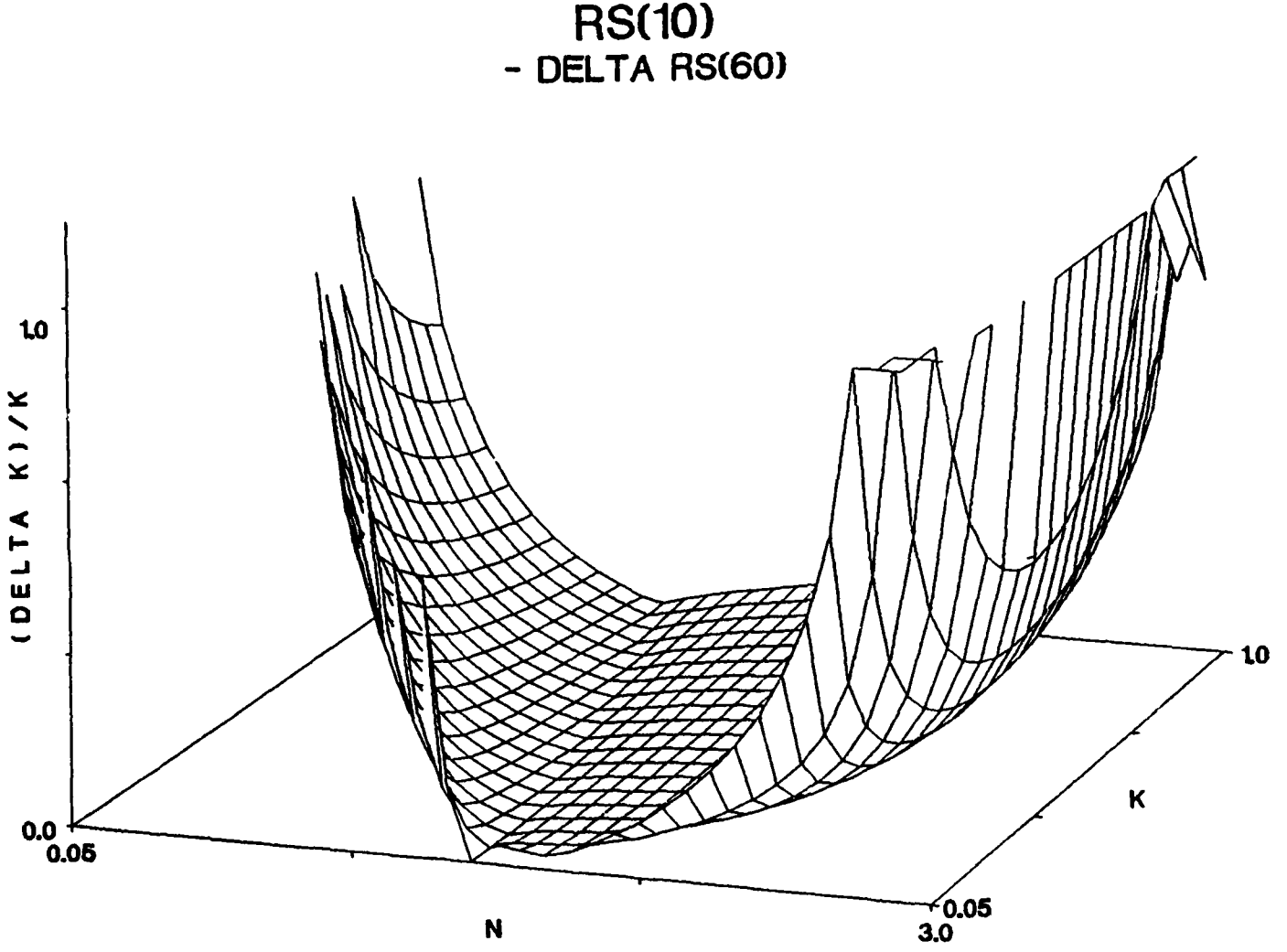

FIG. 4.9 Fractional error in k, $\Delta k/k$ with R_s varied downward by 2% at $\theta = 60^{\circ}$.

VARIATION IN BOTH R_s AT 10^0 AND 60^0

Figs. 4.10 - 4.13 show the error in n and k for a variation in both reflection coefficients, with the sign of the error being the same for both angles of incidence. The error in n is smaller when both uncertainties in R_s are positive than when they are negative. Again the error in k is extremely large and appears to be dominated by the uncertainty in R_s at the 60^0 angle of incidence. The most reasonable error appears to be for n in a narrow range around 2 and for k to range from 0 to 1. Outside of this region the error in n continues to be reasonable but that in k is above 100% for most of the n-k plane that has been observed.

Figs. 4.14 - 4.17 present the error in n and k when the reflection coefficients are adjusted in opposite directions. The errors in n are much larger in this case than when the adjustments were both in the same direction. Although, the error for the case of a reduction in the 10^0 values and an increase in the 60^0 values provides nearly the same error as that discussed in the previous paragraph. Figs. 4.16 and 4.17 again show the sensitivity of k to very small deviations in R_s.

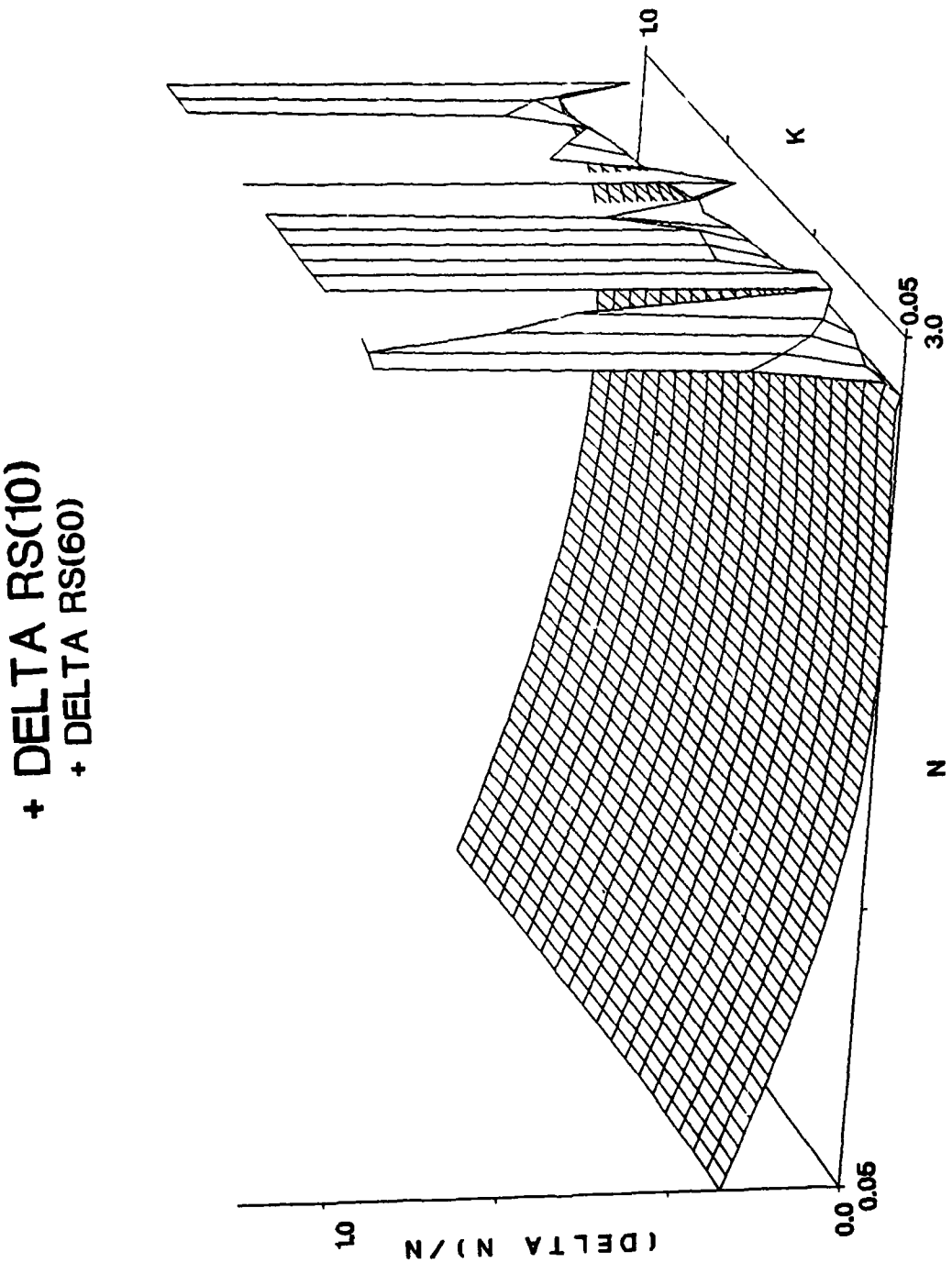

FIG. 4.10 Fractional error in n, $\Delta n/n$, with R_s varied upward by 2% at both $\theta = 10^\circ$ and $\theta = 60^\circ$.

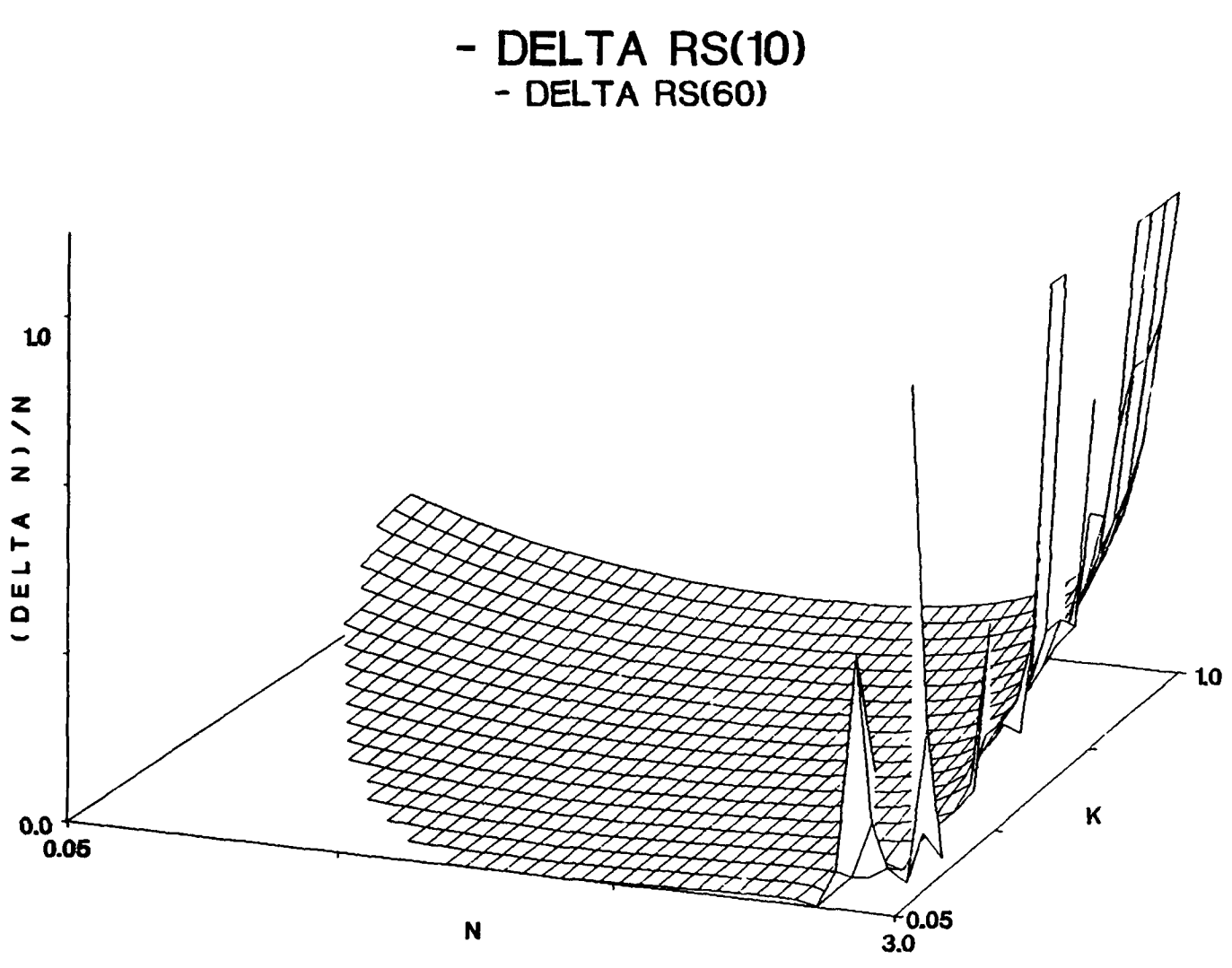

FIG. 4.11 Fractional error in n, $\Delta n/n$, with R_s varied downward by 2% at both $\theta = 10^\circ$ and $\theta = 60^\circ$.

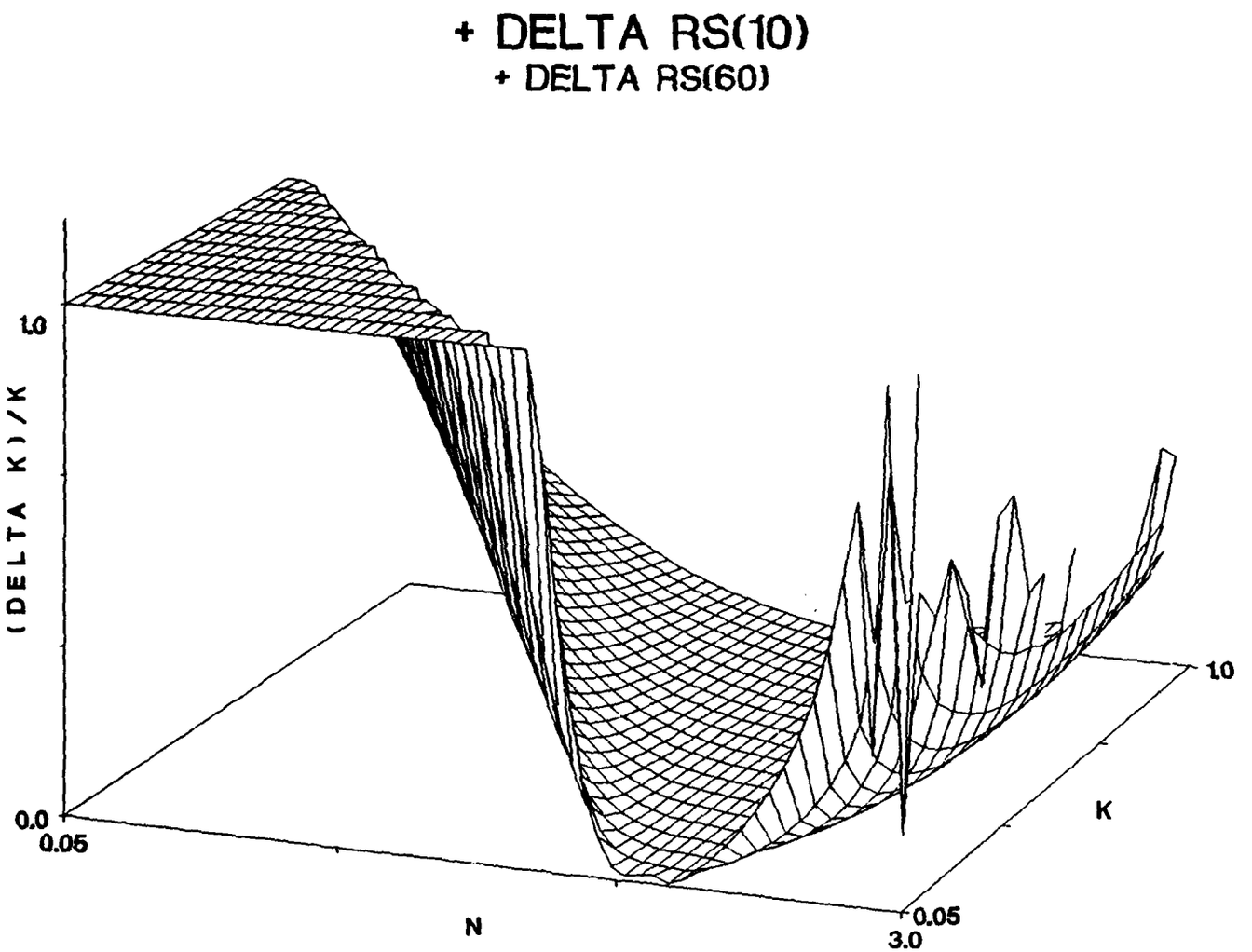

FIG. 4.12 Fractional error in k, $\Delta k/k$, with R_s varied upward by 2% at both $\theta = 10^\circ$ and $\theta = 60^\circ$.

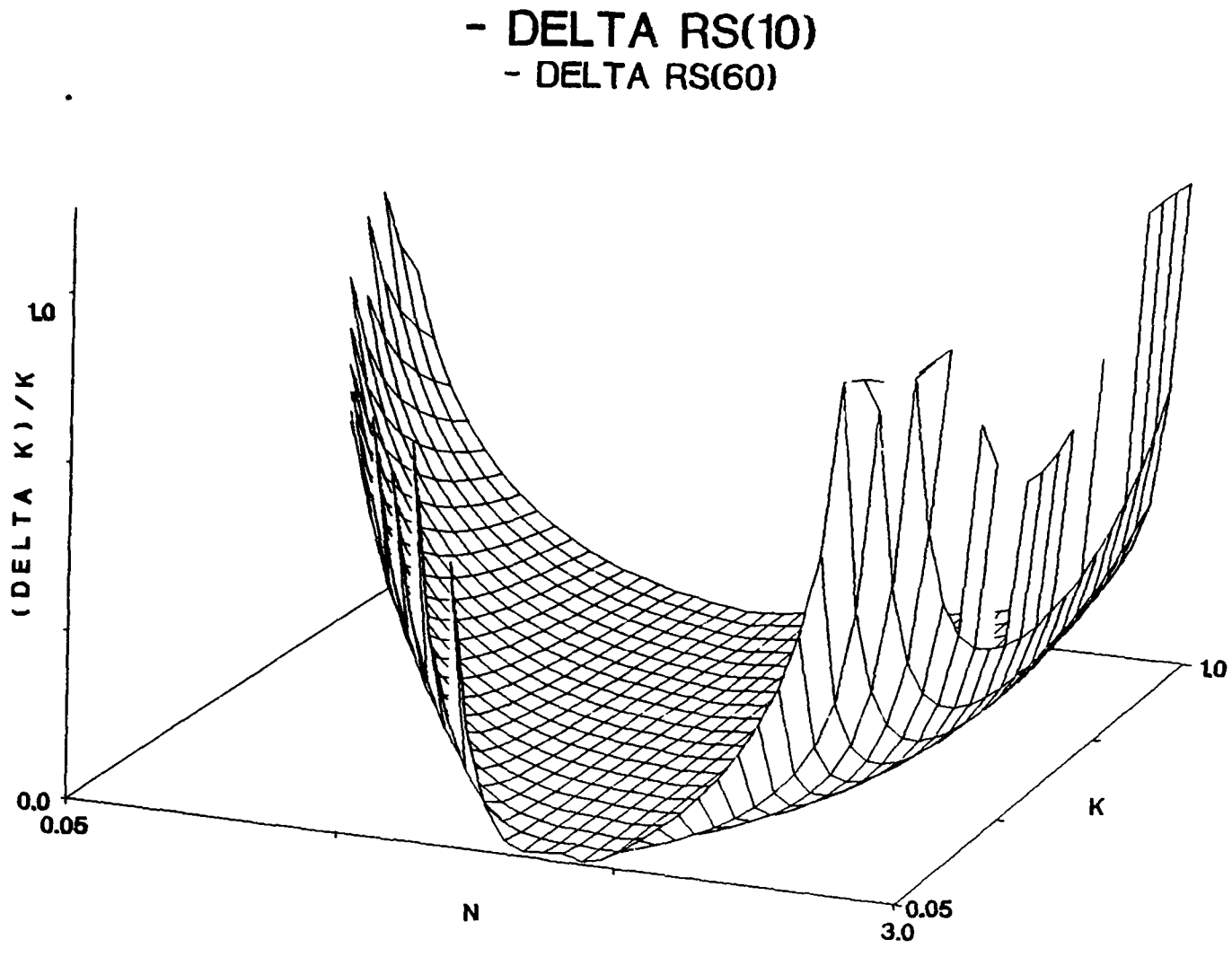

FIG. 4.13 Fractional error in k, $\Delta k/k$, with R_s varied downward by 2% at both $\theta = 10^\circ$ and $\theta = 60^\circ$.

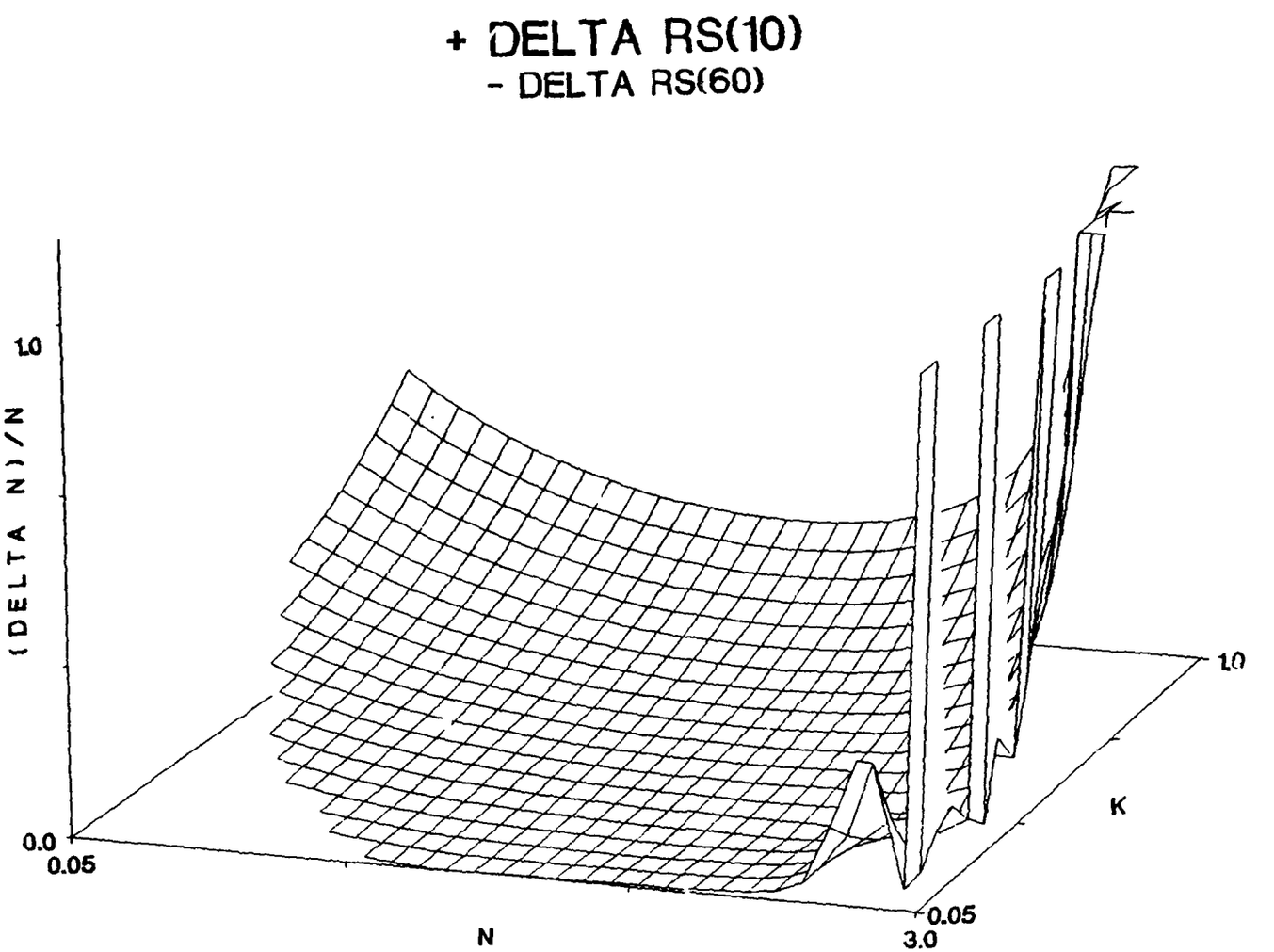

FIG. 4.14 Fractional error in n, $\Delta n/n$, with R_a varied upward by 2% at $\theta = 10^\circ$ and downward by 2% at $\theta = 60^\circ$.

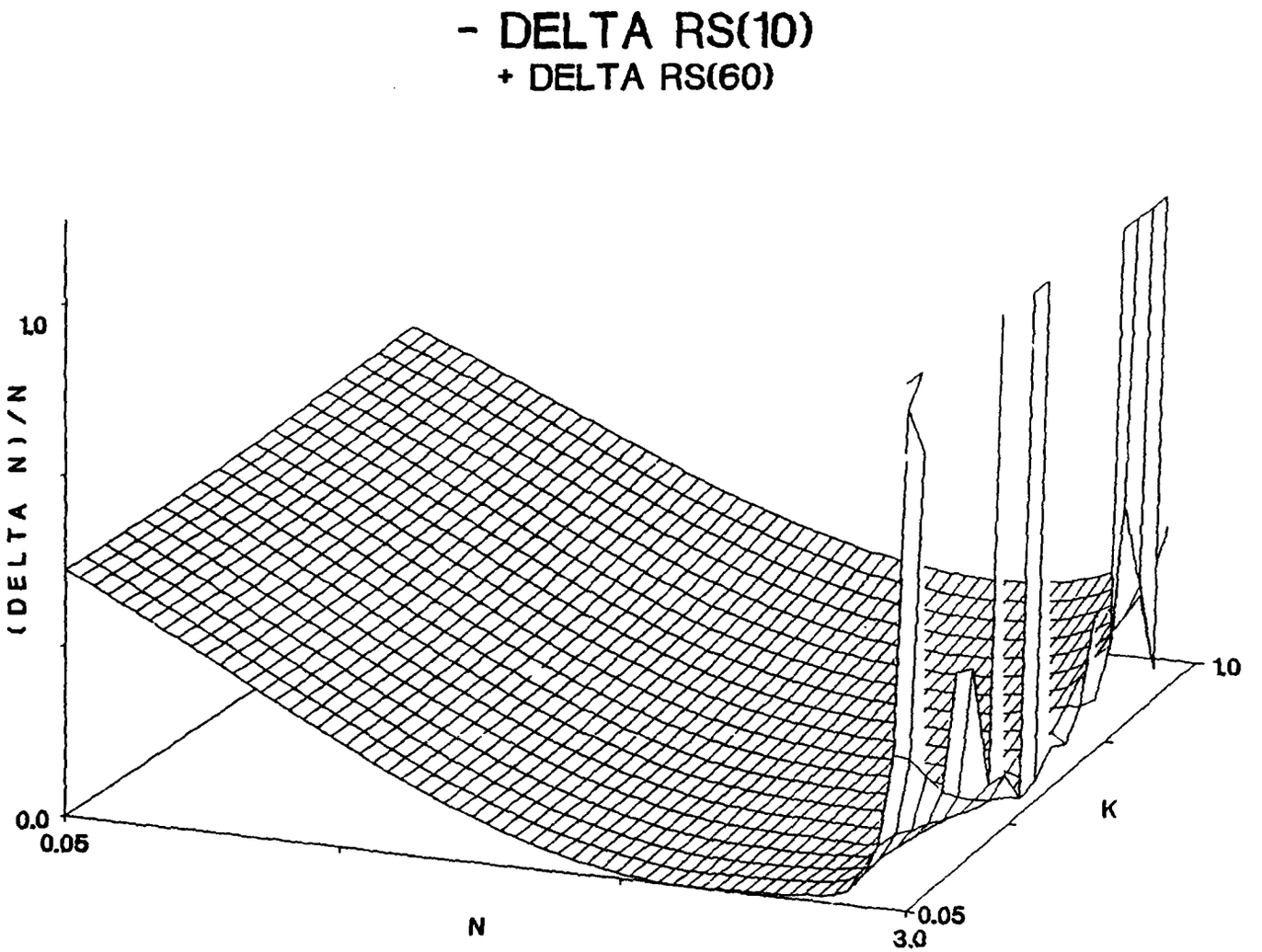

FIG. 4.15 Fractional error in n, $\Delta n/n$, with R_e varied downward by 2% at $\theta = 10^\circ$ and upward at $\theta = 60^\circ$.

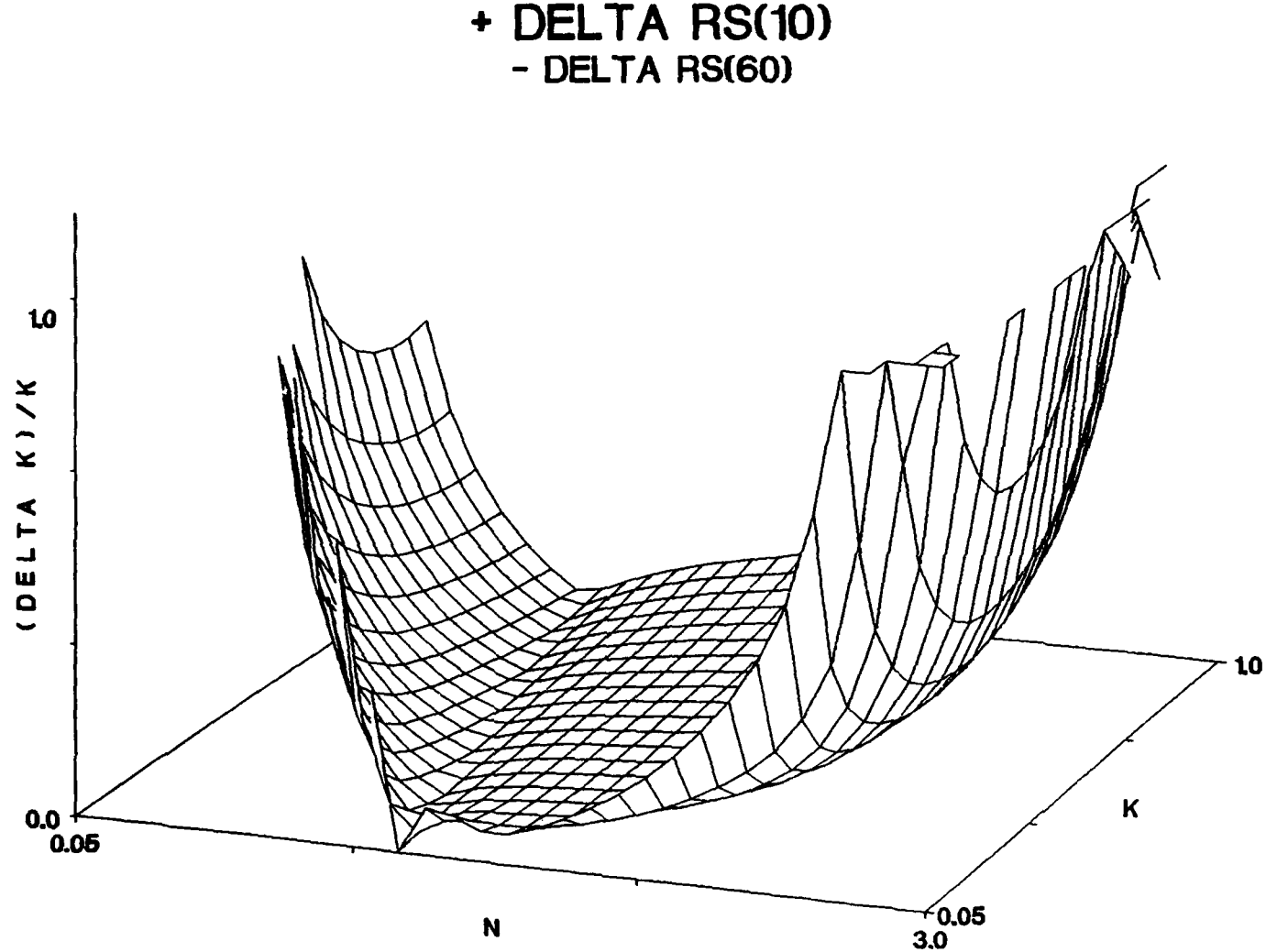

FIG. 4.16 Fractional error in k, $\Delta k/k$, with R_a varied upward by 2% at $\theta = 10^\circ$ and downward at $\theta = 60^\circ$.

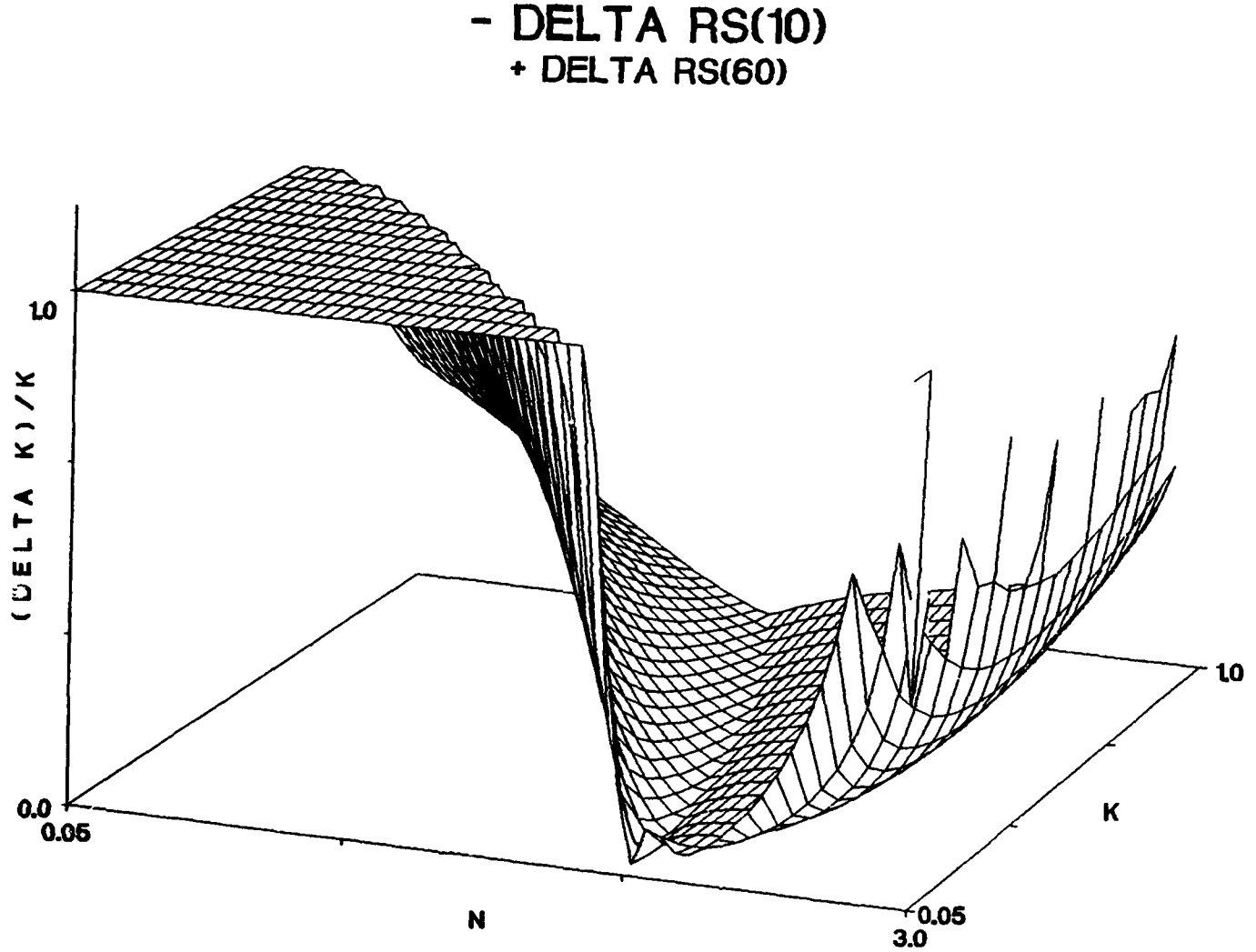

FIG. 4.17 Fractional error in k, $\Delta k/k$, with R_s varied downward by 2% at $\theta = 10^\circ$ and upward at $\theta = 60^\circ$.

The previous figures indicate Avery's technique suffers from similar difficulties as Querry's method. The reflection coefficients must be determined to an uncertainty of less than 1% in order to provide accurate optical constants. In addition, if experimental conditions lead to one reflection coefficient being increased while the value at the second angle decreases we can expect the largest error in the final n and k values.

c. DESCRIPTION OF EQUIPMENT

The equipment employed for Avery's method is the same as that used to perform the experiments necessary for Querry's method. In fact the system was aligned for light polarized perpendicular to the plane of incidence and the measurements were performed, with the resulting reflection coefficients used to determine the compelx refractive index from both theories. Briefly the sample was mounted on a gimble to allow for positioning the sample surface accurately. The IR polarizer was purchased from Cleveland Crystals and mounted in a custom built frame, allowing it to be rotated to provide any linear polarization state desired. Since the polarizers were reflection type the system alignment was extremely difficult. For each desired polarization state the position of the sample had to be adjusted to coincide with the direction of the light path.

d. ACQUISITION OF DATA

All data was acquired under computer control using the program listed in appendix 3.2, AMENU. The data was reduced and n and k was determined by the program AVERY in appendix 4.1. The data necessary to obtain the reflection coefficients was obtained using the following procedure:

1. Polarizer adjusted to provide R_s.
2. With the sample holder empty the intensity of the CO_2 laser was determined as a function of wavelength, I_o.
3. The sample was mounted in the gimble and adjusted to provide an accurate determination of the angle of incidence.
4. The CO_2 laser was tuned to the appropriate line and the dither stabilizer unit was activated.
5. The sample and reference lock-in amplifiers were adjusted with respect to phase, amplitude, and time constant.
6. The operating parameters were input into the computer to be stored with the data.
7. The amplitudes of the lock-ins and the power meter were read and stored to disk.
8. For each wavelength several angles of incidence were used providing the reflection coefficient as a function of angle.
9. The procedure from step 4 was repeated until data was obtained at all possible wavelengths.
10. After obtaining the raw data the files were reduced and a master file containing wavelength, angle of incidence, and R_s was created for each sample.
11. The reflection coefficients were then input into the computer program AVERY for determination of n and k.

Table 4.1 provides a listing of representative data prior to the determination of the reflection coefficients. Notice that several angles of incidence are associated with each wavelength of the incident light.

TABLE 4.1

Raw data for Avery's method

Wavelength (μm)	Angle (degrees)	Sample Lock-in (V)	Reference Lock-in (V)	Power Meter (W)
10.741	16.95	1.164E-02	1.037E-01	2.13
10.741	37.05	1.475E-02	1.014E-01	2.13
10.741	41.00	1.609E-02	1.021E-01	2.14
10.741	45.00	1.827E-02	1.005E-01	2.13
10.741	51.10	2.877E-02	9.878E-02	2.14
10.741	57.10	3.837E-02	9.907E-02	2.14
10.741	61.10	4.216E-02	9.964E-02	2.14
10.741	66.90	5.410E-02	9.831E-02	2.14
10.719	16.80	7.945E-03	4.220E-02	2.41
10.696	17.00	4.543E-02	7.271E-02	2.08
10.696	16.90	4.453E-02	7.354E-02	2.08
10.696	22.85	6.136E-02	1.488E-01	2.08
10.696	37.10	3.506E-02	1.522E-01	2.08
10.696	41.00	3.697E-02	1.541E-01	2.08
10.696	44.85	1.126E-01	1.575E-01	2.07
10.696	51.10	5.466E-02	1.570E-01	2.08
10.696	57.10	6.973E-02	1.593E-01	2.07
10.696	61.00	7.512E-02	1.606E-01	2.07
10.696	67.00	1.273E-01	1.635E-01	2.08
10.632	16.90	2.978E-01	4.998E-01	1.12
10.632	22.85	3.137E-02	2.151E-01	1.11
10.632	37.10	6.759E-02	2.177E-01	1.11
10.632	41.05	4.204E-02	2.197E-01	1.10
10.632	45.00	4.925E-02	2.213E-01	1.10
10.632	50.95	4.164E-02	2.243E-01	1.10
10.632	50.95	1.196E-01	2.245E-01	1.09
10.632	61.10	1.258E-01	2.242E-01	1.09
10.632	67.00	1.587E-01	2.236E-01	1.10
10.571	17.75	3.690E-02	1.853E-01	3.51
10.571	22.95	2.832E-02	1.865E-01	3.53
10.571	36.90	4.732E-02	1.849E-01	3.52
10.571	41.05	3.314E-02	1.859E-01	3.53
10.571	45.05	3.767E-02	1.857E-01	3.53
10.571	51.00	3.748E-02	1.860E-01	3.54
10.571	56.90	9.222E-02	1.855E-01	3.54
10.571	61.00	1.065E-01	1.858E-01	3.55
10.571	67.00	1.070E-01	1.850E-01	3.54

The data from Table 4.1 was then reduced with the I_o data to produce Table 4.2 providing R_s as a function of wavelength and angle of incidence. The values for R_s were then read into a program which reformatted the file providing all distinct combinations of R_s for a given wavelength. The reformated file was then read into the program AVERY and the complex refractive index was computed. Some of the data pairs produced intermediate results which would not allow a final value for n and k to be computed, these pairs were extracted from the data and not used in determining the complex refractive index or the standard deviation associated with it.

TABLE 4.2

Analyzed data for Avery's method

Wavelength (μm)	Angle (Degrees)	R_S
10.741	16.95	2.440E-02
10.741	37.05	3.161E-02
10.741	41.00	3.423E-02
10.741	45.00	3.949E-02
10.741	51.10	6.327E-02
10.741	57.10	8.412E-02
10.741	61.10	9.192E-02
10.741	66.90	1.195E-01
10.696	17.00	6.173E-02
10.696	16.90	5.983E-02
10.696	22.85	4.076E-02
10.696	37.10	2.276E-02
10.696	41.00	2.370E-02
10.696	44.85	7.064E-02
10.696	51.10	3.439E-02
10.696	57.10	4.324E-02
10.696	61.00	4.622E-02
10.696	67.00	7.691E-02
10.632	16.90	1.194E-01
10.632	22.85	2.922E-02
10.632	37.10	6.219E-02
10.632	41.05	3.834E-02
10.632	45.00	4.459E-02
10.632	50.95	3.720E-02
10.632	50.95	1.067E-01
10.632	61.10	1.124E-01
10.632	67.00	1.422E-01
10.571	17.75	5.074E-02
10.571	22.95	3.868E-02
10.571	36.90	6.521E-02
10.571	41.05	4.541E-02
10.571	45.05	5.169E-02
10.571	51.00	5.133E-02
10.571	56.90	1.266E-01
10.571	61.00	1.461E-01
10.571	67.00	1.474E-01

e. RESULTS

The results obtained using the procedure described in the previous sections are presented here in both tabular and graphical format. The complex refractive index as determined using Avery's method is compared to that determined from near normal reflection measurements and Kramers-Kronig analysis[3].

The complex refractive index for Illite is presented in Table 4.3 and in Figs. 4.18 and 4.19. The table fives n and k as a function of wavelength. The standard deviation for each, n and k, is given in columns 4 and 5 of the table, respectively. A standard deviation of 0 indicates that only one pair of angles was used in determining the complex refractive index. The figures represent n and k as functions of wavenumber with the error bars representing +/- one standard deviation. The results are very similar to those obtained using Querry's method, namely an almost constant complex refractive index as a function of wavenumber. The error bars are quite large indicating the tremendous sensitivity of the technique to the measured reflection coefficients. The sparseness of the data indicates, only 16 values from a total experimental set of over 60, the size of the error in the reflection coefficients. If the reflection coefficients have too large of an error the equations as developed by Fahrenfort and Visser[1] cannot be solved.

The complex refractive index for Kaolin is presented in Table 4.4 and in Figs. 4.20 and 4.21. The results are extremely similar to that for illite, indicating poorly determined reflection coefficients. The number of values for the complex refractive index is also reduced to 25 from the over 60 values of the reflected intensity that were measured.

TABLE 4.3

Complex refractive index for Illite

λ (μm)	n	k	Δn	Δk
10.741	0.1007E+01	0.9461E-01	0.0000E+00	0.0000E+00
10.632	0.1033E+01	0.1265E+00	0.2721E+00	0.3707E+00
10.571	0.9673E+00	0.1867E+00	0.1788E+00	0.4105E+00
10.551	0.1092E+01	0.2810E+00	0.3921E+00	0.4900E+00
10.513	0.8183E+00	0.2008E+00	0.4006E+00	0.4122E+00
10.494	0.1002E+01	0.2205E+00	0.1091E+00	0.4397E+00
10.233	0.1233E+01	0.6755E+00	0.8760E+00	0.6591E+00
10.171	0.7022E+00	0.3486E+00	0.6449E+00	0.6198E+00
10.159	0.8641E+00	0.1460E+00	0.4149E+00	0.4193E+00
9.639	0.8717E+00	0.8390E-01	0.0000E+00	0.0000E+00
9.603	0.8258E+00	0.1337E+00	0.4230E+00	0.3646E+00
9.586	0.1673E+01	0.4717E-01	0.0000E+00	0.0000E+00
9.569	0.1160E+01	0.2603E+00	0.7338E+00	0.5891E+00
9.552	0.3393E+00	0.2637E+00	0.4035E+00	0.3381E+00
9.536	0.8440E+00	0.1194E+00	0.4442E+00	0.3907E+00

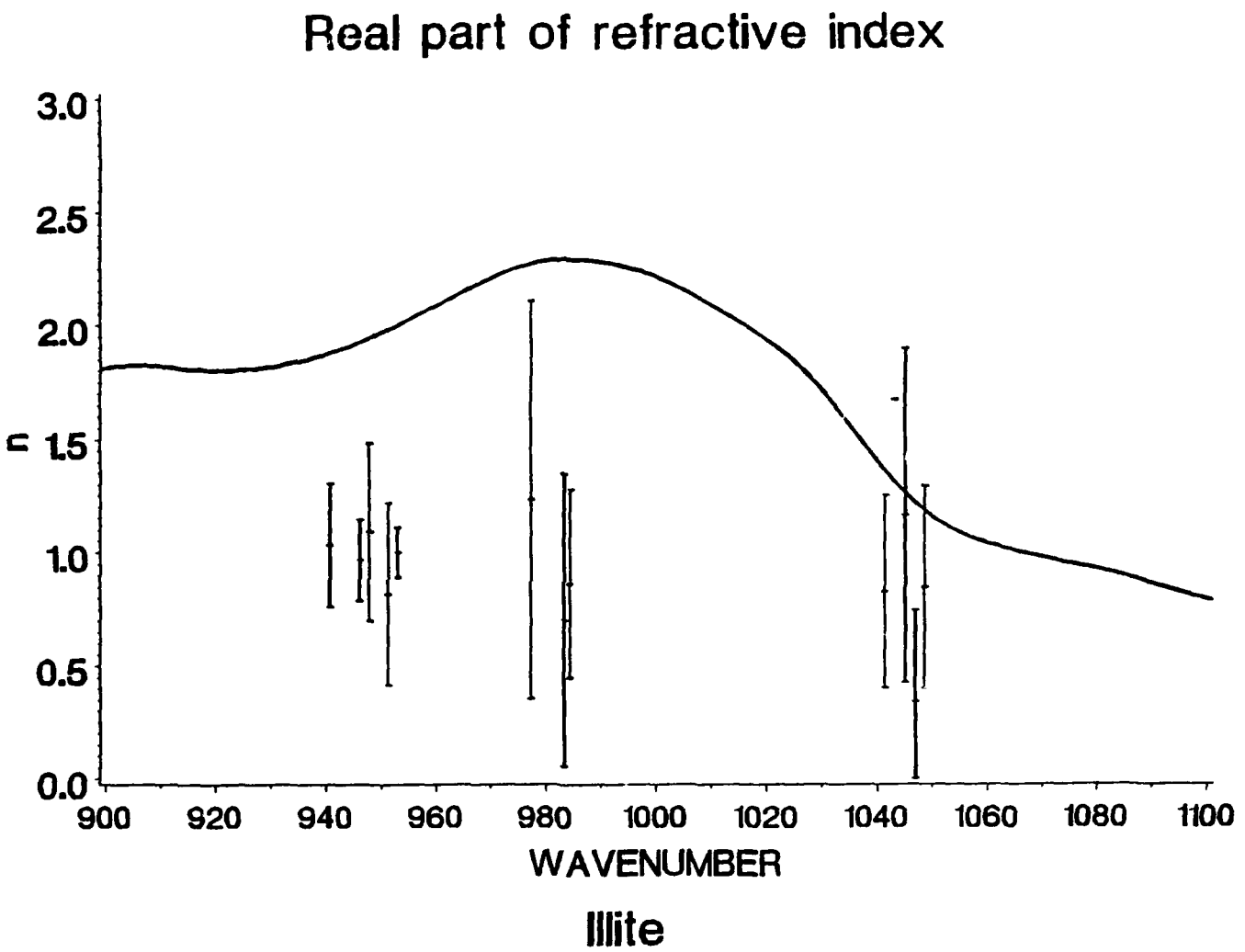

FIG. 4.18 Refractive index for Illite in the spectral region 900 to 1100 cm^{-1}. The laser data is represented by the symbols with the error bars representing +/- one standard deviation. The solid line is from Querry.

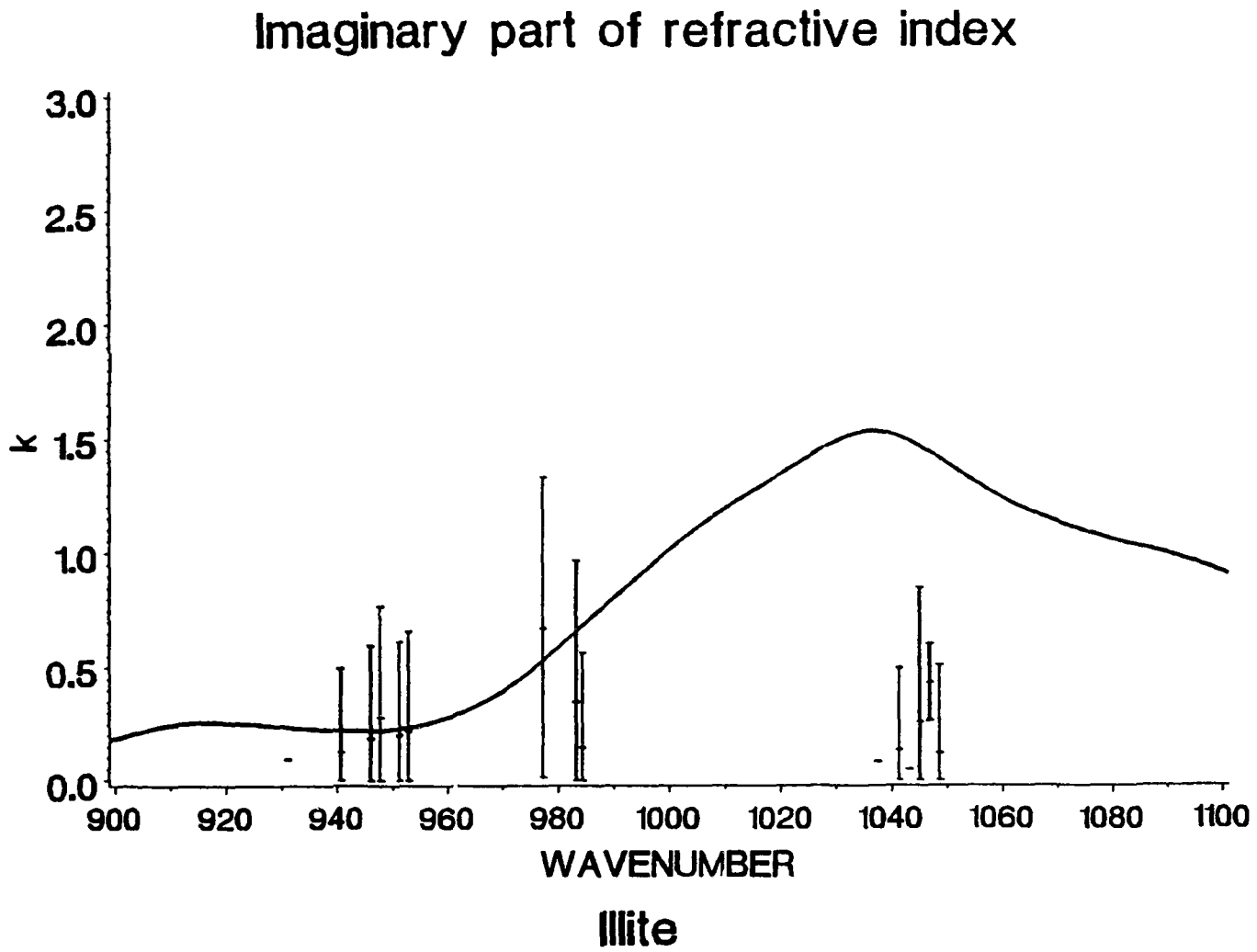

FIG. 4.19 Extinction coefficient for Illite in the spectral region 900 to 1100 cm^{-1}. The laser data is represented by the symbols with the error bars representing +/- one standard deviation. The lower limit of the error bars has not been allowed to go below k=0.0. The solid line is from Querry.

TABLE 4.4

Complex refractive index for Kaolin

λ (μm)	n	k	Δn	Δk
10.741	0.8499E+00	0.5358E+00	0.0000E+00	0.0000E+00
10.719	0.1507E+01	0.6633E+00	0.1039E+01	0.4516E+00
10.571	0.1156E+01	0.4859E+00	0.5473E+00	0.4929E+00
10.551	0.1132E+01	0.5731E+00	0.4672E+00	0.5134E+00
10.513	0.1597E+01	0.2847E+00	0.1396E+01	0.5606E+00
10.494	0.1030E+01	0.3426E+00	0.2972E+00	0.5008E+00
10.289	0.9425E+00	0.4959E+00	0.0000E+00	0.0000E+00
10.247	0.1056E+01	0.5777E+00	0.5762E+00	0.5032E+00
10.233	0.1342E+01	0.7753E+00	0.9498E+00	0.3755E+00
10.220	0.1090E+01	0.3876E+00	0.4130E+00	0.5137E+00
10.195	0.1150E+01	0.5354E+00	0.7914E+00	0.6033E+00
10.182	0.9383E+00	0.5500E+00	0.4762E+00	0.4307E+00
10.171	0.1049E+01	0.5787E+00	0.0000E+00	0.0000E+00
10.159	0.1109E+01	0.7142E+00	0.5686E+00	0.4347E+00
10.148	0.9417E+00	0.2424E+00	0.1934E+00	0.4616E+00
9.657	0.6672E+00	0.2229E+00	0.4023E+00	0.2576E+00
9.639	0.4773E+00	0.5323E+00	0.2761E+00	0.8256E+00
9.586	0.6489E+00	0.4945E+00	0.4339E+00	0.4253E+00
9.552	0.4388E+00	0.3319E+00	0.0000E+00	0.0000E+00
9.536	0.4830E+00	0.7431E+00	0.4975E+00	0.3256E+00
9.519	0.7709E+00	0.7413E+00	0.2292E+00	0.1411E+00
9.504	0.4753E+00	0.2514E+00	0.9584E-01	0.2255E+00
9.488	0.5800E+00	0.1390E+00	0.4189E+00	0.2965E+00
9.473	0.6185E+00	0.4048E+00	0.6776E+00	0.6890E+00
9.305	0.5686E+00	0.1824E+00	0.4832E+00	0.2806E+00

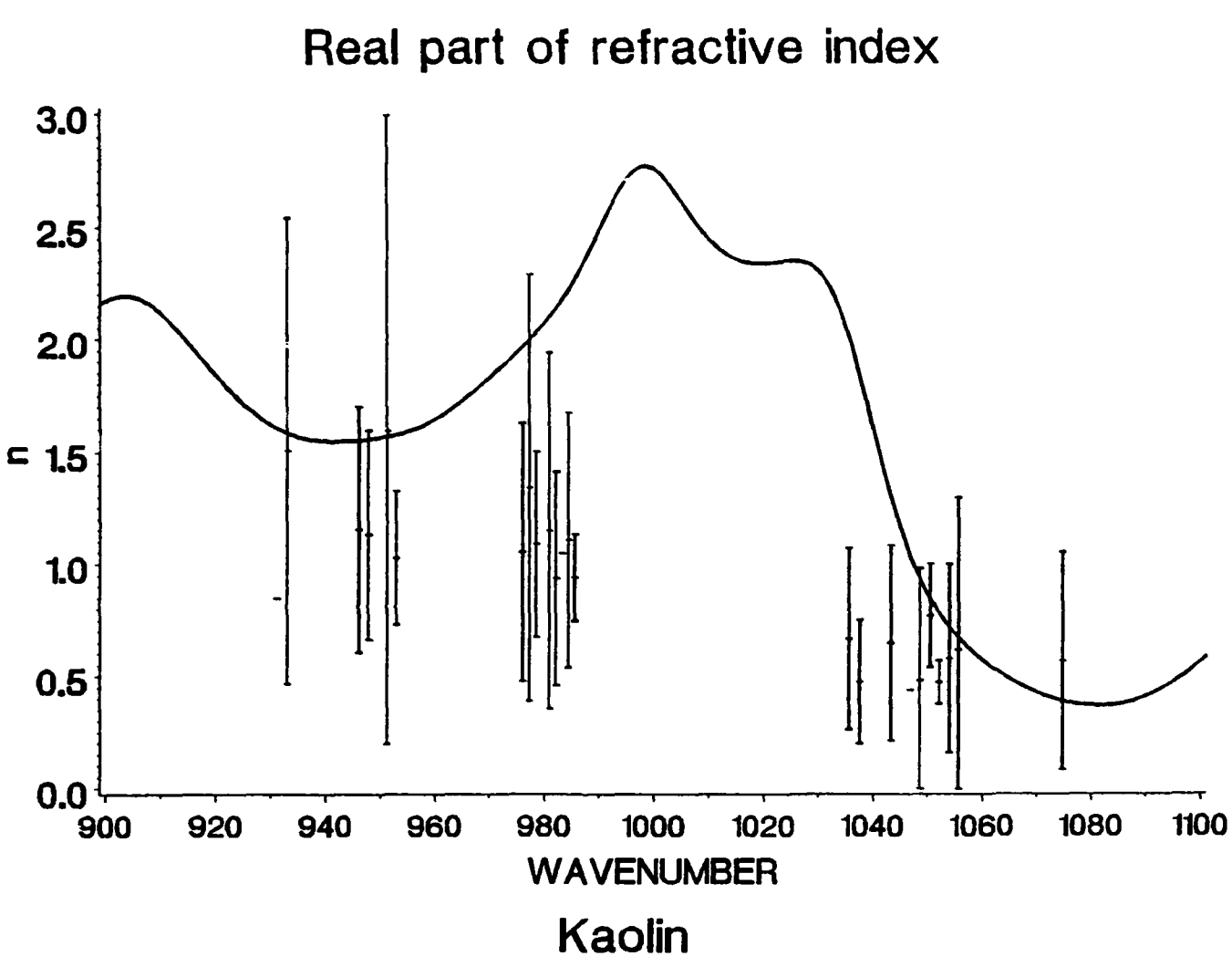

FIG. 4.20 Refractive index for Kaolin in the spectral region 900 to 1100 cm^{-1}. The laser data is represented by the symbols with the error bars representing +/- one standard deviation. The solid line is from Querry.

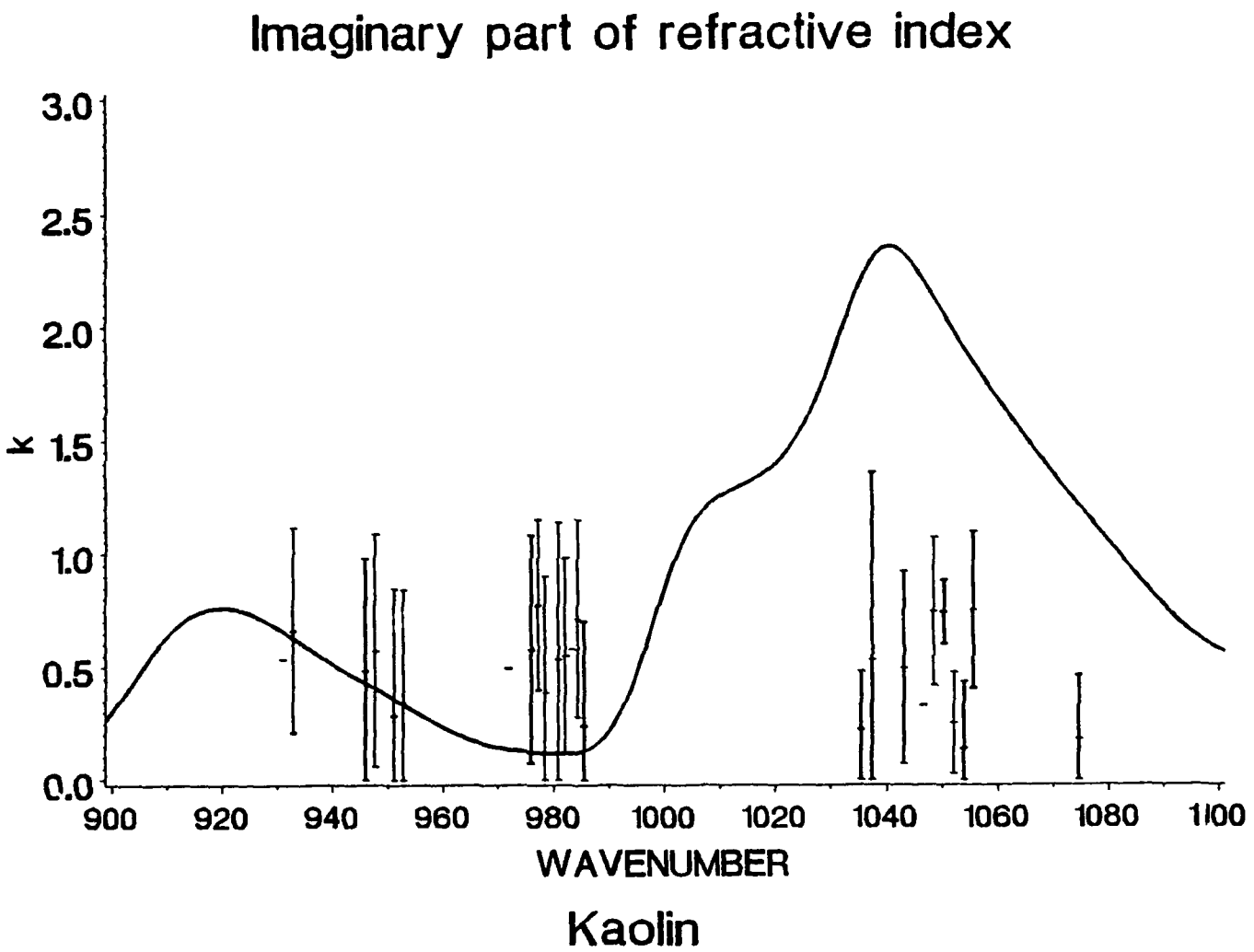

FIG. 4.21 Extinction coefficient for Kaolin in the spectral region 900 to 1100 cm^{-1}. The laser data is represented by the symbols with the error bars representing +/- one standard deviation. The lower limit of the error bars has not been allowed to go below k=0.0. The solid line is from Querry.

The complex refractive index for Montmorillinite is presented in Table 4.5 and in Figs. 4.22 and 4.23. The results are extremely poor. Any agreement between the complex refractive index as determined using Avery's method and those determined by Kramers-Kronig analysis is purely coincidental.

TABLE 4.5

Complex refractive index for Montmorillinite

λ (μm)	n	k	Δn	Δk
10.741	0.9317E+00	0.1842E+00	0.1890E+00	0.3969E+00
10.719	0.8431E+00	0.1706E+00	0.3678E+00	0.3761E+00
10.632	0.9629E+00	0.1427E+00	0.1831E+00	0.3537E+00
10.571	0.9525E+00	0.1339E+00	0.2106E+00	0.3483E+00
10.551	0.9654E+00	0.1286E+00	0.1153E+00	0.3486E+00
10.513	0.8528E+00	0.2642E+00	0.3483E+00	0.4393E+00
10.494	0.1025E+01	0.1820E+00	0.2733E+00	0.4450E+00
10.247	0.9508E+00	0.2125E+00	0.2449E+00	0.4605E+00
10.220	0.9995E+00	0.2309E+00	0.1043E+00	0.5097E+00
10.195	0.8221E+00	0.2162E+00	0.3858E+00	0.4329E+00
10.182	0.9997E+00	0.1517E+00	0.1524E+00	0.4108E+00
10.171	0.7869E+00	0.1107E+00	0.5011E+00	0.3764E+00
10.148	0.9742E+00	0.3482E+00	0.1773E+00	0.4475E+00
9.657	0.9741E+00	0.3937E+00	0.2661E+00	0.5319E+00
9.639	0.9180E+00	0.2763E+00	0.7469E-01	0.4615E+00

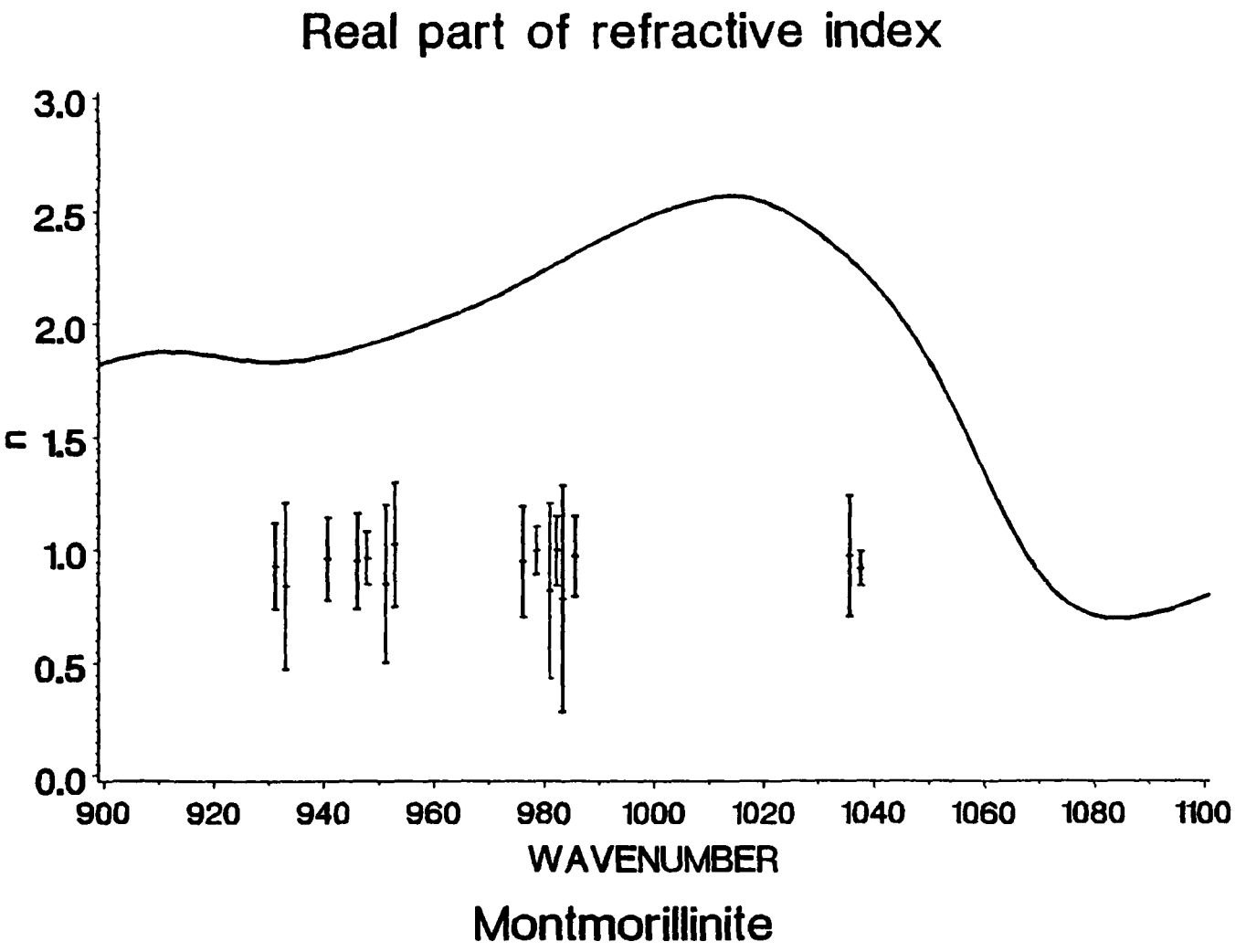

FIG. 4.22 Refractive index for Montmorillinite in the spectral region 900 to 1100 cm^{-1}. The laser data is represented by the symbols with the error bars representing +/- one standard deviation. The solid line is from Querry.

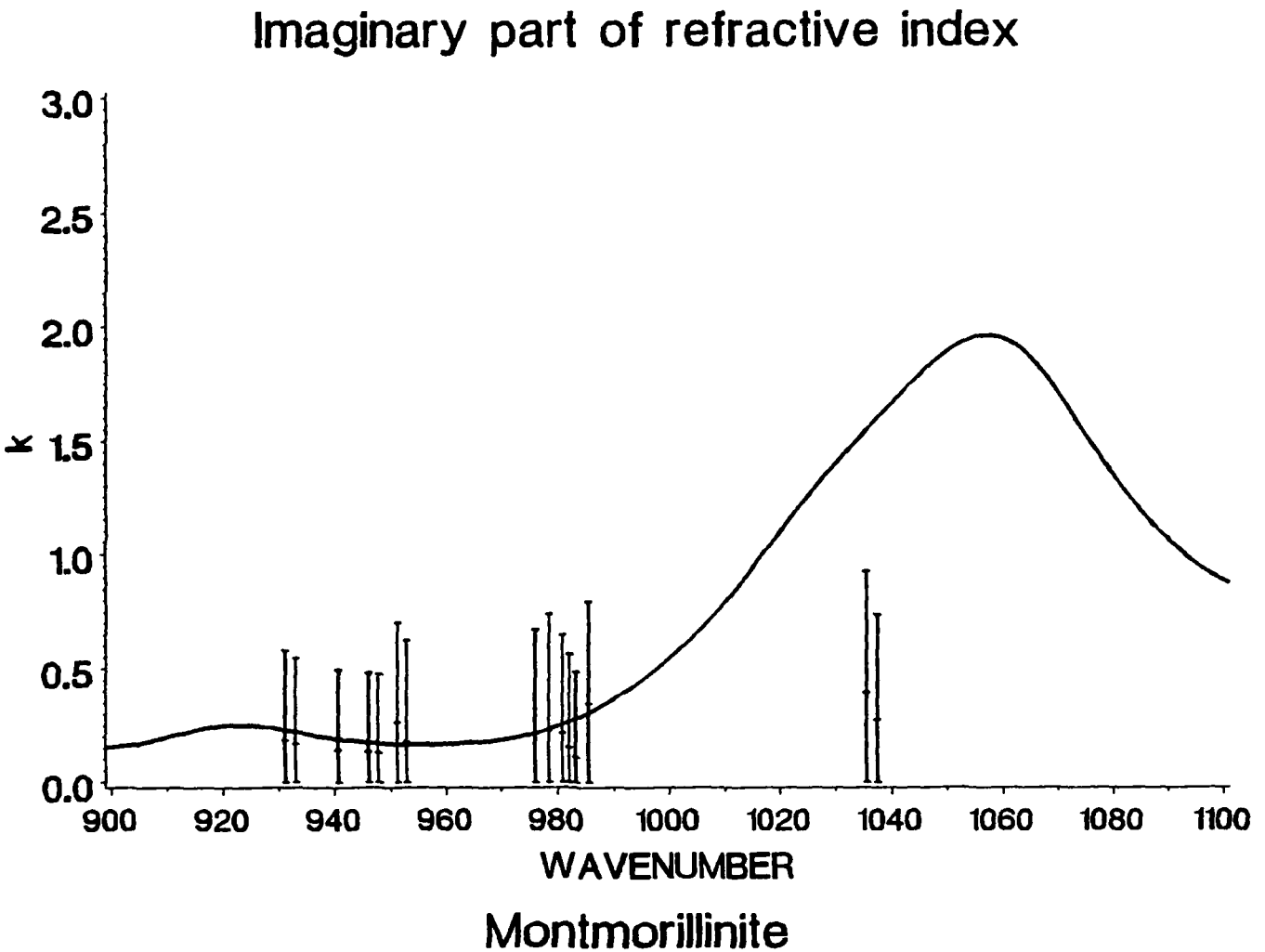

FIG. 4.23 Extinction coefficient for Montmorillinite in the spectral region 900 to 1100 cm^{-1} The laser data is represented by the symbols with the error bars representing +/- one standard deviation. The lower limit of the error bars has not been allowed to go below k=0.0. The solid line is from Querry.

f. CONCLUSION

The results presented are indicative of the sensitivity of the Avery method. The graphs of the fractional uncertainty in n and k, presented in the section on error analysis, show the refrective index to be very sensitive to variations in the reflection coefficients. In addition to the samples being pressed pellets, providing some diffuse reflection, the equipment problem continues to plague the experimental setup. As with the wedge-shaped cell, ATR and Querry's method the intensities cannot seem to be measured accurately enough. We are at a loss as to the source of the error in the system. Although, several tests have been performed to try to narrow the range of possible problems we still cannot pinpoint the problem. As suggested in the conclusion for the chapter on Querry's method one possibility is to coat the pellet surface with aluminum after the reflection measurements are performed on the pellet. This woul at least provide a scaling for the surface roughness. It will not account for the equipment problem, as this appears to be a random effect.

[1]D.G. Avery, Proc. Phys. Soc. (London) B 65. 425 (1952)

[2]J. Fahrenfort and W.M. Visser, Spectrochimica Acta, 18, 1103 (1962)

[3]Marvin R. Querry, private communication

g. APPENDIX 4.1

Program AVERY

g. APPENDIX 4.1

Program AVERY

```
C*************************************************************************
C   THIS PROGRAM IS TO COMPUTE THE COMPLEX REFRACTIVE INDEX USING THE ANGLE
C   METHOD. THE DETAIL DISCUSSION OF THE DERIVATION IS GIVEN IN
C   REFERENCE [2].
C*************************************************************************
C*************************************************************************
C  AIS1 AND AIS2 ARE REFLECTANCES OBTAINED FROM THE MEASUREMENTS. ANGLE1 AND
C  ANGLE1 ARE THE INCIDENT ANGLES. THE FIRST PART OF THE PROGRAM IS READ IN.
C*************************************************************************
      DIMENSION WN(4000),AIS1(4000),AIS2(4000),ANGLE1(4000),ANGLE2(4000)
      I=1
  10  READ(54,*,END=20) WN(I),ANGLE1(I),AIS1(I),ANGLE2(I),AIS2(I)
      ANGLE1(I)=ANGLE1(I)*3.141592654/180.0
      ANGLE2(I)=ANGLE2(I)*3.141592654/180.0
      I=I+1
      GOTO 10
  20  CONTINUE
      J=I-1
C*************************************************************************
C     CALCULATION OF A,B,C AND D IN [2].
C*************************************************************************
      DO 100 I=1,J
      COA=COS(ANGLE1(I))
      COB=COS(ANGLE2(I))
      A1=(1.0-AIS1(I))**4/AIS1(I)
      B1=(1.0+AIS1(I))**2*COA**4
      C1=((1.0-AIS1(I))*COA)**2
      D1=AIS1(I)*COA**4
      A2=(1.0-AIS2(I))**4/AIS2(I)
      B2=(1.0+AIS2(I))**2*COB**4
      C2=((1.0-AIS2(I))*COB)**2
      D2=AIS2(I)*COB**4
      G=C1*D2-C2*D1
C*************************************************************************
C     CALCULATION OF P AND Q IN [2].
C*************************************************************************
      P=(A1*D2-A2*D1)/G
      Q=(B1*D2-B2*D1)/G
C*************************************************************************
C     CALCULATION OF X, Y AND Z IN [2].
C*************************************************************************
      X=0.25*(A1-C1*P+0.25*D1*P**2)
      Y=4.0*(-B1+C1*Q-0.5*D1*P*Q)
      Z=16.0*D1*Q**2
C*************************************************************************
C     CALCULATION OF M, u and w IN [2].
C*************************************************************************
```

```
      IF ((Y**2-4.0*X*Z).LT.0.0) GOTO 50
      AM=(-Y-SQRT(Y**2-4.0*X*Z))/(2.0*X)
      U=Q-P*AM/16.0
      W1=(AM-U**2)
      IF (W1.LT.0.0) GOTO 50
      W=SQRT(W1)
C*****************************************************************************
C     CALCULATION OF THE COMPLEX REFRACTIVE INDEX N AND K.
C*****************************************************************************
      E=U-1.0
      AK1=(E+SQRT(E**2+W**2))/W
      IF (W/AK1.LT.0.0) GOTO 50
      AN=SQRT(W/(2.0*AK1))
      AK=AN*AK1
C*****************************************************************************
C     OUTPUT VALUES OF N AND K AS AN AND AK RESPECTIVELY
C*****************************************************************************
      WRITE(55,*) WN(I),AN,AK
   50 CONTINUE
  100 CONTINUE
      END
```


★ U.S. GOVERNMENT PRINTING OFFICE: 1990 261-016/20098